

The Synthesis of Amphiphilic Glycolipids as Potential Inhibitors of Bacterial Adhesion

A thesis submitted to the National University of Ireland in fulfilment of the requirements for the degree of

Doctor of Philosophy

by

Lorna Abbey, B.Sc.



NUI MAYNOOTH

Ollscoil na hÉireann Má Nuad

Department of Chemistry,
National University of Ireland Maynooth,
Maynooth, Co. Kildare, Ireland

September 2013

Research Supervisor: Dr. Trinidad Velasco-Torrijos

Head of Department: Dr. John Stephens

***To my parents and Conor,
Thank you for everything.***

Contents

Acknowledgements.....	i
Declaration.....	iii
Abstract.....	iv
Abbreviations.....	v
Chapter 1: Introduction.....	1
1.1 Glycolipids and their biological importance.....	2
1.2 Glycolipids as potential anti-adhesion agents.....	2
1.2.1 Anti-adhesion therapy.....	2
1.2.3 The multivalent glycoside effect.....	4
1.2.4 Glycoconjugates as inhibitors of <i>Burkholderia cenocepacia</i> adhesion.....	6
1.2.5 Glyconjugates as inhibitors of <i>Pseudomonas aeruginosa</i> adhesion.....	8
1.3 Glycolipids as immunomodulators.....	9
1.3.1 The immune response.....	9
1.3.2 Natural Killer T-Cells.....	10
1.3.3 α -Gal-Cer.....	10
1.3.4 Synthetic analogues of α -GalCer.....	11
1.4 Thesis objectives.....	13
Chapter 2: Alkyl glycolipids as novel soft materials.....	15
2.1 Amphiphilic glycolipids.....	16
2.2 Gelator molecules.....	17
2.2.1 Low molecular weight gelators (LMWG).....	17
2.2.1.1 The non-covalent interactions involved in gel formation.....	18
2.2.2 Non-carbohydrate gelators.....	18
2.2.3 Carbohydrate-based gelators.....	19
2.3 Glycomimetics.....	20
2.3.1 Glycolipid mimetics.....	21
2.3.2 Glycosphingolipid glycomimetics.....	22
2.4 Chapter objective.....	23
2.5 The synthesis of first generation aspartic acid-based β -O-glycolipids 2.26 , 2.27 and 2.28	25
2.5.1 Initial synthesis of β -O-glycolipid 2.26	26
2.5.1.1 Synthesis of galactosyl amine 2.33	27
2.5.1.2 Synthesis of acylated aspartic acid glycolipid 2.50	29
2.5.2 Alternative route to form β -O-glycolipid 2.26-2.28	32

2.5.3 Synthesis of β - <i>O</i> glycolipid 2.27 and 2.28	34
2.6 Synthesis of second generation glycolipids	36
2.6.1 Synthesis of bivalent β - <i>O</i> -glycolipid 2.29	36
2.6.2 Synthesis of β - <i>O</i> -glycolipid 2.31	37
2.6.3 Synthesis of disaccharide β - <i>O</i> -glycolipid 2.32	39
2.6.3.1 Synthesis of Lactosyl amine 2.70	39
2.6.3.2 Synthesis of aspartic acid building block 2.35	40
2.6.4 Synthesis of C-6 functionalised β - <i>O</i> -glycolipid 2.30	41
2.6.4.1 Attempted synthesis of C-6 functionalised galactose building block 2.83	43
2.7 Gelation and self-assembly properties of β - <i>O</i> -glycolipids 2.26-2.32	47
2.7.1 Gelation and self-assembly properties of first generation of β - <i>O</i> -glycolipids	47
2.7.1.1 SEM on <i>O</i> -glycolipids 2.55 , 2.61 , and 2.90	51
2.7.1.2 Spectroscopic studies on glycolipid 2.55 and 2.61	55
2.7.2 Gelation and self-assembly properties of second generation β - <i>O</i> -glycolipids	61
2.7.3 Ability of selected <i>O</i> -glycolipids to act as hydrogelators	64
2.8 Incorporation of glycolipid 2.55 into a giant unilamellar vesicle (GUV)	68
2.9 Conclusion	69
Chapter 3: Synthesis of malonamide glycoconjugates as potential anti-adhesion agents	71
3.1 Introduction	72
3.1.1 Malonates and their potential application	72
3.1.2 Non-carbohydrate-based malonamides	73
3.1.3 Carbohydrate-based malonamides	76
3.2 Chapter Objective	77
3.3 The synthesis of malonyl-based glycoconjugates 3.32 , 3.33 and 3.34	79
3.3.1 Attempted synthesis of β - <i>O</i> -glycoconjugate 3.33 via alkylation followed by amide coupling	80
3.3.2 Decarboxylation of malonic acid derivatives	81
3.3.3 Attempted Knoevenagel synthesis of β - <i>O</i> -glycoconjugate 3.43 via alkylation followed by amide coupling	84
3.3.4 Hydrolysis of alkylidene malonate 3.48	86
3.3.5 Amidation reactions of malonic esters	87
3.3.6 Malonyl chloride and malonic acid as precursors for the synthesis of malonamides	88
3.4 Synthesis of <i>O</i> -glycoconjugate 3.33	90
3.4.1 DMTMM as an alternative peptide coupling reagent	90
3.5 Synthesis of <i>N</i> -glycoconjugate 3.32	92

3.5.1 Synthesis of galactosyl amine 3.66	92
3.6 Synthesis of Malonyl-based <i>O</i> -glycoconjugate 3.44	93
3.7 Conclusion	95
Chapter 4: Synthesis of glycolipids-based on aromatic scaffolds as potential anti-adhesion agents	96
4.1 Introduction	97
4.2 Aromatic-based glycolipids and their biological importance	98
4.2.1 Synthesis and application of divalent glycoconjugates	98
4.2.2 Synthesis and applications of trivalent glycoconjugates	100
4.2.3 Synthesis and applications of oligovalent glycoconjugates	102
4.2.4 Synthesis and applications of glycolipids based around an aromatic core	103
4.3 Chapter objective	104
4.3 The synthesis of the first generation of glycolipids 4.38 and 4.39 based on aromatic scaffolds	106
4.3.1 Synthesis of <i>O</i> -glycoconjugate 4.38	107
4.3.1.1 Initial synthesis of aromatic backbone 4.47 utilising trimesoyl chloride.....	108
4.3.1.2 Attempted Synthesis of aromatic backbone 4.47 utilising trimesic acid.....	112
4.3.1.3 Synthesis of glycolipid 4.48 via pentafluorophenyl (PFP) esters	114
4.3.2 Synthesis of <i>O</i> -glycoconjugate 4.39	116
4.3.2.1 Synthesis of aromatic core 4.72	116
4.4 The synthesis of first generation triazole containing glycolipids 4.40 and 4.41 based on aromatic scaffolds.....	118
4.4.1 Cu catalysed azide-alkyne cycloaddition (CuAAC)	119
4.4.2 Synthesis of β - <i>O</i> -glycoconjugate 4.40	121
4.4.3 Synthesis of β - <i>O</i> -glycoconjugate 4.41	122
4.5 The synthesis of the second generation of glycolipids-based on aromatic scaffolds 4.36 and 4.37	123
4.5.1 Synthesis of <i>N</i> -Glycoconjugate 4.36	124
4.5.2 Synthesis of <i>N</i> -glycoconjugate 4.37	125
4.6 The synthesis of the second generation triazole containing glycolipid 4.42 based on an aromatic scaffold	126
4.7 The synthesis of second generation glycoconjugate 4.43 based on an aromatic scaffold	128
4.7.1 Initial synthesis of glycoconjugate 4.43	129
4.7.2 Attempted synthesis of glycoconjugate 4.43 using pentafluorophenyl esters	130
4.7.3 Synthesis of glycoconjugate 4.43	131

4.8 The synthesis of monovalent aromatic glycolipid 4.44	132
4.9 The synthesis of non-symmetrical glycolipids based on an aromatic scaffolds 4.116 and 4.117	133
4.9.1 Synthesis of non-symmetrical aromatic glycolipid 4.116	135
4.9.2 Synthesis of non-symmetrical aromatic glycoconjugate 4.117	137
4.10 The synthesis of glycoconjugates with more complex carbohydrate epitopes.....	139
4.10.1 Synthesis of glycosyl donor 4.129	140
4.10.2 Synthesis of glycosyl acceptor 4.130	141
4.10.3 α -Galactosylation between glycosyl donor 4.129 and glycosyl acceptor 4.130	142
4.11 Spectroscopic analysis on selected glycolipids	145
4.11.1 Concentration studies on first generation glycolipids 4.48 and 4.116	145
4.11.2 Concentration studies on second generation glycolipids 4.109 , 4.125 and 4.126	147
4.12 Conclusions	149
Chapter 5: Evaluation of glycolipids as potential inhibitors of bacterial adhesion	151
5.1 Cystic Fibrosis.....	152
5.1.1 CFTR protein.....	152
5.1.2 CF and bacterial infections.....	153
5.2 <i>Burkholderia cenocepacia</i> complex (<i>Bcc</i>).....	153
5.2.1 Virulence of <i>Bcc</i>	155
5.3 Bacterial adhesion to cell surfaces.....	155
5.3.1 <i>Bcc</i> invasion of epithelial cells.....	156
5.4 Chapter Objective	157
5.5 Anti-adhesion assay	158
5.6 Biological evaluation of glycolipids 2.26 and 2.29 based on aspartic acid scaffolds	159
5.7 Biological evaluation of glycolipids 3.32 and 3.34 based on aliphatic scaffolds.....	161
5.8 Biological evaluation of glycolipids based on aromatic scaffolds 4.27-4.34	163
5.8.1 Rigid N-glycolipids 4.36 and 4.37 versus flexible O-glycolipids 4.38 and 4.39	163
5.8.2 1,2,3-Triazole-containing O-glycolipids 4.40 and 4.41 and N-glycolipids 4.42	166
5.8.3 Biological evaluation of O-glycolipid 4.43 and N-glycolipid 4.44	169
5.9. Conclusions based on structural-activity relationship.....	170
5.9.1 Multivalent versus monovalent:	170
5.9.2 Flexibility versus rigidity:.....	171
5.9.3 Importance of hydrophobic chain.....	172
5.10 Conclusions	174

Chapter 6: Experimental details	175
6.1 General Procedure and Instrumentation.....	176
6.2 Experimental procedures.....	177
6.2.1 Experimental procedures for Chapter 2	177
6.2.2 Experimental procedures for Chapter 3	212
6.2.3 Experimental procedures for Chapter 4	224
6.2.4 Experimental procedures and materials for Chapter 5	261
Bibliography	265
Author Publications	275

Acknowledgements

Firstly I would like to thank my supervisor Dr. Trinidad Velasco-Torrijos. It has been an honour to work with you over the last few years and I sincerely thank you for all the support and encouragement you have given me. To all lecturing staff at NUIM, a huge thank you for helping me to get to where I am today! To the technical staff, for their extreme patience when analysing our often difficult samples, hopefully the mass spectrometer will stay pyridine free for the foreseeable future. To Noel for all the technological advice and for keeping my computer running smoothly. To Dr. John O'Brien for performing NMR experiments, and to Dr. Siobhan McClean for hosting me in your lab in ITT.

To all the post graduate students past and present, a huge thank for making the last few years so enjoyable. I will certainly miss the random conversations and tasty treats which used to await me in the coffee room. To Rob, my symbiosis sidekick, you have been there through it all. Thank you for the support, the laughs, and even the abuse. You really have always been here for me and I couldn't ask for a truer friend (I am holding you to that Hebrew prayer!). To Roisin, my evil enantiomer, thank you so much for everything. You were an immense help right from the start, and certainly kept us all entertained with your ridiculous sayings and statements. I think I owe you a few nights B and B for the amount of times you gave me a bed! To Ursula, for keeping me company on the many late nights, I can truly say I am not just friends with you because you are Walshy's missus. To Dec for the endless abuse, hilarious stories and home cooked meals, Foxy for the cakes, coffee breaks and many chats, John W for the insults only he could get away it, Lynn for the power ballads, Valeria for highlighting just how bad my eating habits are and Gillian for coming back to us, don't let me down with them carbohydrates!! You really are a great bunch. I also want to thank Ross for educating me on music and Finno for giving me an interesting internet browsing history! To the past post graduate students, Colin for his funny impressions, John for when he was Greg, and Dennis for the quote wall, it has been memorable. To the Velasco gang Carol, Roisin, Gama and Andrew thank you for everything. Andrew, I only hope you enjoy your time here as much as I did. To my write up room buddies, Keely, Wayne, Niall and Haixin, thanks for the advice and chats! To everyone I didn't mention personally, thanks a million, I hope you realise how much easier you's made it.

Thanks also to all the post graduate students in ITT, Ruth, Sarah, Minu, Mark, Luke, Loiuise and Niamh. It is thanks to you that I am now half a biologist, even if it did initially look doubtful! At least my antics kept you's entertained.

To my girls Aisling, Michelle, Roisin and Danielle, I am sorry I haven't been around much the last year but I promise from now on you will be sick of the sight of me. Thank you for the distractions and for keeping me sane.

To Conor, what can I say, you have been my rock. Over the last eight years you have provided me with unending love and encouragement. You have been such an emotional, physical and even financial support, and words cannot express how grateful I am. As a wise women once said "every women should have a Conor in their lives". I think a few trips to Old Trafford are definitely in order.

Finally to huge thank you to my family. To my Mam and Dad for their continuing love and support throughout the years. Even as children you both always encouraged us in everything we did, and for that, I will be eternally grateful. Oh and don't worry Dad I am sure will move out eventually! A huge thank you to Wendy, Gav, Keith and Marion for always looking out for their little sister, but more importantly for my adorable nieces and nephews. Cian, Lexi and Craig, you always managed to bring a smile to my face and truly were the most welcome distraction.

Declaration

I declare that the work presented in this thesis was carried out in accordance with the regulations of NUI Maynooth. The work is original, except where indicated by reference, and has not been submitted before, in whole or in part, to this or any other university for any other degree.

Signed: _____

Date: _____

Abstract

The synthesis of glycolipids as potential anti-bacterial agents and glycolipid mimetics is the main focus of the research presented in this thesis. A variety of glycolipids based around an aspartic acid, aliphatic or aromatic scaffold were investigated.

Chapter 1 describes the biological importance of glycolipids and how they can be utilised as anti-adhesion agents and immunomodulators. The concept of multivalency is also discussed, with specific examples relating to the anti-adhesion approach.

A variety of *O*-glycolipids based around an aspartic acid scaffold were constructed in chapter 2. Based on a modular approach, a diverse range of glycolipids were synthesised. They exhibited variations in hydrocarbon chain length, number of hydrocarbon chains, connectivity of carbohydrate moiety and the carbohydrate moiety used. Although originally designed to act as immunomodulators their ability to inhibit bacterial adhesion in immunocompromised individuals was also investigated. Furthermore the glycolipids were tested as low molecular weight organogelators (LWOG), and promising results were obtained.

Chapter 3 deals with the synthesis of *O*- and *N*-glycolipids built around an aliphatic core. Initially the synthesis proved problematic but success was achieved utilising DMTMM as the coupling reagent. Similarly to the aspartic acid analogues, the glycolipids exhibited variation in the chemical nature of the spacer groups used to link the carbohydrate to the aliphatic core. The *O*- and *N*-glycolipids were synthesised with a view to examine their ability to inhibit bacterial adhesion in Cystic Fibrosis (CF) patients.

The synthesis of a range of glycolipids based around an aromatic core is discussed in chapter 4. Again variation in the linker utilised to connect the carbohydrate moiety and the aromatic core is explored. This time the importance of the presence of the hydrocarbon chain was also investigated. Therefore variation in the connectivity of the lipidic chain is explored, and analogues of varying hydrocarbon chain length were synthesised. The *O*- and *N*-glycolipids were synthesised as potential anti-adhesion agents in order to determine a structural activity relationship.

The biological evaluation of selected glycolipids is discussed in chapter 5. Selected aspartic acid, aliphatic and aromatic glycolipids are investigated as potential inhibitors of *Burkholderia multivorans* adhesion to a model of lung epithelial cells of CF patients. Promising preliminary results were obtained for both a mono- and di-valent aromatic-based glycolipid.

Abbreviations

Ac = Acetyl

Ac₂O = Acetic anhydride

AcCl = Acetyl chloride

ANOVA = Analysis of variance

APC = Antigen presenting cell

Aq = Aqueous

Atm = Atmospheric pressure

Bcc = Burkholderia cepacia complex

BnBr = Benzyl Bromide

Boc = *t*-Butyloxycarbonyl

°C = Degrees Celsius

Cbz = Benzyloxycarbonyl

CD1 = Cluster of differentiation

CDCl₃ = Deuterated chloroform

CDMT = 2-Chloro-4,6-dimethoxy-1,3,5-triazine

CF = Cystic Fibrosis

CFTR = Cystic fibrosis transmembrane conductance regulator

COSY = Correlation spectroscopy

Con A = *Concanavalin A*

CTB = Cholera toxin B

CuAAC = Copper(I)-catalysed azide-alkyne cycloaddition

*d*₅-Pyr = Deuterated pyridine

DBU = 1,8,-Diazabicyclo[5.4.0]undec-7-ene

DCM = Dichloromethane

DCC = *N,N*-Dicyclohexylcarbodiimide

DEPT = Distortionless enhancement by polarization transfer

DIPEA = *N,N*-Diisopropylethylamine

DMAP = Dimethylaminopyridine

DMF = Dimethylformamide

DMSO = Dimethylsulfoxide

DMTMM = 4-(4,6-Dimethoxy-1,3,5-triazin-2-yl)-4-methylmorpholinium chloride

Et₂O= Diethyl ether

EtOAc = Ethyl acetate

EtOH = Ethanol

FT-IR = Fourier transfer infrared spectrometry

α-GalCer = α-Galactosylceramide

GMB = Gram negative bacteria

GSL = Glycosphingolipid

GUV = Giant unilamellar vesicle

h = Hours

HBD = Hydrogen bond donor

HBA = Hydrogen bond acceptor

HAT = Histone acetyltransferases

HCl = Hydrochloric acid

HOBT = Hydroxybenzotriazole

HR-MS = High resolution mass spectrometry

HSQC = Heteronuclear single quantum coherence

Hz = Hertz

IC₅₀ = The concentration of compound that's results in 50% inhibition

iNKT = invariant Natural killer T

IR = Infrared spectroscopy

KBr = Potassium bromide

LMWG = Low molecular weight gelator

LMWOG = Low molecular weight organogelators

MeCN = Acetonitrile

MeOH = Methanol

MGC = Minimum gelation concentration
MIC = Minimum inhibitory concentration
Min = Minutes
MS = Molecular sieves
NaOMe = Sodium methoxide
NEt₃ = Triethylamine
NIS = *N*-Iodosuccinimide
NMR = Nuclear magnetic resonance
NMM = *N*-Methylmorpholine
Pd(C) = Palladium on activated charcoal
Pet Ether = Petroleum ether
ppm = Parts per million
p-TsOH = *p*-Toluenesulfonic acid
Pyr = Pyridine
Rt = Room temperature
SAR = Structure-activity relationship
Sat. = Saturated
SEM = Scanning electron microscopy
TBTU = (*O*-Benzotriazol-1-yl)-1,1,3,3-tetramethyluronium hexafluorophosphate
TCR = T cell receptor
TFA = Trifluoroacetic acid
T_{gs} = Gel to sol temperature
T_H1 = T helper 1
T_H2 = T helper 2
THF = Tetrahydrofuran
TLC = Thin layer chromatography
TMS = Trimethylsilyl
TMSCl = Trimethylsilyl chloride

TMSN₃ = Trimethylsilyl azide

TMSOTf = Trimethylsilyl trifluoromethanesulfonate

TOF = Time of flight

Chapter 1: Introduction

1.1 Glycolipids and their biological importance

Glycolipids, as their name implies, are lipids that are attached to a carbohydrate moiety.^[1] Glycolipids are amphiphilic in nature, and can be divided into different sub-classes depending on 1) the organism in which they are found,^[2] and 2) their structure and function.^[3] Glycolipids found in animals generally belong to the glycosphingolipid family and are important membrane components (Figure 1.1).^[3] Glycolipids found in plants generally belong to the glycoacylglycerolipids family.^[2]

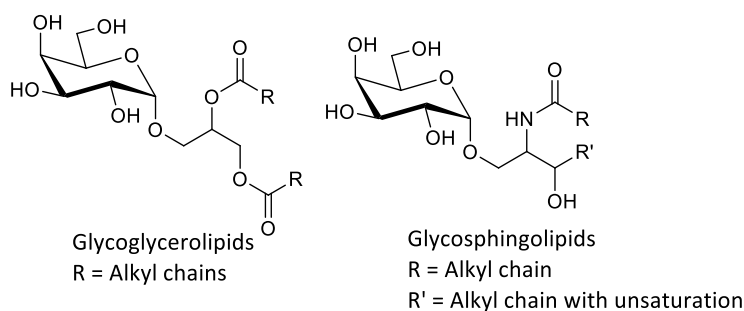


Figure 1.1 General structure of glycoacylglycerolipids and glycosphingolipids.

Glycolipids are an essential component of cell membranes^[4] and are normally found at the outer surface. They play a vital role in a number of cellular functions, including cell adhesion, cell-cell communication, signal transduction, protein sorting^[2] and cell pathogen interactions.^[4-5]

The hydrophobic lipid part of the glycolipid buries itself in the outer lipid layer of the cell membrane, whereas the hydrophilic carbohydrate portion extends from the phospholipids bilayer into the aqueous environment outside the cell.^[6] It can then act as a recognition site for specific chemicals, help maintain the stability of the membrane and also play a role in tissue formation.^[6-7]

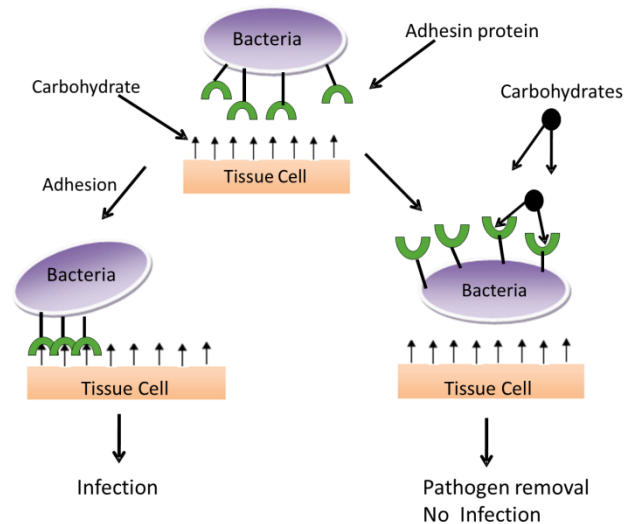
1.2 Glycolipids as potential anti-adhesion agents

1.2.1 Anti-adhesion therapy

The alarming rate at which bacterial antibiotic resistance is increasing has made it vital to intensify the search for new means of combating bacterial infections.^[8] A strategy which does not kill the pathogens but still interferes with their pathogenicity may provide a much needed alternative.^[9] One such approach, which has proved highly promising, is anti-adhesion therapy.^[8-9]

The anti-adhesion approach inhibits bacterial adhesion to the host cell by using agents (particularly carbohydrate) to bind to the adhesin proteins present on the pathogen, therefore preventing the bacteria from attaching to the carbohydrates present on the surface of the cell

(Scheme 1.1). Bacterial adhesion is often the prerequisite for the later stages of infection including colonisation and invasion of tissues, thus this approach is highly advantageous. The non-adhering bacteria can then be removed by the regular cleansing mechanisms of the body.^[9] As the bacteria are not killed, but rendered ineffective, they are not under selection pressure and as a result, bacterial resistance to these anti-adhesive drugs evolves slowly.^[10]



Scheme 1.1 Bacterial adhesion to the cell can result in infection (left). Free carbohydrates binding to the pathogen (right) prevent bacterial adhesion to the cells, therefore preventing infection.^[9]

The key to using carbohydrates for the anti-adhesion approach is that, when the bacteria mutate and lose their affinity for the carbohydrate drug (i.e. become resistant), they also lose their ability to bind to the native carbohydrates present on host cells.^[11] Also, as many of the saccharides that inhibit bacterial adhesion are found on cell surfaces or in body fluids, they are unlikely to be toxic or immunogenic and are ideal for using as anti-adhesion agents.^[12] Another benefit comes from the specificity exhibited by the bacterial adhesins. Individual microbe species bind to different carbohydrate sequences, therefore the carbohydrate-based drugs can be used to target only the species that requires elimination. This is not the case with conventional antibiotics, which can also kill and target non-pathogenic, normal microbial flora.^[13]

An important hurdle in the development of this area is the limited affinity of monovalent carbohydrates for the target proteins that are often multivalent. Multivalent inhibitors seem a logical step to overcome the limitation.^[9]

1.2.3 The multivalent glycoside effect

Protein-carbohydrate interactions are responsible for the initiation of a number of crucial events in a variety of biological processes including cell–cell communication, fertilisation, host–pathogen interactions, and immune response.^[14] However, a major problem lies in the fact that individual carbohydrates tend to bind weakly to their complementary multivalent proteins. To overcome this, multivalent scaffolds containing a number of carbohydrates have been utilised.^[15] It has been shown that multivalent glycosides bind with greater affinities to their polyvalent protein receptors.^[16] This phenomenon, which was first noted by Lee and co-workers is known as the “cluster” or “multivalent” glycoside effect,^[17] and has found a wide range of applications in biology and medicine. Some examples are discussed below.

Adhesin proteins present on uropathogenic *Escherichia coli* recognise and bind to galabiose (Gal- α 1-4Gal)-containing structures present on cell surfaces. It is by this mechanism that the bacteria adhere to the host cells. Pieters and coworkers synthesised a variety of galabiose containing multivalent glycoconjugates **1.1-1.4** (Figure 1.2) and investigated their potential as inhibitors of *E. coli* adhesion.^[18] They also investigated their potential anti-adhesion properties against *Streptococcus suis*.

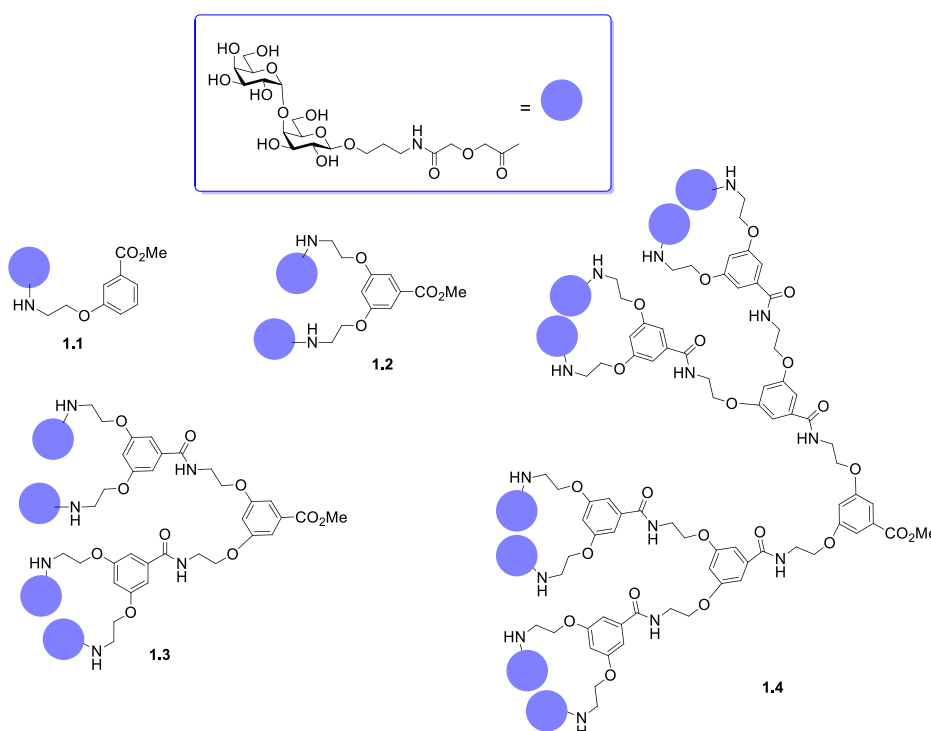


Figure 1.2 Variety of galabiose multivalent ligands tested as potential inhibitors of *E. coli* adhesion to host cells.^[18]

A number of assays were performed, and it was found that the mono- and multivalent galabiose derivatives **1.1-1.4** inhibited bacterial adhesion in a concentration-dependent manner. The multivalent effect was also prominent as the octavalent derivative **1.4** proved to

be a much better inhibitor than the tetravalent derivative **1.3**, which was in turn superior to the bivalent derivative **1.2** and so on (Table 1.1). Interestingly, the multivalent effect was much more pronounced for the inhibition of *S. suis* adhesion in comparison to the *E. coli*.

	<i>E. coli</i> Relative potency	<i>E. coli</i> potency per sugar	<i>S. suis</i> Relative potency	<i>S. suis</i> potency per sugar
Monovalent (1.1)	1.0	1.0	1.0	1.0
Divalent (1.2)	2.6	1.3	13	6.7
Tetravalent (1.3)	7.7	1.9	250	63
Octavalent (1.4)	43	5.3	310	39

Table 1.1. The relative inhibitory potency [IC_{50} (monovalent compound)/ IC_{50} (multivalent compound)] of galabiose derivatives in surface plasmon resonance (SPR) adhesion assay with *E. coli* and *S. suis*. To calculate the potency per sugar unit, the relative potency was divided by the valency of the compound.

Pieters and his group have carried out much research in this area and have synthesised a variety of different ligand collections consisting of compound with varying valency.^[18-19] Each collection is based around the same dendrimer scaffold but contains different carbohydrate moieties and also different linker structures.^[19] One such example is the synthesis of a variety of lactose-containing dendrimers **1.5-1.9** (Figure 1.3), with each one exhibiting a different valency. The ability of the ligands to bind the cholerae toxin B (CTB) subunit were evaluated.^[20]

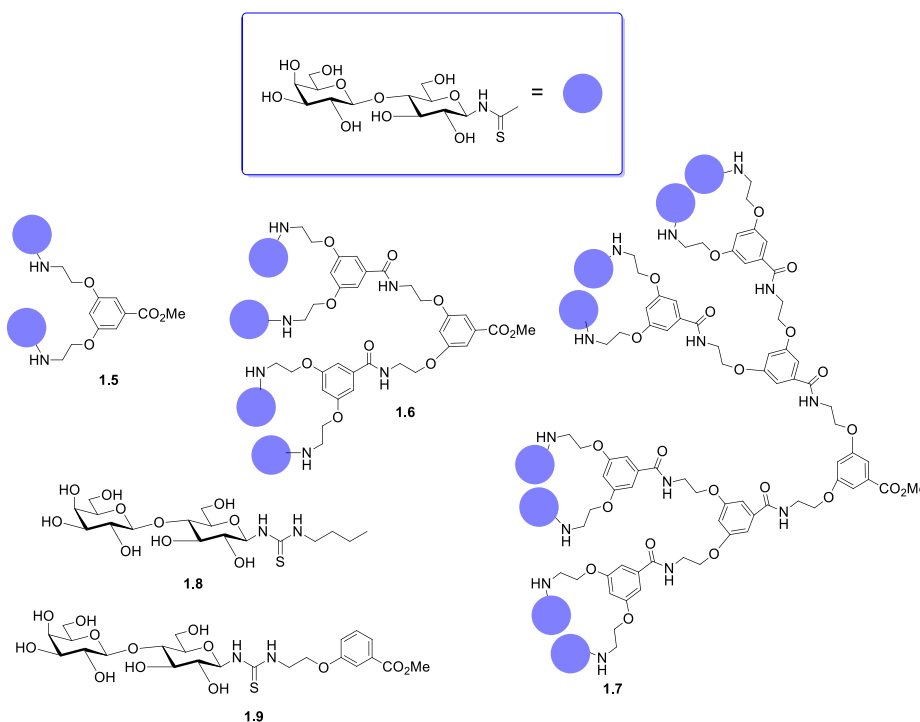


Figure 1.3 Variety of lactose multivalent ligands tested as potential binders of the cholerae toxin B subunit.^[20]

As with the previous example, the multivalent effect is extremely evident. All multivalent derivatives were able to bind to the CTB and therefore led to an increase in inhibition of bacterial binding to the host cells (Table 1.2). They also found that the binding of CTB increased with increasing valency. As expected, the octavalent ligand **1.7** displays the strongest binding with a K_d of 33 mM. Surprisingly the results for the monovalent ligand **1.9** were also quite promising, as it had a K_d of 248 mM, making it 73 times more potent than lactose alone. Pieters *et al.* suggest that this increase in affinity is due to additional interactions which can occur between the aglycone and the protein. The difference in binding affinity between the mono- **1.9** and di-valent ligand **1.5** is only very minimal. This could be due to the linker length, as it may not have allowed both carbohydrate moieties to bind simultaneously to adjacent subunits. This highlights the importance of considering binding site spacing when designing dendrimers for multivalent inhibition.^[21]

Compound	K_d [μ m]	Relative potency	Relative potency per lactose
Lactose	18000	1	1
1.8	2700	7	7
1.9	248	73	73
1.5	235	77	38
1.6	99	182	46
1.7	33	545	68

Table 1.2 Apparent dissociation constants of the binding of various lactose derivatives to CTB.

1.2.4 Glycoconjugates as inhibitors of *Burkholderia cenocepacia* adhesion

Burkholderia cenocepacia complex (Bcc) is a group of opportunistic pathogens associated with infections in immunocompromised individuals which have underlying lung disease e.g. CF (discussed further in Chapter 5, section 5.1).^[22] Bcc is often resistant to common antibiotics, and therefore utilising multivalent carbohydrates as inhibitors of the bacterial adhesion would be highly advantageous.

McClellan and co-workers previously showed that terminal galactose-containing glycolipids present on the surface of the host cell mediate bacterial adhesion and therefore facilitate the invasion of the lungs.^[23] With this in mind, ligands containing terminal galactose moieties could potentially be utilised to reduce bacterial adhesion. One such example comes from Murphy and co-workers.^[24] Bivalent lactosides **1.10-1.12** (Figure 1.4) were synthesised and tested as potential inhibitors of *Burkholderia multivorans* bacterial adhesion. Results showed that

lactoside **1.10** strongly inhibited the binding of *B. multivorans* to lung epithelial cells at a range of concentrations. In comparison, the more rigid derivative **1.11** was unable to inhibit adhesion. In fact, at certain concentrations it led to an increase in bacterial adhesion to the epithelial cells. Finally the tertiary amide derivative **1.12** decreased attachment at low concentrations, but at higher concentrations, it led to an increase in bacterial attachment.^[24]

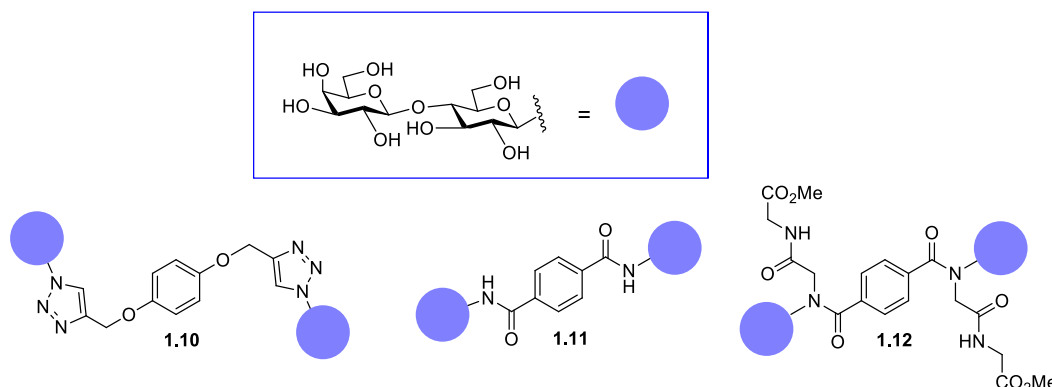


Figure 1.4 Selection of bivalent lactosyl glycoconjugates synthesised and tested against *B. multivorans*.

One of the soluble lectins (discussed in detail in chapter 5) of *Burkholderia cenocepacia* is BC2L-A, and it has been shown to exhibit a strong affinity for α -D-mannosides, with methyl α -D-mannopyranoside displaying a K_d value of $2\mu\text{m}$.^[25] Lameignere *et al.* tested a variety of α -D-mannosides and investigated their affinity for the BC2-A lectin (Figure 1.5). The bivalent compound **1.15** with a rigid linker displayed high binding affinities in comparison to the more flexible bivalent derivative **1.14** and the trismannoside **1.16**, which both only exhibited moderate affinities. The rigid compound **1.15** had an affinity ten times greater than the flexible compound **1.14** and it is believed this difference is due to the inability of the flexible compound to cross-link the lectins. It was observed that both the flexible derivative **1.14** and the trismannoside **1.16** bind as monomers. Lameignere *et al.* postulated that the flexible compound **1.14** can fold on the BC2L-A structure and as a result, it does not interact with neighbouring proteins. If this is the case, a rigid linker which efficiently presents the second mannose far from the first binding site can result in a higher cross-linking effect, and therefore resulting in higher affinities.

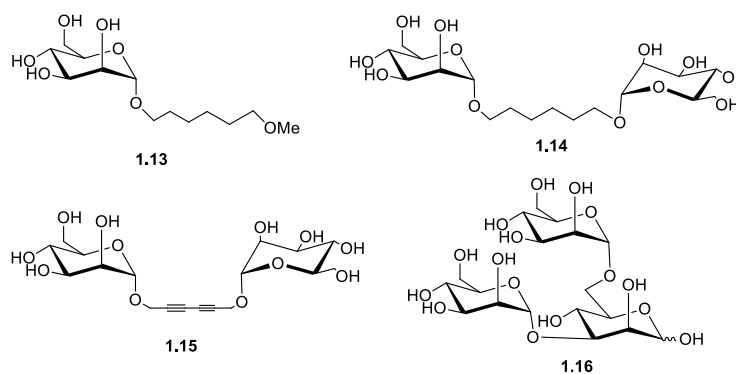


Figure 1.5 Selection of α -D-mannosides tested for the affinity for the BC2L-A lectin.^[25]

1.2.5 Glycoconjugates as inhibitors of *Pseudomonas aeruginosa* adhesion

P. aeruginosa is an opportunistic pathogen associated with causing chronic airway infections in immunocompromised individuals, most notably cystic fibrosis patients. *P. aeruginosa* contains two lectins, LecA and LecB, which play a major role in the infection process.^[22] It has been shown that LecA recognises galactose derivatives and LecB recognises fucose derivatives. Glycoconjugates containing galactose and fucose have exhibited a therapeutic effect against *P. aeruginosa* pneumonia in both mice models^[26] and cystic fibrosis patients.^[27]

A variety of multivalent glycoconjugates have been synthesised for inhibiting the binding of LecA to galactosylated surfaces and some representative examples **1.17-1.19** are shown in Figure 1.6. Similarly, a variety of multivalent glycoconjugates have been found to be LecB high affinity ligands and again representative examples are shown in Figure 1.6.

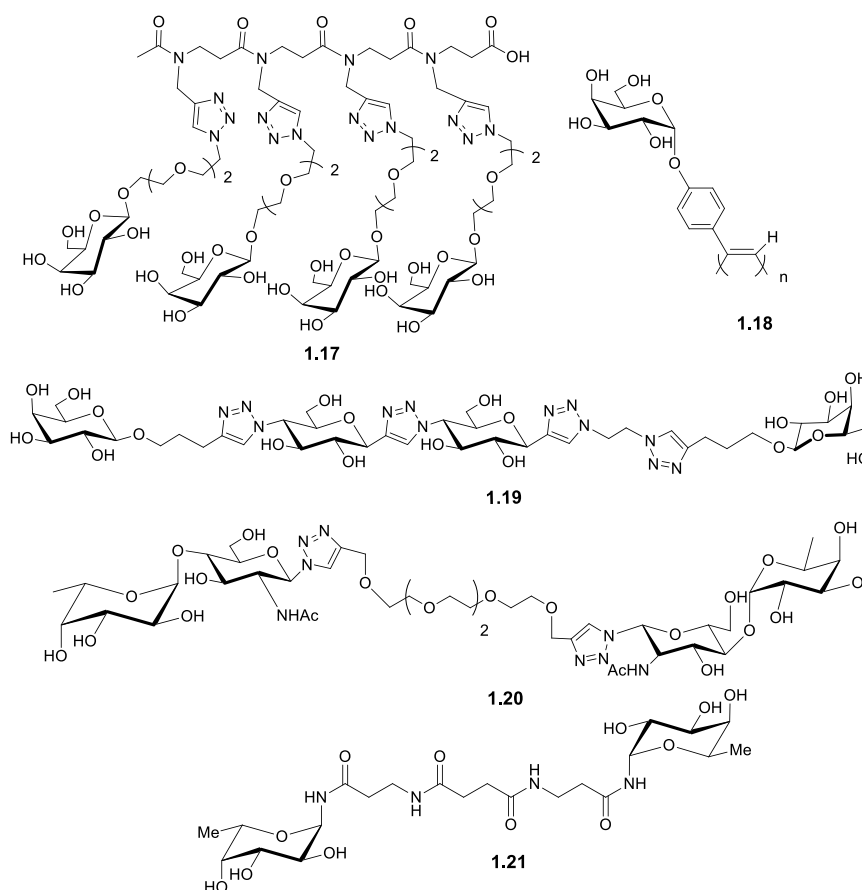


Figure 1.6 Representative examples of multivalent glycoconjugates **1.17**,^[28] **1.18** (monomer, from which polymer was synthesised)^[29] and **1.19**^[30] which are LecA high affinity ligands. Representative examples of multivalent glycoconjugates **1.20**^[31] and **1.21**^[32] which are LecB high affinity ligands.

1.3 Glycolipids as immunomodulators

1.3.1 The immune response

The human mammalian immune system has two components; the innate or non-specific immune system and the adaptive or specific immune system.^[33] The innate immune system is the first line of defence against invading pathogens and foreign bodies (Table 1.3). The adaptive immune system is the second line of defence and only comes into effect if the innate immune system is overwhelmed or circumvented. Both immune systems utilise cellular and humoral components to carry out their protective function, however the innate immune system also includes physical barriers such as skin. The innate immune system provides a fast, non-specific response to an unknown pathogen. In comparison, the adaptive immune system provides a slower specific response as it needs to produce lymphocytes with specific antigen receptors such as T-cells receptors (TCR). As these lymphocytes can retain a memory of the invading organism, the host can recognise these pathogen if re-infected and therefore produce a faster response.^[34]

Innate or non-specific immunity	Adaptive or specific immunity
Response is antigen-independent	Response is antigen-dependent
Fast response	Slow response
Not antigen-specific	Antigen specific
No immunologic memory	Immunologic memory

Table 1.3 Key differences between innate and adaptive immunity.

1.3.2 Natural Killer T-Cells

Natural killer T (NKT) cells are a subset of T cells, which share characteristics of both Natural Killer (NK) cells and T-cells.^[35] T-cells recognise fragments of foreign molecules that are presented to the host by antigen-presenting cells (APC).^[36] The major difference between T-cells and NKT cells is that T-cells detect antigens presented by conventional major histocompatibility (MHC) molecules, whereas, NKT cells recognise lipid antigens presented by the non-traditional MHC molecule CD1d.^[37] CD1d is a member of the CD1 family. The binding of the NKT cells and the CD1d protein leads to the rapid secretion of cytokines.^[36] Cytokines are small, cell-signalling proteins used extensively in intercellular communication and they are secreted by a number of cells. The secretion of cytokines is discussed more in the next section.

1.3.3 α -Gal-Cer

In 1993, during a screen for reagents that prevent tumour metastases in mice, researchers at the Pharmaceutical division of the Kirin Brewery company reported the isolation of Agelasphin-9b from a marine sponge, *Agelas mauritianus*.^[38] Although work had previously been carried out on sponges of this type, this isolation was of significant interest as the compound displayed potent anti-tumour and immunostimulatory properties. Various structure-activity studies were carried out and as a result the candidate molecule for immunology researchers became the synthetic material, known as KRN7000 or α GalCer (Figure 1.7).^[36]

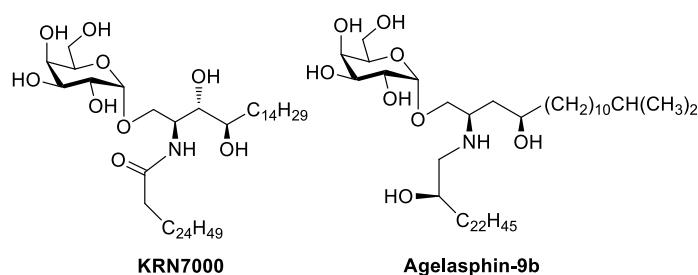


Figure 1.7 Structure of KRN7000 (synthetic α -GalCer compound) and Agelasphin 9b (one of the original compounds isolated from the *Agelas mauritianus*).^[36]

Numerous mechanistic immunological studies have shed some light onto the mode of action of α -GalCer. It has been shown that two consecutive cellular recognition events are necessary to exhibit activity.^[36, 39] First, the α -GalCer binds to the CD1d protein, forming a binary complex. This binary complex is then recognised by the T cell receptor (TCR) located on the surface of the invariant natural killer T (*i*NKT) cells to form the active ternary complex. This recognition leads to the activation of the immune response through the secretion of cytokines.^[36, 39-40] The secretion of a range of cytokines including interferon- γ (IFN γ) (T_H1 cytokine) and interleukin-4 (T_H2 cytokine) is initiated by the *i*NKT cells.^[40] T_H1 cytokines are believed to be involved in antitumor and antimicrobial activity, whereas T_H2 cytokines may play a role in alleviating autoimmune diseases.^[41]

Although promising results for KRN7000 were observed in pre-clinical trials on mice,^[42] phase 1 clinical trials on 24 patients suffering from refractory solid tumours didn't give promising results. In fact, the patients showed no partial or complete response to the treatment.^[43] As a result, clinical trials were terminated. Another complication that has hampered the use of KRN7000 as a therapeutic agent is the fact that it leads to the release of both T_H1 and T_H2 cytokines. It has been revealed that, when released together, their effects oppose one another, and can lead to unpredictable biological responses.^[40] Therefore the main focus on current KRN7000 research is to find a synthetic analogue that can effectively activate *i*NKT cells but with a bias towards either a T_H1 or T_H2 response.

1.3.4 Synthetic analogues of α -GalCer

Since its discovery, numerous analogues of KRN700 have been synthesised. The main sites of modifications are highlighted in Figure 1.8 and representative examples are discussed below (Figure 1.9).

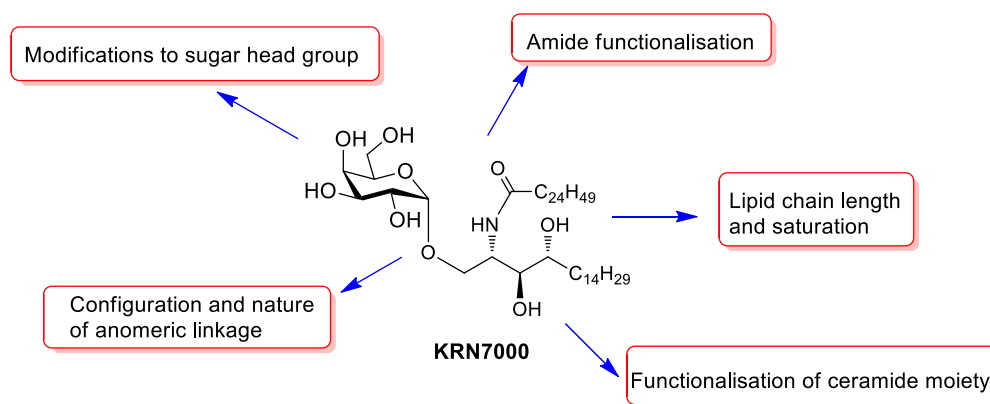


Figure 1.8 Modifications investigated on KRN7000.

In glycolipid **1.22** Lee and colleagues replaced the amide functionality of the phytosphingosine backbone with a triazole ring containing a long hydrocarbon chain.^[44] In vivo studies were performed on mice, and they found that the analogue exhibited an improved bias towards T_H2 cytokine production compared to KRN7000. Another promising analogue is the β -glycolipid **1.23**. Although evidence suggests that β -glycolipid analogues have potential as immune regulating compounds, there has been little interest in the synthesis and evaluation of such analogues. In vitro studies on glycolipid **1.23** showed it to be a promising anti-tumour agent.^[45] In the final glycolipid analogue shown, **1.24**, an aromatic group together with a long alkyl chain was introduced at the amino acid functionality.^[46] This resulted in an increase bias towards T_H1 cytokine production in comparison to KRN7000.

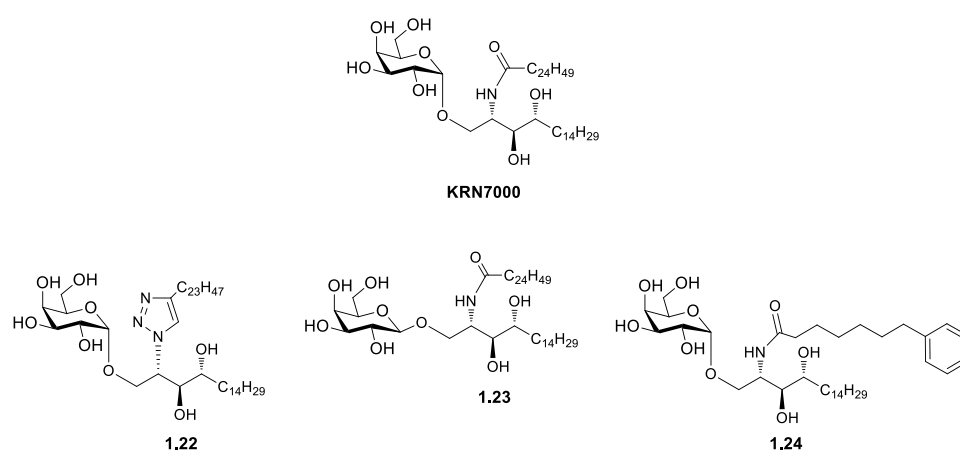


Figure 1.9 Synthetic analogues of the glycolipid KRN7000 with modifications of the amide functionality **1.22**,^[44] anomeric linkage **1.23**^[45] and lipid chain **1.24**.^[46]

The hydroxy group on the C-6 position of galactose is the only sugar alcohol not involved in any hydrogen bonding between α -GalCer and the CD1d protein. For this reason huge interest lies in the synthesis of analogues with modifications in this position^[47]. Two examples are shown below in Figure 1.10; a 6-ureido analogues with a bulky 1-naphthyl group linked to the 6'-ureido-6'-deoxy- α -GalCer **1.26**,^[48] and a highly soluble analogue which has an acetamide group in the C6 position of galactose and a *cis*-double bond in the acyl chain of KRN7000 **1.25**.^[49] Compound **1.25** was shown to activate both murine and human NKT cells more effectively than KRN7000. **1.26** showed a slight T_H1 bias with IFN- γ stimulation comparable or possibly greater than KRN7000 with reduced IL-4 production.^[47] However a stronger T_H1 bias was obtained with the 3-CF₃, 4-Cl benzamide substituent **1.27**^[48] on the 6-position. The compound, **1.27**, induced IFN- γ levels comparable to α -GalCer and only marginal levels of IL-4.

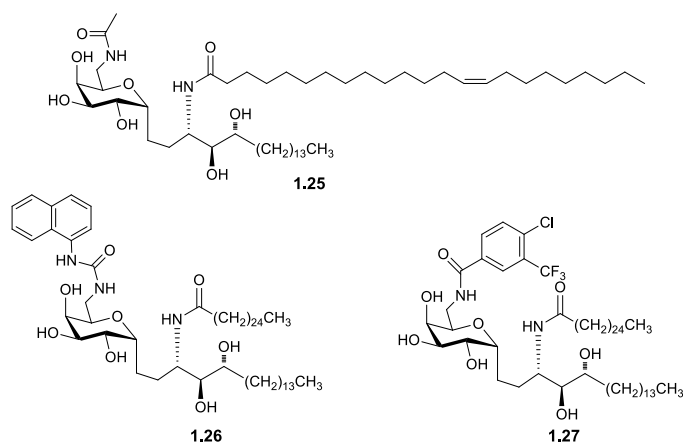


Figure 1.10 Modifications of the 6-position of the galactose moiety in α -GalCer which led to improved immunological activity.

1.4 Thesis objectives

As discussed previously, glycolipids are extremely important and are involved in a variety of biological processes. Despite this, their structural complexity and amphiphilic nature can make isolation and synthesis problematic. With this in mind, the efficient synthesis of glycolipid mimetics which resemble naturally occurring glycolipids is advantageous and could provide a useful tool in aiding investigation into their biological relevance. We aimed to synthesise a collection of glycolipid mimetics and investigate their potential as both anti-adhesion agents and immunomodulators.

The alarming rate at which bacterial antibiotic resistance is increasing, especially among Gram-negative bacteria (GNB), has made it vital to intensify the search for new means of combating bacterial infections.^[8] We wanted to investigate the ability of the selected glycolipids to inhibit the adhesion of *Burkholderia multivorans* to the epithelial cells of patients with cystic fibrosis (CF), thus, reducing bacterial infections. This approach is extremely valuable as there are no drugs against resistant GNB currently in development.^[50]

Although numerous multivalent ligands have been examined as potential inhibitors of bacterial adhesion, limited examples of glycolipids have been investigated for this purpose. We wanted to explore how the lipidic component of the glycolipid may influence the bacterial adhesion process. There are a number of reasons as to how the lipidic component may influence the biological activity of the compounds. They are lipophilic and may insert into the cell membrane of the cells. This could result in the glycolipids aiding the adhesion of the bacteria to the host cells by acting as a bridge between the bacteria and the cell. The presence of lipidic chains may also lead to increased steric hinderence. This could affect both the conformation of the

molecule and also how it interacts with the bacterial lectin involved in the adhesion process. Finally, the presence of lipidic chains may lead to the formation of micelles. This would result in a supramolecular, multivalent presentation of the glycolipids to the bacteria and may lead to an increased biological activity.

Our investigation focused around the construction of galactosyl ligands, as it has been shown that terminal galactosyl-containing glycolipids mediate bacterial adhesion to the host cells.^[23] Structural information on the bacterial lectin involved in the adhesion process is limited, therefore the rationale design of synthetic anti-adhesion ligands is extremely difficult. For this reason, a wide range of structurally diverse glycoconjugates have been examined in an attempt to identify possible structural requirements necessary to exhibit anti-adhesion properties.

Our research focused on the synthesis of glycolipids around an aspartic acid scaffold (chapter 2), malonyl scaffold (chapter 3) or an aromatic core (chapter 4). Representative based examples have been investigated as potential inhibitors of bacterial adhesion and preliminary results are discussed in chapter 5.

During the course of our research it was observed that some of the glycolipids had the ability to act as low molecular weight gelators (LMWG). This was further investigated and the results are presented in chapter 2.

Chapter 2: Alkyl glycolipids as novel soft materials

2.1 Amphiphilic glycolipids

Amphiphilic compounds such as glycolipids are used as surfactants in industry. Due to the unique physicochemical properties that arise from the coexistence of the hydrophilic head group and the hydrophobic moiety, surfactants reduce the interfacial tension and facilitate the formation of emulsions between immiscible liquids of different polarities. They can also be adsorbed between different phases (e.g. liquid-liquid or liquid-solid) and reduce the tension between these phases. Owing to these properties, surfactants are utilised in the polymer, plastic, textile, paper, cosmetics and pharmaceutical industries.^[51]

The majority of commercial surfactants are chemically synthesised from petroleum derivatives^[52] and prolonged usage can lead to significant environmental problems. As a result of this, surfactants which are derived from natural products pose fewer environmental problems and as a result are of great interest.^[51b] Biosurfactants are surfactants produced by microorganisms. As they are extracted from renewable sources, have high purity, low toxicity, and are biodegradable, they are extremely advantageous, and this has led to huge commercial interest.^[53] Examples of biosurfactants include glycolipids, lipopeptides, fatty acids and phospholipids. Due to their biocompatibility, biological activities, biodegradability and physicochemical properties glycolipids are the most widely used surfactants in the cosmetic industry. Examples of types of glycolipid biosurfactants include sophorolipids, rhamnolipids and mannosylerythritol lipids (Figure 2.1).^[51b]

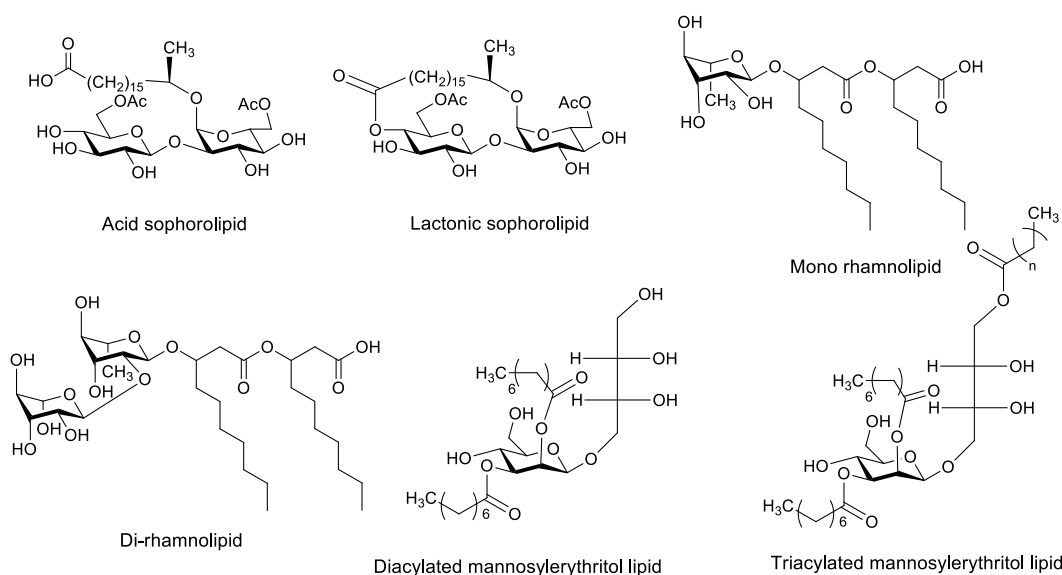


Figure 2.1 Examples of structures of sophorolipids, rhamnolipids and mannosylerythritol lipids extracted from microorganisms.^[51b]

2.2 Gelator molecules

In the 1920's, J.Lloyd made a predictive statement whereby he described gel as materials "easier to recognize than define".^[54] In the years that followed various definitions were presented. Nowadays it is generally accepted that gels are solid-like materials comprised of an elastic cross-linked network and a solvent (major component). By weight gels are mostly liquid, yet they behave like solids due to the entrapment of the solvent in a three-dimensional gelator network within the liquid.^[55] Gels can be formed *via* self-assembly (supramolecular gels) or *via* polymerisation of the gelator (polymer gels) molecule. A supramolecular gel, is a semi solid material which is composed of gelator molecules in relatively low concentrations. In the presence of an appropriate solvent, a supramolecular gelator can prevent liquid flow as a result of surface tension. This surface tension is caused by self-assembly which leads to an extensive three dimensional network of intertwined gelator fibre.^[54] Polymer gels are created from two components: a polymer network and a solvent. A polymer network envelops the liquid and prevents it from escaping. The properties of a gel depend largely on the structure of the gelator network that makes up the gel and the interaction of the network and the solvent.^[56]

2.2.1 Low molecular weight gelators (LMWG)

Low molecular weight gelators (LMWGs) have received a great deal of interest in recent years due to their potential for creating novel soft materials which have applications in the environmental, cosmetics, and biomedical industries. LMWG are small molecules which can self-assemble through noncovalent interactions to form fibrous networks which are able to entrap solvent molecules in their matrix. This leads to the formation of thermally reversible supramolecular gels, which can occur in both organic solvents (organogels) and aqueous solutions (hydrogels).^[57] The non-covalent interactions involved in gel formation include H-bonding, π stacking, electrostatic interactions and Van der Waals forces.^[58] These gels are usually prepared by heating the gelator in an appropriate solvent and cooling the resulting supersaturated solution to rt. When the hot solution is cooled, the molecules start to condense and there are three possible outcomes (Figure 2.2): (1) a highly ordered aggregation which results in the formation of crystals; (2) a random aggregation which results in an amorphous precipitate; or (3) an aggregation process intermediate between these two, which yields a gel.^[55]

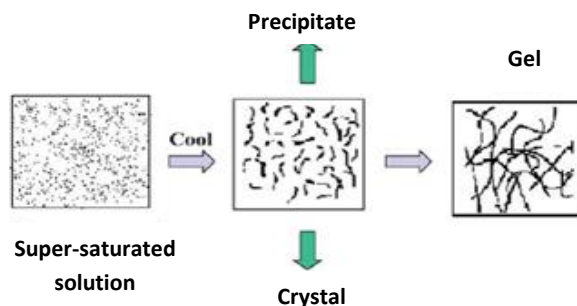


Figure 2.2 Schematic representation of gelation process.^[59]

Organogels are of interest due to their potential uses as sensors, cosmetics, separation systems, biomimetics and templates for material synthesis. Arguably the most important application of organogels is for drug delivery.^[58b]

Low molecular weight organogelators (LMWOG) can be further divided into two main groups, H-bond gelators and non H-bond gelators.^[58b, 58c] H-bonding is responsible for gelation when induced by compounds containing amide bonds such as peptides^[60] and compounds which contain hydroxyl groups such as carbohydrates.^[61] On the other hand, cholesterol derivatives,^[62] anthracene and tropone derivatives are classified as non-H bond gelators.^[58b]

2.2.1.1 The non-covalent interactions involved in gel formation

H-bonding interactions take place between an electron-rich heteroatom and electron-deficient hydrogen. The group that provides the hydrogen atom is termed the hydrogen bond donor (HBD) and the heteroatom that receives the hydrogen is known as the hydrogen bond acceptor.^[63] H-bonding between the gelator molecules themselves and also between the gelator molecule and the solvent can play a role in the formation of a gel.^[64]

Van der Waals forces are another important non-covalent interaction which plays a role in the formation of gels.^[65] The electron density of the hydrophobic regions of a molecule is never evenly distributed. Instead, transient areas of higher and lower electron density exist. This leads to temporary dipoles being present in the molecule. The presence of these transient dipoles can induce dipole formation in the hydrophobic region of another molecule. The interaction between these two dipoles is what is known as Van der Waals forces.^[63]

2.2.2 Non-carbohydrate gelators

There are many examples of LMWGs described in the literature. Initially, most were discovered through serendipity rather than design. However, due to an increased interest in this field, researchers are now attempting to synthesise “designed” gelators to examine the relationship between chemical structure and gelation ability.

Although we are primarily interested in carbohydrate-based gelators there are many examples in the literature of non-carbohydrate gelators. As can be seen from the representative examples shown in Figure 2.3, many LMWGs contain either an aromatic ring or an amide bond.

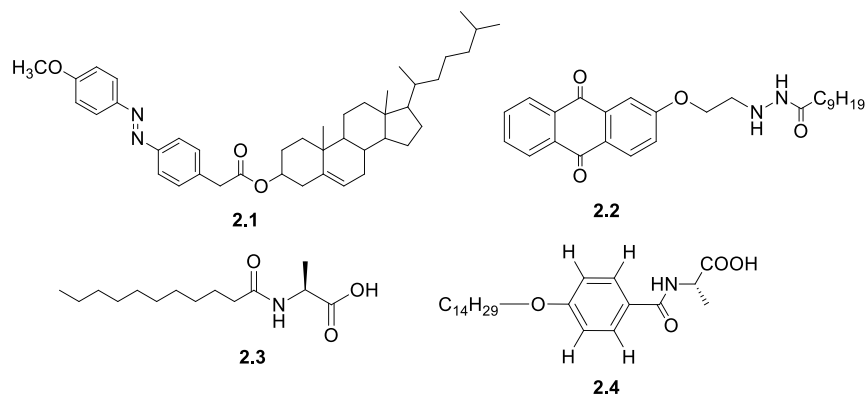


Figure 2.3 Chemical structure of some representative examples of LMWG: cholesterol derivative **2.1**,^[66] hydrazine derivative **2.2**,^[67] fatty acid amide **2.3**^[68] and a L-alanine derivative **2.4**.^[58b]

2.2.3 Carbohydrate-based gelators

The presence of stereogenic centres has been shown to affect the ability to form gels.^[69] Chirality also plays a crucial role and is involved in the assembly processes that take place on surfaces to form supramolecular gels.^[58b] For these reasons carbohydrates have commonly been used in the synthesis of LMWGs. They are also naturally abundant and can be selectively functionalised because they contain multiple chiral centres.^[57] Wang *et al.* have found that glucose is a versatile building block for synthesising carbohydrate organogelators, as substituted products can be obtained easily by selectively functionalising the anomeric position and the 4- and 6- hydroxyl groups.^[57] Examples of these functionalised glucose derivatives, **2.5** and **2.8**, are shown in Figure 2.4. Amino acids are also popular in the synthesis of LMWGs as they allow for the introduction of hydrocarbon chains (important for non-polar Van der Waal type interactions) and also the formation of amide bonds (**2.6** and **2.7** Figure 2.4). Finally, selected triazole-containing molecules **2.9** have also proven to be efficient gelators.

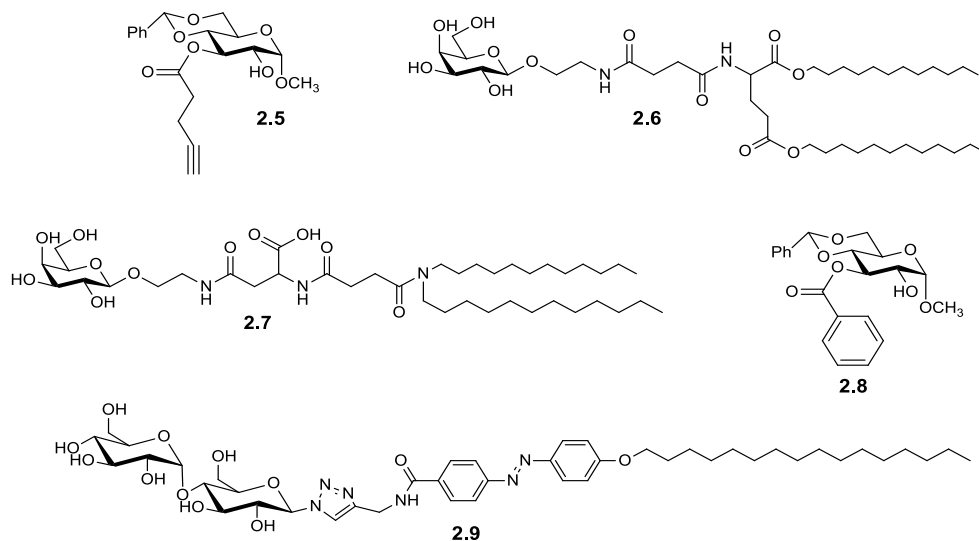


Figure 2.4 Chemical structure of carbohydrate-based gelators, a functionalised glucose **2.5**,^[57] a glycolipid amino acid **2.6**,^[70] a glycolipid aspartic acid derivative **2.7**,^[71] a simpler functionalised glucose **2.8**,^[72] and a maltose compound containing a triazole and azobenzene moiety **2.9**.^[73]

2.3 Glycomimetics

Glycomimetics are small organic molecules that have structures similar to carbohydrates, but with some modification which normally results in improved pharmacological properties. They are designed to mimic the bioactive function of naturally occurring carbohydrates and yet address the drawbacks of carbohydrate leads, namely their low bioavailability and insufficient drug-like properties.^[74] Strong interest lies in the rational design of glycomimetic drugs as alternatives to complex and naturally occurring oligosaccharides. Glycomimetic drugs currently approved and on the market include glycosidase inhibitors that prevent the digestion of carbohydrates for the treatment of diabetes (Voglibose)^[75] and also prevent influenza virus infections (Oseltamivir).^[76] Other examples include carbohydrate-derived drugs that are used to treat Gaucher's disease (Miglustat),^[77] and epilepsy (Topiramate).^[78] The structures of these compounds are shown in Figure 2.5.

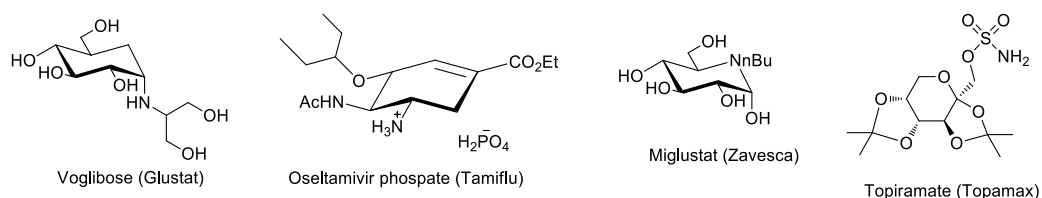


Figure 2.5 Examples of some glycomimetic drugs currently on the market. Their trade name is given in brackets.^[74]

2.3.1 Glycolipid mimetics

Glycolipids contain one or more saccharide units linked to a hydrophobic lipid chain. Due to their involvement in a variety of processes in bacteria, plants and animals, there is strong interest in, not only the synthesis of naturally occurring glycolipids, but also the design and preparation of glycolipid mimetics. Glycolipids are structurally complex, therefore their synthesis can often be demanding. This is why simpler mimetics of naturally occurring glycolipids are advantageous. As glycolipids can interact with both the polar and non-polar regions in their receptors, they often exhibit high activity in many biological processes such as inhibition of microbial adhesion.^[79] Moreover, due to their amphiphilic nature, glycolipids can form supramolecular structures, such as micelles or liposomes^[80] (section 2.1.3), and this feature may be employed for drug delivery approaches^[81] or to enhance biological activity through multivalent presentation of carbohydrate ligands.^[82]

There are limited examples of glycolipid mimetics reported in the literature. In one such example, Dubber *et al.* synthesised a variety of functionalised glycolipid mimetics, including a variety of monosaccharide building blocks.^[79] Their structures can be seen in Figure 2.6.

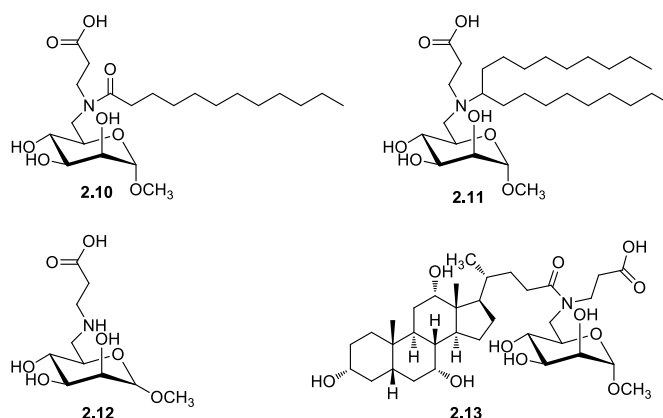


Figure 2.6 Series of glycolipid mimetics synthesised by Dubber *et al.*^[79]

More examples of simple glycolipid mimetics are shown in Figure 2.7. *Escherichia coli* urinary tract infections are initiated by adhesion of uropathogenic bacteria to uroplankin receptors in the uroepithelium. This adhesion is mediated by the FimH adhesin which is located at the tips of the mannose-binding type 1 pili. Blocking of bacterial adhesion is achieved by binding these pili with a functionalised free mannose structure therefore preventing infection. Bouckaert *et al.* synthesised glycolipid mimetics **2.14-2.23** and investigated their potency as FimH antagonists.^[83] Experiments showed heptyl α -D-mannopyranoside as the best binder.

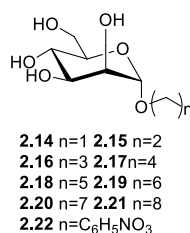


Figure 2.7 Glycolipid mimetics against *E. Coli* urinary tract infections.^[83]

An example of a more structurally complicated glycocluster mimetic is shown below (Figure 2.8). This novel palmitylated cluster **2.23** exhibits surfactant properties which was determined by surface tension measurements of aqueous solutions.^[84]

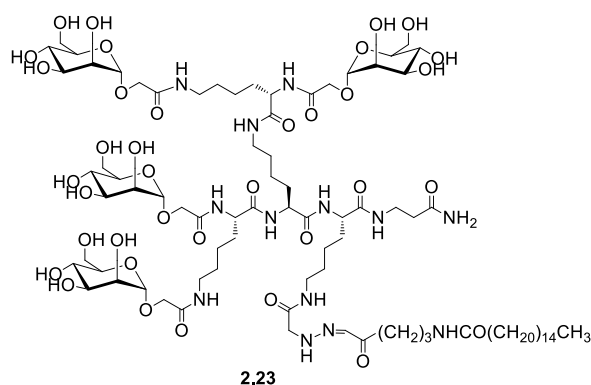


Figure 2.8 Example of surfactant glycocluster mimetic **2.23**.^[84]

2.3.2 Glycosphingolipid glycomimetics

Glycosphingolipids (GLS) consist of glycosylated sphingolipids. They are bioactive molecules which are ubiquitous in eukaryotic cell membranes. They are essential to many biological processes such as cell signalling, proliferation, differentiation and cell recognition. They also play a role in cell pathogen interactions. Due to their biological importance and complexity the preparation of synthetic analogues of GLS is highly advantageous.^[85]

Due to the range of therapeutic applications displayed by the synthetic glycosphingolipid KRN7000 (discussed in Chapter 1), much research has centred on synthesising mimetics of this compound. In addition to the examples described earlier, Kinjo and colleagues synthesised a carboxylic glycosphingolipid **2.24** (Figure 2.9) and observed that the compound displayed improved *i*NKT cell stimulatory properties compared to the parent compound.^[35] Franck and Tsuji reported the synthesis of α -C-galactosylceramide **2.25**, and provided evidence that the C-analogue is superior to the O-analogue in both immunological activity and stability.^[36]

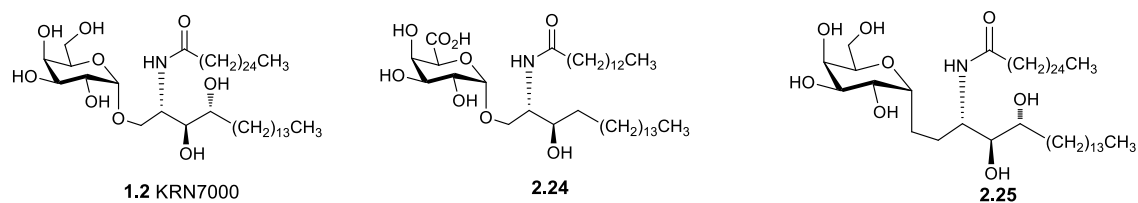


Figure 2.9 Synthetic α -GalCer analogue KRN700 **1.2**, Glycosphingolipid mimetic **2.24**^[35] with improved immunological activity and α -C-galactosylceramide derivative **2.25**.^[36]

2.4 Chapter objective

This chapter deals with the synthesis of a variety of L-aspartic acid *O*-linked glycolipids, as mimetics of glycolipids and more specifically glycosphingolipids. Although glycosphingolipids have been shown to exhibit a variety of biological activities, the isolation and purification of natural glycosphingolipids has proven very difficult. For this reason, synthetic mimetics are extremely advantageous. As peptide coupling methodologies are well developed, we chose to base our approach on amino acids, and more specifically on aspartic acid. We chose aspartic acid as it features an acid group on its side chain and a carboxylic acid and amino group at the α -carbon and therefore would allow the introduction of functionality easily. Owing to this, it would provide access to a range of structurally diverse glycoconjugates which could be investigated for potential biological activities. We followed a modular approach utilising a key set of protection, deprotection and coupling strategies which allowed us to achieve diversity easily and also enable sufficient scale up. We aimed to synthesise a collection of compounds which exhibited variations in hydrocarbon chain length, quantity of hydrocarbon chains, connectivity of carbohydrate moiety and variation in the carbohydrate moiety used. Our objective was to examine if and how these changes affected the biological and physicochemical properties of the glycolipids.

The core building block structure can be seen in Figure 2.10. It is clear that the aspartic acid linker would remain constant in all analogues and that variation could be achieved at three potential sites.

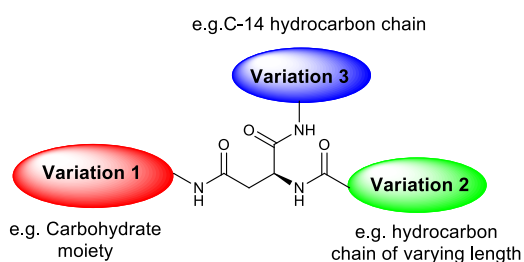


Figure 2.10 Core building block structure of L-aspartic acid *O*-linked glycolipids.

The structures of the desired glycolipids are shown in Figure 2.11. Variation site 1 allowed for differences in the carbohydrate moiety used. In most cases, a galactosyl moiety was used, however a lactosyl moiety (as in **2.32**) and a functionalised galactose moiety (as in **2.30**) were also exploited. The carbohydrate connectivity could also be modified (as in **2.31**), where the carbohydrate moiety was replaced by a C-14 lipidic chain. Variation site 2 allowed for changes in the hydrocarbon chain length. Analogues with a short C-10, medium C-16 and large C-24 hydrocarbon chain were prepared. Variation site 3 allowed different amines to be coupled to the α -carboxylic acid. In most cases, tetradecylamine was used. This position also allowed for the number of hydrocarbon chains coupled to be varied. Glycolipid **2.29** has a slightly different structure to the others in that there are two galactosyl moieties coupled to the aspartic acid core and only one hydrocarbon chain.

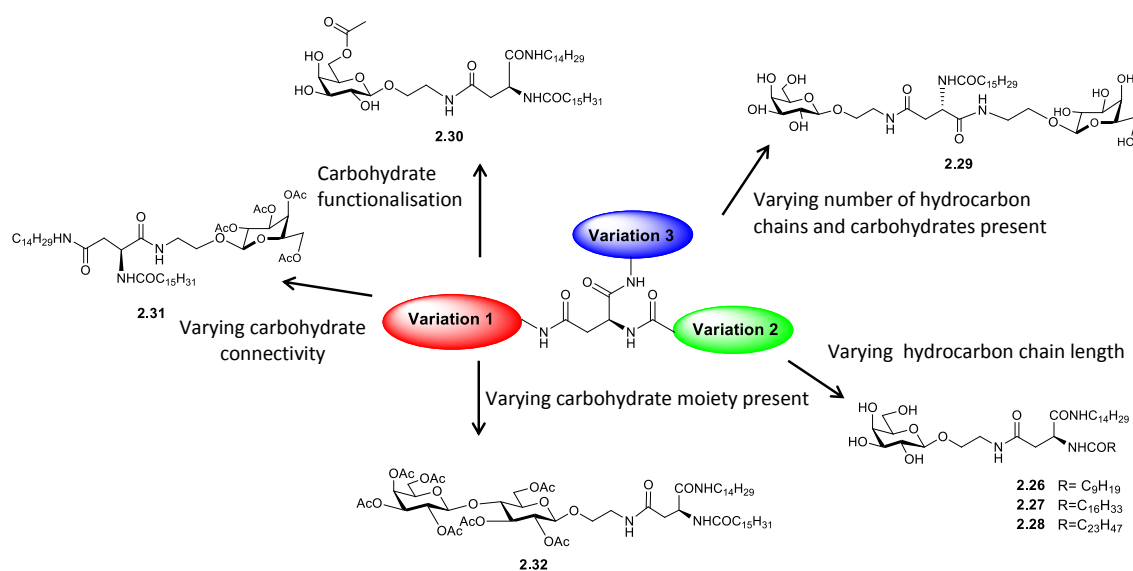


Figure 2.11 Structure of glycolipid analogues **2.26-2.32** generated from an aspartic acid core.

During the course of the synthesis it was observed that some of the analogues were able to induce gelation of the solvents used in their purification. As a result, these amphiphilic glycolipids were investigated as LMWGs in a range of organic solvents of different polarities. We envisaged that hydrocarbon chain length, number of hydrocarbon chains present, and general conformational differences would influence the gelation ability. Finally, the ability of the glycolipids to form giant unilamellar vesicles (GUV's) to further examine their potential as biomedical agents was investigated by Urzula Miggis in the laboratory of Dr. Jennifer Mc Manus in NUI Maynooth.

2.5 The synthesis of first generation aspartic acid-based β -O-glycolipids 2.26, 2.27 and 2.28

The structures of the L-aspartic acid-based *O*-glycolipids **2.26**, **2.27** and **2.28** were designed to act as glycosphingolipid mimetics, where the sphingosine backbone of the glycosphingolipids would be replaced by an acylated amino acid core. The idea was to introduce a spacer group that would allow the functionalisation of the glycolipids with two hydrocarbon chains. The naturally occurring amino acid L-aspartic acid was chosen as it features an acid group on its side chain, which would allow for connectivity to the galactosyl moiety through the formation of an amide bond. It also contains a carboxylic acid and amino group at the α -carbon which would allow for the introduction of hydrocarbon chains through the formation of amide bonds. The tetradecylamide hydrocarbon chain remained constant in analogues **2.26-2.28** to mimic the sphingosine hydrocarbon chain length in glycosphingosines (Figure 2.12).

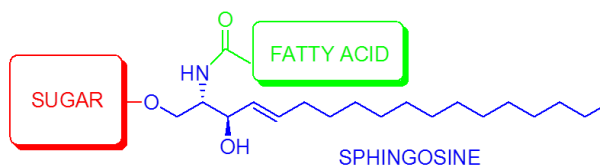
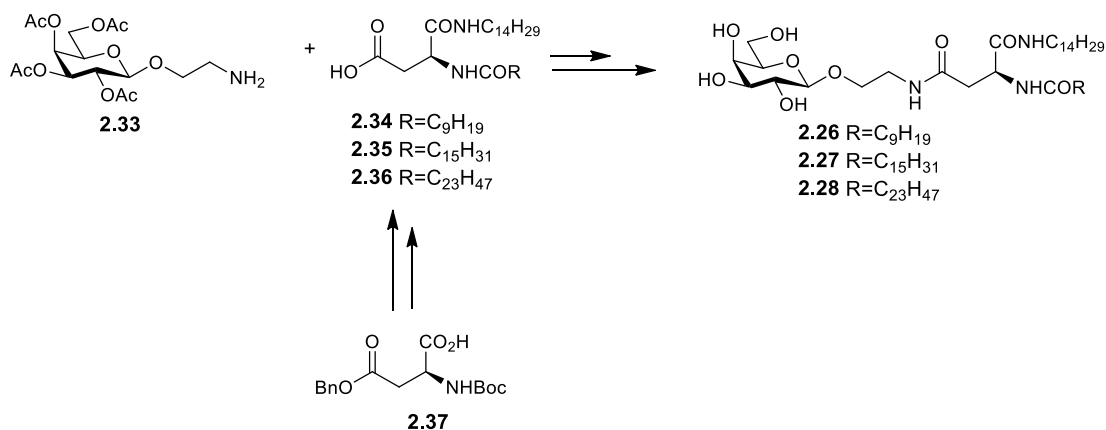


Figure 2.12 General structure of glycosphingosines.

Initial investigations led us to design the synthetic pathway as in Scheme 2.1 whereby the easily accessible β -*O*-ethyl-galactosyl amine **2.33** and the commercially available protected aspartic acid derivative **2.37** would serve as suitable building blocks. The tetradecylamide chain would be introduced first using standard peptide coupling conditions. The deprotection of the *N*-Boc protecting group would provide the free amine which would allow for introduction of the second hydrocarbon chain, again using standard peptide coupling conditions. Finally, deprotection of the benzyl ester protecting group would yield the free acid in the aspartic acid building blocks **2.34-2.36** which is ready for coupling with galactosyl amine **2.33**, again using standard coupling conditions. In this way a range of analogues could be synthesised in a straightforward manner by exploiting a key set of protection/deprotection and coupling strategies which are already widely accepted and utilised.



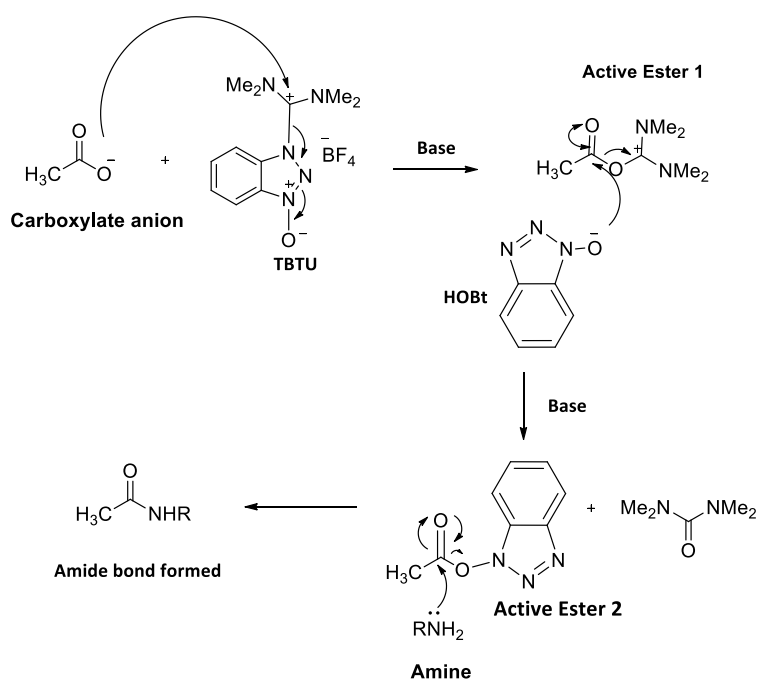
Scheme 2.1 Key building blocks and intermediates for the synthesis of glycolipids **2.26-2.28**.

2.5.1 Initial synthesis of β -O-glycolipid **2.26**

Amide bond formation is one of the most commonly used transformations in the synthesis of pharmaceuticals, fine chemicals and polymers.^[86] Amides are widely utilised as they are more stable to hydrolysis than esters, yet still accepted to be biodegradable. It is estimated that more than 25% of known drugs contain an amide bond.^[86] For this reason, there are a plethora of methods for amide bond formation reported in the literature.^[87] The most frequently used procedures for amide formation involve the reaction of an amine (including ammonia) with either activated carboxylic acid derivatives or reaction with carboxylic acids mediated by a coupling reagent. Various different coupling methodologies have been developed using azides, active esters, acyl halides, anhydrides, carbodiimides, immonium and aminium salts to name but a few. The use of acid chlorides and activated esters is discussed in chapter 4, however for the purpose of this chapter only aminium coupling reagents will be discussed. TBTU (*O*-benzotriazol-1-yl)-1,1,3,3-tetramethyluronium hexafluorophosphate) (Scheme 2.2) is an extremely popular aminium coupling reagent. It was originally believed to have an uronium structure but crystallography data and solution studies revealed it actually has an aminium structure.^[88] TBTU is commonly used in conjunction with HOBt. HOBt acts as a racemisation suppressant, therefore when used together minimal racemisation occurs in the amide bond formation. HOBt is also used in conjunction with a variety of other carbodiimide coupling reagents such as DCC.

A reaction mechanism for the coupling of a carboxylic acid and an amine with TBTU and HOBt is proposed in Scheme 2.2. The mechanism proceeds with the attack of the carboxylate anion (generated in basic conditions) at the TBTU aminium carbocation to form an active ester species. Subsequent attack of the HOBt to the electrophilic carbon of the active ester, again in basic conditions yields a second active ester intermediate which then reacts with the amine to

lead to the formation of a new amide bond. However, it is important to highlight, that this is not the only pathway possible and the amide product can be formed via a number of routes. Direct attack of the amine at the acylaminium intermediate (active ester 1) generating the amide product is also possible. Finally, the carboxylate anion can also attack the active ester to form an anhydride, which can subsequently react with the amine to form the amide product.



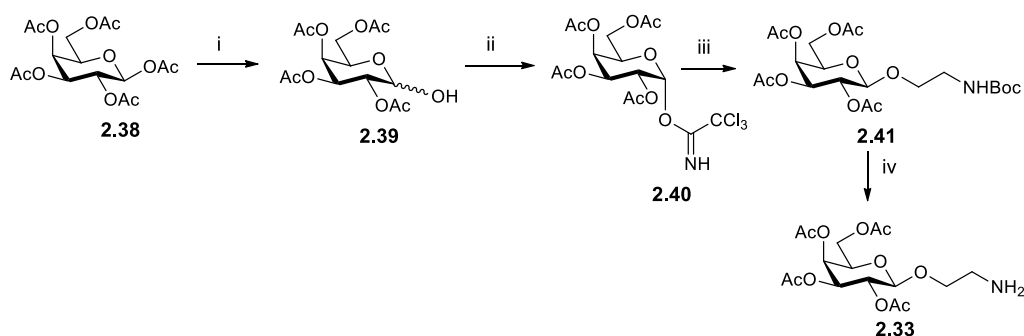
Scheme 2.2 Mechanism of TBTU and HOBT coupling reagents to form a new amide bond.

It was decided to use the TBTU/HOBT coupling methodology as there are many advantages over the use of other standard reagents, including the easy removal of by-products.

2.5.1.1 Synthesis of galactosyl amine 2.33

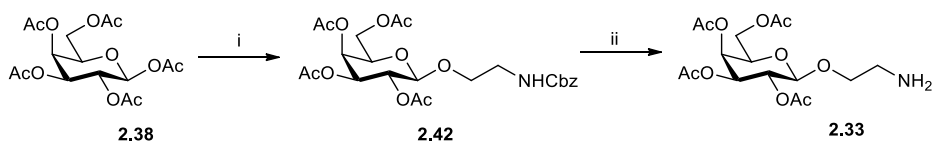
The synthesis of β -galactosyl amine **2.33** was attempted through a variety of synthetic routes (Schemes 2.3-2.5). The first route examined (Scheme 2.3) involved the use of the well-established trichloroacetimidate donor developed by Schmidt and colleagues in 1980.^[89] Due to their excellent yields and stereoselectivities, trichloroacetimidates are well regarded and extensively used in carbohydrate chemistry.^[90] The galactosyl trichloroacetimidate donor **2.40** was prepared as described in the literature from 1,2,3,4,6-penta-*O*-acetyl- β -D-galactose **2.38**.^[91] Selective deacetylation of the anomeric position of the galactose pentacetate, using Me_2NH , yielded the galactose hemiacetal **2.39**. The free hydroxyl group of the hemiacetal intermediate **2.39** was then treated with trichloroacetonitrile and DBU to yield the α -galactosyl trichloroacetimidate **2.40** exclusively. The α -anomer, which is the thermodynamically favoured product, is obtained due to the use of a strong base (DBU) for deprotonation of the anomeric hydroxyl group. The glycosylated product **2.41** was obtained in 40% yield, by reacting the

glycosyl donor (**2.40**) and the glycosyl acceptor *N*-Boc ethanolamine under Lewis acid (TMSOTf) activation. The final step involved the deprotection of the *N*-Boc protecting group using TFA to yield the free amine **2.33** in 93% yield. Although the synthesis was successful, it was found that excess acid from the final deprotection step was hampering successive reactions which involved basic conditions. For this reason it was decided to investigate an alternative synthetic route.



Scheme 2.3 Reagents and conditions: i) Me₂NH, CH₃CN, rt, 24 h, 91%; ii) CCl₃CN, DBU, DCM, 3 Å MS, N₂, 3.5 h, 83%; iii) 0.04 N TMSOTf, *tert*-Butyl *N*-(2-hydroxyethyl)carbamate, 3 Å MS, DCM, 0°C-rt, N₂, 18 h, 40%; iv) TFA, DCM, rt, 3 h, 93%.

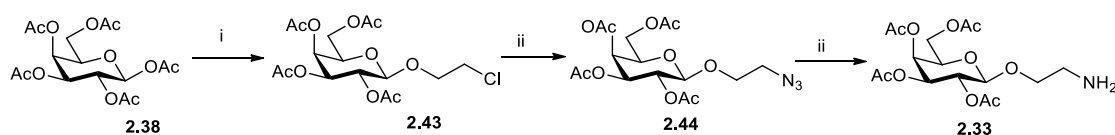
In order to optimise the reaction and also to shorten the reaction steps required, we decided to attempt the direct activation of the 1,2,3,4,6-penta-*O*-acetyl-β-*D*-galactose **2.38** using the Lewis acid BF₃·O(Et)₂ as the promoter (Scheme 2.4).^[92] This time, in order to avoid acidic deprotection conditions, an acceptor which had the amine protected as a benzyloxy carbamate (*N*-CBz) was utilised. The galactoside **2.42** was obtained in 36% yield. It was observed that the use of BF₃·O(Et)₂ may have been too harsh for the acetyl protecting groups as ¹H NMR analysis showed a partially deacetylated galactoside product was also isolated. Reacetylation of the resulting crude mixture using Ac₂O and pyridine for 1 h led to an improved yield of 57% of the desired glycoside **2.42**. The final step involved hydrogenolysis of the *N*-CBz protecting group using Pd/C which afforded the free amine product **2.33** in 91% yield.



Scheme 2.4 Reagents and conditions: i) 1) BF₃·OEt₂, benzyl *N*-(2-hydroxyethyl)carbamate, DCM, rt, 16 h, 2) Ac₂O, Pyr, 1 h, 57%; ii) Pd/C, H₂, EtOH, rt, 4 h, 91%.

Galactosyl amine **2.33** was obtained in only moderate yields using carbamate protected (*N*-Boc or *N*-CBz) ethanolamines as the glycosyl acceptors. It is possible that these may be quite deactivating towards glycosylation. For this reason it was decided to attempt the synthesis of

the amine **2.33** via one more synthetic approach (Scheme 2.5). As in the previous route, the glycosylation reaction was carried out directly from the 1,2,3,4,6-penta-*O*-acetyl- β -D-galactoside **2.38** under Lewis acid $\text{BF}_3 \cdot \text{O}(\text{Et})_2$ activation. This time, 2-chloroethanol was used as the glycosyl acceptor and a few changes were made regarding the addition of $\text{BF}_3 \cdot \text{O}(\text{Et})_2$. 6 eq were used instead of the 3 eq used previously, and it was added in a 50% solution of $\text{BF}_3 \cdot \text{O}(\text{Et})_2$ in DCM at 0 °C over a period of 30 min. The desired galactoside **2.43**^[93] was obtained in 78% yield, and no partially deacetylated product was detected by TLC. The reaction was repeated using 3 eq of $\text{BF}_3 \cdot \text{O}(\text{Et})_2$ added dropwise over 30 min and a similar result was observed. The chloride group of glycoside **2.43** was then substituted with an azido moiety by reaction of NaN_3 in DMF at 110 °C, to yield the galactosyl azide intermediate **2.44**^[93] in 81% yield. The final step involved the reduction of the azide to the amine using H_2 , Pd/C in EtOH to yield the free amine **2.33** in 89% yield.

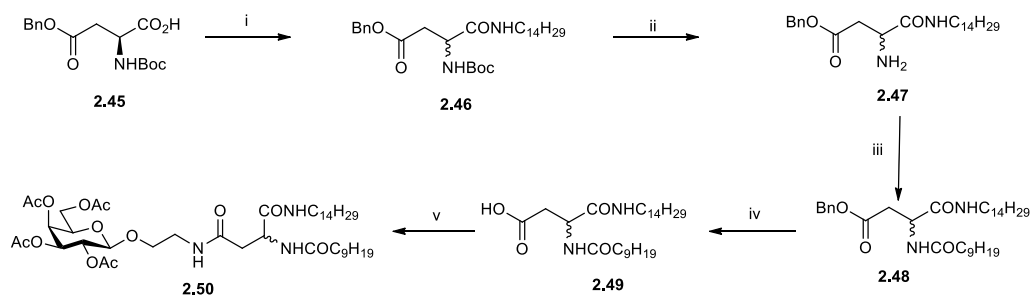


Scheme 2.5 Reagents and conditions: i) $\text{BF}_3 \cdot \text{OEt}_2$, 2-chloroethanol, DCM, rt, 16 h, 78%; ii) NaN_3 , DMF, 110 °C, 3 h, 81%; iii) Pd/C, H_2 , EtOH, rt, 16 h, 89%.

Although similar yields were obtained for the glycosylation reactions in route one (scheme 2.3) and route three (scheme 2.5), route three required less steps and was therefore more efficient. Another advantage of route three is that the galactose azide **2.44** could also be utilised as a synthetic intermediate. For these reasons route three was chosen as the optimum synthetic route.

2.5.1.2 Synthesis of acylated aspartic acid glycolipid **2.50**

The synthesis of the L-aspartic acid derivative **2.50** commenced with the amide coupling of the commercially available *N*-Boc-L-aspartic acid-4-benzyl ester **2.45** with tetradecylamine using TBTU and HOBt (Scheme 2.6). This reaction was initially carried out in the presence of a base (NEt_3) to yield the desired product **2.46**^[94] in 87% yield. Subsequent removal of the *N*-Boc protecting group with TFA afforded the amine **2.47** which was acylated with decanoic acid using the above mentioned TBTU/HOBt methodology to give derivative **2.48** in 94% yield. Hydrogenolysis of the side chain benzyl ester of glycoside **2.48**, (carried out at 50 °C to enhance solubility) afforded the desired L-aspartic acid building block **2.49**, which was then coupled to the primary amine galactosyl derivative **2.33** to yield the acylated glycolipid **2.50** in 60% yield.



Scheme 2.6 Reagents and conditions: i) TBTU, HOBT, $C_{14}H_{29}NH_2$, NEt_3 , DMF, 4 Å MS, N_2 , rt, 18 h, 87%; ii) TFA, DCM, rt, 1.5 h, 93%; iii) TBTU, HOBT, $CH_3(CH_2)_8COOH$, NEt_3 , DMF, 4 Å MS, N_2 , rt 16 h, 94%; iv) H_2 , Pd/C, EtOAc, 50 °C, 4 h, 85%; v) TBTU, HOBT, **2.33**, NEt_3 , DMF, 4 Å MS, N_2 , 50 °C, 16 h, 60%.

However, the 1H NMR spectrum of glycolipid **2.50** showed distinct duplication of the expected signals in a 1:1 ratio (Figure 2.13). Duplication of the amide protons is the most obvious, but the signals corresponding to the β -protons* and also the anomeric proton (H-1) suggested the presence of a mixture of diastereoisomers.

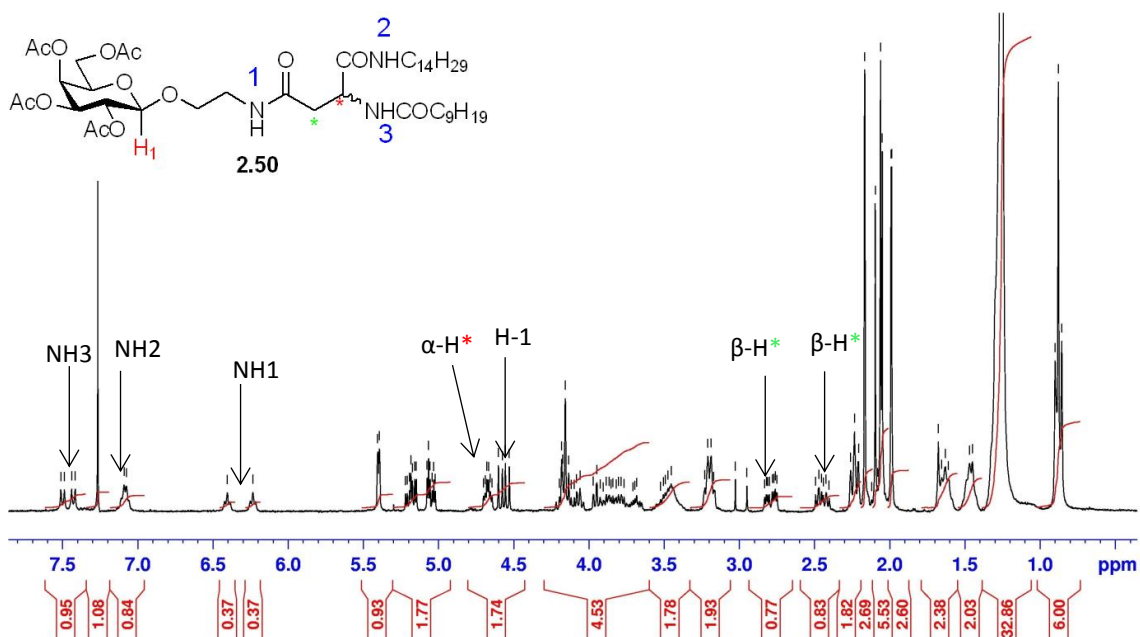
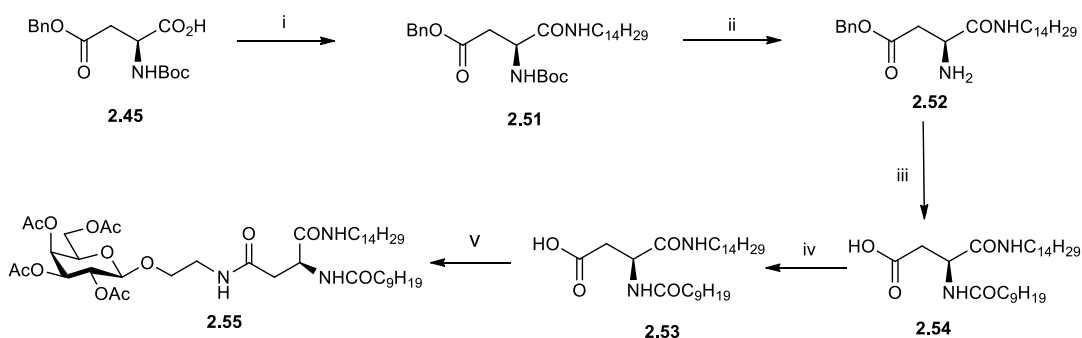


Figure 2.13 1H NMR spectrum of β -O-glycolipid **2.50** ($CDCl_3$, 300 MHz). The duplication of signals suggests the presence of a mixture of diastereoisomers.

To rule out possible conformational exchange equilibria, variable temperature 1H NMR spectra of compound **2.50** were recorded in d_6 -DMSO. No coalescence of the signals was observed at temperatures as high as 80 °C. This suggested that at some point during the synthesis of the glycolipid racemisation had occurred, and glycolipid **2.50** was in fact, a mixture of diastereoisomers.

It is believed that the unexpected racemisation of the chiral carbon of the L-aspartic acid derivative **2.50** takes place in the first step of the synthesis upon activation of the α -carboxylic acid. Although the use of TBTU and HOBt as coupling reagents is commonplace in peptide synthesis, the activation of the α -carboxylic acid using these conditions may increase the acidity of the α -proton and it may be abstracted in the presence of a base such as NEt_3 . This is further supported by the disappearance of the optical activity of compound **2.46** $[[\alpha]^{22}_{\text{D}} = 0$ (c 1.55, CHCl_3)]. If the coupling reaction is repeated in the absence of NEt_3 (Scheme 4.5), a specific optical rotation value of $[[\alpha]^{22}_{\text{D}} = +2.5$ (c 1.55, CHCl_3) is obtained for the L-enantiomer, compound **2.51**. Most of the published procedures reporting amide bond formation of *N*-Boc aspartic acid **2.45** involve the use of carbodiimide-type coupling reagents,^[95] formation of activated esters, such as pentafluorophenyl derivatives,^[96] or mixed anhydrides.^[97] The coupling of the aspartic acid building block **2.45** has been reported in the literature using the conditions described above. However, to the best of our knowledge no compromise of the optical purity of the resulting aspartate derivatives when using uronium-type reagents (such as TBTU or HBTU) has been explicitly reported prior to our report.^[94, 98]

The L-enantiomeric glycolipid **2.55** was obtained from repeating the synthetic sequence as described above, but in this case the initial coupling reaction was carried out in the absence of base. Although this route allowed access to sufficient amounts of diastereomerically pure **2.55**, the initial coupling of the α -carboxylic acid results in a lower yield in the absence of NEt_3 (Scheme 2.7).



Scheme 2.7 Reagents and conditions: i) TBTU, HOBt, $\text{C}_{14}\text{H}_{29}\text{NH}_2$, DMF, rt, 16 h, 37%; ii) TFA, DCM, rt, 83%; iii) (1) TBTU, HOBt, $\text{C}_{10}\text{H}_{20}\text{O}_2$, NEt_3 , DMF, rt, 62%; (2) H_2 , Pd/C, EtOAc, 50 °C, 76%; iv) TBTU, HOBt, **2.33**, NEt_3 , DMF, 50 °C, 69%.

The ^1H NMR spectrum of the diastereomerically pure glycolipid **2.55** is shown in Figure 2.14. This time no duplication of the expected signals was observed, confirming the presence of a single diastereoisomer **2.55**.

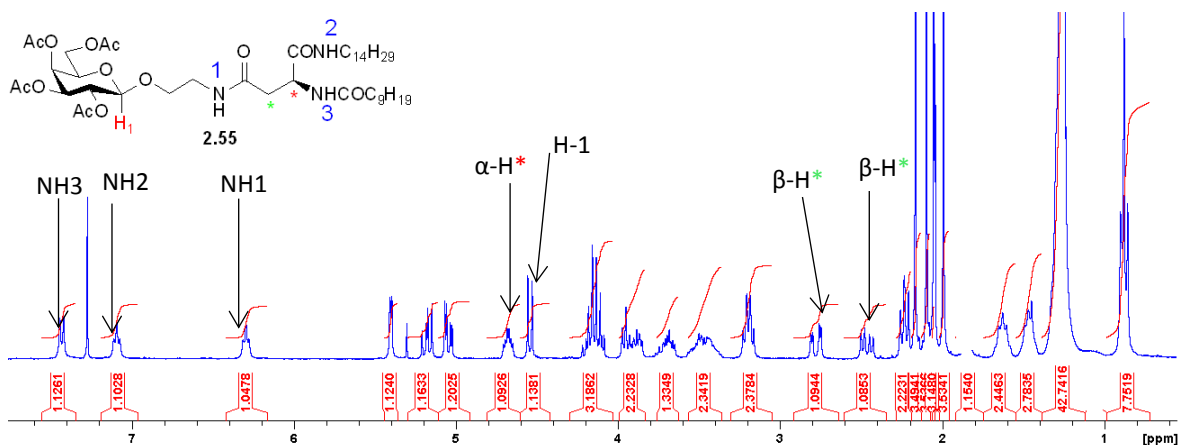
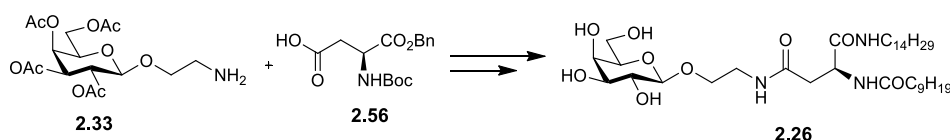


Figure 2.14 ^1H NMR spectrum of glycolipid **2.55** (CDCl_3 , 300 MHz) with characteristic signals assigned. Solvent under peak at 1.25 affecting integration.

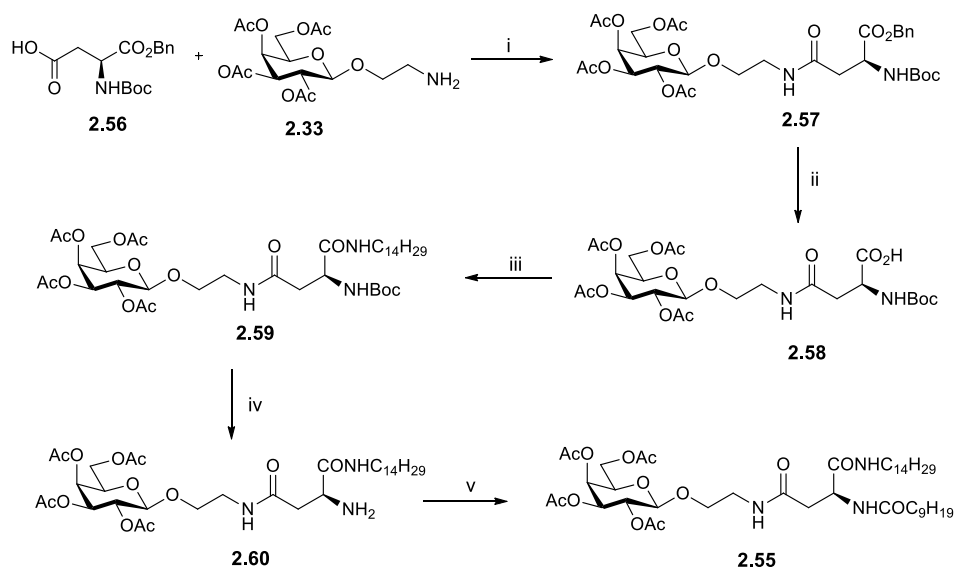
2.5.2 Alternative route to form β -O-glycolipid 2.26-2.28

Upon these unexpected drawbacks, we decided to use an alternative synthetic approach as in Scheme 2.8. We chose to introduce the galactosyl moiety early on in the synthesis so we could observe if racemisation was occurring by ^1H NMR analysis. For this reason, the commercially available *N*-Boc-L-aspartic acid-1-benzyl ester **2.56** was utilised. In this starting material the carboxylic acid at the α -carbon is benzyl ester protected and the side chain is a free carboxylic acid. In order to maintain the L-configuration at the α -position of the aspartic acid derivative **2.26**, upon activation with TBTU/HOBt, we chose to carry out this step in the absence of base.



Scheme 2.8 Alternative synthetic approach for β -O-glycolipid **2.26**.

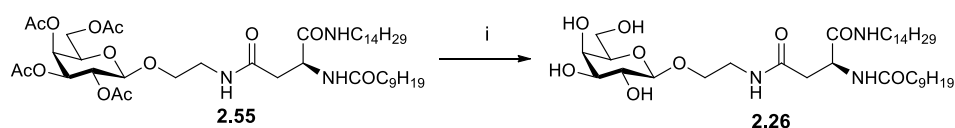
The synthesis proceeded with the coupling of the galactosyl amine **2.33** and the *N*-Boc-L-aspartic acid-1-benzyl ester **2.56**, using TBTU/HOBt to give the orthogonally protected compound **2.57** in 76% yield (Scheme 2.9). Deprotection of the benzyl ester was performed using H_2 and Pd(C) in EtOAc and the resulting crude carboxylic acid **2.48** was carefully reacted with tetradecylamine using TBTU/HOBt system. To avoid racemisation of the chiral carbon in this crucial step, the reaction was carried out in the absence of base. Under these conditions, diastereomerically pure glycolipid **2.59** was successfully obtained, albeit in a moderate yield of 56%. Subsequent removal of the *N*-Boc protecting group with TFA afforded the amine **2.60** which was acylated with pre-activated decanoic acid using the above mentioned TBTU/HOBt methodology. The diastereomerically pure, protected glycolipid **2.55** was successfully obtained in 63% yield.



Scheme 2.9 Reagents and conditions: i) TBTU, HOBT, NEt_3 , DMF, 4 Å MS, N_2 , rt, 16 h, 76%; ii) H_2 , Pd/C, EtOAc, rt, 4 h, 90%; iii) TBTU, HOBT, $\text{C}_{14}\text{H}_{29}\text{NH}_2$, DMF, 4 Å MS, N_2 , rt, 16 h, 56%; iv) TFA, DCM, 50 °C, 1.5 h, 74%; v) TBTU, HOBT, $\text{CH}_3(\text{CH}_2)_8\text{COOH}$, DMF, 4 Å MS, N_2 , rt, 16 h, 63%.

Structural elucidation of the acetyl protected glycolipid **2.55** was carried out and we observed that the ^1H NMR spectrum obtained was identical to the spectrum shown in Figure 2.14. This proved that carrying out the synthesis *via* a different approach still yielded the desired product **2.55**.

Finally, selective deprotection of the acetyl protecting groups was performed under mildly basic conditions. Catalytic NEt_3 in a heterogenous solvent system (DCM/MeOH/ H_2O , 1:2:1) at 40 °C afforded the deprotected glycolipid **2.26** as a white precipitate in 83% yield (Scheme 2.10). Mild deprotection conditions were chosen preferentially over the harsher, but more commonly employed Zémlen conditions,^[99] which may have resulted in degradation of the glycolipid.



Scheme 2.10 Reagents and conditions: i) NEt_3 , DCM/MeOH/ H_2O , 40 °C, 18 h, 83%.

The best solvent for ^1H NMR analysis of the deprotected glycolipids, in terms of solubility and resolution, was found to be d_5 -Pyr. The ^1H NMR of the *O*-glycolipid **2.26**, is shown in Figure 2.15. Characteristic peaks are highlighted, including the amide protons (NH), the anomeric proton (H-1), and the α^* and β^* -protons.

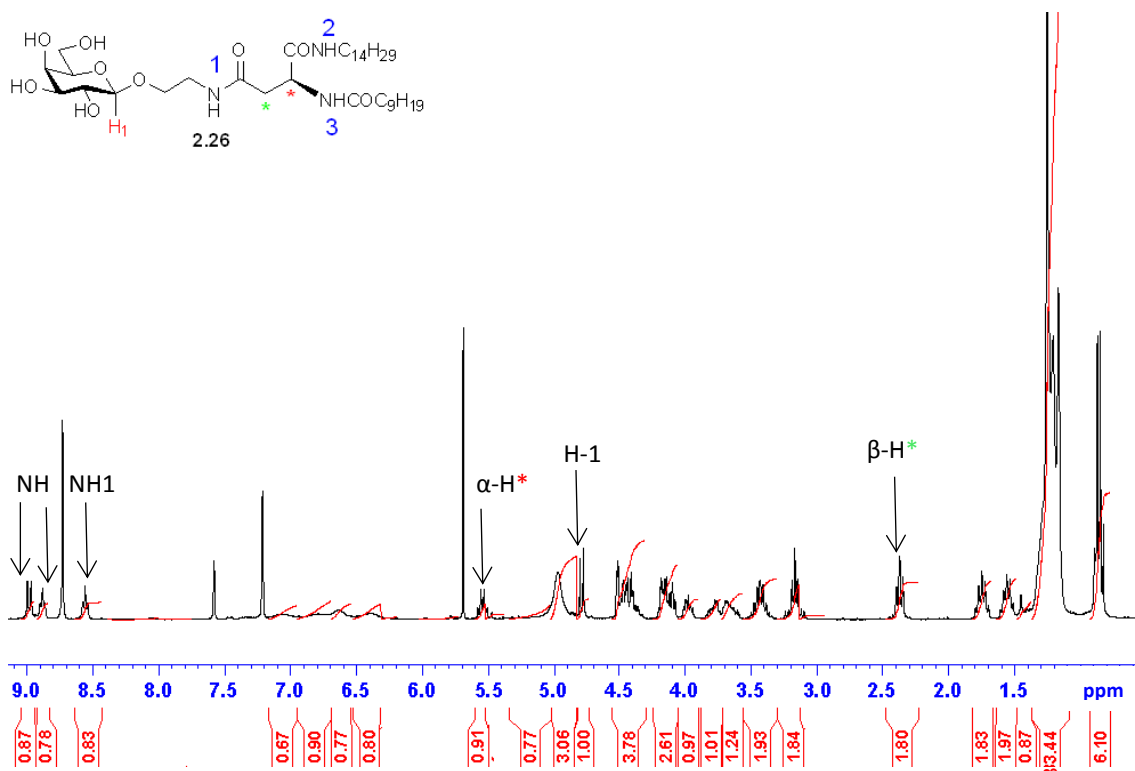
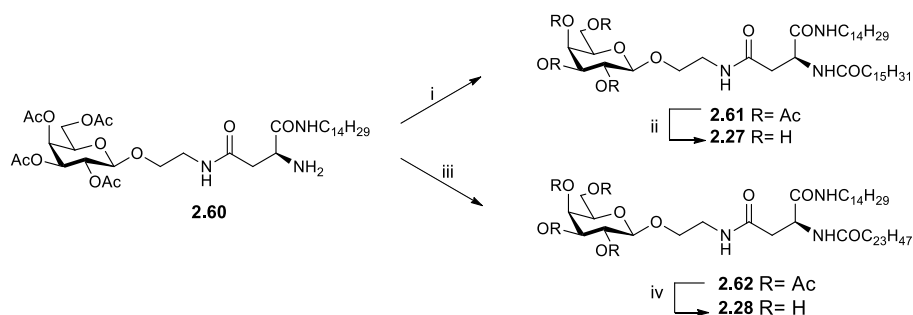


Figure 2.15 ^1H -NMR spectrum of deprotected glycolipid **2.26** (d_5 -Pyr, 300 MHz) with characteristic signals assigned.

2.5.3 Synthesis of β -O glycolipid **2.27** and **2.28**

The synthesis of glycolipids **2.27** and **2.28** began from the synthetic intermediate **2.60**, which was used previously. The free amine **2.60** was acylated with either hexadecanoyl chloride or tetracosanoic acid using the TBTU/HOBt methodology, to yield diastereomerically pure glycolipid **2.61** (87% yield) and glycolipid **2.62** (40% yield), respectively (Scheme 2.11). The moderate yield of **2.62** is due to the poor solubility of tetracosanoic acid in DMF.



Scheme 2.11 Reagents and conditions: i) NEt_3 , $\text{CH}_3(\text{CH}_2)_{14}\text{COCl}$, DCM, N_2 , rt, 16 h, 87%; ii) NEt_3 , DCM/MeOH/ H_2O , 40°C , 18 h, 52%; iii) TBTU, HOBt, NEt_3 , DMF, 4 \AA MS, N_2 , rt, 6 h, 40%; iv) NEt_3 , DCM/MeOH/ H_2O /THF, 40°C , 18 h, 38%.

Deprotection of the O -glycolipid **2.61** using NEt_3 afforded the novel O -glycolipid **2.27** as a white precipitate in a moderate yield of 52% (Scheme 2.11). The ^1H NMR spectrum of O -glycolipid **2.27** is displayed in Figure 2.16. Characteristic peaks are highlighted in the figure, including the

amide protons (NH), the anomeric proton (H-1), and the α^* and β^* -protons. Again the best solvent for ^1H NMR analysis, in terms of solubility and resolution, was found to be d_5 -Pyr.

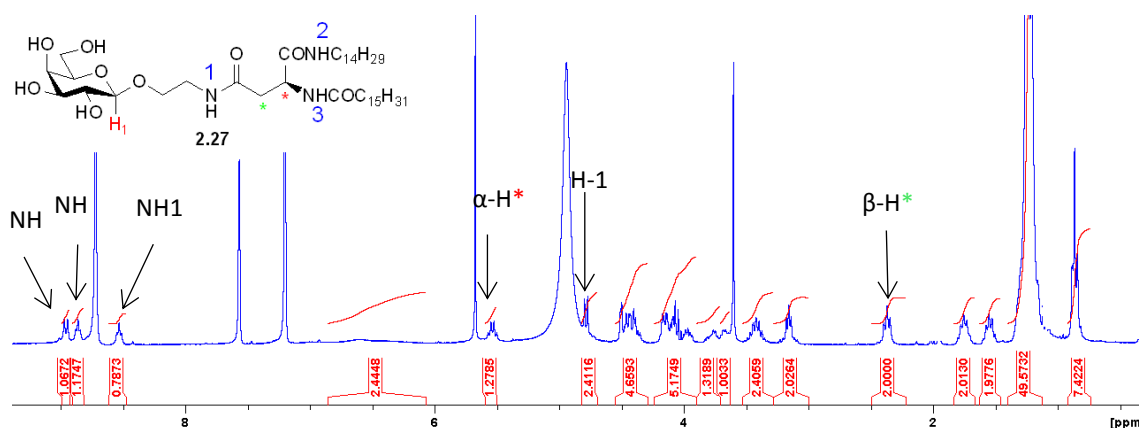


Figure 2.16 ^1H NMR spectrum of glycolipid **2.27** (d_5 -Pyr, 300 MHz) with characteristic peaks assigned. Presence of solvent effecting integration of H-1 and α -H.

Deprotection of tetracosanoyl derivative **2.62** proved a lot more difficult. The mildly basic conditions of NEt_3 in a heterogenous solvent mixture, which had worked for glycolipids **2.26** and **2.27**, was unsuccessful. Although partial deacetylation was observed by TLC, full deprotection was not achieved. Other common methods were also attempted such as Zémlen conditions and reaction with hydrazine, but these proved to be too harsh and degradation of compound **2.62** was observed in both cases. We believed that the problems encountered were due to poor solubility of the partially deacetylated compound, as the reaction mixture became cloudy after overnight stirring. Upon careful consideration the mild conditions of NEt_3 in $\text{MeOH}/\text{H}_2\text{O}/\text{DCM}$ was reinvestigated and the solvent systems were varied in an attempt to achieve greater solubility. This time THF (1 mL) was added to the already heterogenous solvent system of DCM , H_2O and MeOH (1 mL, 1 mL, 2 mL). As before, a precipitation, which was assumed to be the partially deprotected glycolipid, was observed after 1 h (reaction mixture became cloudy). The reaction was continued and 1 mL of THF was added every time a precipitate was formed. This process continued for 72 h until no starting material could be visualised by TLC. The reaction was quenched by evaporation and triturated using $\text{DCM}/\text{Et}_2\text{O}$ to yield the desired fully deprotected compound **2.28** as a white solid in 38% yield.

Due to the extremely poor solubility of glycolipid **2.28**, structural elucidation was very difficult. Like glycolipids **2.26** and **2.27**, glycolipid **2.28** was partially soluble in d_5 -Pyr, therefore ^1H NMR analysis was carried out and the structure confirmed. The ^1H NMR spectrum of *O*-glycolipid

2.28 is displayed in Figure 2.17. Characteristic peaks are highlighted in the Figure, including the amide protons, the anomeric proton, and α and β -protons.

Insufficient material was soluble in d_5 -Pyr to enable us to obtain a clear ^{13}C NMR spectrum. However comparisons of the ^1H NMR spectrum to the shorter chain analogues **2.26** and **2.27**, gave sufficient evidence that the desired compound **2.28** was present. This was further confirmed by HR-MS analysis.

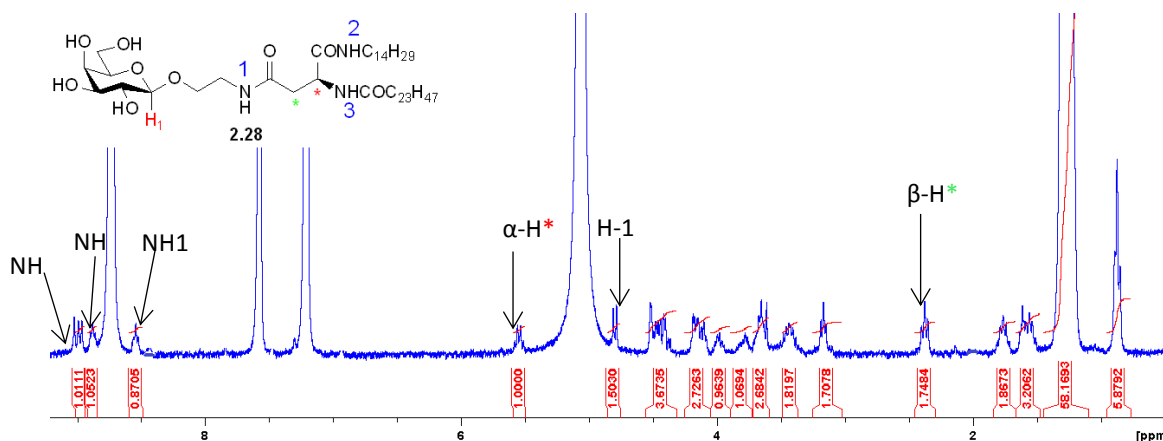


Figure 2.17 ^1H NMR spectrum of deprotected glycolipid **2.28** (d_5 -Pyr, 300 MHz) with characteristic peaks assigned. Solvent under peak at ~ 1.25 ppm affecting integration.

2.6 Synthesis of second generation glycolipids

2.6.1 Synthesis of bivalent β -O-glycolipid **2.29**

Due to the solubility issues encountered with the previous glycolipids **2.26**–**2.28**, we wished to investigate alternative glycolipid structures. As aspartic acid contains two carboxylic acid groups there are two potential sites for acylation. We wanted to investigate if acylating at both sites with the galactosyl amine (therefore having only one lipidic chain present) would improve solubility and lead to different physicochemical properties and self-assembly behaviour. Glycolipid **2.29** was prepared as a representative example (Figure 2.18).

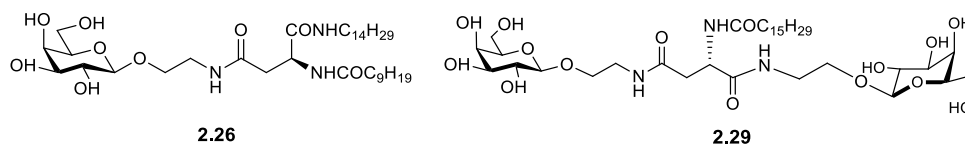
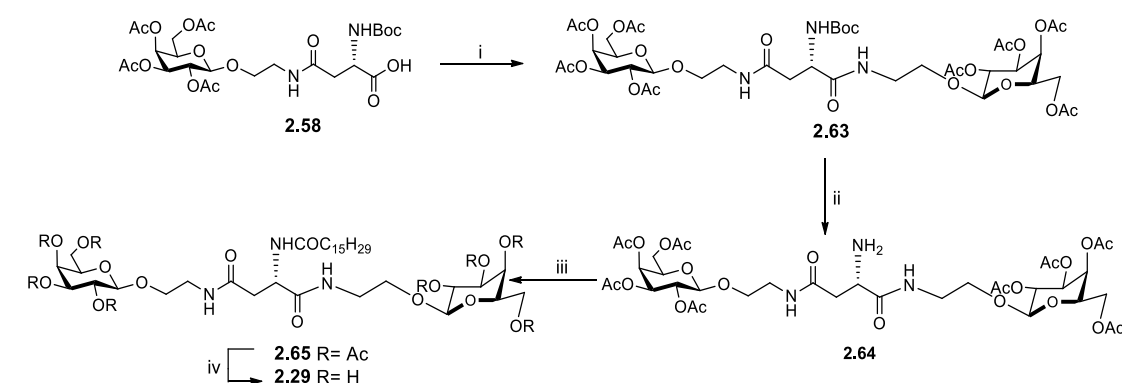


Figure 2.18 Structural comparison between the structure of glycolipids **2.26** and **2.29**.

The synthesis started with galactosylated carboxylic acid intermediate **2.58** synthesised previously as described in section 2.5.2. Coupling of the free acid building block **2.58** with the galactosyl amine **2.33** using TBTU/HOBt methodology afforded 61% of the bivalent molecule

2.63 (Scheme 2.12). Subsequent removal of the *N*-Boc protecting group with TFA afforded the amine **2.64** which was acylated with hexadecanoyl chloride in the presence of base. The diastereomerically pure protected glycolipid **2.65** was successfully obtained in 58% yield. Due to the increased solubility of glycolipid **2.65** the removal of the acetyl protecting groups proceeded very smoothly and the deprotected bivalent β -*O*-glycolipid was obtained as a white solid in 86% yield. The ^1H NMR spectrum of the deprotected bivalent β -*O*-glycolipid **2.29** is shown in Figure 2.19.



Scheme 2.12 Reagents and conditions: i) TBTU, HOBT, DMF, 4 Å MS, N_2 , rt, 18 h, 61%; ii) TFA, DCM, rt, 3.5 h, 61%; iii) NET_3 , $\text{CH}_3(\text{CH}_2)_{14}\text{COCl}$, DCM, N_2 , rt, 16 h, 58%; iv) NET_3 , DCM/MeOH/ H_2O , 40 °C, 18 h, 86%.

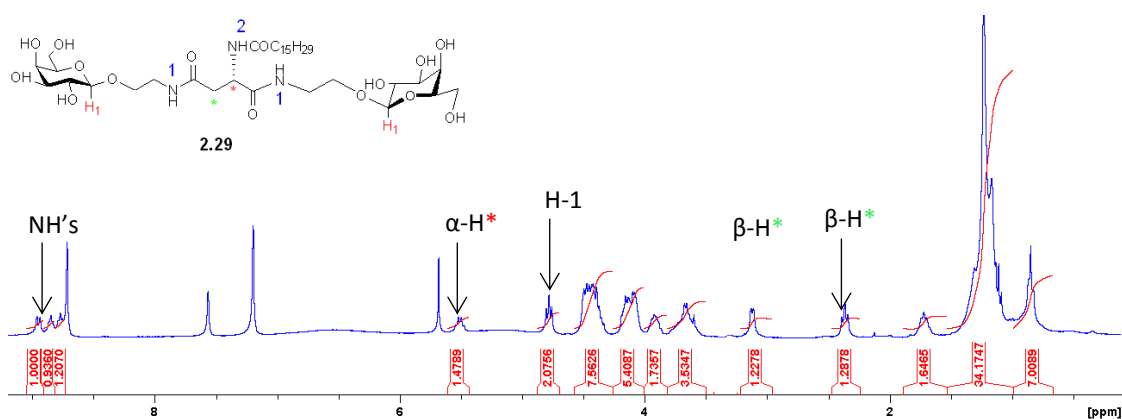


Figure 2.19 ^1H NMR spectrum of deprotected bivalent β -*O*-glycolipid **2.29** (d_5 -Pyr, 300 MHz).

2.6.2 Synthesis of β -*O*-glycolipid **2.31**

A further structural variation was investigated around the aspartic acid linker. We wanted to examine if varying the position of both the galactosyl moiety and the tetradecyl chain would affect the physicochemical properties and gelation ability. Therefore, we attempted the synthesis of β -*O*-glycolipid **2.31**, which differs from glycolipid **2.55** as the galactose moiety is in the C-4 position of the aspartic acid rather than the C-1 position. Compared to glycolipid **2.55**, the lipid chains are no longer branching off from the same carbon (Figure 2.20).

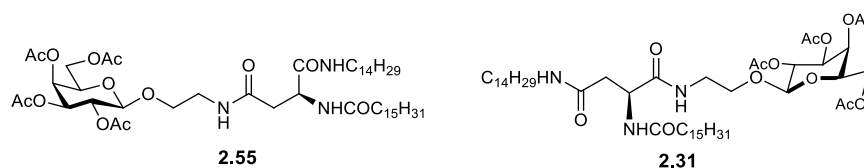
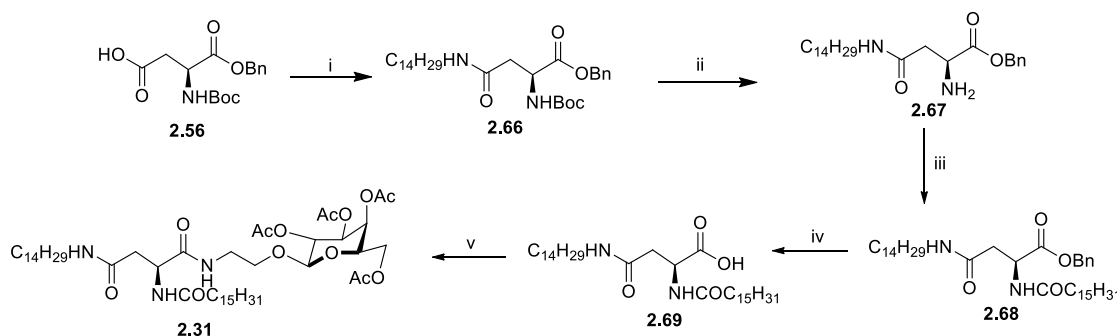


Figure 2.20 Comparison between the structure of glycolipids **2.55** and **2.31**.

The synthesis proceeded with the coupling of tetradecylamine and the commercially available *N*-Boc-L-aspartic acid-1-benzyl ester **2.56** using TBTU/HOBt in DMF to give the orthogonally protected compound **2.66** in 84% yield (Scheme 2.13). Removal of the *N*-Boc protecting group with TFA afforded the amine **2.67** which was acylated with hexadecanoyl chloride using base to give compound **2.68**. Deprotection of the benzyl ester was performed using H₂ bubbled through a solution of **2.68** in EtOAc at 50 °C in the presence of Pd(C). The resulting carboxylic acid **2.69** was carefully reacted with the galactosyl amine **2.33** again using the TBTU/HOBt system. To avoid racemisation of the chiral carbon in this crucial step, the reaction was carried out in the absence of external base. Under these conditions, diastereomerically pure **2.31** was successfully obtained, in a moderate yield of 63%. Despite the moderate yield of the final step, all other synthetic steps exhibited high yields, we therefore concluded that the synthetic approach was advantageous.



Scheme 2.13 Reagents and conditions: i) TBTU, HOBt, DMF, 4 Å MS, N₂, rt, 18 h, 84%; ii) TFA, DCM, ,2.5 h, 73%; iii) TBTU, HOBt, CH₃(CH₂)₁₄COCl, DMF, 4 Å MS, N₂, rt, 16 h, 87%; iv) H₂, Pd/C, EtOAc, 50 °C, 4 h, 94%; v) TBTU, HOBt, **2.33**, DMF, 4 Å MS, N₂, rt, 18 h, 63%.

The ¹H NMR spectrum of glycolipid **2.31** can be seen in Figure 2.21. Characteristic signals are assigned which include the amide protons (NH), the anomeric proton (H-1), and the α* and β*-protons. The ¹H NMR spectrum shows no evident differences to the corresponding one of glycolipid **2.55**.

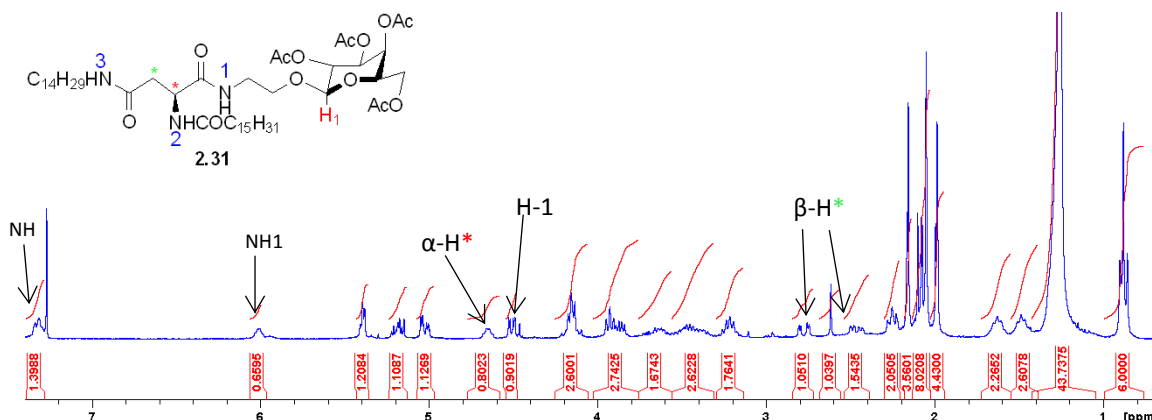
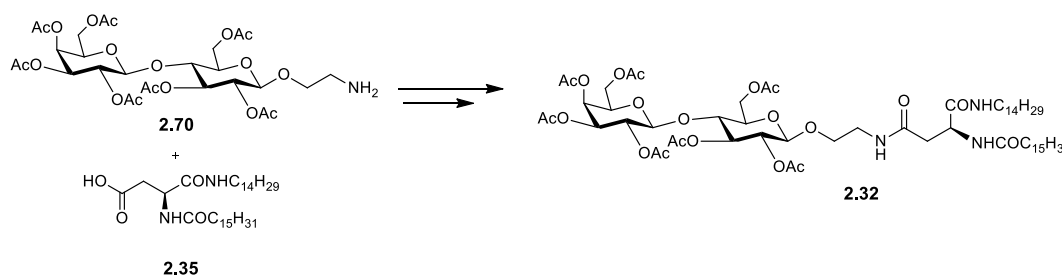


Figure 2.21 ^1H NMR spectrum of acetylated β -O-glycolipid of **2.31** (CDCl_3 , 300 MHz).

2.6.3 Synthesis of disaccharide β -O-glycolipid **2.32**

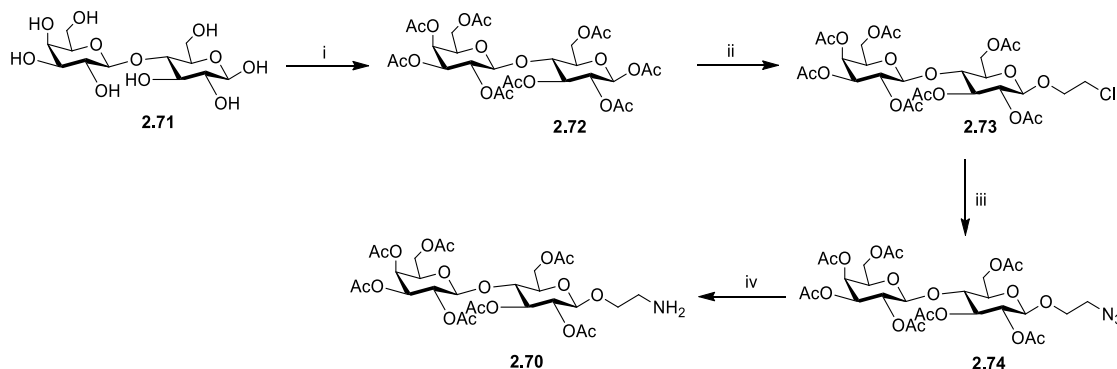
The next synthesis investigated was the disaccharide aspartic acid derivative **2.32**. Like the previous mimetics discussed, this variation was chosen as we wanted to examine whether the presence of a disaccharide (a higher percentage of polarity) would influence gelation ability in a range of solvents of different polarities, including H_2O . Initial investigations led us to approach the synthesis *via* a modular approach as shown in Scheme 2.14, whereby the easily accessible β -O-ethyl-lactosyl amine **2.70** and aspartic acid derivative **2.35** would serve as suitable building blocks.



Scheme 2.14 Aspartic acid **2.35** and lactosyl amine **2.70** building blocks used for the synthesis of glycolipid **2.32**.

2.6.3.1 Synthesis of Lactosyl amine **2.70**

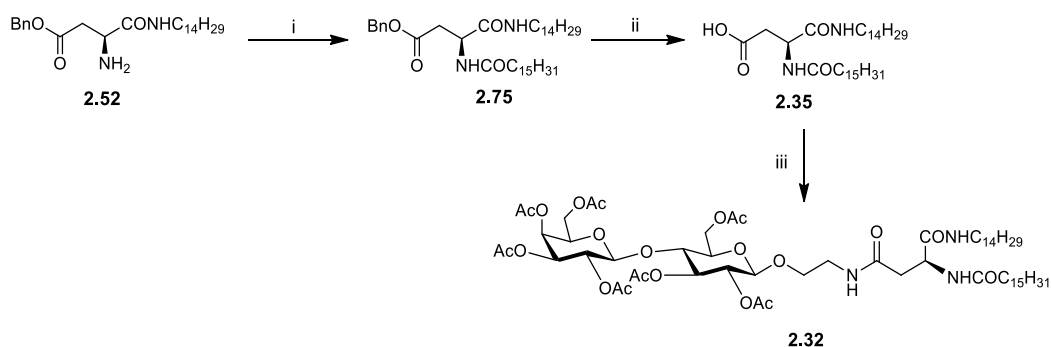
The synthesis followed the same methodology as the galactosyl amine **2.33** described in section 2.2.1.1. The hydroxyl groups of commercially available D-lactose **2.72** were acetylated and a direct glycosylation reaction with 2-chloroethanol was carried out on the anomeric position of the *per*-acetylated donor **2.72** (Scheme 2.15). This yielded 47% of the β -lactoside **2.73** exclusively. A substitution reaction was then performed and the chloride atom of the ethyl linker was replaced with an azide group. Hydrogenolysis afforded the final lactosyl amine **2.70** in 73% yield.



Scheme 2.15 Reagents and conditions: i) NaOAc, Acetic anhydride, 0-110 °C, 18 h, 80%; ii) 2-chloroethanol, $\text{BF}_3 \cdot \text{O}(\text{Et}_2)$, DCM, N_2 , rt, 16 h, 47%; iii) NaN_3 , DMF, 110 °C, 3 h; 74% iv) H_2 , Pd/C, EtOH, 5 h, 73%.

2.6.3.2 Synthesis of aspartic acid building block 2.35

The synthesis commenced with the same reaction conditions that were initially used for the C-10 glycolipid **2.26** (section 2.5.1.2, Scheme 2.7). Coupling of the free amine building block **2.52** with hexadecanoyl chloride afforded 68% of the desired compound **2.75** (Scheme 2.16). Subsequent removal of the benzyl ester protecting group with H_2 bubbled through Pd/C afforded the free acid aspartic acid building block **2.35**. The free acid **2.35** was coupled with the lactosyl amine **2.70** using TBTU/HOBt coupling methodology (Scheme 2.16). The enantiomerically pure protected glycolipid **2.32** was successfully obtained in 29% yield. The poor yield was due to poor solubility of the aspartic acid building block **2.35** with the long hydrophobic chains. The ^1H NMR spectrum of *O*-glycolipid **2.32** is displayed in Figure 2.22. Characteristic peaks are highlighted in the figure, including the amide protons, the anomeric proton, and the α and β -protons. Deprotection of glycolipid **2.32** was attempted using NEt_3 in a heterogenous solvent system however full deprotection, without degradation of the compound, could not be achieved.



Scheme 2.16 Reagents and conditions: i) TBTU, HOBt, $\text{CH}_3(\text{CH}_2)_{14}\text{COCl}$, NEt_3 , DMF, N_2 , rt, 68%; ii) H_2 , Pd/C, EtOAc, 50 °C, 5 h, 90%; iii) TBTU, HOBt, NEt_3 , DMF, 50 °C-rt, 18 h, 29%.

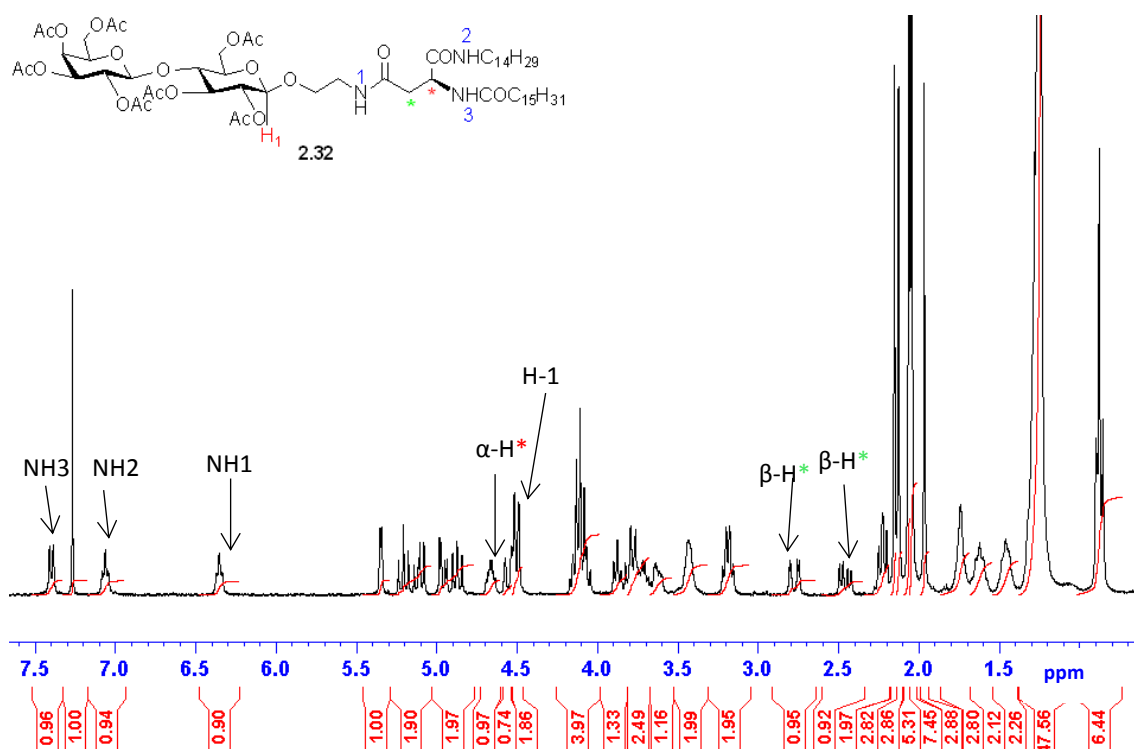


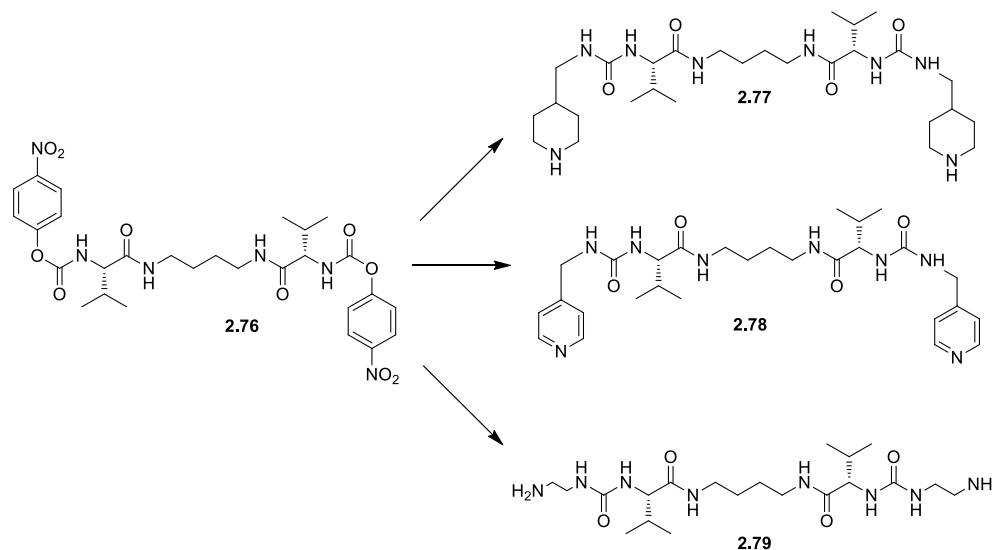
Figure 2.22 $^1\text{H-NMR}$ spectrum of acetylated disaccharide glycolipid **2.70** (CDCl_3 , 300 MHz) with characteristic peaks assigned.

2.6.4 Synthesis of C-6 functionalised $\beta\text{-O}$ -glycolipid **2.30**

Literature research has shown that there is a great deal of interest in compounds which form gels as a result of an external stimulus.^[67, 73] One way this can be achieved is by functionalising the gelator molecule with a group that can be activated by external conditions and therefore lead to stimuli responsive gels. One example that is commonly reported in the literature is the use of azobenzenes. Azobenzenes undergo photoreversible *cis-trans* isomerism: *trans-cis* isomerisation is achieved by UV irradiation and *cis-trans* isomerisation takes place upon visible light irradiation. Many groups have exploited this ability and produced gelator molecules containing azobenzene whereby the gels collapse under UV irradiation and reform by visible light irradiation.^[55]

Another approach reported by Miravet and Escuder^[100] involves the synthesis of reactive gels. Using this method, the already assembled gels can be further reacted with other functional groups to produce new gel materials that have different properties to that of the original gel. This means the pre-assembled gel acts as scaffold for the synthesis of the new gel.

Some selected examples are shown below in Scheme 2.17. The reactive organogel **2.76** was reacted with a variety of primary amines to obtain a number of new bis-urea gel materials **2.77-2.79** which exhibited increased thermal stability.



Scheme 2.17 Synthesis of a variety of new bis urea gels **2.77-2.79** from reactive organogel **2.76**.^[100]

We wanted to examine if functionalising the C-6 position on the galactose moiety of the glycolipid **2.27** would result in different physicochemical properties and self-assembly behaviour. Our aim was to investigate if we could improve gelation ability or synthesise a stimuli responsive gelator by replacing the hydroxyl group on the C-6 position of galactose with a variety of functional groups, which could lead to a reactive organogel system.

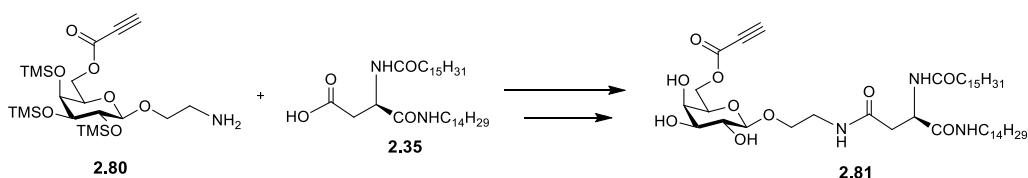
As we had previously synthesised the free acid aspartic acid building block **2.35** featuring both the tetradecyl and hexadecanoyl chain (discussed in section 2.2.6), it was decided to use this building block and again follow a modular approach. This way we could focus on the functionalisation of the carbohydrate moiety.

As aromatic groups have been reported to stabilise gel formation as a result of π - π stacking,^[73] our initial idea was to introduce a group capable of forming a triazole moiety into the C-6 position of the analogue. In order to achieve this, it was decided to functionalise the C-6 position of the galactose with an alkyne group. The alkyne moiety of the galactose could then react with an azide-containing molecule in a 1,3 dipolar cycloaddition to form the desired triazole functionality.

For this synthesis the free hydroxyl groups at the C-2, C-3 and C-4 positions need to be protected (to prevent unwanted coupling reactions) and the C-6 position needs to bear a free hydroxyl group. Fernández *et al.* demonstrated selective deprotection of a primary C-6 trimethyl silyl (TMS) ether in the presence of secondary TMS groups on galactose.^[101] Jervis *et al.* further proved this methodology.^[40] Owing to their ease of introduction into the galactose starting material, the ability to selectively deprotect the primary silyl ether at the C-6 and

finally, due to the ease with which the remaining silyl ether groups can be removed when required, protection with TMS group appeared to be ideal for this type of approach.

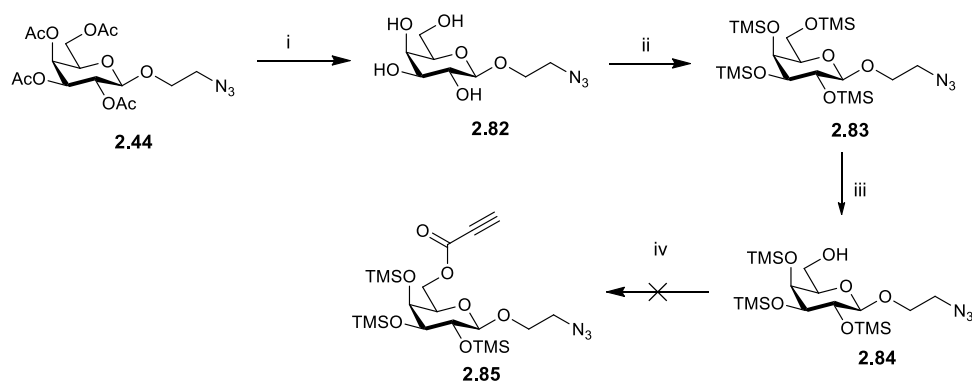
The synthetic approach had to be considered carefully. Introduction of an alkyne group, such as propiolic acid, to the selectively TMS protected galactoside could be carried out *via* a Steglich esterification. This would yield a functionalised galactose building block such as **2.80** ready for coupling with the free acid aspartic acid derivative **2.35**. The alkyne of glycolipid **2.81** could then react with an azide-containing molecule in a 1,3 dipolar cycloaddition, in the presence of a Cu(I) source, to form the desired triazole functionality. The initial synthetic pathway can be seen below in Scheme 2.18.



Scheme 2.18 Key building block in the synthesis of glycolipid **2.78**.

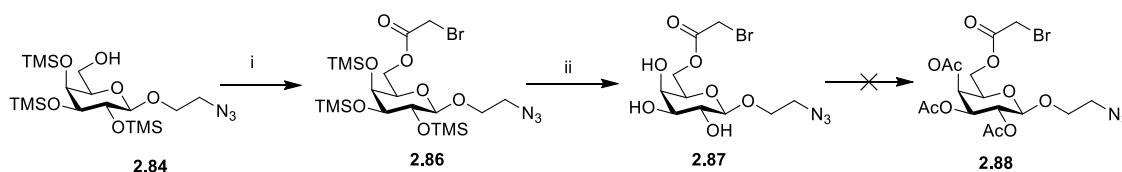
2.6.4.1 Attempted synthesis of C-6 functionalised galactose building block **2.83**

The synthesis of galactosyl amine **2.83** started with the acetylated galactosyl azide building block **2.44** (discussed previously in section 2.5.1.1), which was deprotected using methanolic NaOMe (Scheme 2.19). The resulting compound **2.82** was then reacted with chlorotrimethylsilane and hexamethyl disilazane in pyridine to yield compound **2.83** in 76% yield. Selective deprotection of the TMS ether in the C-6 position using acetic acid in MeOH/acetone afforded the alcohol **2.84** in 75% yield. The final step was the Steglich esterification with propiolic acid, *N,N'*-dicyclohexylcarbodiimide (DCC) and 4-dimethylaminopyridine (DMAP) in DCM. However, no desired product **2.85** was obtained. This reaction was repeated in the absence of DMAP but still remained unsuccessful. Instead, due to the presence of the labile TMS ethers, a complicated mixture of products and deprotected galactose azide **2.82** was obtained. It is possible that the primary alcohol of the galactose was attacking the terminal alkyne of the propiolic acid in a Micheal type reaction and therefore preventing the formation of the product **2.85**. There are examples of this type of reactivity in the literature and ways to circumvent this problem include cooling the reaction, and also allowing the alcohol to react with the DCC and DMAP prior to addition of the alkyne.^[102] Both conditions were attempted but again, no product was obtained.



Scheme 2.19 Attempted synthesis of galactosyl azide building block **2.83** *Reagents and conditions:* i) NaOMe, DCM, MeOH, N₂, rt, 1 h, 91%; ii) TMSCl, HMDS, pyr, 0 °C → rt, overnight, 76%; iii) AcOH, acetone:MeOH, 2 h, 75%; iv) propiolic acid, DCC, DMAP, DCM, N₂, rt/0 °C.

Due to the problems encountered above, possibly due to the side reactivity of propiolic acid, it was decided to instead attempt to incorporate the azide functionality onto the C-6 position of the galactoside building block. As the molecule already contained an azide group, which needed to be reduced to the free amine for coupling to the aspartic acid, we needed to introduce an orthogonal group that could be converted to the azide at a later stage. For this reason we chose to functionalise the galactoside **2.87** with bromoacetic acid. The revised synthetic route can be observed below in Scheme 2.20. The synthesis started with the C-6 free hydroxyl galactoside **2.84** (discussed above). Steglich esterification with bromoacetic acid this time afforded the desired functionalised product **2.86** in 61% yield. The ¹H NMR spectrum of the galactosyl azide building block **2.86** is shown below in Figure 2.23.



Scheme 2.20. *Reagents and conditions:* i) DCC, DMAP, DCM, N₂, rt/0 °C, 18 h, 61%; ii) (1) 2% TFA in DCM, 1 h, 96%; (2) Dowex, MeOH, 1 h, 98%.

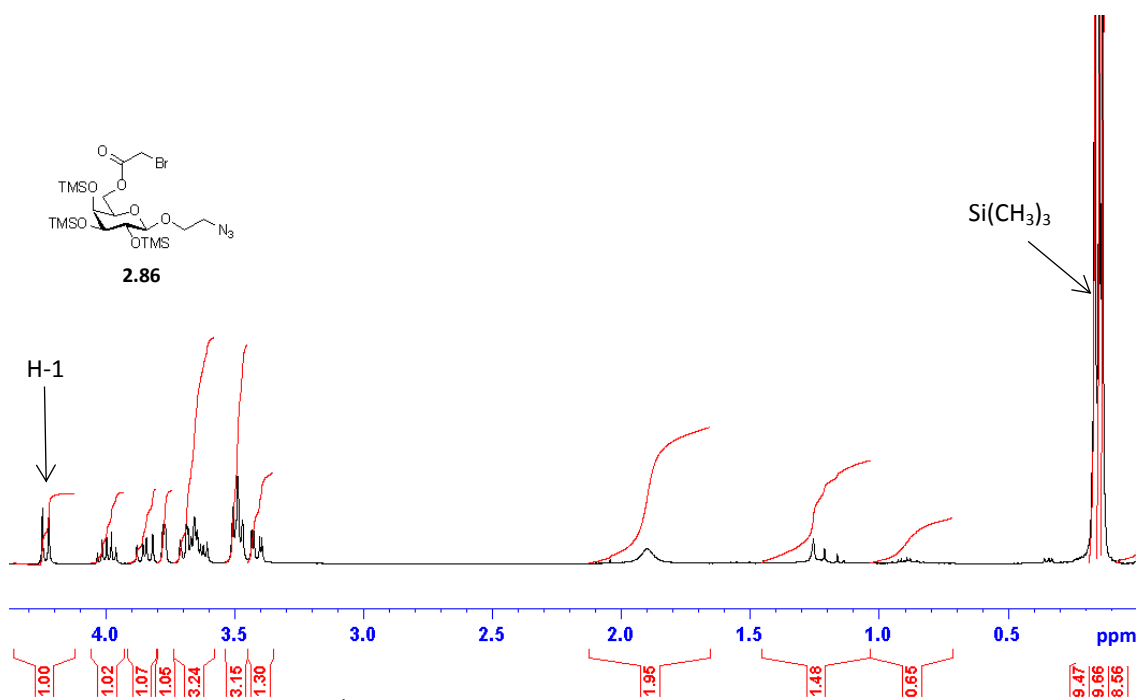
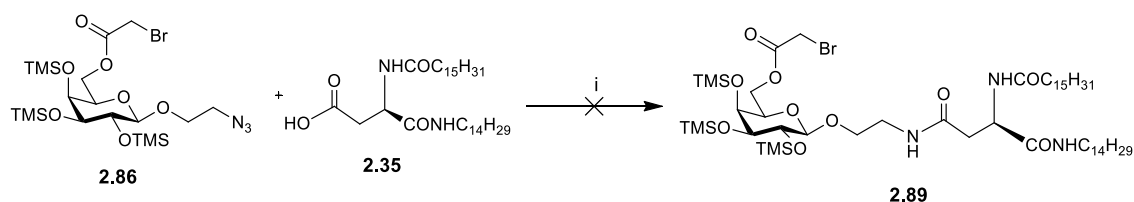


Figure 2.23 ^1H NMR spectrum of galctosylazide building block **2.86**.

Owing to the constraints of working with the labile TMS protecting groups, it was decided to attempt their removal at this point and then reprotect the sugar hydroxyl groups using a more robust protecting group. The use of acetyl protecting groups was investigated for comparison with the glycolipid described in earlier sections. Initial deprotection of the remaining TMS ethers was achieved using a 2% solution of TFA in DCM to yield compound **2.87**. However, reprotection using acetyl protecting conditions to give galactoside **2.88** could not be achieved. A number of common acetylation conditions were attempted including; acetic anhydride and pyridine, acetic anhydride, pyridine and DMAP, and acetyl chloride and NEt_3 . All reactions were carried out at both rt and reflux but in all cases, no desired product was obtained. We believed that this may have been due to residual acid from the preceding deprotection step. Therefore, we attempted the deprotection using the milder conditions of Dowex in MeOH, as Gervay-Hague and Witschi had reported the successful deprotection of TMS ethers on a similar substrate using the same conditions.^[103] Again the desired deprotected product **2.90** was obtained, however acetylation still remained unsuccessful.

As a result of these setbacks, we again had to address our synthetic approach. We opted to maintain the TMS protected galactose moiety **2.86** and carry on with the synthesis. The functionalised galctosyl azide **2.86** was reduced to the amine using, Pd/C in EtOAc and subsequently *in situ* coupled to the aspartic acid building block **2.35** using TBTU/HOBt methodology. Unfortunately, under these conditions no desired product **2.89** was obtained (Scheme 2.21).



Scheme 2.21 Attempted synthesis of C-6 functionalised glycolipid **2.89** Reagents and conditions: i) (1) H_2 , Pd/C, EtOAc, 2.5 h; (2) HOBT, TBTU, NEt_3 , DMF, N_2 , rt, 16 h.

Instead, the product of these reactions appeared to have an acetyl group in the C-6 position of the galactose as in glycolipid **2.30** (Figure 2.24), and cleavage of the TMS ethers was also observed. We postulated that the bromo-carbon bond had undergone hydrogenolysis when reduction of the azide was taking place, as many examples of halogen hydrogenolysis have been carried out with Pd/C in the literature.^[104] Structural elucidation using ^1H NMR, ^{13}C NMR spectroscopy and HR-MS confirmed the presence of compound **2.30**. The ^1H NMR spectrum of this compound is shown below (Figure 2.25), with characteristic peaks assigned.

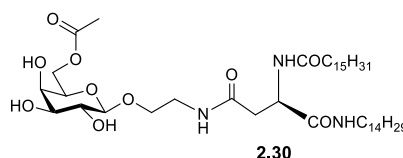
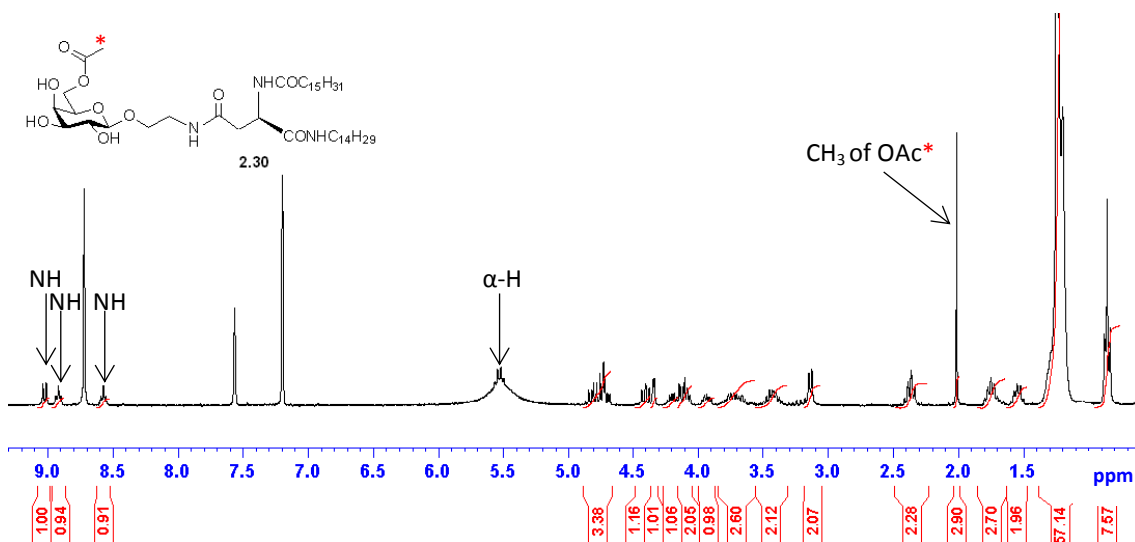


Figure 2.24 Structure of glycolipid **2.30** obtained from the hydrogenolysis of **2.89** and subsequent *in situ* coupling with the aspartic derivative **2.35**.



2.7 Gelation and self-assembly properties of β -O-glycolipids 2.26-2.32

As discussed earlier, the ability of a molecule to induce gelation of a certain solvent has a wide range of applications in the chemical industry including their use as soft materials, drug delivery systems and H₂O purification systems. During the synthesis of glycolipid **2.27** we observed that it was able to induce gelation in certain solvents used for chromatographic purification. This serendipitous observation prompted us to review the literature and recognise the potential applications of *O*-glycolipid **2.27** to act as a LMWG. With this in mind we decided to examine the gelation abilities of a range of different glycolipids, and investigate some of the structural features that may affect gelation ability including hydrophobic chain length, and the effect of chirality. All of the compounds tested are amphiphilic in nature and feature the presence of one or two saturated hydrocarbon chains varying in length.

2.7.1 Gelation and self-assembly properties of first generation of β -O-glycolipids

Our aim was to investigate how alterations in the glycolipid structure could influence their ability to induce gelation (Figure 2.26). We also wanted to examine if changes in the glycolipid structure affected the stability of the gels. The first variation investigated was hydrophobic chain length. As discussed previously, (section 2.2.1.1), Van der Waals forces of hydrophobic regions in a molecule play a role in the formation of gels. Therefore, we strived to determine if the length of the hydrophobic chain influenced self-assembly and gelation ability of the glycolipids. For this comparison, we chose glycolipid **2.55** which contained the C-10 chain and glycolipid **2.61** which contained the C-16 chain. The second structural feature chosen to examine was how chirality in the molecule altered gelation ability. For this, we chose to compare the diastereomerically pure glycolipid **2.26** and the mixture of diastereomers, glycolipid **2.90**. The final variant we opted to assess was how the presence of acetyl or hydroxyl groups affected the solubility, and therefore changed self-assembly behaviour. H-bonding between gelator molecules and also between the gelator molecule and the solvent are important in gel formation. It was believed the presence of the hydroxyl groups would lead to more H-bond donors being available for H-bonding and therefore, could result in more thermally stable gels. For this evaluation we compared the acetyl protected glycolipid **2.61**, and the deprotected glycolipid **2.27**.

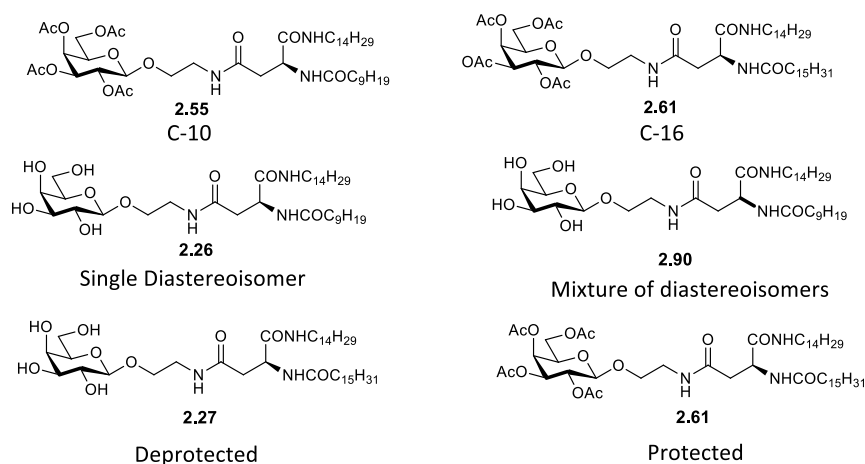


Figure 2.26 Structure of compounds **2.26**, **2.27**, **2.55**, **2.61**, and **2.90** tested for their gelation ability in a variety of organic solvents.

Gelation tests were performed using an “inverted test-tube method” as described by Tanake *et al.*^[105] The glycolipids and solvents (20 mg mL⁻¹) were placed in screw cap glass vials and heated until all solid had dissolved (apart from the insoluble compounds). The solution was then cooled to rt and left to stand for 2 h. Their gelation ability was assessed by inverting the vials and examining the absence of the gravitational flow of solvents. If the solvent did not flow upon inversion, but instead remained at the bottom of the vial, the molecule was classified as a gelator. If there was gravitational flow of liquid upon inversion of the vial, the compound was determined to be a non-gelator. Based on our observations, the term non-gelator was further categorised. If the compound was determined to be a non-gelator and dissolved fully in the solvent, it is classified as soluble in the gelation table. However, if the glycolipid never solubilised in the solvent, it was classified as insoluble in the gelation table. Another term used is aggregates, which implies that the glycolipid was initially soluble in the given solvent but upon standing at rt it precipitated as a more defined, self-assembled structure. The final term utilised is partial gelation. In some cases we found that, although there was a presence of liquid flow upon inversion of the vial, small localised gelled areas could also be observed. Images of the self-assembly behaviour in different solvents are portrayed in Figure 2.27.

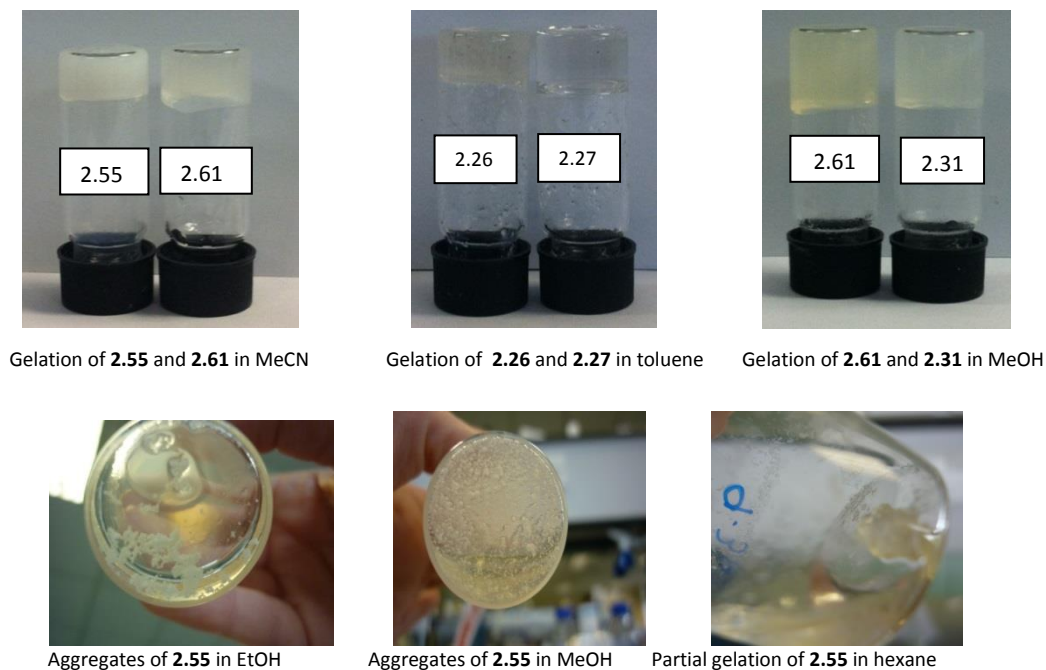


Figure 2.27 Images of self-assembly of selected glycolipids in various solvents.

The ability of the glycolipids to induce gelation was tested in a variety of organic solvents and the results are presented in Table 2.1. The minimum gelation concentrations (MGC) were also calculated for all gelators in their various solvents. The MGC indicates the minimum concentration of gelator molecule (mg) required to induce full gelation in a given volume of solvent (1 mL).^[106]

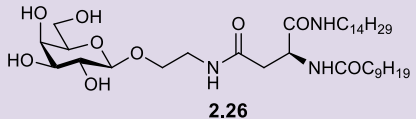
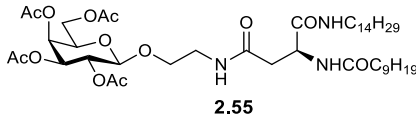
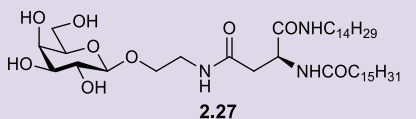
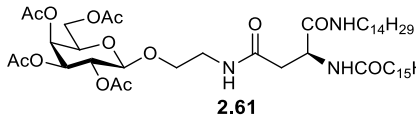
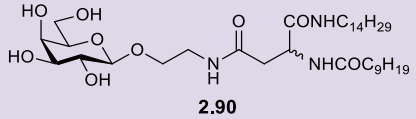
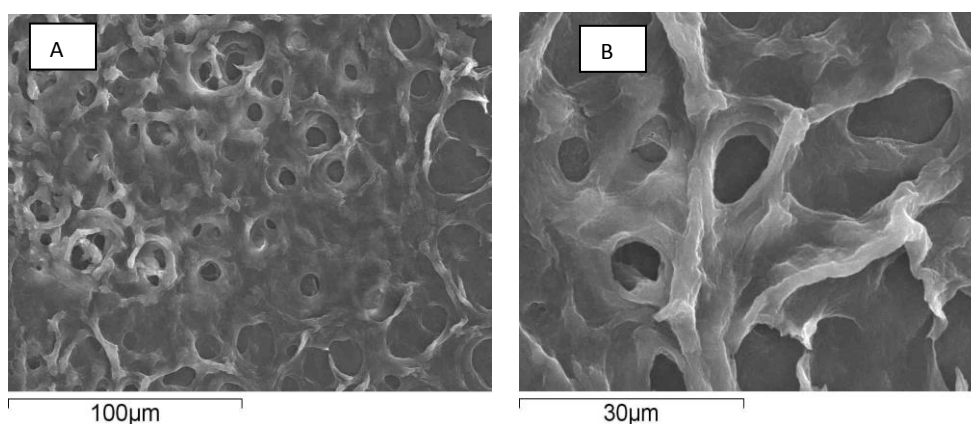
	DCM	Toluene	MeCN	MeOH	EtOH	H ₂ O	EtOAc	Hexane	CHCl ₃
 <p>2.26</p>	I	P.G	I	A	A	I	I	I	I
 <p>2.55</p>	S	S	G(14)	A	A	I	S	P.G	S
 <p>2.27</p>	I	G(13)	I	A	A	I	I	I	I
 <p>2.61</p>	S	G(17)	G(15)	G(20)	G(8)	I	S	I	S
 <p>2.90</p>	I	P.G	P.G	A	A	I	I	I	G(20)

Table 2.1 Gelation abilities of glycolipids in various solvents. All compounds were tested using the inverted test tube method at 20 mg mL⁻¹. Values refer to critical gel concentration (MGC) (mg per mL). Aggregates=A, Gelation=G, Partial Gelation=P.G, Insoluble=I, Soluble=S, Partial soluble=P.S.

2.7.1.1 SEM on O-glycolipids 2.55, 2.61, and 2.90

Scanning Electron microscopy (SEM) is a technique commonly employed to give information about a samples morphology. To gain a microscopic insight into the self-assembled structures of **2.55** and **2.61** when acting as LMWGs, the morphologies of galactosyl aspartic acid derivatives were observed by SEM as xerogels using the drop casting method. The drop-cast technique involved the gelling of a small amount of solvent directly onto the silicon wafer used in SEM analysis. The corresponding xerogel was formed by allowing the sample solvent to evaporate at rt overnight.

The SEM images of the xerogel from MeCN of glycolipid **2.55** are shown in micrograph A and B of Figure 2.28. The SEM image in micrograph A shows that evaporation of the solvent leaves behind a porous structure characteristic of xerogels. On magnification, the formation of a network of thick fibres, which enables the trapping of solvent and leads to the formation of the gel can be observed (micrograph B). These observations are in line with those reported, as SEM images of organogelators are commonly encountered as three dimensional fibrous networks.^[107] A very different morphology is observed when examining the aggregates formed by glycolipid **2.55** in EtOH. Micrograph B (Figure 2.29) depicts a very compact three dimensional network containing long thin fibrils that are woven tightly together with a defined structure. Again, this is in line with morphologies described in the literature and it is believed that these thinner fibrils can further aggregate forming highly entangled and more dense fibrous bundles.^[68] No pores can be observed in the SEM image of the aggregates and this explains why gelation is not observed in this solvent. These pores represent pockets where the solvent becomes trapped as the gel is being formed and remain visible after the solvent has evaporated.



MeCN xerogel of glycolipid **2.55**

Magnification of MeCN xerogel of glycolipid **2.55**

Figure 2.28 SEM micrographs of xerogel of glycolipid **2.55** in MeCN.

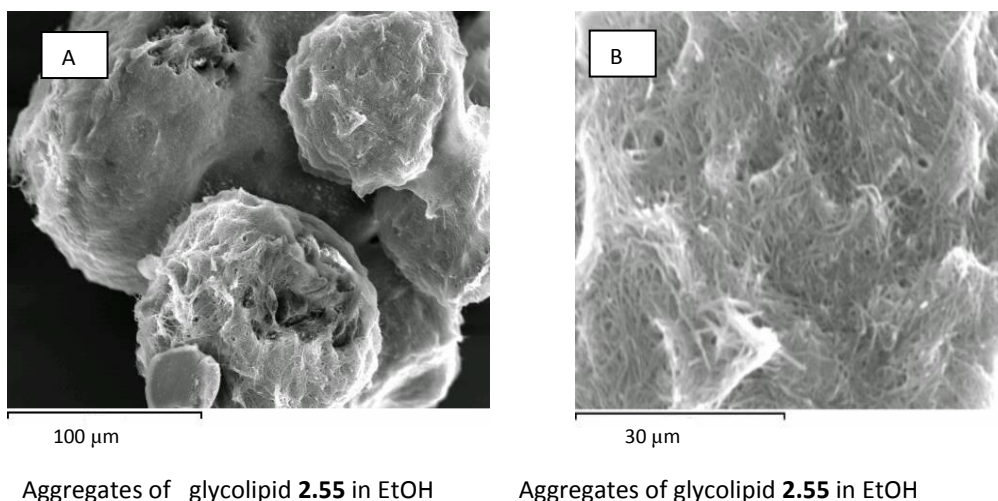


Figure 2.29 SEM micrographs of aggregates of glycolipid **2.55** in EtOH.

Remarkably, the mixture of diastereoisomeric glycolipids **2.90** was capable of inducing the gelation of CHCl_3 , whereas the single diastereoisomer **2.26** was insoluble in this solvent. The SEM images of the xerogel of glycolipids **2.90** in CHCl_3 are shown below in Figure 2.30. Again, the images depict the formation of a three dimensional fibrous network, however, this time the fibrils are much thinner and the structure is much more porous in comparison to the images of the xerogel of **2.55** in MeCN (Figure 2.28).

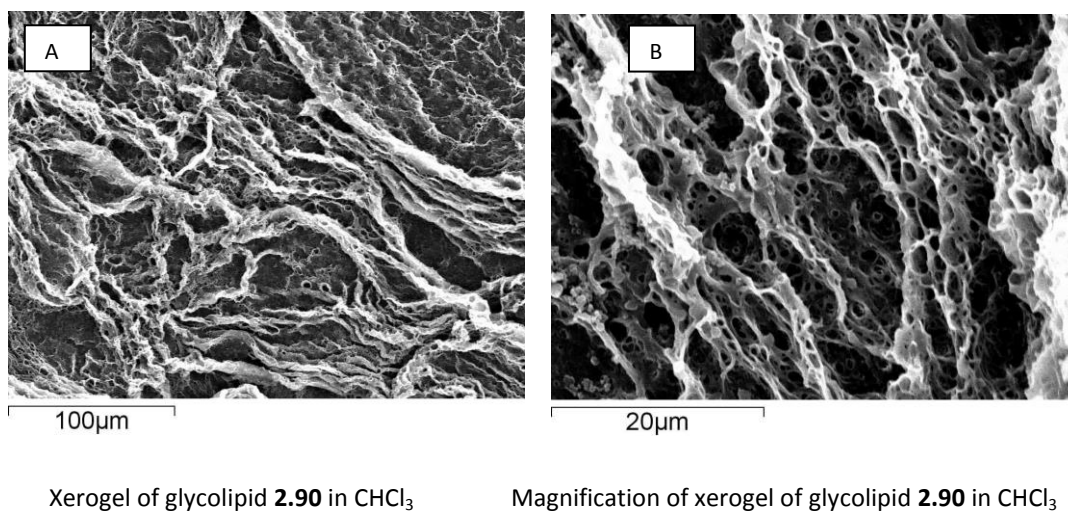


Figure 2.30 SEM micrographs of xerogel of glycolipid **2.90** in CHCl_3 .

It is very clear from the above images that the morphology of the xerogels differs greatly depending on both the molecule inducing gelation and the solvent used for gelation. The single diastereoisomer, protected C-10 glycolipid **2.55**, forms much thicker fibres with the pores very evenly distributed. In contrast, the deprotected mixture of diastereoisomeric C-10 glycolipids **2.90** appears to form a three dimensional network saturated with pores formed by much

thinner fibrils. This is supported by data from gelation Table 2.1 which shows that although the deprotected glycolipids **2.26**, **2.27** and **2.90** exhibit self-assembly behaviour in certain solvents, in general, the protected compounds **2.55** and **2.61** induce gelation in a wider variety of solvents. However, we observed that the deprotected glycolipids formed more stable gels than their acetylated counterparts. This implies that H-bonding of the free hydroxyl on the galactose moiety may be important in the self-assembly process. This was further supported by examination of the *gel-sol* transition temperature (T_{gs}). The formation of all the gels was found to be thermo-reversible, i.e. they turned into solutions upon heating and slowly gelled upon cooling. The *gel-sol* transition temperature indicates the temperature for the phase transition at which the gel breaks down and changes back into a solution. For the gel of the protected glycolipid **2.61** in toluene, the T_{gs} was observed to be 36 °C, however, the gel of the deprotected glycolipid **2.27** in the same solvent showed a T_{gs} of 46 °C.

The SEM micrograph of the xerogel of C-16 glycolipid **2.61** in MeCN is similar to that of glycolipid **2.55** (Figure 2.31). Micrograph A shows the presence of numerous pores distributed on an otherwise dense structure. On magnification (40 μm) we can see that the self-association leads to an ordered three dimensional network made up of thick fibres interwoven to form solvent pores (Micrograph B). Micrograph A and B of Figure 2.32 show the xerogel of glycolipid **2.61** in EtOH. This time a very different morphology is observed. Although thick fibres and large solvent pores can still be observed, we also see the presence of globular domains dotted throughout the structure.

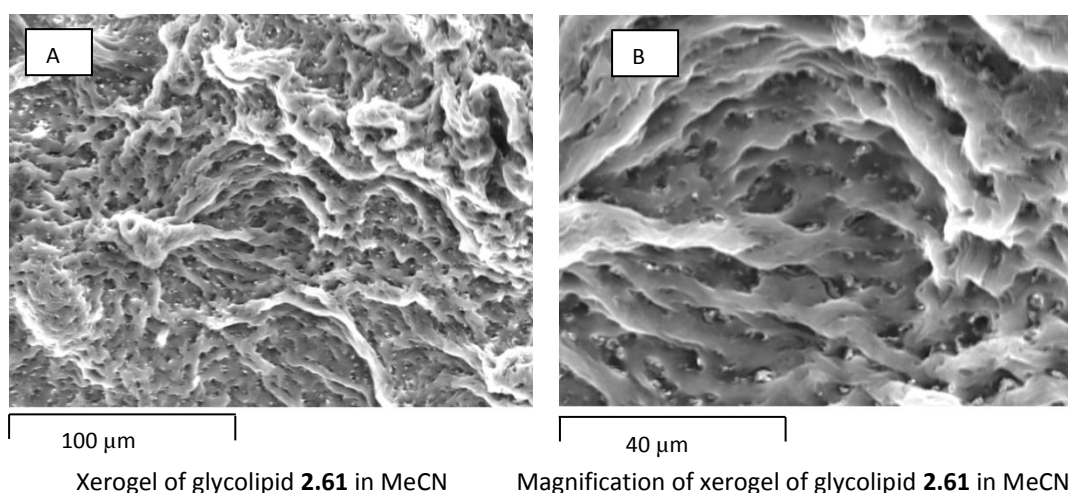


Figure 2.31 SEM micrographs of xerogel of glycolipid **2.61** in MeCN.

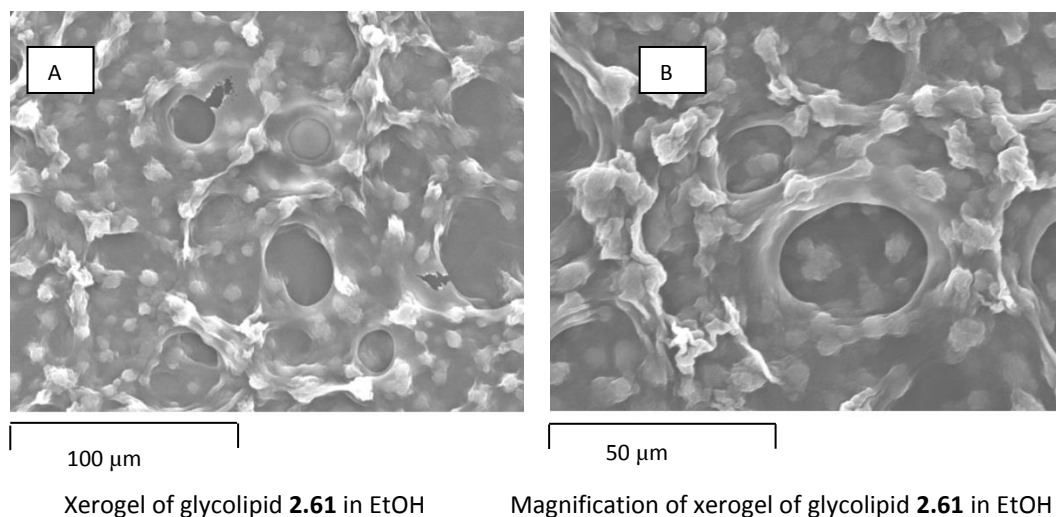


Figure 2.32 SEM micrographs of Xerogel **2.61** in EtOH.

These micrographs provide an excellent example of how morphology of the xerogels differs depending on both the glycolipid inducing gelation and the solvent involved in the self-assembly process. In comparison to the C-10 glycolipid **2.55**, the C-16 glycolipid **2.61** forms a complex three dimensional structure with much thicker fibres, tightly interwoven to form smaller pores. The results presented in Table 2.1 show that the C-16 glycolipid **2.61** is able to induce gelation in a wider variety of solvents (toluene, MeOH, EtOH and MeCN) than its C-10 counterpart **2.55** (MeCN). The ability of the glycolipid **2.61** to induce gelation in EtOH is particularly interesting as EtOH is a biocompatible solvent therefore, the organogelator could potentially be used in drug delivery systems. These results indicate the importance of non-polar, Van der Waals type interactions caused by the hydrocarbon chains, in the self-assembly process. In polar and non-polar solvents, the longer the alkyl chain, the better the molecule is at inducing gelation in the selected example. The importance of non-polar interactions was further cemented by comparison of the T_{gs} of the C-10 **2.55** and C-16 **2.61** glycolipids in MeCN, which were found to be 15 °C and 52 °C, respectively. This showed that the C-16 induced gels had a greater thermal stability. This is in line with what is reported in the literature. Zweep *et al.*^[65] reported that the MGC and T_{gs} of a group of cyclohexane-based bisamide organogelators in polar solvents, increased with increasing alkyl chain length. They postulated that it was as a result of increased gelator-gelator interactions together with decreasing interactions between the hydrophobic chains and the polar solvent molecules.

2.7.1.2 Spectroscopic studies on glycolipid **2.55** and **2.61**

As discussed above, interactions between the gelator compound and solvent are crucial in the self-assembly and gelation process. In order to gain insight into the role of the gelator molecules in this regard, a series of spectroscopic studies using different techniques were performed.

The first spectroscopic technique we used was ^1H NMR analysis. H-bonding has been shown to play an important role in the self-assembly process and we sought to examine if H-bonding could be observed in our samples. Concentration studies were carried out and ^1H NMR spectra on the C-10 glycolipid **2.55** in CDCl_3 were recorded at different concentrations. The variation in the chemical shifts of the signals corresponding to the different N-H protons of glycolipid **2.55** were examined (Figure 2.33). The bottom spectrum represents the least concentrated sample and the top spectrum represents the most concentrated sample. The biggest change observed relates to the amide connecting the galactosyl moiety to the aspartic acid side chain (labelled N-H1). It resonates at 6.26 ppm in the dilute sample and shifts to a higher chemical shift of 6.37 ppm in the more concentrated sample. This implies that the amide is involved in intermolecular H-bonding, which could be contributing to self-assembly of the molecule. As CHCl_3 is a relatively non-polar solvent, H-bonding between the glycolipid is accentuated. Intramolecular H-bonding may be taking place in amides labelled N-H2 and N-H3, as the resonances for the amides of both the tetradecyl and decanoic chain occur at relatively high chemical shift.

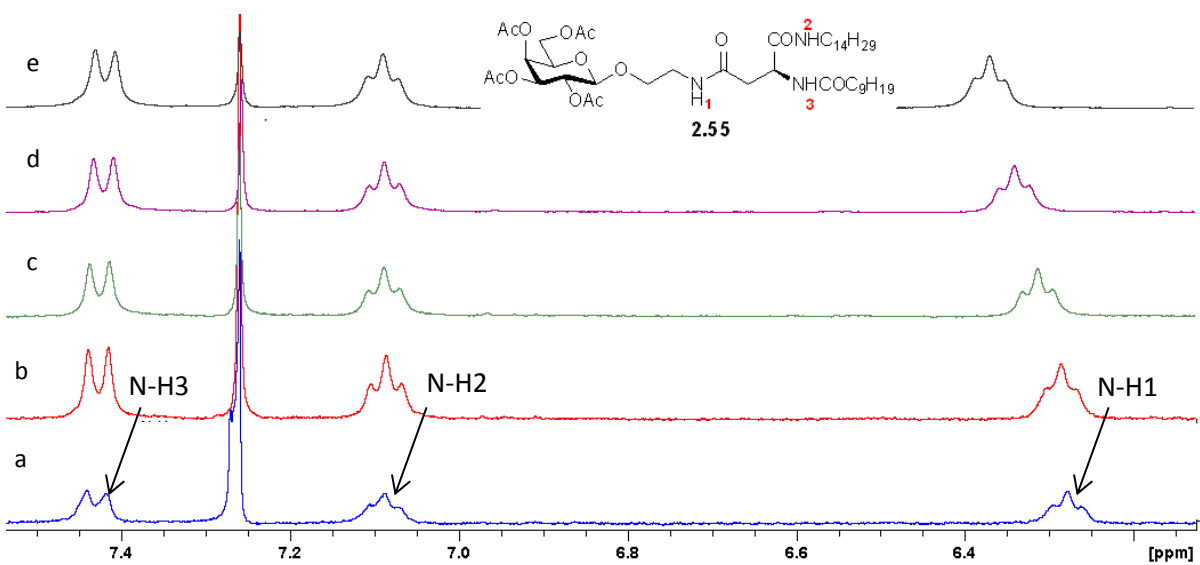


Figure 2.33 ^1H NMR concentration studies on **2.55** in CDCl_3 : a) 2 mg mL^{-1} , b) 4 mg mL^{-1} , c) 6 mg mL^{-1} , d) 9 mg mL^{-1} , e) 12 mg mL^{-1} .

Although H-bonding of glycolipid **2.55** is detected in CHCl_3 , self-assembly behaviour is not observed (i.e. no gel or aggregates are formed). CHCl_3 is a non-polar solvent and this may result in the glycolipid **2.55** being almost too soluble when dissolved in it. As a result, the glycolipid may be extremely solvated leading to a reduction in gelator-gelator interactions, therefore, resulting in no self-assembly behaviour.

In order to further examine the interaction between the solvent and gelator molecule we compared the ^1H NMR spectra of **2.55** in CDCl_3 (where it is soluble), CD_3CN (where it acts as a gelator) and MeOD (where aggregates are formed) (Figure 2.34). Clear differences between the spectra are evident, with the most obvious being the shifting of the amide protons. When comparing the values of the ^1H NMR spectra recorded in CDCl_3 and CD_3CN a change in the values of the chemical shifts for the amide protons is observed (Table 2.2).

	CDCl_3 (ppm)	CD_3CN (ppm)	$\Delta \delta =$ (ppm)
N-H1	6.30	6.60	0.30
N-H2	7.11	6.82	0.29
N-H3	7.44	7.06	0.38
H-1	4.53	4.62	0.09
α-H	4.66	4.57	0.09
β-H	2.77, 2.45	2.55	0.22, 0.10

Table 2.2 Chemical shifts for selected protons in CDCl_3 and CD_3CN .

MeCN is a polar, aprotic solvent which can act as an H-bond acceptor and compete for H-bonding with the amides of the glycolipid. This may result in some of the intermolecular and intramolecular H-bonds between the gelator molecules being broken and therefore results in the values for the N-H signals shifting to a lower chemical shift. This does not rule out H-bonding completely, but merely implies that different interactions can take place in MeCN, resulting in the glycolipid **2.55** being able to adopt a different conformation, leading to differences in chemical shifts, most notably with the β -protons. This conformational difference observed in MeCN allows non-polar interactions (due to the hydrocarbon chains) to become more prominent and leads to the formation of gels.

When comparing the ^1H NMR spectra of **2.55** in CD_3CN and MeOD only minor differences are observed, however, the outcome is completely different (gel in MeCN and aggregates in EtOH). MeOH is a polar protic solvent, acting as both a H-bond donor and acceptor. This means it can compete even more severely than MeCN for H-bonding with the amides of the molecule. As before, this leads to a non-polar interaction becoming more important, however, in this case the glycolipid is solvated differently. As MeOH is more polar than MeCN, glycolipid **2.55** is likely

to be more insoluble in MeOH. This may result in the non-polar interactions being too strong, leading to the formation of a three dimensional network which is not robust enough to entrap solvent molecules and thus leading to the formation of aggregates.

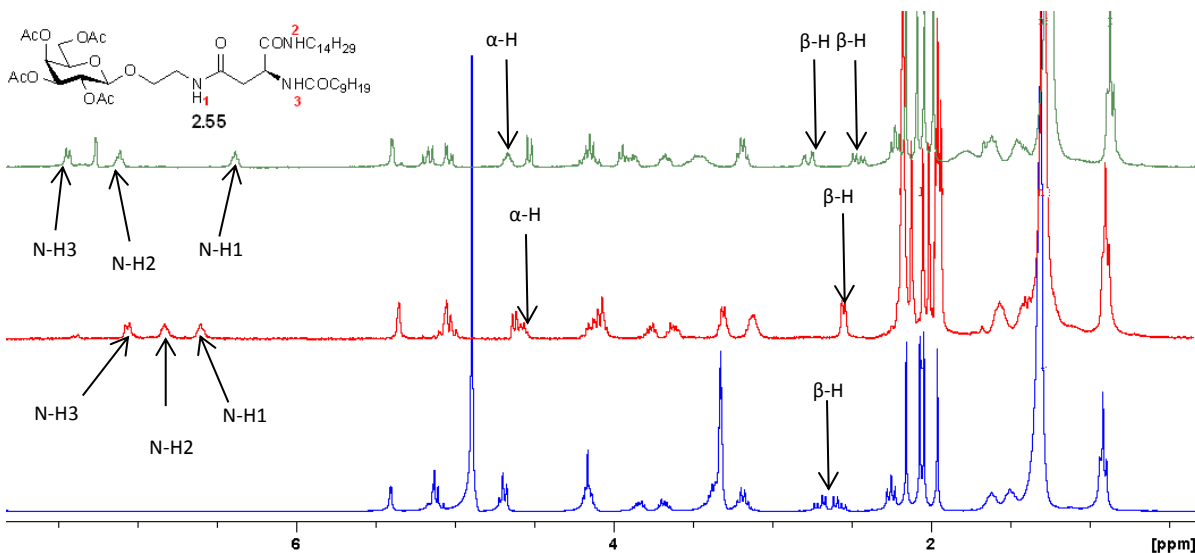


Figure 2.34 ^1H NMR spectrum of **2.55** in CDCl_3 (green) versus CD_3CN (red) and MeOD (blue).

In addition, FT-IR analysis was performed as it is extremely sensitive to H-bonding interactions. The self-assembly behaviour of the C-10 aspartic acid derivative **2.55** and C-16 aspartic acid derivative **2.61** were investigated to examine the possibility that an intermolecular H-bonding network was contributing to gelation. When comparing the FT-IR spectra of the LMWG in solution and in the gel phase, the differences in the frequencies of some bands can be attributed to differences in H-bonding patterns.^[61] For C-10 derivative **2.55** the sample was dissolved in MeCN, heated, and FT-IR analysis was performed in real time as the gel was being formed. The FT-IR spectra can be seen in Figures 2.35 and 2.36. The frequencies of the functional groups in the gel state (green line) were compared to those in the solution state (pink line). Significant differences in both wavenumbers and band intensity were observed. In the spectrum of the MeCN gel the emergence of two broad N-H amide bands at 3614 and 3552 cm^{-1} is an indication that H-bonding of the compound **2.55** is playing a significant role in the gelation process. Similarly, one of the bands belonging to the carbonyl amides of the solution spectrum (1673 cm^{-1}) has increased in intensity and shifted to a lower frequency (1635 cm^{-1}). A low frequency shift is indicative of H-bonding in the formation of the gel of **2.55** in MeCN. These data correlates well with those reported in the literature.^[108]

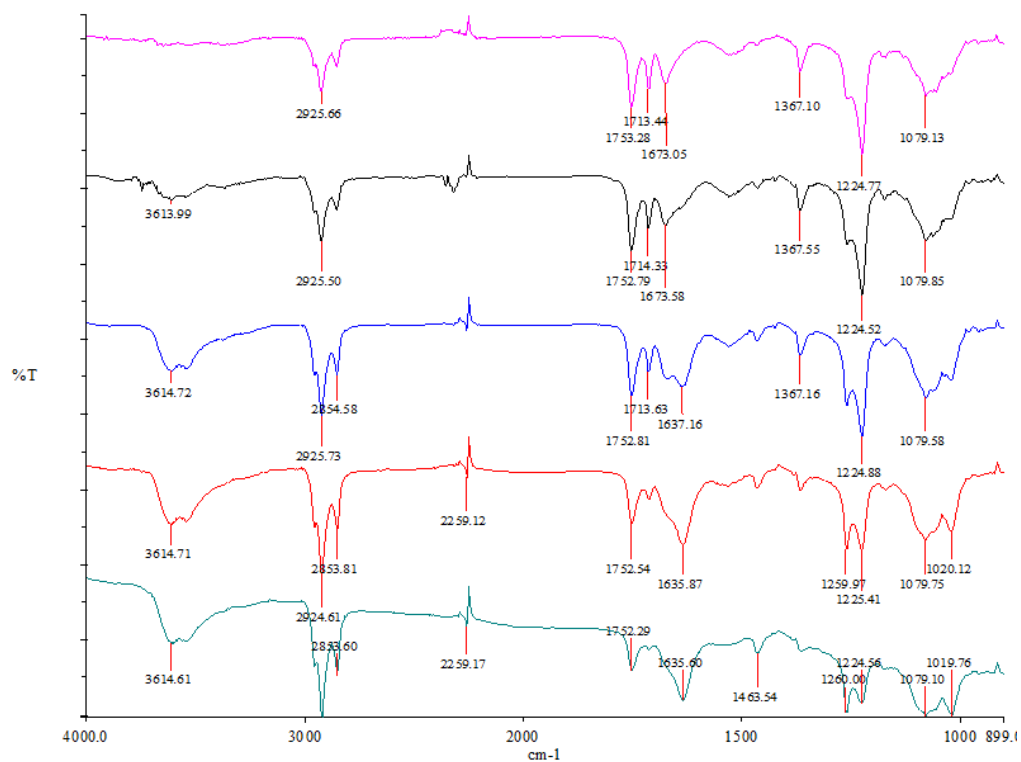


Figure 2.35 FT-IR spectra of glycolipid **2.55**, from solution to gel in MeCN, spectra recorded at intervals of 2 min. The pink line indicates first measurement (solution) while the green line indicates final measurement (gel). The MeCN background is subtracted.

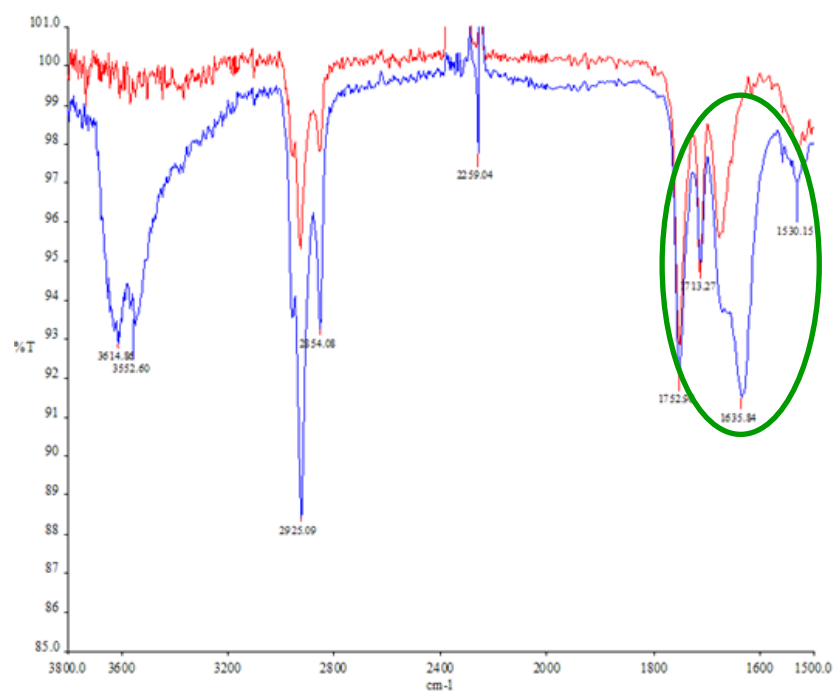


Figure 2.36 Zoomed in FT-IR spectra of the carbonyl region of **2.55**, showing difference in intensities between solution and gel state.

For the C-16 derivative **2.61** the sample was dissolved in MeCN, heated, and FT-IR analysis was performed in real time as the organogel was being formed. The FT-IR spectra can be seen in Figure 2.37. The bands corresponding to certain functional groups in the gel state (black line) were compared to those in the solution state (red line). In this case, the differences in both wavenumbers and band intensity between the gel and solution phase spectra were less noticeable. The C-16 aspartic acid derivative **2.61** is an extremely good gelator and always gelled almost instantaneously, it is therefore assumed that there was not sufficient time to obtain a spectrum before gelation occurred. This explains why differences between the spectra are not as clear. In the spectrum of the gel phase the emergence of a broad N-H amide band at 3615 cm^{-1} is representative for the formation of H-bonds involving organogelator **2.61**. In this case, little or no difference can be seen in the carbonyl amides between the gelled and solution spectra. In fact, besides the appearance of the broad peak at 3615 cm^{-1} no differences can be observed between the two spectra. However, the carbonyl amide appears at a frequency of 1643 cm^{-1} which is in the region that implies it is participating in H-bonding.

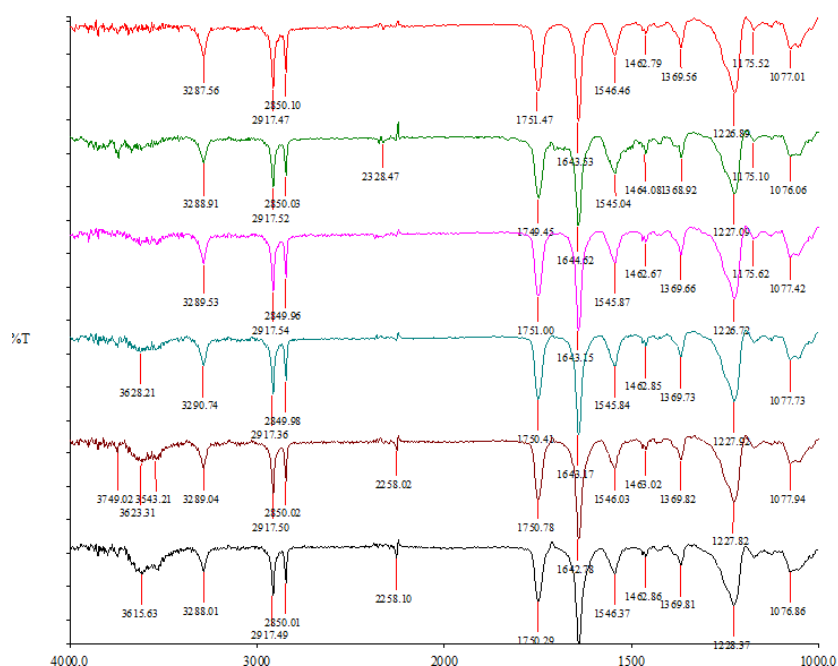


Figure 2.37 FT-IR spectra of LMWG **2.61** formation from solution to gel in MeCN. The red line indicates first measurement (solution) while the black line indicates final measurement (gel).

The role of H-bonding in the gelation process was further investigated by an experiment which showed the competing effects of solvent on the protected C-10 derivative **2.55**. As indicated earlier in Table 2.1, glycolipid **2.55** formed aggregates in 100% EtOH, however, in 100% MeCN gelation was observed (Figure 2.38). The self-assembly behaviour in varying percentages of MeCN and EtOH was then investigated and the results can be seen in Table 2.3.

Glycolipid Amount	MeCN (mL)	EtOH (mL)	Result
20 mg	100%	-	Gelation
20 mg	90%	10%	Gelation
20 mg	80%	20%	Gelation
20 mg	50%	50%	Soluble
20 mg	-	100%	Aggregates

Table 2.3 Gelation results of glycolipid **2.55** in varying percentages of MeCN and EtOH.

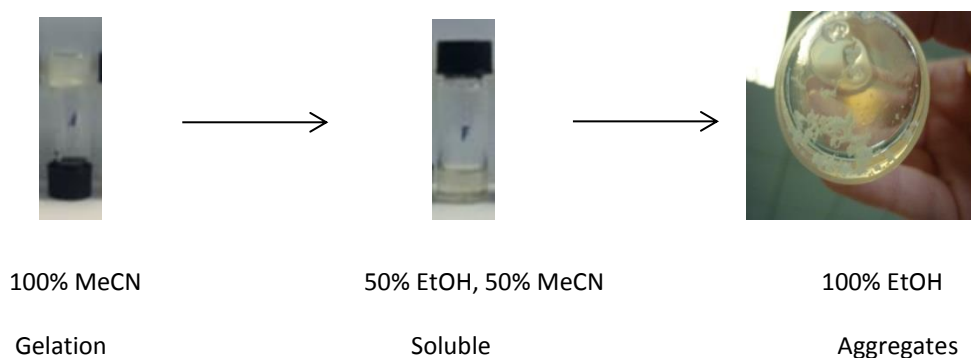


Figure 2.38 The competing effects of EtOH and MeCN on glycolipid **2.55**.

As stated already, EtOH is a polar, protic solvent and it can be considered as a “competing” solvent. It has the ability to act as a H-bond donor and acceptor. In EtOH, the H-bonding between the amides of the glycolipid is being interrupted by H-bonding between the glycolipid and the solvent. Also, the glycolipid is more insoluble in EtOH than it is in MeCN, leading to differences in the solvation of the glycolipid, which can lead to increased gelator-gelator interactions. As a result the glycolipid is subjected to different interactions when EtOH is the solvent. A fine balance between H-bonding, non-polar interactions and solubility is required in order for the self-assembly process to lead to gelation. In the MeCN:EtOH 1:1 mixture this balanced is not achieved, therefore, the glycolipid remains in solution. In this mixture, the solvent nature and composition leads to the glycolipid again being solvated in a different manner. The H-bonding ability of EtOH may interfere with H-bonding occurring between the amides of the glycolipids. Similarly, the increased solvation (due to the MeCN) may lead to decreased Van der Waals forces between the lipidic portions of the glycolipids. All this suggests that in this mixture of solvents the interactions required to induce gelation are prohibited and the self assembly process required to induce gelation does not occur.

The formation of organogels involves gelator-gelator interactions and solvent-gelator interactions.^[109] H-bonding and Van der Waals interactions seem to be the most important interactions contributing to the self-assembly and gelation process of the glycolipids described.

Solubility also plays a crucial role because if the molecule is really soluble it can become effectively solvated and therefore, prevent the gelator-gelator interactions. In the above glycolipids the carbohydrate moiety and the aspartic acid linker provide the source for H-bonding donors and acceptors, whereas the lipidic chains are responsible for the non-polar Van der Waals type interactions.

2.7.2 Gelation and self-assembly properties of second generation β -O-glycolipids

In order to support the results discussed above a second generation of potential organogelators were synthesised and investigated (Figure 2.39). Initially we set out to examine the importance of the sugar moiety in the gelation process. For this investigation two non-glycosidic controls were examined: compound **2.75**, which was an intermediate in the synthesis of the disaccharide **2.32** (Section 2.6.3.2) and compound **2.91**, which was easily synthesised by the reaction of hexadecanoyl chloride and propyl amine.

We also wanted to examine whether the number of monosaccharide's and type of linkage present affected the gelation ability. Therefore, compound **2.65** was synthesised (Figure 2.39), which has two galactosyl moieties and only the C-16 chain (section 2.2.5). Compound **2.31** was also synthesised, which had the galactose moiety linked through the C-1 position of the aspartic acid linker instead of the C-4 position, as in previous examples (section 2.5.2 and section 2.5.3). Another variation we wanted to investigate was whether changing the carbohydrate moiety affected the gelation ability. Compound **2.32** was synthesised for this comparison, which has a lactose moiety and two hydrophobic chains (section 2.2.6). Finally, we wanted to examine if functionalising the C-6 position on the galactose moiety of the C-16 aspartic acid derivative **2.61**, as described earlier (Section 2.5.3), affected its gelling ability (compound **2.30**, section 2.6.4).

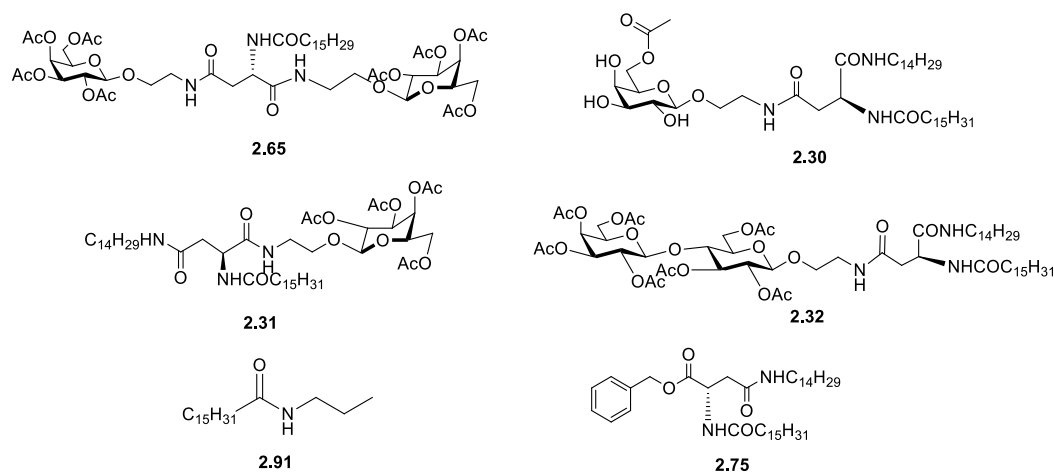


Figure 2.39 Second generation of potential aspartic acid derived LWMGs.

The gelation ability of the above compounds was tested in a range of solvents using the inverted test tube method as described in section 2.3.1. The results are presented in Table 2.4 below.

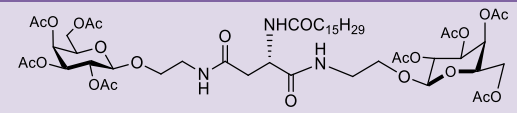
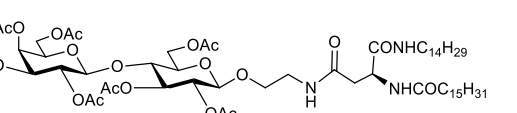
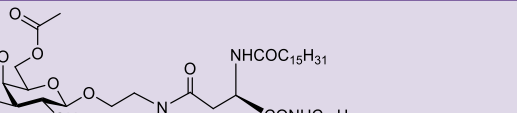
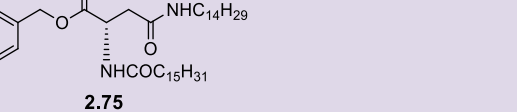
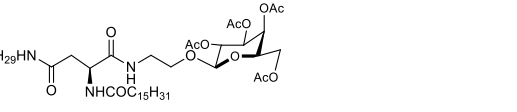
	DCM	Toluene	MeCN	MeOH	EtOH	H ₂ O	EtOAc	Hexane	CHCl ₃
 <p style="text-align: center;">2.65</p>	S	S	S	S	S	I	S	I	S
 <p style="text-align: center;">2.32</p>	S	P.S	G(6)	G(10)	G(8)	I	S	I	S
 <p style="text-align: center;">2.30</p>	-	G(35)	-	-	-	-	-	-	-
 <p style="text-align: center;">2.91</p>	S	G(16)	A	S	S	I	S	I	S
 <p style="text-align: center;">2.75</p>	S	S	A	P.G	G(20)	I	S	I	S
 <p style="text-align: center;">2.31</p>	S	G(10)	A	G(10)	G(8)	I	S	P.G	S

Table 2.4 Gelation abilities of second generation glycolipids in various solvents. All compounds were tested using the inverted test tube method at 20 mg mL⁻¹. Values refer to Minimum Gelation concentration (mg mL⁻¹). Aggregates=A, G=Gelation, P.G= Partial Gelation, Insoluble=I, Soluble=S, Partially soluble=P.S, Non-tested = -.

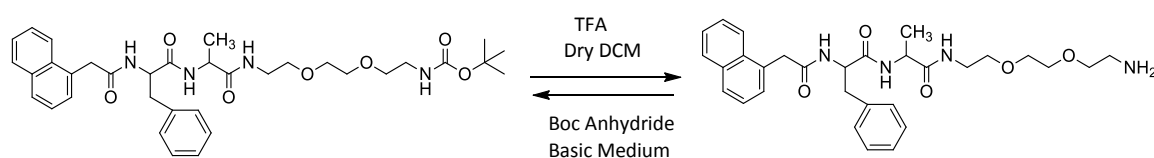
A number of conclusions could be drawn from the results.

- i) The galactosyl moiety was required in order to increase the stability of the gel, although not necessarily to induce its formation. Although the non-glycosidic controls **2.89** and **2.75** still possessed some self-association behaviour (**2.91** gelled in toluene and **2.75** gelled in EtOH) it was observed that the thermal stability of the gels was much lower, so much so that even holding the vial could cause the gel to collapse.
- ii) We also concluded that Van der Waals non-polar interactions were extremely important in the gelation process, and two lipidic chains were necessary for gelation. Compound **2.65**, which contained one lipidic chain, did not exhibit any self-association behaviour, whereas compound **2.32** which contained two lipid chains and a lactosyl moiety, exhibited similar behaviour to the galactosyl derivatives which contained two lipidic chains **2.55** and **2.61**. Gel formation was observed in MeCN, MeOH and EtOH. The gels were also very stable, with T_{gs} values of 45 °C in MeCN, and 47 °C in EtOH, which is slightly lower than the T_{gs} value of 52 °C obtained for the galactose C-16 derivative **2.61**.
- iii) Regarding the differences observed when altering the sugar moiety, the lactose derivative **2.32** gelled in the same solvents as **2.61** (its galactosyl counter-part). However it had significantly lower MGC values in MeOH and MeCN, which is beneficial (i.e. a lower concentration of compound was required to induce gelation).
- iv) The position of the sugar moiety in the aspartic acid scaffold also influenced the self-assembly behaviour. Compound **2.31** exhibited self-assembly behaviour in a variety of solvents including, EtOH, MeOH and toluene and exhibited lower MGC values than **2.61**. However the thermal stability of the EtOH gel was much lower, with a T_{gs} value of 33 °C compared to **2.61** (T_{gs} of 42 °C).
- v) The final conclusion drawn was that functionalising the C-6 position of the galactose moiety did affect its gelation ability. Although the molecule did act as a LMWG in toluene its MGC was much higher than its fully deprotected counterpart **2.27**, which was less beneficial as a higher concentration of compound was required to induce gelation.

2.7.3 Ability of selected O-glycolipids to act as hydrogelators

A hydrogel may be defined as a semi-solid formulation having an external aqueous phase which is immobilised within the available spaces of a three dimensional network structure.^[110] As a result of their high H₂O content they are extremely biocompatible and therefore, have been considered for use in a wide range of biomedical and pharmaceutical applications. Applications of hydrogels include contact lenses, biosensors, sutures, dental materials, and controlled drug delivery devices.^[111]

In 2011 work by Kar *et al.*^[112] demonstrated the transformation of an organogel to a hydrogel by using simple protecting group removal. They reported the development of a series of amino acid/peptide-based amphiphilic molecules which could induce gelation of both H₂O and organic solvents. If the molecule contained a *tert*-butyloxycarbonyl (*t*-Boc) protecting group at the primary amine of the hydrophilic ethyleneoxy unit at the C terminus, the compound acted as an organogelator. Whereas deprotection of the *N*-Boc moiety under acidic conditions to yield the primary amine resulted in the molecule acting as a hydrogelators (Scheme 2.22).



Scheme 2.22 Example of transformation between organogelator and hydrogelators.^[112]

Due to the high biocompatibility and numerous applications of hydrogels, it was decided to test the potential of our glycolipids to act as hydrogelators. Their gelation ability was tested as previously described^[105] and the results are presented in Table 2.5. Initially, all compounds tested were insoluble in H₂O, and no hydrogels were formed. It was believed that the long hydrophobic chains were driving the high insolubility and therefore, they could not interact with the solvent to form the complex, three dimensional structures required to form a gel. Due to the previous positive results obtained with EtOH, it was decided to test the ability of the compounds to induce gelation in a mixture of EtOH and H₂O. These conditions proved slightly more successful. Glycolipid **2.31** and **2.55** induced gelation in a 1:1 mixture of H₂O /EtOH. Varying the proportions of a H₂O /EtOH mixture was attempted but only the 1:1 ratio induced full gelation. These optimised conditions were investigated for all glycolipids described earlier, however only glycolipid **2.31** and **2.55** induced gelation.

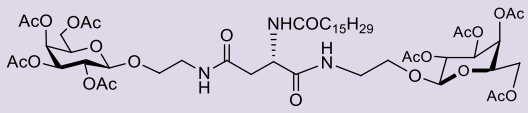
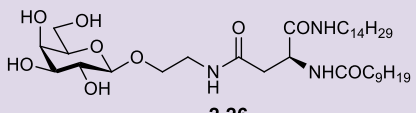
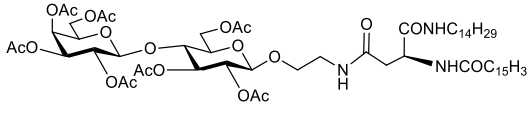
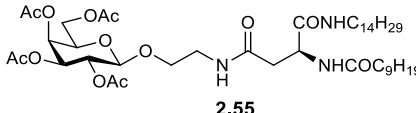
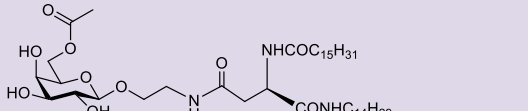
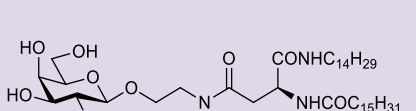
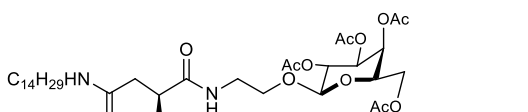
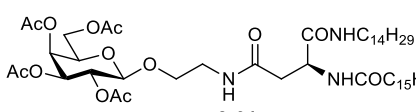
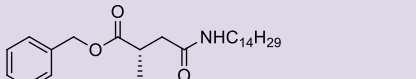
	H ₂ O	H ₂ O /EtOH (1:1)		H ₂ O	H ₂ O /EtOH (1:1)
 <p style="text-align: center;">2.65</p>	I	I	 <p style="text-align: center;">2.26</p>	I	I
 <p style="text-align: center;">2.32</p>	I	I	 <p style="text-align: center;">2.55</p>	I	G(4)
 <p style="text-align: center;">2.30</p>	I	I	 <p style="text-align: center;">2.27</p>	I	I
 <p style="text-align: center;">2.31</p>	I	G(8)	 <p style="text-align: center;">2.61</p>	I	I
 <p style="text-align: center;">2.91</p>	I	I	 <p style="text-align: center;">2.75</p>	I	I

Table 2.5 Gelation abilities of second generation glycolipids in various solvents. All compounds were tested using the inverted test tube method at 20 mg mL⁻¹. Values refer to Minimum Gelation concentration (mg mL⁻¹). Aggregates=A, G=Gelation, P.G= Partial Gelation, Insoluble=I, Soluble=S, Partially soluble=P.S.

Liu *et al.*^[67] recently published an article highlighting the ability of ultrasonication to induce gelation in some cases. They found that a selection of hydrazide compounds could not induce gelation in polar solvents by the usual heating and cooling process. However if the cooling process was carried out in the presence of ultrasound, stable gels were formed. With this in mind, we decided to again test the ability of the glycolipids to induce the formation of hydrogels. This time we allowed the cooling process to occur in the presence of ultrasound. However, as before, the formation of hydrogels was still not observed for all compounds investigated (Table 2.5). Using ultrasound it was found that the deprotected glycolipids, **2.26** and **2.27**, were able to induce gelation in MeOH, which they had not been able to do using the heating and cooling method. The thermal stability of the gels was greatly increased in MeOH (carried out under same conditions). The T_{gs} value of the C-16 derivative **2.27** was 70 °C in MeOH and only 46 °C in toluene.

A summary of all T_{gs} values is shown in table 2.6.

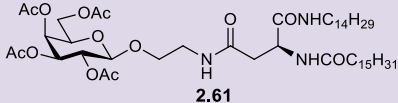
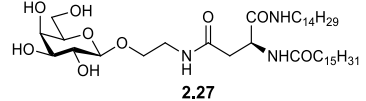
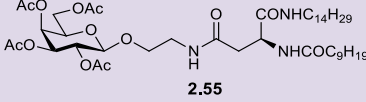
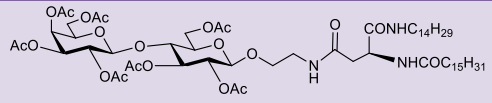
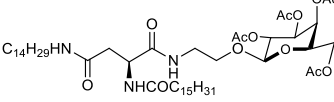
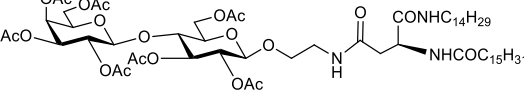
Compound	Solvent	T_{gs}
 2.61	Toluene	36 °C
 2.27	Toluene	46 °C
 2.55	MeCN	15 °C
2.61	MeCN	52 °C
 2.32	MeCN	45 °C
 2.31	EtOH	33 °C
2.61	EtOH	42 °C
 2.32	MeOH	70 °C

Table 2.6 Comparison of T_{gs} values of various glycolipids in different solvents.

2.8 Incorporation of glycolipid 2.55 into a giant unilamellar vesicle (GUV)

Amphiphilic glycolipids assemble into a variety of structures in aqueous solution (Figure 2.40). The shape of the structures depends mainly on the geometry and properties of the lipids involved in their formation. The most commonly occurring aggregates include a bilayer, micelle and liposome.^[80] The lipid molecules are organized in such way that the hydrophilic head groups are in contact with the aqueous solution and the hydrophobic tails are interacting with each other.

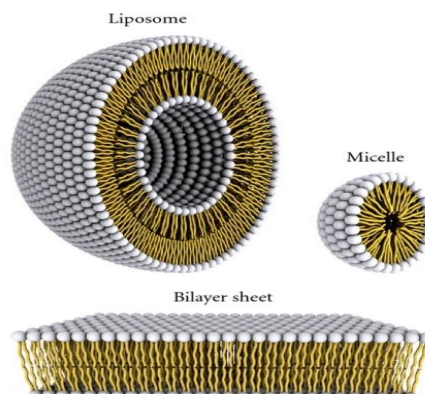


Figure 2.40 Shapes of lipid aggregation in an aqueous environment.^[113]

Micelles are mainly formed by lipids with large head groups and one hydrocarbon chain, which is usually unsaturated and pointing towards the centre of the structure. Bilayers and liposomes are formed by lipid amphiphiles containing two fatty acid chains.^[80]

A vesicle is a lipid bilayer rolled up into a spherical shell. The centre of the vesicle is H₂O filled and is surrounded by a single lipid bilayer (unilamellar vesicle) or by more than one (multilamellar vesicle).^[114] Giant unilamellar vesicles (GUVs) range in size from 1-300 μm ^[81] and were first observed by Bangham in the 1950's.^[115] Their size allows for their manipulation by micropipettes and visualisation under light microscope. GUVs are extensively used in studying the physical and chemical properties of biological membranes. The vesicle membrane mimics the lipid bilayer of the plasma membrane and they can be utilised to study biochemical reactions and self-assembly processes that occur on the membrane.^[116]

Vesicles are also used as drug delivery vehicles. They can be prepared from lipids naturally occurring in mammalian cells, which make them highly biocompatible.^[81] Also, incorporation of receptors, ligands, addressins, poly-ethylene glycol (PEG) and other molecules would allow for the targeting of a specific site or organ within the body. The incorporation of certain glycolipids into the vesicles allow for targeting specific tissues or cells (for example cancer or metastatic cells). Interesting examples include the development of liposomes containing carbohydrate-

functionalised β -cyclodextrins designed for drug delivery into liver cells,^[117] and GUVs containing glycolipid specific for activated platelets which is a promising method for drug delivery in cardiovascular diseases.^[118]

In view of the ability of our synthetic glycolipids to self-assemble, and in order to expand the scope of the applications, the formation of GUVs in the presence of these compounds was explored. The acetylated glycolipid **2.55** was successfully incorporated into GUVs formed with DOPC, DPPC and cholesterol. In studies carried out by Ms Ursula Miggas and Dr. Jennifer McManus at NUI Maynooth, a series of phase condensation phenomena, which is believed to be induced by the presence of the glycolipid, were observed at the surface of the GUVs. Detailed investigations are currently underway.

2.9 Conclusion

Despite the initial problem of racemisation that occurred during the synthesis of acylated aspartic acid derivative **2.34**, careful consideration of the synthetic approach resulted in the synthesis of the diastereomerically pure aspartic acid derivatives, **2.26-2.28**. Following the same modular approach, we described the successful synthesis of a variety of L-aspartic acid derivatives, **2.29-2.32**, utilising a key set of reaction conditions.

The gelation abilities of a range of glycolipid derivatives were examined in a variety of solvents, and some of the structural features that may affect gelation ability, including hydrophobic chain length and chirality, were investigated. We found that the acetylated galactosyl C-16 analogue **2.61** and the acetylated lactosyl C-16 analogue **2.32** were the best gelators as they were able to induce gelation in the widest number of solvents. The lactosyl derivative **2.32** exhibited lower MGC values in MeOH and MeCN than its galactosyl counterpart **2.61**, however, the galactosyl derivative produced more thermally stable gels.

Spectroscopic analysis provided evidence for the importance of H-bonding and non-polar Van der Waals interactions in the self-assembly and gelation process. However, we also confirmed that solvation and solubility plays a crucial role. A fine balance between all these factors is necessary to induce effective gelation.

Structural analysis indicated that, for the glycolipids investigated, two lipidic chains were crucial for the self assembly process. This was evident as when a derivative containing two galactose moieties and one lipidic chain **2.29** was investigated no self-assembly or gelation was observed. The C-16 derivatives always performed better than their C-10 counterparts and this suggested that Van der Waals forces are also important in the self assembly process as the

hydrophobic chain length can influence the gelation ability. The acetylated analogues were able to induce gelation in a wider variety of solvents than the free hydroxyl analogues which indicated that a certain degree of solubility is required for the self-assembly process. Finally, we determined that although the carbohydrate moiety was not necessarily required to induce gelation however, it was required for stability. As the control compounds **2.89** and **2.77** both formed gels which collapsed upon moving of the vial.

The ability of the glycolipids to acts as hydrogels was also examined. Although none of the glycolipids were able to induce gelation in H₂O, we found that with 1:1 mixtures of EtOH and H₂O the acetylated galactose C-10 derivative **2.55** was able to induce gelation with an extremely low MGC value of 4 mg mL⁻¹.

Chapter 3: Synthesis of malonamide glycoconjugates as potential anti-adhesion agents

3.1 Introduction

Due to the presence of two carboxylic acid side groups, which can be easily functionalised, malonic acid is an ideal scaffold for the synthesis of a wide range of divalent molecules. Owing to the short methylene linker connecting the two acid groups, there is provision for access to short bivalent glycoconjugates. Also, further functionalisation can be achieved at the α carbon, with the possibility of adding side groups or alkyl chains depending on the compound of interest.

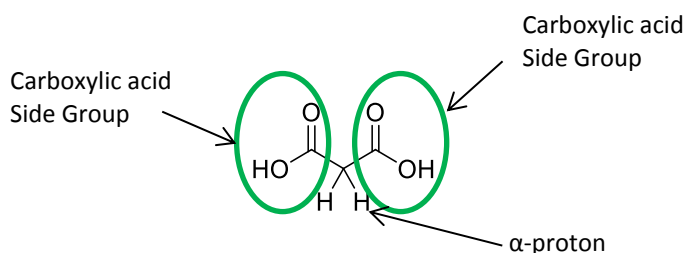


Figure 3.1 Structure of malonic acid and sites for functionalisation.

Despite the fact that malonic acid and its various esters are readily available and easily functionalised, there are limited examples of malonamide synthesis reported in the literature. More specifically, examples of malonamides used as glycoconjugate scaffolds are limited. The synthesis of malonate derivatives is somehow more common, however, again reports in the literature are sparse.

3.1.1 Malonates and their potential application

Malonate esters have been used extensively as intermediates in the synthesis of complex molecules. In many cases, one carboxylic acid is lost through decarboxylation and this phenomenon is discussed further in section 3.2.1.1. The synthesis of simple malonate esters is discussed below. Sbardella *et al.*^[119] synthesised a series of long chain alkylidenemalonates **3.1-3.5** (Figure 3.2) and examined their potential as modulators of histone acetyltransferases (HATs). Compounds **3.1-3.5**, are structurally related and simplified analogues of anacardic acid, which is a known inhibitor of HATs.

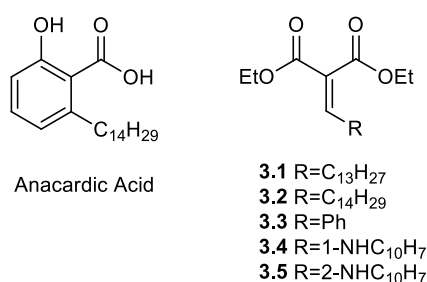
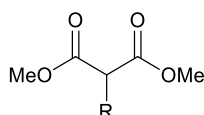


Figure 3.2 Structure of long chain alkylidenemalonates **3.1-3.5**, and Anacardic acid (a known HAT inhibitor).^[120]

During nucleosome assembly, DNA repair and other genomic processes, HATs regulate transcription and histone deposition by acetylating the ϵ -amino groups of specific lysines in histones.^[121] They are also responsible for acetylating transcription factors (e.g. p53)^[122] and other nuclear proteins (e.g. α -tubulin).^[123] A limited number of HAT inhibitors have been identified.

The compounds **3.1-3.5** were pre-screened for their effects on cell-cycle and apoptosis induction in the human leukemia cell line U937. The inhibiting capability of the more active derivatives was then investigated against HAT enzymes. Malonates **3.1** and **3.2** were able to both arrest cell cycle and induce apoptosis, whereas the other derivatives had very minimal effects. Pentadecyldenemalonate **3.2** was further identified as the first molecule able to both activate and inhibit HATs.^[119]

Kolb and Meier also published a report on the synthesis of a series of malonate derivatives bearing long aliphatic chains ranging in length from C₆-C₁₆ (Figure 3.3).^[124]



- 3.6** R= C₆H₁₃
- 3.7** R= C₈H₁₇
- 3.8** R= C₁₀H₂₁
- 3.9** R= C₁₂H₂₅
- 3.10** R= C₁₄H₂₉
- 3.11** R= C₁₆H₃₃

Figure 3.3 Malonate-derived monomers **3.6-3.11**.^[124]

These alkyl malonate derivatives had a completely different application and were polymerised to yield polyesters and polyamides. The use of degradable polymers has become very topical in order to minimise polymer waste management caused by non-degradable polymers. Due to their biodegradability, biocompatibility, hydrolytic degradability and suitable mechanical strength, synthetic aliphatic polyesters are promising candidates for degradable polymer materials.^[124-125]

3.1.2 Non-carbohydrate-based malonamides

Malonamides are derivatives of malonic acid, whereby an amide functionality replaces the carboxylic acid groups. The hydrolysis of malonamides does not proceed as easily as that of malonate esters, therefore, they have not been exploited as synthetic intermediates. Some selected examples of non-carbohydrate malonamides are discussed below.

A family of *N,N'*-di-substituted malonamides were prepared as potential silver(I)-selective chelating ligands, and a selection of representative examples are shown in Figure 3.4.^[126]

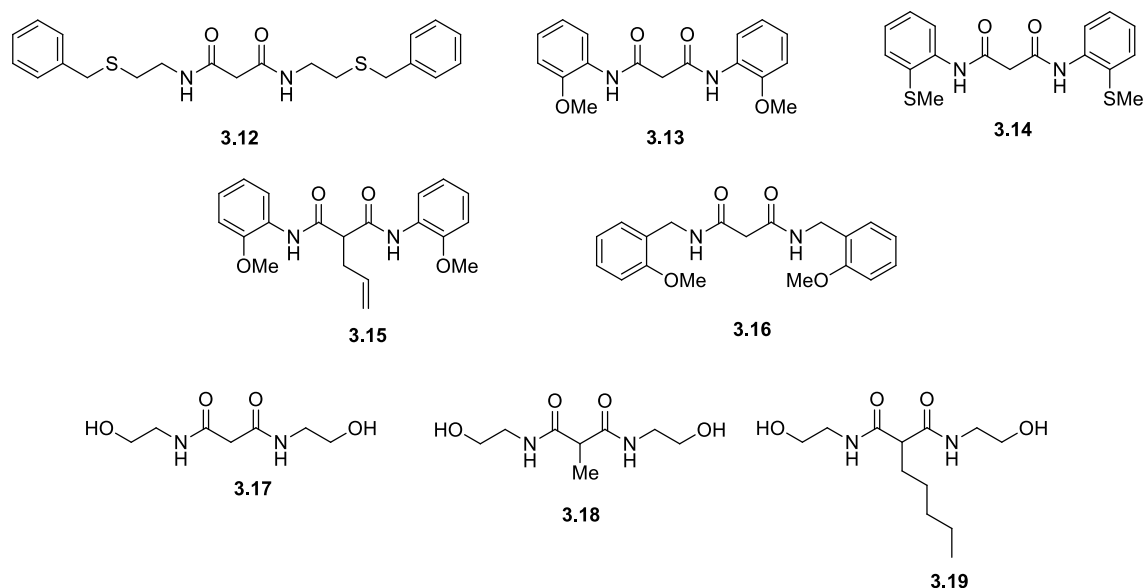
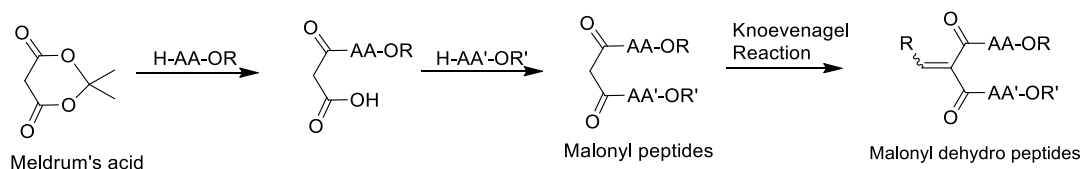


Figure 3.4 Disubstituted malonamides as potential silver(I) selective ligands.^[126]

Metal-selective ligands have applications in solvent extraction and Daubinet and Kaye aimed to develop ligands capable of extracting silver(I) selectively from ore-leached solutions containing metal-based contaminants. Initial results indicated that although substituted malonamides **3.12-3.16** exhibited some selectivity for silver(I) over copper(II) and lead(II), **3.12** gave the best results as it exhibited remarkably high selectivity and excellent efficiency.^[126a] A second generation of analogues was synthesised and examined (representative examples **3.17-3.19**), however, the original substituted malonamides proved to be more efficient ligands.^[126b]

Fioravanti *et al.* discussed the use of Meldrum's acid as a scaffold to obtain non-symmetric disubstituted malonyl peptides (Scheme 3.1).^[127] They aimed to further functionalise these disubstituted malonyl peptides and synthesise malonyl dehydro peptides, using Knoevenagel reactions (Scheme 3.1), which could be potential scaffolds for peptidomimetics.^[128]



Scheme 3.1 Synthesis of malonyl peptides and malonyl dehydro peptides as potential scaffolds for the construction of peptidomimetics.^[127]

The use of natural peptides is limited by their poor bioavailability and susceptibility to proteolysis. Therefore, the synthesis of peptidomimetics, by structural manipulation of the natural peptide backbone, is highly advantageous. One modification that can be made in the peptide chain is reversal of the amide bond. This alteration increases the peptides resistance to biodegradation without decreasing the receptor binding ability and biological response.

Some selected examples of malonyl dehydro peptides are shown in Figure 3.5. These can be regarded as important synthetic targets, not only for the construction of novel peptidomimetics but also for their potential biological applications. Also, due to the double bond, they can be further functionalised to synthesise more complex molecules. Figure 3.5 also highlights the difference between natural dehydro peptides and the synthetic malonyl dehydro peptides.^[128]

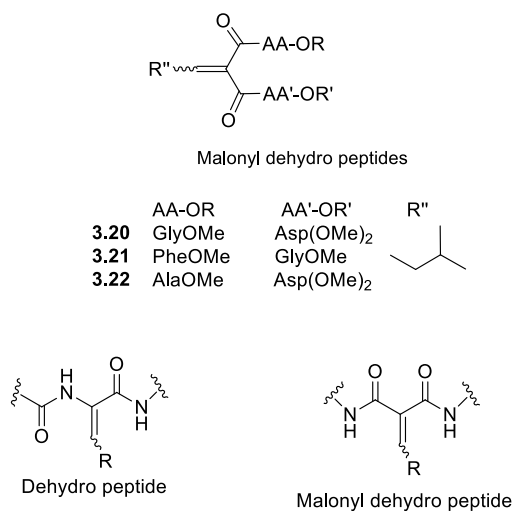


Figure 3.5 Selected examples of synthesised malonyl dehydro peptides, and the difference between malonyl dehydro peptide and natural dehydro peptide.^[127-128]

It is important to highlight that more complicated bicyclic malonamides have also been utilised in the literature, surprisingly, however, examples are limited. One such example, reported by Parks *et al.*, involves the synthesis of a series of 6,6-bicyclic malonamides as ligands for the binding of f-block metals (Figure 3.6).^[129]

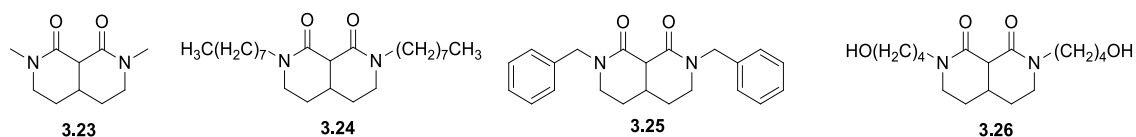


Figure 3.6 Selection of 6,6-bicyclic ligands synthesised as potential ligands for the binding of f-block ions.^[129]

3.1.3 Carbohydrate-based malonamides

As stated previously, there are a limited examples of carbohydrate-based malonamides reported in the literature. Kato *et al.* described the synthesis of bis(α -D-mannopyranosyl)malonamide **3.27** which was further reacted with C₆₀ to afford the fullerene glycoconjugate **3.28** (Figure 3.7).^[130]

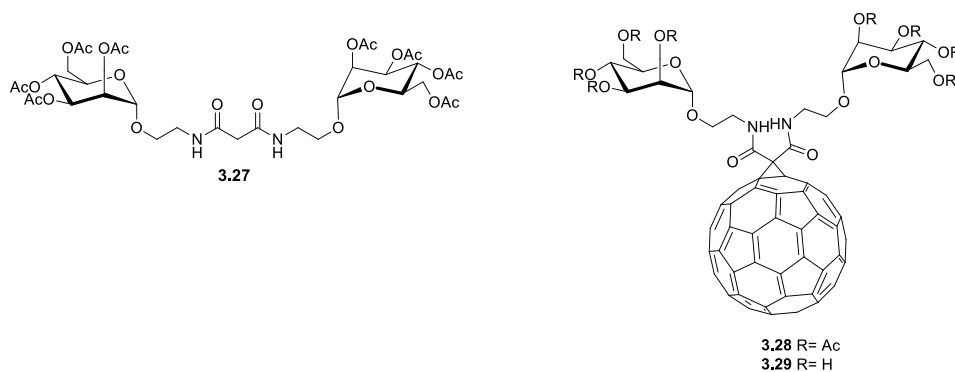


Figure 3.7 Structure of carbohydrate malonamide **3.27** and protected and deprotected fullerene sugar **3.28**, **3.29**, synthesised from bis(α -D-mannopyranosyl)malonamide **3.27** and C₆₀.^[130]

The first fullerene sugars were described by Vaselle and Diederich in 1992,^[131] and since then a variety of fullerene glycoconjugates have been designed and characterised. They are extremely important as they have potential applications in both the biomedical and materials industries.^[130]

Another paper which was published by Isaad *et al.*^[132] concerns the synthesis of carbohydrate-based malonamides. However, in this case the sugars are utilised to aid the water solubility of naturalised dyes. Disperse dyes are commonly used in the dyeing of many materials. Due to their insoluble nature in water, however, additives are regularly used in conjunction with the dyes to enable them to approach the hydrophobic fibres and dye them.^[133] This practice causes great concern owing to the large quantities of additives that are necessary for dyeing in water and also because of the environmental impact of both the dyes and the additives. Isaad *et al.*^[132] have developed a new class of dyes termed “naturalised dyes” which reduce environmental impact, as no additives are required for the dyeing process. This also enables the dyeing process to be carried out at lower temperatures and over a shorter period of time.

Two potential soluble naturalised dyes were synthesised^[132]: the mono-glycoconjugated derivative, **3.30**, and the double-glycoconjugated derivative **3.31** (Figure 3.8).

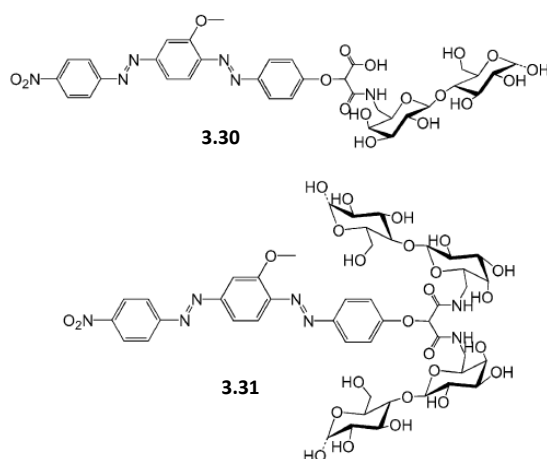


Figure 3.8 Structure of mono and double-glycoconjugated dyes **3.30** and **3.31**.^[132]

The mono-glycoconjugate **3.30** was still insoluble in water, however, the double-glycoconjugate **3.31** was water soluble. A mixed derivative, which has one lactose and one galactose moiety attached, was also synthesised but exhibited limited solubility in water. This shows that a minimum percentage weight of 50% of the glycidic moiety is required for solubility, since at 40% they are still completely insoluble.^[132]

3.2 Chapter Objective

This chapter deals with the synthesis of a variety of malonamide glycoconjugates as potential anti-adhesion agents. Although examples of similar compounds are minimal in the literature, we chose malonamides as we envisaged a symmetric, aliphatic scaffold that could be easily functionalised. As stated previously, malonic acid is an ideal building block in the synthesis of these bivalent aliphatic ligands. It features two carboxylic acid side groups and an acidic α -proton and therefore, allows the easy introduction of functionality. Owing to this, it would provide access to a range of structurally diverse glycoconjugates which could be investigated for potential biological activities. The design of the ligands involved the use of an aliphatic scaffold that would enable the synthesis of a bivalent galactose system but also allow for the introduction of a lipidic chain. As with the previous chapter, we followed a modular approach utilising a key set of reaction conditions which allowed us to achieve diversity quickly and easily, and also allowed for sufficient scale up.

The core building block structure can be seen in Figure 3.9. It is clear from the figure that the malonyl backbone would remain constant in all analogues and that variation could be achieved at three potential sites.

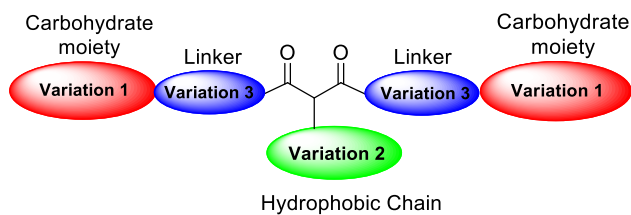


Figure 3.9 Core scaffold utilised for the synthesis of malonamide glycoconjugates.

Promising anti-adhesion activity has been achieved using a variety of synthetic multivalent compounds, and there are numerous examples discussed throughout this report. However, in most of these cases, the structure of the bacterial lectin of interest is known. This makes the discovery of efficient synthetic ligands simpler, as they can be specifically designed for optimum binding. In our case, minimal structural information is known about the bacterial lectins of *Burkholderia. Multivorans* which are involved in the recognition of glycolipids present on the surface of the cell. This makes the design of synthetic ligands as anti-adhesion agents extremely difficult. For this reason, we chose to synthesise a variety of structurally diverse ligands, and aimed to examine their structure-activity relationships.

For the purpose of our research, we chose to investigate how linker length, chemical structure and flexibility influenced the presentation of the carbohydrate moieties and thus, the biological activity. For this reason, variation site 1 always remained as a galactosyl moiety, although it could be expanded to a different carbohydrate moiety if required. At variation site 2, a C-10 lipidic chain was kept constant but again it could be altered to a hydrophobic chain of varying length if desired. The main variations focused on the chemical structure of the linker. We aimed to examine three types of amide linkage between the galactosyl moiety and the malonyl backbone. In the first linkage envisaged, the galactosyl moiety is coupled directly to the malonyl scaffold *via* an *N*-glycosidic bond (compound **3.32**, Figure 3.10). For the second linkage, we intended to utilise an ethyl linker functionalised with a primary amine to connect the galactose and malonyl backbone *via* an amide bond (compound **3.33**, Figure 3.10). The final linker we aimed to investigate exploits a triazole moiety to pin the galactose moiety and the malonyl building block (**3.34**, Figure 3.10).

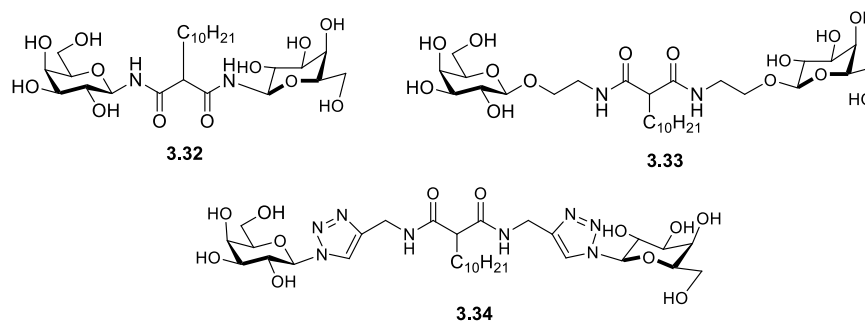


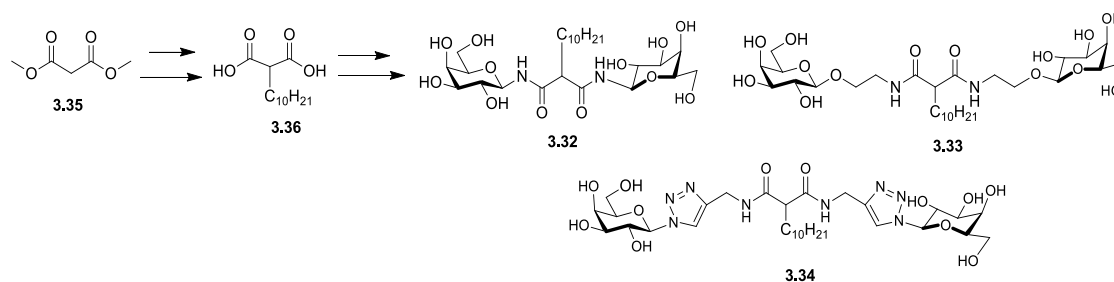
Figure 3.10 Structures of galactosyl malonamides **3.32-3.34**.

3.3 The synthesis of malonyl-based glycoconjugates **3.32**, **3.33** and **3.34**

The malonyl-based *N*-glycoconjugates **3.22** and *O*-glycoconjugates **3.33** and **3.34** were designed to act as potential anti-bacterial agents. Their biological activity will be discussed in Chapter 5 (section 5.7). A suitable starting material for their synthesis is methyl malonate **3.35**, as it features an acidic α -proton, which would allow for the introduction of a hydrocarbon chain. It also contains two ester groups on its side chain, which upon hydrolysis would allow for connectivity to the galactosyl moiety through the formation of an amide bond.

Two routes for the synthesis of the bivalent aliphatic glycoconjugates were explored: 1) alkylation of the α -proton followed by the amide coupling of the desired amine and the free carboxylic acid groups, or 2) amide coupling with the desired amine, followed by alkylation of the α -carbon.

Initial investigations led us to design the synthetic pathway shown in Scheme 3.2, whereby the easily accessible amines and the commercially available dimethyl malonate **3.35** would serve as suitable building blocks. The decyl chain would be introduced first *via* alkylation of the α -carbon. Subsequent hydrolysis of the methyl esters would provide the carboxylic acid side groups which would allow for introduction of the galactosyl moiety using standard peptide coupling conditions. Based on this approach, a variety of analogues could be easily synthesised by utilising a key set of reaction conditions which are already widely accepted and utilised.

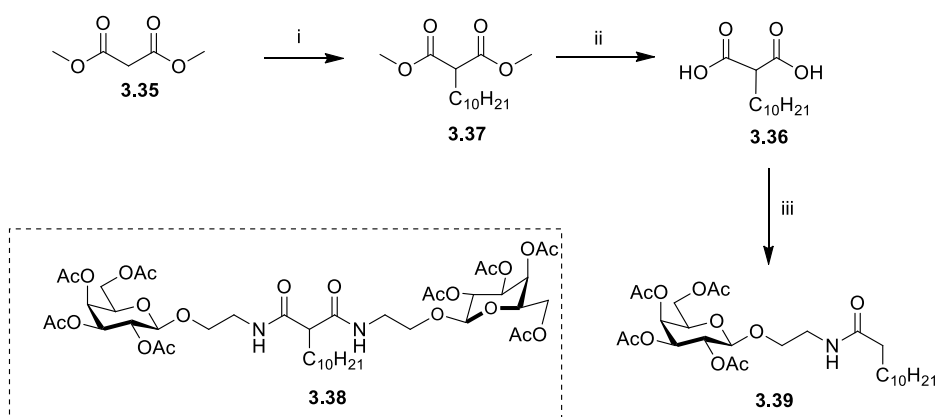


Scheme 3.2 Initial synthetic route for synthesis of glycoconjugates **3.32-3.34**.

3.3.1 Attempted synthesis of β -O-glycoconjugate **3.33 via alkylation followed by amide coupling**

The malonamide O-glycoconjugate **3.33** was designed as a flexible molecule. We believed that the ethyl linker would allow for a certain amount of flexibility of the galactosyl moieties.

The synthesis commenced with the alkylation of the commercially available dimethyl malonate **3.35** with 1-bromodecane using K_2CO_3 to give ester **3.37** (Scheme 3.3).^[134] Hydrolysis, utilising 15% NaOH in EtOH, afforded the di-acid **3.36**, which was ready for coupling with the galactosyl amine **2.33** using standard TBTU/HOBt methodology, as discussed previously (Chapter 2, section 2.5). Unfortunately, this coupling reaction did not yield the desired product **3.38**.



Scheme 3.3 Reagents and conditions: i) $CH_3(CH_2)_9Br$, K_2CO_3 , CH_3CN , $80\text{ }^\circ\text{C}$, 36 h, 80%; ii) 15% NaOH, EtOH, $80\text{ }^\circ\text{C}$, 18 h, 50%; iii) HOBt, TBTU, DMF, NEt_3 , N_2 , rt, 16 h, 78%.

Instead, the major product obtained appeared to be the decarboxylated derivative **3.39**. The 1H NMR spectrum of **3.39** is shown in Figure 3.11 with characteristic peaks assigned. The signal corresponding to the α -proton is absent from the 1H NMR spectrum, and instead the methylene protons* can be seen resonating at 2.16-2.12 ppm. This was very much unexpected because although decarboxylation can occur in the presence of base, it usually requires thermal conditions.^[135] The coupling reaction was repeated, this time in the absence of base but nonetheless the decarboxylated product **3.39** was obtained.

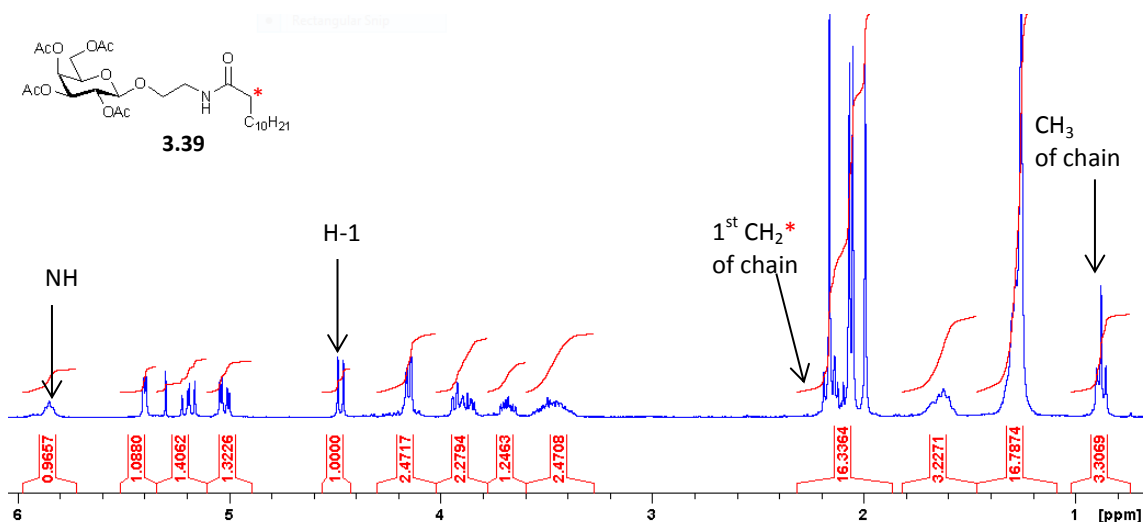
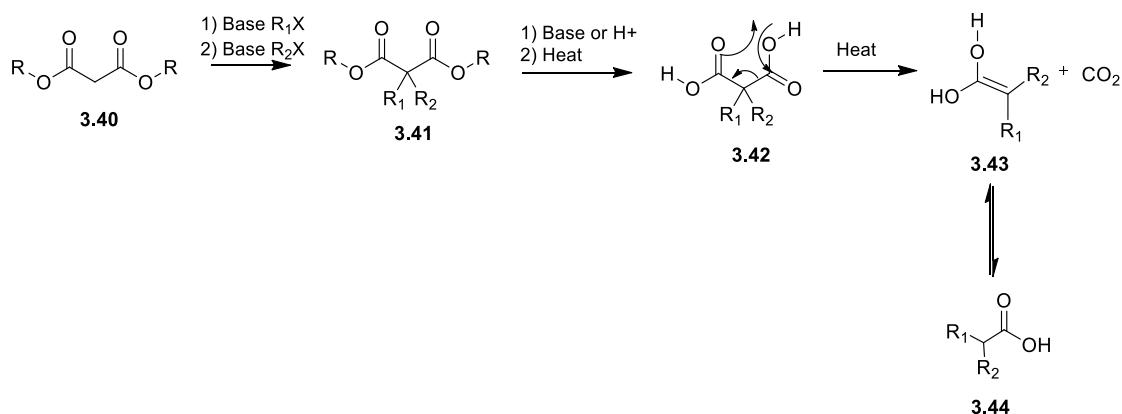


Figure 3.11 ^1H NMR spectrum of decarboxylated derivative **3.39** (300 MHz, CDCl_3).

To rule out possible steric issues arising from the bulky carbohydrate, a test reaction was carried out. Propyl amine was reacted with the malonyl backbone **3.36**, under the same conditions but again the ^1H NMR spectrum indicated that only one propyl group had been attached. This result indicated that steric issues were not the problem and that decarboxylation was occurring due to some other factor.

3.3.2 Decarboxylation of malonic acid derivatives

It is well established that malonic acid derivatives can undergo decarboxylation to form carboxylic acids (Scheme 3.4).^[135-136] In fact, it is this feature which makes malonic acids such useful synthetic reagents in what has famously been named the Malonic Ester Synthesis (MES).^[137] The MES reaction mechanism is described below (Scheme 3.4). The malonic ester **3.40** is first alkylated using mild basic conditions to yield derivative **3.41**. Hydrolysis promoted by either acidic or basic conditions, affords the di-carboxylic acid **3.42** which can then undergo thermal decarboxylation to yield the enol **3.43** and CO_2 . In the final step, the enol tautomerises to the carboxylic acid derivative **3.44**.^[135]



Scheme 3.4 Synthesis of carboxylic acid derivatives *via* malonic ester alkylation, hydrolysis and decarboxylation, i.e. the malonic ester synthesis.^[135]

As a result of this phenomenon it was decided to re-examine the hydrolysis step of our synthetic route and ensure decarboxylation was not occurring at this point. The ^1H NMR spectrum of the alkylated malonic acid **3.36** exhibited a signal for the α -proton at 3.44 ppm (Figure 3.12), while the 2D COSY spectrum showed distinct coupling between the α -proton and first methylene of the decyl chain (Figure 3.13). The presence of the compound was also confirmed by HR-MS analysis. As stated already, the α -proton resonates downfield at 3.44 ppm in the carboxylic acid derivative **3.36**, whereas the first methylene proton of the decarboxylated derivative **3.39** (Figure 3.11) resonates upfield at 2.12 ppm.

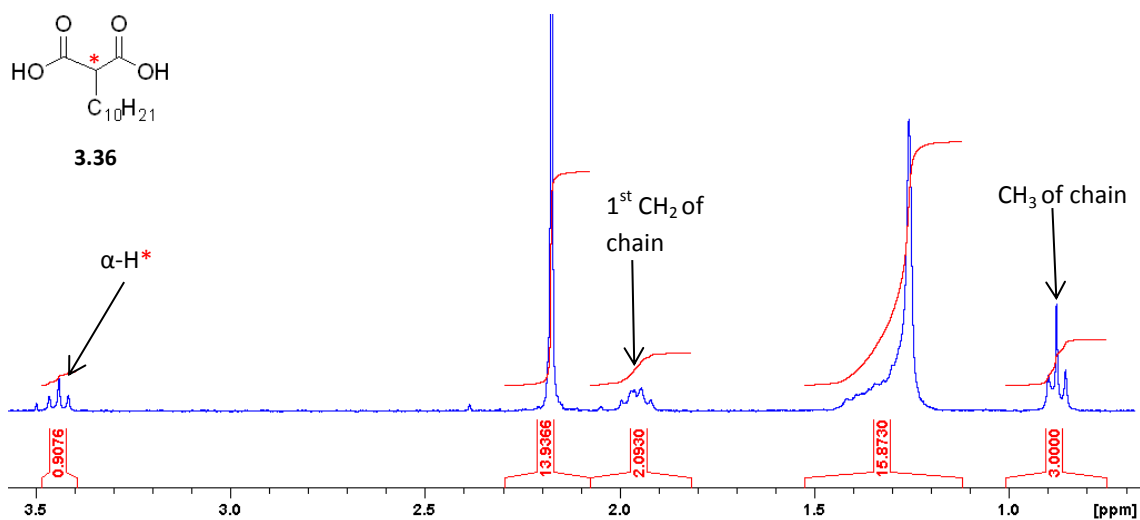


Figure 3.12 ^1H NMR spectrum of the malonyl backbone **3.36** (MeOD, 300 MHz).

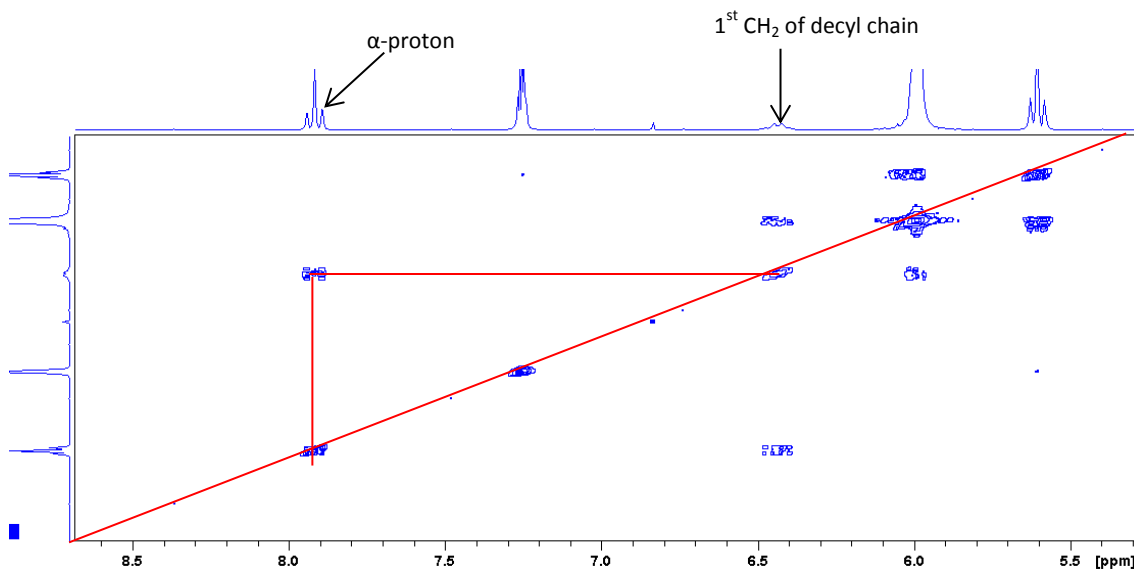
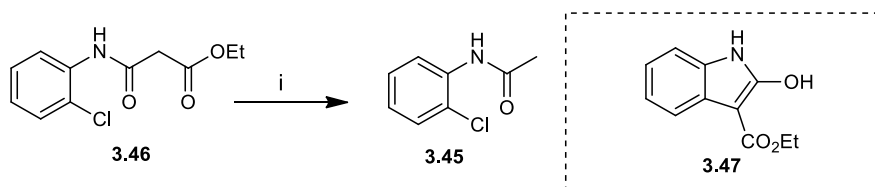


Figure 3.13 ^1H NMR COSY spectrum of carboxylic acid derivative **3.36** which shows the α -proton coupling to the first methylene of the decyl chain (300 MHz, CDCl_3).

This confirmed that the decarboxylation was in fact occurring during the amide coupling reaction between the galactosyl amine **2.33** and the malonyl backbone **3.36**.

As mentioned above, this decarboxylation of malonic acids *via* Malonic Ester Synthesis has been exploited for the synthesis of substituted carboxylic acids since 1901.^[138] On the other hand, the synthesis of amides from malonyl esters never emerged as a universal and efficient methodology. Recently, Majahan *et al.* reported a general methodology for the synthesis of amides utilising malonic esters.^[137] Originally they were attempting to synthesise the indole alkaloid derivative **3.47** using intramolecular, copper-catalysed α -arylation of malonates **3.46**. However, they observed the formation of decarboxylated product **3.45** instead of the alkaloid derivative **3.47** (Scheme 3.5).



Scheme 3.5 Reagents and conditions: i) CuI (0.10 equiv.), 2-picolinic acid (0.20 equiv.), Cs_2CO_3 (3.0 equiv.), 1,4-dioxane, rt to 70°C , 4 h.^[137]

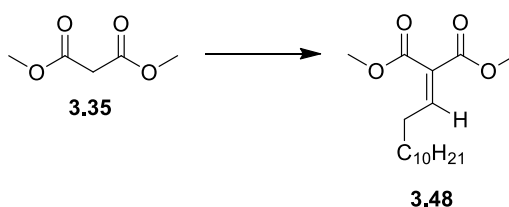
This serendipitous discovery led them to explore this reaction further and examine both the cause of decarboxylation and its potential as a method for amide bond formation. The methodology worked very well for aromatic, hetero-aromatic, primary and secondary amines, however, the conditions did not tolerate the formation of aliphatic amines. Further studies of the reaction and the conditions required for decarboxylation found that the base Cs_2CO_3 was

responsible, although some heterocyclic amines, such as 2-aminopyridine, yielded the decarboxylated amide without the addition of Cs_2CO_3 .

Although this report shows that decarboxylation can occur with amides derived from malonic esters, to the best of our knowledge decarboxylation under the coupling conditions utilised has not been reported in the literature to date.

3.3.3 Attempted Knoevenagel synthesis of β -O-glycoconjugate 3.43 via alkylation followed by amide coupling

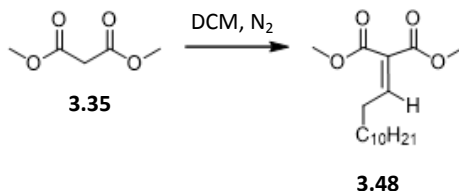
As a result of the problems encountered above, the synthetic route was readdressed and a new approach was taken. We wanted to investigate if the presence of a double bond in the hydrophobic chain could lessen the risk of decarboxylation during the coupling step. With this in mind, a Knoevenagel condensation between the ester **3.35** and an aliphatic aldehyde (dodecanal), was attempted (Scheme 3.6).



Scheme 3.6 Knoevenagel condensation between dodecanal and dimethyl malonate **3.35**.

The Knoevenagel condensation is widely utilised as a carbon-carbon bond forming reaction in organic synthesis.^[139] The reaction is generally catalysed by weak organic bases such as amines, ammonia and ammonium salts,^[140] but acidic conditions can also be exploited.^[139] There are numerous synthetic conditions reported in the literature, however, conventional reagents used as catalysts in this reaction include piperidine,^[141] aluminium oxide^[142] and lithium bromide.^[143] Although there are many examples of Knoevenagel condensations carried out with aromatic aldehydes, the literature on the condensation with aliphatic aldehydes is a lot sparser. In fact there are only isolated reports of the condensation reaction between aliphatic aldehydes and malonic esters,^[139, 144] and even fewer between aliphatic aldehydes and the poorly reactive malonamides.^[128] The biggest challenge lies in the fact that reaction conditions seem to require optimisation for each specific substrate.^[139]

A variety of reaction conditions were attempted for this transformation and the results are summarised in Table 3.1. After extensive optimisation, the desired product **3.48** was isolated in 38% yield (Table 3.1, entry 6), when acetic acid and piperidine were used as catalysts. The purification of **3.48** was complicated by the presence of excess of unreacted aldehyde, which hampered separation by chromatography.

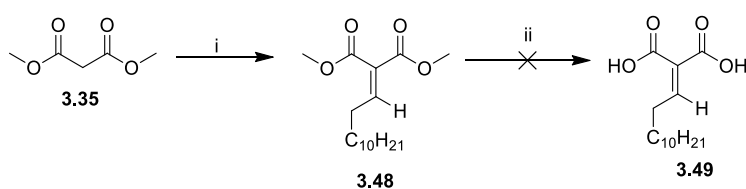


Entry	Reagents	Conditions	Molecular Sieves (4 Å)	Reaction Time	Product
1	Piperidine (1 drop) Acetic Acid ^[119] (1 drop)	3.35 (1 eq) and C ₁₁ H ₂₃ CHO (1 eq) at 0 °C. Reagents added 0 °C for 45 min, then rt.	Yes (added after 45 min)	3 h	3.35 C ₁₁ H ₂₃ CHO
2	LiBr (0.5 eq) Acetic anhydride ^[145] (4.4 eq)	3.35 (1.5 eq) and reagents refluxed at 80 °C for 3 h. C ₁₁ H ₂₃ CHO (1 eq) added and stirred for further 2 h.	No	5 h	3.48:3.35 (10:1 ratio) C ₁₁ H ₂₃ CHO
3	LiBr (0.2 eq) Acetic anhydride ^[140] (2 eq)	3.35 (1 eq) and reagents refluxed at 80 °C for 4 h. C ₁₁ H ₂₃ CHO (3 eq) added and stirred for 2 h.	No	6 h	3.48:3.35 (8:1 ratio) C ₁₁ H ₂₃ CHO
4	Acetic Acid (0.2 eq) Piperidine (0.2 eq)	3.35 (1 eq) and C ₁₁ H ₂₃ CHO (1.1 eq). Reagents added and stirred at rt overnight.	Yes (from start)	16 h	3.48:3.35 (1: 2 ratio) C ₁₁ H ₂₃ CHO
5	Acetic Acid (1 eq) Piperidine (1 eq)	3.35 (1 eq) and C ₁₁ H ₂₃ CHO (1.1 eq). Reagents added and stirred at 90 °C overnight.	Yes (from start)	16 h	Decomposed
6	Acetic Acid (2 drops) Piperidine (2 drops)	3.35 (1 eq) and C ₁₁ H ₂₃ CHO (1.1 eq) on ice. Reagents added and stirred at 0 °C for 45 min. Sieves added and stirred at rt overnight.	Yes (after 45 min)	16 h	3.48 (38%) C ₁₁ H ₂₃ CHO

Table 3.1 Various reaction conditions attempted for the Knoevenagel condensation between **3.35** and dodecanal.

3.3.4 Hydrolysis of alkylidenmalonate 3.48

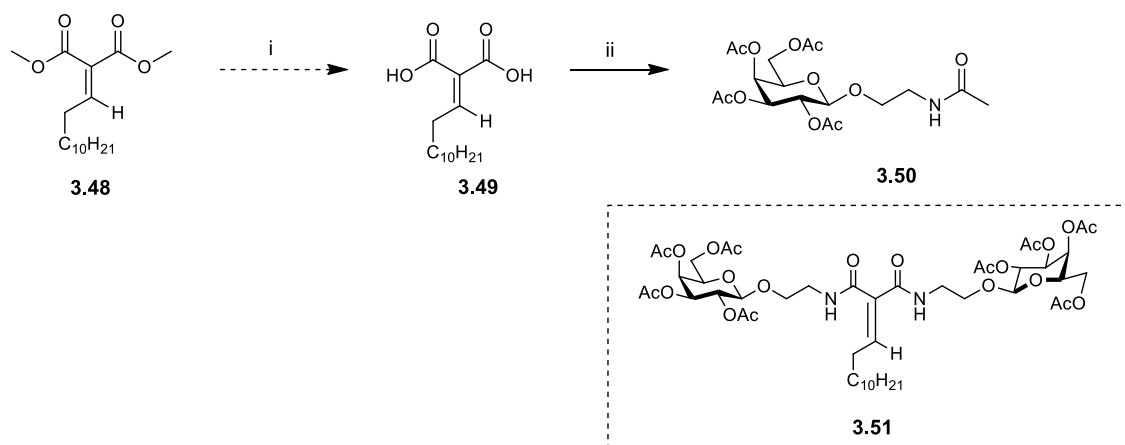
The next step required hydrolysis of the methyl esters in **3.48** to yield the carboxylic acid derivative **3.49**. Unfortunately, problems were again encountered. Various hydrolysis conditions were examined, which included the use of LiOH, NaOH or formic acid but in all cases the compound appeared to decompose. Ester hydrolysis is a widely utilised reaction in organic synthetic chemistry and the transformation is most commonly carried out under basic conditions such as NaOH or LiOH (Scheme 3.7). These hydroxides have high basicity and nucleophilicity and therefore, can be classed as unsuitable reagents when sensitive substrates are being hydrolysed.^[145] In our case, the presence of the double bond seemed to induce the degradation of the molecule, and a complex crude 1H NMR spectrum that no desired product or decarboxylated product was obtained.



Scheme 3.7 Reagents and Conditions: i) Piperidine, CH₃COOH, C₁₁H₂₃COH, 0 °C-rt, 18 h, 38%; ii) see Table 3.1.

Based on this information, a milder hydrolysis method was obviously required. In 1960, Elsingher *et al.* reported the selective hydrolysis of methyl esters using lithium iodide.^[146] Since then, there has been a number of reports on the use of lithium salts for the mild hydrolysis of esters.^[145, 147] Lithium iodide is a mild, neutral reagent and therefore, can hydrolyse esters in the presence of a variety of functional groups.

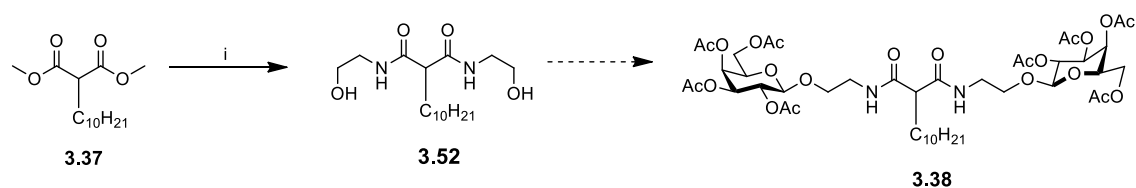
With this in mind, hydrolysis of the alkylidene malonate **3.48** was attempted using lithium iodide. At first, the results appeared promising, but upon closer inspection the crude mixture was extremely complex and purification proved difficult. We next investigated a one pot reaction, whereby the alkylidene malonate **3.48** was hydrolysed and coupled to the galactosyl ethyl amine **2.33** *in situ* (Scheme 3.8). Unfortunately, the reaction did not proceed as expected. The crude sample appeared to consist of a variety of unknown compounds. Upon purification by column chromatography the major product was identified as the decarboxylated derivative **3.50**, which was confirmed by HR-MS. The presence of the double bond did not appear to lessen the risk of decarboxylation as expected. Instead, the alkene chain was also lost. This was unexpected, and as the reaction was carried out *in situ*, it is difficult to identify whether it occurred during the hydrolysis or coupling reaction.



Scheme 3.8 Reagents and Conditions: i) LiI, EtOAc, N₂, 60 °C, overnight; ii) HOBt, TBTU, NEt₃, **2.33**, DMF, rt, 16 h, 63%.

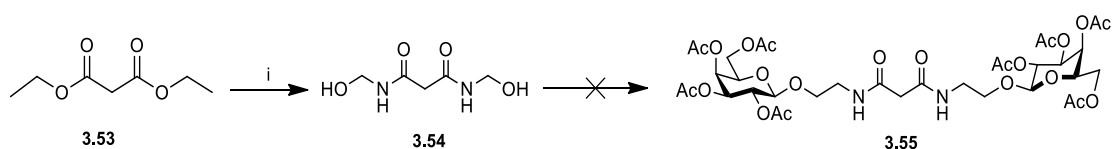
3.3.5 Amidation reactions of malonic esters

To circumvent the problems we again had to alter our synthetic method. The amidation of malonic esters has been previously reported^[126] and provides a convenient route for accessing malonamides from malonic esters. Our initial approach involved the amidation of ethanolamine with the alkylated malonic ester **3.37** (Scheme 3.9) which could be later reacted with two galactosyl donors in a glycosylation reaction to give compound **3.38**.



Scheme 3.9 Reagents and conditions: i) NH₂CH₂CH₂OH, DCM, rt, 3 days, 62%.

Amidation of the alkylated malonic ester **3.37** afforded the desired *N,N*-bis(2-hydroxyethyl)malonamide **3.52** in 62% yield after a period of three days (Scheme 3.9). Unfortunately, compound **3.52** was found to be extremely insoluble in all organic solvents tested, which made any further reactions practically impossible. As a result of this, a different approach was taken. This time the amidation reaction was performed on the diethyl malonate prior to alkylation (Scheme 3.10). We believed this would alleviate solubility issues and enable further functionalisation.

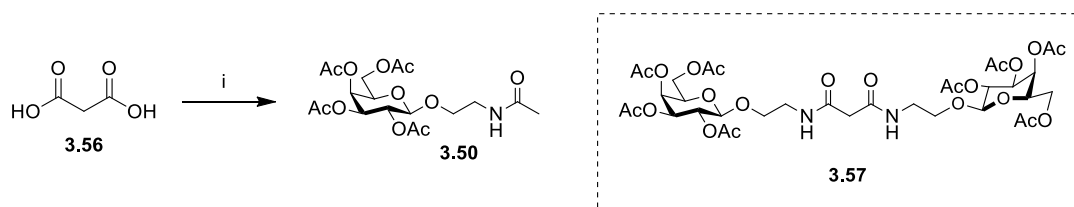


Scheme 3.10 Reagents and conditions: i) NH₂CH₂CH₂OH, rt, 2 h, 85%.

Starting from diethyl malonate **3.53** the desired *N,N*-bis(2-hydroxyethyl)malonamide **3.54** was obtained in 85% yield. While **3.54** exhibited improved solubility in relation to the alkylated derivative **3.52**, it was still limited to a number of solvents including DMF and THF. The next step, which was the glycosylation reaction, raised more problems. Although various synthetic approaches were examined the desired bis-galactosylated product **3.55** could not be obtained. With Schmidt glycosylation conditions (see Chapter 2, section 2.5.1.1), a mixture of compounds, which could not be identified, were observed. Direct glycosylation from the β -pentacetate galactoside **2.38** was also attempted but no reaction appeared to take place and only starting material was observed in the crude mixture. A direct amidation reaction between diethyl malonate **3.53** and the galactose ethyl amine **2.33** was also attempted, but even after 3 days TLC analysis indicated that only starting material was present.

3.3.6 Malonyl chloride and malonic acid as precursors for the synthesis of malonamides

The report by Kato *et al.* (discussed in section 3.1.3) described the synthesis of mannose malonamides from malonic acid **3.56** using standard peptide coupling conditions.^[130] This led us to examine the synthesis of galactosyl malonamides from malonic acids (Scheme 3.11). We then attempted to form the galactosyl malonamide **3.57** first, with alkylation of the α -carbon to introduce the aliphatic chain being carried out at a later stage.



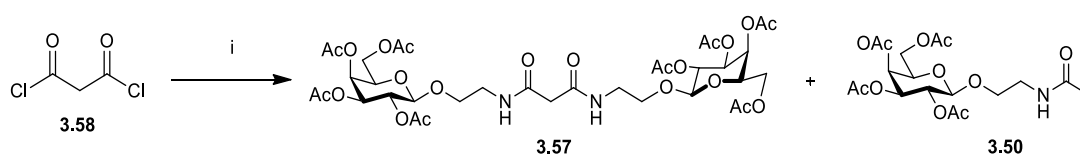
Scheme 3.11 Reagents and Conditions: i) HOBt, TBTU, DIPEA, **2.33**, N₂, 0 °C-rt, 16 h, 72%.

Despite our renewed optimism, we did not obtain the di-substituted product **3.57**. Instead, we again isolated the decarboxylated derivative **3.50** in a high yield of 72%. The synthesis was carried out as per standard peptide coupling conditions, i.e. activation of the acid with HOBt, TBTU and DIPEA prior to addition of the amine. As it is possible that decarboxylation occurred during this activation process, the reaction was repeated with no prior activation, but, as before, the decarboxylated product was obtained and no di-substituted product **3.57** observed.

In order to examine the effect of base on decarboxylation, the reaction was repeated in the presence of NEt₃. Similar results were observed and although the decarboxylated product **3.50** was still the major product, small amounts of the disubstituted product **3.57** could be detected

in the ^1H NMR spectrum. The presence of the di-substituted product was confirmed by HR-MS. Optimisation of the reaction failed to improve on this result and even at reduced temperatures ($-10\text{ }^\circ\text{C}$) the decarboxylated derivative **3.50** was the major product. Kato *et al.* did not report any observation of decarboxylation and appear to only obtain disubstituted product. Therefore, our observations were highly unexpected.

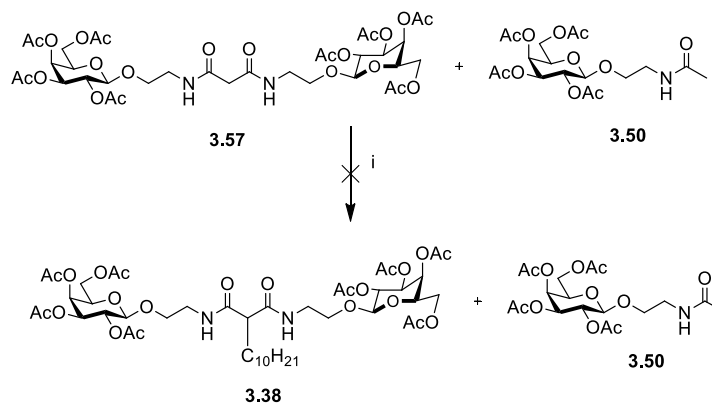
We next looked to malonyl chlorides as precursors for the synthesis of di-substituted galactosyl malonamides, as these type of transformations have been previously reported in the literature.^[148] Malonyl chloride **3.58** was reacted with the galactosyl amine **2.33**, in the presence of base (NEt_3) and yielded both the disubstituted **3.57** and decarboxylated derivatives **3.50** in a 1:1 ratio (Scheme 3.12). Various purification methods were attempted, including recrystallisation and column chromatography, but the two compounds could not be separated. HR-MS confirmed the presence of both products.



Scheme 3.12 Reagents and Conditions: i) **2.33**, DCM, NEt_3 , N_2 , $0\text{ }^\circ\text{C}$ -rt, 16 h, 60%.

As before, the effect of base on the reaction was examined, and the reaction was repeated using DIPEA. No improvement on the efficiency of the system was observed, and in fact the yield decreased to 45%. The reaction was also attempted at lower temperatures ($-10\text{ }^\circ\text{C}$), and this time improvements were achieved. The ratio of desired product **3.57** to decarboxylated product **3.50** increased from 1:1 to 1.5:1. Further enhancement could be achieved when the reaction time was reduced from 16 h to 4 h, and the ratio increased to 4:1. No further improvements were achieved, and again purification was unsuccessful. Thus, it was decided to continue on with the synthesis, and to attempt the alkylation on the mixture of **3.57** and **3.50**. As only the disubstituted derivative **3.57** was expected to undergo alkylation, we hoped purification may be simpler after this step.

Initially, we followed the same alkylation procedure as previously discussed in section 3.2.1 and the mixture of products was reacted with 1-bromodecane using K_2CO_3 (Scheme 3.13).



Scheme 3.13 Reagents and condition: i) CH₃(CH₂)₉Br, K₂CO₃, CH₃CN, 80 °C, 36 h.

These conditions proved ineffective as no product was isolated and only starting material recovered. However, this is not surprising, as the amide groups are less electron withdrawing than the original esters and this results in the reduced acidity of the α -proton. Therefore, a stronger base is required for deprotonation. With this in mind, the reaction was repeated, this time using NaH as the base, but this led to the partial decomposition of compound **3.57**.

Degradation of the bisamide **3.57** was also observed when Knoevenagel condensation was attempted, using all the conditions described in Table 3.1.

3.4 Synthesis of *O*-glycoconjugate **3.33**

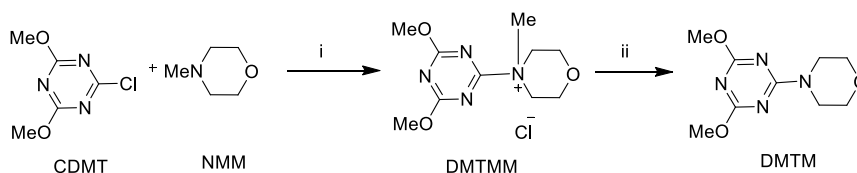
With so many problems to contend with, a change of approach was considered. We finally decided to investigate if coupling conditions other than TBTU/HOBt or acid chlorides would reduce or even eliminate decarboxylation. Rather than using other conventional coupling reagents, such as carbodimides, we focused on the use of 4-(4,6-dimethoxy-1,3,5-triazin-2-yl)-4-methylmorpholinium chloride (DMTMM), which has previously been used in the synthesis of malonamide glycoconjugates.^[132]

3.4.1 DMTMM as an alternative peptide coupling reagent

DMTMM has been highlighted as an effective activating agent for amide bond formation and peptide synthesis.^[149] Although initially reported by Kaminski *et al.* in 1998,^[150] it was not until Kunishima and co-workers^[151] optimised its usage that it began receiving interest as an alternative reagent for amide bond formations.

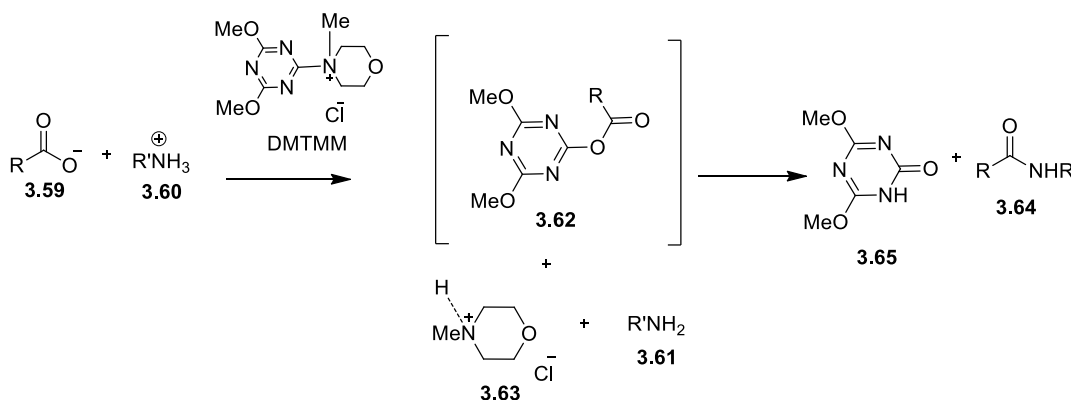
DMTMM, which is a white solid, is synthesised by the reaction of 2-chloro-4,6-dimethoxy-1,3,5-triazine (CDMT) with *N*-methylmorpholine (NMM) in THF at rt (Scheme 3.14). It is extremely easy to purify as the solid product precipitates readily. However, it can be unstable and can only be stored and used for one month after synthesis. As shown below, it can

undergo demethylation at the morpholinium nitrogen when suspended in DCM, while in THF it was found to be stable with only 13% DMTM detected after 13 h (Figure 3.14).^[151b]



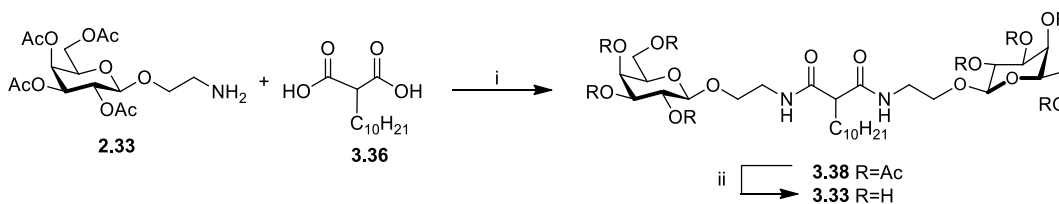
Scheme 3.14 Reagents and conditions: i) THF, rt, 30 min, 100%, ii) rt, DCM, 3 h, 100%.

The reaction mechanism is similar to other activating agents. The DMTMM reacts with the carboxylate ion **3.59** in a S_NAr transformation to form the activated ester **3.62** (Scheme 3.15), and regenerated NMM **3.63**. The amine then attacks and displaces the activated ester to form the amide **3.64** and the triazinone by-product **3.65**.



Scheme 3.15 Mechanism of DMTMM activated coupling.^[151]

The synthesis started with alkylated malonic acid **3.36** as described in section 3.2.1. The acid **3.36** was coupled to the galactosyl amine **2.33** using DMTMM and NMM and to our delight the desired bis-substituted product **3.38** was obtained (Scheme 3.16), albeit in a low yield of 30% and with a number of impurities. In the procedure reported by Isaad and co-workers,^[132] NMM and DMTMM were utilised, however, it is known from the mechanism that NMM is generated during the reaction. For this reason, the reaction was repeated without the addition of base and this resulted in both an increase in yield (55%) and a decrease in side-product formation.



Scheme 3.16 Reagents and Conditions: i) 1) DMTMM, NMM, THF, 16 h, rt, 37%; or DMTMM, THF, 16 h, 55%; ii) NEt_3 , DCM/MeOH/ H_2O , 40 °C, 18 h, 78%.

The deprotection of the malonyl-based glycoconjugate **3.38** using NEt_3 afforded the novel *O*-glycoconjugate **3.33** as a white precipitate in a yield of 78% (Scheme 3.16). The ^1H NMR spectrum of *O*-glycoconjugate **3.33** is displayed in Figure 3.14 and diagnostic signals, including the amide protons (N-H), the anomeric (H-1) proton and the α -proton*, are assigned.

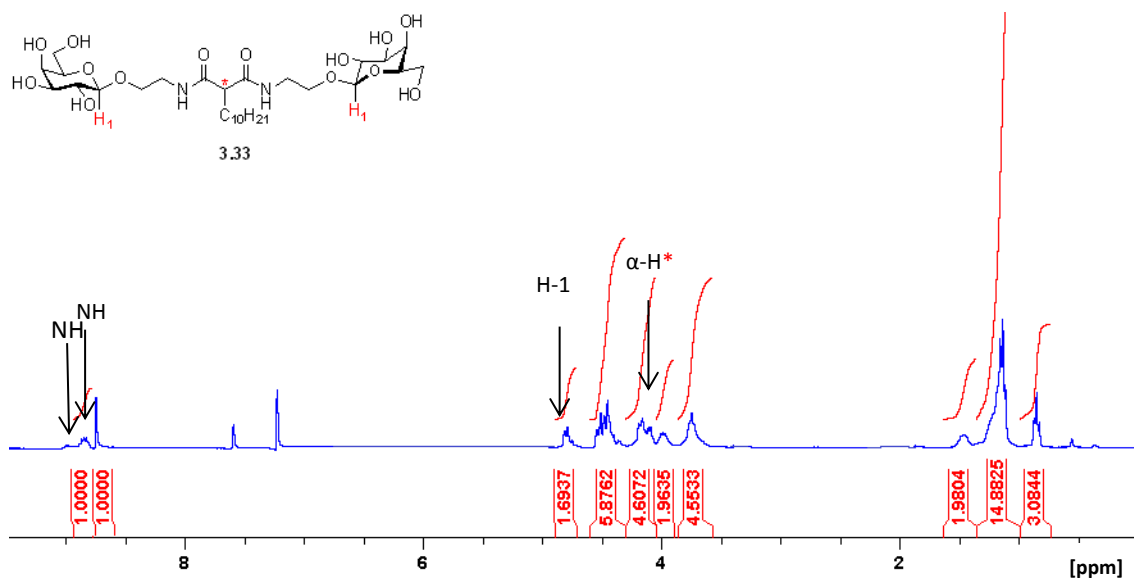


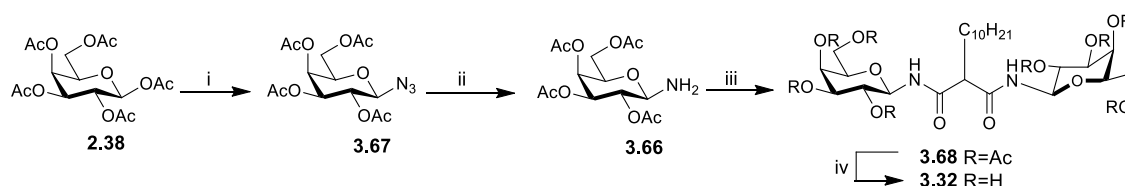
Figure 3.14 ^1H NMR spectrum of deprotected *O*-glycoconjugate **3.33** (300 MHz, d_5 -Pyr).

3.5 Synthesis of *N*-glycoconjugate **3.32**

Once a successful synthetic route was established, the preparation of the other malonamides could be attempted. The malonamide glycoconjugate **3.32** was designed to act as a more rigid molecule compared to the *O*-glycoconjugate **3.33**. The galactose moiety is directly linked to the malonyl backbone *via* an *N*-glycosidic bond. This should exert a certain degree of rigidity in the molecule, as rotation around the amide bond is limited, thus restricting the conformation of the molecule and locking the presentation of the galactosides.

3.5.1 Synthesis of galactosyl amine **3.66**

The synthesis of the known galactosyl amine **3.66** began with the reaction of the per-acetylated galactosyl donor **2.38** with TMSN_3 , promoted by the Lewis acid SnCl_4 to yield 91% of the β -galactosylazide **3.67** (Scheme 3.17). Reduction of the azide by hydrogenation catalysed by Pd/C afforded the galactosyl amine **3.66** in 97% yield.^[152]



Scheme 3.17 Reagents and Conditions: i) SnCl_4 , TMSN_3 , DCM, N_2 , 18 h, 91%; ii) H_2 , Pd/C, EtOAc, rt, 16 h, 97%; iii) **3.66**, DMTMM, THF, rt, 18 h, 56%; iv) NEt_3 , DCM/MeOH/ H_2O , 40 $^\circ\text{C}$, 18 h, 93%.

The galactosyl amine **3.66** was then coupled to the alkylated malonic acid **3.36**, using DMTMM as the activating agent, and the *N*-glycoconjugate **3.68** was obtained in 56% yield. Finally, selective deprotection of the acetyl protecting groups, using catalytic NEt_3 in a heterogenous solvent system (DCM/MeOH/ H_2O , 1:2:1) at 40 °C, afforded the novel *N*-glycoconjugate **3.32** as a white precipitate in 93% yield (Scheme 3.17). These mild deprotection conditions were attempted as we feared that harsher conditions, such as those employed in Zémlen deprotection, may result in degradation of the glycolipid. The ^1H NMR spectrum of the *N*-glycoconjugate **3.32**, is shown in Figure 3.15 with characteristic peaks highlighted.

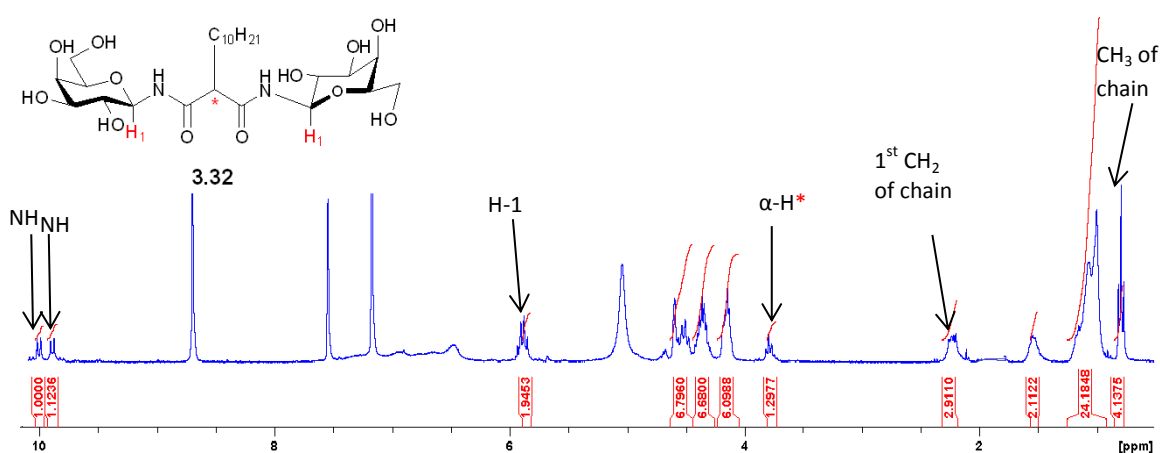


Figure 3.15 ^1H NMR spectrum of deprotected *N*-glycoconjugate **3.32** (300 MHz, d_5 -Pyr).

3.6 Synthesis of Malonyl-based *O*-glycoconjugate **3.44**

As with the *N*-glycoconjugate **3.32** and *O*-glycoconjugate **3.33**, malonyl-based *O*-glycoconjugate **3.34** was designed to act as a potential inhibitor of bacterial adhesion (see Chapter 5). A very different extended linker can be observed in this molecule. Like the malonamide glycoconjugate, **3.33**, it contains the ethyl chain which should allow for a certain degree of conformational flexibility. However, it also contains a triazole moiety, which could influence both the biological activity and conformation of the molecule. Promising anti-microbial results of a triazole-containing glycolipid **3.69** on the bacterium *P. aeruginosa* were reported by Marotte *et al.* (Figure 3.16).^[31]

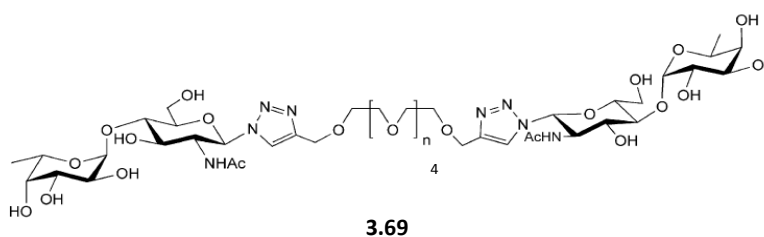
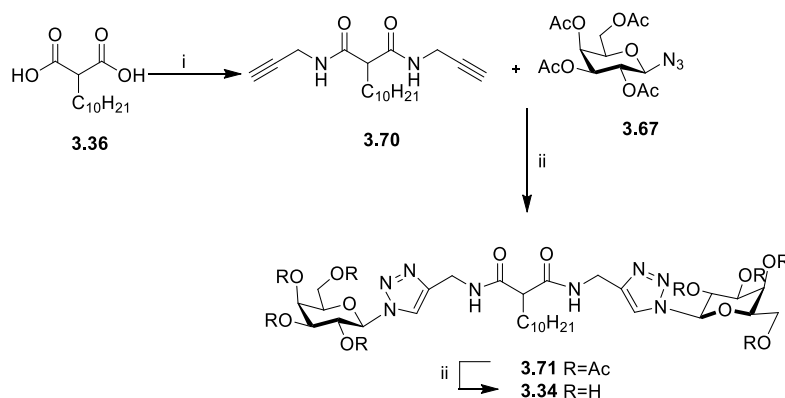


Figure 3.16 Triazole glycolipid **3.69** which showed promising anti-adhesion activity towards *P. aeruginosa*.^[31]

We intended to synthesise the triazole-containing glycoconjugate **3.34** and then compare its ability to inhibit bacterial adhesion with that of glycoconjugates **3.32** and **3.33**. Ultimately we wanted to probe whether introducing aromaticity into the linker of the glycolipid structure would affect its anti-microbial properties.

The synthesis commenced with the coupling of 3-aminopropyne to the malonic acid building block **3.36**, utilising DMTMM as the activating agent. This resulted in the alkylated alkyne malonamide **3.70** (Scheme 3.18). A subsequent Huisgen cycloaddition (discussed in detail in Chapter 4, section 4.4.1) between the galactosyl azide **3.67** and the malonamide alkyne **3.70**, which was catalysed by $\text{CuSO}_4 \cdot 5\text{H}_2\text{O}$ and sodium ascorbate, afforded the 1,4-disubstituted 1,2,3-triazole *O*-glycoconjugate **3.71** in 58% yield.



Scheme 3.18 Reagents and Condition: i) Propargylamine, DMTMM, THF, rt, 16 h, 78%; ii) $\text{CuSO}_4 \cdot 5\text{H}_2\text{O}$, sodium ascorbate, DCM/ H_2O /Acetone, 18 h, 58%; ii) NEt_3 , DCM/ H_2O /MeOH, 40 °C, 20 h, 89%.

Selective deprotection of the *O*-glycoconjugate **3.71** using NEt_3 yielded the novel *O*-glycoconjugate **3.34** as a white precipitate in 98% yield. The ^1H NMR spectrum is displayed in Figure 3.17. Characteristic peaks are highlighted in the figure, including the amide protons (NH), triazole proton (CN_3CH) and α -proton*.

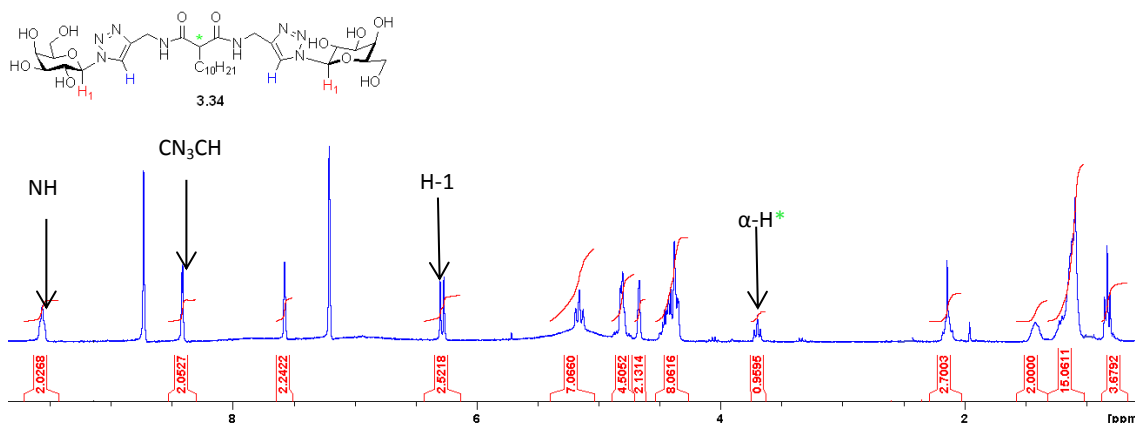


Figure 3.17 ^1H NMR spectrum of deprotected *O*-glycoconjugate **3.34** (300 MHz, d_5 -Pyr).

3.7 Conclusion

The synthesis of the malonyl-based glycoconjugates proved more problematic than anticipated, and a variety of synthetic routes were attempted. The main problem encountered was decarboxylation. We found that although the decarboxylation of malonic acids is widely reported in the literature, it generally occurs during the hydrolysis step. This was not the case for the compounds discussed above as the decarboxylation step appeared to occur during amide bond formation. To the best of our knowledge no decarboxylation has previously been reported using the HOBt/TBTU methodology utilised here. Amidation reactions overcame this decarboxylation, however, the resulting compounds were extremely insoluble and unreactive. A variety of precursors, including malonyl chloride and malonic acid, were utilised, and although some success was achieved, alkylation with the lipid chain then proved difficult due to the decreased acidity of the α -proton.

Finally, the malonyl-based glycoconjugates **3.32-3.34** were successfully synthesised by using DMTMM as an alternative coupling reagent. Following this approach, no decarboxylation was observed. Glycoconjugates exhibiting a variety of linkages to the malonyl backbone were explored, and we found that the best yields were achieved with the triazole-containing derivative **3.34**. The ability of selected malonamides to inhibit bacterial adhesion was also investigated and the results are discussed in Chapter 5.

Chapter 4: Synthesis of glycolipids-based on aromatic scaffolds as potential anti-adhesion agents

4.1 Introduction

Cell surface carbohydrates are important in initiating a vast number of biological and pathological processes.^[153] More specifically, carbohydrate-protein interactions are often responsible for mediating the early stages of the infection process for bacterial pathogens.^[22, 153] One drawback in the synthesis of carbohydrate-based anti-infection agents lies in the fact that individual carbohydrates tend to bind weakly to their corresponding polyvalent protein receptors.^[15] This can be overcome by utilising multivalent carbohydrate ligands which generally result in greater affinity of binding^[15-16] (discussed in detail in Chapter 1 section 1.2.3).

In complex, multiantennary oligosaccharides, only a small number of the carbohydrate residues are directly involved in the protein-carbohydrate interactions. It is believed that the remaining sugars have a purely structural role. It has been suggested that they may act as spacers and ensure optimal protein-carbohydrate interactions by maintaining the sugar epitopes at an appropriate distance. In theory, this suggests that the saccharide moieties responsible for structure could be replaced by other rigid molecules such as aromatic scaffolds.^[154]

Glycoconjugates built around a benzene core are widely explored in the literature. Depending on the analogue utilised, they can lead to the synthesis of divalent, trivalent, tetravalent and even hexavalent molecules. They also allow for the linkage between the sugar moiety and the aromatic scaffold to be varied (e.g. N-, O-, S- or C- linked), and therefore, various reaction conditions can be exploited.

One benzene derivative which has received a great deal of attention is benzene-1,3,5-tricarboxylic acid (trimesic acid, Figure 4.1). Trimesic acid has been widely utilised as an aromatic scaffold for the synthesis of multivalent glycoconjugates. Due to the presence of the three carboxylic acid side groups, which can be easily functionalised, it is an ideal scaffold for the synthesis of a wide range of trivalent molecules through the formation of amide bonds.

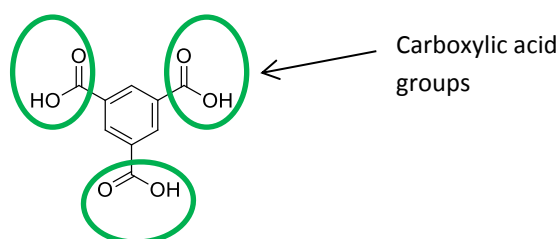


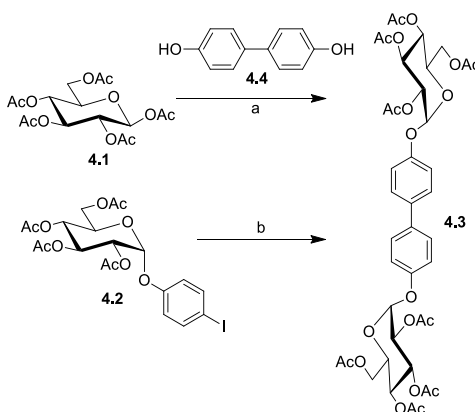
Figure 4.1 Benzene-1,3,5-tricarboxylic acid (trimesic acid).

4.2 Aromatic-based glycolipids and their biological importance

As benzene derivatives are readily available and easily functionalised there are numerous examples of glycoconjugates based on aromatic scaffolds reported in the literature.

4.2.1 Synthesis and application of divalent glycoconjugates

Depending on the valency of the glycoconjugate of interest, different reaction conditions can be exploited. For example, Roy *et al.*^[155] and van Doren *et al.*^[156] both reported the synthesis of a divalent biaryl glucoside **4.3**, yet they both used different synthetic strategies (Scheme 4.1). Van Doren *et al.* utilised a double Lewis acid-catalysed glycosidation (reaction a) and the glucoside **4.3** was obtained in 47% yield, whereas Roy *et al.* utilised an Ullman-type reductive homocoupling (reaction b), and improved this yield to 81%. Glucoside **4.3** displayed strong binding affinities towards the plant lectin Concanavalin A (Con A).



Scheme 4.1 Synthesis of divalent aryl glucoside **4.3** using either a) a double Lewis acid-catalysed glycosidation^[156] or b) an Ullman-type reductive homocoupling strategy.^[155]

Another example of divalent glycoconjugates based around an aromatic scaffold comes from Pagé and Roy.^[157] They reported the synthesis of two, divalent, mannopyranoside clusters **4.5** and **4.6** and investigated their binding affinities towards Con A and pea lectins. Both ligands were designed to display similar structural features by utilising the same aromatic core, one linked *via* an aryl spacer and the other *via* a heteroaliphatic spacer.

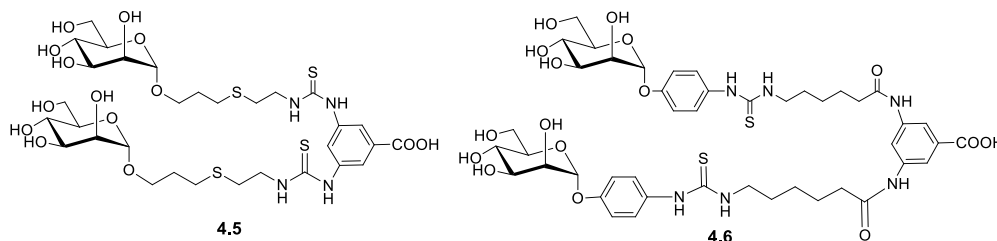


Figure 4.2 Divalent mannopyranoside clusters **4.5** and **4.6** investigated for their binding affinities towards Con A and pea lectins.^[157]

Both divalent compounds were shown to exhibit greatly improved affinities towards the plant lectins, in comparison to the monosaccharide standards (Table 4.1). However, the effect was

more prominent for the tetravalent lectin (Con A) over the divalent pea lectin. Con A exists as tetramers at physiological pH, which enables the formation of a stable, cross-linked lattice with the mannosylated clusters **4.5** and **4.6**. This is not the case for the divalent pea lectin and therefore may explain the difference in affinities.

Compound	Con A IC ₅₀ (μm)	Relative Potency	Pea Lectin IC ₅₀ (μm)	Relative Potency
Methyl α-D-Man	924	1.0	3850	1.0
pNO ₂ -Ph α-D-Man	106	8.7	1500	2.6
Allyl α-D-Man	261	3.5	940	4.1
4.5	30.5	30.3	185	20.8
4.6	36.8	25	575	6.7

Table 4.1 Affinities of bivalent mannosylated clusters **4.5** and **4.6** and their monosaccharide counterparts against plant lectins, Con A and pea lectin.

Aiming to investigate how scaffold flexibility and spatial arrangement of ligands may affect their inhibitory potency against *Viscum album* agglutinin and human galectins, a variety of divalent lactosyl glycoconjugates-based around an aromatic core were synthesised by Murphy and co-workers (scaffolds **1.10-1.12** and **4.7-4.11**, Figure 4.3).^[158]

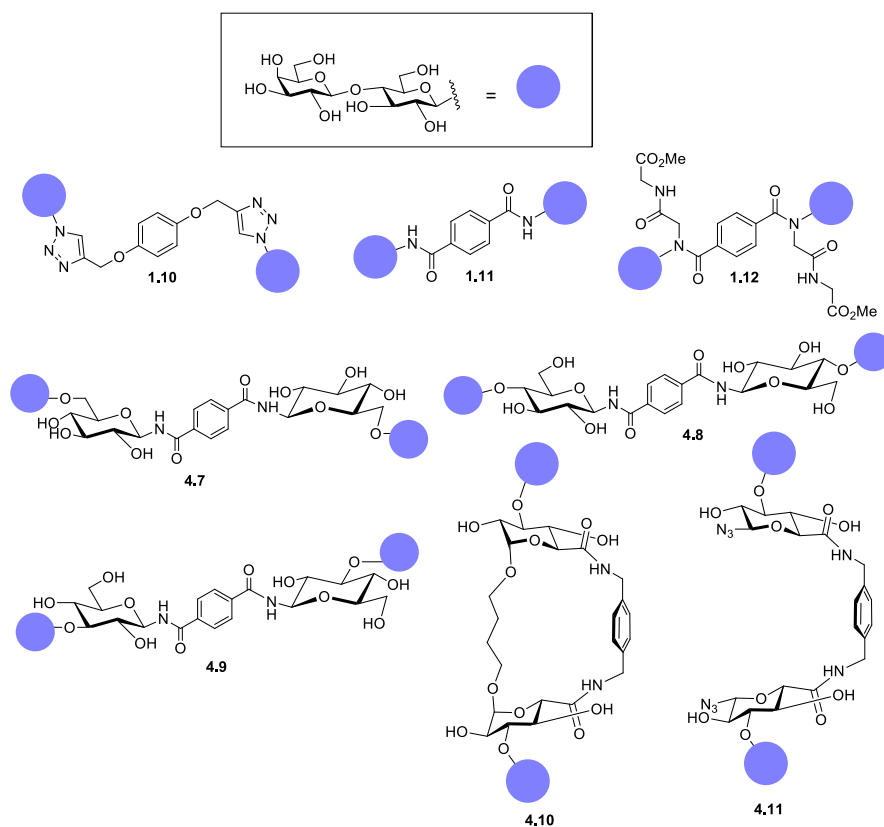


Figure 4.3 Selection of bivalent lactose glycoconjugates **1.10-1.12** and **4.9-4.11** synthesised and tested against *Viscum album* agglutinin and human galectins.^[158]

A number of assays were carried out in order to correlate structural features with bioactivity and a number of conclusions were reached. It was found that the bivalent lactose glycoconjugates were less effective at interfering with glycoprotein binding to the plant toxin than to human lectins. Solid phase and cell surface experiments showed that structural differences in the compounds (secondary amide in **1.11** versus tertiary amide in **1.12**), as well as where the lactose moieties were placed around the common core (substitution at the 6, 4 or 3 position on glucose, **4.7-4.9** respectively), had an influence on binding properties to galectin-3 and galectin-4. This was due to both changes in geometry and inter-epitopes' distance. Significantly, the constrained compound **1.12** displayed the best inhibition with truncated galectin-3 and galectin-4. Conversely, glycoconjugates which were highly flexible exhibited notable ability to protect human cells from plant toxin binding. Results also showed that the more rigid structures led to a loss in biological activity as the acyclic compound **4.11** displayed more optimum activity than the cyclic **4.10** molecule against all lectins investigated.^[158]

4.2.2 Synthesis and applications of trivalent glycoconjugates

Due to the easy functionalisation of commercially available trimesic acid and trimesoyl chloride there are a wide range of trivalent glycoconjugates reported in the literature. Selected examples based on the common core **4.12** can be seen below in Figure 4.4.

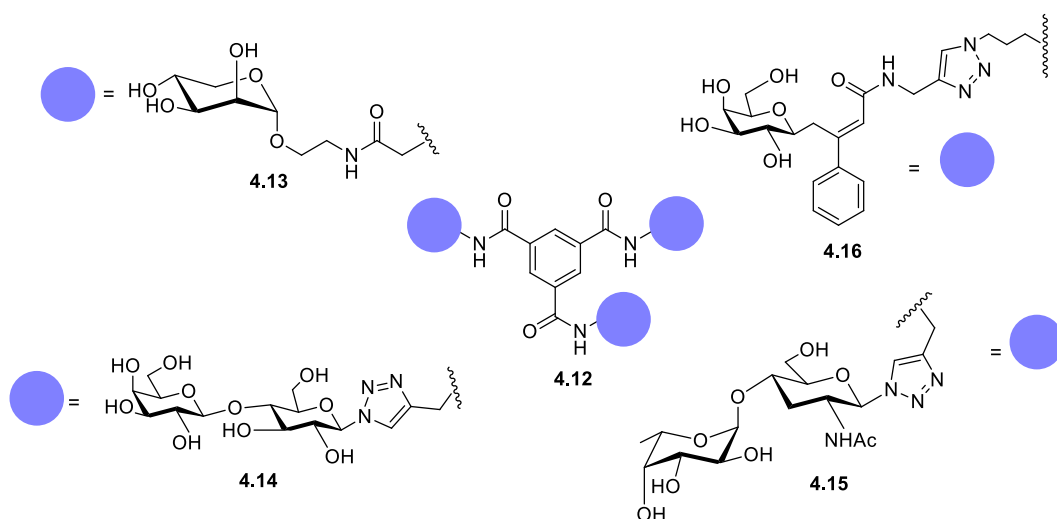


Figure 4.4 Examples of aromatic trivalent glycoconjugates **4.12-4.16** built around trimesic acid.^[31, 159]

The Stoddart group reported one of the first glycoclusters built around benzene-1,3,5 tricarboxylic acid **4.13** in the late 1990's.^[159a] Since then, a variety of trivalent glycoclusters bearing more complex epitopes such as lactosides **4.14**,^[159b] Lewis^a diasaccharides **4.15**^[31] and modified galactoside mimetics **4.16**^[159c] have been synthesised. Reaction of *N,N,N*-tripropargyl-1,3,5-carboxamidobenzene with the corresponding azido glycosides using CuAAC methodology

afforded the trivalent glycoconjugates **4.14-4.16** in high yields. The inhibitory properties of these glycoclusters towards different galectins and bacterial lectins have been investigated. Trivalent lactoside **4.14** exhibited high affinity against galectin-1 and -3, and IC_{50} values implied enhanced activity compared to free lactose.^[159b] Lewis^a disaccharide derivative **4.15** was tested for its inhibitory properties towards PA-IIL, which is a fucose binding lectin found in *P. aeruginosa*. Results showed, however, that the trivalent glycocluster did not exhibit higher affinity over the Lewis^a trisaccharides or their PEGylated dimers.^[31] The Chabre and Roy group^[159c] then attempted to combine aromatic glycomimetics and multivalency in order to synthesise glycoclusters with increased potency and affinities towards the PA-IL bacterial lectin, which is a glucose binding lectin. They synthesised **4.16** by reacting the propargylated C-galactoside, which contained hydrophobic aglycones in the anomeric position, to the elongated triazide derivative of trimesic acid again using CuAAC methodology. The presence of aglycones has led to enhanced binding properties and experiments have shown a 127-fold overall enhancement of affinity towards PA-IL compared to the controls. This experiment highlighted the benefits of utilising both glycomimetics and multivalency in the synthesis of carbohydrate ligands.^[154, 159c]

Not all linkages to the core aromatic scaffold occur *via* the formation of amide bonds. Alternative linkages such as ethers, as in the general core structure **4.17**, have also been utilised and some examples are shown in Figure 4.5.^[160]

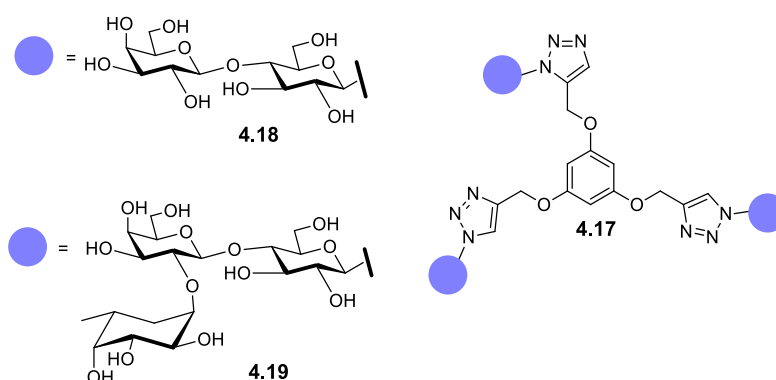


Figure 4.5 Selection of trivalent glycoconjugates **4.18** and **4.19** where an ether linkage connects the aromatic scaffold and the glucosides.^[160]

A large selection of glycoconjugates were synthesised in the group of Chabre and evaluated as potential inhibitors of the interaction between biotinylated plant, human and chicken galectins and the surface-immobilised asialofetuin (ASF).^[154] Derivative **4.19** showed the best results against the full length chicken galectin-3, with a 10-fold improvement in affinity when compared to derivative **4.18** and a 63- and 18-fold enhancement when compared to the

controls, lactose and 2'-fucosyllactose.^[160] Similar results were also observed for the human galectins but the enhancements were not as distinct.

4.2.3 Synthesis and applications of oligovalent glycoconjugates

By utilising a variety of benzene derivatives a large selection of diverse glycoconjugates with varying valencies can be synthesised quite easily. This highlights the advantages of building glycoconjugates around an aromatic core, as it allows for flexibility in both the number of epitopes added, and the connectivity between the glycan and aromatic scaffold. A selection of multivalent glycoconjugates can be seen in Figure 4.6.

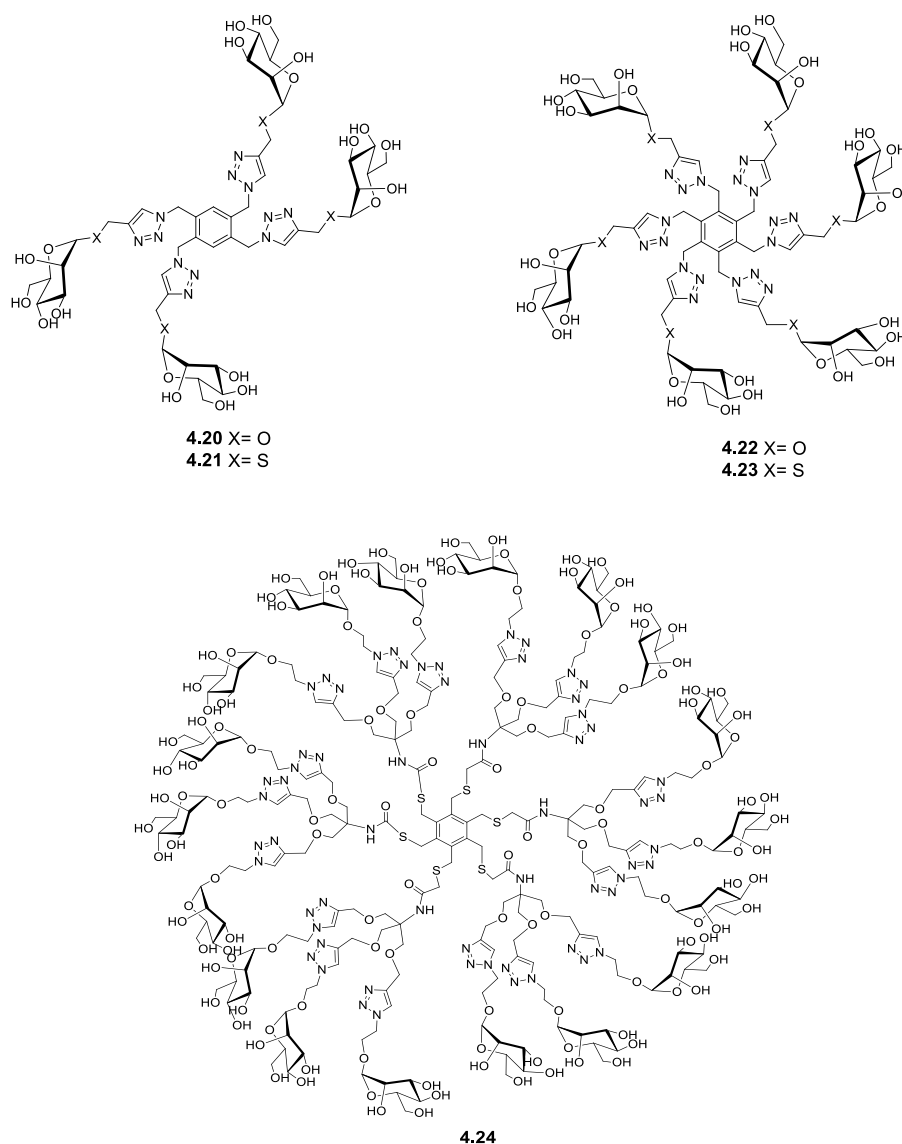


Figure 4.6 Selected examples of tetra-valent **4.20** and **4.21**,^[161] hexa-valent **4.22** and **4.23**,^[161] and octa-deca-valent **4.24**^[162] glycoconjugates.

Santoyo-Gonzalez *et al.* synthesised a variety of multivalent mannose (α -Man)-containing glycoconjugates which centred around either an aliphatic, aromatic, or carbohydrate core. Two tetra-valent compounds (**4.20** and **4.21**) and two hexa-valent compounds (**4.22** and **4.23**)

derivatives based around an aromatic core can be seen in Figure 4.6. The ability of the glycoconjugates to bind Con A was evaluated and results showed that the aromatic conjugates exhibited enhanced binding in comparison to their aliphatic counterparts and also that the aromatic thioglycosides analogues **4.21** and **4.23** showed more promising results.^[161]

The octadecavalent glycocluster **4.24** was synthesised by Roy *et al.* as part of a study in order to examine the effects of multivalent mannose glycoconjugates on bacterial adhesion.^[162] Initial results against the BclA lectin of *Burkholderia cenocepacia* showed that some of the ligands had micromolar affinities towards the lectin, and that these affinities increased with increasing valency.^[154]

4.2.4 Synthesis and applications of glycolipids based around an aromatic core

Although there are many examples of aromatic-based glycoconjugates reported in the literature,^[154, 163] examples of analogues which contain both a carbohydrate moiety and a lipidic chain are limited. Some monovalent examples can be seen below in Figure 4.7.

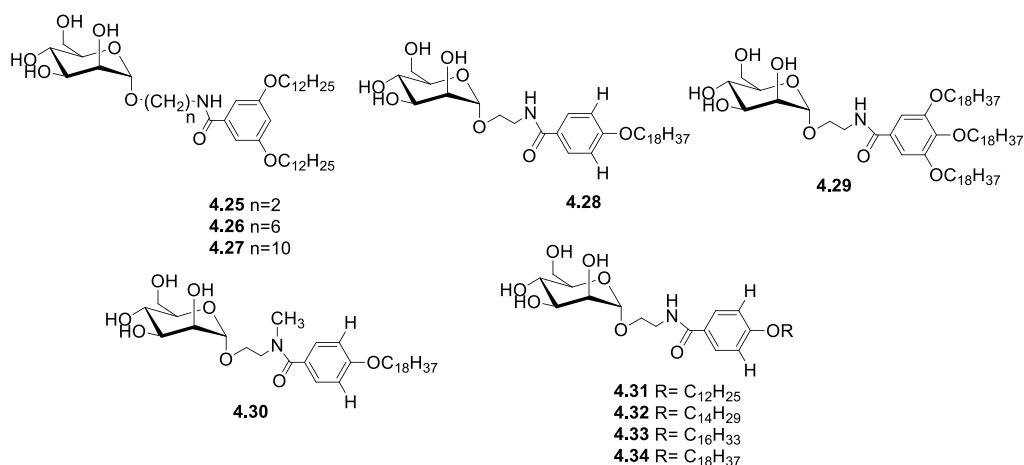


Figure 4.7 Examples of glycolipid analogues possessing one carbohydrate moiety and either one (**4.328**,^[164] **4.31-4.34**^[164]), two (**4.25-4.27**^[165]), or three **4.29**^[164] lipidic chains.

Analogues **4.25-4.27** were synthesised by Tamiaki *et al.* The glycolipids were incorporated into a L- α -phosphatidylcholine liposome and were able to interact with a specific lectin to form liposomal assemblies.^[165] In order to assist in the understanding of protein-carbohydrate interactions, the remaining glycolipid analogues **4.28-4.34** were synthesised as models for natural glycolipids.^[164]

The literature is even sparser with regards to multivalent aromatic glycoconjugates possessing a lipidic chain. One example involves the synthesis of a divalent neoglycopeptide possessing a tetradecylamine chain, **4.35**, is shown in Figure 4.8.^[153] Glycolipid **4.35** was investigated as a potential inhibitor of the binding of verotoxin globotriosylceramide (Gb3) and showed promising results ($IC_{50} = 0.2$ mM).

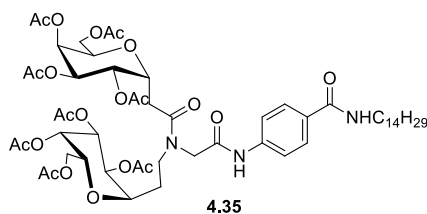


Figure 4.8 Example of divalent glycoconjugate possessing a lipidic chain.^[153]

4.3 Chapter objective

This chapter deals with the synthesis of a variety of aromatic-based glycolipids as potential inhibitors of bacterial adhesion. As can be seen from the introduction, there are extensive examples of these types of compounds reported in the literature, and huge interest lies in the synthesis of glycoconjugates built around an aromatic scaffold. We chose an aromatic-based core as we required a rigid scaffold for comparison against the more flexible aliphatic derivatives described in chapter 3. The objective was to introduce an aromatic scaffold that would allow the synthesis of a bivalent galactosyl ligand but also enable for the introduction of a lipidic chain. As discussed previously, trimesic acid and its derivatives are ideal building blocks in the synthesis of aromatic glycoconjugates. Another appropriate building block for this purpose is the aniline derivative, 5-aminoisophthalic acid, which features two carboxylic acid side groups and a primary amine. This allows for the easier sequential functionalisation of different positions in the aromatic core. Owing to this, both building blocks would provide access to a range of structurally diverse glycolipids which could be investigated for potential biological activities. As before, the aim was to adopt a modular approach utilising a key set of reaction conditions which would enable us to achieve diversity quickly and easily, and also allow for sufficient scale up.

The core building block structures can be seen below in Figure 4.9, where it is clear that the aromatic core would remain constant in all analogues and that variation could be achieved at three potential sites.

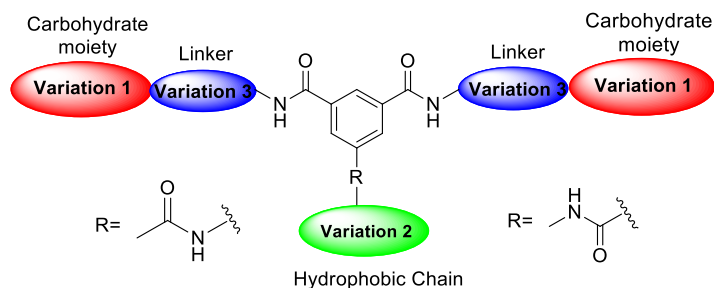


Figure 4.9 Core scaffold utilised for the synthesis of aromatic-based glycoconjugates.

As stated previously, structural information on the bacterial lectins involved in the adhesion process of *B. multivorans* is limited, so the rational design of synthetic ligands as anti-adhesion agents is extremely difficult. For this reason, we aimed to synthesise a variety of ligands and examine how the structure influences the biological activity. As with the aliphatic bivalent ligands (discussed in chapter 3), we sought to investigate how linker length, structure and flexibility influenced the presentation of the carbohydrate moieties and thus the biological result. In addition, we intended to examine whether hydrophobic chain length also played a role in the activity of the aromatic glycoconjugates. For this reason, variation site 1 always remained as a galactosyl moiety, although it could be extended to a different carbohydrate moiety if required. At variation site 2, a hydrophobic chain of varying length (C-3 compared to C-16 and C-14) was utilised. As before, the main variation focused on the chemical structure of the linker. In order to investigate how linker flexibility/rigidity and length affected the conformation and thus the biological activity, we aimed to synthesise a variety of structurally diverse glycoconjugates with different amide linkages between the galactosyl moiety and the aromatic backbone.

In the first type of linkage envisaged, the galactosyl moiety is coupled directly to the aromatic scaffold *via* an *N*-glycosidic bond (**4.36**, **4.37**, Figure 4.10). For the second type of spacer we intended to utilise an ethylene group functionalised with a primary amine to connect the galactose and aromatic core *via* an amide bond (**4.38**, **4.39**, Figure 4.10). With the third type of linker, we aimed to exploit both a triazole moiety and an ethylene group to join the galactose moiety and the aromatic building block (**4.40**, **4.41**, Figure 4.10). In the fourth type of linkage we looked at connecting the galactose to the aromatic scaffold again *via* an *N*-glycosidic bond and a triazole moiety (**4.42**, Figure 4.10). For the final linkage, a glycine-based spacer and an ethylene group were exploited to link the aromatic backbone to the carbohydrate moiety (**4.43**, Figure 4.10).

The ability of the glycoconjugates to act as potential inhibitors of bacterial adhesion was investigated and the results are discussed in chapter 5 (section 5.8). In order to test the multivalent effect we also synthesised a monovalent version of the glycolipid which showed the most promising results (**4.44**, Figure 4.10).

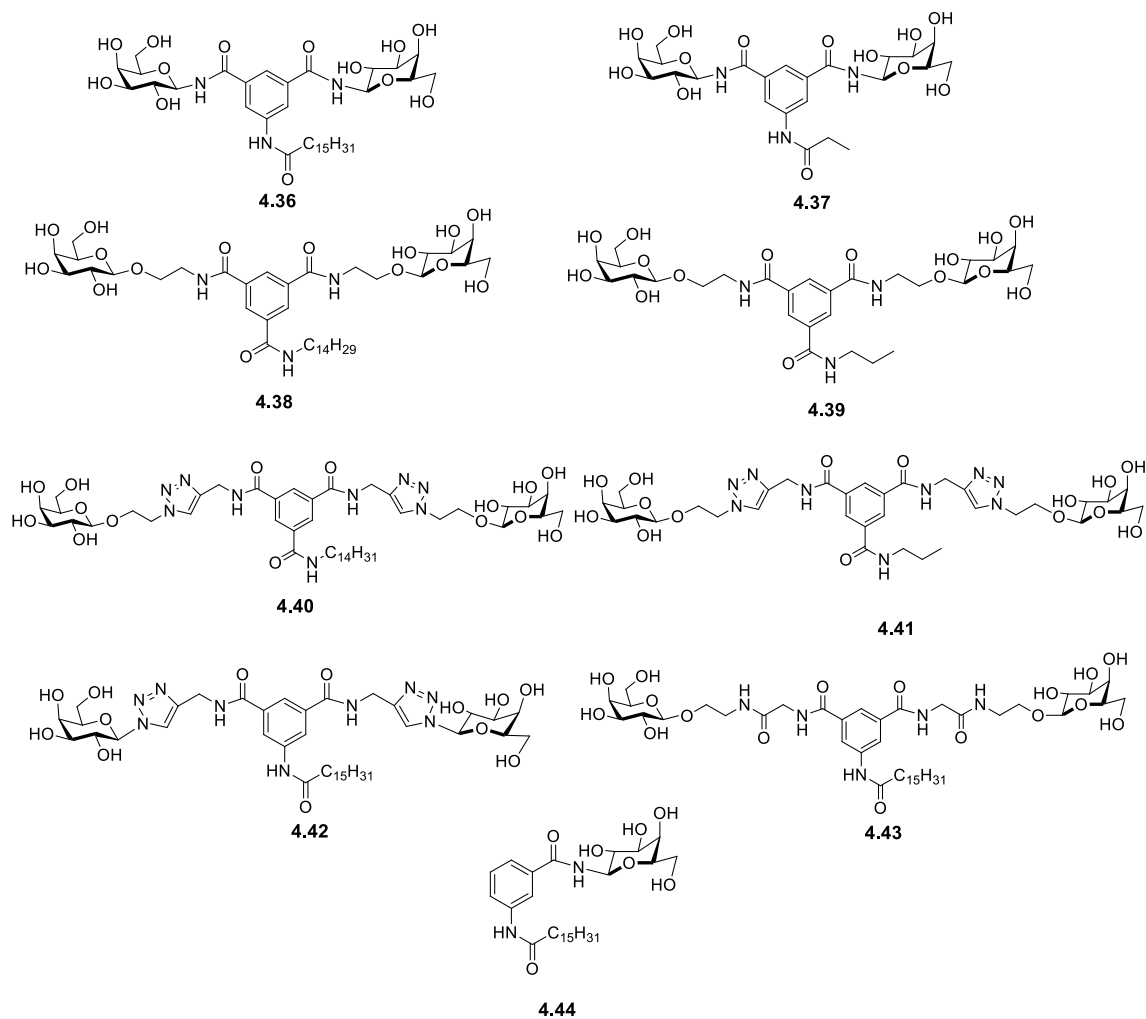


Figure 4.10 Structure of glycoconjugates 4.36-4.44 generated from an aromatic core.

4.3 The synthesis of the first generation of glycolipids 4.38 and 4.39 based on aromatic scaffolds

The aromatic-based *O*-glycolipids analogues 4.38 and 4.39 were designed to act as potential anti-bacterial agents (see chapter 5). Initially the readily available trimesoyl chloride was chosen as the starting material, as it features three acid chloride side groups which would allow for the formation of amide bonds with galactosyl moieties featuring amino groups. Trimesic acid was also utilised, as it contains three carboxylic acid groups which could be activated and again, would enable easy functionalisation. As trimesoyl chloride and trimesic acid were utilised in the synthesis of the first generation derivatives, all first generation glycolipids are connected to the lipidic chain *via* an amide bond of the form ArCONHR (4.45 a, Figure 4.11). In contrast, 5-aminoisophthalic acid is used in the synthesis of the second generation derivatives, therefore, the lipidic chain is linked to the aromatic scaffold *via* an amide bond of the form ArNHCOR (4.45 b, Figure 4.11). These different amide bond forms lead to differences in the distribution of the electron density on the aromatic ring. The anilide of

the second generation derivatives can donate electrons into the aromatic ring leading to more electron-rich aromatic rings in comparison to the first generation derivatives.

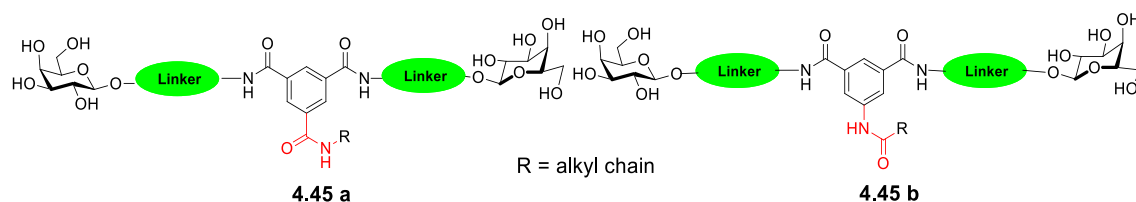
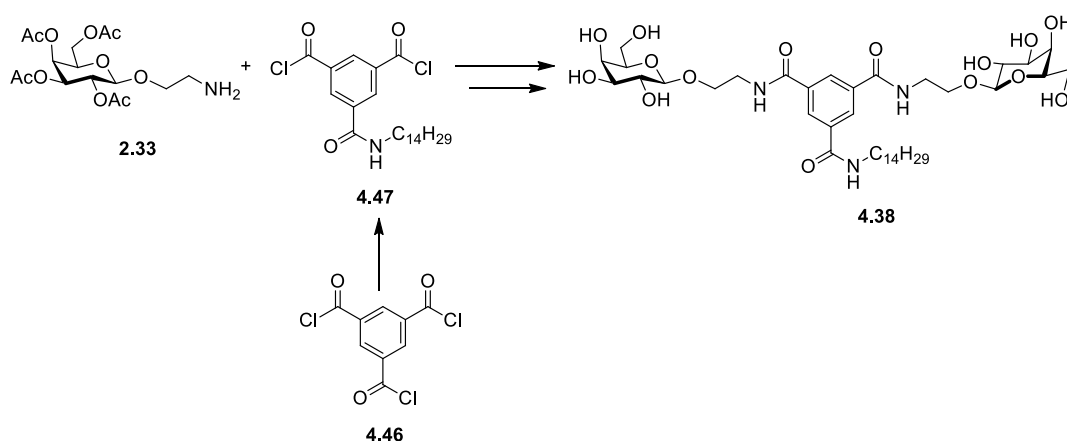


Figure 4.11 Contrasting amide bond formation of first generation **4.45 a** and second generation glycolipids **4.45 b**.

Initial investigations led us to design the synthetic pathway as shown in Scheme 4.2, whereby the easily accessible β -*O*-galactosyl amine **2.33** and the commercially available trimesoyl chloride **4.46** would serve as suitable building blocks. The tetradecylamine chain would be introduced first by careful stoichiometric adjustment, followed by an *in situ* reaction with the galactosyl amine to yield the desired glycoconjugate **4.38** in one easy step. Based on this approach a variety of analogues could be synthesised, although the formation of side products may complicate the purification of the desired products.



Scheme 4.2 Initial synthetic route for synthesis of glycoconjugate **4.38**.

4.3.1 Synthesis of *O*-glycoconjugate **4.38**

The aromatic *O*-glycoconjugate **4.38** was designed as a flexible ligand (Figure 4.12). We believed that the ethylene linker would allow for a certain amount of flexibility for the presentation of the galactosyl moieties.

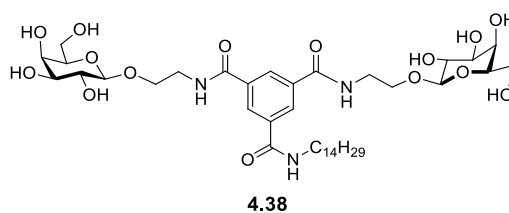
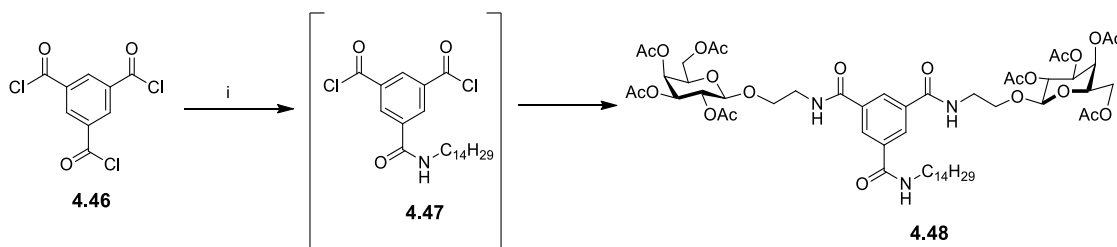


Figure 4.12 Structure of β -glycoconjugate **4.38**.

4.3.1.1 Initial synthesis of aromatic backbone 4.47 utilising trimesoyl chloride

The synthesis of the aromatic backbone **4.47** commenced with the reaction of tetradecylamine with the commercially available trimesoyl chloride **4.46** using NEt_3 (Scheme 4.3). To promote reaction with only one of the three acid chlorides, an *in situ* reaction with the galactosyl amine **2.33** (whose synthesis was discussed in section 2.5.1.1) was carried out. This afforded the desired bivalent glycoconjugate **4.48**, albeit the yield was very low and a variety of by-products were also obtained.



Scheme 4.3 Reagents and Conditions: i) 1) $\text{NH}_2\text{C}_{14}\text{H}_{29}$ (1 eq), NEt_3 , THF, N_2 , 0 °C- rt, 3 h, 2) **2.33** (2 eq), NEt_3 , THF, N_2 , rt, 16 h, 8%.

This result was not totally surprising. There are many examples reported in the literature which utilise trimesoyl chloride for the synthesis of functionalised aromatic analogues.^[159c, 166] In most examples, however, all three acid chloride groups are being reacted with the same amine. In our case, selective functionalisation is challenging, as two different amines are being utilised and this can therefore lead to a mixture of products.

The main product isolated was the tri-tetradecyl substituted derivative **4.50** (Figure 4.13). The benzene derivative, containing one galactose moiety and two lipidic chains, **4.49**, was also obtained.

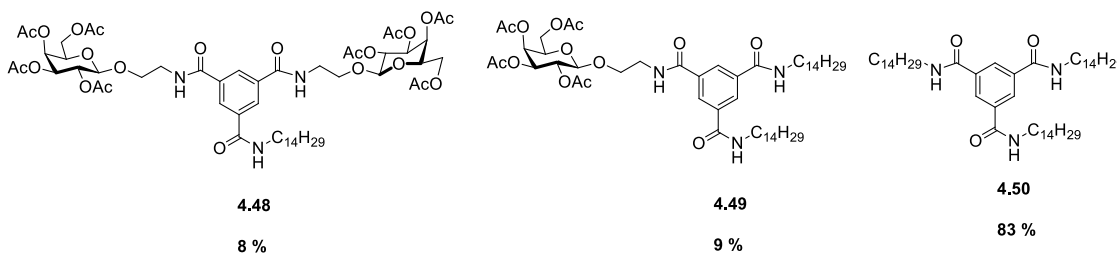
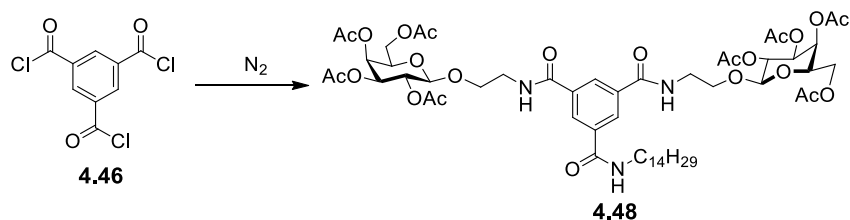


Figure 4.13 Structure of by-products isolated from reaction of trimesoyl chloride with tetradecylamine and the galactosyl amine **2.33**.

With this in mind, we decided to readdress our synthetic approach and a variety of different reactions and conditions were attempted. The results are summarised in Table 4.2.



Entry	NH ₂ C ₁₄ H ₂₉	Addition conditions	Galactose ethyl amine 2.33	Addition conditions	Solvent	MeOH	Product
1	1 eq	added over 3 h at 0 °C at high dilution	N/a	N/a	THF	No	4.50 (56%)
2	0.33 eq	added over 3 h at 0 °C at high dilution	N/a	N/a	THF	No	4.50-4.52 (did not isolate)
3	0.33 eq	over 3 h at 0 °C at high dilution	N/a	N/a	THF	Yes	4.53-4.55 (could not separate)
4	1 eq	added second after 2.33 at medium dilution	2 eq	added first over 3 h at 0 °C at high dilution	THF	No	4.50, 4.49, 4.48 (39%, 22%, 18%)
5	0.33 eq	added first over 3 h at 0 °C at high dilution	2 eq	added second, quickly at rt at low dilution	THF	No	4.50, 4.49, 4.48 (6:2:1 ratio)
6	1 eq	added first over 3 h at 0 °C at high dilution	2 eq	added second, quickly at rt at low dilution	DCM	No	4.50, 4.49, 4.48 (8:1:0.5 ratio)

Table 4.2 Reaction conditions attempted for the formation of divalent glycolipid **4.48**

Additional by-products formed during the attempted synthesis of glycolipid **4.48** are shown in Figure 4.14.

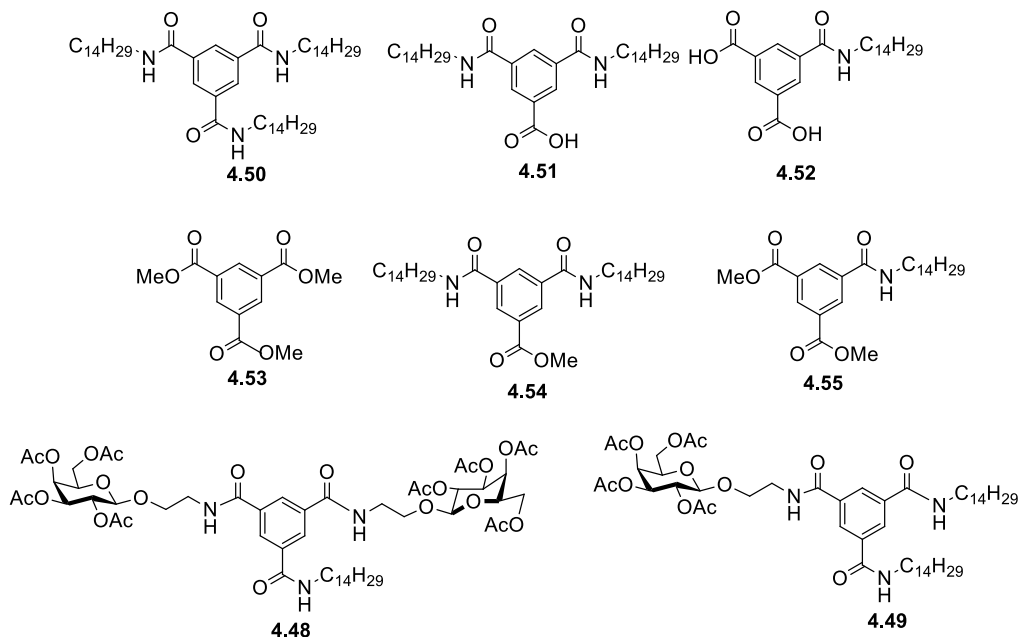


Figure 4.14 Additional products formed in the synthesis of glycolipid **4.48** using a variety of reaction conditions.

For our next approach, the synthesis again started with the trimesoyl chloride, but unlike previously we attempted to isolate the diacid mono-tetradecyl derivative **4.52** prior to reaction with the galactose ethyl amine **2.33** (Table 4.2, entry 1). The reaction was carried out in a 1:1 ratio of trimesoyl chloride and tetradecylamine and this time the addition of the amine was carried out at a high dilution over a period of 3 h at 0 °C. Nevertheless, upon purification the tri-substituted derivative **4.50** was still isolated as the major product. The reaction was repeated, using a 3:1 ratio of trimesoyl chloride to tetradecylamine. We hoped this would lessen the formation of the tri-substituted derivative **4.50** (Table 4.2, entry 2). Under these conditions the results slightly improved and the mono-, di- and tri-substituted products **4.50-4.52** were obtained. However, we hypothesised that the acid chlorides had hydrolysed during isolation of the products and this led to difficulties in purification. HR-MS confirmed this hydrolysis.

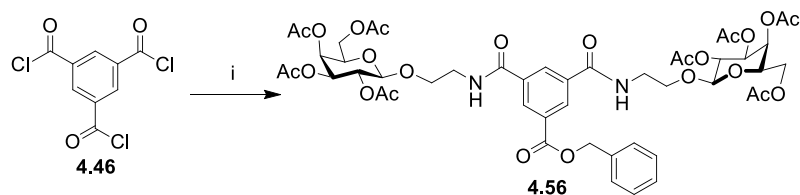
Due to the purification problems posed by the hydrolysis of the acid chlorides, a new approach was required. The reaction was carried out as before (3:1 ratio), but this time MeOH was added to the crude mixture after the reaction was complete (Table 4.2, entry 3). We believed that the addition of MeOH would result in the formation of methyl esters, which may enable more efficient separation of the reaction products. To our delight a white solid precipitated upon addition of the MeOH, and a large singlet at 4 ppm in the ^1H NMR spectrum indicated the

presence of methyl esters. Unfortunately, purification still proved problematic. Although the presence of the mono-substituted **4.54** and di-substituted **4.55** products were confirmed by HR-MS, the compounds could not be separated using column chromatography as the two products eluted together.

Finally, we reverted back to the original one pot reaction method, and attempted to optimise the reaction conditions. A number of variations were examined including addition order and alteration of the number of eq. and solvent used (Table 4.2, entries 4-6). Even with the alterations in the reaction conditions, the tri-substituted tetradecyl derivative was always the major product **4.50**. This led us to believe that the poor nucleophilicity of the galactose ethyl amine **2.33** may also be a factor in the poor yields of the product.

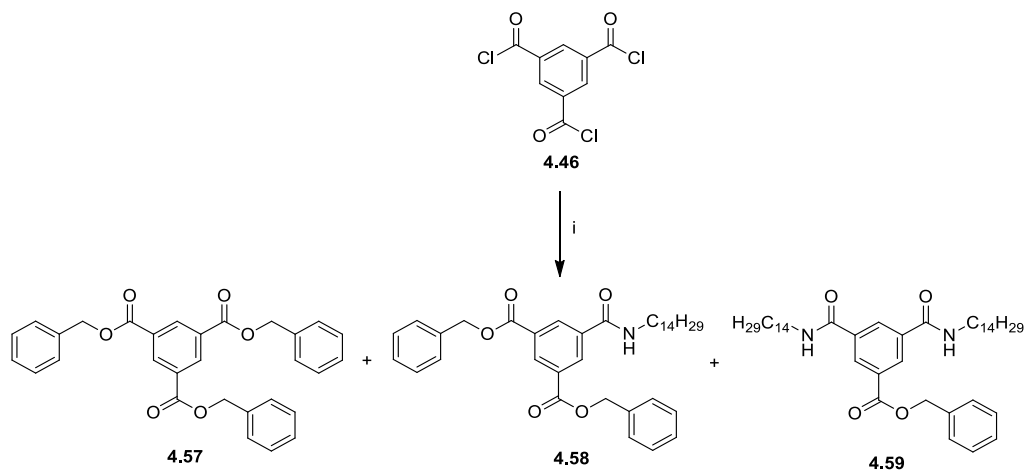
As a result of the problems encountered it was decided to re-address the synthetic route. In order to avoid preferential formation of the tri-substituted product **4.50**, we attempted to temporarily protect one of the carboxylic acids groups as a benzyl ester, which could be removed at a later stage.

For this approach, phenylmethanol was reacted with trimesoyl chloride **4.46** in the presence of base (Scheme 4.4). The reaction was carried out in a 1:1 ratio and as before the benzyl alcohol was added in high dilution at 0 °C over a period of 3 h. An *in situ* reaction with the galactose ethyl amine **2.33** was then performed (the galactosyl amine **2.33** was added in very low dilution very quickly in order to increase the chance of reaction with the acid chloride). The desired di-substituted galactose glycoconjugate **4.56** was obtained in 7% yield.



Scheme 4.4 Reagents and Conditions: i) 1) C₆H₅CH₂OH (1 eq), DIPEA, THF, N₂, 0 °C- rt, 3 h, 2) **2.33** (2 eq), DIPEA, THF, N₂, rt, 16 h, 7%.

Nonetheless, a low yield was again observed and implied that the nucleophilicity of the galactose ethyl amine **2.33** was a problem. Following on from this, the next reaction attempted was between phenylmethanol and trimesoyl chloride followed by the *in situ* addition of tetradecylamine (Scheme 4.5). Nevertheless, like with so many previous reactions, ¹H NMR analysis indicated that a mixture of products **4.57-4.59** formed and which could not be separated.

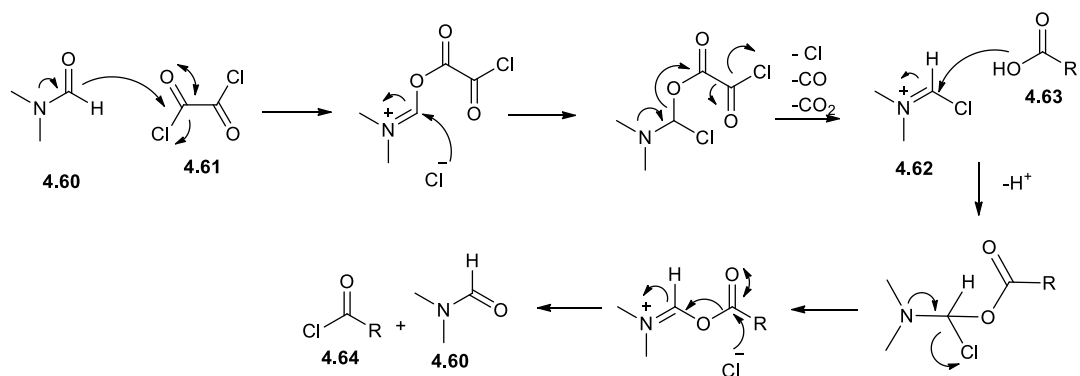


Scheme 4.5 Reagents and Conditions: i) 1) C₆H₅CH₂OH (2 eq), DIPEA, THF, N₂, 0 °C- rt, 3 h, 2) NH₂C₁₄H₂₉ (1 eq), DIPEA, THF, N₂, rt, 16 h.

4.3.1.2 Attempted Synthesis of Aromatic backbone 4.47 utilising trimesic acid

The results from the experiments above show that the trimesoyl chloride seems to be extremely susceptible to reaction with the tetradecylamine and phenylmethanol. The high reactivity of acid chlorides is widely reported in the literature, and supports why they are commonly utilised in amide bond forming reactions.^[167] Nonetheless, one drawback lies in their susceptibility to hydrolysis. In our case, the high reactivity of the trimesoyl chloride is a disadvantage, as it means achieving selective mono-substitution may be difficult. Trimesic acid has also been widely utilised in the synthesis of aromatic glycoconjugates.^[163b, 168] Therefore, we again re-addressed our synthetic approach and attempted using trimesic acid as an alternative to trimesoyl chloride. The idea was to activate only one of the three carboxylic acid side groups, therefore, making mono-substitution more likely. Two approaches were attempted: i) activation *via* standard HOBt, TBTU methodology, and ii) activation *via* formation of one acid chloride.

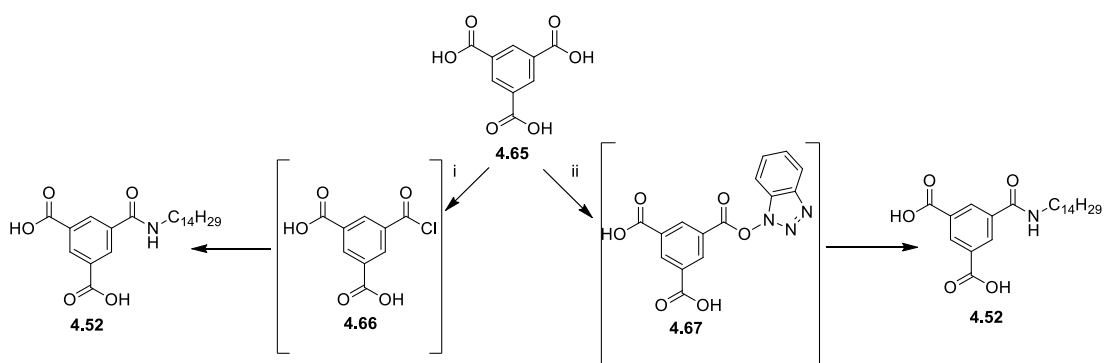
The activation of carboxylic acids using HOBt and TBTU was previously discussed in Chapter 2 (section 2.5.1). The formation of acid chlorides is one of the easiest ways to activate a carboxylic acid and make it more susceptible to nucleophilic attack.^[87] Reagents commonly used to generate acid chlorides from their corresponding acids include thionyl chloride,^[169] oxalyl chloride,^[170] phosphorus oxychloride^[171] and phosphorus pentachloride. In our case, oxalyl chloride with catalytic DMF was used. The mechanism is shown in Scheme 4.6.



Scheme 4.6 Mechanism of acid chloride formation using oxalyl chloride and catalytic DMF.

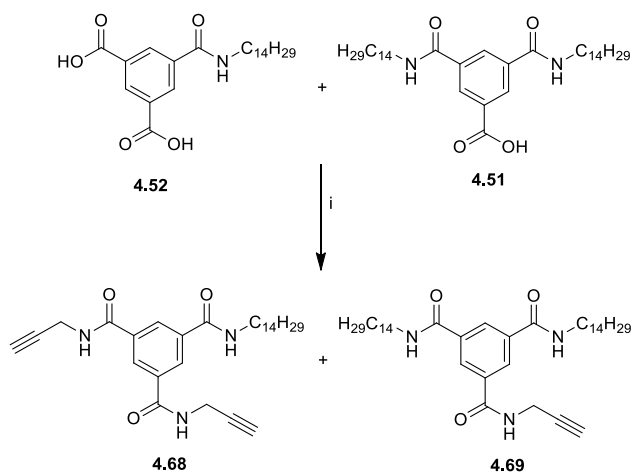
In the first step, the oxalyl chloride **4.61** reacts with DMF **4.60** to yield the iminium intermediate **4.62**, with loss of CO , CO_2 and Cl^- which then reacts with the carboxylic acid **4.63** to form the acid chloride **4.64** and the regenerated DMF catalyst.

Scheme 4.7 depicts the outcome of attempted activation of one of the carboxylic acids of trimesic acid **4.65** utilising both acid chloride formation (reaction conditions i) or HOBT/TBTU methodology (reaction conditions ii). The active intermediates generated would be the corresponding acid chloride **4.66** and active ester **4.67**, respectively.



Scheme 4.7 Reagents and Conditions: i) 1) Oxalyl chloride, DMF, DCM, N_2 , 0°C , 1 h, 2) $\text{NH}_2\text{C}_{14}\text{H}_{29}$, NEt_3 , 0°C - rt, 16 h; ii) HOBT (1 eq), TBTU (1 eq), DMF, NEt_3 , N_2 , 10 min, 2) $\text{NH}_2\text{C}_{14}\text{H}_{29}$, 16 h.

In both cases, we encountered the same problems as before. The crude mixtures showed a number of products, and ^1H NMR analysis indicated the presence of both the mono-substituted **4.52** and di-substituted **4.51** compounds. In order to fully confirm the presence of the two compounds we decided to react both crude mixtures with propargylamine using HOBT and TBTU in the presence of base, and attempt separation afterwards (Scheme 4.8).



Scheme 4.8 Reagents and conditions: i) 1) HOBt (3 eq), TBTU (3 eq), DMF, NEt_3 , N_2 , 10 min, 2) $\text{HCCCH}_2\text{NH}_2$ (3 eq), 16 h, 8% and 11%.

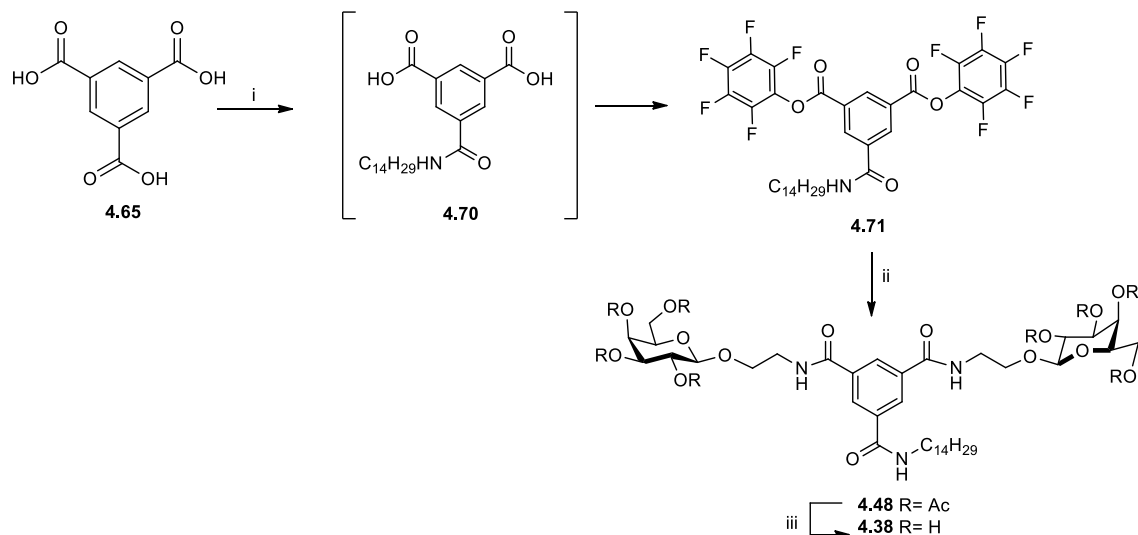
The reaction confirmed what we had expected and both the mono-substituted tetradecyl derivative **4.68** and the di-substituted tetradecyl derivative **4.69** were observed in the crude reaction mixture. Unfortunately, purification still proved difficult. Integration of the corresponding signals in the ^1H NMR spectrum implied that the di-substituted derivative **4.69** was obtained in a slightly higher conversion of 11% in comparison to 8% of the mono-substituted product **4.68**, but the low yields demonstrated the difficulties in the approach.

4.3.1.3 Synthesis of glycolipid **4.48** via pentafluorophenyl (PFP) esters

Further literature research led to our interest in the use of activated esters in amide bond forming reactions. Activated esters are extremely advantageous as they can be isolated and purified. This means they can be synthesised in advance and stored over a period of time.^[87] They are generally prepared using standard ester-formation reagents such as DCC and DIC.^[172] Activated esters react more cleanly with amines under mild conditions and therefore produce fewer side reactions during coupling.^[167] One of the most commonly used active esters is pentafluorophenyl esters,^[173] which have been commonly utilised since they were first reported in 1974.^[174]

Owing to this, we attempted to synthesise the pentafluorophenyl ester of aromatic diacid **4.70**. We hoped that subsequent reaction with the galactose ethyl amine **2.33** would thus lead to an improved yield of the desired bivalent glycolipid **4.48**. The synthesis commenced with the selective activation of trimesic acid (discussed previously, section 4.3.1.2) using HOBt and TBTU to give diacid **4.70**. This time, the HOBt/TBTU, base and tetradecylamine were added to trimesic acid solution portion-wise. The resulting crude reaction mixture was dissolved in dry THF along with pentafluorophenol, and DIC was added dropwise at 0°C .^[175] Following column

chromatography the desired mono-substituted, di-activated derivative **4.71** was obtained in 24% yield over two steps (Scheme 4.9). Formation of a number of other by-products, including the corresponding tri-pentafluorophenyl ester, was also observed, albeit, the products were not isolated.



Scheme 4.9 Reagents and Conditions: i) 1) HOBT, TBTU, DMF, NEt_3 , N_2 , 10 min, $\text{NH}_2\text{C}_{14}\text{H}_{29}$, 16 h 2) THF, $\text{C}_6\text{F}_5\text{OH}$, DIC, 0°C – rt, 3 h, 24% over two steps; ii) **2.33**, THF, NEt_3 , N_2 , 16 h, 47%; iii) NEt_3 , DCM/ H_2O / MeOH , 40°C , 20 h, 78%.

The pentafluorophenyl ester derivative **4.71** was then reacted with the galactosyl amine **2.33** in the presence of base to yield the divalent galactose glycolipid **4.48** in an improved yield of 47%. Finally, selective deprotection of the acetyl groups using catalytic NEt_3 in a heterogeneous solvent system (DCM/ MeOH / H_2O , 1:2:1) at 40°C afforded the novel *O*-glycoconjugate **4.38** as a white precipitate in 78% yield (Scheme 4.9). As discussed in earlier chapters, mild deprotection conditions were attempted as we feared the harsher conditions, such as Zémlen conditions, may result in degradation of the glycolipid. The ^1H NMR spectrum of the deprotected *O*-glycoconjugate, **4.38**, is shown in Figure 4.15, with characteristic peaks such as the amide (NH), aromatic (ArH*), anomeric (H-1) and tetradecyl protons highlighted. It is clear from the ^1H NMR spectrum that the desired bivalent glycolipid has been synthesised, since all expected peaks are present and integrate correctly. For example, the anomeric proton of the galactose moiety (labelled H-1 on ^1H NMR spectrum) integrates for two protons, indicating that two galactose moieties are in fact present. In comparison, the terminal methyl group of the tetradecyl chain integrates for three protons confirming the presence of only one hydrocarbon chain.

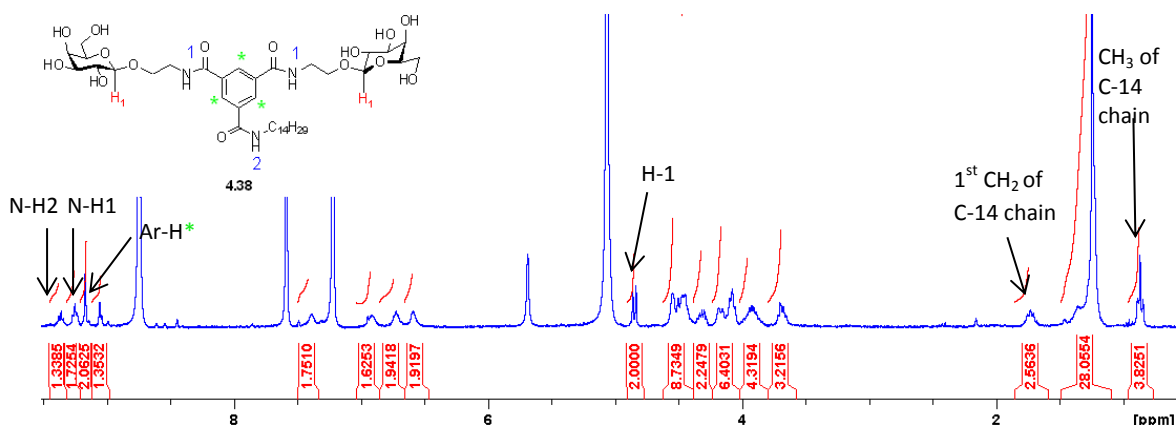


Figure 4.15 ^1H NMR spectrum of bivalent deprotected *O*-glycolipid **4.38** (300 MHz, d_5 -Pyr).

4.3.2 Synthesis of *O*-glycoconjugate **4.39**

In order to investigate the effect of the hydrocarbon chain length on the activity of the glycoconjugate, the aromatic *O*-glycoconjugate **4.39** was synthesised (Figure 4.16). Again It was designed to act as a flexible molecule utilising the same ethyl linker as glycoconjugate **4.38**, though this time the glycolipid contains a short C-3 hydrophobic chain instead of the longer C-14 one.

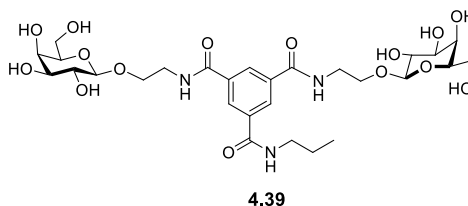
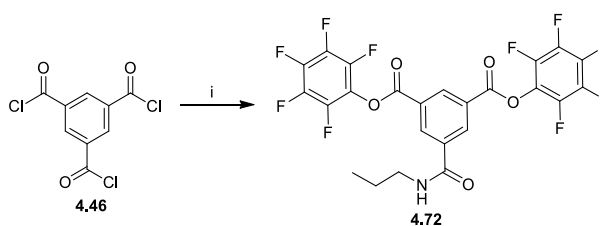


Figure 4.16 Structure of β -*O*-glycoconjugate **4.39**.

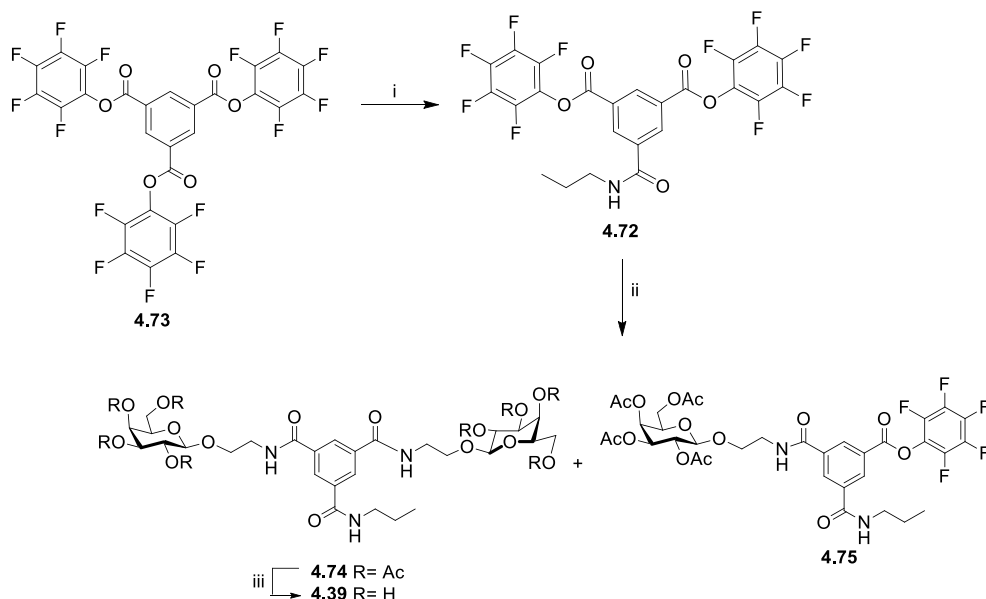
4.3.2.1 Synthesis of aromatic core **4.72**

We followed the same approach as discussed above for the synthesis of glycoconjugate **4.38** and utilised the active pentafluorophenyl esters to attain coupling to the galactose ethyl amine **2.33**. The synthesis started with nucleophilic addition of propylamine to trimesoyl chloride in the presence of base. As before, the propylamine was added in high dilution, at 0 °C over a period of 3 h. An *in situ* reaction with pentafluorophenol yielded the aromatic scaffold **4.72**, but in a low yield of 20% (Scheme 4.10).



Scheme 4.10 Reagents and Conditions: i) DIPEA, $\text{NH}_2\text{C}_3\text{H}_7$, THF, N_2 , 0 °C, 3 h, 2) $\text{C}_6\text{F}_5\text{OH}$, DIPEA, rt, 16 h, 20% over two steps.

Surprisingly, the main product isolated was the aromatic derivative containing three pentafluorophenyl esters **4.73**. This was in complete contrast to what was previously observed, as usually the tri-amide was found to be the major product. We chose to use this to our advantage and reacted the tri-pentafluorophenyl derivative **4.73** with 1 eq of propylamine in the presence of base. To our delight, the desired mono-substituted derivative **4.72** was attained in a high yield of 88% (Scheme 4.11).



Scheme 4.11 Reagents and Conditions: i) DIPEA, $\text{NH}_2\text{C}_3\text{H}_7$, THF, N_2 , 0°C , 16 h, 88%; ii) **2.33**, DIPEA, THF, N_2 , rt, 18 h, 40% (**4.74**) and 36% (**4.75**); iii) NEt_3 , $\text{DCM}/\text{H}_2\text{O}/\text{MeOH}$, 40°C , 20 h, 98%.

The desired short chain, bivalent galactose glycoconjugate **4.74** was obtained in a moderate yield of 40% by reaction of the galactose ethyl amine **2.33** with the pentafluorophenyl ester **4.72** in the presence of base (Scheme 4.11). A monovalent galactose derivative **4.75**, with one pentafluorophenol ester still remaining, was also isolated but in a lower yield of 30%. This again highlighted the poor nucleophilicity of the galactose ethyl amine **2.33**. This monovalent derivative **4.75** was also a very interesting product, as it meant the synthesis of asymmetric glycoconjugates may also be possible, following this approach. This was investigated and is discussed in section 4.9.

Deprotection of the aromatic-based glycoconjugate **4.74** using NEt_3 afforded the novel *O*-glycoconjugate **4.39** as a white precipitate in 98% yield. The ^1H NMR spectrum of *O*-glycoconjugate **4.39** is displayed in Figure 4.17, with significant peaks, including the amide (NH), anomeric (Ar-H) and aromatic (H-1) protons, highlighted.

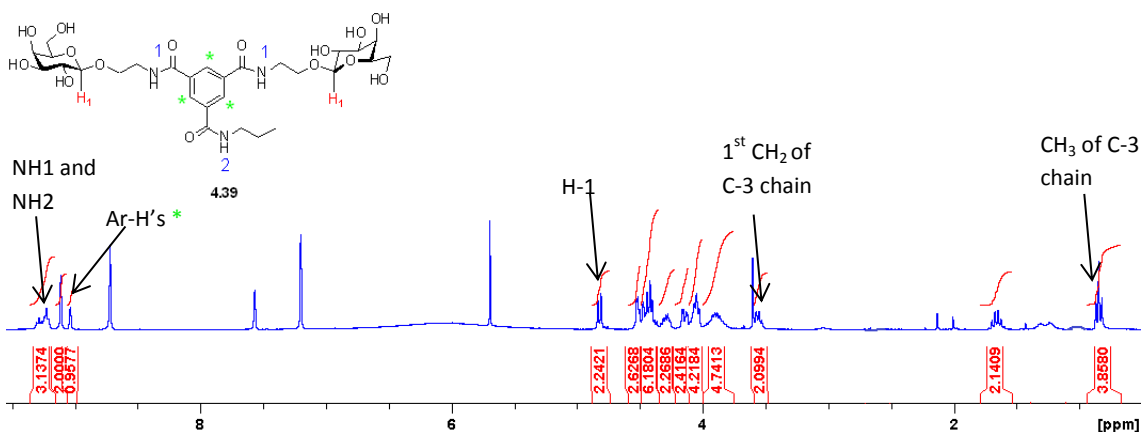


Figure 4.17 ^1H NMR spectrum of bivalent deprotected *O*-glycolipid **4.39** (300 MHz, d_5 -Pyr).

4.4 The synthesis of first generation triazole containing glycolipids **4.40** and **4.41** based on aromatic scaffolds

As part of our on-going studies into the potential anti-microbial activity of bivalent aromatic glycoconjugates, we were interested in synthesising the 1,4 di-substituted 1,2,3-triazole *O*-glycolipids **4.40** and **4.41** (Figure 4.18). There are many examples of triazole-containing compounds, as discussed in the introduction to this chapter, and in most cases high affinities towards the lectin of interest were observed. 1,4-Disubstituted 1,2,3-triazoles are of high biological interest as they possess high chemical stability, display aromatic character and can act as hydrogen bond acceptors.^[176] This means they can mimic the electronic properties and atom arrangement of peptide bonds, without being susceptible to hydrolytic cleavage.^[177] Ultimately, these glycoconjugates **4.40-4.41** were designed to probe how introducing aromaticity into the linker may affect their anti-microbial activity.

As with the glycoconjugates discussed previously, the *O*-glycoconjugates **4.40** and **4.41** are linked to the aromatic scaffold *via* an ethylene chain which should allow for a certain degree of conformational flexibility. The spacer also contains a triazole moiety which can impart a certain amount of rigidity to the molecule. Therefore, the presence of the triazole moiety could influence the conformation of the glycoconjugate and thus its biological activity. Glycolipids **4.40** and **4.41** (Figure 4.18) differ only by the length of lipidic chain attached, as again we wanted to investigate how hydrophobic chain length influenced anti-microbial activity.

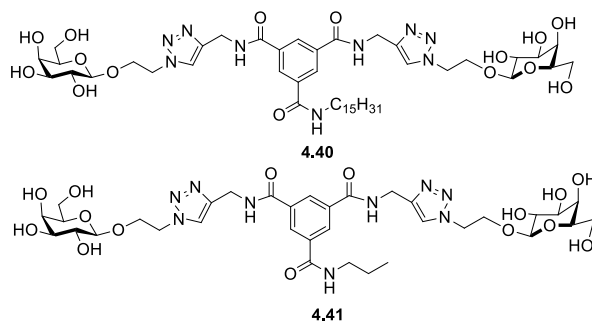
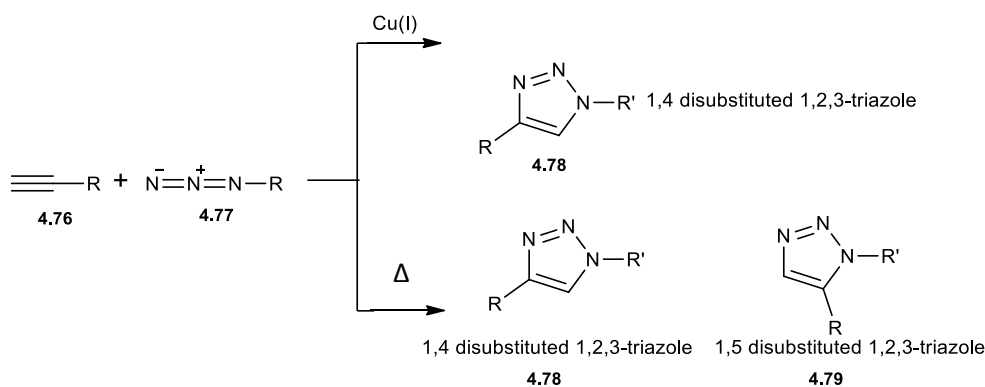


Figure 4.18 Structure of triazole-containing glycoconjugates **4.40** and **4.41**.

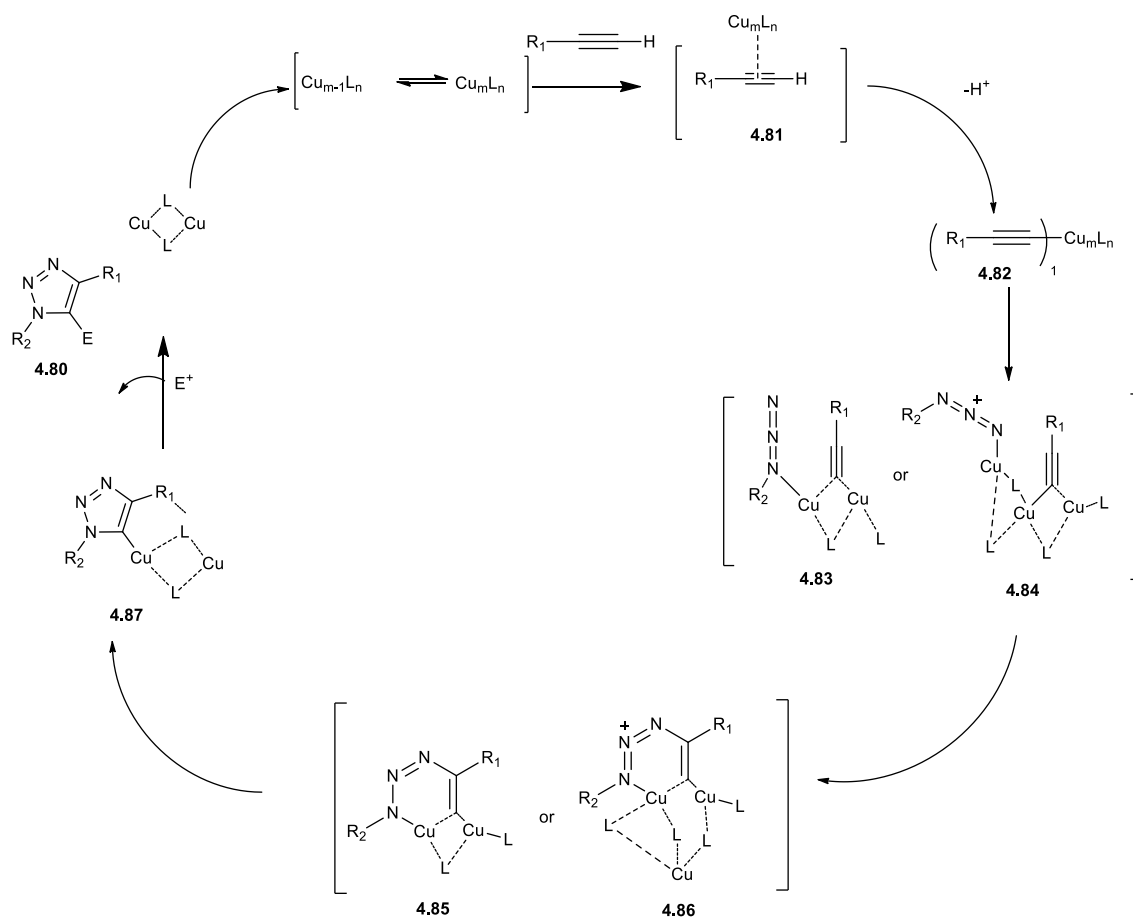
4.4.1 Cu catalysed azide-alkyne cycloaddition (CuAAC)

The synthesis of 1,4 di-substituted 1,2,3-triazoles occurs *via* a copper(I) catalysed azide-alkyne cycloaddition (CuAAC) reported independently by the Meldal group in Denmark,^[178] and Sharpless and Fokin in the U.S.^[179] Prior to their reports, the uncatalysed Huisgen 1,3-dipolar cycloaddition was utilised in the synthesis of substituted triazoles. However, it had many drawbacks.^[180] The Huisgen 1,3-dipolar cycloaddition required high temperatures, long reaction times and provided mixtures of 1,4- and 1,5-triazole regioisomers (**4.78** and **4.79**, respectively). In contrast, the copper catalysed reaction transforms organic azides (**4.77**) and terminal alkynes (**4.76**) into the 1,4 di-substituted 1,2,3-triazoles (**4.78**) exclusively, without the need for elevated temperatures (Scheme 4.12).^[176]



Scheme 4.12 Huisgen 1,3-dipolar cycloaddition of azides and alkynes usually requires prolonged heating and results in mixtures of both 1,4- and 1,5-regioisomers (bottom), whereas CuAAC produces only 1,4-di-substituted-1,2,3-triazoles in excellent yields at rt (top).

The proposed mechanism for the CuAAC reaction is shown in Scheme 4.13.^[181] The classical thermal cycloaddition proceeds *via* a concerted mechanism, however, DFT calculations provided evidence that the CuAAC reaction follows a stepwise mechanism.^[182]

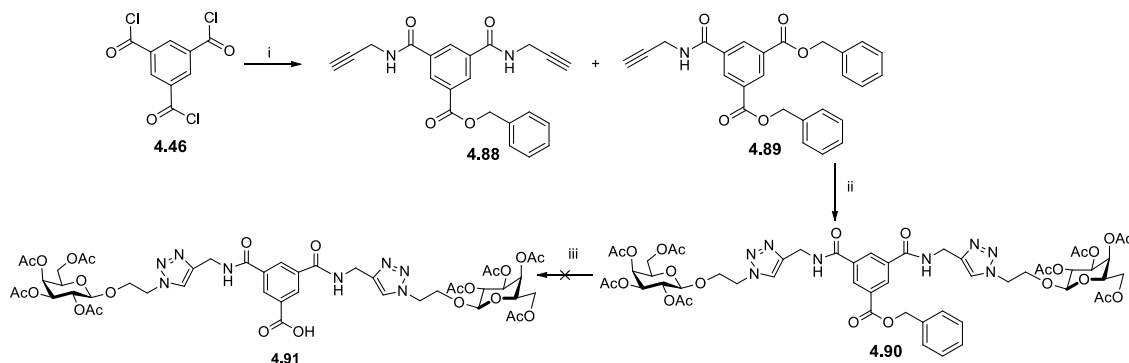


Scheme 4.13 Outline of plausible mechanism for the Cu(I) catalyzed reaction between organic azides and terminal alkynes.^[183]

π coordination of the terminal alkyne to a copper(I) species to form the copper(I) acetylide complex **4.81** initiates the catalytic cycle. As a result, the alkyne proton becomes more acidic and can therefore be abstracted (generally under basic conditions) to form the δ -acetylide intermediate **4.82**. In the next step, a copper ion coordinates to the azide group as shown in transition states **4.83** and **4.84**.^[182] Kinetic studies and structural evidence suggest that the acetylide and azide may not be bound to the same copper atoms as in **4.83**, but instead to two different copper atoms as in **4.84**.^[178] During the transition state, two possibilities for coordination and delivery of the azide to the alkyne have been suggested **4.85** or **4.86**. It is believed that complexation between the azide and copper atom leads to the azide being susceptible to nucleophilic attack at the secondary carbon of the acetylide, generating the regioselective metallocene intermediates **4.85** and **4.86**. Ring contraction yields the metallated triazole **4.87**. Finally, electrophilic attack at the triazole yields the desired 1,2,3-triazole **4.80**, with dissociation leading to the regeneration of the copper catalyst, thus ending the catalytic cycle.^[181-183]

4.4.2 Synthesis of β -O-glycoconjugate **4.40**

The synthesis began with the reaction of trimesoyl chloride and benzyl alcohol using DIPEA, followed by an *in situ* reaction with propargylamine to yield the di-alkynyl derivative **4.88** in a low yield of 20% (Scheme 4.14). As discussed for the previous reactions, the mono-substituted alkynyl derivative **4.89** was also isolated, albeit in a lower yield of 9%.

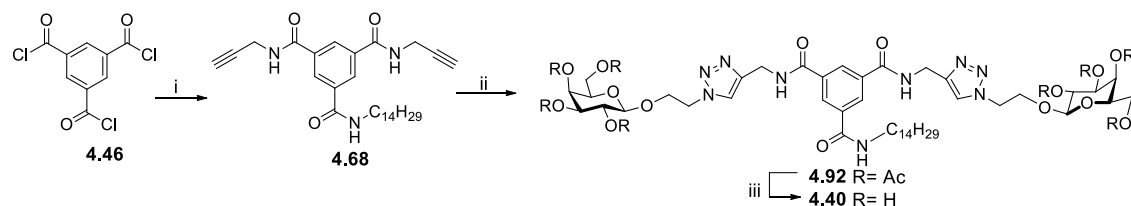


Scheme 4.14 Reagents and Conditions: i) 1) $C_6H_5CH_2OH$ (1 eq), THF, DIPEA, N_2 , 0 °C, 3h, 2) NH_2CH_2CCH (2 eq), DIPEA, rt, 16 h, 20%; ii) **2.44**, $CuSO_4 \cdot 5H_2O$, Sodium ascorbate, DCM/Acetone/ H_2O , 20 h, 58%; iii) H_2 , Pd/C, EtOAc, 4-48 h.

A subsequent CuAAC reaction with the galactosyl azide **2.44** (previously synthesised in Chapter 2, section 2.5.1.1) using a promoter system of $CuSO_4 \cdot 5H_2O$ and sodium ascorbate, afforded the 1,4-di-substituted 1,2,3-triazole glycolipid **4.90** in a regiospecific manner and in a moderate yield of 58%. Unfortunately, the next step which involved hydrogenolysis of the benzyl ester using H_2 and Pd/C, proved unsuccessful. The reaction was attempted at rt, with bubbling H_2 through the reaction mixture and utilising EtOH as the solvent, but in all cases the desired product **4.91** was not obtained. Instead, only the starting material **4.90** was isolated. Increasing the reaction temperature to 50 °C also proved unsuccessful and a further increase to 70 °C resulted in the degradation of compound **4.90**.

As a result of the problems encountered our synthetic approach was modified. It was decided to utilise the di-alkynyl derivative **4.68** discussed previously in section 4.2.1, however, this time the compound was synthesised *via* an alternative method. Trimesoyl chloride was reacted directly with the tetradecylamine followed by the addition of propargylamine after a period of 3 h. Nonetheless, a mixture of products was obtained and isolation of the desired derivative **4.68** was complicated by the presence of side-products. However, as 1H NMR spectral analysis indicated that the desired di-alkynyl **4.68** was the major product the crude mixture was reacted on without further purification. A CuAAC reaction with the galactose ethyl azide **2.44**, using $CuSO_4 \cdot 5H_2O$ and sodium ascorbate as promoters afforded the desired bivalent galactose glycolipid **4.92** in 54% yield. Global deacetylation using catalytic NEt_3 in a heterogenous solvent

system (DCM/MeOH/H₂O, 1:2:1) at 40 °C afforded the novel *O*-glycoconjugate **4.40** as a white precipitate in 90% yield (Scheme 4.15).



Scheme 4.15 Reagents and conditions: i) NH₂C₁₄H₂₉, THF, DIPEA, N₂, 0 °C, 3h, NH₂CH₂CCH, DIPEA, rt, 16 h; ii) **2.44**, CuSO₄·5H₂O, Sodium ascorbate, DCM/Acetone/H₂O, 20 h, 54% over two steps; iii) NEt₃, DCM/H₂O/MeOH, 40 °C, 20 h, 90%.

The ¹H NMR spectrum of β-*O*-glycolipid **4.40** can be seen in Figure 4.19. Characteristic peaks, including the anomeric proton (H-1), aromatic protons (Ar-H*), amide protons (N-H), and triazole protons (CCHN₃*), are assigned.

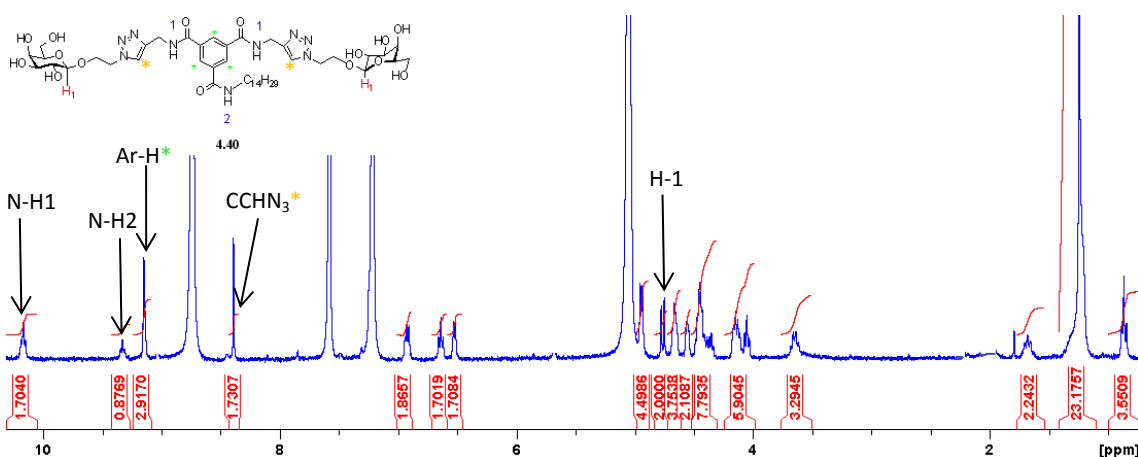
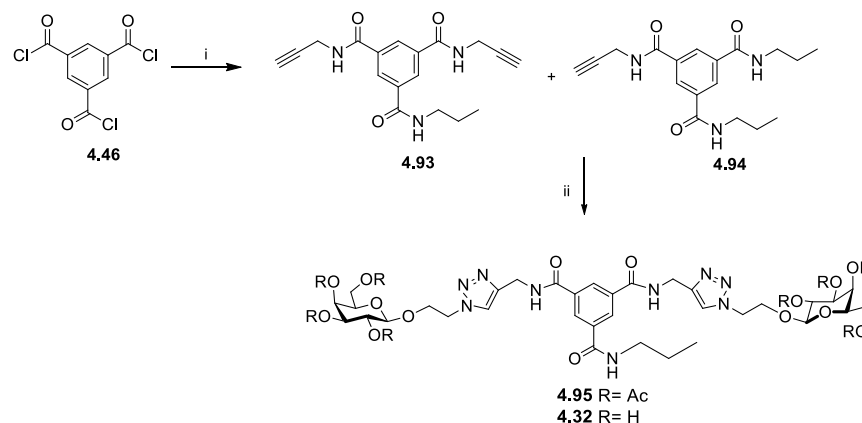


Figure 4.19 ¹H NMR spectrum of bivalent deprotected *O*-glycolipid **4.40** (300 MHz, *d*₅-Pyr).

4.4.3 Synthesis of β-*O*-glycoconjugate **4.41**

Following the same approach as described above, the synthesis of glycoconjugate **4.41** proceeded smoothly. Propylamine was added over a period of 3 h to trimesoyl chloride **4.46** in the presence of base. An *in situ* reaction with propargylamine afforded a mixture of products which was used without further purification (Scheme 4.16). A successive Cu(I) catalyzed cycloaddition using a promoter system of CuSO₄·5H₂O and sodium ascorbate yielded 57% of the protected β-*O*-glycoconjugate **4.95**. Finally, selective deprotection using the mild conditions of NEt₃ in a heterogeneous solvent system (DCM/MeOH/H₂O, 1:2:1) led to the synthesis of the deprotected, bivalent β-*O*-glycoconjugate **4.41** in a high yield of 93%. The ¹H NMR spectrum of *O*-glycoconjugate **4.41** is displayed in Figure 4.20 with significant peaks assigned.



Scheme 4.16 Reagents and conditions: i) $\text{NH}_2\text{C}_3\text{H}_7$, THF, DIPEA, N_2 , 0°C , 3h, $\text{NH}_2\text{CH}_2\text{CCH}_3$, DIPEA, rt, 16 h; ii) **2.44**, $\text{CuSO}_4 \cdot 5\text{H}_2\text{O}$, sodium ascorbate, DCM/Acetone/ H_2O , 20 h, 57%; iii) NEt_3 , DCM/ H_2O /MeOH, 40°C , 20 h, 93%.

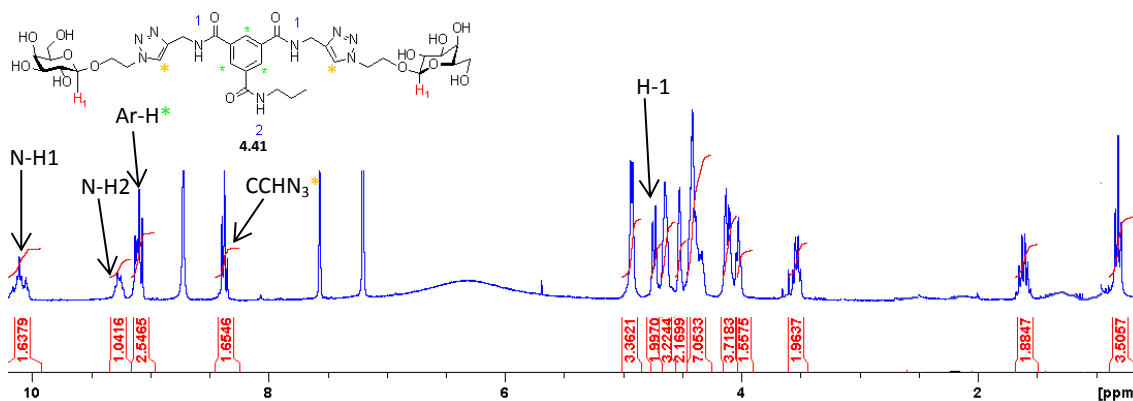
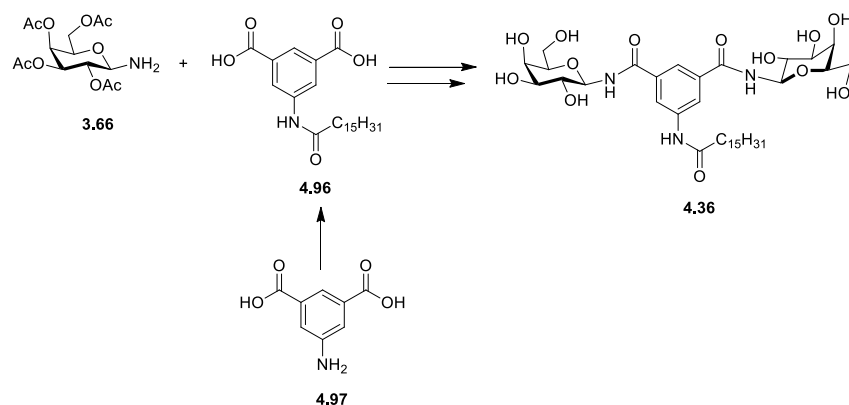


Figure 4.20 ^1H NMR spectrum of bivalent deprotected *O*-glycolipid **4.41** (300 MHz, d_5 -Pyr).

4.5 The synthesis of the second generation of glycolipids-based on aromatic scaffolds **4.36** and **4.37**

When trimesoyl chloride and trimesic acid were exploited in the synthesis of the aromatic glycoconjugates, a variety of side-products, which complicated purification and reduced the yield, was always observed. Although the desired products were still obtainable, we opted to construct an alternative approach and investigate methods to potentially reduce this by-product formation, therefore making the synthesis more efficient.

The use of aniline derivatives in the synthesis of aromatic glycoconjugates is well reported in the literature.^[93, 153, 172] We therefore chose 5-aminoisophthalic acid as our aromatic building block starting material. This way, functionalisation with the lipidic chain could be achieved prior to coupling of the galactosyl moieties. The revised synthetic route can be seen in Scheme 4.17. This alternative approach would also provide access to an important building block **4.96**, which could be easily functionalised with a variety of carbohydrate-based amines to yield a number of structurally diverse glycoconjugates.



Scheme 4.17 Revised synthetic approach for the synthesis of the second generation of glycoconjugates based around an aromatic scaffold.

As well as exhibiting different connectivity in the amide linkage to the hydrocarbon chain, the *N*-glycoconjugates **4.36** and **4.37** (Figure 4.21) were designed to act as more rigid ligands than the ones described in the previous sections, since the galactose is connected to the aromatic core directly *via* an *N*-glycosidic bond. As before, in order to investigate how chain length influenced the biological activity C-16 and C-3 hydrocarbon derivatives were synthesised.

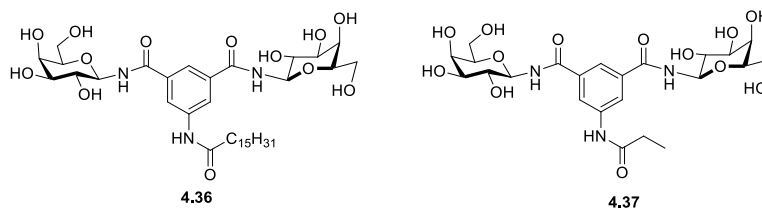
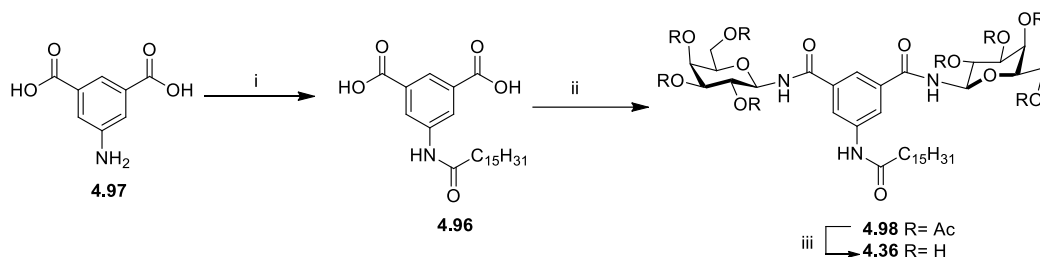


Figure 4.21 Structure of second generation *N*-glycolipids **4.36** and **4.37**.

4.5.1 Synthesis of *N*-Glycoconjugate **4.36**

The synthesis of the galactose amine **3.66** was discussed previously in Chapter 3 (section 3.5.1).

Hexadecanoyl chloride was reacted with 5-aminophthalic acid **4.97** in the presence of base to yield the di-acid building block **4.96** in 81% yield (Scheme 4.18). The di-acid derivative was then activated using DMF and oxalyl chloride to yield the di-acid chloride intermediate. A succeeding *in situ* reaction with the galactose amine **3.66** yielded the *N*-glycoconjugate **4.98** in a moderate yield of 45%. Finally, selective deprotection using the mild conditions of catalytic NEt_3 led to 93% of the desired deprotected *N*-glycoconjugate **4.36**.



Scheme 4.18 Reagents and conditions: i) $\text{ClOC}_{15}\text{H}_{31}$, NEt_3 , THF, DMF, N_2 , 18 h, 81%; ii) 1) Oxalyl chloride, DMF, DCM, N_2 , 0°C , 1 h, 2) **3.66**, NEt_3 , 0°C -rt, 16 h, 45% over two steps; iii) NEt_3 , DCM/ H_2O / MeOH , 40°C , 20 h, 93%.

The ^1H NMR spectrum of the deprotected *N*-glycoconjugate **4.36** is shown in Figure 4.22 with characteristic peaks assigned. It is clear from the ^1H NMR spectrum that the anilide proton of the second generation derivatives resonates at a higher ppm, in comparison to the lipidic amide of the first generation derivatives. We can also see a difference in the chemical shift of the methylene protons of the lipidic chain. The first methylene group resonates further upfield at a lower ppm of 2.52 than what was observed for the first generation derivatives (3.70 ppm).

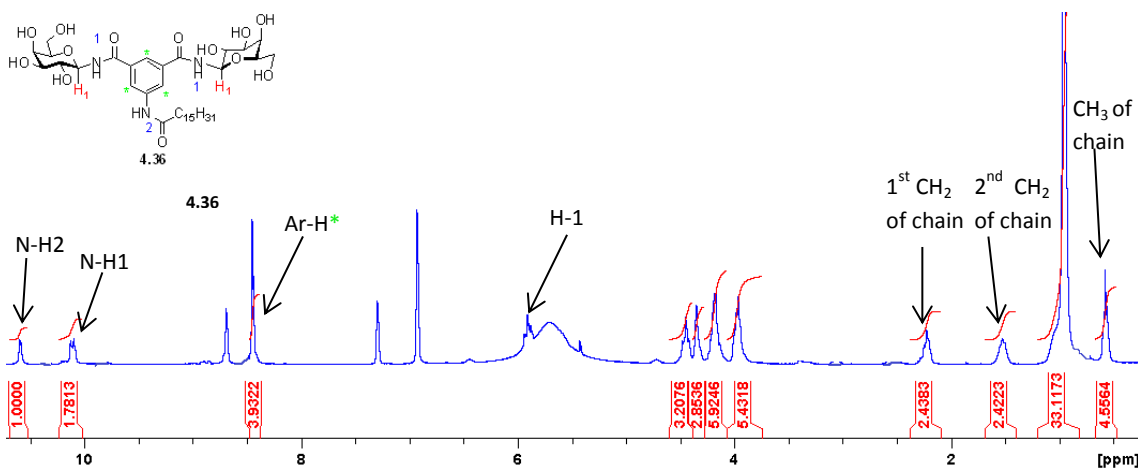
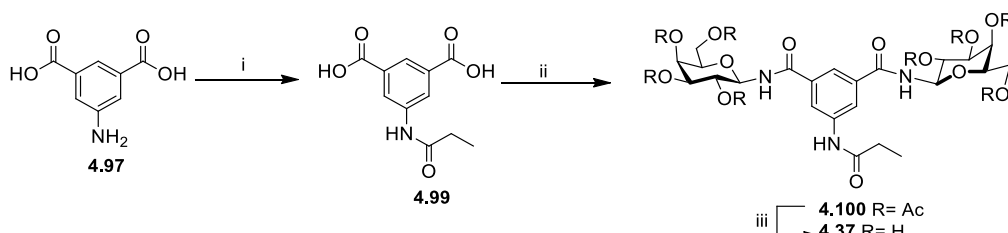


Figure 4.22 ^1H NMR spectrum of bivalent deprotected *N*-glycolipid **4.36** (300 MHz, d_5 -Pyr).

4.5.2 Synthesis of *N*-glycoconjugate **4.37**

The synthesis of the shorter chain *N*-glycolipid **4.37** proceeded *via* a similar route as discussed earlier. 5-Aminoisophthalic acid **4.97** was reacted with propionic chloride and afforded the di-acid **4.99** in 89% yield (Scheme 4.19). ^1H NMR spectral analysis also indicated the presence of some propionic acid. Purification proved unsuccessful so it was decided to proceed on with the crude compound **4.99**. The di-acid derivative was coupled to the galactose amine **3.66** using HOBt/TBTU methodology and the protected, bivalent glycoconjugate **4.100** was acquired in a low yield of 20%. The low yield indicated that both the electrophilicity of the carbonyl carbon, and nucleophilicity of the amine are extremely important in the synthesis of aromatic glycoconjugates. Due to the higher yield achieved in the synthesis of the C-16 derivative, discussed in section 4.5.1, it was believed that converting the acids into acid chlorides is the

optimum approach. Nevertheless, as we had obtained enough sample to carry out biological analysis no further optimisation of the reaction was attempted.



Scheme 4.19 Reagents and Conditions: i) ClOC_2H_5 , NEt_3 , THF, DMF, N_2 , 18 h, 89%; ii) HOBt, TBTU, NEt_3 , DMF, N_2 , **3.66**, rt, 16 h, 20%; iii) NEt_3 , DCM/ H_2O /MeOH, 40 °C, 20 h, 96%.

Global deprotection was achieved using catalytic NEt_3 in a heterogeneous solvent system to yield the deprotected *N*-glycoconjugate **4.37** in 96% yield. The ^1H NMR spectrum can be seen in Figure 4.23, with significant peaks including the anomeric proton (H-1), amide protons (N-H) and aromatic protons (Ar-H) highlighted.

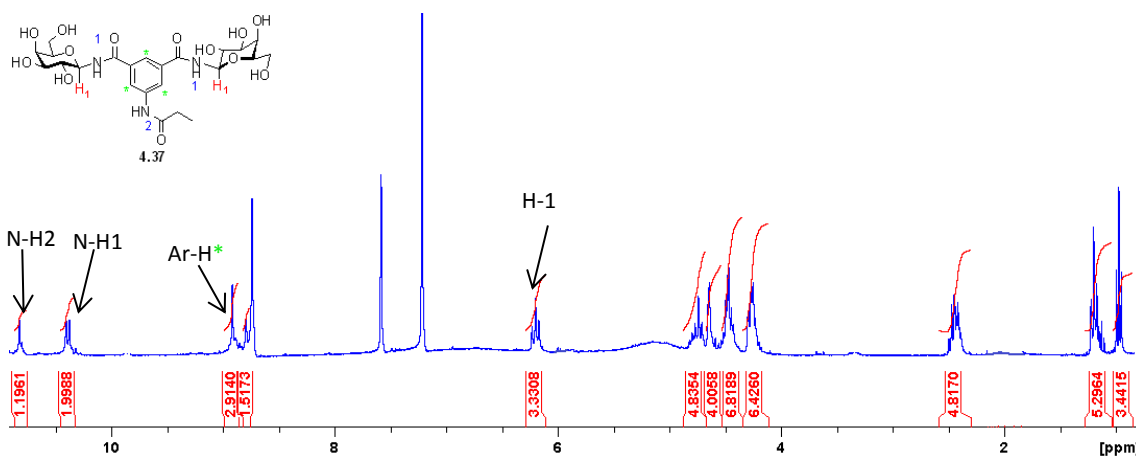


Figure 4.23 ^1H NMR spectrum of bivalent, deprotected *N*-glycolipid **4.37** (300 MHz, d_5 -Pyr).

4.6 The synthesis of the second generation triazole containing glycolipid **4.42** based on an aromatic scaffold

Similarly to the first generation of 1,4-di-substituted 1,2,3-triazole *O*-glycoconjugates discussed previously in section 4.4, the *N*-glycoconjugate **4.42** (Figure 4.24) was designed to act as a potential inhibitor of bacterial adhesion. In this case, the *N*-glycoconjugate **4.42** was intended to act as a more rigid molecule than glycolipids **4.40** and **4.41**, as no ethyl linker is used and the galactose moiety is directly attached to the triazole moiety *via* an *N*-glycosidic bond. As discussed previously, glycoconjugates containing triazole moieties are of high biological interest.

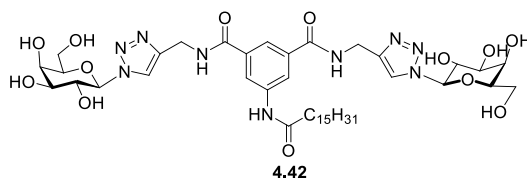
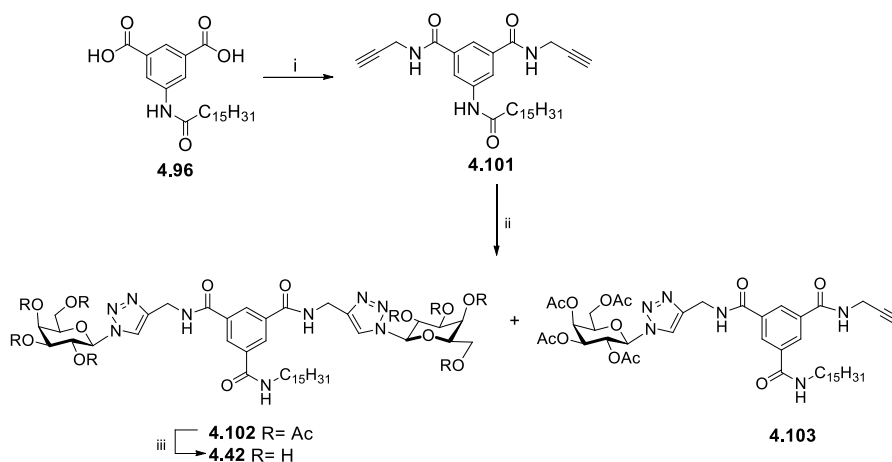


Figure 4.24 Structure of second generation 1,4-di-substituted 1,2,3-triazole glycoconjugate **4.42**.

The synthesis started with the di-acid **4.96** intermediate synthesised previously in section 4.4.1. Coupling of the free acid building block **4.96** with propargylamine using TBTU/HOBt methodology afforded the di-alkyne intermediate **4.101** in 62% yield (Scheme 4.20). A subsequent CuAAC reaction with the galactosyl azide **3.67** (previously synthesised in Chapter 3, section 3.5.1) using a promoter system of $\text{CuSO}_4 \cdot 5\text{H}_2\text{O}$ and sodium ascorbate afforded the 1,4-di-substituted 1,2,3-triazole *N*-glycolipid **4.102** in a regioselective manner and in a moderate yield of 58%. The monovalent derivative **4.103** was also isolated in 22% yield. Again, this was extremely interesting as it could be employed as a precursor in the synthesis of asymmetric aromatic glycoconjugates. Finally, mildly basic cleavage of the acetyl protecting groups was performed with catalytic NEt_3 in a heterogeneous solvent system (DCM/MeOH, H_2O , 1:2:1) at 40 °C to yield the divalent *N*-glycolipid **4.42** in a 98% yield after 18 h.



Scheme 4.20 Reagents and conditions: i) HOBt, TBTU, NEt_3 , DMF, N_2 , $\text{NH}_2\text{CH}_2\text{CCH}$, rt, 16 h, 62%; ii) **3.67**, $\text{CuSO}_4 \cdot 5\text{H}_2\text{O}$, Sodium ascorbate, DCM/Acetone/ H_2O , 20 h, 58%; iii) NEt_3 , DCM/ H_2O /MeOH, 40 °C, 20 h, 98%.

Structural elucidation was carried out and the ^1H NMR spectrum of deprotected glycolipid **4.42** is shown in Figure 4.25. Characteristic signals, including the anomeric proton (H-1), aromatic (Ar-H) protons, amide protons (NH) and the triazole proton (CCHN₃), are highlighted in the figure.

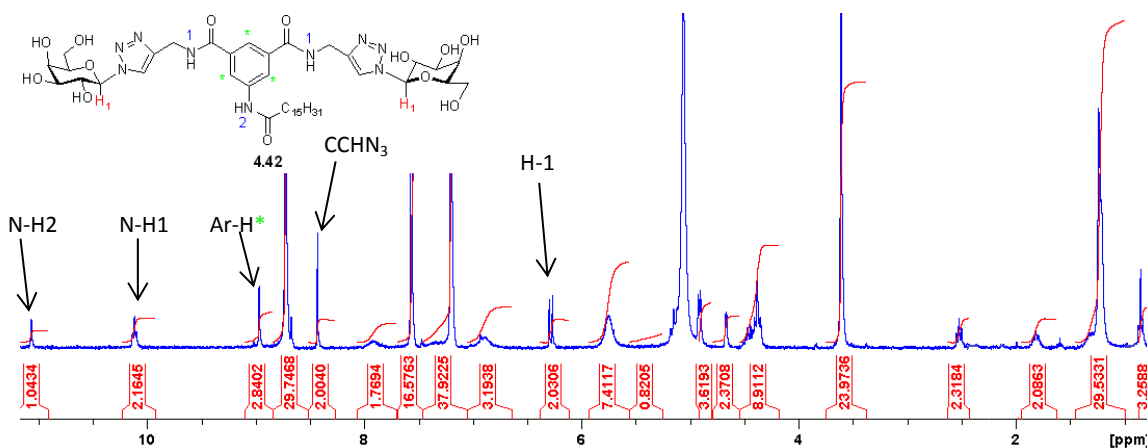


Figure 4.25 ^1H NMR spectrum of bivalent deprotected *N*-glycolipid **4.42** (300 MHz, d_5 -Pyr).

4.7 The synthesis of second generation glycoconjugate **4.43** based on an aromatic scaffold

As mentioned previously, the exact structure of the bacterial receptor of *B. multivorans* which is involved in the adhesion process is not known. This makes the design of synthetic ligands difficult, and instead a variety of ligands have to be synthesised and evaluated. It is very clear from Figure 4.26 that the chemical nature of the linker groups between the aromatic core and the galactosyl moieties are significantly different for all glycoconjugates designed. This should be reflected in a different three-dimensional presentation of the carbohydrate epitopes in each of the glycoconjugates. However, precise structural information on these ligands would require crystallography data and conformational studies. It is also clear from Figure 4.26 that an obvious relationship between linker length and resulting flexibility/rigidity of the ligands cannot be realised. A more “extended” structure would not necessarily present the galactose groups at a further distance from each other.

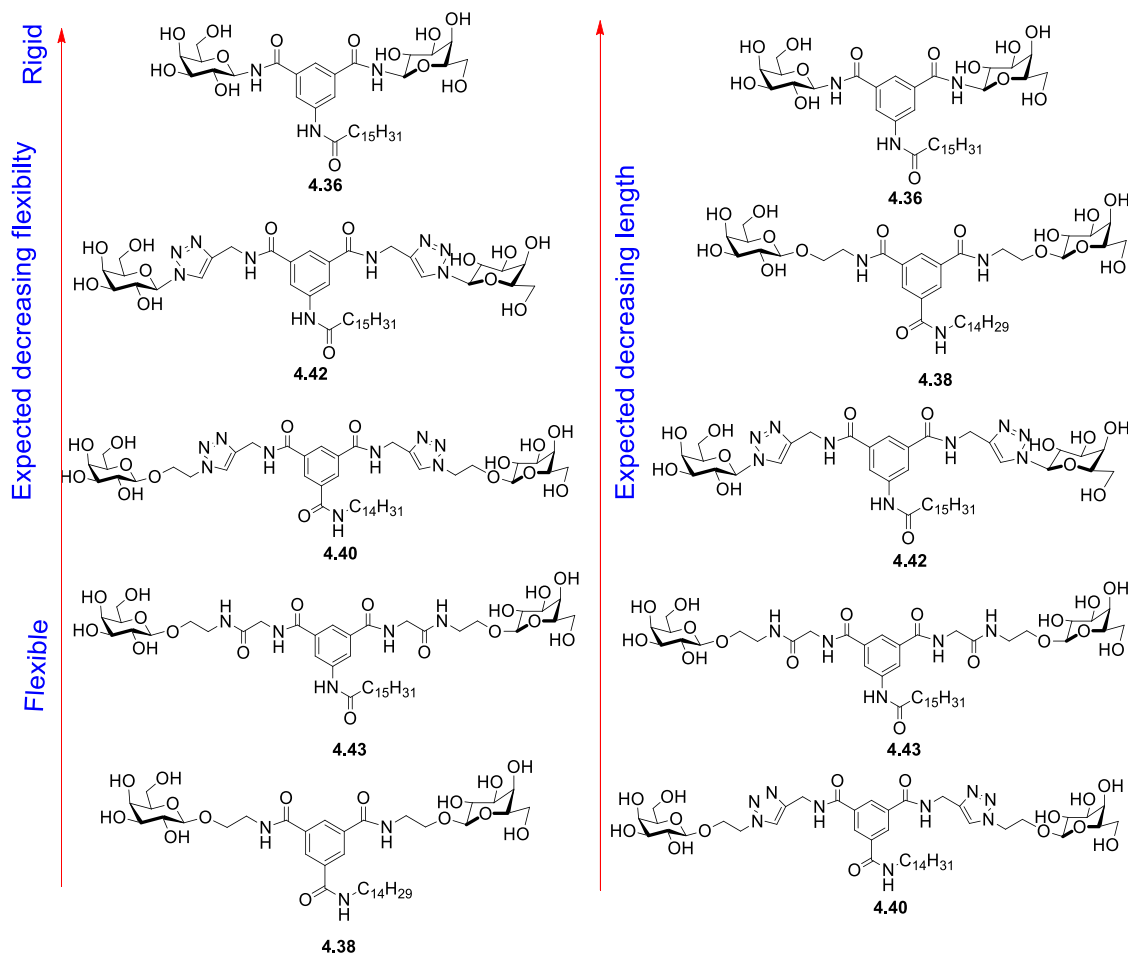
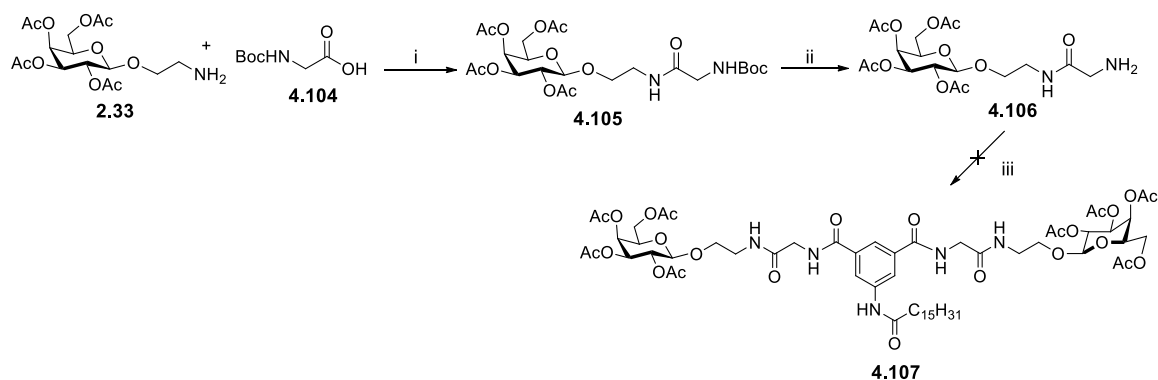


Figure 4.26 Difference between linker flexibility/rigidity and distance between the galactose epitopes.

With these observations in mind, glycoconjugate **4.43** (Figure 4.26) was designed. The galactose molecule is linked to the aromatic core *via* an ethylene chain and a glycine amino acid. The presence of the second peptide bond may impart additional conformational constraints to the glycoconjugate, which could influence the presentation of the galactose epitopes compared to the triazole-containing glycolipids **4.40** and **4.42**.

4.7.1 Initial synthesis of glycoconjugate **4.43**

The synthesis of glycoconjugate **4.43** commenced with the amide coupling of the commercially available *N*-Boc-glycine **4.104** with the galactose ethyl amine **2.33** using TBTU and HOBT (Scheme 4.21). The desired galactose building block **4.105** was afforded in 62% yield. Subsequent removal of the *N*-Boc protecting group with TFA afforded the amine **4.106** which was then reacted with di-acid aniline derivative **4.96**, synthesised previously (section 4.5.1). Unfortunately, the reaction was unsuccessful and a mixture of inseparable compounds was obtained.



Scheme 4.21 Reagents and Conditions: i) HOBt, TBTU, DMF, NEt_3 , N_2 , 16 h, rt, 62%; ii) TFA, DCM, 0°C – rt, 5 h, 74%; iii) 1) **4.96**, oxalyl chloride, DMF, DCM, N_2 , 0°C , 1 h, 2) **4.106**, NEt_3 , 0°C –rt, 16 h.

It is possible that unfavourable intramolecular H-bonding (Figure 4.27) was occurring in the free amine derivative **4.106**. This H-bonding leads to a decrease in the nucleophilicity of the amine **4.106** and therefore could explain why the reaction did not proceed as expected.

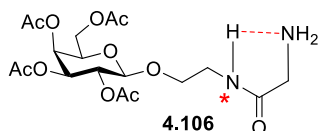


Figure 4.27 Unfavourable intramolecular H-bonding of amine derivative **4.106**.

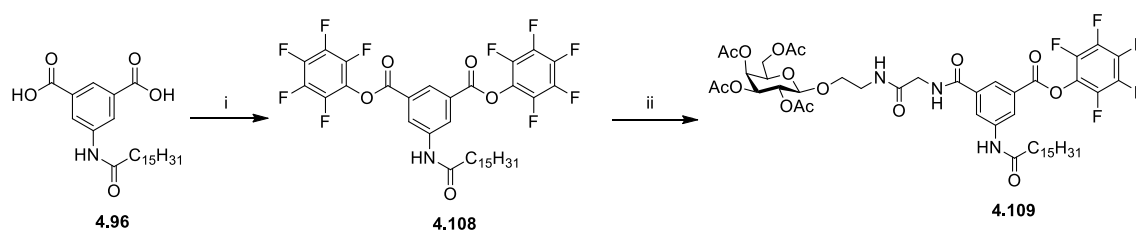
^1H NMR spectral analysis provided an indication for this H-bonding. In the ^1H NMR spectrum of the *N*-Boc derivative **4.105** the sugar amide * resonates at 6.5 ppm, whereas, in the ^1H NMR spectrum of the free amine derivative **4.106** the amide peak shifts upfield to 7.5 ppm.

To circumvent this problem, we altered our synthetic route. The reaction was repeated but this time the coupling of the free amine **4.106** to di-acid aniline derivative **4.96** was attempted using HOBt and TBTU in DMF. As DMF is a polar aprotic solvent we hoped that it would compete with these intramolecular H-bonds therefore increasing the nucleophilicity of the amine. Unfortunately, this proved fruitless and again a mixture of products was observed in the crude sample. Column chromatography was attempted and a small amount of potential product **4.107** was isolated, although some impurities still remained.

4.7.2 Attempted synthesis of glycoconjugate **4.43** using pentafluorophenyl esters

Due to the problems encountered above, we opted to alter our synthetic approach and convert the di-acids **4.96** into activated pentafluorophenyl esters. The diacid **4.96** was reacted with pentafluorophenol and DIC and the di-ester derivative **4.108** was obtained in a moderate yield of 46% (Scheme 4.22). Remarkably, a subsequent reaction with the free amine **4.106**, in the presence of base, yielded the mono-substituted galactose derivative **4.109**, exclusively. Although unexpected, this was extremely interesting and again provided a potential building block for the synthesis of asymmetric aromatic glycoconjugates (discussed in section 4.9). We

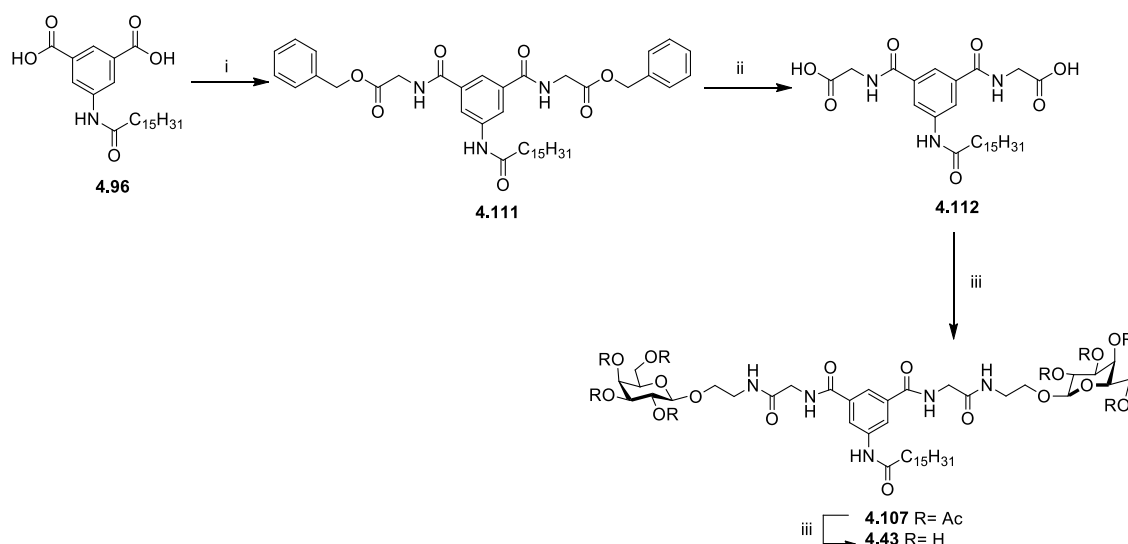
decided to further explore this reaction and found that if the reaction mixture was heated to 50 °C, the di-substituted derivative **4.107** was obtained. However, a number of side-products were also obtained and purification proved unsuccessful.



Scheme 4.22 Reagents and Conditions: i) C₆F₅OH, DIC, DIPEA, THF, N₂, 0 °C, 1 h, rt, 4 h, 46%; ii) **4.106**, DIPEA, THF, N₂, 16 h, rt, 45%.

4.7.3 Synthesis of glycoconjugate **4.43**

With so many problems to contend with, a complete change of approach was considered and it is shown in Scheme 4.23. The di-acid C-16 aniline **4.96** was first reacted with the HCl salt of the glycine benzyl ester **4.110** to yield the bi-substituted amide derivative **4.111**. Hydrogenolysis of the benzyl ester using H₂ and Pd/C catalyst afforded the novel di-acid compound **4.112** in 78% yield. The di-acid **4.112** was then reacted with the galactose ethyl amine **2.33** using HOBT and TBTU to yield the desired bivalent glycoconjugate **4.107**, albeit in a low yield of 15%. Global deprotection was achieved using catalytic NEt₃ to afford the deprotected glycoconjugate **4.43** in quantitative yield.



Scheme 4.23 Reagents and conditions: i) TBTU, HOBT, NEt₃, DMF, N₂, NH₂CH₂COOCH₂C₆H₅·HCl, rt, 16 h, 54%; ii) H₂, Pd/C, EtOAc, 78%; iii) TBTU, HOBT, NEt₃, DMF, N₂, **2.33**, rt, 18 h, 15%; iv) NEt₃, DCM/H₂O/MeOH, 40 °C, 20 h, quant.

The ¹H NMR spectrum of the deprotected, bivalent galactose derivative can be seen in Figure 4.28, and characteristic peaks including the aromatic protons (Ar-H), amide protons (NH) and anomeric protons (H-1) are highlighted.

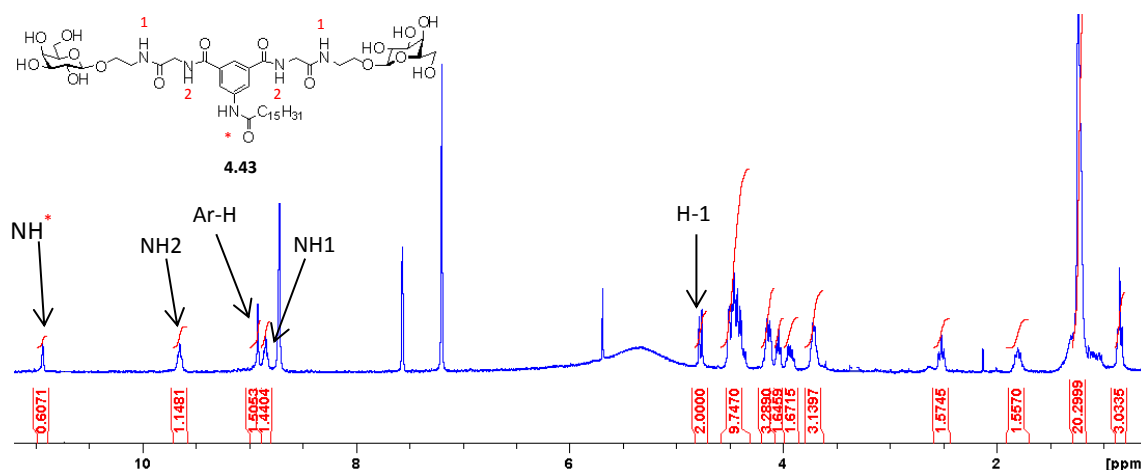


Figure 4.28 ^1H NMR spectrum of bivalent, deprotected *O*-glycolipid **4.43** (300 MHz, d_5 -Pyr).

4.8 The synthesis of monovalent aromatic glycolipid **4.44**

The concept of multivalency has been previously discussed in detail in Chapter 1 and also briefly in the introduction to this chapter. There are many reviews on the topic published in the literature.^[184] In order to confirm that a true multivalent effect was occurring for our bivalent, aromatic glycoconjugates, it was necessary to synthesise a monovalent derivative for direct comparison. As will be discussed in Chapter 5, the rigid, aromatic, bivalent glycoconjugate **4.36** gave the most promising anti-microbial results. Therefore, we opted to attempt the synthesis of a monovalent comparison for glycoconjugate **4.36** (Figure 4.29).

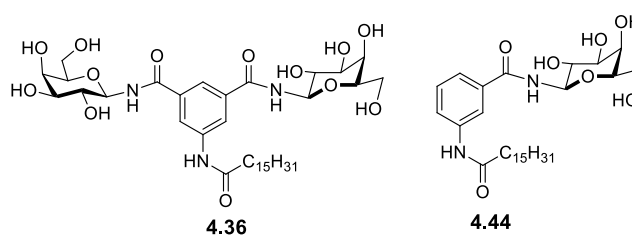
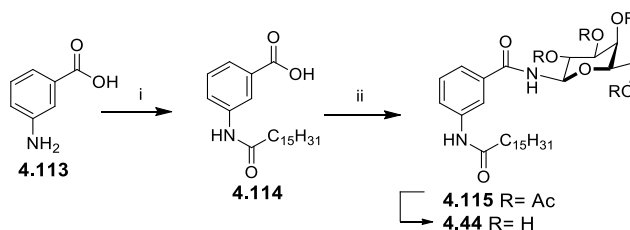


Figure 4.29 Bivalent **4.36** and monovalent **4.44** version of rigid aromatic glycoconjugate.

The synthesis proceeded smoothly following a similar approach as used for the synthesis of **4.36** (section 4.5.1). 3-Aminobenzoic acid **4.113** was reacted with hexadecanoyl chloride in the presence of base to yield 75% of the mono-acid building block **4.114** (Scheme 4.24). The mono-acid derivative was then reacted with the galactose amine **3.66** using HOBt and TBTU to attain the monovalent *N*-glycoconjugate **4.115** in a moderate yield of 65%. Finally, selective deprotection using the mild conditions of catalytic NEt_3 led to the desired deprotected *N*-glycoconjugate **4.44** in 92% yield. The ^1H NMR spectrum of the deprotected monovalent glycoconjugate **4.24** with characteristic peaks assigned is shown in Figure 4.30.



Scheme 4.24 Reagents and conditions: i) ClCOC₁₅H₃₁, NEt₃, THF, DMF, N₂, 18 h, 75%; ii) HOBT, TBTU DMF, N₂, NEt₃, **3.66**, rt, 16 h, 65%; iii) NEt₃, DCM/H₂O/MeOH, 40 °C, 20 h, 99%.

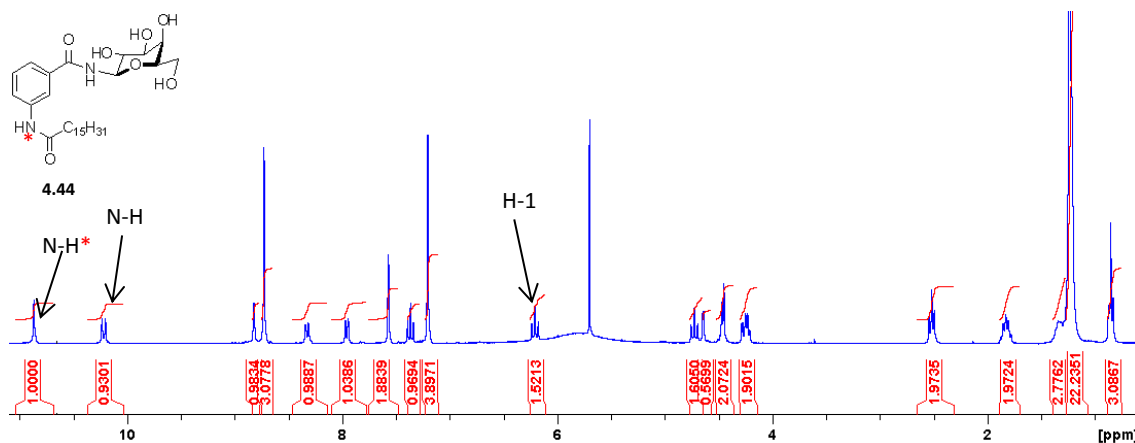


Figure 4.30 ¹H NMR spectrum of monovalent deprotected *N*-glycolipid **4.44** (300 MHz, *d*₅-Pyr).

4.9 The synthesis of non-symmetrical glycolipids based on an aromatic scaffolds **4.116** and **4.117**

During the synthesis of bivalent glycolipids **4.39** and **4.43** we found that the mono pentafluorophenyl esters **4.75** and **4.109** could also be isolated and purified (section 4.3.2 and section 4.7.2, respectively). This led us to examine the possibility of synthesising non-symmetrical, aromatic glycoconjugates, which could be of high biological interest.

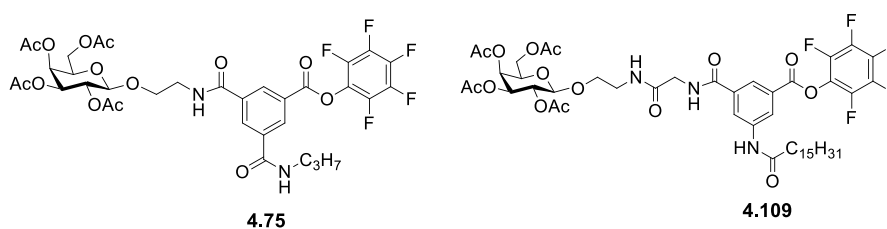


Figure 4.31 Monovalent derivatives isolated during the synthesis of bivalent glycoconjugates.

As discussed previously, individual carbohydrate interactions with their complementary protein, which are essential for a number of biological processes, tend to be very weak. To overcome this, multivalent carbohydrate systems have been widely explored,^[154] and it has been shown that multivalency generally leads to increased binding affinities.^[15] To date, most interest has centred around the synthesis of multivalent systems composed of identical carbohydrate entities linked to an appropriate scaffold.^[154] Although beneficial and successful,

this approach does not take the glycoheterogeneity of carbohydrate-protein binding into account. In order to understand this biological heterogeneity further, efficient methodologies for the successful synthesis of scaffolds displaying different carbohydrate ligands (heteroglycans, heteroglycoclusters and heteroglycoassemblies) are of extreme importance.^[15] Some examples are shown in Figure 4.32.

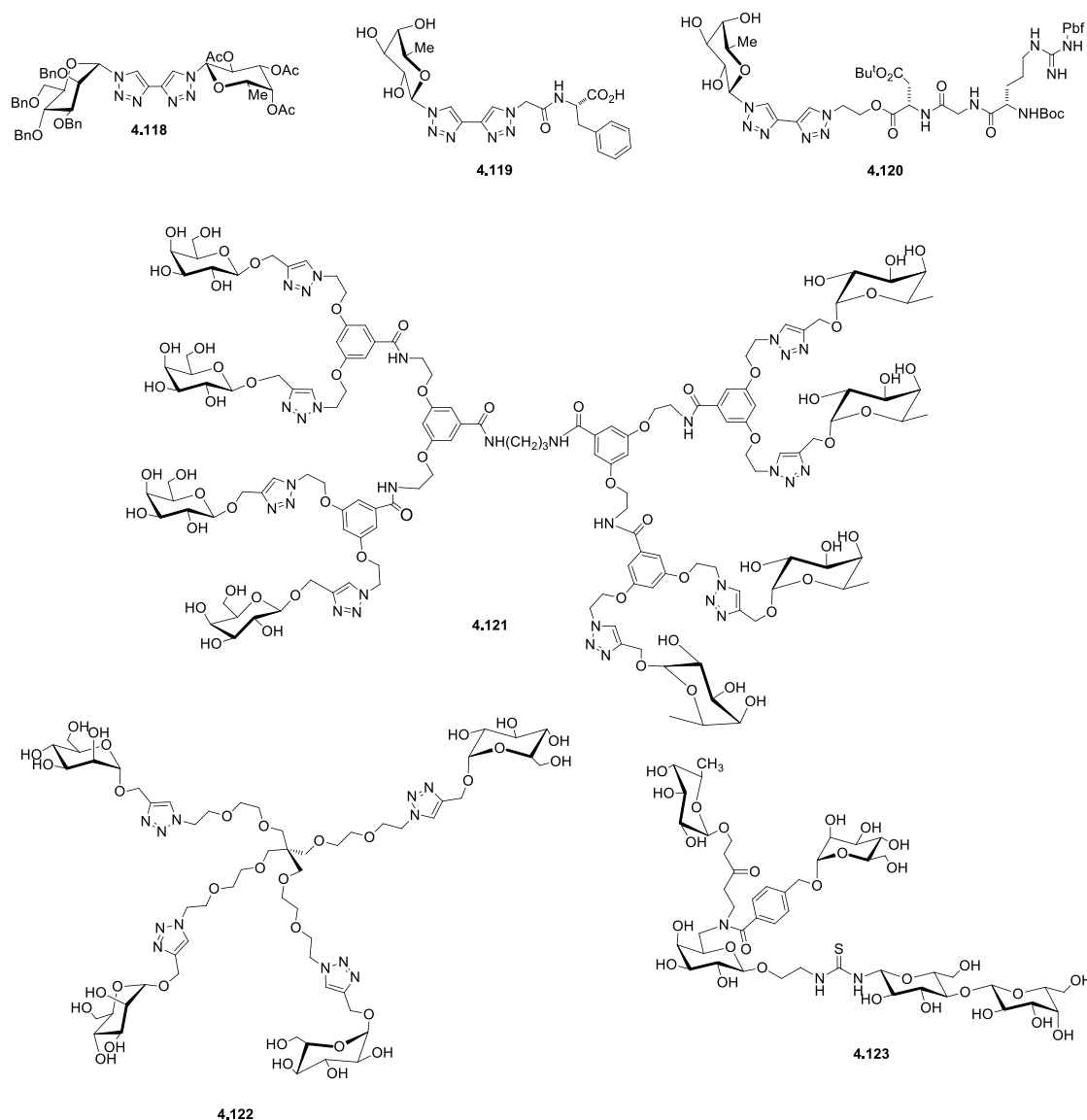


Figure 4.32 Examples of selected heteroglycans, Lindhorst *et al.* **4.123**,^[185] Roy *et al.* **4.121**,^[186] Aizpurua *et al.* **4.118-4.120**,^[187] and Santoyo-Gonzalez *et al.* **4.122**.^[188]

In 2002, Lindhorst and co-workers successfully synthesised a novel hetero-glycocluster **4.123** using an approach based on the orthogonal derivatisation of D-galactose to attach different carbohydrate moieties.^[185] Later, in 2007, Roy *et al.* explored the possibility that heteromultivalent glycoconjugates may be able to cross-link two different lectins, if each of the lectins was specific for one of the saccharide units.^[186] They successfully demonstrated this principle and the heteromultivalent glycodendrimer **4.121**, which contained four α-fucose and

four β -galactose residues on opposite sides of the scaffold, displayed fast cross-linking abilities with both the PA-IL and PA-III *P. aeruginosa* ligands. In 2010, Aizpurua *et al.* published the first report on the synthesis of non-symmetrical *bis*(1,2,3-triazoles).^[187] Some selected examples of the non-symmetrical *bis*(1,2,3-triazoles) they synthesised included compounds **4.118-4.120** (Figure 4.32). Santoyo-Gonzalez and co-workers exploited the CuAAC reaction to synthesise multivalent heteroglycans incorporating two different monosaccharides, including D-mannose, D-glucose, D-glucosamine, onto a variety of scaffolds.^[188] One such example of a pentaerythritol scaffold bearing 2 α -mannose and 2 α -glucose moieties is glycocluster **4.122**. The ability of the compounds to bind Con A was evaluated and it was found that even though α -mannose is a much better ligand than α -glucose for binding Con A, the relative potency per α -mannose unit was 1.5-fold higher for the $(\alpha\text{Man})_2(\alpha\text{Glc})_2$ derivative as compared to the $(\alpha\text{Man})_4$ homoconjugate.

4.9.1 Synthesis of non-symmetrical aromatic glycolipid 4.116

As stated above, during the synthesis of the bivalent glycoconjugate **4.39** the monovalent counterpart **4.75** was also isolated. The clear differences between the ^1H NMR spectra of the two compounds can be seen in Figure 4.33. The red spectrum corresponds to the protected divalent glycoconjugate **4.74**, and shows that in this case the aromatic protons appear equivalent and resonate together as a broad singlet at 8.35 ppm. In contrast the blue spectrum, which corresponds to the monovalent derivative **4.75**, shows that the aromatic protons no longer appear equivalent. The aromatic H1 and H2 atoms are now in close proximity to the electron-withdrawing pentafluorophenyl ester and, as a result, they have shifted to a higher ppm value of 8.77. The H3 atom remains in a similar environment as in compound **4.74** and therefore shifts upfield only slightly to 8.44 ppm.

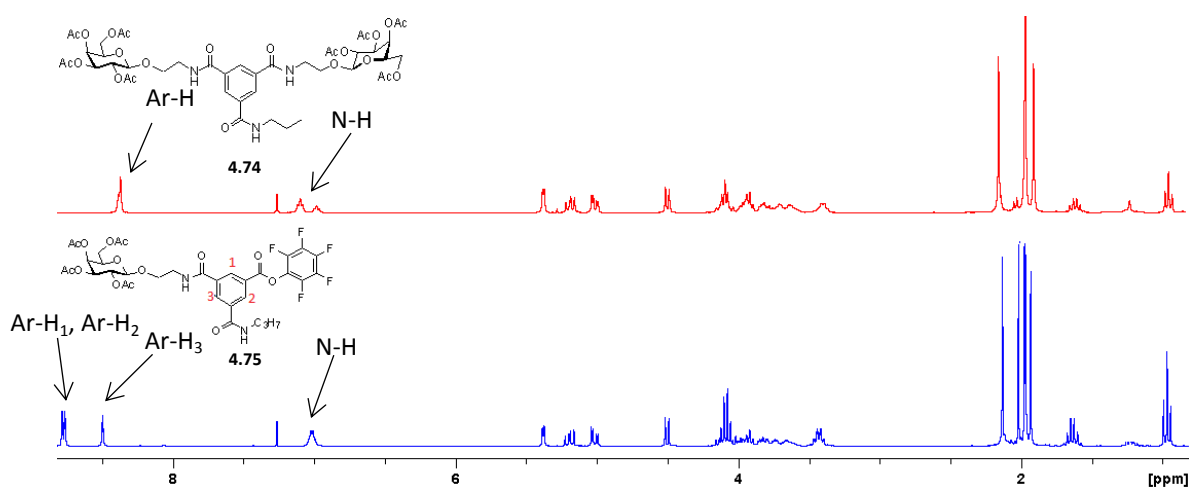


Figure 4.33 ^1H NMR spectra of divalent glycoconjugate **4.74** (red) and its monovalent counterpart **4.75** (blue).

Although the synthesis of heteroglycans is advantageous, we decided to continue with the galactose moiety and synthesise a non-symmetrical molecule containing two galactose moieties connected to the aromatic backbone *via* a different linker. The compound we aimed to synthesise was glycolipid **4.116**, which was a hybrid between glycoconjugate **4.39** and **4.41** (Figure 4.34).

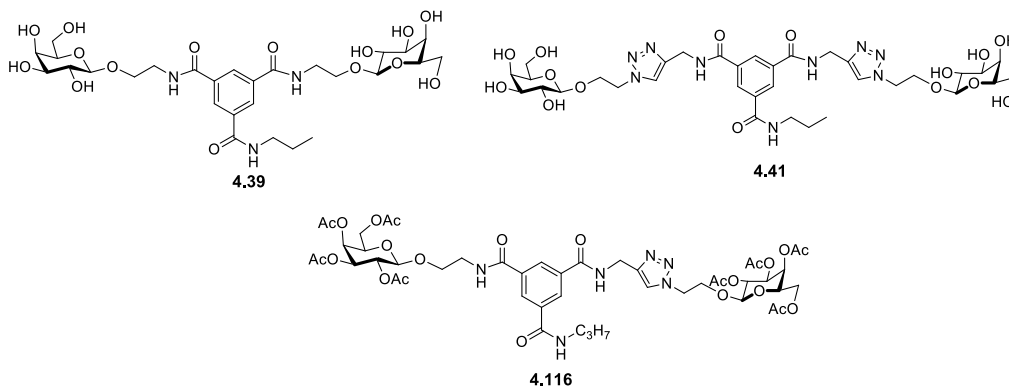
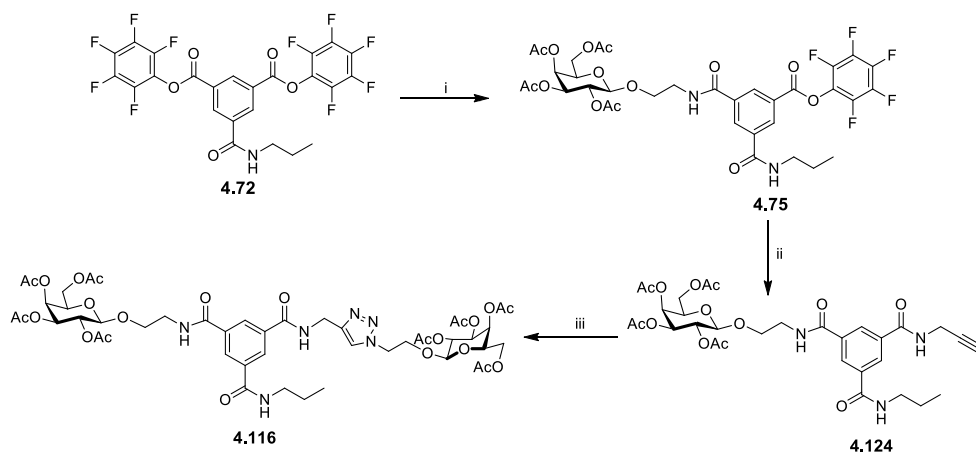


Figure 4.34 Structure of non-symmetrical glycolipid **4.116**, which is a cross between glycolipids **4.30** and **4.32**.

When carrying out the synthesis of the divalent glycolipid **4.39**, a 30% yield of the monovalent counterpart **4.75** was obtained. Aiming to improve this yield, the reaction was repeated using less equivalents of galactose ethyl amine **2.33**, and with dropwise addition of the amine to the reaction mixture (Scheme 4.25). Nevertheless the yield only increased to 36%, and no divalent glycolipid **4.39** was detected by ^1H NMR spectral analysis. The monovalent derivative **4.75** was reacted with propargylamine to afford the alkyne intermediate **4.124** in 66% yield. A subsequent CuAAC reaction with the galactosyl azide **2.44** using a promoter system of $\text{CuSO}_4 \cdot 5\text{H}_2\text{O}$ and sodium ascorbate afforded the non-symmetrical glycolipid **4.116** in a regioselective manner and in a good yield of 72%. Removal of the acetyl protecting groups of glycolipid **4.116** was not attempted in this case as the compound would not be tested for antimicrobial activity.



Scheme 4.25 Reagents and Conditions: i) **2.33**, DIPEA, THF, N₂, rt, 18 h, 36%; ii) NH₂CH₂CCH, THF, DIPEA, N₂, rt, 3h, 66%; ii) **2.44**, CuSO₄·5H₂O, sodium ascorbate, DCM/Acetone/H₂O, 20 h, 72%.

Although the non-symmetrical glycolipid **4.116** contains two galactose moieties, this approach proves that the synthesis of a variety of heteroglycans can be easily achieved by simply varying the carbohydrate azide utilised in the CuAAC reaction. The ¹H NMR spectrum of the protected glycolipid **4.116** is shown in Figure 4.35 with characteristic signals assigned.

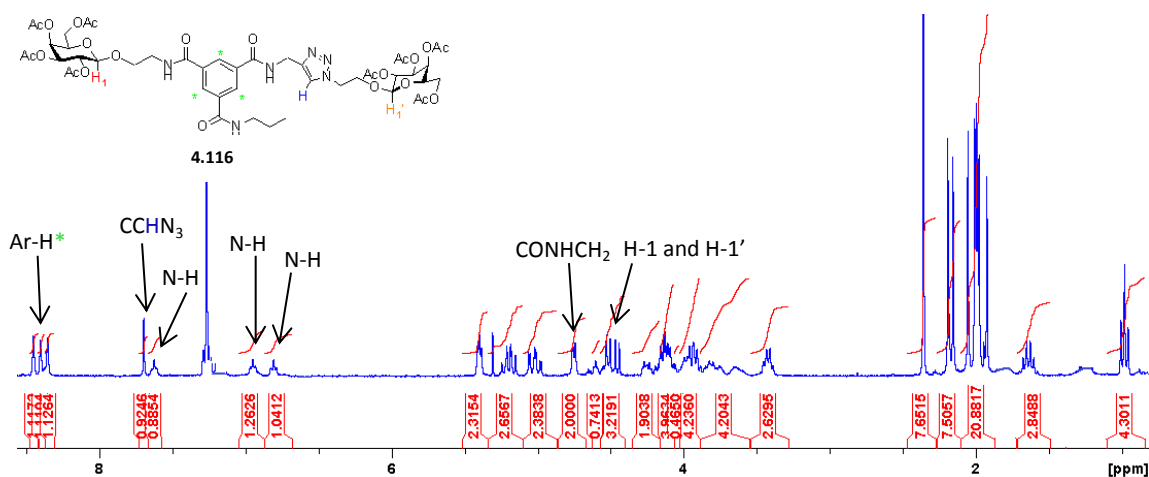


Figure 4.35 ¹H NMR spectrum of non-symmetrical glycolipid **4.116** (300 MHz, CDCl₃).

4.9.2 Synthesis of non-symmetrical aromatic glycoconjugate **4.117**

Like glycoconjugate **4.116**, non-symmetrical glycolipid **4.117** was designed to be a hybrid between two previously synthesised glycoconjugates, **4.42** and **4.43** (Figure 4.36). We wanted to synthesise a non-symmetrical molecule whereby the two galactose moieties were connected to the aromatic scaffold *via* a different linker. The idea was to prove that this methodology would be effective, and that the monovalent derivatives could be utilised to synthesise a variety of diverse heteroglycans.

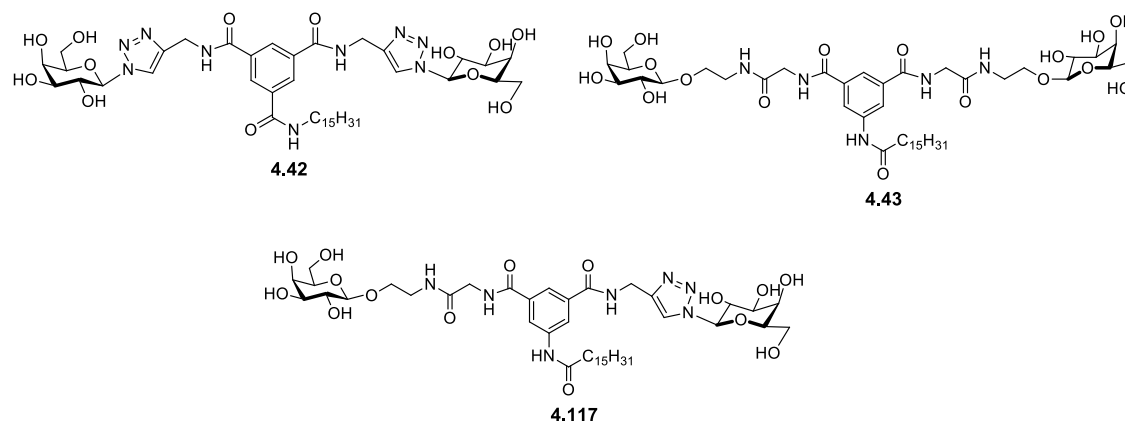


Figure 4.36 Structure of non-symmetrical glycolipid **4.117**, which is a cross between glycolipids **4.42** and **4.43**.

As mentioned previously (section 4.7.2), the monovalent counterpart **4.109** was obtained exclusively in a 45% yield while trying to synthesise the bivalent glycine derivative **4.43**. Again this was evident from the ^1H NMR spectrum (Figure 4.37). Due to the electron-withdrawing pentafluorophenyl ester group the aromatic protons of the monovalent derivative **4.109** (red) resonates at a higher chemical shift compared to the bivalent derivative **4.107** (blue).

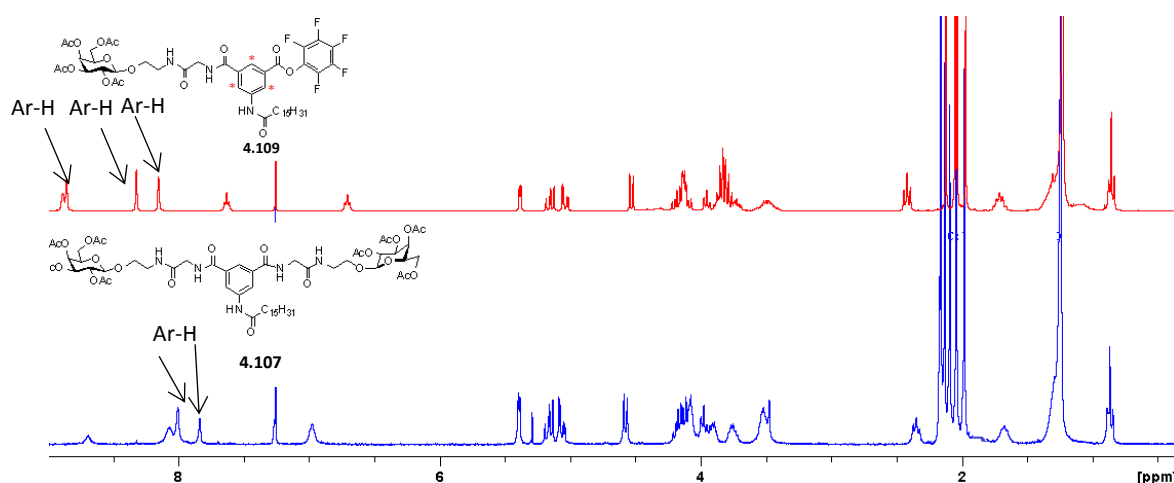
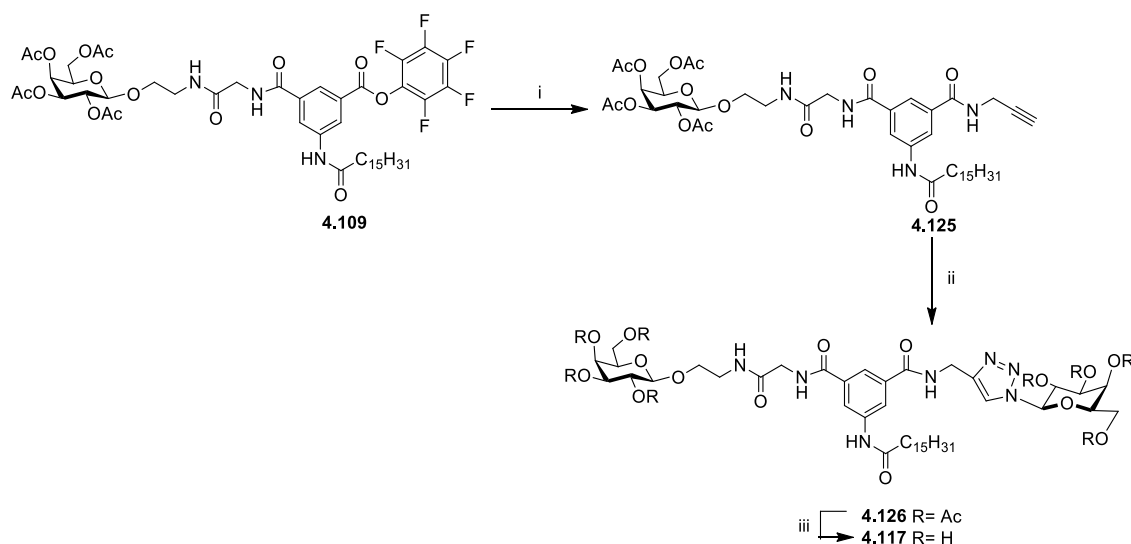


Figure 4.37 ^1H NMR spectra of divalent glycoconjugate **4.107** (blue) and its monovalent counterpart **4.109** (red).

The synthesis of the non-symmetrical glycolipid **4.117** started with the reaction of the monovalent derivative **4.109** with propargylamine using NEt_3 to yield the alkynyl derivative **4.125** in 68% yield (Scheme 4.26). The alkyne derivative was then reacted with galactose azide **3.67** in a Cu(I) catalysed azide-alkyne cycloaddition, and the protected non-symmetrical glycolipid **4.126** was attained in 65% yield. Global acetyl deprotection was achieved using catalytic NEt_3 in a heterogeneous solvent system, to give the final deprotected, non-symmetrical glycolipid **4.117** in 88% yield.



Scheme 4.26 Reagents and Conditions: i) $\text{NH}_2\text{CH}_2\text{CCH}$, THF, DIPEA, N_2 , rt, 3h, 68%; ii) **3.67**, $\text{CuSO}_4 \cdot 5\text{H}_2\text{O}$, Sodium ascorbate, DCM/Acetone/ H_2O , 20 h, 65%; iii) NEt_3 , DCM/ H_2O /MeOH, 40°C , 20 h, 88%.

The ^1H NMR spectrum of the deprotected glycolipid can be seen in Figure 4.38. Characteristic signals are highlighted including the amide protons (NH), the triazole proton (CN_3CH), the two anomeric protons (H-1 and H-1') and finally the aromatic protons (Ar-H).

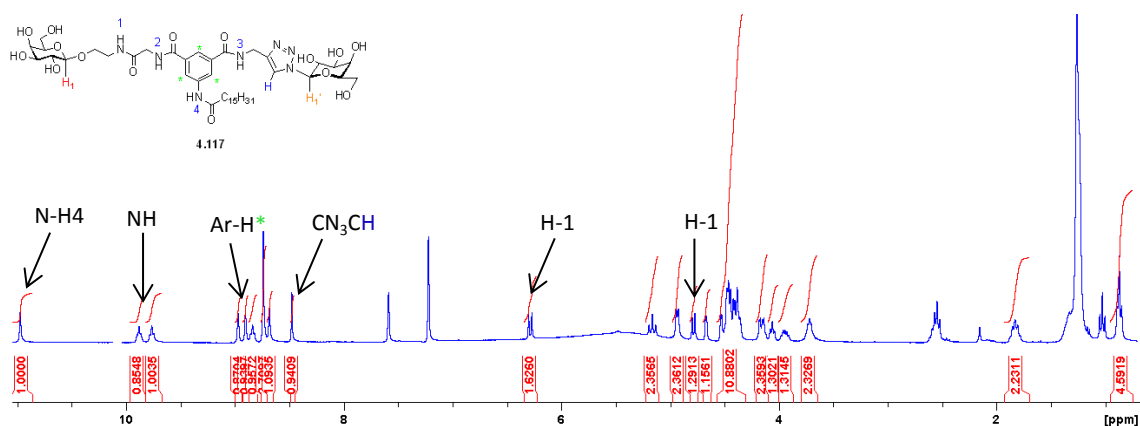


Figure 4.38 ^1H NMR spectrum of bivalent glycolipid **4.117** (300 MHz, d_5 -Pyr).

4.10 The synthesis of glycoconjugates with more complex carbohydrate epitopes

Finally, it was decided to attempt the synthesis of aromatic glycoconjugates with more complex carbohydrate moieties present, and investigate how this would affect the binding to the bacterial proteins and thus influence the biological activity. We chose the disaccharide galabiose (also known as Gal(α ,1-4)gal), as it contains a terminal galactose moiety which should be recognised by the bacterial proteins (Figure 4.39). Glycoconjugates-containing this disaccharide have been shown to be inhibitors of both *E. coli* and *S. suis* adhesins.^[10] There are many examples of both monovalent and multivalent glycoconjugates-containing galabiose reported in the literature and in many cases they have been utilised to inhibit bacterial adhesion to human cells.^[10, 22, 189]

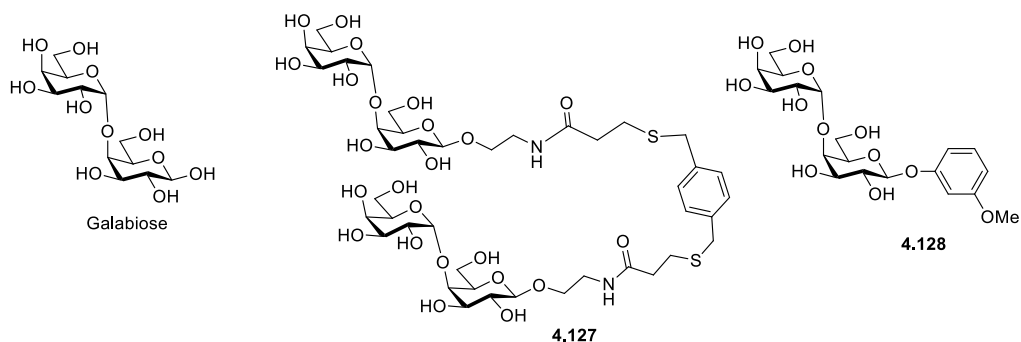
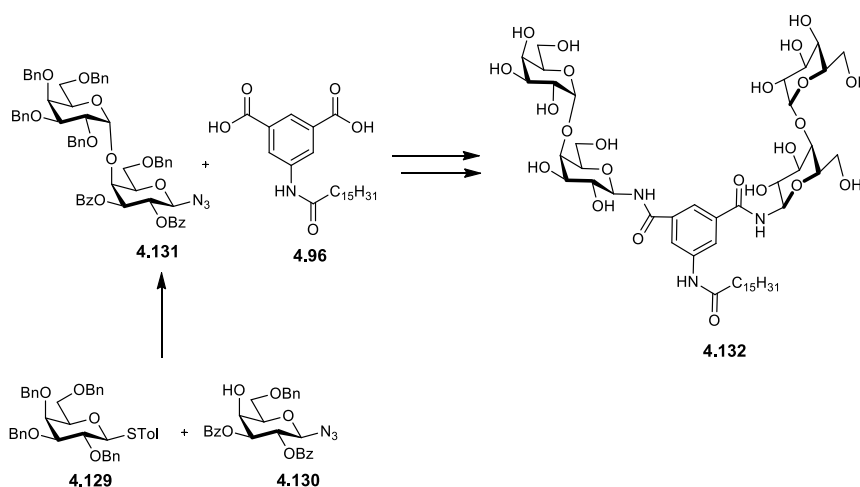


Figure 4.39 Representative examples of monovalent **4.128**^[10] and bivalent **4.127**^[190] glycoconjugates containing the disaccharide galabiose which have been utilised to inhibit bacterial adhesion to human cells.

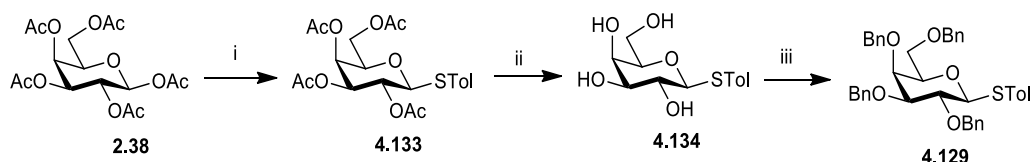
Initial investigations led us to design the synthetic pathway shown in Scheme 4.27, whereby the easily accessible glycosyl donor **4.129** and acceptor **4.130** would serve as suitable building blocks in the synthesis of the novel galabiose diasaccharide **4.131**. The carbohydrate moiety could then be coupled to the aromatic backbone **4.96**, synthesised previously in section 4.5.1, to yield the more complex glycoconjugate **4.132**. Galabiosyl azide **4.131** could also be used as a building block in the synthesis of other glycoconjugates using the methodologies discussed in the previous sections.



Scheme 4.27 Proposed synthetic pathway for the synthesis of the more complex bivalent glycoconjugate **4.132**.

4.10.1 Synthesis of glycosyl donor **4.129**

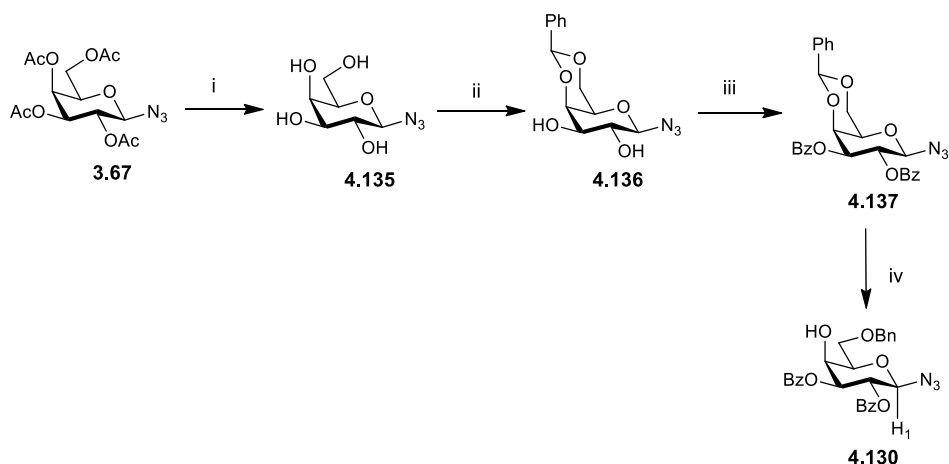
Following a procedure reported by Wang *et al.*, the known compound **4.129** was successfully synthesised.^[191] Commercially available β -D-Galactose pentacetate **2.38** was reacted with *p*-toluenethiol under Lewis acid $\text{BF}_3 \cdot \text{O}(\text{Et})_2$ activation and the desired galactoside **4.133** was obtained in 69 % yield (Scheme 4.28). Global deprotection using methanolic NaOMe afforded the deprotected compound **4.134** which was subsequently reacted with NaH and benzyl bromide to attain the benzylated glycosyl donor **4.129**^[192] in a yield of 80%.



Scheme 4.28 Reagents and conditions; i) $\text{BF}_3 \cdot \text{OEt}_2$, p-toluenethiol, DCM, 0°C - rt, 20 h, 69%; ii) NaOMe, DCM, MeOH, N_2 , rt, 1 h, 85%; iii) NaH, BnBr, DMF, N_2 , 0°C - rt, 18 h, 80%.

4.10.2 Synthesis of glycosyl acceptor 4.130

The synthesis of the known compound **4.130** commenced with the deprotection of the galactose azide **3.67** which was previously discussed in Chapter 3, section 3.2.6.1 (Scheme 4.29). Following a literature procedure, the hydroxyl groups at the C-4 and C-6 position of the resulting compound **4.135** were selectively protected using a benzylidene acetal to give intermediate **4.136**.^[193] The remaining hydroxyl groups were then benzoylated by treatment with benzoyl chloride in pyridine, and the desired galactoside **4.137** was obtained in 75% yield. When benzyl groups are present on the acceptor, they increase its nucleophilicity and lead to higher yields in glycosylation reactions. However, Ohlsson and Nilsson reported a series of α -galactosylations using a variety of acceptors, and a donor closely related to **4.129**. They found that although the yields were higher when the acceptor contained all benzyl groups, the α/β selectivity was much lower. They achieved the best results utilising the acceptor **4.130**, with a yield of 67% and a α/β selectivity of 25:1.^[189] Regioselective reduction of the benzylidene under acidic conditions by NaCNBH_3 initially proved unsuccessful. However following a procedure reported by Xia *et al.*, whereby methyl orange was used as a pH indicator^[194], the known galactosyl acceptor **4.130**^[189] was obtained in a yield of 73%. This compound is mentioned in the literature but no experimental data is given. The ^1H NMR spectrum of the acceptor **4.130** is shown in Figure 4.40.



Scheme 4.29 Reagents and conditions; i) NaOMe, DCM, MeOH, N_2 , rt, 1 h, 83%; ii) $\text{C}_6\text{H}_5\text{CH}(\text{OCH}_3)_2$, $\text{CH}_3\text{C}_6\text{H}_4\text{SO}_3\text{H}$, DMF, N_2 , 20 h, NEt_3 , 83%; iii) $\text{C}_6\text{H}_5\text{COCl}$, Pyr, 0°C - rt, 16 h, 84%; iv) NaCNBH_3 , HCl, methyl orange, THF, rt, 4 h, 73%.

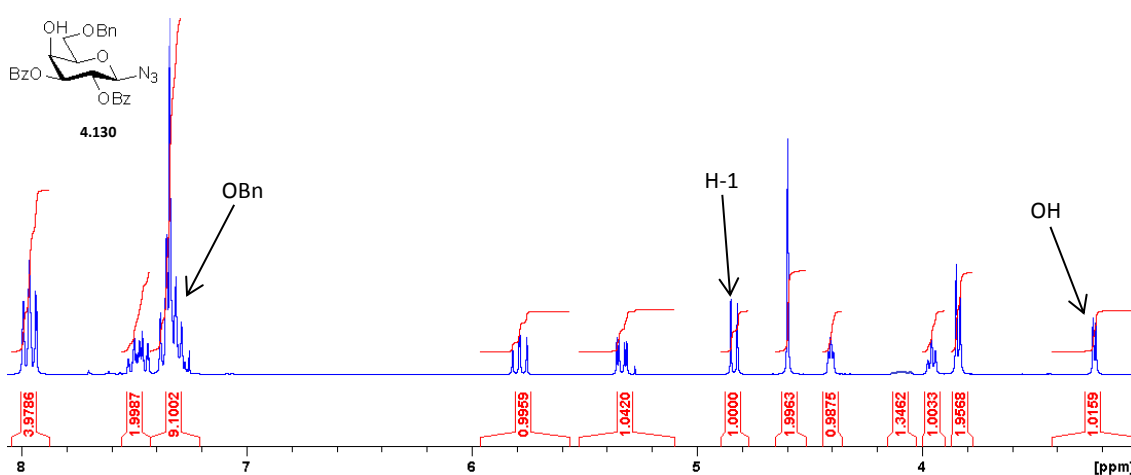


Figure 4.40 ^1H NMR spectrum of glycosyl acceptor **4.130** (300 MHz, CDCl_3).

4.10.3 α -Galactosylation between glycosyl donor **4.129** and glycosyl acceptor **4.130**

The next step was the α -galactosylation between the glycosyl donor **4.129** and acceptor **4.130**. Following a procedure from Ohlsson and Magnusson the galactosylation was carried out at $-55\text{ }^\circ\text{C}$ using a promoter system of TMSTOf and NIS in a mixture of DCM and Et_2O .^[195] The galabiose diasaccharide **4.131** was obtained in 41% yield (Scheme 4.30). The ^1H NMR spectrum of compound **4.131** is shown in Figure 4.41. Unreacted donor and acceptor were also recovered, however, interestingly only small amounts of the β -diasaccharide were recovered (< 1%).

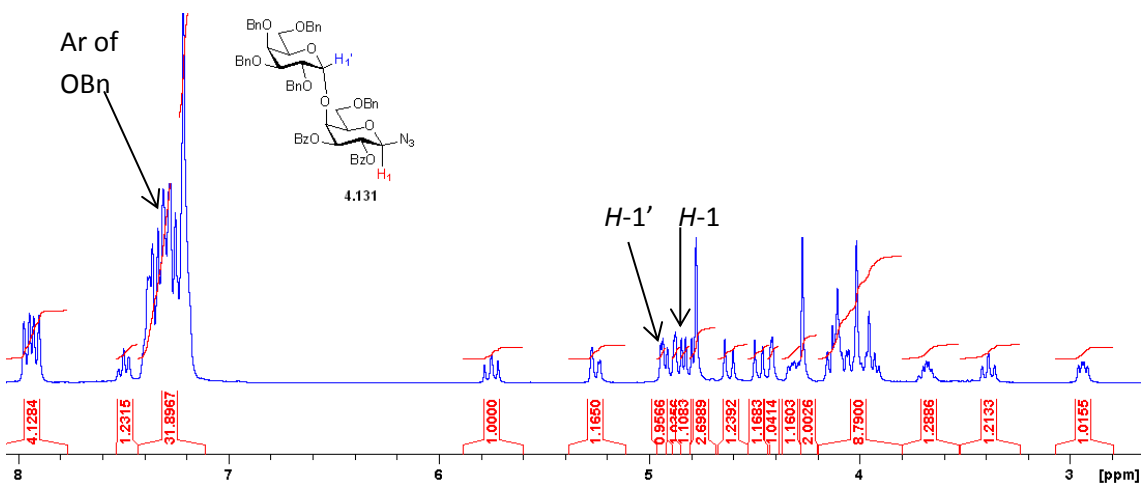
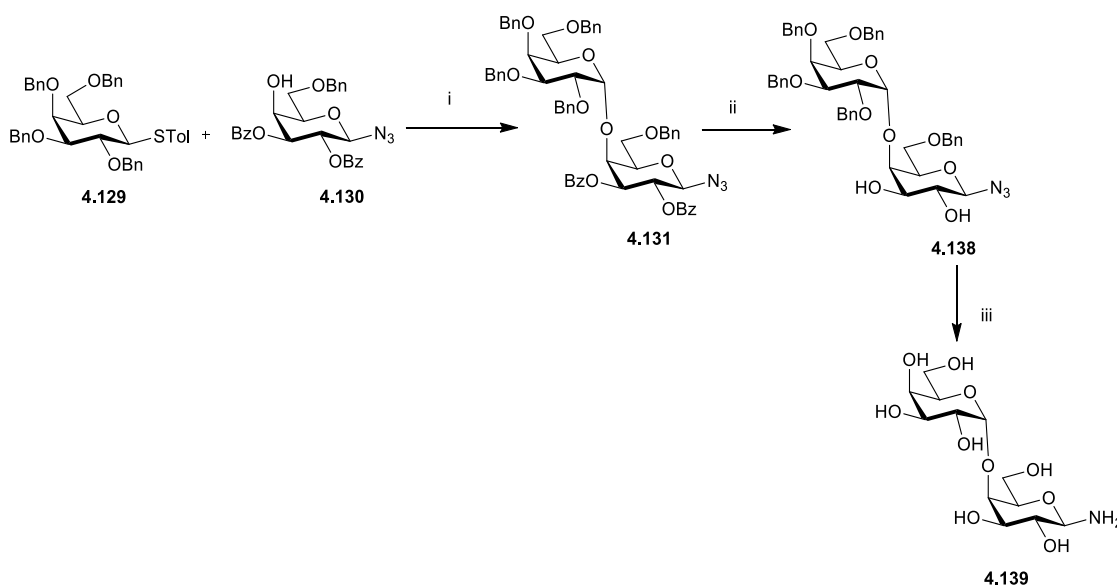


Figure 4.41 ^1H NMR spectrum of protected galabiose derivative **4.131** (300 MHz, CDCl_3).

The α -anomer **4.131** was found to be the major product as the non-ester benzyl protecting groups do not allow for neighbouring group participation. This means that the glycosylation reaction can follow either a $\text{S}_{\text{N}}1$ or $\text{S}_{\text{N}}2$ mechanism, which can result in a mixture of anomers. By controlling the temperature, solvent and reaction conditions used, the formation of one anomer over the other can be favoured.^[196] However, this can be extremely difficult and thus

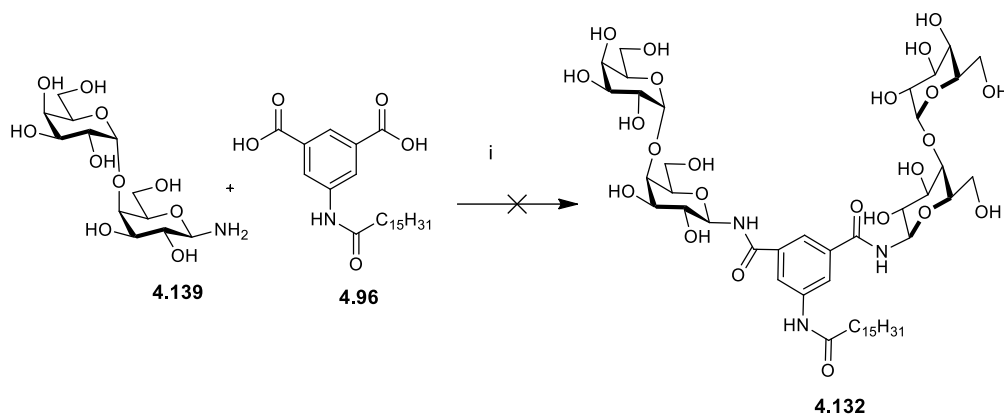
in the majority of cases the synthesis of 1,2-*trans* glycosides (β -anomer) involves simpler purification of products and more efficient procedures than for the corresponding 1,2-*cis* glycosides (α -anomer). Other groups have previously synthesised the Gal(α , 1-4)gal linkage and optimum conditions have already been established.^[195]

The next synthetic steps required careful consideration. The reduction of the azide in **4.131** to the amine group was required for coupling to the aromatic scaffolds; however, the benzyl and benzoyl groups also needed to be removed. The deprotection conditions of the benzoyl groups are quite harsh and require reflux in NaOMe. If this was carried out after the coupling reaction we would risk hydrolysis of the newly formed amide bonds. With this in mind, we decided to first remove the benzoyl groups and then reduce the azide. Deprotection of the benzoyl groups by refluxing with NaOMe yielded 91% of compound **4.138**. Subsequent hydrogenolysis using H₂ and Pd/C led to both the reduction of the azide and removal of the benzyl groups, and afforded a 98% yield of compound **4.139**.



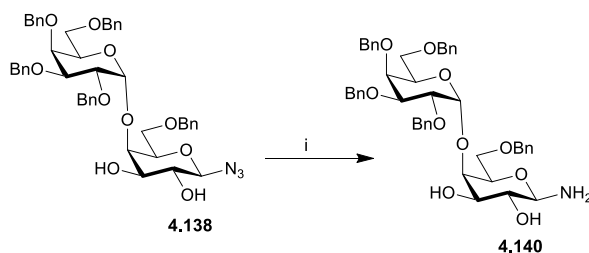
Scheme 4.30 Reagents and conditions; i) TMSOTf, NIS, DCM, Et₂O, Ar, -55 °C, 2 h, 41%; ii) NaOMe, MeOH, 90 °C, 4 h, 91%; iii) H₂, Pd/C, MeOH, HCl, 2 h, 98%.

Unfortunately, the final step, which involved coupling of the free amine **4.139** to the aromatic backbone proved extremely problematic. For our first attempt, the aromatic scaffold was activated using TBTU/HOBt, followed by addition of the galabiosyl amine **4.139** (Scheme 4.31). The reaction was unsuccessful and a complex mixture of products was obtained. The reaction was repeated but this time the carboxylic acids were converted into acid chlorides prior to addition of the amine, nevertheless, the desired product was not obtained. On closer inspection, we observed that the galabiosyl amine **4.139** was extremely insoluble and was therefore posing problems for the reaction.



Scheme 4.31 Reagents and conditions: i) 1) HOBt, TBTU, DMF, NEt_3 , N_2 , 16 h; or 2) Oxalyl chloride, DMF, DCM, N_2 , 0°C , 1 h, **4.216**, 0°C -rt, 16 h.

To circumvent this problem, we re-addressed our synthetic route and attempted the reduction of the azide in compound **4.138** using Ph_3P (Scheme 4.32). With this method, only the azide would be reduced and the benzyl groups would remain intact, therefore improving the solubility in organic solvents. The reaction appeared to go to completion, however, when purification was attempted the galabiosyl amine **4.140** could not be eluted from the column. A variety of solvent systems were attempted and NEt_3 was also added but this was to no avail. It was decided to repeat the reaction and carry on the synthesis without further purification. Unfortunately, this approach was also unsuccessful and when both reaction conditions (HOBt/TBTU or oxalyl chloride mediated couplings) were re-attempted, similar results were observed. The ^1H NMR spectrum showed a complex mixture of products, including unreacted starting material **4.215**.



Scheme 4.32 Reagents and conditions: i) Ph_3P , THF, H_2O , rt, 18 h.

As previously stated, numerous times throughout this chapter the electrophilicity of the carbonyl carbon of the aromatic scaffold and the nucleophilicity of the carbohydrate amine is extremely important in the synthesis of aromatic scaffolds. The reaction conditions appear to be substrate specific, consequently attaching a more complex epitope such as galabiose would require careful optimisation that will be carried out in the future.

4.11 Spectroscopic analysis on selected glycolipids

During the synthesis of some of the glycolipids described so far, we observed that the ^1H NMR spectra appeared to vary greatly with concentration. In order to gain a further insight into this phenomenon, a series of spectroscopic studies were performed.

Concentration studies were carried out on a selection of glycolipids including first generation glycoconjugates **4.48** and **4.93**, and second generation glycoconjugates **4.109**, **4.125** and **4.126** (Figure 4.42). With these studies, we expected to get some information on how the molecule conformation was influenced by the chemical nature of the linkers and also whether the amide bond form of the lipidic chain (i.e. first generation analogues versus second generation analogues) influenced conformation.

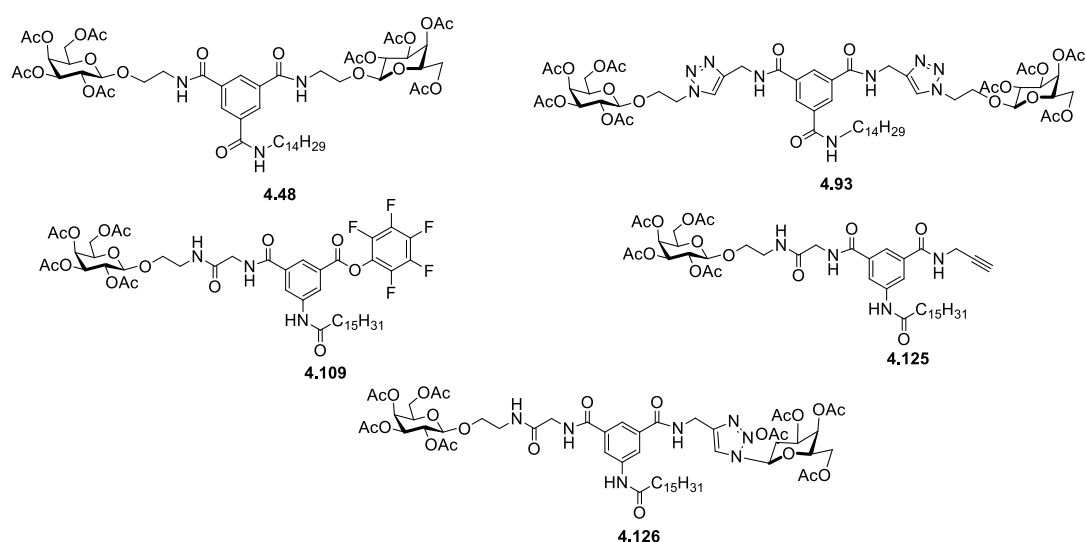


Figure 4.42 First generation glycolipids **4.48** and **4.93**, and second generation glycolipids **4.109**, **4.125** and **4.126** selected for spectroscopic analysis.

4.11.1 Concentration studies on first generation glycolipids **4.48** and **4.116**

Concentration studies were carried out and ^1H NMR spectra of the C-14 flexible glycolipid **4.48** in CDCl_3 were recorded at different concentrations. The variation in the chemical shifts of the signals corresponding to the different N-H signals in glycolipid **4.48** was examined (Figure 4.43). The bottom spectrum represents the least concentrated sample (blue) and the top spectrum represents the most concentrated sample (black). It is very clear that minimal differences are observed between the spectra. The tetradecyl amide proton (N-H2) resonates at 6.77 ppm in the most dilute spectrum and 6.81 ppm in the most concentrated spectrum. This implies that this amide may be weakly involved in intermolecular H-bonding. An even smaller shift is observed for the sugar amide proton (N-H1), which resonates at 6.99 ppm in the dilute spectrum and only moves to 7.0 ppm in the more concentrated sample.

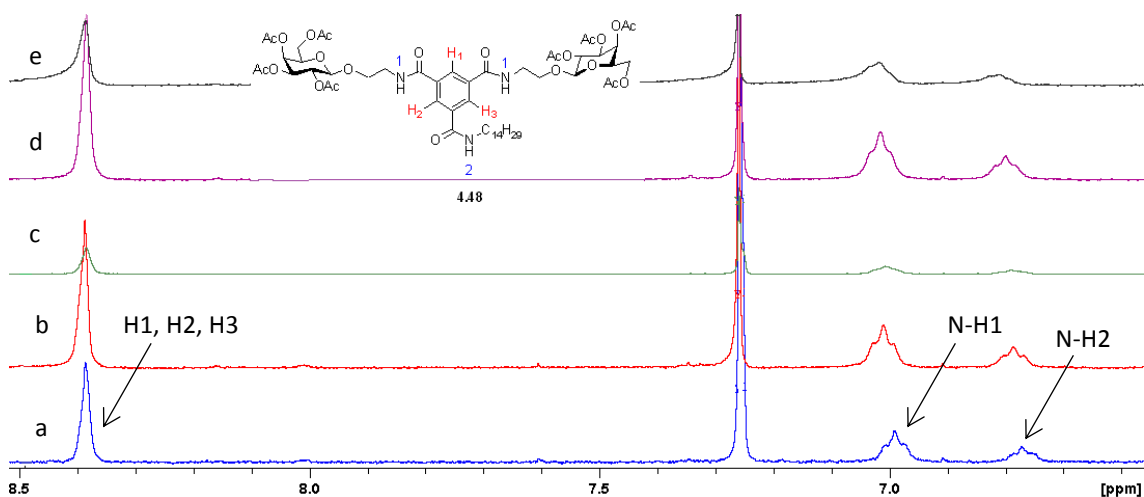


Figure 4.43 ^1H NMR concentration studies on **4.48** in CDCl_3 : a) 4 mg mL^{-1} , b) 9 mg mL^{-1} , c) 13 mg mL^{-1} , d) 16 mg mL^{-1} , e) 23 mg mL^{-1} .

Conversely, much bigger differences are observed between the dilute (blue) and concentrated (pink) spectra of the more rigid, triazole-containing glycolipid **4.116** in CDCl_3 (Figure 4.44). Clear differences between the chemical shifts of the amide protons can be seen in the least concentrated sample (bottom), and the most concentrated sample (top).

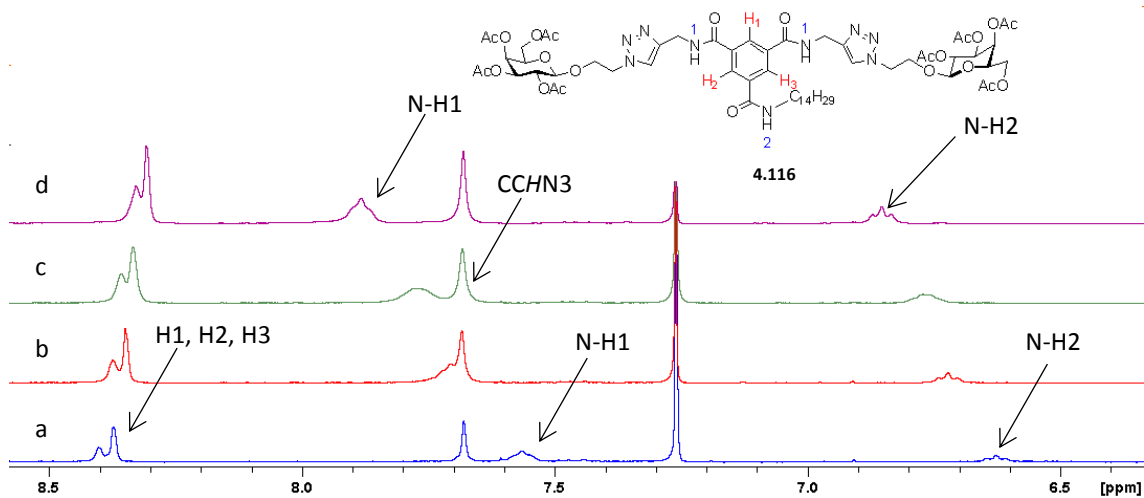


Figure 4.44 ^1H NMR concentration studies on **4.116** in CDCl_3 : a) 4 mg mL^{-1} , b) 8 mg mL^{-1} , c) 11 mg mL^{-1} , d) 18 mg mL^{-1} .

The biggest change observed relates to the amide proton connecting the triazole moiety to the aromatic scaffold (N-H1). It resonates at 7.56 ppm in the dilute sample and shifts to a higher ppm value of 7.88 in the more concentrated sample. This implies that the amide is involved in intermolecular H-bonding. As CHCl_3 is a non-polar solvent, H-bonding between the glycolipid is accentuated. The tetradecyl amide proton (N-H2) also shifts to a higher ppm value going from the dilute spectra to the more concentrated. It resonates at 6.62 ppm in the dilute spectrum and 6.85 ppm in the concentrated spectra. Interestingly, the aromatic protons shift to a lower

ppm value with increasing concentration. This could imply that the aromatic rings are participating in aromatic π stacking interactions.^[197]

4.11.2 Concentration studies on second generation glycolipids **4.109**, **4.125** and **4.126**

The second generation derivative **4.109** showed even bigger variations in the chemical shifts of the signals corresponding to the different amide protons. Most notably, the anilide proton exhibited the biggest variation, as the more acidic NH protons exhibit the stronger H-bonds.^[198] As before, concentration studies were carried out and ^1H NMR spectra of the monovalent pentafluorophenyl derivative **4.109** in CDCl_3 were recorded at different concentrations. The variation in the chemical shifts of the signals corresponding to the different protons in glycolipid **4.109** was examined (Figure 4.45).

The bottom spectrum represents the least concentrated sample (blue) and the top spectrum represents the most concentrated sample (green). Full NMR analysis was carried out by Dr. John O'Brien in Trinity College Dublin, and enabled assignment of all signals.

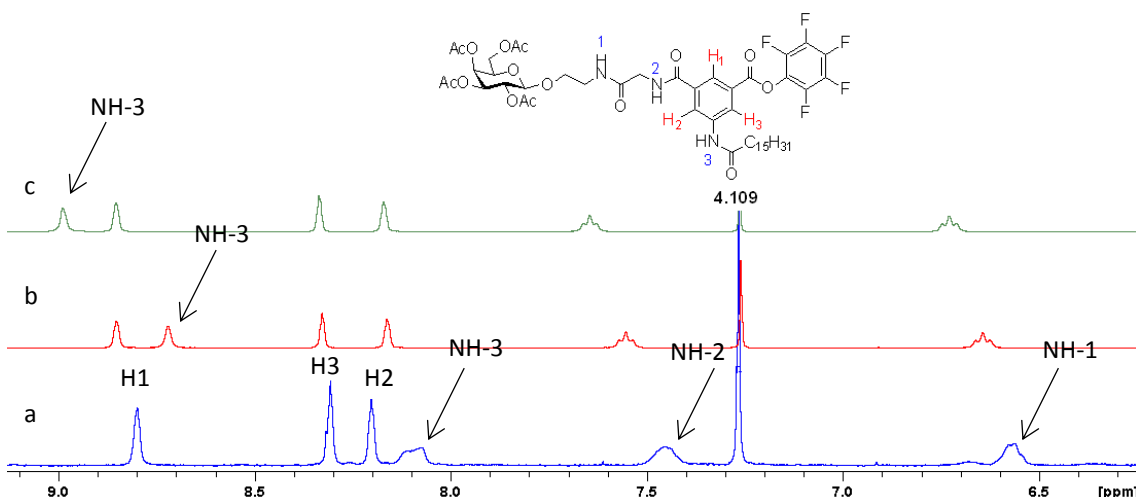


Figure 4.45 ^1H NMR concentration studies on **4.109** in CDCl_3 : a) 5 mg mL^{-1} , b) 10 mg mL^{-1} , c) 15 mg mL^{-1} .

Similar studies were carried out on monovalent glycolipid **4.125** and the non-symmetrical glycolipid **4.126** and the variation in chemical shifts is summarised in Table 4.3. As with glycolipid **4.109**, the resonances for the anilide proton showed the highest chemical shift variation (Figure 4.46). This is not the case for the first generation derivatives where much smaller chemical shift differences are observed for the tetradecyl amide proton. While the pentafluorophenyl derivative **4.109** and divalent galactosyl **4.126** showed similar variation patterns in the chemical shifts for the amide protons, the signals corresponding to the monovalent, non-symmetrical glycolipid **4.126** registered the most significant differences in the dilute and concentrated spectra. This implies that compound **4.126** may participate more readily in intermolecular associations, mediated to some extent by H-bond formation.

Glycolipid	N-H1	N-H1	Δ	N-H2	N-H2	Δ	N-H3	N-H3	Δ	N-H4	N-H4	Δ
	Dilute	Conc.		Dilute	Conc.		Dilute	Conc.		Dilute	Conc.	
	ppm	ppm	ppm									
<p>4.109</p>	6.57	6.73	0.16	7.46	7.67	0.21	8.10	8.99	0.89	-----	-----	-----
<p>4.125</p>	6.69	6.97	0.28	7.53	8.13	0.60	8.12	8.97	0.85	7.09	7.56	0.49
<p>4.126</p>	6.86	7.01	0.15	8.09	8.228	0.19	8.38	8.75	0.37	7.83	7.96	0.13

Table 4.3 Summary of ^1H NMR spectral concentration studies which shows the variations in the chemical shift of the different N-H signals in both dilute and concentrated samples.

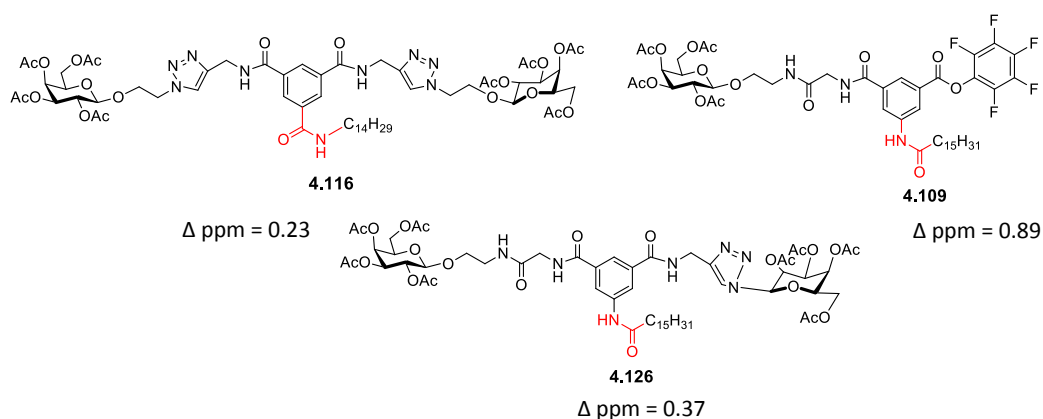


Figure 4.46 Differences in the chemical shift of the lipidic amides for the first generation derivative **4.116** and the second generation derivatives **4.109** and **4.126**.

We can therefore conclude that the type of amide linkage between the lipidic chain and the aromatic scaffold does play a role in H-bonding ability and thus it contributes to the intermolecular interactions between the ligands. A much bigger chemical shift difference is observed for the second generation derivatives, whereby the lipidic chain is linked to the aromatic scaffold *via* an amide bond of the form ArNHCOR, in comparison to the first generation glycolipids which are connected to the lipidic chain *via* an amide bond of the form ArCONHR.

Another conclusion which can be drawn from these data is that the substituents present around the aromatic core also influence the glycolipids ability to form intermolecular associations. With the flexible first generation molecule **4.48**, minimal differences between the amides resonances were observed in the dilute and concentrated spectra. The triazole-containing molecule **4.116** exhibited higher chemical shift differences, but the real substituent effect can be observed in Table 4.3. The difference in the chemical shift of the amides varied depending on whether the pentafluorophenyl ester, alkyne group, or galactosyl triazole were present.

4.12 Conclusions

A collection of bivalent, aromatic glycoconjugates **4.36-4.44** were successfully synthesised. Linkers of varying structure, length and flexibility were exploited to produce a range of glycolipids which offered different presentations of the carbohydrate moiety, thus potentially leading to different biological activities. Two different aromatic scaffolds were also employed, 1) trimesic acid and its derivatives and 2) 5-aminoisophthalic acid, and this led to different amide bond forms being utilised to connect the lipidic chain (ArCONHR, or ArNHCOR). The use

of 5-aminoisophthalic acid proved to be the more efficient synthetic approach, exhibiting higher yields and a decrease in side-product formation.

Following a modular approach, two non-symmetrical glycoconjugates **4.116** and **4.117** were successfully synthesised and using this synthetic route a variety of bivalent heteroglycans could also be potentially prepared.

Spectroscopic analysis was carried out on selected glycolipids and it was found that the first and second generation derivatives behaved quite differently in solution in chloroform. In both cases, the lipidic amide appeared to participate in intermolecular H-bonding, however the anilide proton of the second generation glycolipids exhibited the highest chemical shift difference in ^1H NMR concentration studies. This may imply that the glycoconjugates are involved in intermolecular association as a result of both H-bonding and aromatic interactions.

Studies towards the synthesis of glycoconjugates containing more complex carbohydrate epitopes such as galabiose, has been investigated. However, further optimisation will be necessary.

Finally, for comparison with the bivalent ligands, a monovalent derivative was synthesised and the ability of selected aromatic glycoconjugates to inhibit bacterial adhesion was investigated. The results are discussed in chapter 5.

Chapter 5: Evaluation of glycolipids as potential inhibitors of bacterial adhesion

5.1 Cystic Fibrosis

Cystic fibrosis (CF) is a genetic, life-threatening disease that causes severe lung damage by the recurrence of lower respiratory tract infections.^[199] It is the most common autosomal recessive disease in people of European ancestry and it affects 1 in 2500-3000 live births.^[200] It is caused by a mutation in a *CFTR* gene which encodes the cystic fibrosis transmembrane conductance regulator (CFTR) protein.^[201] Both environmental and inherited factors determine the severity and course of the disease, and it can even differ between siblings that exhibit the same mutations.^[202] Cystic fibrosis does not only affect the respiratory tract but it also leads to the impairment of other organs including the pancreas, sweat glands, vas deferens, bile duct and the large and small bowel.^[201]

5.1.1 *CFTR* protein

The CFTR protein (found in the apical plasma membrane) is a member of the ATP-binding cassette (ABC) superfamily of proteins^[203] and primarily regulates the movement of chloride ions across epithelial membranes. It also regulates the transport of other ions, including sodium.^[204] This regulation of the movement of chloride and sodium ions is extremely important, as it aids in the clearance of mucus by controlling the volume of liquid present on the airway surfaces.^[205]

Mutations in the *CFTR* gene disrupt the function of the chloride and sodium channels. This leads to a decrease in chloride secretion into the airways and an increase in sodium absorption from the airways.^[204] As a result, the airway mucous becomes dehydrated, and therefore leads to the accumulation of mucous which is unusually thick and sticky. This mucous clogs the airways leading to breathing difficulties and susceptibility to bacterial infections.^[206]

Several different mutations of the *CFTR* gene can occur and each mutation leads to a different defect in the CFTR protein. These different defects can result in a milder or more severe form of the disease.^[201] The most common mutation which accounts for about two-thirds of mutated alleles in northern Europe and America, is the deletion of phenylalanine at position 508 ($\Delta F508$).^[201] $\Delta F508$ results in a mutant CFTR protein that does not properly fold and therefore is degraded by the cell. In general, mutations in CFTR gene lead to the production of proteins which are misfolded. The cell protein quality control recognises this misfolded protein and either retains and degrades it, or the abnormal protein is trafficked to the apical plasma membrane where it functions abnormally (Figure 5.1).^[203]

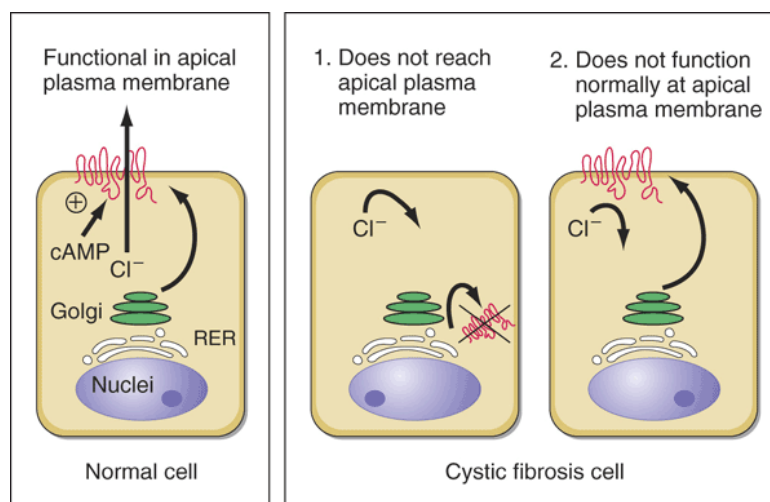


Figure 5.1 In a normal cell (left), the CFTR protein is synthesised in the rough endoplasmic reticulum, glycosylated in the Golgi apparatus and then transported to the apical plasma membrane where it functions as a ion channel regulator. The diagram on the right shows two possible outcomes that can occur with mutations in the CF gene. (1) The mutation can lead to protein mis-folding, e.g., the ΔF_{508} mutation. When this occurs the CFTR is degraded intracellularly and no protein is transported to the apical plasma membrane. (2) With other mutations, the abnormal protein is still processed and transported to the apical plasma membrane where it functions abnormally.^[203]

5.1.2 CF and bacterial infections

Chronic pulmonary infections caused by bacterial pathogens are the leading cause of death among CF patients.^[208] Common bacterial pathogens found in CF airways include *P. aeruginosa* and *B. cepacia* complex.^[209] *B. cepacia* complex (*Bcc*) is a group of opportunistic pathogens classified into at least 17 species. However, with regards to CF infections, *B. cenocepacia* and *B. multivorans* are the most significant.^[208] Although *Pseudomonas* infections are much more common in CF patients, *Bcc* is much more worrying as it is particularly virulent in the CF airway and is often more difficult to eradicate.^[204] Many of the *Bcc* species are highly transmissible and exhibit resistance to multiple antibiotics.^[201] Once a CF patient becomes colonised with *Bcc* the infection is rarely eradicated, and can occasionally lead to the deterioration of the patient.^[201, 204] For these reasons, *Burkholderia* is a pathogen which cannot be ignored.

5.2 *Burkholderia cenocepacia* complex (*Bcc*)

Bcc is a group of genetically distinct and ubiquitous Gram-negative bacteria. Although known to be beneficial to the environment they are also associated with causing severe lung infections in immunocompromised individuals.^[210]

B. cepacia was originally identified by Walter H. Burkholder over 50 years ago as a plant pathogen which caused onion rot. Since then, many environmental benefits have been discovered. *Bcc* can prevent certain plant diseases (including root-rot^[211]), inhibit the growth of

mould on fruit,^[212] act as a chemical fungicide and utilise many different carbon compounds as energy sources.^[213] Some *Bcc* strains can even increase crop production by acting as nitrogen fixers^[214] (Figure 5.2). Despite its obvious environmental advantages, the pathogenesis of *Bcc* in susceptible individuals still remains a major concern, and the risks of using *Bcc* strains in agriculture remains uncertain.

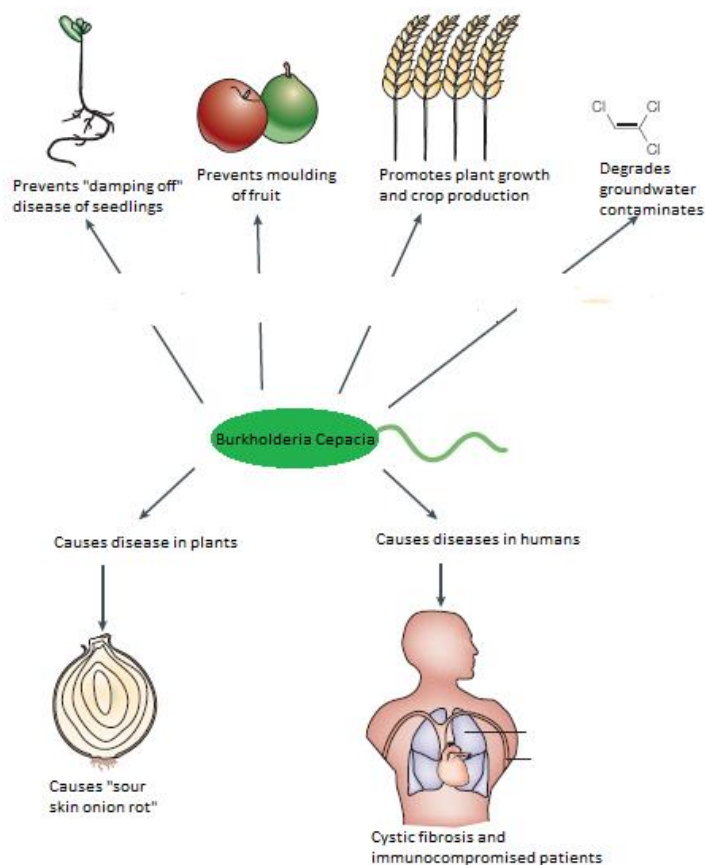


Figure 5.2 Environmental advantages and worrying pathogenesis of the *B. cepacia* complex.^[215]

As stated earlier, the *P. aeruginosa* pathogen accounts for the majority of infections in CF patients, in fact only 3.5% of CF infections worldwide are due to *Bcc*.^[216] Although the incidence of *Bcc* infections is much lower than the more common *P. aeruginosa*, patients colonised with *Bcc* suffer a more rapid decline in health and for this reason *Bcc* infections are particularly feared by CF patients and their carers.^[208, 216] Initially, *B. cenocepacia* was the most common species isolated from CF patients. However, more recently, short term segregation reduced the patient-to-patient transmissibility of *B. cenocepacia*. As *B. multivorans* can be acquired from the environment, it has surpassed *B. cenocepacia* and become the most common *Bcc* species isolated in CF patients in both America and the United Kingdom.^[217]

5.2.1 Virulence of *Bcc*

There are many reasons why *Bcc* is such a virulent group of pathogens. Firstly, they are intrinsically resistant to most antimicrobial treatments available, including aminoglycosides, quinolones, polymyxins and β -lactams.^[218] Even more, increased resistance is observed upon formation of *Bcc* biofilms *in vitro*.^[219] This resistance can be attributed to: 1) the presence of various efflux pumps which can remove antibiotics from the cell, 2) the formation of biofilms, which leads to decreased contact between the antibiotics and the cell surface and 3) decreased permeability of the cell membrane making it less susceptible to the antibiotic.^[204] Secondly, *Bcc* strains are highly transmissible between CF patients.^[216] In one instance, a strain of *B. cenocepacia* (ET12) was isolated from patients residing on different sides of the Atlantic.^[215] Although it is believed that transmission results from direct contact, the exact method by which *Bcc* spreads between CF patients is not known. Finally, infection with *Bcc* strains can lead to the 'cepacia syndrome'. The cepacia syndrome results in a rapid decline in the patient's health and can even lead to death. It occurs when the bacteria enters the bloodstream and is characterised by fever, pneumonia, septicemia and bacteremia.^[210, 220]

Bcc strains can also exhibit a wide variety of virulence factors which enhance its pathogenicity. These include the lipopolysaccharide, secretion of proteins, iron acquisition, formation of biofilm, adhesion proteins and quorum sensing.^[215-217] The lipopolysaccharide can lead to the induction of a strong immune response that results in damage of the host cell,^[210] it also plays a role in antimicrobial peptide resistance.^[221] Quorum sensing is the phenomenon by which bacterial cells can communicate with each other. Acyl-homoserine lactones (AHLs), which are cell-cell signalling molecules, are released by the bacterial cells and then can diffuse into neighbouring cells where they can modulate gene expression including many virulence associated genes.^[215]

5.3 Bacterial adhesion to cell surfaces

Infectious diseases occur when microorganisms colonise host surfaces and grow to a sufficient number to produce clinical symptoms.^[8] For colonisation to occur, pathogens must adhere to the cell surface so that they do not become washed away by the body's regular cleansing mechanisms.^[222] Therefore, the adhesion of pathogenic organisms to host tissues is often the prelude for the majority of infectious diseases.^[222b] As stated previously, this adhesion is largely governed by protein-protein and/or protein-carbohydrate interactions and determines the species specificity of many pathogens and also their preference for certain tissue types.^[9]

One of the phenomena leading to bacterial adhesion involves binding of lectin proteins, present on the surface of the infectious organism, to the carbohydrate portion of glycolipids and glycoproteins present on the surface of the host tissues.^[12, 222b] Lectins are structurally diverse molecules, they are of non-immune origin and do not include enzymes.^[8] Lectins have shallow binding sites but yet are highly specific in their recognition of multivalent complex carbohydrates. They contain a carbohydrate-binding domain (CRD) and binding occurs largely due to hydrogen-bonding between the backbone and side chain carbonyl groups of the protein and the hydroxyl groups of the carbohydrate molecules and non-polar interactions with lipophilic side chains.^[6]

For our research, we are primarily interested in the inhibition of the adhesion of bacterial pathogens. Bacterial lectins are called adhesins and like all lectins they mediate binding to the host cell surface through recognition and binding of specific carbohydrate structures.^[8] They can be described as a bacterial virulence factor due to their ability to mediate adhesion and mutants deficient in the lectin proteins are often unable to initiate infection.^[12, 222b] Bacterial lectins are generally surface-bound and are typically found in fimbriae or pilli.^[12]

Studies as far back as 1979 have shown that soluble carbohydrates recognised by the bacterial surface lectins block the adhesion of bacteria to animal cells *in vitro*.^[222b, 223] Sharon *et al.* found that upon co-administration of methyl α -mannoside and type 1 fimbriated *E. coli* into the urinary bladder of mice, the rate of urinary tract infection decreased by two thirds.^[223] This research showed the potential in using carbohydrates to block bacterial adhesion and led to the examination of new therapies for combating bacterial infections.

5.3.1 *Bcc* invasion of epithelial cells

Bcc adheres to host epithelial cells using both protein and glycolipid receptors which are present on the host cell membrane.^[216] However the exact mechanisms employed by *Bcc* strains to invade the lung epithelial cells are not well understood. There is also some disagreement in the literature. In studies performed by Sylvester *et al.*, it was found that *Bcc* strains bind preferentially to galactose-containing glycolipids, particularly globosides Gb2 and Gb3,^[224] whereas Krivan *et al.* found preferential binding to galactose-containing asialo-GM1 and asialo-GM2.^[225] Neither study showed structural data for the receptors playing a role in invasion of the epithelial cell.

Developing on these findings, McClean and co-workers were the first group to provide direct evidence that galactose-containing glycolipids played a role in the invasion of *Bcc* isolates into

epithelial cells.^[23] They found that preincubation of the lung epithelial cells with either α -galactosidase or β -galactosidase resulted in complete inhibition of invasion by the *B. multivorans* isolate LMG13010 and the *B. cenocepacia* isolate BC7. These results clearly demonstrate that both terminal α - and β -galactose-containing receptors are involved in the invasion process.^[23] In another study, McClean and co-workers^[226] tested the ability of simple sugars (galactose, glucose, mannose, lactose and xylitol) to block the receptors on the bacterial cell, thus inhibiting subsequent binding to the host cell. It was found that competition with lactose was the most effective, however, high concentrations (mmol range) were required. In a follow on study, the same research group reported that glycoconjugates-containing terminal galactose moieties displayed promising anti-adhesion activity and were able to reduce *B. multivorans* adherence to lung epithelial cells (discussed in Chapter 1, section 1.2.4).^[24] With this in mind, the design of galactose-containing glycolipids, which could potentially inhibit bacterial adherence to lung cells of CF patients, and thus reduce infection, is extremely beneficial and could lead to new therapeutic approaches.

5.4 Chapter Objective

This chapter deals with the biological evaluation of a variety of aromatic, aliphatic and aspartic acid-based glycolipids as potential inhibitors of bacterial adhesion. Based on the anti-adhesion approach we wanted to investigate the structure-activity relationship of the selected glycolipids. The work was undertaken in the laboratory of Dr. Siobhan McClean at the Institute of Technology Tallaght, Dublin. As discussed previously, the use of carbohydrates to inhibit bacterial adhesion, and thus reduce infection, is extremely advantageous, and there are numerous examples reported in the literature. However, there are limited examples of compounds containing both a bivalent carbohydrate system and a hydrophobic lipidic chain. Furthermore, to the best of our knowledge there are no examples of these bivalent glycolipid compounds being utilised as potential inhibitors of bacterial adhesion. We hypothesise that the presence and length of the lipidic chain would influence the aggregation of the glycoconjugates in an aqueous environment, and thus influence the presentation of the carbohydrate-binding epitopes.

As discussed earlier, we chose to base our glycolipid analogues around an aromatic, aliphatic or amino acid core (Figure 5.3). The idea was to introduce a scaffold that would allow the synthesis of a bivalent galactose system but also enable the introduction of a lipidic chain. The rigid aromatic compounds could serve as a good comparison to the more flexible aliphatic-based glycolipids.

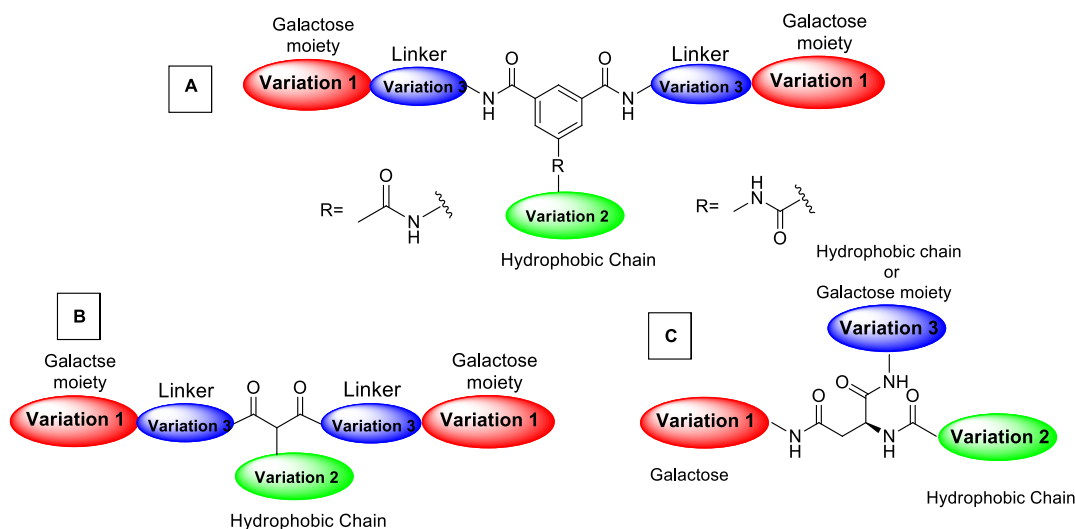


Figure 5.3 General structures of aromatic-based glycolipids (A), aliphatic-based glycolipids (B) and aspartic acid glycolipids (C).

As the lectins of the *B. multivorans* (which recognises glycolipids present on the host cell surface) have not been identified, the rational design of synthetic ligands is extremely difficult. With this in mind, we decided to synthesise a range of glycolipids of diverse chemical structure and investigate how core scaffold, distance between epitopes, linker length and structure, and flexibility influenced the conformation of the ligand and therefore the presentation of the carbohydrate moieties and thus the biological activity. In other words, we wanted to investigate how the structure of the glycolipid affected its biological activity. We also wanted to examine if the presence of the lipidic chain influenced the biological outcome.

As can be seen from Figure 5.3, all of the chosen glycolipids contained a terminal galactose moiety. This was due to the work by McClean *et al.* (discussed in section 5.3.1) which showed that terminal galactose-containing glycolipids present on the host cell mediated adhesion of *Bcc* isolates and facilitated invasion of the lung epithelial cells. We aimed to examine the ability of our synthetic, soluble glycolipids to bind preferentially to the galactose receptors present on the bacterial pathogen, therefore preventing them from binding to the galactosides on the surface of the host cell. In other words, we aimed to prevent colonisation using the anti-adhesion approach.

5.5 Anti-adhesion assay

Biological evaluation was carried out using the clinically relevant LMG13010 isolate. This is a representative strain of *B. multivorans* and is the most frequently acquired *Bcc* species in the last decade. The human epithelial cells (CFBE41o-) used were donated by Dr. Dieter Gruenert

of California Pacific Medical Centre Research Institute, San Francisco, USA. The cells are transformed human bronchial epithelial cells expressing the $\Delta F508$ mutation of the CF transmembrane conductance regulator (CFTR) gene). Therefore, they display the most common mutation observed in CF patients (75% worldwide).

The bacteria were pre-treated with the glycolipids, applied to the cells and the percentage of bacterial adhesion to the epithelial cells evaluated. Epithelial cells incubated with bacteria alone were utilised as a control, and the % of inhibition of adhesion was calculated.

5.6 Biological evaluation of glycolipids 2.26 and 2.29 based on aspartic acid scaffolds

To examine the potential of aspartic acid-based glycolipids to inhibit bacterial adhesion to the lung epithelial cell, *O*-glycolipids, **2.26** and **2.29**, were chosen as representative examples. The C-10 derivative **2.26** was chosen as a representative example as solubility issues were encountered with the C-16 and C-23 derivatives. In order to examine the multivalent effect, bivalent glycolipid **2.29** was also chosen. The results are presented below in Figure 5.5.

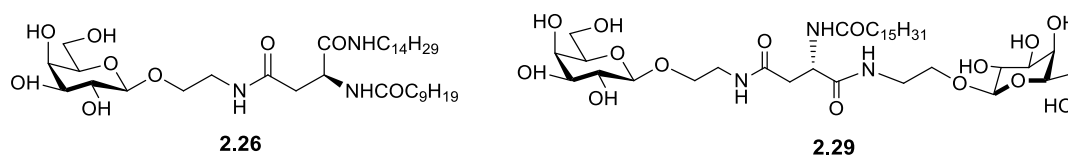


Figure 5.4 Structure of aspartic acid *O*-glycolipids **2.26** and **2.29** selected for biological evaluation.

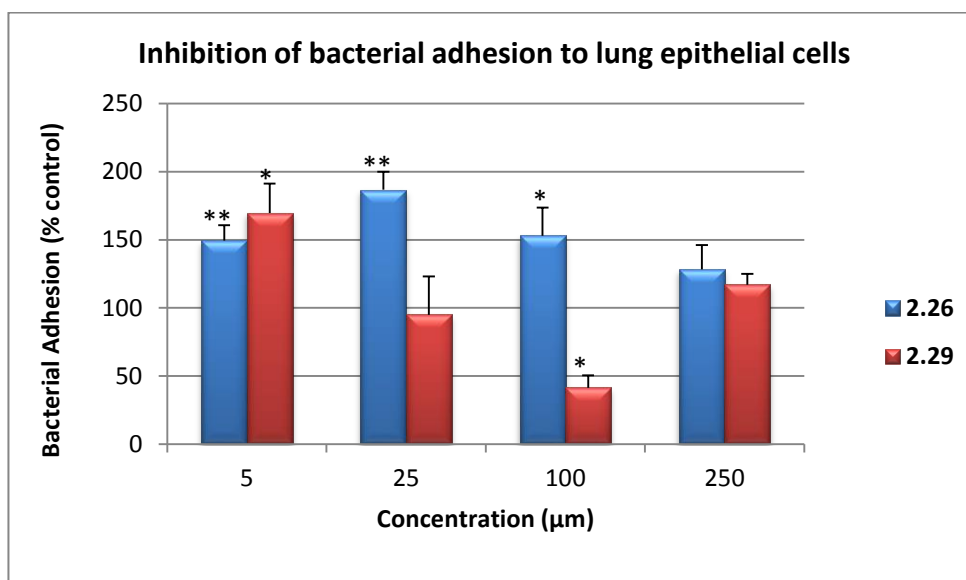


Figure 5.5 Adhesion of LMG13010 bacteria to lung epithelial cells upon treatment with either *O*-glycolipid **2.26** or **2.29**. Bars represent the mean % binding relative to inhibitor-free control (100%) from four separate experiments for each monosaccharide. Error bars represent the standard error of the mean (SEM). * $P < 0.05$, ** $P < 0.01$, *** $P < 0.001$ using a one-way ANOVA and Tukey's post-test, compared to inhibitor-free control.

The results indicate that at all concentrations investigated, the *O*-glycolipid **2.26** appeared to aid bacterial adhesion to the epithelial cells. This phenomenon has been previously reported in the literature and presumably occurs by the glycolipid acting as a 'bridge' between the bacteria and the host cell.^[24] The highest increase in bacterial adhesion (186%) was observed at 25 μm ($p = 0.003$). Glycolipid **2.26** is the only glycolipid tested which presents two lipidic chains. As the concentration increases above 25 μm , a decrease in this effect is observed. This could be due to the ability of this compound to self-assemble into aggregates that precipitate out of solution, as discussed in chapter 2.

Slightly more promising results were observed for the bivalent *O*-glycolipid **2.29**. At a higher concentration of 100 μm bacterial adhesion to the epithelial cell significantly decreased to 40% ($p = 0.003$). In contrast, at a lower concentration of 5 μm , the glycolipid **2.29** appeared to aid adhesion as bacterial adhesion increased to 169% ($p = 0.03$). Statistically significant effects were not observed at all other concentrations examined. The significant decrease in bacterial adherence at 100 μm supports the hypothesis that the bacteria binds to glycolipids present on the host cell surface. With this in mind, it is possible to postulate that synthetic, soluble glycolipids can be used to bind to the bacterial lectins, reducing their ability to adhere to the host cell and rendering them ineffective.

As the bivalent glycolipid **2.29** gave better results, we can postulate that the presence of two carbohydrates favours anti-adhesion and also that the hydrophobic chains affects the biological outcome. The long hydrophobic chains may penetrate into the phospholipid bilayer of the cell membrane exposing the galactose moieties on the surface of the cell. The galactose moieties could then be recognised by the glycolipid receptors present on the bacterial pathogen, and therefore facilitate adhesion.

In order to ensure that the observed biological activity was due to decreased adhesion of the bacteria to the epithelial cells, as opposed to the glycolipids killing the bacteria, minimum inhibitory concentration studies were also carried out. The desired glycolipid was applied to the bacteria at a range of concentrations. The control consisted of the bacteria with no glycolipid applied. The bacterium was incubated for 24 h at 37 °C and the absorbance was read. The % survival was calculated based on the control. The results are shown in Figure 5.6.

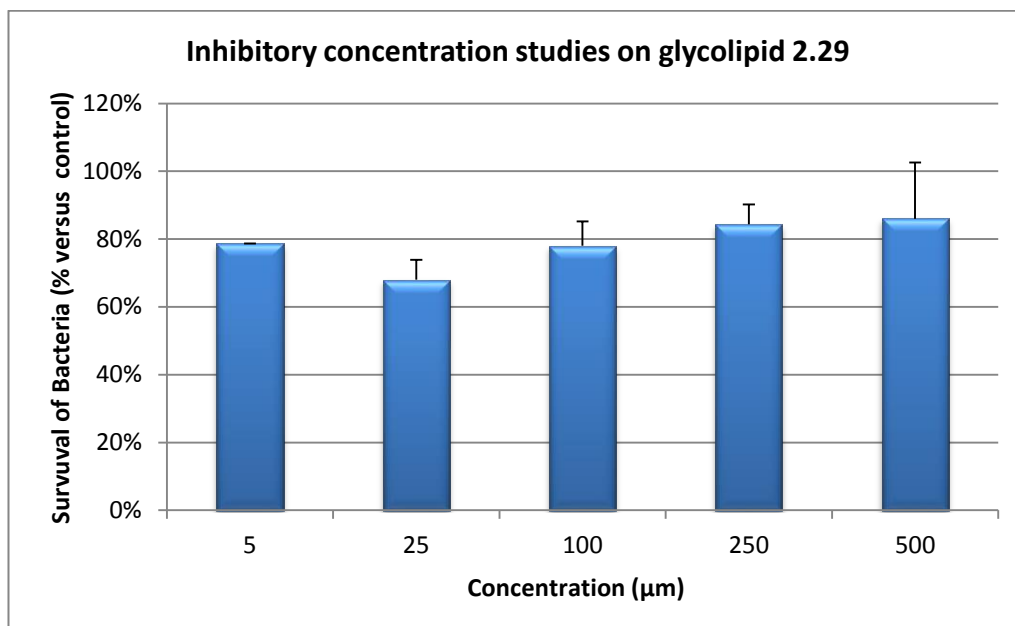


Figure 5.6 Survival of bacteria after overnight incubation (37 °C) with bivalent glycolipid **2.29**. Bars represent the mean% survival relative to inhibitor-free control (100%) from four separate experiments for disaccharide **2.29**. Error bars represent the standard error of the mean (SEM).

Statistically significant effects were not observed at all concentrations examined. This indicates the bacteria survival after overnight incubation with the glycolipid **2.29** is similar to the inhibitor-free control. These data also indicates that the biological activity observed was a real anti-adhesion effect.

5.7 Biological evaluation of glycolipids **3.32** and **3.34** based on aliphatic scaffolds

To examine the potential of aliphatic bivalent glycolipids to inhibit bacterial adhesion to the lung epithelial cell, *N*-glycolipids **3.32** and **3.34** (Figure 5.7) were chosen as representative examples.

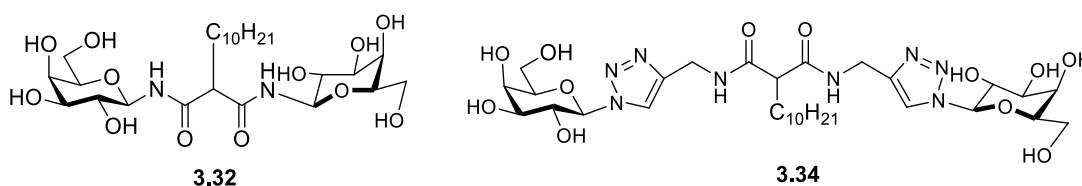


Figure 5.7 Structure of aliphatic *N*-glycolipids **3.32** and **3.44** selected for biological evaluation.

We chose *N*-glycolipid **3.34** to investigate if introducing a triazole moiety into the molecule would influence the biological activity, as has been reported in the literature.^[31] Due to the isosteric relationship between 1,4-di-substituted 1,2,3-triazoles and the amide bond, many biological applications for triazole-containing molecules have been explored.^[227] The results are presented in Figure 5.8.

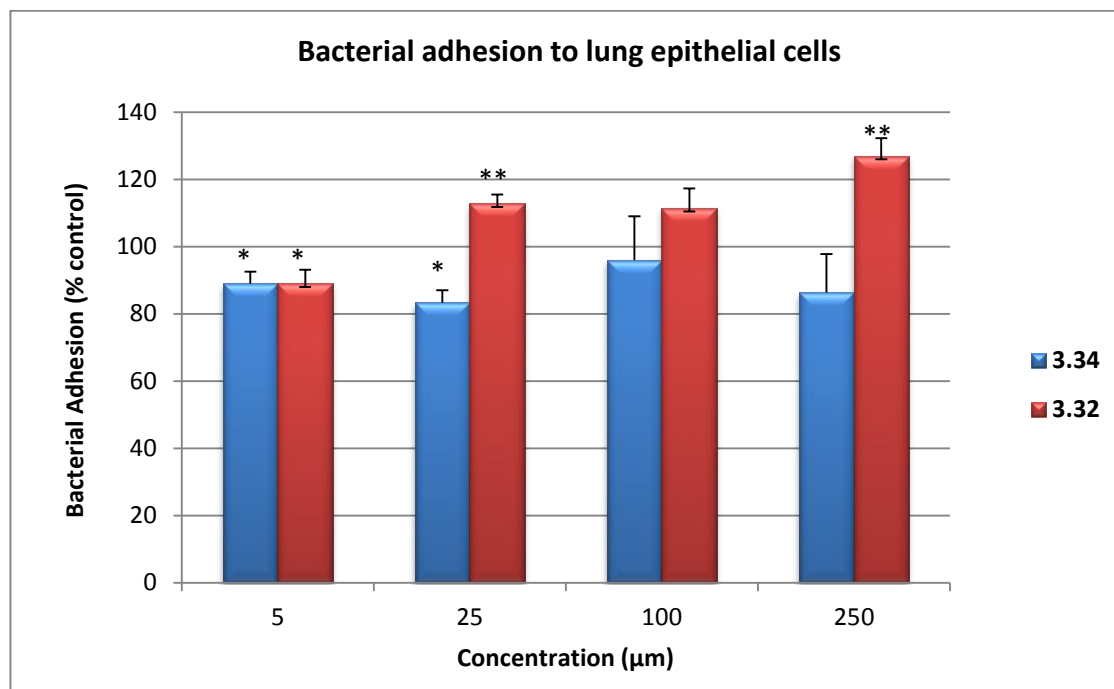


Figure 5.8 Adhesion of LMG13010 bacteria to lung epithelial cell upon treatment with either *N*-glycolipid **3.42** or **3.44**. Bars represent the mean% binding relative to inhibitor free control (100%) from four separate experiments for each disaccharide. Error bars represent the standard error of the mean (SEM). * $P < 0.05$, ** $P < 0.01$, *** $P < 0.001$ using a one-way ANOVA and Tukey's post-test, compared to inhibitor free control.

Preliminary results indicate that the 1,2,3-triazole moiety did in fact influence the biological activity, as the triazole-containing *N*-glycolipid **3.34** gave more promising results than the *N*-glycolipid **3.32**. Although only minimal, and not statistically significant ($p = 0.5$), a reduction in bacterial adhesion to the epithelial cells was observed at all concentrations tested in comparison to glycolipid **3.32**. The more rigid *N*-glycolipid **3.32** appeared to aid the adhesion process at all concentrations, except at 5 μm. The highest increase in bacterial adhesion to the host cell is observed a 250 μm (127%, $p = 0.002$). As with the aspartic acid glycolipids **2.26** and **2.29** (discussed in section 5.5) the **3.32** molecule could be acting as a “bridge” between the bacteria and the host cell and facilitating adhesion. Also It is believed that when a high concentration of glycolipids is present the bacteria can utilise them as a carbon source to provide energy.

Unlike the aspartic acid glycolipids **2.26** and **2.29** previously discussed, the results do not follow the expected concentration-dependent pattern. In fact for the triazole-containing glycolipid **3.34**, glycolipid concentration had a limited effect on the results, and similar adhesion levels were observed at all concentrations examined.

As before, inhibitory concentration studies were also carried out, and the results are shown in Figure 5.9. High survival rates of bacteria were achieved after overnight incubation with the corresponding glycolipid. One way ANOVA shows no statistically significant difference between the inhibitor free control and the bacteria incubated with varying concentrations of the glycolipids **3.32** and **3.34**. These results indicate that the glycolipids **3.32** and **3.34** slightly interfere with bacterial adhesion to the epithelial cell, but exhibit no toxicity towards the bacteria.

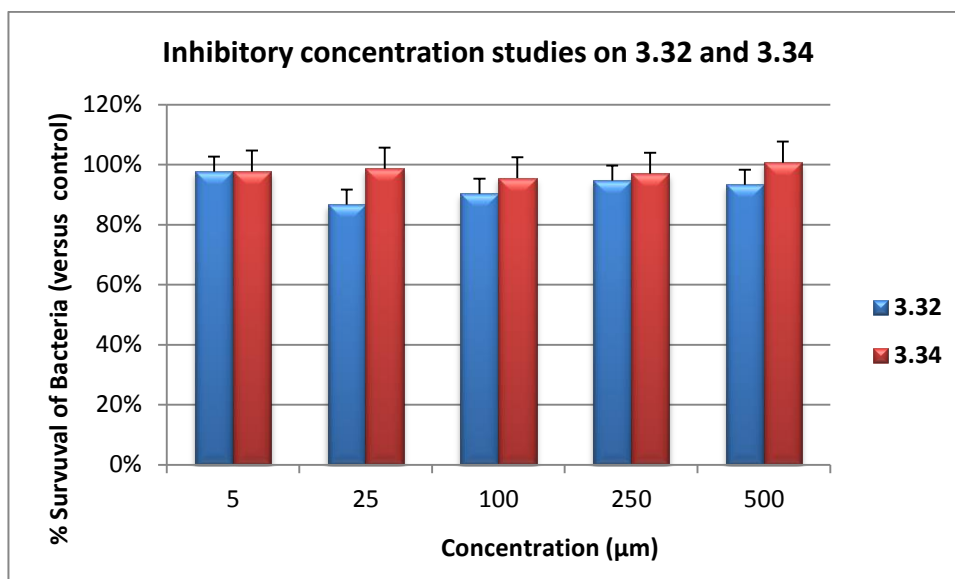


Figure 5.9 Survival of bacteria after overnight incubation with glycolipids **3.33** and **3.34**. Bars represent the mean% survival relative to inhibitor free control (100%) from four separate experiments for each disaccharide. Error bars represent the standard error of the mean (SEM).

5.8 Biological evaluation of glycolipids based on aromatic scaffolds 4.27-4.34.

To examine the potential of aromatic-based glycolipids to inhibit bacterial adhesion to the lung epithelial cell, a wide variety of structurally diverse molecules were analysed. In order to compare how linker length and structure, and also flexibility influenced the presentation of the carbohydrate moieties and thus the biological activity, glycolipids-containing structurally diverse linkers were evaluated.

5.8.1 Rigid *N*-glycolipids 4.36 and 4.37 versus flexible *O*-glycolipids 4.38 and 4.39

The rigid *N*-glycolipids **4.36** and **4.37** served as a good comparison to the more flexible *O*-linked glycolipids **4.38** and **4.39**. We also wanted to examine how hydrophobic chain length alters the biological activity so both short (**4.27** and **4.39**) and long (**4.36** and **4.38**) chain derivatives were synthesised (Figure 5.10). The effect of the aromatic scaffold (trimesic derivatives **4.36** and **4.39**, versus isophthalic derivatives **4.37** and **4.38**) were also evaluated. The assay was performed as before and the results are presented in Figure 5.11.

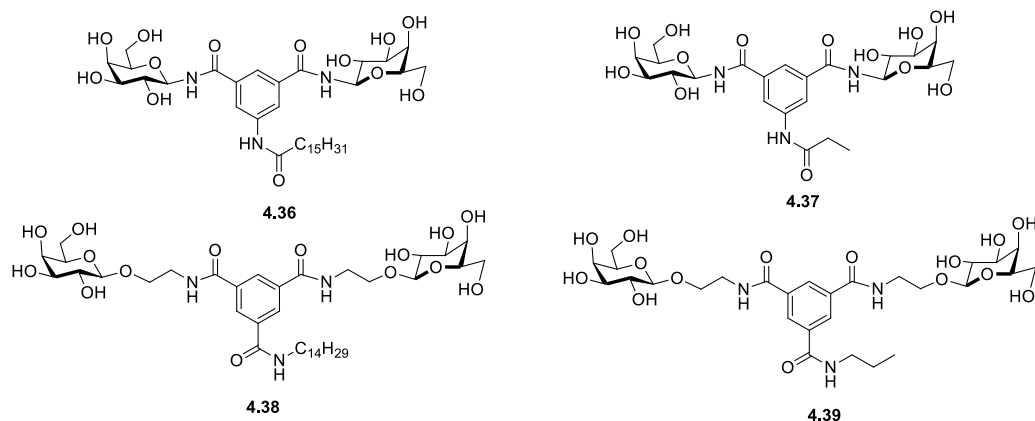


Figure 5.10 Structures of aromatic, rigid *N*-glycolipids **4.36** and **4.37**, and flexible *O*-glycolipids **4.38** and **4.39** selected for biological evaluation.

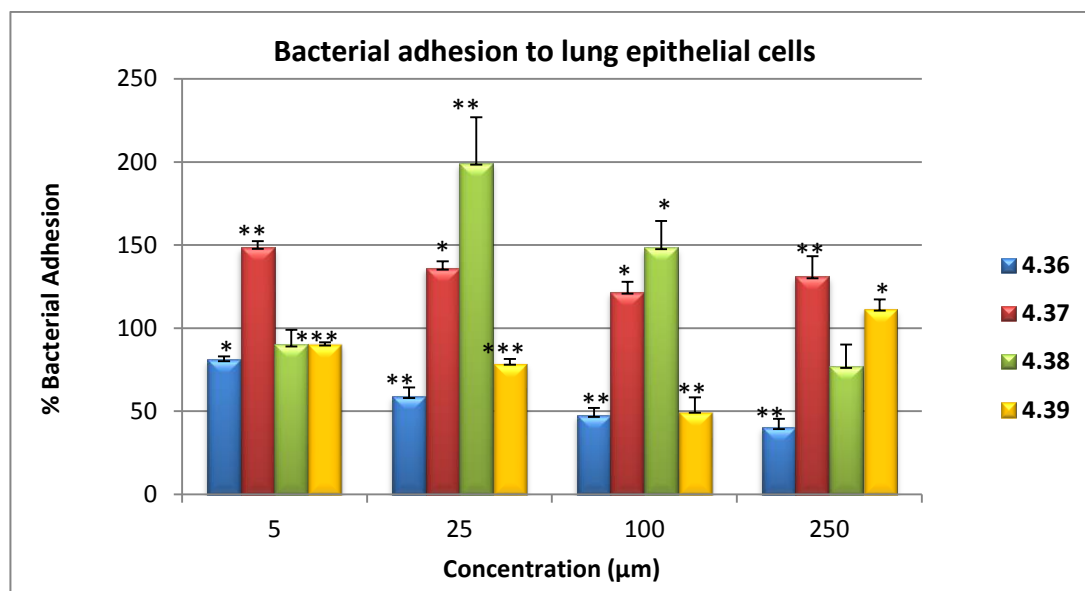


Figure 5.11 Adhesion of LMG13010 bacteria to lung epithelial cell upon treatment with either *N*-glycolipid **4.36** or **4.37**, or *O*-glycolipid **4.38** or **4.39**. Bars represent the mean% binding relative to inhibitor-free control (100%) from four separate experiments for each bivalent glycolipid. Error bars represent the standard error of the mean (SEM). * $P < 0.05$, ** $P < 0.01$, *** $P < 0.001$ using a one-way ANOVA and Tukey's post-test, compared to inhibitor free control.

The results show that the C-16 rigid glycolipid **4.36** displayed optimum biological activity. At all concentrations tested, a reduction in bacterial adhesion was observed. One way ANOVA analysis indicated that these biological data differed significantly ($p = 0.009$). Further, Tukey *post hoc* analysis indicated that the activity observed at 25, 100 and 250 μm is significantly different to the inhibitor-free control. The highest inhibition was achieved at 250 μm where bacterial adhesion to the epithelial lung cell significantly decreased to 40% ($p = 0.006$). As expected, the results were inversely proportional and as the glycolipid concentrated decreased the% of bacterial adhesion increased. In contrast, the C-3 rigid derivative **4.37** seemed to increase bacterial adhesion at all concentrations tested ($p = 0.003$). Like before, we believe the

glycolipid aids adhesion by acting as a “bridge” between the bacteria and the host cell. Interestingly, these results indicate that the hydrophobic chain may play a role in the inhibition process, maybe by altering the molecule conformation and/or leading to the formation of intermolecular assembles and thus influencing the presentation of the carbohydrate moieties.

Unexpectedly, the results for the more flexible *O*-glycolipids **4.38** and **4.39** follow an opposite pattern. This time, the C-3 flexible derivative **4.39** provides the more promising results. At all concentrations (apart from 250 μm) a decrease in bacterial adhesion is observed. The highest reduction is observed at 100 μm where the bacterial adhesion decreases to 50% ($p = 0.008$). Again, the results follow an inversely proportional pattern and the bacterial adhesion increases with decreased glycolipid concentration. The fact that the bacterial adhesion increases at 250 μm and decreases at lower concentrations is not unusual. As mentioned previously it is believed that when a high concentration of glycolipids is present the bacteria can utilise them as a carbon source to provide energy. The C-14 flexible derivative **4.38** shows a dramatic increase in bacterial adhesion at 25 and 100 μm ($p = 0.01$, $p = 0.02$ respectively), whereas at 250 and 5 μm a statistically significantly effect is not observed.

With these contradicting results a direct conclusion is difficult. While it is clear that the rigid C-16 derivative **4.36** gave the most promising results, the C-3 flexible derivative **4.39** also led to a slight decrease in bacterial adhesion. We can therefore assume that the biggest influence on the biological activity lies in the conformation of the molecule, intermolecular interactions and thus the presentation of the terminal galactose moieties. In the case of the rigid derivatives **4.36** and **4.37**, the C-16 derivative resulted in a more optimum presentation of the galactose moieties and thus an optimum biological activity. In contrast for the more flexible derivatives **4.38** and **4.39** the C-3 derivative led to a more optimum presentation of the galactose moieties and therefore an increased biological activity. It is also possible that the shorter distance between the galactose moieties is more optimum for the rigid derivative **4.36** and rigidity does not play as big a role as believed.

Inhibitory concentration studies were also carried out, and the results are shown in Figure 5.12. The results indicate that the inhibition of bacterial adhesion observed was a real effect as statistically significantly differences in bacterial survival were not observed at the relevant concentrations.

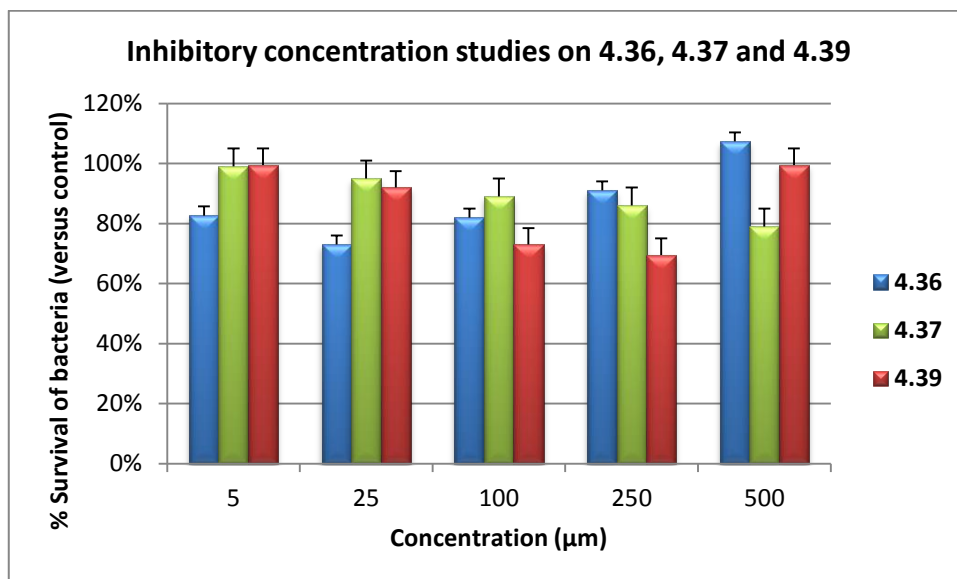


Figure 5.12 Survival of bacteria after overnight incubation with glycolipids **4.36**, **4.37** and **4.39**. Bars represent the mean% survival relative to inhibitor free control (100%) from three separate experiments for each bivalent glycolipid. Error bars represent the standard error of the mean (SEM).

5.8.2 1,2,3-Triazole-containing *O*-glycolipids **4.40** and **4.41** and *N*-glycolipids **4.42**

As before, we wanted to examine how introducing a triazole moiety into the molecule would influence the biological activity. For this analysis, the more flexible *O*-glycolipids **4.40-4.41** and rigid *N*-glycolipid **4.42** (Figure 5.13) were chosen as representative examples. The presence of a triazole moiety can aid binding to the bacterial receptor, as aromatic stacking can occur with aromatic moieties present on the lectin. It is also important to highlight that introducing the triazole moiety alters the distance between the aromatic core and the carbohydrate epitope. This results in an increased distance between the carbohydrate epitopes and thus can influence how they are presented to the bacterial receptor and therefore the biological result. We also wanted to investigate how hydrophobic chain length alters the biological activity, so both short (**4.41**) and long (**4.40**) chain derivatives were synthesised.

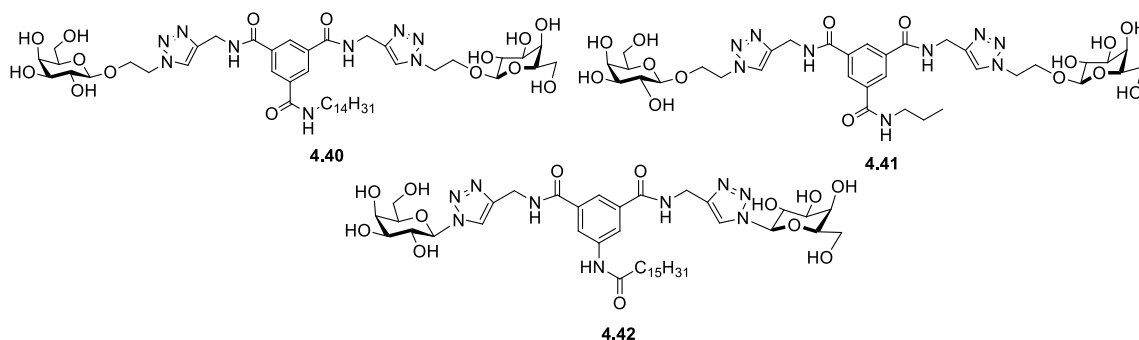


Figure 5.13 Structure of aromatic flexible *O*-glycolipids **4.40** and **4.41**, and rigid *N*-glycolipids **4.42** selected for biological evaluation.

The assay was performed as before and the results are presented in Figure 5.14.

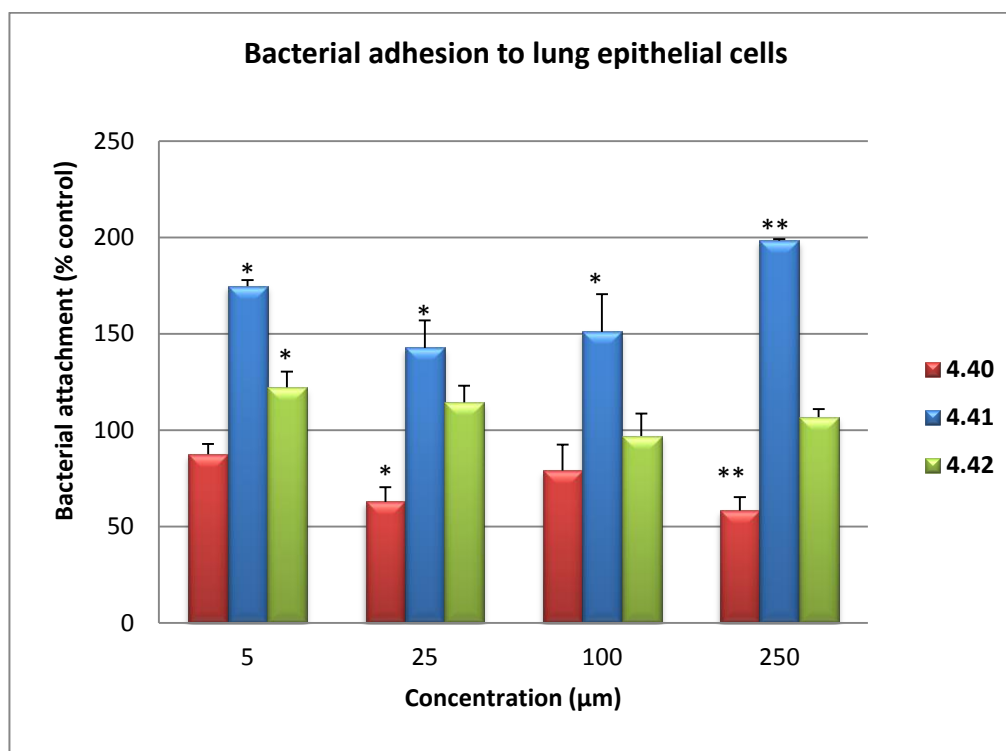


Figure 5.14 Adhesion of LMG13010 bacteria to lung epithelial cell upon treatment with either *O*-glycolipid **4.40** or **4.41**, or *N*-glycolipid **4.42**. Bars represent the mean% binding relative to inhibitor-free control (100%) from four separate experiments for each bivalent glycolipid. Error bars represent the standard error of the mean (SEM). * $P < 0.05$, ** $P < 0.01$, *** $P < 0.001$ using a one-way ANOVA and Tukey's post-test, compared to inhibitor free control.

The results indicate that the C-14, flexible, triazole-containing derivative **4.40** exhibited the best biological activity, as bacterial adhesion to the epithelial cells decreased at all concentrations tested. However, at some concentrations (5 and 100 µm) the reduction was not statistically significant. The highest reduction was observed at 250 µm (bacterial adhesion decreased to 58% ($p = 0.001$)).

In comparison, the C-3, flexible, triazole-containing derivative **4.41** exhibited the least biological activity as treatment with the compound led to a statistically significant increase in bacterial adhesion at all concentrations tested. In fact, when the bacteria was treated with 250 µm of glycolipid **4.41**, bacterial adhesion to the epithelial cell increased to 170% ($p = 0.004$). For the more rigid C-16 *N*-glycolipid **4.42** the results were also poor. As with derivative **4.41**, the presence of the compound led to an increase in bacterial adhesion at the majority of concentrations tested. However, in this case, the increase in bacterial adhesion to the host cell is fairly minimal and not statistically significant.

Again, these contradictory results led to difficulties in reaching an obvious conclusion. In the case of the more flexible *O*-glycolipid **4.40**, the presence of the triazole moiety does lead to an improved biological activity, as a decrease in bacterial adhesion was observed at all concentrations investigated. At both 250 and 25 μm concentrations the decrease is fairly significant (58% and 62% respectively). These results also highlight the importance of the hydrophobic chain, as the C-3 glycolipid **4.41** performed much worse than its C-14 counterpart **4.40**. In fact, **4.41** promotes a significant increase in bacterial adhesion at all concentrations tested. For the more rigid *N*-glycolipid **4.42**, introducing the triazole moiety into the molecule does not lead to an improved biological result. In fact, it actually had a poorer biological activity. Treatment of the bacteria with glycolipid **4.42** led to an increase in bacterial adhesion at most of the concentrations tested, however, the increase is fairly minimal.

All of this information points to the conclusion that the glycolipid conformation and how they interact with each other in solution are the most important factors, as these factors influence how the galactose moieties are presented to the cell and ultimately the biological activity.

As before, inhibitory concentration studies were also carried out, and the results are shown in Figure 5.15. The graph clearly shows that a real adhesion inhibition effect was in fact observed as high survival rates were obtained after overnight incubation with the desired glycolipid.

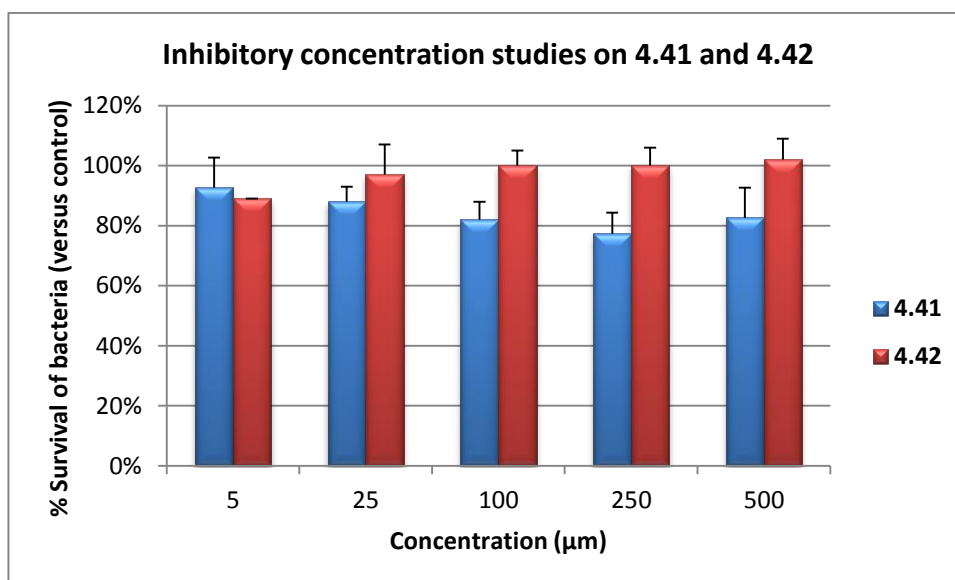


Figure 5.15 Survival of bacteria after overnight incubation with glycolipids **4.41**, and **4.42**. Bars represent the mean% survival relative to inhibitor-free control (100%) from three separate experiments for each bivalent glycolipid. Error bars represent the standard error of the mean (SEM).

5.8.3 Biological evaluation of *O*-glycolipid **4.43** and *N*-glycolipid **4.44**

In an attempt to distinguish between linker length and flexibility/rigidity, the biological evaluation of glycolipid **4.43** (Figure 5.16) was carried out. We also wanted to determine if multivalency was important for the biological activity of glycolipid **4.36**. With this in mind, the rigid, monovalent *N*-glycolipid **4.44** was also evaluated as a potential inhibitor of bacterial adhesion. The assay was performed as before and the results are presented in Figure 5.17.

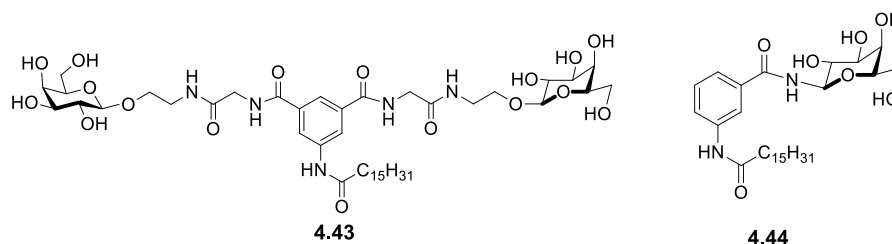


Figure 5.16 Structure of aromatic *O*-glycolipid **4.43** and, and monovalent *N*-glycolipid **4.44** selected for biological evaluation.

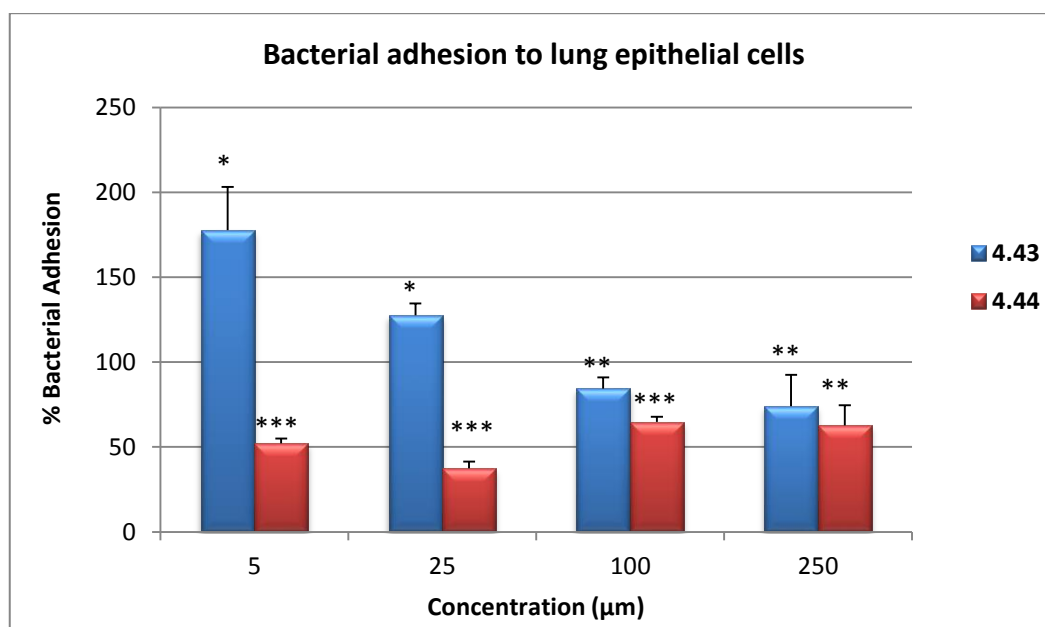


Figure 5.17 Adhesion of LMG13010 bacteria to lung epithelial cell upon treatment with either *O*-glycolipid **4.43**, or *N*-glycolipid **4.44**. Bars represent the mean% binding relative to inhibitor-free control (100%) from four separate experiments for each bivalent glycolipid. Error bars represent the standard error of the mean (SEM). *P < 0.05, **P < 0.01, ***P < 0.001 using a one-way ANOVA and Tukey's post-test, compared to inhibitor free control.

As can be seen from the graph, the biological activity of the elongated *O*-glycolipid derivative **4.43** is concentration dependent. At the higher concentrations of 250 and 100 μm, a decrease in bacterial adhesion to the epithelial lung cells is observed (74% and 84%, respectively, compared to 100% for the control). However, at the lower concentrations of 25 and 5 μm an

increase in bacterial adhesion is clearly seen (127% and 177% respectively). From these data it is evident that concentration plays an important role in the biological activity of glycolipid **4.43**.

For the monovalent *N*-glycolipid **4.44**, the results are a bit more promising. As with its bivalent counterpart **4.36**, the presence of glycolipid **4.44** leads to a reduction in bacterial adhesion at all concentrations investigated. Interestingly, unlike the bivalent glycolipid **4.36**, the results are not inversely proportional to the glycolipid concentration, the largest reduction in bacterial adhesion is actually observed at 25 μm (37%, $p=0.000$).

As with previous glycolipids, inhibitory concentration studies were carried out, and the results are shown in Figure 5.18. From these data, we can conclude that monovalent glycolipid **4.44** was in fact inhibiting bacterial adhesion as nearly 100% bacterial survival is observed at all concentrations after overnight incubation.

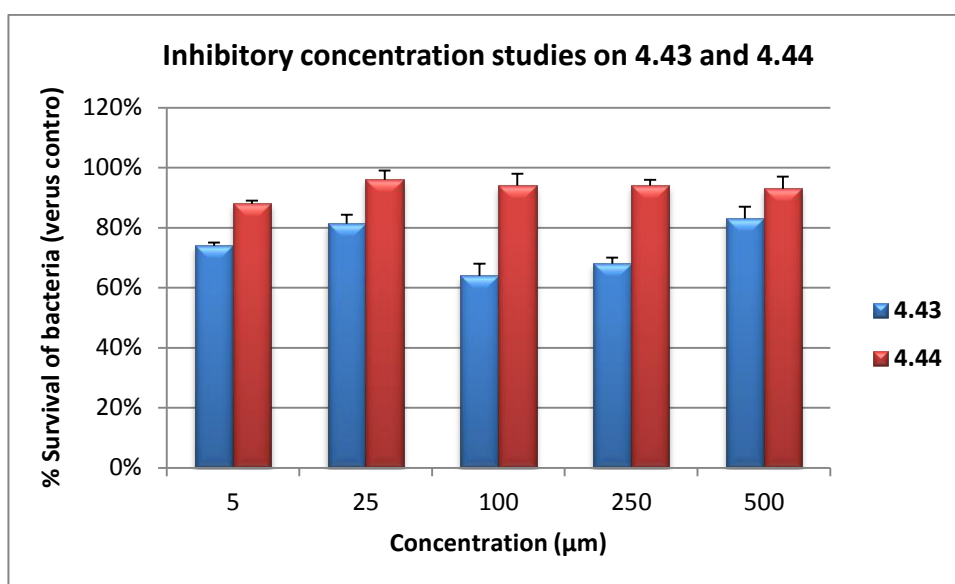


Figure 5.18 Survival of bacteria after overnight incubation with glycolipids **4.43** and **4.44**. Bars represent the mean% survival relative to inhibitor-free control (100%) from three separate experiments for each bivalent glycolipid. Error bars represent the standard error of the mean (SEM).

5.9. Conclusions based on structural-activity relationship

5.9.1 Multivalent versus monovalent:

For glycolipids **2.26** and **2.29**, which were based around aspartic acid scaffolds, the bivalent derivative **2.29** displayed increased biological activity in comparison to the monovalent glycolipid **2.26**. However, for the glycolipids based around an aromatic scaffold, the results are not so clear (Figure 5.19).

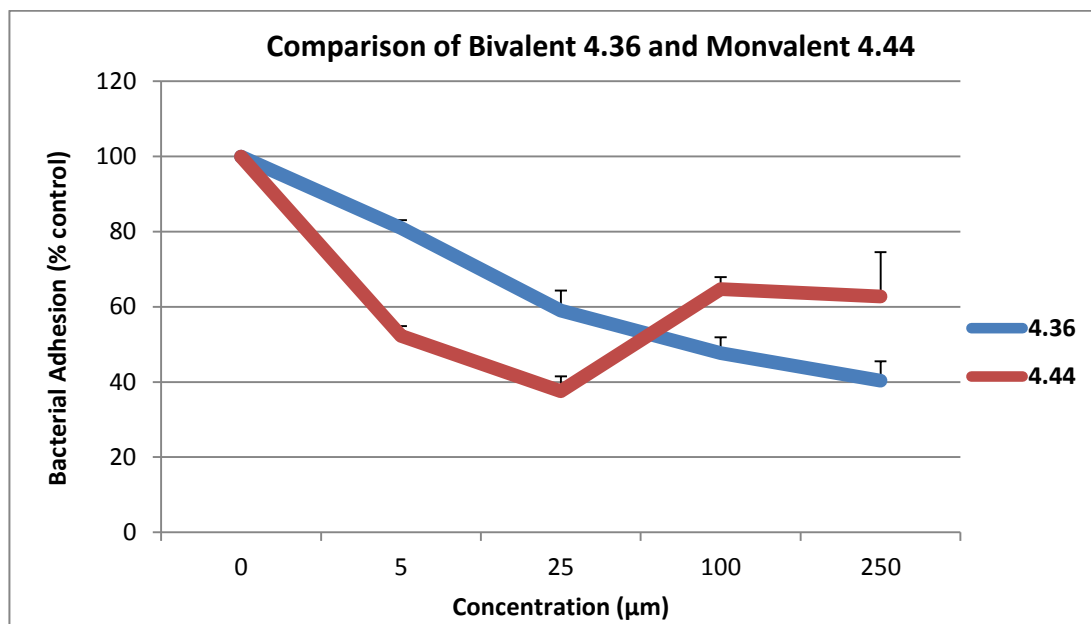


Figure 5.19 Comparison of how bivalent derivative **4.36** and monovalent derivative **4.44** influence bacterial adhesion to epithelial cells.

For both bivalent glycolipid **4.36** and monovalent glycolipid **4.44**, the bacterial adhesion decreases at all concentrations examined. It is clear from Figure 5.19 that the biological activity of bivalent derivative **4.36** is concentration dependent, and the % adhesion is inversely proportional to the glycolipid concentration. This is not the case for the monovalent derivative **4.44**, which shows the best biological activity at 25 µm. With both glycolipid **4.36** and **4.44**, having optimum activities at different concentrations the effect of multivalency is difficult to determine. Nevertheless, statistical analysis shows glycolipid **4.44** to be the better inhibitor of bacterial adhesion, as a more statistically significant difference to the control is observed at all concentrations examined.

5.9.2 Flexibility versus rigidity:

In Figure 5.20, the flexible compounds **4.38** and **4.40** are denoted in red, and the rigid **4.36** and **4.42** compounds are shown in blue. The more transparent colours refer to the triazole-containing compounds, **4.40** and **4.42**.

The non-triazole-containing rigid *N*-glycolipid **4.36** exhibited the best biological activity of all compounds tested. However, when a triazole moiety was introduced into the molecule **4.42**, a reduction in biological activity was observed. In comparison the non-triazole-containing flexible glycolipid **4.38** generally led to increased levels of bacterial adhesion, or at least only minimal levels of decreased bacterial adhesion. With this glycolipid, **4.38**, introducing a triazole moiety (**4.40**) did lead to an increase in biological activity. In fact, glycolipid **4.40** displayed a

high level of biological activity and inhibition of bacterial adhesion was observed at all concentrations.

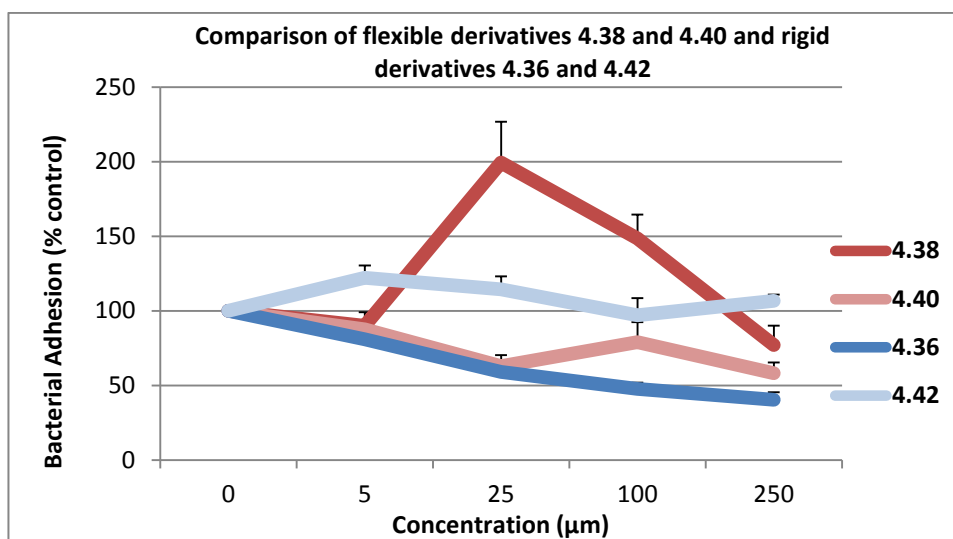


Figure 5.20 Comparison of how rigidity (blue) and flexibility (red) influences the biological activity of the glycolipid.

In summary, for the rigid *N*-glycolipid **4.36**, the introduction of the triazole moiety results in a decrease in biological activity. In contrast, for the more flexible *O*-glycolipid **4.38**, introducing the triazole moiety results in an improved biological activity. All this information leads to the conclusion that rigidity, and thus the “locking” of compound conformation, may be beneficial. This may lead to a more optimum presentation of the galactose moieties and thus increased biological activity. Introducing the triazole moiety will also alter the length of the linker between the scaffold and the carbohydrate epitope. This increase in length will alter the distance between the two galactose moieties and again could influence the presentation of the galactose moieties and thus the biological activity.

5.9.3 Importance of hydrophobic chain

The effect of hydrophobic chains is somewhat conflicting. Our studies indicated that, generally, for the more rigid derivatives, the longer chain analogues **4.36** gave the more promising results. Whereas, for the more flexible derivatives, the shorter chain analogues **4.39** appeared to exhibit a higher biological activity. However, overall it is clear that the presence of hydrophobic chains does influence the biological activity (Figure 5.21 and 5.22).

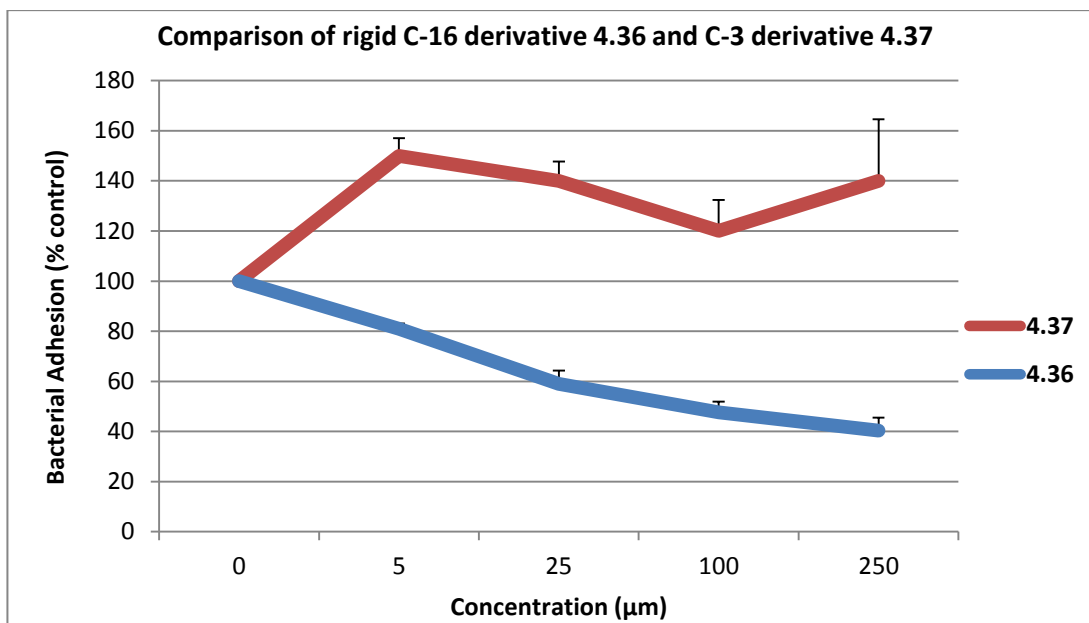


Figure 5.21 Comparison of how C-14 **4.36** (blue) and C-3 **4.37** (red) hydrocarbon chains influence the biological activity of the flexible *O*-glycolipids.

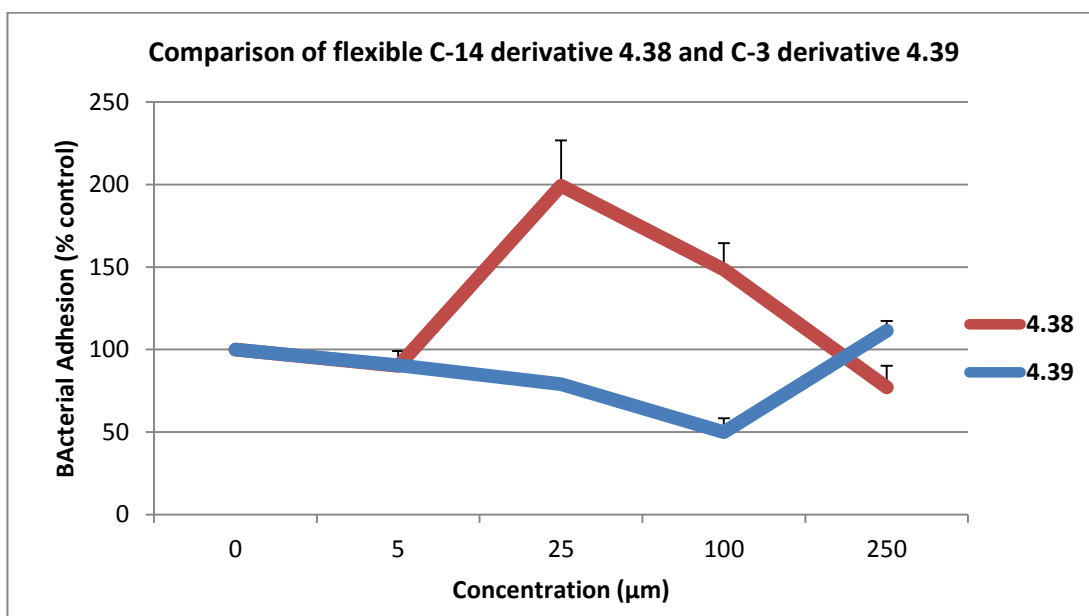


Figure 5.22 Comparison of how C-14 **4.38** (red) and C-3 **4.39** (blue) hydrocarbon chains influence the biological activity of the rigid *N*-glycolipids.

5.10 Conclusions

We have examined the structure-activity relationship of a variety of glycolipids based around either an aspartic acid, aliphatic or aromatic core. The inhibition ability of the glycoconjugates appears to be very specific for each compound. For the majority of the compounds, the ability to influence adhesion is not concentration dependent. For example some compounds promoted inhibition at lower concentrations, but at higher concentrations bacterial adhesion is promoted.

Preliminary results have revealed ligands which can reduce bacterial adhesion to the host epithelial cell in the μm range. It is believed they achieve this by binding to the bacterial receptors thus inhibiting subsequent binding to the host cells. The best inhibitors were identified as the rigid, bivalent *N*-glycolipid **4.36** and the rigid, monovalent *N*-glycolipid **4.44**. Overall, the results are extremely difficult to rationalise and conformational analysis on the glycolipids, as well as more structural information on the lectins of interest, is required in order to establish trends. This highlights the complex nature of the adhesion process. Furthermore, the investigation of micelle formation is also crucial in order to rationalise the results.

In order to improve the anti-adhesion effect, more definite structural information on the receptors involved in the adhesion process is required. This would allow for a more rational design of synthetic ligands.

Chapter 6: Experimental details

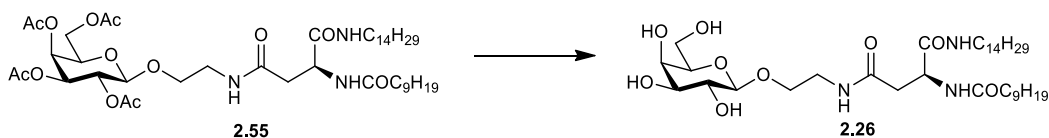
6.1 General Procedure and Instrumentation

All chemicals purchased were reagent grade and used without further purification, unless stated otherwise. DCM was distilled over CaH_2 , MeCN over P_2O_5 , THF over Na wire and benzophenone. Anhydrous DMF and Pyr were purchased from Sigma Aldrich. Molecular sieves (MS) used for glycosylation and coupling were 8-12 Mesh and were flamed dried prior to use. Reactions were monitored using thin layer chromatography (TLC) on Merck Silica Gel F₂₅₄ plates, using mixtures of Pet Ether/EtOAc, unless otherwise stated. Detection was effected either by visualisation in UV light and/or charring in a mixture of 5% sulphuric acid-EtOH or phosphomolybdic acid-EtOH (12 g in 250 mL). Evaporation under reduced pressure was always effected with the bath temperature kept below 40 °C.

NMR spectra were obtained on a Bruker Avance 300 MHz spectrometer operated at 300 MHz for ^1H NMR analysis and 75 MHz for ^{13}C analysis at 298 K, or a Bruker Avance AV-600 MHz spectrometer (Trinity College Dublin) operated at 600 MHz for ^1H and 150 MHz for ^{13}C at 298 K. Proton and carbon signals were assigned with the aid of 2D NMR experiments (COSY, HSQC, TOCSY, ^{14}N HSQC, ROESY, NOESY or HCCOSW) and DEPT experiments for novel compounds. HCCOSW is a HSQC type of experiment. Chemical shifts for ^1H NMR acquired in CDCl_3 are reported in ppm relative to residual solvent proton (δ 7.26 ppm). Flash chromatography was performed according to the method of Still et al. with Merck Silica Gel 60, using adjusted mixtures of Pet Ether/EtOAc, unless otherwise stated.^[228] Optical rotations were obtained using an AA-100 polarimeter. $[\alpha]_D^{25}$ values are given in $10^1\text{cm}^2\text{g}^{-1}$. The melting points were obtained using a Stuart Scientific SMP1 melting point apparatus and are uncorrected. High resolution mass spectra (HR-MS) were performed on an Agilent-L 1200 Series coupled to a 6210 Agilent Time-of-Flight (TOF) mass spectrometer equipped with both a positive and negative electrospray source. Infrared spectra were obtained in the region 4000-400 cm^{-1} on a Nicolet Impact 400D spectrophotometer or using a Perkin Elmer 2000 FTIR spectrometer. SEM was performed using a Hitachi S-3200-N with a tungsten filament and the sample was coated in gold.

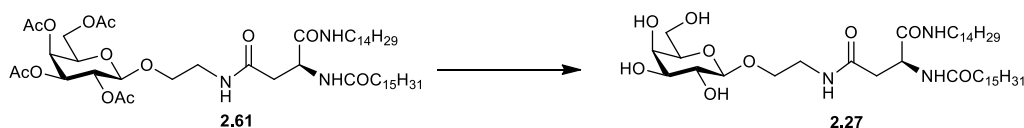
6.2 Experimental procedures

6.2.1 Experimental procedures for Chapter 2



*N*⁴-[2-*O*-(β-*D*-galactopyranosyl)-ethyl]-*N*₂-decanoyl-*L*-asparagine tetradecylamide **2.26**

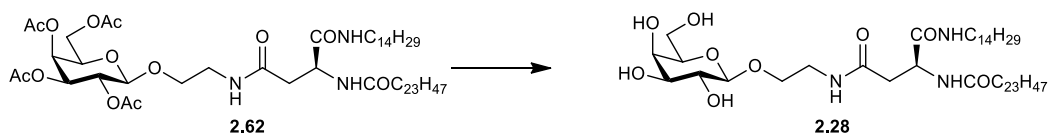
NEt₃ (0.1 mL) was added to a stirring solution of *N*⁴-[2-*O*-(2,3,4,6-tetra-*O*-acetyl-β-*D*-galactopyranosyl)-ethyl]-*N*₂-decanoyl-*L*-asparagine tetradecylamide **2.55** (120 mg, 0.14 mmol) dissolved in DCM/MeOH/H₂O (3 mL/6 mL/3 mL) at 40 °C. The mixture was stirred for 18 h. The reaction mixture was concentrated under reduced pressure to afford the crude solid which was triturated using DCM and EtO₂ to give **2.26** as a white solid (80 mg, 83%); [α]²⁵_D = -6.0 (c, 0.33 in Pyr); ¹H-NMR (300 MHz, *d*₅-Pyr): δ 8.95 (d, *J* = 8.1 Hz, 1 H, NHCOC₉H₁₉), 8.87 (t, *J* = 5.4 Hz, 1 H, CH₂CH₂NHCO), 8.55 (t, *J* = 5.7 Hz, 1 H, CONHC₁₄H₂₉), 7.05, 6.79, 6.63, 6.39 (each bs, 1 H, OH), 5.55–5.53 (m, 1 H, *H*-α), 4.79 (d, *J* = 7.5 Hz, 1 H, *H*-1), 4.51–4.33 (m, 4 H, overlap of *H*-2, *H*-4, *H*-6, *H*-6'), 4.18–4.07 (m, 3 H, overlap of *H*-3, *H*-5, 1 H of OCH₂CH₂NH), 3.99–3.95 (m, 1 H, 1 H of OCH₂CH₂NH), 3.77–3.65 (m, 2 H, OCH₂CH₂NH), 3.22–3.16 (m, 2 H, NHCH₂C₁₃H₂₇), 3.18 (td, *J* = 6.6 Hz, *J* = 1.2 Hz, 2 H, overlap of *H*-β, *H*-β'), 2.36 (t, *J* = 7.5 Hz, 2 H, COCH₂C₈H₁₇), 1.79–1.69 (m, 2 H, COCH₂CH₂C₇H₁₅), 1.60–1.50 (m, 2 H, NHCH₂CH₂C₁₂H₂₅), 1.28–1.10 (m, 34 H, overlap of COC₂H₄(CH₂)₆CH₃, NHC₂H₄(CH₂)₁₁CH₃), 0.85 (m, 6 H, overlap of COC₈H₁₆CH₃, NHC₁₃H₂₆CH₃); ¹³C-NMR (75 MHz, *d*₅-Pyr): δ_c 175.4, 173.9, 173.0 (each CO), 107.7 (*C*-1), 78.9, 77.2, 74.5, 72.2 (*C*-2, *C*-4, *C*-3, *C*-5), 71.7 (OCH₂CH₂NH), 64.5 (*C*-6), 53.3 (*C*-α), 42.5 (each OCH₂CH₂NH), 41.8 (NHCH₂H₁₃H₂₇), 40.7 (*C*-β), 38.5, 38.4, 34.1, 34.0, 32.0, 31.9, 31.9, 31.7, 31.7, 31.6, 31.6, 31.5, 29.2, 28.1 (each CH₂), 18.6 (overlap of COC₈H₁₆CH₃, NHC₁₃H₂₆CH₃); HRMS *m/z* (ESI⁺): 688.5099 (C₃₆H₆₉N₃O₉; [M+H]⁺ requires 688.5107).



*N*⁴-[2-*O*-(β-*D*-galactopyranosyl)-ethyl]-*N*²-hexadecanosyl-*L*-asparagine tetradecylamide **2.27**

Trimethylamine (0.1 mL) was added to a stirring solution of *N*⁴-[2-*O*-(2,3,4,6-tetra-*O*-acetyl-β-*D*-galactopyranosyl)-ethyl]-*N*²-hexadecanosyl-*L*-asparagine tetradecylamide **2.27** (24 mg, 0.020 mmol) dissolved in DCM, /MeOH/H₂O (2 mL/4 mL/2 mL) at 40 °C. The mixture was stirred for 18 h. The reaction mixture was concentrated under reduced pressure to afford the crude solid

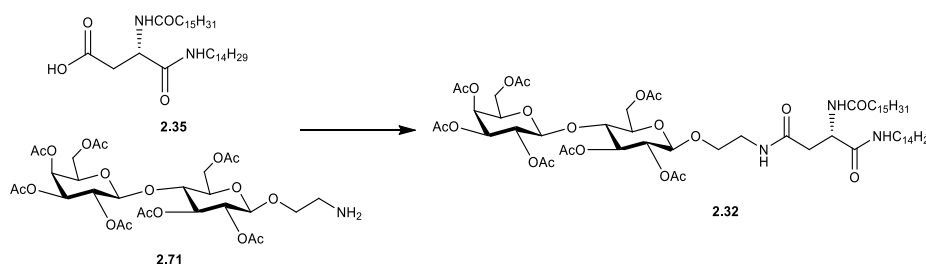
which was triturated using DCM and EtO₂ to give **2.27** as a white solid (10 mg, 52%); $[\alpha]_D^{25} = -20$ (c, 0.1 in Pyr); ¹H-NMR (300 MHz, *d*₅-Pyr): δ 8.95 (d, *J* = 8.1 Hz, 1 H, NHCOC₁₅H₃₁), 8.81 (t, *J* = 5.4 Hz, 1 H, CH₂CH₂NHCO), 8.52 (t, *J* = 5.7 Hz, 1 H, CONHC₁₄H₂₉), 5.57-5.50 (m, 1 H, *H*-α), 4.78 (d, *J* = 7.5 Hz, 1 H, *H*-1), 4.51-4.35 (m, 4 H, overlap of *H*-2, *H*-4, *H*-6 and *H*-6'), 4.17-4.00 (m, 3 H, overlap of *H*-3, *H*-5 and 1 H of CH₂CH₂O), 3.98-3.93 (m, 1 H, 1 H of CH₂CH₂O), 3.80-3.64 (m, 2 H, CH₂CH₂NH), 3.48-3.35 (m, 2 H, NHCH₂C₁₃H₂₇), 3.14 (td, *J* = 6.6 Hz, *J* = 1.2 Hz, 2 H, *H*-β, *H*-β'), 2.36 (t, *J* = 7.5 Hz, 2 H, NHCOC₂H₄(CH₂)₁₂CH₃), 1.80-1.72 (m, 2 H, NHCOC₂H₄(CH₂)₁₂CH₃), 1.59-1.50 (m, NHCH₂CH₂C₁₂H₂₅), 1.22-1.12 (m, 46 H, overlap of NHCOC₂H₄(CH₂)₁₂CH₃, and NHC₂H₄(CH₂)₁₁CH₃), 0.86 (m, 6 H, overlap of NHCOC₁₄H₂₈CH₃ and NHC₁₃H₂₆CH₃); ¹³C-NMR (75 MHz, *d*₅-Pyr): δ_c 175.4, 173.9, 173.0 (each CO), 107.7 (*C*-1), 78.9, 77.2, 74.5, 72.2 (*C*-2, *C*-4, *C*-3, *C*-5), 71.7 (OCH₂CH₂NH), 64.5 (*C*-6), 53.3 (*C*-α), 42.50 (OCH₂CH₂NH), 41.81 (NHCH₂C₁₃H₂₇), 40.7 (*C*-β), 38.5 (NHCOC₂H₄(CH₂)₁₂CH₃), 34.1, 32.04, 31.9, 31.9, 31.8, 31.7, 31.0, 31.6, 29.2 (each s, NHCOC₂H₄(CH₂)₁₂CH₃ and NHCH₂(CH₂)₁₂CH₃), 28.1 (NHCOC₂H₄(CH₂)₁₂CH₃), 24.9 (each s, NHCOC₂H₄(CH₂)₁₂CH₃ and NHCH₂(CH₂)₁₂CH₃), 16.2 (NHCOC₁₄H₂₈CH₃, NHC₁₃H₂₆CH₃); HRMS *m/z* (ESI⁺): 772.606 (C₄₂H₈₂N₃O₉: [M+H]⁺ requires 772.6046).



*N*⁴-[2-*O*-(β-*D*-galactopyranosyl)-ethyl]-*N*₂-tetracosanoyl-*L*-asparagine tetradecylamide **2.28**

NEt₃ (0.1 mL) was added to a stirring solution of *N*⁴-[2-*O*-(2,3,4,6-tetra-*O*-acetyl-β-*D*-galactopyranosyl)-ethyl]-*N*₂-tetracosanoyl-*L*-asparagine tetradecylamide **2.62** (16 mg, 0.015 mmol) dissolved in DCM/MeOH/H₂O/THF (1 mL/2 mL/1 mL/2 mL) at 40 °C. The reaction mixture was stirred and its progress was followed by ¹H-NMR spectra of aliquots. The reaction was deemed complete after 36 h. The reaction mixture was concentrated under reduced pressure to afford the crude solid which was triturated using DCM and EtO₂ to give **2.28** as a white solid (5 mg, 38%); ¹H-NMR (300 MHz, *d*₅-Pyr): δ 9.02–8.96 (m, 1 H, NHCOC₂₃H₄₇), 8.89–8.79 (m, 1 H, CH₂CH₂NHCO), 8.54–8.52 (m, 1 H, CONHC₁₄CH₂₉), 5.54 (dd, *J* = 6.3, 12.9 Hz, 1 H, *H*-α), 4.80 (d, *J* = 7.8 Hz, 1 H, *H*-1), 4.52–4.36 (m, 4 H, overlap of *H*-2, *H*-4, *H*-6, *H*-6'), 4.18–4.10 (m, 3 H, overlap of *H*-3, *H*-5, 1 H of OCH₂CH₂NH), 3.99–3.95 (m, 1 H, 1 H of OCH₂CH₂NH), 3.77–3.65 (m, 2 H, OCH₂CH₂NH), 3.48–3.38 (m, 2 H, NHCH₂C₁₃H₂₇), 3.18 (m, 2 H, *H*-β, *H*-β'), 2.40–2.35 (m, 2 H, COCH₂C₂₂H₄₅), 1.79–1.69 (m, 2 H, COCH₂CH₂C₂₁H₄₃), 1.60–1.50 (m, 2 H, NHCH₂CH₂C₁₂H₂₅), 1.20 (bs, 62 H, overlap of COC₂H₄(CH₂)₂₀CH₃, NHC₂H₄(CH₂)₁₁CH₃), 0.85 (m, 6

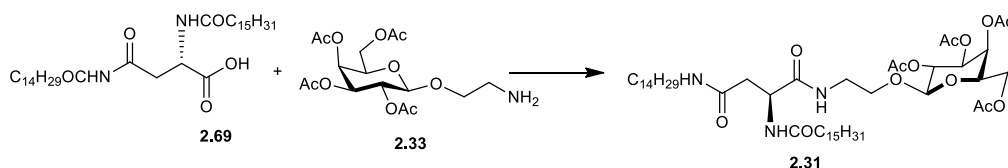
H, overlap of $\text{COC}_2\text{H}_4\text{CH}_3$, $\text{NHC}_{13}\text{H}_{26}\text{CH}_3$); HRMS m/z (ESI+): 884.7278 ($\text{C}_{50}\text{H}_{97}\text{N}_3\text{O}_9$: $[\text{M}+\text{H}]^+$ requires 884.7298).



*N*⁴-[2-*O*-(2,3,6-*tri-O*-acetyl- β -*D*-galactopyranosyl-4-(2,3,4,6-tetra-*O*-acetyl- β -*D*-glucopyranosyl)-ethyl]-*N*²-decanoyl-*L*-asparagine tetradecylamide **2.32**

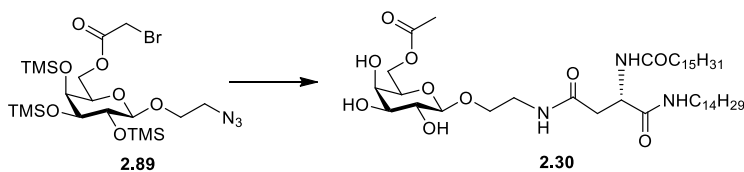
HOBt (17 mg, 0.48 mmol) was added to a stirring solution of carboxylic acid **2.35** (66 mg, 0.11 mmol), TBTU (37 mg, 0.11 mmol) and NEt_3 (0.035 mL 0.26 mmol) dissolved in DMF (6 mL), under N_2 at 50 °C. The mixture was stirred for 10 min and 1-*O*-(2-aminoethyl)-2,2',3,3',4',6,6'-hepta-*O*-acetyl- β -lactoside **2.76** (87 mg, 0.13 mmol) dissolved in DMF (3 mL) was added dropwise. The mixture was stirred overnight at rt. The reaction mixture was concentrated *in vacuo*. Flash chromatography (EtOAc) afforded **2.22** as a white solid (42 mg, 29%); $R_f = 0.4$ (EtOAc); $[\alpha]_D^{25} = +3.6$ (c, 1.1 in DCM); IR ν_{max} (NaCl plate, DCM): 3287.3, 2918.6, 2850.5, 1750.9, 1642.4, 1558.8, 14431.9, 1369.9, 1227.46, 1057.6, 955.0, 903.1, 802.1, 729.8, 719.0, 682.51 cm^{-1} ; $^1\text{H-NMR}$ (300 MHz, CDCl_3): δ 7.39 (d, $J = 6.9$ Hz, 1 H, $\text{NHCOC}_{15}\text{H}_{31}$), 7.06 (t, $J = 5.4$ Hz, 1 H, $\text{CONHC}_{14}\text{CH}_{29}$), 6.34 (t, $J = 5.4$ Hz, 1 H, $\text{CH}_2\text{CH}_2\text{NHCO}$), 5.34 (d, $J = 2.7$ Hz, 1 H, *H*-4 Gal), 5.24-5.18 (m, 1 H, *H*-3 Gluc), 5.11 (dd, $J = 7.8$ Hz, $J = 10.5$ Hz, 1 H, *H*-2 Gal), 4.97 (dd, $J = 3.3$ Hz, $J = 10.5$ Hz, 1 H, *H*-3 Gal), 4.89-4.86 (m, 1 H, *H*-2, Gluc), 4.68-4.64 (m, 1 H, *H*- α), 4.57-4.48 (m, 3 H, overlap of *H*-1 Gal, *H*-1 Gluc and 1 H of *H*-6 Gluc), 4.15-4.04 (m, 3 H, overlap of *H*-6 Gal, and 1 H of *H*-6 Gluc), 3.89-3.85 (m, 1 H, *H*-5 Gal), 3.82-3.60 (m, 4 H, overlap of $\text{OCH}_2\text{CH}_2\text{NH}$, *H*-4 Gluc and *H*-5 Gluc), 3.43 (bs, 2 H, $\text{OCH}_2\text{CH}_2\text{NH}$), 3.19 (m, 2 H, $\text{NHCH}_2\text{C}_{13}\text{H}_{27}$), 2.77 (dd, $J = 3.6$ Hz, $J = 15.3$ Hz, 1 H, *H*- β), 2.45 (dd, $J = 6.9$, $J = 15$, 1 H, *H*- β'), 2.22 (t, $J = 7.2$ Hz, 2 H, $\text{COCH}_2\text{C}_{14}\text{H}_{29}$), 2.15, 2.12, 2.06, 2.04, 1.96 (each s, 6 H, $\text{O}(\text{CO})\text{CH}_3$), 1.62-1.60 (m, 2 H, $\text{COCH}_2\text{CH}_2\text{C}_{13}\text{H}_{27}$), 1.46-1.45 (m, 2 H, $\text{NHCH}_2\text{CH}_2\text{C}_{12}\text{H}_{25}$), 1.20-1.31 (m, 46 H, overlap of $\text{COC}_2\text{H}_4(\text{CH}_2)_{12}\text{CH}_3$, $\text{NHC}_2\text{H}_4(\text{CH}_2)_{11}\text{CH}_3$), 0.87 (t, $J = 6.6$ Hz, 6 H, overlap of $\text{COC}_{14}\text{H}_{28}\text{CH}_3$, $\text{NHC}_{13}\text{H}_{26}\text{CH}_3$); $^{13}\text{C-NMR}$ (75 Hz, CDCl_3): δ_c 172.6, 170.6, 169.6, 169.4, 169.3, 169.1, 169.0, 168.9, 168.7, 168.03 (each CO), 101.0 (*C*-1 gal), 100.7 (*C*-1 Gluc), 76.0 (*C*-5, Gluc), 72.8 (*C*-4, Gluc), 72.6 (*C*-3 Gluc), 71.6 (*C*-2 Gluc), 70.9 (*C*3- Gal), 70.7 (*C*-5 Gal), 69.1 ($\text{OCH}_2\text{CH}_2\text{NH}$), 68.8 (*C*-2 Gal), 66.6 (*C*-4 Gal), 61.7, 60.7 (*C*-6 Gal, *C*-6 Gluc), 49.8 (*C*- α), 39.6 ($\text{NHCH}_2\text{C}_{13}\text{H}_{27}$), 39.4 ($\text{OCH}_2\text{CH}_2\text{NH}$), 36.9 ($\text{COCH}_2\text{C}_{14}\text{H}_{29}$), 36.6 (*C*- β), 31.9, 29.7, 29.5, 29.5, 29.3, 29.3, 26.9, 25.6, 22.6 (overlap of $\text{COC}_2\text{H}_4(\text{CH}_2)_{12}\text{CH}_3$,

$\text{NHC}_2\text{H}_4(\text{CH}_2)_{11}\text{CH}_3$, 20.9, 20.8, 20.7, 20.6, 20.5 ($\text{O}(\text{CO})\text{CH}_3$), 14.11 ($\text{COC}_{14}\text{H}_{28}\text{CH}_3$, $\text{NHC}_{13}\text{H}_{26}\text{CH}_3$); HRMS m/z (ESI+): 1228.7353 ($\text{C}_{62}\text{H}_{106}\text{N}_3\text{O}_{21}$: $[\text{M}+\text{H}]^+$ requires 1228.7313).



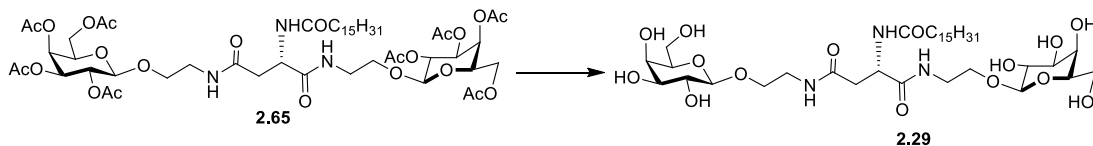
*N*⁴-[2-*O*-(2,3,4,6-tetra-*O*-acetyl- β -*D*-galactopyranosyl)-ethyl]-*N*²-palmitoyl-*L*-asparagine tetradecylamide **2.31**

HOBt (65 mg, 0.48 mmol) was added to a stirring solution of carboxylic acid **2.69** (250 mg, 0.44 mmol) and TBTU (155 mg, 0.48 mmol) dissolved in DMF (20 mL), under N_2 at 50 °C. The solution was stirred for 10 min and 2-aminoethyl 2,3,4,6-tetra-*O*-acetyl- β -*D*-galactopyranoside **2.33** (189 mg, 0.48 mmol) dissolved in DMF (15 mL) was added dropwise. The reaction mixture was stirred overnight at rt and concentrated *in vacuo*. Flash chromatography (EtOAc) afforded **2.31** as a white solid (274 mg, 63%); $R_f = 0.59$ (9:1, DCM:MeOH); $[\alpha]_D^{25} = -1.67$ (c, 1.2 in DCM); ^1H NMR (300 MHz, CDCl_3): δ 7.32-7.27 (m, 2 H, overlap of $\text{NHCOC}_{15}\text{H}_{31}$ and $\text{CONHC}_{14}\text{H}_{29}$), 6.03-5.97 (m, 1 H, $\text{OCH}_2\text{CH}_2\text{NH}$), 5.4-5.37 (m, 1 H, *H*-4), 5.21-5.14 (m, 1 H, *H*-2), 5.04-4.99 (m, 1 H, *H*-3), 4.66-4.61 (m, 1 H, *H*- α), 4.51 (d, $J = 7.8$ Hz, 1 H, *H*-1), 4.18-4.10 (m, 2 H, *H*-6 and *H*-6'), 3.96-3.80 (m, 2 H overlap of *H*-5 and 1 H of $\text{CH}_2\text{CH}_2\text{O}$), 3.65 (m, 3 H, overlap of 1 H of $\text{OCH}_2\text{CH}_2\text{NH}$ and $\text{OCH}_2\text{CH}_2\text{NH}$), 3.25-3.16 (m, 2 H, $\text{NHCH}_2\text{C}_{13}\text{H}_{27}$), 2.61 (dd, $J = 3.3$ Hz, $J = 15.3$, 1 H, *H*- β), 2.45 (dd, $J = 6.9$, $J = 15.6$, 1 H, *H*- β'), 2.27-2.22 (m, 2 H, $\text{NHCOCH}_2\text{C}_{14}\text{H}_{29}$) 2.16, 2.09, 2.04, and 1.9 (each s, 3 H, $\text{O}(\text{CO})\text{CH}_3$), 1.64-1.59 (m, 2 H, $\text{NHCOCH}_2\text{CH}_2\text{C}_{13}\text{H}_{27}$), 1.51-1.46 (m, $\text{NHCH}_2\text{CH}_2\text{C}_{12}\text{H}_{25}$), 1.33-1.24 (m, 46 H, overlap of $\text{NHC}_2\text{H}_4(\text{CH}_2)_{11}\text{CH}_3$, $\text{NHCOC}_2\text{H}_4(\text{CH}_2)_{12}\text{CH}_3$), 0.88 (t, $J = 6.3$ Hz, 6 H, overlap of $\text{NHCOC}_{14}\text{H}_{28}\text{CH}_3$, $\text{CONHC}_{13}\text{H}_{26}\text{CH}_3$); ^{13}C -NMR (75 MHz, CDCl_3): δ_c 173.7, 171.7, 170.4, 170.2, 170.1, (each CO), 101.1 (*C*-1), 70.8, 70.7 (*C*-5, *C*-3), 69.0, (*C*-2), 68.7 ($\text{OCH}_2\text{CH}_2\text{NH}$), 67.0 (*C*-4), 61.3 (*C*-6), 50.0 (*C*- α), 39.7 ($\text{OCH}_2\text{CH}_2\text{NH}$), 37.6 ($\text{NHCH}_2\text{C}_{13}\text{H}_{27}$), 36.6 (*C*- β), 35.6 ($\text{NHCOCH}_2\text{C}_{14}\text{H}_{29}$), 31.9, 29.7, 29.6, 29.6, 29.5, 29.4, 29.3, 29.2, 26.9, 25.6, 22.6 (overlap of $\text{NHCOCH}_2(\text{CH}_2)_{13}\text{CH}_3$ and $\text{NHCH}_2(\text{CH}_2)_{12}\text{CH}_3$), 20.8, 20.7, 20.6, 20.5 (each $\text{O}(\text{CO})\text{CH}_3$), 14.1 (overlap of $\text{COC}_{14}\text{H}_{28}\text{CH}_3$, $\text{NHC}_{13}\text{H}_{26}\text{CH}_3$); HRMS m/z (ESI+): 940.6532 ($\text{C}_{50}\text{H}_{90}\text{N}_3\text{O}_{13}$: $[\text{M}+\text{H}]^+$ requires 940.6468).



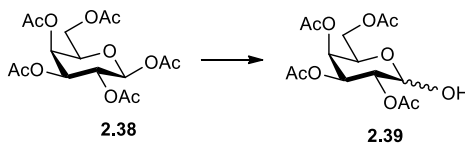
*N*⁴-[2-*O*-(6-*O*-acetyl- β -*D*-galactopyranosyl)-ethyl]-*N*²-hexadecanosyl-*L*-asparagine tetradecylamide **2.30**

To a solution of 1-*O*-(2-azidoethyl) -(2,3,4-tri-*O*-trimethylsilyl, 6-*O* carboxymethylbromide)- β -*D*-galactopyranose **2.89** (138 mg, 0.2 mmol) in absolute EtOH (15 ml), Pd/C (14 mg, 10% w/w) was added. The resulting mixture was stirred under H₂ for 2.5 h. The mixture was then filtered through a Celite cake and the filtrate was concentrated under vacuum to afford the crude product as thick clear oil. An *in situ* reaction with the aspartic acid derivative **2.35** was then carried out. HOBt (16 mg, 0.12 mmol), followed by NEt₃ (0.030 mL, 2.2 mmol), were added to a stirring solution of the carboxylic acid **2.35** (63 mg, 0.11 mmol) and TBTU (39 mg, 1.2 mmol) dissolved in anhydrous DMF (10 mL), under N₂ at rt. The mixture was stirred for 15 min and **2.89** (46 mg, 0.13 mmol) dissolved in anhydrous DMF (1.2 mL) was added dropwise. The mixture was stirred for 18 h upon which a precipitate was observed. Filtration and trituration of the precipitate yielded the pure product **2.30** as a white solid (55 mg, 55%, over two steps); [α]_D²⁵ = 3 (c, 0.5 in Pyr); ¹H-NMR (300 MHz, *d*₅-Pyr): δ 9.02 (d, *J* = 7.8 Hz, 1 H, NHCOC₁₅H₃₁), 8.92 (t, *J* = 5.1 Hz, 1 H, CH₂CH₂NHCO), 8.57 (t, *J* = 5.7 Hz, 1 H, CONHC₁₄H₂₉), 5.55-5.50 (m, 1 H, *H*- α), 4.86-4.67 (m, 3 H, overlap of *H*-1, *H*-6 and *H*-6'), 4.40 (dd, *J* = 7.5 Hz, *J* = 9.3 Hz, 1 H, *H*-2), 4.34 (d, *J* = 3.3 Hz, 1 H, *H*-4), 4.23-4.11 (m, 3 H, overlap of *H*-3, *H*-5 and 1 H of CH₂CH₂O), 3.97-3.89 (m, 1 H, 1 H of OCH₂CH₂NH), 3.83-3.64 (m, 2 H, OCH₂CH₂NH), 3.48-3.35 (m, 2 H, NHCH₂C₁₃H₂₇), 3.13 (d, *J* = 6.6 Hz, 2 H, *H*- β , *H*- β'), 2.41-2.34 (m, 2 H, NHCOCH₂C₁₄H₂₉), 2.2 (s, 3 H, O(CO)CH₃), 1.80-1.72 (m, 2 H, NHCOCH₂CH₂C₁₃H₂₇), 1.57-1.50 (m, NHCH₂CH₂C₁₂H₂₅), 1.24 (46 H, overlap of NHCOC₂H₄(CH₂)₁₂CH₃, and NHC₂H₄(CH₂)₁₁CH₃), 0.86 (t, *J* = 6.3 Hz, 6 H, overlap of NHCOC₁₄H₂₈CH₃ and NHC₁₃H₂₆CH₃); ¹³C-NMR (75 Hz, CDCl₃): δ _c 173.96, 172.5, 171.6, 171.2 (each CO), 105.8 (*C*-1), 75.5 (*C*-5), 74.0 (*C*-3), 72.7 (*C*-2), 70.39 (*C*-4), 69.6 (OCH₂CH₂NH), 65.1 (*C*-6), 55.5 (*C*- α), 40.7 (OCH₂CH₂NH), 40.3 (NHCH₂C₁₃H₂₇), 39.0 (*C*- β), 36.9 (NHCOCH₂C₁₄H₂₉), 32.6, 30.5, 30.4, 30.3, 30.2, 30.1, 30.0, 29.7, 28.4, 27.7, 27.5, 26.6, 26.4, 23.4 (each s, NHCOCH₂(CH₂)₁₃CH₃ and NHCH₂(CH₂)₁₂CH₃), 21.2 (O(CO)CH₃), 16.24 (NHCOC₁₄H₂₈CH₃, NHC₁₃H₂₆CH₃); HRMS *m/z* (ESI⁺): 814.616 (C₄₄H₈₄N₃O₁₀: [M+H]⁺ requires 814.6151).



*N*⁴-[2-*O*-(β-*D*-galactopyranosyl)-ethyl]-*N*²-hexadecanoyl-*N*¹-[2-*O*-(β-*D*-galactopyranosyl)-ethyl] L-asparagine **2.29**

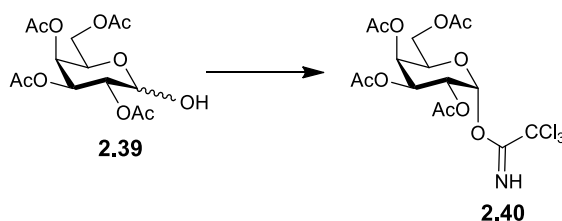
Trimethylamine (0.1 mL) was added to a stirring solution of *N*⁴-[2-*O*-(2,3,4,6-tetra-*O*-acetyl-β-*D*-galactopyranosyl)-ethyl]-*N*²-hexadecanoyl-*N*¹-[2-*O*-(2,3,4,6-tetra-*O*-acetyl-β-*D*-galactopyranosyl)-ethyl] L-asparagine **2.29** (37 mg, 0.040 mmol) dissolved in DCM, /MeOH/H₂O (2 mL/4 mL/2 mL) at 40 °C. The mixture was stirred for 18 h. The reaction mixture was concentrated under reduced pressure to afford the crude solid which was triturated using DCM and EtO₂ to yield **2.29** as a white solid (15 mg, 86%); $[\alpha]_{\text{D}}^{25} = 6$ (c, 0.8 in Pyr); ¹H-NMR (300 MHz, *d*₅-Pyr): δ 8.95 (d, *J* = 7.8 Hz, 1 H, NHCOC₁₅H₃₁), 8.79-8.85-8.71 (m, 2 H, CH₂CH₂NHCO), 5.54-5.48 (m, 1 H, *H*-α), 4.78 (t, *J* = 6.9 Hz, 1 H, *H*-1), 4.53-4.32 (m, 8 H, overlap of *H*-2, *H*-4, *H*-6 and *H*-6'), 4.19-4.08 (m, 6 H, overlap of *H*-3, *H*-5 and 1 H of CH₂CH₂O), 3.94-3.87 (m, 2 H, 1 H of CH₂CH₂O), 3.77-3.60 (m, 4 H, CH₂CH₂NH), 3.12 (d, *J* = 5.4 Hz, 2 H, *H*-β, *H*-β'), 2.37 (t, *J* = 7.2 Hz, 2 H, NHCOC₂H₄(CH₂)₁₃CH₃), 1.74-1.70 (m, 2 H, NHCOC₂H₄(CH₂)₁₂CH₃), 1.30-1.09 (m, 24 H, NHCOC₂H₄(CH₂)₁₂CH₃), 0.85-0.82 (m, 3 H, NHCOC₁₄H₂₈CH₃); ¹³C-NMR (75 MHz, *d*₅-Pyr): δ_c 173.7, 172.5, 171.3 (each CO), 105.9, 105.7 (*C*-1, *C*-1'), 77.2 (*C*-5, *C*-5'), 75.5 (*C*-3, *C*-3'), 72.9, 72.8 (*C*-2, *C*-2'), 70.5 (*C*-4, *C*-4'), 69.8, 66.0 (OCH₂CH₂NH), 66.1, 62.8 (*C*-6, *C*-6'), 55.3 (*C*-α), 40.8, 40.6 (OCH₂CH₂NH), 39.2 (*C*-β), 36.7 (NHCOC₂H₄(CH₂)₁₃CH₃ and NHCH₂(CH₂)₁₂CH₃), 32.4, 30.2, 30.1, 30.0, 29.8, 26.3, 23.2 (each s, NHCOC₂H₄(CH₂)₁₃CH₃ and NHCH₂(CH₂)₁₂CH₃), 21.2 (O(CO)CH₃), 14.5 (NHCOC₁₄H₂₈CH₃, NHC₁₃H₂₆CH₃); HRMS *m/z* (ESI+): 782.4620 (C₃₆H₆₈N₃O₁₅N₃: [M+H]⁺ requires 782.4645).



2,3,4,6-Tetra-O-acetyl- α/β -D-galactopyranose **2.39**

Dimethylamine (3.83 mL, 7.66 mmol) was added to a stirring solution of 1,2,3,4,6-penta-*O*-acetyl- β -D-galactopyranose **2.38** (2 g, 5.12 mmol) in MeCN (20 mL). The solution was heated to 80 °C and stirred for 24 h. The reaction mixture was concentrated *in vacuo*, dissolved in DCM washed with brine and dried (MgSO₄). The solution was filtered, the solvent removed under reduced pressure, and the crude product purified using flash column chromatography (1:1, EtOAc:Hexane) to yield the title compound **2.39** as a brown oil (1.18 g, 66%); *R*_f = 0.28 (1:1, Hexane/EtOAc); IR ν_{max} (NaCl plate, DCM): 3619.6, 3643.1, 3063.3, 2971.8, 2942.7, 2916.7, 2849.2, 2726.0, 2442.3, 2124.9, 191.9, 1747.7, 1648.1, 1434.4, 1372.2, 1231.2, 1155.4, 1127.2, 1052.2 cm⁻¹; ¹H NMR (300 MHz, CDCl₃, α -anomer): δ 5.71-5.72 (m, 1 H, *H*-1), 5.48 (d, *J* = 3.3 Hz, 1 H, *H*-4), 5.43 (dd, *J* = 6.2 Hz, *J* = 12.0 Hz, 1 H, *H*-3), 5.15 (dd, *J* = 3.4 Hz, *J* = 12.0 Hz, 1 H, *H*-2), 4.48 (appt, *J* = 6.0 Hz, 1 H, *H*-5), 4.08-4.16 (m, 2 H, *H*-6, *H*-6'), 2.09, 2.00, 1.98, 1.92 (each s, 3 H, O(CO)CH₃).

The NMR data are in agreement with the reported values.^[229]



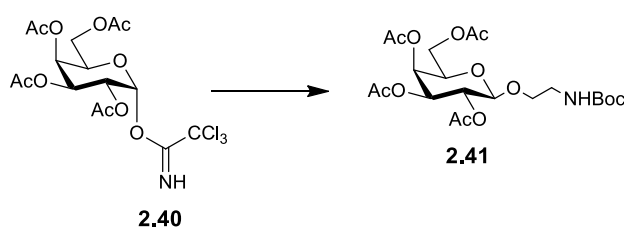
2,3,4,6-Tetra-O-acetyl- α -D-galactopyranosyl-1-trichloroacetimidate **2.40**^{[230]ii}

Trichloroacetonitrile (1.52 mL, 15.18 mmol) and 1,8-diaza bicyclo[5.4.0]undec-7-ene (0.12 mL, 0.792 mmol) was added to a solution of 2,3,4,6-tetra-*O*-acetyl- α/β -D-galactopyranose **2.39** (918 mg, 2.64 mmol) in anhydrous DCM (5 mL) under N₂. The reaction mixture was stirred for 3.5 h. The solvent was evaporated under reduced pressure and the residue obtained

ⁱⁱ A reference preceding the compound title indicates that an experimental procedure was followed as in a publication. It does not implicitly indicate that the exact compound in question was synthesised; only that reagents and conditions were followed.

was purified by column chromatography (4:3, Hexane/EtOAc) to give the title compound **2.40** as a white solid (1.08 g, 83%); $R_f = 0.57$ (1:1, Hexane/EtOAc); ^1H NMR (300 MHz, CDCl_3 , α -anomer): δ 8.66 (s, 1 H, NH), 6.58 (d, $J = 3.2$ Hz, 1 H, $H-1$), 5.54-5.52 (m, 1 H, $H-4$), 5.43-5.28 (m, 2 H, $H-2$, $H-3$), 4.42 (t, $J = 6.5$ Hz, 1 H, $H-5$), 4.17-4.05 (m, 2 H, $H-6$, $H-6'$), 2.1, 2.01, 2.0, 1.99 (each s, 3 H, $\text{O}(\text{CO})\text{CH}_3$); ^{13}C (75 MHz, CDCl_3): δ_c 170.3, 170.1, 170.0, 169.9 (each CO), 160.9 (CNH) 93.5 (C-1), 90.8 (CCl_3), 68.9 (C-5), 67.5 (C-2), 67.4 (C-4), 66.9 (C-3), 61.2 (C-6), 20.7, 20.6, 20.5, 20.5 ($\text{O}(\text{CO})\text{CH}_3$).

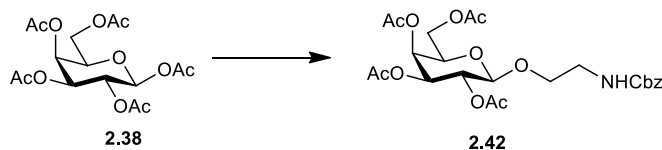
The NMR data are in agreement with the reported values.^[231]



O-(2-*N*-carbobenzyloxyaminoethyl)-(2,3,4,6-tetra-*O*-acetyl)- β -*D*-galactopyranose **2.41**

2,3,4,6-tetra-*O*-acetyl- α -*D*-galactopyranosyl-1-trichloroacetimidate (2.7 g, 5.6 mmol) and *N*-(*tert*-Butoxycarbonyl)ethanolamine (1.36 g, 8.4 mmol) were dissolved in anhydrous DCM under N_2 . TMSOTf (0.21 mL, 1.1 mmol) was added and the reaction mixture was stirred overnight. The solvent was removed under reduced pressure and the resulting residue dissolved in DCM and washed with 1M HCl, aqueous sat. NaHCO_3 , brine and dried over MgSO_4 . Column chromatography afforded the title compound as a white solid (1.12 g, 40%); $R_f = 0.37$ (1:1, Hexane/EtOAc); ^1H NMR (300 MHz, CDCl_3): δ 5.38-5.36 (m, 1 H, $H-4$), 5.21-5.14 (m, 1 H, $H-2$), 5.02-4.97 (m, 1 H, $H-3$), 4.44 (d, $J = 7.9$ Hz, 1 H, $H-1$), 4.14-4.05 (m, 2 H, $H-6$, $H-6'$), 3.92-3.82 (m, 2 H, overlap of $H-5$ and 1 H of $\text{OCH}_2\text{CH}_2\text{NH}$), 3.69-3.59 (m, 1 H, 1 H of $\text{OCH}_2\text{CH}_2\text{NH}$), 3.33-3.25 (m, 2 H, $\text{OCH}_2\text{CH}_2\text{NH}$), 2.1, 2.07, 2.05, 1.99 (each s, 3 H, $\text{O}(\text{CO})\text{CH}_3$), 1.44-1.40 (m, 9 H, $\text{OC}(\text{CH}_3)_3$); ^{13}C (75 MHz, CDCl_3): δ_c 170.5, 170.3, 170.2, 169.7 (each CO), 155.9 ($\text{COOC}(\text{CH}_3)_3$), 101.6 (C-1), 79.7 ($\text{OC}(\text{CH}_3)_3$), 70.7 (C-5, C-3), 69.8 ($\text{OCH}_2\text{C}_2\text{NH}$), 68.8 (C-2), 67.8 (C-4), 60.3 (C-6), 39.3 ($\text{OCH}_2\text{CH}_2\text{NH}$), 27.3 ($\text{OC}(\text{CH}_3)_3$), 20.7, 20.6, 20.5, 20.5 ($\text{O}(\text{CO})\text{CH}_3$).

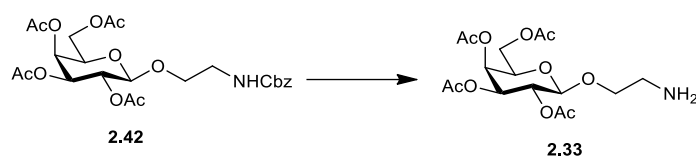
The spectroscopic data are in agreement with the literature.^[185]



2-(Benzyloxycarbonyl)aminoethyl 2,3,4,6-tetra-O-acetyl-β-D-galactopyranose **2.42**^[92]

β-D-galactose pentacetate **2.38** (0.57 g, 1.45 mmol) and benzyl *N*-(2-hydroxyethyl)carbamate (0.34 g, 1.7 mmol) were dissolved in dry DCM (6 mL) under N₂ and BF₃Et₂O (546 mg, 4.35 mmol) was added dropwise at rt. After overnight stirring the reaction mixture was quenched using NEt₃ (1 mL). The solvent was concentrated under vacuum and the crude mixture was acetylated using AcOH (3 mL) and pyridine (9 mL) for 1 h. The solvent was evaporated under reduced pressure to yield a yellow oil that was purified by column chromatography (1:1, EtOAc: Pet Ether). The title compound **2.42** was obtained as thick clear oil (0.42 g, 57%); R_f = 0.53 (6:4, Pet Ether:EtOAc); IR ν_{max} (NaCl plate, DCM): 3394.4, 3065.5, 3034.1, 2953.9, 2888.1, 1751.6, 1534.1, 1455.7, 1432.5, 1370.9, 1227.1, 1173.2, 1060.4, 965.0, 912.7, 776.6, 737.5, 590.3 cm⁻¹; ¹H NMR (300 MHz, CDCl₃): δ 7.35-7.34 (m, 5 H, Ar), 5.37 (dd, *J* = 0.9 Hz, *J* = 3.6 Hz, 1 H, *H*-4), 5.17 (dd, *J* = 7.8 Hz, *J* = 10.5 Hz, 1 H, *H*-2) 5.09 (s, 2 H, PhCH₂), 4.99 (dd, *J* = 3.6 Hz, *J* = 10.5 Hz, 1 H, *H*-3), 4.46 (d, *J* = 7.8 Hz, 1 H, *H*-1), 4.11 (d, *J* = 6.3 Hz, 2 H, *H*-6 and *H*-6'), 3.92-3.86 (m, 2 H, overlapping of *H*-5 and 1 H of OCH₂CH₂NH), 3.69 (m, 1 H, 1 H of OCH₂CH₂NH), 3.41-3.37 (m, 2 H, OCH₂CH₂NH), 2.14, 2.03, 2.02, 1.97 (each s, 3 H, O(CO)CH₃); HRMS *m/z* (ESI⁺): 526.1926 (C₂₄H₃₁NO₁₂: [M+H]⁺ requires 526.1919).

The spectroscopic data are in agreement with the literature.^[92]

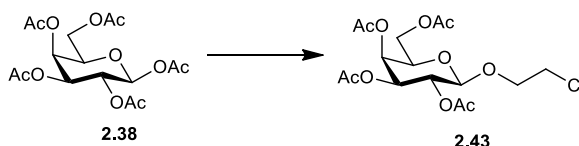


2-Aminoethyl 2,3,4,6-tetra-O-acetyl-β-D-galactopyranoside **2.33**^[92]

To a solution of 2-(Benzyloxycarbonyl)aminoethyl 2,3,4,6-tetra-O-acetyl-β-D-galactopyranose **2.42** (350 mg, 0.6 mmol) in absolute EtOH (20 mL), Pd/C (40 mg, 10% w/w) was added. The resulting mixture was stirred under H₂ for 3 h. The mixture was then filtered through a Celite cake and the filtrate was concentrated under vacuum to afford the pure product **2.33** as thick clear oil (242 mg, 91%); R_f = 0.1 (6:4, Pet Ether:EtOAc); IR ν_{max} (NaCl plate, DCM): 3402.0, 1750.6, 1655.4, 1550.9, 1372.6, 1227.4, 1048.0, 913.3, 738.4, 602.9, 542.5 cm⁻¹; ¹H NMR (300 MHz, CDCl₃): δ 5.32 (d, *J* = 3. Hz, 1 H, *H*-4), 5.13 (dd, *J* = 7.8 Hz, *J* = 10.2 Hz, 1 H, *H*-2), 4.96 (dd, *J*

= 3.6 Hz, $J = 10.5$ Hz, 1 H, $H-3$), 4.45 (d, $J = 7.8$ Hz, 1 H, $H-1$), 4.15-4.03 (m, 2 H, $H-6$ and $H-6'$), 3.89-3.81 (m, 2 H, overlapping of $H-5$ and 1 H of $\text{OCH}_2\text{CH}_2\text{NH}_2$), 3.55-3.50 (m, 1 H, 1 H of $\text{OCH}_2\text{CH}_2\text{NH}_2$), 2.86-2.75 (m, 2 H, $\text{OCH}_2\text{CH}_2\text{NH}_2$), 2.09, 2.00, 1.98, 1.92 (each s, 3 H, $\text{O}(\text{CO})\text{CH}_3$); HRMS m/z (ESI+): 392.157 ($\text{C}_{16}\text{H}_{26}\text{NO}_{10}$: $[\text{M}+\text{H}]^+$ requires 392.1551).

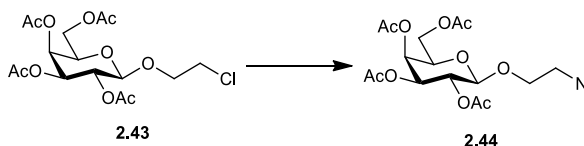
The spectroscopic data are in agreement with the literature.^[92]



2-Chloroethyl 2,3,4,6-tetra-O-acetyl- β -D-galactopyranoside **2.43**^[232]

A solution of β -D-galactose pentacetate **2.38** (5 g, 12.8 mmol) and 2-chloroethanol (1 mL, 15.3 mmol) in dry DCM (50 mL) was stirred under nitrogen and placed on ice. $\text{BF}_3\text{Et}_2\text{O}$ (4.74 mL, 38.4 mmol) was added dropwise over 30 min. After overnight stirring the reaction mixture was concentrated under vacuum to yield a yellow oil that was purified by column chromatography (1:1, hexane/EtOAc). The product **2.43** was obtained as thick clear oil (4.15 g, 78%); $R_f = 0.50$ (1:1, Pet Ether:EtOAc); IR ν_{max} (NaCl plate, DCM): 3469.2, 2968.4, 1747.4, 1432.7, 1372.2, 1233.7, 1152.4, 1049.6, 952.5, 914.8, 736.8, 663.8 cm^{-1} ; ^1H NMR (300 MHz, CDCl_3): δ 5.36 (d, $J = 3.3$ Hz, 1 H, $H-4$), 5.20 (dd, $J = 8.1$ Hz, $J = 10.5$ Hz, 1 H, $H-2$), 4.99 (dd, $J = 3.3$ Hz, $J = 10.5$ Hz, 1 H, $H-3$), 4.53 (d, $J = 8.1$ Hz, 1 H, $H-1$), 4.18-4.08 (m, 2 H, $H-6$ and $H-6'$), 4.06-3.98 (m, 1 H, 1 H of $\text{OCH}_2\text{CH}_2\text{Cl}$), 3.92-3.87 (m, 1 H, $H-5$), 3.69-3.62 (m, 1 H, 1 H of $\text{OCH}_2\text{CH}_2\text{Cl}$), 3.51-3.43 (m, 1 H, 1 H of $\text{OCH}_2\text{CH}_2\text{Cl}$), 3.3-3.23 (m, 1 H, 1 H of $\text{OCH}_2\text{CH}_2\text{Cl}$), 2.12, 2.02, 2.01, 1.95 (each s, 3 H, $\text{O}(\text{CO})\text{CH}_3$); HRMS m/z (ESI+): 411.1065 ($\text{C}_{16}\text{H}_{24}\text{ClO}_{10}$: $[\text{M}+\text{H}]^+$ requires 411.1053).

The spectroscopic data are in agreement with the literature.^[233]

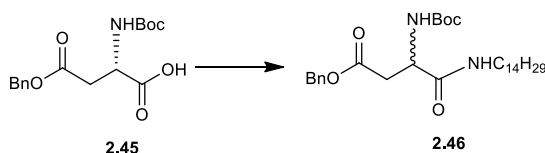


2-Azidoethyl 2,3,4,6-tetra-O-acetyl- β -D-galactopyranoside **2.44**^[234]

2-Chloroethyl 2,3,4,6-tetra-O-acetyl- β -D-galactopyranoside **2.43** (1.5 g, 3.65 mmol) was dissolved in DMF (70 mL) and NaN_3 (443 mg, 7.3 mmol) was added. The mixture was heated to 110°C and stirred for 4 h. The solvent was removed under reduced pressure and the residue dissolved in DCM and washed with H_2O and dried over MgSO_4 . Flash chromatography (1:1,

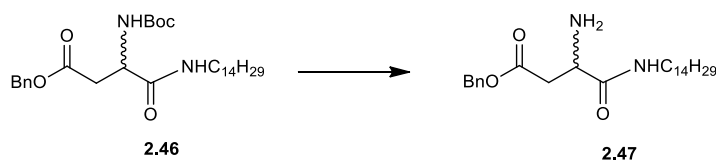
EtOAc:Pet Ether) afforded the pure product **2.44** as an oily solid (1.23 g, 81%); $R_f = 0.50$ (1:1, Pet Ether:EtOAc); IR ν_{\max} (NaCl plate, DCM): 2941.6, 2106.9, 1750.9, 1434.7, 1370.4, 1223.8, 1173.7, 1134.4, 1061.6, 955.6, 899.8 cm^{-1} ; $^1\text{H NMR}$ (300 MHz, CDCl_3): δ 5.38 (d, $J = 3.3$ Hz, 1 H, $H-4$), 5.21 (dd, $J = 7.8$ Hz, $J = 10.5$ Hz, 1 H, $H-2$), 5.02 (dd, $J = 3.3$ Hz, $J = 10.5$ Hz, 1 H, $H-3$), 4.53 (d, $J = 7.8$ Hz, 1 H, $H-1$), 4.20-4.07 (m, 2 H, overlap of $H-6$, $H-6'$ and 1 H of $\text{OCH}_2\text{CH}_2\text{N}_3$), 3.93-3.88 (m, 1 H, $H-5$), 3.69-3.79-3.71 (m, 1 H, 1 H of $\text{OCH}_2\text{CH}_2\text{N}_3$), 3.63-3.60 (m, 1 H, 1 H of $\text{OCH}_2\text{CH}_2\text{N}_3$), 2.14, 2.06, 2.04, 1.97 (each s, 3 H, $\text{O}(\text{CO})\text{CH}_3$); HRMS m/z (ESI+): 440.1263 ($\text{C}_{16}\text{H}_{23}\text{N}_3\text{NaO}_{10}$: $[\text{M}+\text{Na}]^+$ requires 440.1276).

The spectroscopic data are in agreement with the literature.^[93]



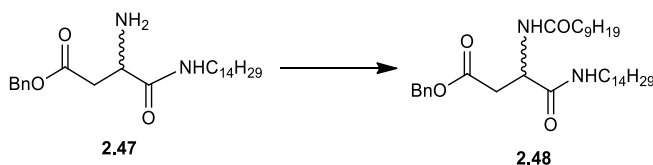
*N*²-*tert*-butoxycarbonyl-*L/D*-asparagine tetradecylamide benzyl ester **2.46**

HOBt (230 mg, 1.7 mmol), *N*-Boc-L-Asp-OBn **2.45** (500 mg, 1.50 mmol) and TBTU (540 mg, 1.7 mmol) were dissolved in DMF (10 mL), under N_2 at rt and NEt_3 (0.646 mL, 4.6 mmol) added. The solution was stirred for 15 min and tetradecylamine (330 g, 1.5 mmol) dissolved in DMF (3 mL) was added. The reaction mixture was stirred for 18 h. The solvent was removed under reduced pressure, and the residue was diluted with DCM and washed successively with 0.1 M HCl, aqueous sat. NaHCO_3 and brine. Flash chromatography (1:1, Pet Ether:EtOAc) afforded **2.46** (680 mg, 87%); $R_f = 0.9$ (1:1, Pet Ether:EtOAc); $[\alpha]_D^{25} = 0$ (c, 1.55 in DCM); IR ν_{\max} (NaCl plate, DCM): 3333.8, 2918.4, 2850.1, 1737.5, 1687.2, 1647.2, 1527.3, 1467.3, 1367.5, 1293.0, 1168.2, 1058.6, 1028.6, 864.4, 732.0, 695.4 cm^{-1} ; $^1\text{H NMR}$ (300 MHz, CDCl_3): δ 7.39-7.32 (m, 5 H, Ar), 6.42 (bs, 1 H, $\text{NHCOC}(\text{CH}_3)_3$), 5.67 (bs, 1 H, $\text{NHC}_{14}\text{H}_{29}$), 5.18-5.08 (m, 2 H, PhCH_2), 4.47 (bs, 1 H, $H-\alpha$), 3.27-3.15 (m, 2 H, $\text{NHCH}_2\text{C}_{13}\text{H}_{27}$), 3.07 (dd, $J = 4.5$ Hz, $J = 17.1$ Hz, 1 H, $H-\beta$), 3.01 (dd, $J = 6.6$ Hz, $J = 17.1$ Hz, 1 H, $H-\beta'$), 1.45 (bs, 11 H, overlap of $\text{NHCH}_2\text{CH}_2\text{C}_{12}\text{H}_{25}$ and $\text{NHCOC}(\text{CH}_3)_3$), 1.25-1.20 (m, 22 H, $\text{NHC}_2\text{H}_4(\text{CH}_2)_{11}\text{CH}_3$), 0.88 (t, $J = 6.6$ Hz, 3 H, $\text{NHC}_2\text{H}_4(\text{CH}_2)_{11}\text{CH}_3$); $^{13}\text{C NMR}$ (75 MHz, CDCl_3): δ_c 170.8, 169.4, (each CO), 134.4 (ArC), 128.6, 128.4, 128.3 (ArCH), 66.8 (PhCH_2), 39.7 ($\text{NHCH}_2\text{C}_{13}\text{H}_{27}$), 31.9, 29.7, 29.6, 29.5, 29.4, 29.4, 29.3, ($\text{NHCH}_2(\text{CH}_2)_{12}\text{CH}_3$), 28.3 ($\text{COC}(\text{CH}_3)_3$), 26.8, 22.7 ($\text{NHCH}_2(\text{CH}_2)_{12}\text{CH}_3$), 14.10 ($\text{NHC}_{13}\text{H}_{26}\text{CH}_3$); HRMS m/z (ESI+): 519.3788 ($\text{C}_{30}\text{H}_{51}\text{N}_2\text{O}_5$: $[\text{M}+\text{H}]^+$ requires 519.3792).



L-asparagine tetradecylamide benzyl ester **2.47**

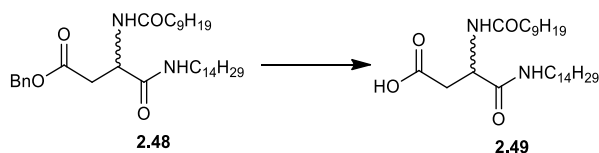
A solution of *N*²-*tert*-butoxycarbonyl-*L*-asparagine tetradecylamide benzyl ester **2.46** (358 mg, 0.69 mmol) in DCM (10 mL) was cooled in an ice bath and 50% TFA in DCM (0.53 ml, 6.9 mmol) was added dropwise. The reaction mixture was stirred at 0 °C for 30 min and then warmed to rt where The mixture was stirred for a further 2 h. The organic solvent was removed *in vacuo* and the residue obtained was diluted with EtOAc and washed with aqueous sat. NaHCO₃ solution, brine, dried over MgSO₄ and concentrated to yield the corresponding deprotected amine **2.47** as an off white solid which was used without further purification (267 mg, 93%); ¹H NMR (300 MHz, CDCl₃): δ 7.38-7.29 (m, 5 H, Ar), 5.18-5.09 (m, 2 H, PhCH₂), 3.70 (bs, 1 H, *H*-α), 3.25-3.18 (m, 2 H, NHCH₂C₁₃H₂₇), 2.99 (dd, *J* = 3 Hz, *J* = 15.3 Hz, 1 H, *H*-β'), 2.66 (dd, *J* = 8.7 Hz, *J* = 15.6 Hz, 1 H, *H*-β'), 1.52-1.42 (m, 2 H, NHCH₂CH₂C₁₂H₂₅), 1.31-1.22 (m, 22 H, NHC₂H₄(CH₂)₁₁CH₃), 0.88 (t, *J* = 6.6 Hz, 3 H, NHC₁₃H₂₆CH₃); HRMS *m/z* (ESI⁺): 419.3288 (C₂₅H₄₃N₂O₃: [M+H]⁺ requires 419.3268).



*N*²-decanoyl-*L*-asparagine tetradecylamide benzyl ester **2.48**

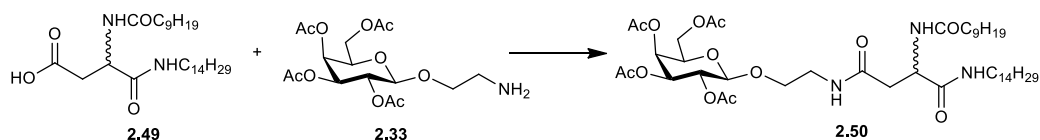
HOBt (192 mg, 1.4 mmol) and NEt₃ (0.54 mL, 3.9 mmol) were added to a stirring solution of decanoic acid (54 mg, 0.31 mmol) and TBTU (110 mg, 0.34 mmol) dissolved in DMF (5 mL), under N₂ at rt. The mixture was stirred for 10 min and *L*-asparagine tetradecylamide benzyl ester **2.47** (543 mg, 1.2 mmol) was dissolved in DMF (5 mL) and added slowly. The mixture was stirred for 18 h. The reaction mixture was concentrated *in vacuo*, diluted with EtOAc, washed with brine, dried over MgSO₄ and concentrated. The residue obtained was purified by flash chromatography (1:1, Pet Ether: EtOAc) to afford **2.48** as a white solid (700 mg, 94%); *R*_f = 0.80 (1:1, Pet Ether:EtOAc); [α]²⁵_D = 0 (c, 1.5 in DCM); IR *v*_{max} (NaCl plate, DCM): 3294.5, 2920.4, 2851.4, 1735.4, 1643.9, 1543.5, 1221.7, 772.6 cm⁻¹; ¹H NMR (300 MHz, CDCl₃): δ 7.38-7.32 (m, 5 H, Ar), 6.79 (d, *J* = 8.1 Hz, 1 H, NHCOC₉H₁₉), 6.51 (bs, 1 H, CONHC₁₄H₂₉), 5.19-5.10 (m, 2 H,

PhCH₂), 4.80-4.74 (m, 1 H, *H*-α), 3.22-3.15 (m, 2 H, NHCH₂C₁₃H₂₇), 2.95 (dd, *J* = 3 Hz, *J* = 15.3 Hz, 1 H, *H*-β), 2.66 (dd, *J* = 8.7 Hz, *J* = 15.6 Hz, 1 H, *H*-β'), 2.22-2.17 (m, 2 H, NHCOCH₂C₈H₁₇), 1.62-1.58 (m, *J* = 6, 2 H, NHCH₂CH₂C₁₂H₂₅), 1.48-1.49 (m, 2 H, NHCOCH₂CH₂C₇H₁₅), 1.33-1.21 (m, 34 H, NHC₂H₄(CH₂)₁₁CH₃ and NHCOC₂H₄(CH₂)₆CH₃), 0.88 (t, *J* = 6.6 Hz, 6 H, NHC₁₃H₂₆CH₃ and NHCOC₉H₁₆CH₃); ¹³C NMR (75 Mhz, CDCl₃): δ_c 173.4, 172.0, 170.2 (each CO), 134.38 (ArC), 128.6, 128.4, 128.3 (ArCH), 66.9 (PhCH₂), 49.2 (*C*-α), 39.7 (NHCH₂C₁₃H₂₇), 36.5 (NHCOCH₂C₈H₁₇), 35.8 (*C*-β), 31.9, 31.8, 29.7, 29.6, 29.6, 29.5, 29.4, 29.3, 29.3, 29.2, 29.2, 28.3, 27.5, 26.8 (NHC₂H₄(CH₂)₁₁CH₃ and NHCOCH₂(CH₂)₇CH₃), 25.6 (NHCH₂CH₂(CH₂)₁₁CH₃), 22.7, 22.6 (NHC₂H₄(CH₂)₁₁CH₃ and NHCOCH₂(CH₂)₇CH₃) 14.1, 14.1 (NHC₁₃H₂₆CH₃ and NHCOC₈H₁₆CH₃); HRMS *m/z* (ESI+): 573.4646 (C₃₅H₆₁N₂O₄: [M+H]⁺ requires 573.4626).



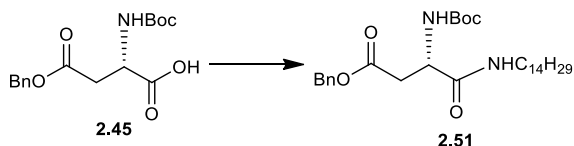
*N*²-decanoyl-*L*-asparagine tetradecylamide **2.49**

To a solution of *N*²-decanoyl-*L*-asparagine tetradecylamide benzyl ester **2.48** (442 mg, 0.77 mmol) in EtOAc (10 mL), Pd/C (44 mg, 10% w/w) was added. The resulting mixture was heated to 50 °C and H₂ bubbled through for 4 h. The mixture was then filtered through a Celite cake and the filtrate was concentrated under vacuum to afford a white solid which was recrystallised in DCM to yield the pure product **2.49** (315 mg, 85%); ¹H NMR (300 MHz, CDCl₃): δ 7.03 (d, *J* = 7.8 Hz, 1 H, NHCOC₉H₁₉), 6.95 (t, *J* = 5.7 Hz, 1 H, NHC₁₄H₂₉), 4.78-4.72 (m, 1 H, *H*-α), 3.24-3.17 (m, 2 H, NHCH₂C₁₃H₂₇), 2.91 (dd, *J* = 3.8 Hz, *J* = 17 Hz, 1 H, *H*-β), 2.67 (dd, *J* = 6.6 Hz, *J* = 16.8 Hz, 1 H, *H*-β'), 2.26-2.19 (m, 2 H, NHCOCH₂C₈H₁₇), 1.64-1.59 (m, 2 H, NHCH₂CH₂C₁₂H₂₅), 1.49-1.44 (m, 2 H, NHCOCH₂CH₂C₇H₁₅), 1.34-1.16 (m, 34 H, NHC₂H₄(CH₂)₁₁CH₃ and NHCOC₂H₄(CH₂)₆CH₃), 0.87 (t, *J* = 6.3 Hz, 3 H, NHC₁₃H₂₆CH₃ and NHCOC₉H₁₆CH₃); HRMS *m/z* (ESI+): 483.4119 (C₂₈H₅₅N₂O₄: [M+H]⁺ requires 483.4156).



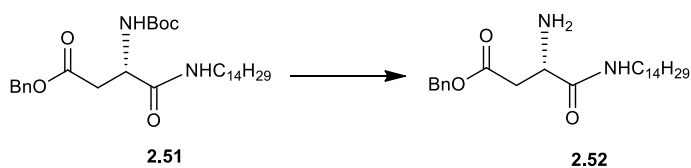
*N*⁴-[2-*O*-(2,3,4,6-tetra-*O*-acetyl- β -*D*-galactopyranosyl)-ethyl]-*N*²-decanoyl-*L*-asparagine tetradecylamide **2.50**

HOBt (137 mg, 1.0 mmol) and NEt₃ (0.387 mL, 3.0 mmol) were added to a stirring solution of *N*²-decanoyl-*L*-asparagine tetradecylamide **2.49** (446 mg, 0.9 mmol) and TBTU (327 mg, 1.0 mmol) dissolved in DMF (15 ml), under N₂ at 50 °C. The mixture was stirred for 10 min and the *O*-(2-aminoethyl)-(2,3,4,6-*O*-tetraacetyl)- β -*D*-galactopyranose **2.33** (435 mg, 1.1 mmol) dissolved in DMF (4 ml) was added dropwise. The mixture was stirred overnight at rt. The reaction mixture was concentrated *in vacuo*. Flash chromatography (EtOAc) afforded **2.50** as a white solid (477 mg, 60%); R_f = 0.46 (EtOAc); [α]_D²⁵ = -2 (c, 1 in CHCl₂); IR ν_{\max} (NaCl plate, DCM): 3295.6, 2922.1, 2852.1, 1754.7, 1641.1, 1553.9, 1468.3, 1371.8, 1224.9, 1058.1, 721.7 cm⁻¹; ¹H-NMR (300 MHz, CDCl₃): δ 7.5 (d, *J* = 6.9 Hz, 0.5 H, NHCOC₉H₁₉), 7.43 (d, *J* = 6.7 Hz, 0.5 H, NHCOC₉H₁₉), 7.19-7.04 (m, 1 H, CONHC₁₄CH₂₉), 6.42 (t, *J* = 5.5 Hz, 0.5 H, CH₂CH₂NHCO), 6.26 (t, *J* = 5.3 Hz, 0.5 H, CH₂CH₂NHCO), 5.39 (d, *J* = 3.2 Hz, 1 H, *H*-4), 5.2-5.14 (m, 1 H, *H*-2), 5.07-5.01 (m, 1 H, *H*-3), 4.69-4.63 (m, 1 H, *H*- α), 4.58 (d, *J* = 7.8 Hz, 0.5 H, *H*-1), 4.53 (d, *J* = 7.8 Hz, 0.5 H, *H*-1), 4.21-4.03 (m, 2 H, overlap of *H*-6, *H*-6'), 3.96-3.94 (m, 1 H, *H*-5), 3.92-3.64 (m, 2 H, OCH₂CH₂NH), 3.53-3.36 (m, 2 H, OCH₂CH₂NH), 3.22-3.15 (m, 2 H, NHCH₂C₁₃H₂₇), 2.83-2.74 (m, 1 H, *H*- β), 2.49-2.40 (m, 1 H, *H*- β '), 2.25-2.20 (m, 2 H, COCH₂C₈H₁₇), 2.16, 2.10, 2.05, 1.98 (each s, 3 H, O(CO)CH₃), 1.64-1.60 (m, 2 H, COCH₂CH₂C₇H₁₅), 1.50-1.45 (m, 2 H, NHCH₂CH₂C₁₂H₂₅), 1.32-1.23 (m, 34 H, overlap of COC₂H₄(CH₂)₆CH₃, NHC₂H₄(CH₂)₁₁CH₃), 0.87 (t, *J* = 6.6 Hz, 6 H, overlap of COC₈H₁₆CH₃, NHC₁₃H₂₆CH₃); ¹³C-NMR (75 Hz, CDCl₃): δ_c 173.7, 171.7, 170.6, 170.4, 170.2, 170.1, 169.9 (each CO), 101.3 (C-1), 70.8, 70.7 (C-5, C-3), 69.0, (C-2), 68.5 (OCH₂CH₂NH), 67.0 (C-4), 61.3 (C-6), 49.7 (C- α), 39.7 (OCH₂CH₂NH), 37.4 (NHCH₂C₁₃H₂₇), 36.6 (C- β), 31.9, 29.7, 29.6, 29.6, 29.5, 29.4, 29.3, 28.3, 26.9, 25.6, 22.6 (each CH₂), 20.9-20.8 (overlap of O(CO)CH₃), 14.1 (overlap of COC₈H₁₆CH₃, NHC₁₃H₂₆CH₃); HRMS *m/z* (ESI+): 856.5507 (C₄₄H₇₈N₃O₁₃: [M+H]⁺ requires 856.5529).



*N*²-*tert*-butoxycarbonyl-*L*-asparagine tetradecylamide benzyl ester **2.51**

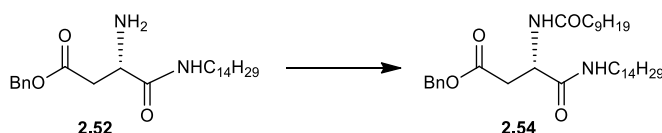
HOBt (230 mg, 1.7 mmol), *N*-Boc-*L*-Asp-OBn **2.45** (500 mg, 1.50 mmol), TBTU (540 g, 1.7 mmol) and tetradecylamine (330 g, 1.5 mmol) were dissolved in DMF (10 mL), under N₂ at rt. The reaction mixture was stirred for 18 h and concentrated under reduced pressure. The residue obtained was diluted with DCM and washed successively with 0.1 M HCl, aqueous sat. NaHCO₃ and brine. Flash chromatography (1:1, Pet Ether:EtOAc) afforded the title compound **2.51** as a white solid (298 mg, 37%); R_f = 0.9 (1:1, Pet Ether:EtOAc); [α]²⁵_D = +2.5 (c, 1.6 in DCM); IR ν_{max} (NaCl plate, DCM): 3333.7, 2918.4, 2850.1, 1737.5, 1687.2, 1647.2, 1527.3, 1467.34, 1367.4, 1293.1, 1168.2, 1058.6, 1028.6 cm⁻¹; ¹H NMR (300 MHz, CDCl₃): δ 7.39-7.62 (bs, 5 H, Ar), 6.43 (bs, 1 H, NHCOC(CH₃)₃), 5.60 (bs, 1 H, NHC₁₄H₂₉), 5.17-5.08 (m, 2 H, PhCH₂), 4.47 (bs, 1 H, *H*-α), 3.25-3.16 (m, 2 H, NHCH₂C₁₃H₂₇), 3.04 (dd, *J* = 4.5 Hz, *J* = 17.1 Hz, 1 H, *H*-β), 2.71 (dd, *J* = 6.3 Hz, *J* = 17.1 Hz, 1 H, *H*-β'), 1.48-1.41 (m, 11 H, overlap of NHCH₂CH₂C₁₂H₂₅ and NHCOC(CH₃)₃), 1.33-1.22 (m, 22 H, NHC₂H₄(CH₂)₁₁CH₃), 0.88 (t, *J* = 6.6 Hz, 3 H, NHC₂H₄(CH₂)₁₁CH₃); ¹³C NMR (75 MHz): δ_c 171.8, 170.4 (each CO), 135.4 (ArC), 128.6, 128.4, 128.2 (ArCH), 66.7 (CH₂Ph), 39.6 (NHCH₂C₁₃H₂₇), 31.8, 29.7, 29.6, 29.6, 29.5, 29.4, 29.3, 29.2 (NHCH₂(CH₂)₁₂CH₃), 28.2 (COC(CH₃)₃), 26.80, 22.7 (NHCH₂(CH₂)₁₂CH₃), 14.1 (NHC₁₃H₂₆CH₃); HRMS *m/z* (ESI⁺): 541.3602 (C₃₀H₅₀N₂NaO₅: [M+Na]⁺ requires 541.3612).



L-asparagine tetradecylamide benzyl ester **2.52**

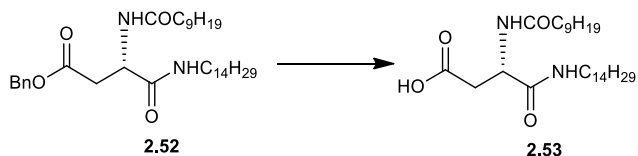
A solution of *N*²-*tert*-butoxycarbonyl-*L*-asparagine tetradecylamide benzyl ester **2.51** (216 mg, 0.4 mmol) in DCM (4 mL) was cooled in an ice bath and 50% TFA in DCM (0.32 mL, 4.1 mmol) was added dropwise. The reaction mixture was stirred at 0 °C for 30 min and then warmed to rt where The mixture was stirred for a further 2 h. The organic solvent was removed *in vacuo* and the residue obtained was diluted with EtOAc and washed with aqueous sat. NaHCO₃ solution, brine, dried over MgSO₄ and concentrated to yield the corresponding deprotected amine **2.52** as a white solid which was used without further purification (144 mg, 83%); ¹H

NMR (300 MHz, CDCl₃): δ 7.39-7.32 (m, 5 H, Ar), 6.77 (bs, 1 H, NHC₁₄H₂₉), 5.20-5.12 (m, 2 H, PhCH₂), 3.88-3.79 (m, 1 H, H- α), 3.22-3.18 (m, 2 H, NHCH₂C₁₃H₂₇), 2.66 (dd, $J = 3.6$ Hz, $J = 15.6$ Hz, 1 H, H- β'), 2.46 (dd, $J = 8.6$ Hz, $J = 15.6$ Hz, 1 H, H- β'), 1.48-1.42 (m, 2 H, NHCH₂CH₂C₁₂H₂₅), 1.32-1.20 (m, 22 H, NHC₂H₄(CH₂)₁₁CH₃), 0.88 (t, $J = 6.6$ Hz, 3 H, NHC₁₃H₂₆CH₃); HRMS m/z (ESI+): 419.3288 (C₂₅H₄₃N₂O₃: [M+H]⁺ requires 419.3268).



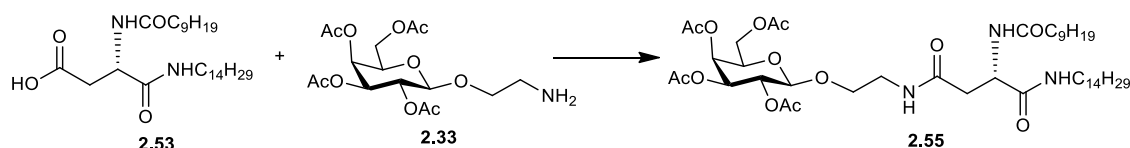
*N*²-decanoyl-L-asparagine tetradecylamide benzyl ester **2.54**

HOBt (46 mg, 0.34 mmol) was added to a stirring solution of decanoic acid (54 mg, 0.31 mmol) and TBTU (110 mg, 0.34 mmol) dissolved in DMF (5 mL), under N₂ at rt. The mixture was stirred for 10 min and L-asparagine tetradecylamide benzyl ester **2.52** (140mg, 0.31 mmol) was dissolved in DMF (5 mL) and added slowly. The reaction mixture was stirred for 18 h, concentrated *in vacuo* and diluted with EtOAc. It was then washed with brine, dried (MgSO₄) and concentrated. The residue obtained was purified by flash chromatography (1:1, EtOAc:Pet Ether) to afford compound **2.54** as a white solid (115 mg, 62%); R_f = 0.82 (1:1, Pet Ether:EtOAc); $[\alpha]_D^{25} = -20$ (c, 1.1 in DCM); IR ν_{\max} (NaCl plate, DCM): 3294.5, 2920.4, 2851.4, 1735.4, 1643.9, 1543.5, 1221.7, 772.6 cm⁻¹; ¹H NMR (300 MHz, CDCl₃): δ 7.34-7.32 (m, 5 H, Ar), 6.83 (d, $J = 8.1$ Hz, 1 H, NHCOC₉H₁₉), 6.60 (bs, 1 H, CONHC₁₄H₂₉), 5.18-5.09 (m, 2 H, PhCH₂), 4.82-4.75 (m, 1 H, H- α), 3.22-3.15 (m, 2 H, NHCH₂C₁₃H₂₇), 2.95 (dd, $J = 3$ Hz, $J = 15.3$ Hz, 1 H, H- β), 2.66 (dd, $J = 8.7$ Hz, $J = 15.6$ Hz, 1 H, H- β'), 2.18 (t, $J = 7.2$ Hz, 2 H, NHCOCH₂C₈H₁₇), 1.59-1.57 (m, $J = 6$, 2 H, NHCH₂CH₂C₁₂H₂₅), 1.44 (bs, 2 H, NHCOCH₂CH₂C₆H₁₅), 1.28-1.20 (m, 34 H, NHC₂H₄(CH₂)₁₁CH₃ and NHCOC₂H₄(CH₂)₆CH₃), 0.87 (t, $J = 6.6$ Hz, 6 H, NHC₁₃H₂₆CH₃ and NHCOC₉H₁₆CH₃); ¹³C NMR (75 MHz, CDCl₃): δ_c 173.4, 171.9, 170.2 (each CO), 134.4 (ArC), 128.6, 128.4, 128.3 (ArCH), 66.9 (PhCH₂), 49.2 (C- α), 39.7 (NHCH₂C₁₃H₂₇), 36.5 (NHCOCH₂C₈H₁₇), 35.8 (C- β), 31.9, 31.9, 29.7, 29.7, 29.6, 29.6, 29.5, 29.4, 29.3, 29.2, 29.2, 28.3, 27.5, 26.8 (NHC₂H₄(CH₂)₁₁CH₃ and NHCOCH₂(CH₂)₇CH₃), 25.6 (NHCH₂CH₂(CH₂)₁₁CH₃), 22.7, 22.6 (NHC₂H₄(CH₂)₁₁CH₃ and NHCOCH₂(CH₂)₇CH₃), 14.1, 14.1 (NHC₁₃H₂₆CH₃ and NHCOC₈H₁₆CH₃); HRMS m/z (ESI+): 573.4646 (C₃₅H₆₀N₂O₄: [M+H]⁺ requires 573.4626).



*N*²-decanoyl-L-asparagine tetradecylamide **2.53**

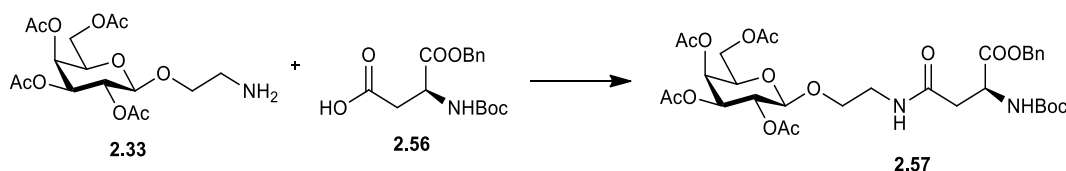
To a solution of *N*²-decanoyl-L-asparagine tetradecylamide benzyl ester **2.53** (115 mg, 0.2 mmol) in EtOAc (10 mL), Pd/C (12 mg, 10% w/w) was added. The resulting mixture was heated to 50 °C and H₂ bubbled through for 4 h. The mixture was then filtered through a Celite cake and the filtrate was concentrated under vacuum to afford a white solid which was recrystallised in DCM to yield the pure product **2.53** (73 mg, 76%); ¹H NMR (300 MHz, CDCl₃): δ 7.02 (d, *J* = 7.8 Hz, 1 H, NHCOC₉H₁₉), 6.96-6.89 (m, 1 H, NHC₁₄H₂₉), 4.84-4.73 (m, 1 H, *H*-α), 3.24-3.18 (m, 2 H, NHCH₂C₁₃H₂₇), 2.92-2.87 (m, 1 H, *H*-β), 2.68 (dd, *J* = 6.6 Hz, *J* = 16.8 Hz, 1 H, *H*-β'), 2.24 (t, *J* = 7.2 Hz, 2 H, NHCOCH₂C₈H₁₇), 1.67-1.57 (m, 2 H, NHCH₂CH₂C₁₂H₂₅), 1.53-1.42 (m, 2 H, NHCOCH₂CH₂C₆H₁₅), 1.32-1.19 (m, 34 H, NHC₂H₄(CH₂)₁₁CH₃ and NHCOC₂H₄(CH₂)₆CH₃), 0.87 (t, *J* = 6.3 Hz, 6 H, NHC₁₃H₂₆CH₃ and NHCOC₉H₁₆CH₃); HRMS *m/z* (ESI⁺): 483.4147 (C₂₈H₅₅N₂O₄: [M+H]⁺ requires 483.4156).



*N*⁴-[2-*O*-(2,3,4,6-tetra-*O*-acetyl-β-*D*-galactopyranosyl)-ethyl]-*N*²-decanoyl-L-asparagine tetradecylamide **2.55**

HOBt (230 mg, 0.17 mmol) was added to a stirring solution of *N*²-decanoyl-L-asparagine tetradecylamide **2.53** (73 mg, 0.15 mmol) and TBTU (54 mg, 0.17 mmol) dissolved in DMF (5 mL), under N₂ at 50 °C. The mixture was stirred for 10 min and 2-Aminoethyl 2,3,4,6-tetra-*O*-acetyl-β-*D*-galactopyranoside **2.33** (71 mg, 0.18 mmol) was dissolved in DMF (4 mL) and added dropwise. The mixture was stirred overnight at rt. The reaction mixture was concentrated *in vacuo*. Flash chromatography (EtOAc) afforded **2.55** as a white solid (87 mg, 69%); *R*_f = 0.64 (EtOAc); [α]_D²⁵ = +5.8 (c, 0.8 in DCM); IR *v*_{max} (NaCl plate, DCM): 3289.5, 3098.3, 2919.3, 2850.8, 1750.8, 168.1, 1646.5, 1542.4, 1467.4, 1370.4, 1225.5, 1174.9, 1058.5 cm⁻¹; ¹H-NMR (300 MHz, CDCl₃): δ 7.43 (d, *J* = 6.9 Hz, 1 H, NHCOC₉H₁₉), 7.08 (t, *J* = 5.4 Hz, 1 H, CONHC₁₄H₂₉), 6.26 (t, *J* = 5.4 Hz, 1 H, CH₂CH₂NHCO), 5.40 (d, *J* = 2.4 Hz, 1 H, *H*-4), 5.18 (dd, *J* = 7.8 Hz, *J* = 10.5 Hz, 1 H, *H*-2), 5.04 (dd, *J* = 3.3 Hz, *J* = 10.5 Hz, 1 H, *H*-3), 4.70-4.64 (m, 1 H, *H*-α), 4.54 (d, *J* = 7.8 Hz, 1 H, *H*-1), 4.22-4.11 (m, 2 H, overlap of *H*-6, *H*-6'), 3.97-3.94 (m, 1 H, *H*-5), 3.92-3.85 (m, 1 H, 1

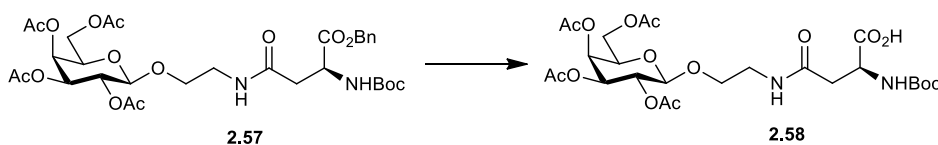
H of $\text{OCH}_2\text{CH}_2\text{NH}$), 3.69–3.64 (m, 1 H, 1 H of $\text{OCH}_2\text{CH}_2\text{NH}$), 3.57–3.39 (m, 2 H, $\text{OCH}_2\text{CH}_2\text{NH}$), 3.22–3.16 (m, 2 H, $\text{NHCH}_2\text{C}_{13}\text{H}_{27}$), 2.81 (dd, $J = 3.3$ Hz, $J = 15.3$ Hz, 1 H, H- β), 2.46 (dd, $J = 6.9$, $J = 15.6$, 1 H, H- β'), 2.25–2.20 (t, $J = 7.5$ Hz, 2 H, $\text{COCH}_2\text{C}_8\text{H}_{17}$), 2.16, 2.09, 2.05, 1.9 (each s, 3 H, $\text{O}(\text{CO})\text{CH}_3$), 1.62–1.60 (m, 2 H, $\text{COCH}_2\text{CH}_2\text{C}_7\text{H}_{15}$), 1.46–1.45 (m, 2 H, $\text{NHCH}_2\text{CH}_2\text{C}_{12}\text{H}_{25}$), 1.30–1.18 (m, 34 H, overlap of $\text{COC}_2\text{H}_4(\text{CH}_2)_6\text{CH}_3$, $\text{NHC}_2\text{H}_4(\text{CH}_2)_{11}\text{CH}_3$), 0.87 (t, $J = 6.6$ Hz, 6 H, overlap of $\text{COC}_8\text{H}_{16}\text{CH}_3$, $\text{NHC}_{13}\text{H}_{26}\text{CH}_3$); ^{13}C -NMR (75 Hz, CDCl_3): δ_{c} 173.7, 171.7, 170.6, 170.4, 170.2, 170.1, 169.9 (each CO), 101.3 (C-1), 70.8, 70.7 (C-5, C-3), 69.0, (C-2), 68.5 ($\text{OCH}_2\text{CH}_2\text{NH}$) 67.0 (C-4), 61.3 (C-6), 49.7 (C- α), 39.7 ($\text{OCH}_2\text{CH}_2\text{NH}$), 39.3 ($\text{NHCH}_2\text{C}_{13}\text{H}_{27}$), 37.0 (C- β), 36.6 ($\text{COCH}_2\text{C}_8\text{H}_{17}$), 31.9, 29.7, 29.6, 29.6, 29.5, 29.4, 29.3, 28.3, 26.9, 25.6, 22.6 ($\text{COC}_2\text{H}_4(\text{CH}_2)_6\text{CH}_3$, $\text{NHC}_2\text{H}_4(\text{CH}_2)_{11}\text{CH}_3$), 20.87–20.85 (overlap of $\text{O}(\text{CO})\text{CH}_3$), 14.1 (overlap of $\text{COC}_8\text{H}_{16}\text{CH}_3$, $\text{NHC}_{13}\text{H}_{26}\text{CH}_3$); HRMS m/z (ESI $^+$): 856.5492 ($\text{C}_{44}\text{H}_{77}\text{N}_3\text{O}_{13}$: $[\text{M}+\text{H}]^+$ requires 856.5529).



*N*⁴-[2-*O*-(2,3,4,6-tetra-*O*-acetyl- β -*D*-galactopyranosyl)-ethyl]-*N*²-tert-butoxycarbonyl-*L*-asparagine benzylester **2.57**

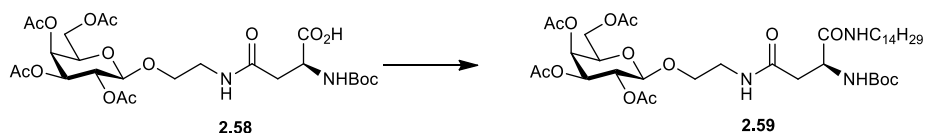
HOBt (90 mg, 0.68 mmol), followed by NEt_3 (0.18 mL, 1.23 mmol), were added to a stirring solution of *N*-Boc-*L*-Asp-OBn **2.56** (0.2 g, 0.61 mmol) and TBTU (220 mg, 0.6 mmol) dissolved in anhydrous DMF (10 mL), under N_2 at rt. The mixture was stirred for 30 min and 2-aminoethyl 2,3,4,6-tetra-*O*-acetyl- β -*D*-galactopyranoside **2.33** (290 mg, 0.74 mmol) dissolved in anhydrous DMF (1.2 mL) was added dropwise. The mixture was stirred for 18 h. The reaction mixture was concentrated under reduced pressure, diluted with EtOAc and washed successively with 0.1 M HCl, aqueous sat. NaHCO_3 solution and brine. Flash chromatography (1:1, EtOAc:Pet Ether) afforded **2.57** as a white solid (330 mg, 76%); $R_f = 0.76$ (EtOAc); $[\alpha]_{\text{D}}^{25} = +6.9$ (c, 1.35 in DCM); IR ν_{max} (NaCl plate, DCM): 3374.7, 2978.0, 1750.7, 1665.8, 1499.3, 1368.8, 1224.3, 1167.9, 1124.3, 1057.2 cm^{-1} ; ^1H -NMR (300 MHz, CDCl_3) δ 7.34–7.33 (m, 5 H, Ar), 6.01 (t, $J = 5.1$ Hz, 1 H, $\text{CH}_2\text{CH}_2\text{NHCO}$), 5.76 (d, $J = 8.1$ Hz, 1 H, $\text{NHCOC}(\text{CH}_3)_3$), 5.39 (dd, $J = 0.6$ Hz, $J = 3.3$ Hz, 1 H, *H*-4), 5.20–5.16 (m, 3 H, overlap of *H*-2, PhCH_2), 5.02 (dd, $J = 3.3$ Hz, $J = 10.2$ Hz, 1 H, *H*-3), 4.57–4.54 (m, 1 H, *H*- α), 4.44 (d, $J = 7.8$ Hz, 1 H, *H*-1), 4.18–4.13 (m, 2 H, overlap of *H*-6, *H*-6'), 3.93–3.89 (m, 1 H, *H*-5), 3.86–3.80 (m, 1 H, 1 H of $\text{OCH}_2\text{CH}_2\text{NH}$), 3.66–3.59 (m, 1 H, 1 H of $\text{OCH}_2\text{CH}_2\text{NH}$), 3.46–3.38 (m, 2 H, $\text{OCH}_2\text{CH}_2\text{NH}$), 2.91 (dd, $J = 5.7$ Hz, $J = 17.4$ Hz, 1 H, *H*- β), 2.71 (dd, $J = 4.5$ Hz, $J = 15.9$ Hz, 1 H, *H*- β'), 2.15 (s, 3 H, $\text{O}(\text{CO})\text{CH}_3$), 2.05 (s, 6 H, $\text{O}(\text{CO})\text{CH}_3$), 1.99 (s, 3 H, $\text{O}(\text{CO})\text{CH}_3$)

1.42 (s, 9 H, $\text{COC}(\text{CH}_3)_3$); ^{13}C -NMR (75 MHz, CDCl_3): δ_c 171.4, 170.4, 169.8 (each CO), 155.5 (Ar-C), 128.5, 128.1 (Ar-CH), 101.4 (C-1), 79.0 ($\text{COC}(\text{CH}_3)_3$), 70.9 (C-5), 70.7 (C-2), 68.9 (C-3), 67.2 ($\text{OCH}_2\text{CH}_2\text{NH}$), 67 (C-4), 61.3 (C-6), 50.5 (C- α), 39.2 (each $\text{OCH}_2\text{CH}_2\text{NH}$), 37.7 (CH_2Ph), 37.1 (C- β), 28.3 ($\text{COC}(\text{CH}_3)_3$), 20.8, 20.6 (each $\text{O}(\text{CO})\text{CH}_3$); HRMS m/z (ESI+): 697.2800 ($\text{C}_{32}\text{H}_{45}\text{N}_2\text{O}_{15}$: $[\text{M}+\text{H}]^+$ requires 697.2814).



*N*⁴-[2-*O*-(2,3,4,6-tetra-*O*-acetyl- β -*D*-galactopyranosyl)-ethyl]-*N*²-*tert*-butoxycarbonyl-*L*-asparagine **2.58**

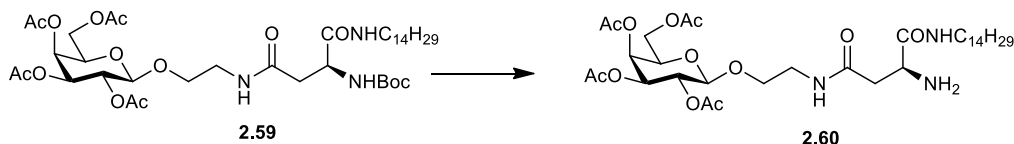
To a solution of *N*⁴-[2-*O*-(2,3,4,6-tetra-*O*-acetyl- β -*D*-galactopyranosyl)-ethyl]-*N*²-*tert*-butoxycarbonyl-*L*-asparagine benzylester **2.57** (120 mg, 0.17 mmol) in EtOAc (6 mL), Pd/C (12 mg, 10% w/w) was added. The resulting mixture was stirred under H_2 gas for 4 h. The mixture was then filtered through a Celite cake and the filtrate was concentrated under vacuum to afford the corresponding carboxylic acid **2.58** as an off-white solid, which was used without further purification (94 mg, 90%); ^1H -NMR (300 MHz, CDCl_3): δ 6.53 (bs, 1 H, $\text{CH}_2\text{CH}_2\text{NHCO}$), 5.86 (d, $J = 5.4$ Hz, 1 H, $\text{NHCOC}(\text{CH}_3)_3$), 5.41 (d, $J = 3.3$ Hz, 1 H, *H*-4), 5.17 (dd, $J = 7.8$ Hz, $J = 10.2$ Hz, 1 H, *H*-2), 5.00 (dd, $J = 3.3$ Hz, $J = 10.2$ Hz, 1 H, *H*-3), 4.49 (d, $J = 7.8$ Hz, 1 H, *H*-1), 4.45–4.42 (m, 1 H, *H*- α), 4.20–4.11 (m, 2 H, overlap of *H*-6, *H*-6'), 3.96–3.92 (m, 1 H, *H*-5) 3.90–3.85 (m, 1 H, 1 H of $\text{OCH}_2\text{CH}_2\text{NH}$), 3.75–3.68 (m, 1 H, 1 H of $\text{OCH}_2\text{CH}_2\text{NH}$), 3.54–3.39 (m, 2 H, $\text{OCH}_2\text{CH}_2\text{NH}$), 2.91 (d, $J = 15.6$ Hz, 1 H, *H*- β), 2.72 (dd, $J = 8.49$ Hz, $J = 15.9$ Hz, 1 H, *H*- β'), 2.17, 2.13, 2.05, 1.98 (each s, 3 H, $\text{O}(\text{CO})\text{CH}_3$), 1.42 (s, 9 H, $\text{COC}(\text{CH}_3)_3$); HRMS m/z (ESI+): 645.1899 ($\text{C}_{25}\text{H}_{38}\text{N}_2\text{KO}_{15}$: $[\text{M}+\text{K}]^+$ requires 645.1904).



*N*⁴-[2-*O*-(2,3,4,6-tetra-*O*-acetyl- β -*D*-galactopyranosyl)-ethyl]-*N*²-*tert*-butoxycarbonyl-*L*-asparagine tetradecylamide **2.59**

HOBt (34 mg, 0.25 mmol) was added to a stirring solution of the *N*⁴-[2-*O*-(2,3,4,6-tetra-*O*-acetyl- β -*D*-galactopyranosyl)-ethyl]-*N*²-*tert*-butoxycarbonyl-*L*-asparagine **2.58** (140 mg, 0.23 mmol), tetradecylamine (60 mg, 0.28 mmol), and TBTU (81 mg, 0.25 mmol) dissolved in anhydrous DMF, (12 mL) at rt. The mixture was stirred for 18 h. The reaction mixture was

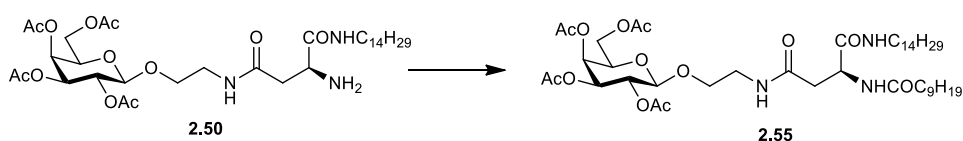
concentrated *in vacuo*, diluted with EtOAc and washed with brine. Flash chromatography (EtOAc) afforded **2.59** as a white solid (120 mg, 56%); $R_f = 0.65$ (EtOAc); $[\alpha]_D^{25} = +8.8$ (c, 0.75 in DCM); IR ν_{\max} (NaCl plate, DCM): 3316.3, 3091.3, 2919.9, 2851.3, 1748.0, 1687.1, 1646.1, 1548.9, 1524.1, 1467.4, 1434.6, 1369.2, 1368.8, 1230.2, 1171.0, 1055.3 cm^{-1} ; $^1\text{H-NMR}$ (300 MHz, CDCl_3): δ 6.87 (bs, 1 H, $\text{CONHC}_{14}\text{H}_{29}$), 6.23 (t, $J = 10.5$ Hz, 1 H, $\text{CH}_2\text{CH}_2\text{NHCO}$), 6.14 (d, $J = 8.1$ Hz, 1 H, $\text{NHCOC}(\text{CH}_3)_3$), 5.38 (d, $J = 2.7$ Hz, 1 H, $H-4$), 5.15 (dd, $J = 7.8$ Hz, $J = 10.5$ Hz, 1 H, $H-2$), 5.01 (dd, $J = 2.7$ Hz, $J = 10.5$ Hz, 1 H, $H-3$), 4.49 (d, $J = 7.8$ Hz, 1 H, $H-1$), 4.40–4.39 (m, 1 H, $H-\alpha$), 4.15–4.11 (m, 2 H, overlap of $H-6$, $H-6'$), 3.94–3.87 (m, 1 H, $H-5$), 3.86–3.81 (m, 1 H, 1 H of $\text{OCH}_2\text{CH}_2\text{NH}$), 3.67–3.60 (m, 1 H, 1 H of $\text{OCH}_2\text{CH}_2\text{NH}$), 3.49–3.34 (m, 2 H, $\text{OCH}_2\text{CH}_2\text{NH}$), 3.22–3.15 (m, 2 H, $\text{NHCH}_2\text{C}_{13}\text{H}_{27}$), 2.71 (dd, $J = 4.2$ Hz, $J = 15.6$ Hz, 1 H, $H-\beta$), 2.51 (dd, $J = 6.6$ Hz, $J = 15.6$ Hz, 1 H, $H-\beta'$), 2.14, 2.07, 2.02, 1.96 (each s, 3 H, $\text{O}(\text{CO})\text{CH}_3$), 1.42 (m, 11 H, overlap of $\text{COC}(\text{CH}_3)_3$, $\text{NHCH}_2\text{CH}_2\text{C}_{12}\text{H}_{25}$), 1.29–1.17 (m, 22 H, $\text{NHC}_2\text{H}_4(\text{CH}_2)_{11}\text{CH}_3$), 0.85 (t, $J = 6.6$ Hz, 3 H, $\text{NHC}_{13}\text{H}_{26}\text{CH}_3$); $^{13}\text{C-NMR}$ (75 MHz, CDCl_3): δ_c 171.2, 170.9, 170.3, 170.2, 170.0, 169.8, 155.7 (CO), 101.3 (C-1), 80.1 ($\text{COC}(\text{CH}_3)_3$), 70.8, 70.7 (C-5, C-3), 68.9 (C-2), 68.6 ($\text{OCH}_2\text{CH}_2\text{NH}$), 67 (C-4), 61.3 (C-6), 51.1 (C- α), 39.6 ($\text{OCH}_2\text{CH}_2\text{NH}$), 39.2 ($\text{NHCH}_2\text{C}_{13}\text{H}_{27}$), 37.5 (C- β), 31.9, 29.7, 29.6, 29.6, 29.5, 29.4, 29.3, 29.2 ($\text{NHC}_2\text{H}_4(\text{CH}_2)_{11}\text{CH}_3$), 28.3 ($\text{COC}(\text{CH}_3)_3$), 26.8, 22.7 ($\text{NHC}_2\text{H}_4(\text{CH}_2)_{11}\text{CH}_3$), 20.8, 20.7, 20.6, 20.5 (each $\text{O}(\text{CO})\text{CH}_3$), 14.93 ($\text{NHC}_{13}\text{H}_{26}\text{CH}_3$); HRMS m/z (ESI+): 802.4685 ($\text{C}_{39}\text{H}_{67}\text{N}_3\text{O}_{14}$: $[\text{M}+\text{H}]^+$ requires 802.4696).



N^4 -[2-O-(2,3,4,6-tetra-O-acetyl- β -D-galactopyranosyl)-ethyl]- N^2 -L-asparagine tetradecylamide
2.60

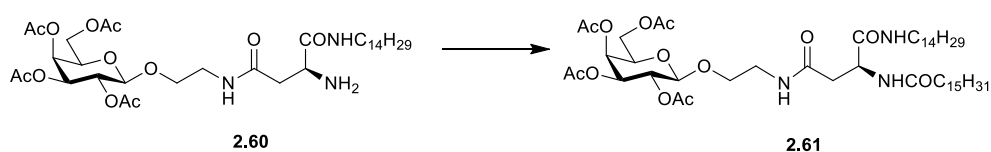
A solution of N^4 -[2-O-(2,3,4,6-tetra-O-acetyl- β -D-galactopyranosyl)-ethyl]- N^2 -tert-butoxycarbonyl-L-asparagine tetradecylamide **2.59** (110 mg, 0.13 mmol) in anhydrous DCM, (6 mL) was cooled in an ice bath and TFA (0.15 mL, 1.37 mmol) was added. The reaction mixture was heated to 50 °C and stirred for 1.5 h. The organic solvent was removed *in vacuo* and the residue obtained was diluted with EtOAc and washed with aqueous sat. NaHCO_3 solution, brine, dried over MgSO_4 and concentrated to yield the corresponding deprotected amine **2.60** as a brown oil, which was used without further purification (71 mg, 74%); $^1\text{H-NMR}$ (300 MHz, CDCl_3): δ 7.41–7.40 (m, 1 H, $\text{CONHC}_{14}\text{H}_{29}$), 6.42 (t, $J = 5.1$ Hz, 1 H, $\text{CH}_2\text{CH}_2\text{NHCO}$), 5.38 (d, $J = 3.3$ Hz, 1 H, $H-4$), 5.16 (dd, $J = 7.8$ Hz, $J = 10.5$ Hz, 1 H, $H-2$), 5.01 (dd, $J = 3.3$ Hz, $J = 10.5$ Hz, 1 H,

H-3), 4.48 (d, $J = 7.8$ Hz, 1 H, *H*-1), 4.2–4.1 (m, 2 H, overlap of *H*-6, *H*-6'), 3.94–3.89 (m, 1 H, *H*-5) 3.87–3.82 (m, 1 H, 1 H of $\text{OCH}_2\text{CH}_2\text{NH}$), 3.67–3.64 (m, 2 H, overlap of 1 H of $\text{OCH}_2\text{CH}_2\text{NH}$, *H*- α), 3.42–3.46 (bm, 2 H, $\text{OCH}_2\text{CH}_2\text{NH}$), 3.20–3.22 (m, 2 H, $\text{NHCH}_2\text{C}_{13}\text{H}_{27}$), 2.68 (dd, $J = 3.9$ Hz, $J = 15$ Hz, 1 H, *H*- β), 2.46 (dd, $J = 7.8$ Hz, $J = 15$ Hz, 1 H, *H*- β'), 2.15, 2.07, 2.03, 1.97 (each s, 3 H, $\text{O}(\text{CO})\text{CH}_3$), 1.50–1.43 (m, 2 H, $\text{NHCH}_2\text{CH}_2\text{C}_{12}\text{H}_{25}$), 1.33–1.20 (m, 22 H, $\text{NHC}_2\text{H}_4(\text{CH}_2)_{11}\text{CH}_3$), 0.85 (t, $J = 6.6$ Hz, 3 H, $\text{NHC}_{13}\text{H}_{26}\text{CH}_3$); HRMS m/z (ESI⁺): 702.4159 ($\text{C}_{34}\text{H}_{59}\text{N}_3\text{O}_{12}$: $[\text{M}+\text{H}]^+$ requires 702.4172).



*N*⁴-[2-*O*-(2,3,4,6-tetra-*O*-acetyl- β -*D*-galactopyranosyl)-ethyl]-*N*²-decanoyl-*L*-asparagine tetradecylamide

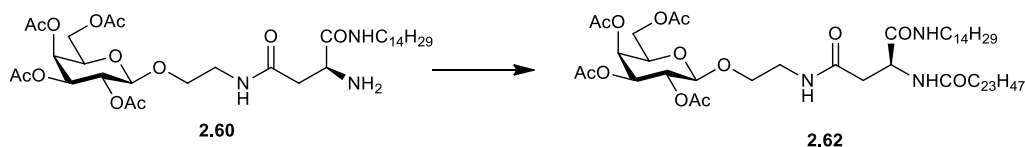
HOBt (41 mg, 0.3 mmol) was added to a stirring solution of decanoic acid (48 mg, 0.27 mmol) and TBTU (98 mg, 0.3 mmol) dissolved in DMF (6 mL), under N_2 at rt. The mixture was stirred for 10 min and *N*⁴-[2-*O*-(2,3,4,6-tetra-*O*-acetyl- β -*D*-galactopyranosyl)-ethyl]-*N*²-*L*-asparagine tetradecylamide **2.60** (60 mg, 0.28 mmol) dissolved in anhydrous DMF (8 mL) was added slowly. The mixture was stirred for 18 h. The reaction mixture was concentrated *in vacuo*, diluted with EtOAc, washed with brine, dried over MgSO_4 and concentrated. The residue obtained was purified by flash chromatography (EtOAc) to afford **2.55** as a white solid (150 g, 63%). The spectroscopic data is identical to that discussed earlier for glycolipid **2.55**.



*N*⁴-[2-*O*-(2,3,4,6-tetra-*O*-acetyl- β -*D*-galactopyranosyl)-ethyl]-*N*²-hexadecanoyl-*L*-asparagine tetradecylamide **2.61**

NEt_3 (0.013 mL, 0.098 mmol) was added to *N*⁴-[2-*O*-(2,3,4,6-tetra-*O*-acetyl- β -*D*-galactopyranosyl)-ethyl]-*N*²-*L*-asparagine tetradecylamide **2.60** (76 mg, 0.108 mmol,) dissolved in DCM (6 mL) under Ar. The reaction mixture was allowed to stir for 10 min, and hexadecanoyl chloride (0.029 mL, 0.098 mmol) was added. The reaction mixture was stirred at rt overnight. The solvent was concentrated *in vacuo*, diluted with EtOAc, washed with 0.1 M HCl, aqueous sat. NaHCO_3 , brine and dried over MgSO_4 . Flash chromatography (EtOAc)

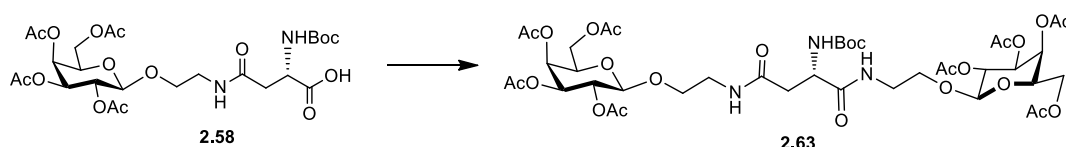
afforded **2.61** as a white solid (80 mg, 87%); $R_f = 0.43$ (EtOAc); $[\alpha]^{25}_D = -3.5$ (c, 1.4 in DCM); IR ν_{\max} (NaCl plate, DCM): 3290.7, 3098.1, 2917.9, 2850.3, 1751.1, 1642.4, 1543.3, 1462.4, 1370.5, 1225.6, and 1079.9 cm^{-1} ; ^1H NMR (300 MHz, CDCl_3): δ 7.41 (d, $J = 6.9$ Hz, 1 H, $\text{NHCOCH}_{15}\text{H}_{31}$), 7.08 (t, $J = 5.1$ Hz, 1 H, $\text{CONHC}_{14}\text{H}_{29}$), 6.30 (bs, 1 H, $\text{OCH}_2\text{CH}_2\text{NH}$), 5.39 (d, $J = 3.3$ Hz, 1 H, $H-4$), 5.16 (dd, $J = 7.8$ Hz, $J = 10.5$ Hz, 1 H, $H-2$), 5.03 (dd, $J = 3.3$ Hz, $J = 10.5$ Hz, 1 H, $H-3$), 4.68-4.63 (m, 1 H, $H-\alpha$), 4.52 (d, $J = 7.8$ Hz, 1 H, $H-1$), 4.20-4.10 (m, 2 H, $H-6$ and $H-6'$), 3.96-3.84 (m, 2 H overlap of $H-5$ and 1 H of $\text{OCH}_2\text{CH}_2\text{NH}$), 3.70-3.64 (m, 1 H, $\text{OCH}_2\text{CH}_2\text{NH}$), 3.53-3.44 (m, 2 H, $\text{OCH}_2\text{CH}_2\text{NH}$), 3.18 (q, $J = 6.6$ Hz, 2 H, $\text{NHCH}_2\text{C}_{13}\text{H}_{27}$), 2.76 (dd, $J = 3.3$ Hz, $J = 15.3$, 1 H, $H-\beta$), 2.46 (dd, $J = 6.9$, $J = 15.6$, 1 H, $H-\beta'$), 2.23 (t, $J = 7.5$ Hz, 2 H, $\text{NHCOCH}_2\text{C}_{14}\text{H}_{29}$), 2.14, 2.08, 2.04, and 1.9 (each s, 3 H, $\text{O}(\text{CO})\text{CH}_3$), 1.62-1.58 (m, 2 H, $\text{NHCOCH}_2\text{CH}_2\text{C}_{13}\text{H}_{27}$), 1.46-1.45 (m, 2 H, $\text{NHCH}_2\text{CH}_2\text{C}_{12}\text{H}_{25}$), 1.18-1.31 (m, 46 H, overlap of $\text{NHC}_2\text{H}_4(\text{CH}_2)_{11}\text{CH}_3$, $\text{NHCOC}_2\text{H}_4(\text{CH}_2)_{12}\text{CH}_3$), 0.87 (t, $J = 6.3$ Hz, 6 H, overlap of $\text{NHCOC}_{14}\text{H}_{28}\text{CH}_3$, $\text{CONHC}_{13}\text{H}_{26}\text{CH}_3$); ^{13}C NMR (75 MHz, CDCl_3): δ_c 172.6, 170.7, 169.6, 169.3, 169.2, 169.0, 168.89 (each CO), 100.3 (C-1), 69.8, 69.7 (C-5 and C-3), 67.9 (C-2), 67.5 ($\text{OCH}_2\text{CH}_2\text{NH}$), 65.9 (C-4), 60.3 (C-6), 48.7 (C- α), 38.6 ($\text{OCH}_2\text{CH}_2\text{NH}$), 38.3 ($\text{NHCH}_2\text{C}_{13}\text{H}_{27}$), 35.9 (C- β), 35.6 ($\text{NHCOCH}_2\text{C}_{14}\text{H}_{29}$), 30.9, 28.7, 28.6, 28.5, 28.5, 28.4, 28.3, 28.3, 25.9, 24.6, and 21.6 ($\text{NHCOCH}_2(\text{CH}_2)_{13}\text{CH}_3$ and $\text{NHCH}_2(\text{CH}_2)_{12}\text{CH}_3$), 19.8, 19.6 and 19.5 (each $\text{O}(\text{CO})\text{CH}_3$), 13.1 (overlap of $\text{NHCOC}_{14}\text{H}_{28}\text{CH}_3$, $\text{NHC}_{13}\text{H}_{26}\text{CH}_3$); HRMS m/z (ESI $^+$): 940.650 ($\text{C}_{50}\text{H}_{89}\text{N}_3\text{O}_{13}$: $[\text{M}+\text{H}]^+$ requires 940.6468).



N^4 -[2-*O*-(2,3,4,6-tetra-*O*-acetyl- β -*D*-galactopyranosyl)-ethyl]- N^2 -tetracosanoyl-*L*-asparagine tetradecylamide **2.62**

HOBt (220 mg, 0.16 mmol) was added to a stirring solution of tetracosanoic acid (56 mg, 0.15 mmol) and TBTU (56 mg, 0.16 mmol) dissolved in anhydrous DMF (6 mL), under N_2 at rt. The mixture was stirred for 10 min and N^4 -[2-*O*-(2,3,4,6-tetra-*O*-acetyl- β -*D*-galactopyranosyl)-ethyl]- N^2 -*L*-asparagine tetradecylamide **2.60** (128 mg, 0.18 mmol) was dissolved in anhydrous DMF (8 mL) and added slowly. The reaction mixture was stirred for 3 h, concentrated *in vacuo*, diluted with EtOAc, washed with brine, dried over MgSO_4 . The resulting solution was concentrated and the residue obtained was purified by flash chromatography (EtOAc) to afford **2.62** as a white solid, (63 mg, 40%); $R_f = 0.51$ (EtOAc); $[\alpha]^{25}_D = +3.8$ (c, 0.83 in DCM); IR ν_{\max} (NaCl plate, DCM): 3423.0, 2918.4, 2850.3, 1749.6, 1644.4, 1543.1, 1465.6, 1369.9, 1223.4,

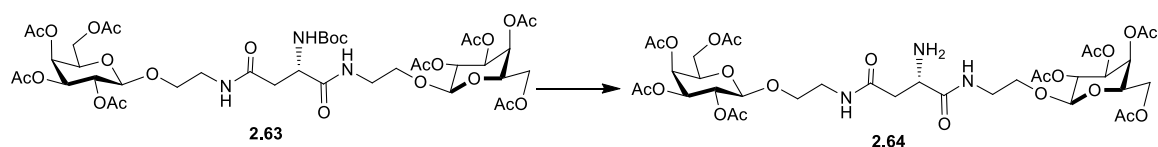
1058.3 cm^{-1} ; $^1\text{H-NMR}$ (300 MHz, CDCl_3): δ 7.44 (d, $J = 6.9$ Hz, 1 H, $\text{NHCOC}_{23}\text{H}_{47}$), 7.09 (t, $J = 4.8$ Hz, 1 H, $\text{CONHC}_{14}\text{CH}_{29}$) 6.26 (bs, 1 H, $\text{CH}_2\text{CH}_2\text{NHCO}$), 5.40 (d, $J = 2.7$ Hz, 1 H, $H-4$), 5.17 (dd, $J = 7.8$ Hz, $J = 10.5$ Hz, 1 H, $H-2$), 5.04 (dd, $J = 2.7$ Hz, $J = 10.5$ Hz, 1 H, $H-3$), 4.70–4.64 (m, 1 H, $H-\alpha$), 4.53 (d, $J = 7.8$ Hz, 1 H, $H-1$), 4.21–4.10 (m, 2 H, overlap of $H-6$, $H-6'$), 3.97–3.92 (tm, 1 H, $H-5$) 3.90–3.85 (m, 1 H, 1 H of $\text{OCH}_2\text{CH}_2\text{NH}$), 3.71–3.64 (m, 1 H, 1 H of $\text{OCH}_2\text{CH}_2\text{NH}$), 3.54–3.44 (m, 2 H, $\text{OCH}_2\text{CH}_2\text{NH}$), 3.22–3.15 (m, 2 H, $\text{NHCH}_2\text{C}_{13}\text{H}_{27}$), 2.77 (dd, $J = 3.3$ Hz, $J = 15.3$ Hz, 1 H, $H-\beta$), 2.45 (dd, $J = 6.9$ Hz, $J = 15.6$ Hz, 1 H, $H-\beta'$), 2.23 (t, $J = 7.5$ Hz, 2 H, $\text{COCH}_2\text{C}_{22}\text{H}_{45}$), 2.16, 2.09, 2.04, 1.90 (each s, 3 H, $\text{O}(\text{CO})\text{CH}_3$), 1.62–1.59 (m, 2 H, $\text{COCH}_2\text{CH}_2\text{C}_{21}\text{H}_{43}$), 1.46–1.45 (m, 2 H, $\text{NHCH}_2\text{CH}_2\text{C}_{12}\text{H}_{25}$), 1.31–1.22 (m, 62 H, overlap of $\text{COC}_2\text{H}_4(\text{CH}_2)_{20}\text{CH}_3$, $\text{NHC}_2\text{H}_4(\text{CH}_2)_{11}\text{CH}_3$), 0.87 (t, $J = 6.3$ Hz, 6 H, overlap of $\text{NHCOC}_{22}\text{H}_{44}\text{CH}_3$, $\text{NHC}_{13}\text{H}_{26}\text{CH}_3$); $^{13}\text{C-NMR}$ (75 MHz, CDCl_3): δ_c 173.6, 171.7, 170.6, 170.4, 170.2, 170.1, 169.9 (each CO), 101.3 (C-1), 70.8, 70.7 (C-5, C-3), 69.0, (C-2), 68.5 ($\text{OCH}_2\text{CH}_2\text{NH}$), 67 (C-4), 61.3 (C-6), 49.7 (C- α), 39.7 ($\text{OCH}_2\text{CH}_2\text{NH}$), 38.5 ($\text{NHCH}_2\text{C}_{13}\text{H}_{27}$), 36.9 (C- β), 36.6 ($\text{NHCOCH}_2(\text{CH}_2)_{21}\text{CH}_3$), 31.9, 31.8, 29.6, 29.5, 29.4, 29.3, 29.2, 26.8, 22.6, 22.6 ($\text{NHCOCH}_2(\text{CH}_2)_{21}\text{CH}_3$, $\text{NHCH}_2(\text{CH}_2)_{12}\text{CH}_3$), 20.9 (overlap of $\text{O}(\text{CO})\text{CH}_3$), 14.1 (overlap of $\text{COC}_2\text{H}_4\text{CH}_3$, $\text{NHC}_{13}\text{H}_{26}\text{CH}_3$); HRMS m/z (ESI+): 1052.775 ($\text{C}_{58}\text{H}_{105}\text{N}_3\text{O}_{13}$: $[\text{M}+\text{H}]^+$ requires 1052.7720).



*N*⁴-[2-*O*-(2,3,4,6-tetra-*O*-acetyl- β -*D*-galactopyranosyl)-ethyl]-*N*²-tert-butoxycarbonyl-*N*¹-[2-*O*-(2,3,4,6-tetra-*O*-acetyl- β -*D*-galactopyranosyl)-ethyl] *L*-asparagine **2.63**

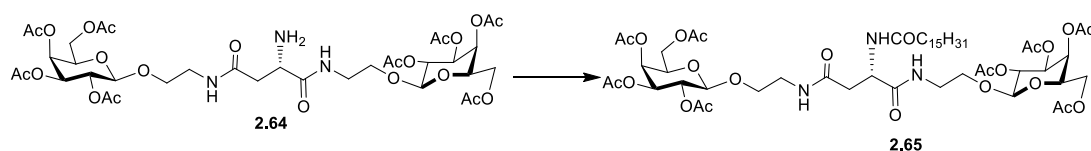
HOBt (161 mg, 1.2 mmol) was added to a stirring solution of *N*⁴-[2-*O*-(2,3,4,6-tetra-*O*-acetyl- β -*D*-galactopyranosyl)-ethyl]-*N*²-tert-butoxycarbonyl-*L*-asparagine **2.58** (673 mg, 1.1 mmol) TBTU (391 mg, 1.2 mmol) and *O*-(2-aminoethyl)-(2,3,4,6-*O*-tetracetyl)- β -*D*-galactopyranose **2.33** (521 mg, 1.3 mmol) dissolved in DMF (15 mL), under N_2 at rt. The mixture was stirred for 18 h. The reaction mixture was concentrated under reduced pressure, diluted with EtOAc and washed successively with 0.1 M HCl, aqueous sat. NaHCO_3 solution, and brine. Flash chromatography (EtOAc) afforded **2.63** as an oily solid (0.750 g, 61%); $R_f = 0.27$ (EtOAc); $[\alpha]^{25}_D = +14.9$ (c, 1 in DCM); IR ν_{max} (NaCl plate, DCM): 3370.2, 2979.7, 1750.1, 1662.4, 1528.9, 1369.6, 1224.2, 1171.1, 1057.02 cm^{-1} ; $^1\text{H NMR}$ (300 MHz, CDCl_3): δ 7.06 (bs, 1 H, $\text{CH}_2\text{CH}_2\text{NH}'$), 6.19 (t, $J = 5.1$ Hz, 1 H, $\text{CH}_2\text{CH}_2\text{NH}$), 5.99 (bs, 1 H, $\text{NHCOC}(\text{CH}_3)_3$), 5.36 (t, $J = 3.3$ Hz, 2 H, overlap of $H-4$ and $H-4'$), 5.19–5.10 (m, 2 H, overlap of $H-2$ and $H-2'$), 5.05–5.01 (m, 2 H, overlap of $H-3$

and $H-3'$), 4.54 (d, $J = 7.8$ Hz, 1 H, $H-1'$), 4.48 (d, $J = 8.1$, 1 H, $H-1$), 4.41 (bs, 1 H, $H-\alpha$), 4.18-4.07 (m, 4 H, overlap of $H-6$ and $H-6'$), 3.92 (m, 1 H, overlap of $H-5$ and $H-5'$) 3.86-3.82 (m, 2 H, 1 H of each OCH_2CH_2NH), 3.67-3.60 (m, 2 H, 1 H of each OCH_2CH_2NH), 3.54-3.29 (m, 4 H, OCH_2CH_2NH), 2.87-2.80 (m, 1 H, $H-\beta$), 2.51 (dd, $J = 6.0$ Hz, $J = 15.6$ Hz, 1 H, $H-\beta'$), 2.13, 2.12, 2.07, 2.06, 2.02, 2.01, 1.96 and 1.95 (each s, 3 H, $O(CO)CH_3$), 1.42 (s, 9 H, $COC(CH_3)_3$); ^{13}C NMR (75 MHz, $CDCl_3$): δ_c 171.2, 171.1, 170.8, 170.3, 170.3, 170.2, 170.1, 170.0, 169.8, 169.56 (CO), 101.3 ($C-1$), 101.1 ($C-1'$), 80.3 ($COC(CH_3)_3$), 70.9, 70.8 ($C-5$ and $C-5'$), 70.7, 68.9 ($C-3'$ and $C-3$), 68.8, 68.6 ($C-2'$ and $C-2$), 68.3 (OCH_2CH_2NH), 67.1, 66.9 ($C-4'$ and $C-4$), 61.3, 60.4 ($C-6'$ and $C-6$), 51.1 ($C-\alpha$), 39.6 (OCH_2CH_2NH), 39.2 ($C-\beta$), 28.3 ($COC(CH_3)_3$), 20.8, 20.8, 20.6 and 20.5 ($O(CO)CH_3$); HRMS m/z (ESI+): 980.3721 ($C_{41}H_{62}N_3O_{24}$: $[M+H]^+$ requires 980.3718).



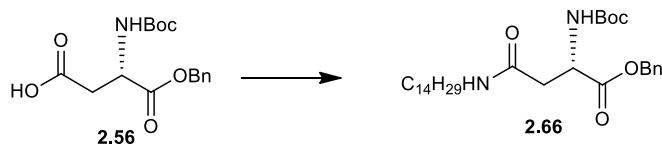
N^4 -[2-*O*-(2,3,4,6-tetra-*O*-acetyl- β -*D*-galactopyranosyl)-ethyl]- N^1 -[2-*O*-(2,3,4,6-tetra-*O*-acetyl- β -*D*-galactopyranosyl)-ethyl] *L*-asparagine **2.64**

A solution of N^4 -[2-*O*-(2,3,4,6-tetra-*O*-acetyl- β -*D*-galactopyranosyl)-ethyl]- N^2 -*tert*-butoxycarbonyl- N^1 -[2-*O*-(2,3,4,6-tetra-*O*-acetyl- β -*D*-galactopyranosyl)-ethyl] *L*-asparagine **2.63** (650 mg, 0.66 mmol) in anhydrous DCM (10 mL) was cooled in an ice bath and 50% TFA in DCM (0.260 mL, 3.3 mmol) was added. The reaction mixture was stirred for 30 min at rt, placed on ice and 50% TFA in DCM (0.260 mL, 3.3 mmol) was again added. The reaction mixture was stirred at rt for 1.5 h, placed on ice and a final portion of 50% TFA in DCM was added (0.260 mL, 3.3 mmol). The organic solvent was removed *in vacuo* and the residue obtained was diluted with EtOAc and washed with aqueous sat. $NaHCO_3$ solution, brine, dried over $MgSO_4$ and concentrated to yield the corresponding deprotected amine **2.64** as a white solid, which was used without further purification (396 mg, 61%). 1H NMR (300 MHz, $CDCl_3$): δ 7.06 (bs, 1 H, CH_2CH_2NH'), 6.19 (t, $J = 5.1$ Hz, 1 H, CH_2CH_2NH), 5.41 (bs, 2 H, overlap of $H-4$ and $H-4'$), 5.17-5.02 (m, 4 H, overlap of $H-2$ and $H-2'$ and $H-3$ and $H-3'$), 4.52-4.57 (m, 2 H, overlap of $H-1$ and $H-1'$), 4.27-4.10 (m, 4 H, overlap of $H-6$ and $H-6'$), 3.96-3.87 (m, 3 H, overlap of $H-5$, $H-5'$ and α - H) 3.66-3.62 (m, 1 H, 1 H of OCH_2CH_2), 3.67-3.60 (m, 1 H, 1 H of each OCH_2CH_2), 3.47-3.46 (m, 4 H, OCH_2CH_2NH), 2.97 (s, 1 H, $H-\beta$), 2.81 (bs, 1 H, $H-\beta'$), 2.15 (s, 6 H, $O(CO)CH_3$), 2.06 (s, 12 H, $O(CO)CH_3$), 1.99 (s, 6 H, $O(CO)CH_3$); HRMS m/z (ESI+): 880.3206 ($C_{36}H_{54}N_3O_{22}$: $[M+H]^+$ requires 880.3193).



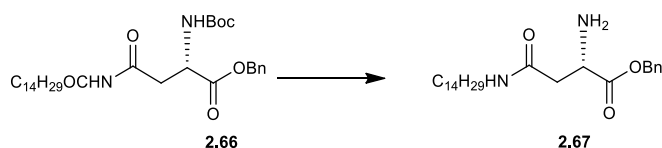
*N*⁴-[2-*O*-(2,3,4,6-tetra-*O*-acetyl-β-*D*-galactopyranosyl)-ethyl]-*N*²-hexadecanoyl- *N*¹-[2-*O*-(2,3,4,6-tetra-*O*-acetyl-β-*D*-galactopyranosyl)-ethyl] L-asparagine **2.65**

*N*⁴-[2-*O*-(2,3,4,6-tetra-*O*-acetyl-β-*D*-galactopyranosyl)-ethyl]-*N*¹-[2-*O*-(2,3,4,6-tetra-*O*-acetyl-β-*D*-galactopyranosyl)-ethyl] L-asparagine **2.64** (396 mg, 0.45 mmol) was dissolved in dry THF (15 mL) under N₂ and hexadecanoyl chloride (0.12 mL, 0.40 mmol) was added. The reaction was left stirring for 10 min and then NEt₃ added (0.057 mL, 0.40 mmol). The reaction mixture was stirred at rt overnight. Gradient elution chromatography (EtOAc-MeOH) yielded the pure product **2.65** as an off white solid (270 mg, 58%); R_f = 0.20 (EtOAc); [α]²⁵_D = +3.8 (c, 0.7 in DCM); IR ν_{max} (NaCl plate, DCM): 3291.9, 2924.5, 2853.67, 1751.3, 1645.5, 1543.1, 1370.4, 1224.1, 1173.5, 1077.07 cm⁻¹; ¹H NMR (300 MHz, CDCl₃): δ 7.26 (bs, 2 H, overlap of CH₂CH₂NH' and NHCOC₁₅H₃₁), 6.25 (t, *J* = 5.4 Hz, 1 H, CH₂CH₂NH), 5.40-5.37 (m, 2 H, overlap of *H*-4 and *H*-4'), 5.19-5.13 (m, 2 H, overlap of *H*-2 and *H*-2'), 5.05-4.99 (m, 2 H, overlap of *H*-3 and *H*-3'), 4.73-4.67 (m, 1 H, *H*-α), 4.52 (d, *J* = 1.8 Hz, 1 H, *H*-1'), 4.50 (d, *J* = 1.8 Hz, 1 H, *H*-1), 4.21-4.08 (m, 4 H, overlap of *H*-6 and *H*-6'), 3.96-3.84 (m, 4 H, overlap of *H*-5, *H*-5' and 1 H of OCH₂CH₂), 3.70-3.57 (m, 2 H, 1 H of OCH₂CH₂), 3.53-3.34 (m, 4 H, OCH₂CH₂NH), 2.79 (dd, *J* = 3.6 Hz, *J* = 15.6 Hz, 1 H, *H*-β), 2.48 (dd, *J* = 6.6 Hz, *J* = 15.6 Hz, 1 H, *H*-β'), 2.24 (t, *J* = 6.9 Hz, 2 H, NHCOC₂H₄(CH₂)₁₂CH₃), 2.16, 2.15, 2.09, 2.08, 2.04, 2.04, 1.98 and 1.97 (each s, 3 H, O(CO)CH₃), 1.64-1.59 (m, 2 H, NHCOC₂H₄(CH₂)₁₃CH₃), 1.29-1.18 (m, 24 H, NHCOC₂H₄(CH₂)₁₂CH₃), 0.87 (t, *J* = 6.3 Hz, 3 H, NHCOC₁₄H₂₈CH₃); ¹³C NMR (75 MHz, CDCl₃): δ_c 173.5, 171.3, 171.0, 170.4, 170.2, 170.2, 170.1, 170.1, 169.9, 169.72 (CO), 101.3 (*C*-1), 101.1 (*C*-1'), 70.9 and 70.8 (*C*-5 and *C*-5'), 70.8 and 70.7 (*C*-3' and *C*-3), 68.9, 68.8 (*C*-2' and *C*-2), 68.6 and 68.1 (OCH₂CH₂NH), 67.1, 66.9 (*C*-4' and *C*-4), 61.3 (*C*-6' and *C*-6), 49.6 (*C*-α), 39.4 and 39.3 (OCH₂CH₂NH), 37.2 (*C*-β), 36.56 (NHCOC₂H₄(CH₂)₁₃CH₃), 39.1, 29.7, 29.7, 29.5, 29.4, 29.3 and 25.6 28.3 (NHCOC₂H₄(CH₂)₁₃CH₃), 20.9, 20.9, 20.8 and 20.7 (O(CO)CH₃), 14.1 (NHCOC₁₄H₂₈CH₃); HRMS *m/z* (ESI⁺): 1118.5502 (C₅₂H₈₄N₃O₂₃: [M+H]⁺ requires 1118.5490).



*N*²-*tert*-butoxycarbonyl-L-asparagine tetradecylamide benzyl ester **2.66**

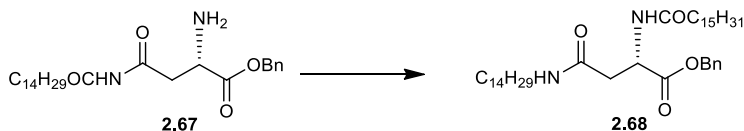
HOBt (680 mg, 5.1 mmol), *N*-Boc-L-Asp-OBn **2.56** (1.5 g, 4.60 mmol) and TBTU (1.6 g, 5.1 mmol) were dissolved in DMF (30 mL), under N₂ at rt. The mixture was stirred for 15 min and tetradecylamine (1.99 g, 5.1 mmol) dissolved in DMF (20 mL) was added dropwise. The mixture was stirred for 18 h. The reaction mixture was concentrated under reduced pressure, diluted with DCM and washed successively with 0.1 M HCl, aqueous sat. NaHCO₃ and brine. Flash chromatography (1:1, EtOAc: Pet Ether) afforded the title compound **2.66** (2.03 g, 84%); R_f = 0.9 (1:1, Pet Ether:EtOAc); IR ν_{max} (NaCl plate, DCM): 3332.8, 2918.5, 2850.6, 1737.2, 1687.4, 1645.2, 1524.4, 1467.3, 1367.4, 1293.1, 1168.7, 1058.3, 1028.3 cm⁻¹; ¹H NMR (300 MHz, CDCl₃): δ 7.34-7.32 (m, 5 H, Ar), 5.80 (d, *J* = 7.8 Hz, 1 H, NHCOC(CH₃)₃), 5.63-5.56 (m, 1 H, NH(CH₂)₁₃CH₃), 5.23-5.12 (m, 2 H, PhCH₂), 4.55-4.49 (m, 1 H, *H*-α), 3.21-3.13 (m, 2 H, NHCH₂(CH₂)₁₂CH₃), 2.89-2.80 (m, 1 H, *H*-β), 2.75-2.73-2.64 (m, 1 H, *H*-β), 1.47-1.39 (m, 9 H, COC(CH₃)₃), 1.32-1.23 (m, 22 H, NHCH₂CH₂(CH₂)₁₁CH₃), 0.88 (t, *J* = 6.6 Hz, 3 H, NHCH₂CH₂(CH₂)₁₁CH₃); HRMS *m/z* (ESI⁺): 1075.7058 (C₆₀H₁₀₀N₄O₁₀: [2M+K]⁺ requires 1075.7071).



L-asparagine tetradecylamide benzyl ester **2.67**

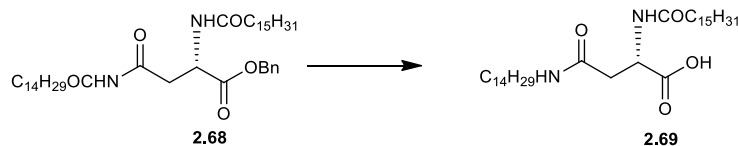
A solution of *N*²-*tert*-butoxycarbonyl-L-asparagine tetradecylamide benzyl ester **2.66** (576 mg, 1.1 mmol) in DCM (6 mL) was cooled in an ice bath and 50% TFA in DCM (0.85 mL, 11.1 mmol) was added dropwise. The reaction mixture was stirred at 0 °C for 30 min and then warmed to rt where The mixture was stirred for a further 2 h. The organic solvent was removed *in vacuo* and the residue obtained was diluted with EtOAc and washed with aqueous sat. NaHCO₃ solution, brine, dried over MgSO₄ and concentrated to yield the corresponding deprotected amine **2.67** as a white solid which was used without further purification (377 mg, 73%). ¹H NMR (300 MHz, CDCl₃): δ 7.37-7.32 (m, 5 H, Ar), 6.81-6.73 (m, 1 H, NHC₁₄H₂₉), 5.20-5.12 (m, 2 H, PhCH₂), 3.91-3.67 (m, 1 H, *H*-α), 3.24-3.17 (m, 2 H, NHCH₂(CH₂)₁₂CH₃), 2.66 (dd, *J* = 3 Hz, *J* =

15.3 Hz, 1 H, *H*-β), 2.47 (dd, *J* = 8.7 Hz, *J* = 15.6 Hz, 1 H, *H*-β'), 1.49-1.41 (t, *J* = 6, 2 H, NHCH₂CH₂(CH₂)₁₁CH₃), 1.32-1.22 (m, 22 H, NHCH₂CH₂(CH₂)₁₁CH₃), 0.88 (t, *J* = 6.6 Hz, 3 H, NHCH₂CH₂(CH₂)₁₁CH₃); HRMS *m/z* (ESI+): 419.3288 (C₂₅H₄₂N₂O₃: [M+H]⁺ requires 419.3268).



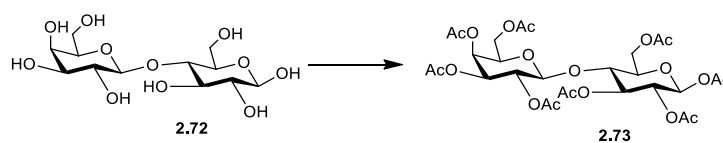
*N*²-hexadecanosyl-*L*-asparagine tetradecylamide benzyl ester **2.68**

NEt₃ (0.129 mL, 0.93 mmol,) was added to *L*-asparagine tetradecylamide benzyl ester **2.67** (357 mg, 0.8 mmol,) dissolved in DCM (11 mL) under Ar. The reaction mixture was allowed to stir for 10 min, placed on ice and hexadecanosyl choride (0.235 mL, 0.77 mmol,) was added. The reaction mixture was stirred at rt overnight. The solvent was concentrated *in vacuo*, diluted with EtOAc, washed with 0.1 M HCl, NaHCO₃, brine and dried (MgSO₄). Column chromatography (EtOAc) afforded **2.68** as a white solid (490 mg, 87%); *R*_f = 0.67 (1:1, Pet Ether:EtOAc); [α]_D²⁵ = +7.5 (c, 1.75 in DCM); IR *v*_{max} (NaCl plate, DCM): 3290.0, 2917.0, 2849.4, 1738.8, 1651.0, 1545.2, 1433.6, 1377.9, 1240.0, 1128.8, 721.5, 695.2 cm⁻¹; ¹H NMR (300 MHz, CDCl₃): δ 7.35-7.30 (m, 5 H, Ar), 6.83 (d, *J* = 7.8 Hz, 1 H, NHCOC₁₅H₃₁), 5.69-5.60 (m, 1 H, NHC₁₄H₂₉), 5.23-5.13 (m, 2 H, PHCH₂), 4.85-4.79 (m, 1 H, *H*-α), 3.20-3.12 (m, 2 H, NHCH₂C₁₃H₂₇), 2.89 (dd, *J* = 4.5 Hz, *J* = 15.6 Hz, 1 H, *H*-β), 2.69 (dd, *J* = 4.5 Hz, *J* = 15.6 Hz, 1 H, *H*-β'), 2.20 (t, *J* = 7.2 Hz, 2 H, NHCOCH₂C₁₄H₂₉), 1.65-54 (m, 2 H, NHCH₂CH₂C₁₂H₂₅), 1.47-1.39 (m, 2 H, NHCOCH₂CH₂C₁₃H₂₇), 1.35-1.18 (m, 46 H, NHC₂H₄(CH₂)₁₁CH₃ and NHCOC₂H₄(CH₂)₁₂CH₃), 0.88 (t, *J* = 6.6 Hz, 6 H, NHC₁₃H₂₆CH₃ and NHCOC₁₄H₂₈CH₃); ¹³C NMR (75 MHz, CDCl₃): δ_c 173.2, 171.0, 169.8 (each CO), 135.43 (ArC), 128.5, 128.3, 128.2 (ArCH), 67.4 (PhCH₂), 49.1 (*C*-α), 39.7 (NHCH₂C₁₃H₂₇), 36.6 (NHCOCH₂C₈H₁₇), 35.8 (*C*-β), 31.9, 29.7, 29.6, 29.6, 29.5, 29.5, 29.4, 29.3, 29.2, 29.2, 29.1, 28.3, 26.9, 25.6 and 22.68 (NHCH₂(CH₂)₁₂CH₃ and NHCOCH₂(CH₂)₇CH₃), 14.1, (NHC₁₃H₂₆CH₃ and NHCOC₈H₁₆CH₃); HRMS *m/z* (ESI+): 658.5588 (C₄₁H₇₃N₂O₄: [M+H]⁺ requires 658.5565).



*N*²-hexadecanosyl-L-asparagine tetradecylamide **2.69**

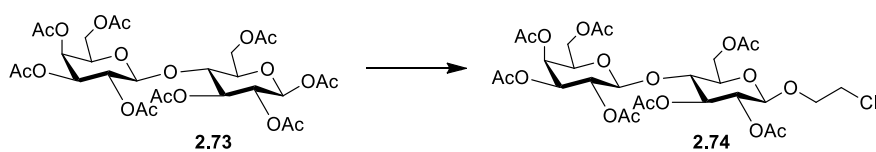
To a solution of *N*²-hexadecanosyl-L-asparagine tetradecylamide benzyl ester **2.68** (450 mg, 0.6 mmol) in EtOAc (35 mL), Pd/C (45 mg, 10% w/w) was added. The resulting mixture was heated to 50 °C and H₂ bubbled through for 4 h. The mixture was then filtered through a Celite cake and the filtrate was concentrated under vacuum to afford a white solid which was recrystallised in DCM to yield the product **2.69** as a white solid (366 mg, 94%); ¹H NMR (300 MHz, CDCl₃): δ 6.97 (d, *J* = 5.1 Hz, 1 H, NHCOC₁₅H₃₁), 6.81-6.77 (m, 1 H, NHC₁₄H₂₉), 4.55-4.49 (m, 1 H, *H*-α), 3.34-3.22 (m, 2 H, NHCH₂C₁₃H₂₇), 2.96-2.91 (m, 1 H, *H*-β), 2.66 (dd, *J* = 6.6 Hz, *J* = 16.8 Hz, 1 H, *H*-β'), 2.24 (t, *J* = 7.2 Hz, 2 H, NHCOCH₂C₁₄H₂₉), 1.65-1.49 (m, 4 H, overlap of NHCH₂CH₂C₁₂H₂₅ and NHCOCH₂CH₂C₁₃H₂₇), 1.32-1.24 (m, 46 H, NHC₂H₄(CH₂)₁₁CH₃ and NHCOC₂H₄(CH₂)₁₂CH₃), 0.88 (t, *J* = 6.3 Hz, 6 H, NHC₁₃H₂₆CH₃ and NHCOC₁₄H₂₈CH₃); HRMS *m/z* (ESI⁺): 567.5087 (C₃₄H₆₇N₂O₄: [M+H]⁺ requires 567.5095).



β-D-Lactose octaacetate **2.73**

D-Lactose (5 g, 13.8 mmol) and NaOAc (1.13 g, 13.8 mmol) was added to a round bottom and placed on ice. Acetic anhydride (13 mL, 13.8 mmol) was added and the reaction mixture was heated to 110 °C and stirred overnight. The mixture was poured into ice H₂O (20 mL) and the resulting gum was filtered and columned in (1:1, EtOAc: Pet Ether) to yield the pure product **2.73** as a white solid (8.5 g, 80%); Mp = 97-95 °C (lit 96-95 °C)^[232]; ¹H NMR (300 MHz, CDCl₃): δ 5.66 (dd, *J* = 1.5 Hz, *J* = 8.1 Hz, 1 H, *H*-1 Gluc), 5.33 (bs, 1 H, *H*-4 Gal), 5.26-5.19 (m, 1 H, *H*-3 Gluc), 5.14-4.91 (m, 3 H, overlap of *H*-2 Gluc, *H*-2 Gal and *H*-3 Gal), 4.48-4.42 (m, 2 H, overlap of *H*-1 Gal and 1 H of *H*-6 Gluc), 4.14 (m, 3 H, overlap of 1 H of *H*-6 Gluc and *H*-6, *H*-6' Gal), 3.88-3.73 (m, 3 H, overlap of *H*-4 Gluc, *H*-5 Gluc and *H*-5 Gal), 2.13, 2.10, 2.07, 2.04, 2.03, 2.02, 2.01, 1.94 (each s, 3 H, O(CO)CH₃); HRMS *m/z* (ESI⁺): 701.1185 (C₂₈H₃₈NaO₁₉: [M+Na]⁺ requires 701.1900).

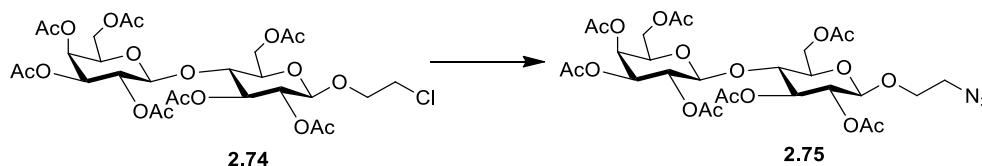
Spectroscopic data is in agreement with the literature.^[232]



2-Chloroethyl 2,2',3,3',4',6,6'-hepta-O-acetyl- β -lactoside **2.74**

A solution of β -D-Lactose octaacetate **2.73** (3.5 g, 5.1 mmol) and 2-chloroethanol (0.415 mL, 6.1 mmol) in dry DCM (10 mL) was stirred under N_2 and placed on ice. 50% BF_3Et_2O (4.74 mL, 38.4 mmol) in DCM was added dropwise over 30 min. The reaction was stirred overnight, poured into 15 mL ice H_2O , extracted with DCM (3x15 mL) and washed with aqueous sat. $NaHCO_3$, H_2O and dried over $MgSO_4$. Flash chromatography (1:1, EtOAc:Pet Ether) afforded the pure product **2.74** as fluffy white solid (1.7 g, 47%); IR ν_{max} (NaCl plate, DCM): 3448.0, 2114.4, 1751.1, 1642.3, 1432.0, 1370.8, 1227.6, 1171., 1136.7, 1056.3, 954.3, 902.2, 736.1 cm^{-1} ; 1H -NMR (300 MHz, $CDCl_3$): δ 5.34 (d, $J = 2.7$ Hz, 1 H, $H-4$ Gal), 5.23-5.17 (m, 1 H, $H-3$ Gluc), 5.10 (dd, $J = 7.8$ Hz, $J = 10.5$ Hz, 1 H, $H-2$ Gal), 4.97-4.88 (m, 2 H, overlap of $H-2$ Gluc and $H-3$ Gal), 4.54-4.47 (m, 3 H, overlap of $H-1$ Gal, $H-1$ Gluc and 1 H of $H-6$ Gluc), 4.15-4.00 (m, 4 H, overlap of $H-6$ Gal, 1 H of $H-6$ Gluc and 1 H of OCH_2CH_2NH), 3.89-3.85 (m, 1 H, $H-5$ Gal), 3.82-3.70 (m, 2 H, overlap of OCH_2CH_2NH and $H-5$ Gluc), 3.63-3.58 (m, 3 H, overlap of $H-4$ Gluc and OCH_2CH_2NH), 2.15, 2.12, 2.06, 2.04, 2.04, 2.03 1.96 (each s, 3 H, $O(CO)CH_3$); ^{13}C -NMR (75 MHz, $CDCl_3$): δ_c 100.9 ($C-1$ gal), 100.7 ($C-1$ Gluc), 76.2 ($C-5$, Gluc), 72.7 ($C-3$, Gluc), 72.6 ($C-4$ Gluc), 71.5 ($C-2$ Gluc), 70.9 ($C-3$ - Gal), 70.7 ($C-5$ Gal), 69.9 (OCH_2CH_2Cl), 69.1 ($C-2$ Gal), 66.6 ($C-4$ Gal), 61.8, 60.8 ($C-6$ Gal, $C-6$ Gluc), 41.9 (OCH_2CH_2Cl), 20.8, 20.8, 20.7, 20.6 and 20.5 ($O(CO)CH_3$); HRMS m/z (ESI+): 721.1714 ($C_{28}H_{39}ClNaO_{18}$: $[M+Na]^+$ requires 721.1717).

The spectroscopic data are in agreement with the literature.^[235]

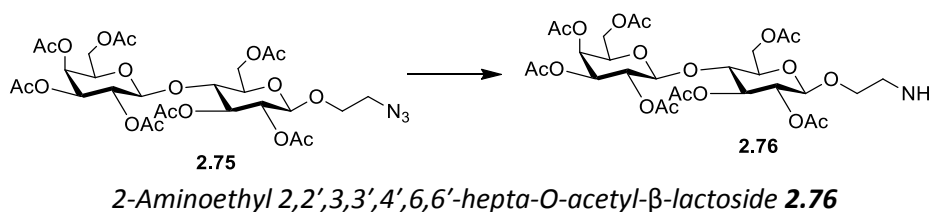


2-Azidoethyl 2,2',3,3',4',6,6'-hepta-O-acetyl- β -lactoside **2.75**^[234]

2-Chloroethyl 2,2',3,3',4',6,6'-hepta-O-acetyl- β -lactoside **2.74** (1 g, 1.5 mmol) was dissolved in DMF (20 mL) and sodium azide (205 mg, 3.1 mmol) was added. The mixture was heated to 110 $^{\circ}C$ for 3 h. The solvent was removed under reduced pressure and the residue dissolved in EtOAc washed with H_2O and dried with $MgSO_4$. Flash chromatography (3:1, EtOAc:Pet Ether)

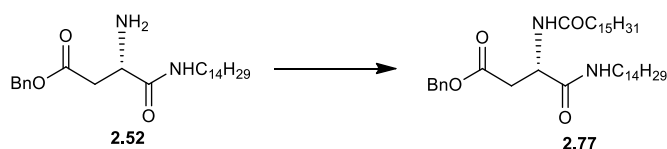
afforded the pure product **2.75** as a fluffy solid (833 mg, 74%); IR ν_{\max} (NaCl plate, DCM): 3443.2, 1750.7, 1642.6, 1433.2, 1370.5, 1226.5, 1170.7., 1132.9, 1055.7, 954.0 cm^{-1} ; $^1\text{H-NMR}$ (300 MHz, CDCl_3): δ 5.31-5.29 (m, 1 H, *H*-4 Gal), 5.19-5.13 (m, 1 H, *H*-3 Gluc), 5.06 (dd, $J = 7.8$ Hz, $J = 10.5$ Hz, 1 H, *H*-2 Gal), 4.94-4.85 (m, 2 H, overlap of *H*-2 Gluc and *H*-3 Gal), 4.54-4.45 (m, 3 H, overlap of *H*-1 Gal, *H*-1 Gluc and 1 H of *H*-6 Gluc), 4.10–3.92 (m, 4 H, overlap of *H*-6 Gal, 1 H of *H*-6 Gluc and 1 H of $\text{OCH}_2\text{CH}_2\text{N}_3$), 3.86–3.75 (m, 2 H, overlap of *H*-5 Gal and *H*-5 Gluc), 3.68–3.56 (m, 2 H, overlap of $\text{OCH}_2\text{CH}_2\text{N}_3$ and *H*-4 Gluc), 3.47-3.39 (m, 1 H, 1 H of $\text{OCH}_2\text{CH}_2\text{N}_3$), 3.47-3.39 (m, 1 H, 1 H of $\text{OCH}_2\text{CH}_2\text{N}_3$), 2.13, 2.11, 2.08, 2.02 (each s, 3 H, $\text{O}(\text{CO})\text{CH}_3$), 2.04 (s, 6 H, $\text{O}(\text{CO})\text{CH}_3$), 1.92 (s, 3 H, $\text{O}(\text{CO})\text{CH}_3$); $^{13}\text{C-NMR}$ (75 Hz, CDCl_3): δ_c 170.3, 170.1, 170.0, 169.7, 169.6, 169.0 (each CO), 100.9 (*C*-1 gal), 100.3 (*C*-1 Gluc), 76.1 (*C*-5, Gluc), 72.8 (*C*-3, Gluc), 72.7 (*C*-4 Gluc), 71.4 (*C*-2 Gluc), 70.9 (*C*-3 Gal), 70.6 (*C*-5 Gal), 60.0 (*C*-2 Gal), 68.6 ($\text{OCH}_2\text{CH}_2\text{N}_3$), 66.6 (*C*-4 Gal), 61.7, 60.8 (*C*-6 Gal, *C*-6 Gluc), 50.4 ($\text{OCH}_2\text{CH}_2\text{N}_3$), 21.0, 20.8, 20.7, 20.7, 20.6 and 20.4 ($\text{O}(\text{CO})\text{CH}_3$); HRMS m/z (ESI+): 728.2099 ($\text{C}_{28}\text{H}_{39}\text{N}_3\text{NaO}_{18}$: $[\text{M}+\text{Na}]^+$ requires 728.2121).

The spectroscopic data are in agreement with the literature.^[235]



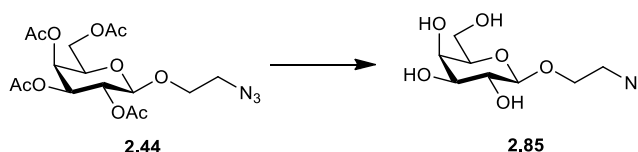
To a solution of 2-aminoethyl 2,2',3,3',4',6,6'-hepta-O-acetyl- β -lactoside **2.75** (100 mg, 0.14 mmol) in absolute EtOH (20 mL), Pd/C (10 mg, 10% w/w) was added. The resulting mixture was stirred under hydrogen gas for 5 h. The mixture was then filtered through a Celite cake and the filtrate was concentrated under vacuum to afford the pure product **2.76** as thick clear oil (87 mg, 73%); $^1\text{H-NMR}$ (300 MHz, CDCl_3): δ 5.28-5.27 (m, 1 H, *H*-4 Gal), 5.17-5.10 (m, 1 H, *H*-3 Gluc), 5.07-5.01 (m, 1 H, *H*-2 Gal), 4.92-4.81 (m, 2 H, overlap of *H*-2 Gluc and *H*-3 Gal), 4.47-4.43 (m, 3 H, overlap of *H*-1 Gal, *H*-1 Gluc and 1 H of *H*-6 Gluc), 4.10–4.0 (m, 4 H, overlap of *H*-6 Gal, 1 H of *H*-6 Gluc and 1 H of $\text{OCH}_2\text{CH}_2\text{NH}_2$), 3.85–3.71 (m, 2 H, overlap of *H*-5 Gal and *H*-5 Gluc), 3.62–3.50 (m, 2 H, overlap of $\text{OCH}_2\text{CH}_2\text{NH}_2$ and *H*-4 Gluc), 2.85-2.73 (m, 2 H, $\text{OCH}_2\text{CH}_2\text{NH}_2$), 2.09, 2.06, 2.0, (each s, 3 H, $\text{O}(\text{CO})\text{CH}_3$), 1.98 (s, 9 H, $\text{O}(\text{CO})\text{CH}_3$), 1.90 (3 H, $\text{O}(\text{CO})\text{CH}_3$).

The spectroscopic data are in agreement with the literature.^[234]



*N*²-palmitoyl-*L*-asparagine tetradecylamide benzyl ester **2.77**

Free amine **2.52** (1.4 g, 3.3 mmol) was dissolved in dry THF (15 mL) under N₂ and hexadecanoyl chloride (1.01 mL, 3.3 mmol) was added. The reaction was left stirring for 10 min and then NEt₃ added (0.46 mL, 3.3 mmol). The reaction mixture was left stirring at rt overnight. Flash Chromatography (2:1, EtOAc:Pet ether) yielded the pure product **2.77** as a white solid (1.5 g, 68%); R_f = 0.52 (2:1, Pet Ether:EtOAc); [α]²⁵_D = -11.2 (c, 1 in DCM); IR ν_{max} (NaCl plate, DCM): 3292.9, 2917.0, 2849.7 1733.4, 1642.8, 1656.9, 1642.8, 1544.0, 1468.2, 1373.2, 1355.9, 1338.6, 1286.6, 1221.0, 113.5, 1145.4, 1113.2, 1100.2, 1030.6, 937.9, 970.5, 740.1, 720.6, 740.1 cm⁻¹; ¹H NMR (300 MHz, CDCl₃): δ 7.34 (bs, 5 H, Ar), 6.95 (d, *J* = 8.1 Hz, 1 H, NHCOC₁₅H₃₁), 6.66-6.64 (m, 1 H, CONHC₁₄H₂₉), 5.17-5.08 (m, 2 H, CH₂Ph), 4.83-4.76 (m, 1 H, *H*-α), 3.20-3.10 (m, 2 H, NHCH₂C₁₃H₂₇), 2.93 (dd, *J* = 4.5 Hz, *J* = 16.8 Hz, 1 H, *H*-β), 2.67 (dd, *J* = 7.2 Hz, *J* = 16.8 Hz, 1 H, *H*-β'), 2.18 (t, *J* = 7.2 Hz, 2 H, NHCOCH₂C₁₄H₂₉), 1.59-1.57 (m, *J* = 6 Hz, 2 H, NHCH₂CH₂C₁₂H₂₅), 1.44 (bs, 2 H, NHCOCH₂CH₂C₁₃H₂₇), 1.25 (s, 36 H, NHC₂H₄(CH₂)₁₁CH₃ and NHCOC₂H₄(CH₂)₁₂CH₃), 0.87 (t, *J* = 6.6 Hz, 6 H, NHC₁₃H₂₆CH₃ and NHCOC₁₄H₂₈CH₃); ¹³C NMR (75 MHz, CDCl₃): δ_c 171.9, 170.3, 135.4 (each CO), 128.6, 128.4, 128.3 (C-Ph), 66.9 (CH₂Ph), 49.2 (C-α), 39.7 (NHCH₂C₁₃H₂₇), 36.5 (NHCOCH₂C₁₄H₂₉), 35.9 (C-β), 31.9, 29.7, 29.7, 29.6, 29.5, 29.36, 29.3, 29.2, 29.1, 28.3, 25.6, 22.7 (NHCH₂(CH₂)₁₂CH₃, NHCOCH₂(CH₂)₁₃CH₃), 13.1 (NHC₁₃H₂₆CH₃, NHCOC₁₄H₂₈CH₃); HRMS *m/z* (ESI⁺): 657.5577 (C₄₁H₇₃N₂O₄: [M+H]⁺ requires 657.5565).

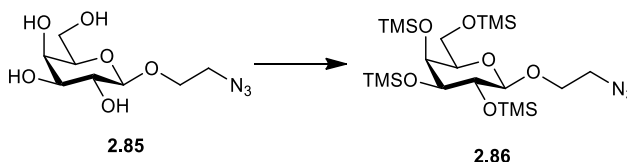


2-Azidoethyl-β-*D*-galactopyranoside **2.85**

2-Azidoethyl 2,3,4,6-tetra-*O*-acetyl-β-*D*-galactopyranoside **2.44** (1.00 g, 2.3 mmol) was dissolved in MeOH (14 mL) and DCM (20 mL) and placed under N₂. 5.40 M NaOMe (0.22 mL, 1.1 mmol) was added at rt. The reaction was stirred for 1 h, neutralised with Amberlite IR-120, filtered and evaporated under reduced pressure to yield the product as a viscous colourless oil (0.54 g, 91%). The product was used without further purification; ¹H NMR (300 MHz, MeOD): δ 4.27 (d, *J* = 7.2 Hz, 1 H, *H*-1), 4.06-3.99 (m, 1 H, OCH₂CH₂NH), 3.3 (d, *J* = 1.8 Hz, 1 H, *H*-4), 3.78-3.67 (m, 3 H, overlap of 1 H of OCH₂CH₂NH and *H*-6, *H*-6'), 3.57-3.43 (m, 5 H, overlap of *H*-3,

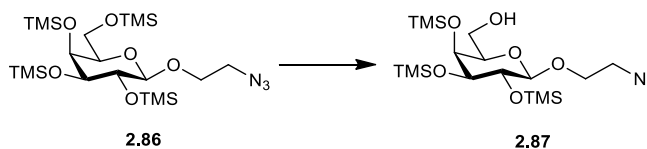
H-2, *H*-5 and OCH₂CH₂NH); ¹³C-NMR (75 MHz, MeOD): δ_c 103.7 (*C*-1), 75.3, 73.3, 71.1 (*C*-2, *C*-3 and *C*-5), 68.8 (*C*-4), 67.8 (OCH₂CH₂NH), 61.1 (*C*-6), 50.5 (OCH₂CH₂NH); HRMS *m/z* (ESI+): 272.0867 (C₈H₁₅N₃NaO₆: [M+Na]⁺ requires 272.0853).

The NMR Data is in agreement with the reported values.^[236]



2-Azidoethyl 2,3,4,6-tetra-*O*-trimethylsilyl-β-*D*-galactopyranoside **2.86**^[101]

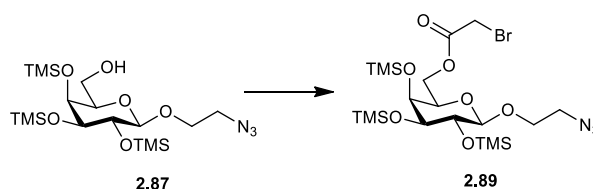
A mixture of chlorotrimethylsilane (1.6 mL, 13 mmol) and hexamethyl disilazane (0.98 mL, 4.4 mmol) was carefully added to a stirred solution of 1-*O*-(2-azidoethyl)-β-*D*-galactopyranose **2.85** (0.540 g, 2.2 mmol) in pyridine (12 mL) at 0 °C. The reaction was allowed to return to rt at stirred overnight. The solvent was removed under reduced pressure and the resulting residue was dissolved in DCM, washed with H₂O, dried (MgSO₄) and concentrated to afford the pure product **2.86** as a clear oil (0.89 g, 76%); *R*_f = 0.90 (1:1, Pet Ether:EtOAc); [α]²⁵_D = -4 (c, 1 in DCM); IR ν_{max} (NaCl plate, DCM): 2958.3, 2879.3, 2104.4, 1439.9, 1399.5, 1374.8 1345.1, 1251.5, 1170.6, 1105.1, 1076.0, 11014.9, 958.3, 978.3, 877.2, 841.2, 751.0, 686.1, 625.8 cm⁻¹; ¹H NMR (300 MHz, CDCl₃): δ 4.19 (d, *J* = 7.5 Hz, 1 H, *H*-1), 4.0-3.93 (m, 1 H, 1 H of OCH₂CH₂NH), 3.83 (d, *J* = 1.8 Hz, 1 H, *H*-4), 3.70-3.58 (m, 3 H, overlap of 1 H of OCH₂CH₂NH, *H*-2 and *H*-6, *H*-6'), 3.48-3.28 (m, 4 H, overlap of *H*-3, *H*-5 and OCH₂CH₂NH), 0.16, 0.14, 0.13 and 0.11 (each s, 9 H, Si(CH₃)₃); ¹³C-NMR (75 MHz, CDCl₃): δ_c 103.4 (*C*-1), 74.6 (*C*-5, *C*-3), 71.0 (*C*-2) 70.9 (*C*-4), 70.6 (*C*-3), 67.1 (OCH₂CH₂NH), 60.4 (*C*-6), 50.1 (OCH₂CH₂NH), 0.0, -0.2 and -1.1 (Si(CH₃)₃); HRMS *m/z* (ESI+): 536.2471 (C₂₀H₄₆N₃O₆Si₄: [M-H]⁻ requires 536.2469).



2-Azidoethyl 2,3,4-tri-*O*-trimethylsilyl-β-*D*-galactopyranoside **2.87**^[101]

2-azidoethyl 2,3,4,6-tetra-*O*-trimethylsilyl-β-*D*-galactopyranose **2.86** (0.99 g, 1.84 mmol) was dissolved in acetone (3 mL) and MeOH (4 mL) and placed on ice. AcOH (0.210 mL, 3.6 mmol) was added and the reaction mixture was allowed to stir for 2 h. NaHCO₃ was added and the solvent removed under reduced pressure. The residue obtained was dissolved in DCM washed

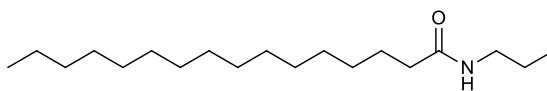
with NaHCO₃, dried (MgSO₄) and concentrated to afford the pure product **2.87** as a clear oil (0.644 g, 75%); R_f = 0.78 (1:1, Pet Ether:EtOAc); [α]²⁵_D = -3.7 (c, 0.9 in DCM); IR ν_{max} (NaCl plate, DCM): 3441.9, 2957.7, 2104.3, 1729.0, 1399.1, 1373.0, 1249.8, 1168.2, 1117.0, 971.7, 895.9, 839.9, 751.4 cm⁻¹; ¹H NMR (300 MHz, CDCl₃): δ 4.22 (d, *J* = 7.5 Hz, 1 H, *H*-1), 4.02-3.95 (m, 1 H, 1 H of OCH₂CH₂NH), 3.88-3.81 (m, 1 H, *H*-6), 3.76 (d, *J* = 2.1 Hz, 1 H, *H*-4), 3.70-3.62 (m, 3 H, overlap of 1 H of OCH₂CH₂NH, *H*-2 and *H*-6'), 3.48-3.46 (m, 3 H, overlap of *H*-5 and OCH₂CH₂NH), 3.64 (dd, *J* = 2.7 Hz, *J* = 9 Hz, 1 H, *H*-3), 0.022, 0.00 and -0.254 (each s, 9H, Si(CH₃)₃); ¹³C-NMR (75 MHz, CDCl₃): δ_c 103.5 (*C*-1), 74.6 (*C*-5), 74.5 (*C*-3), 71.7 (*C*-4) 70.9 (*C*-2), 67.1 (OCH₂CH₂NH), 62.1 (*C*-6), 50.1 (OCH₂CH₂NH), 0.3, 0.2, 0.00 (Si(CH₃)₃); HRMS *m/z* (ESI⁺): 464.2073 (C₁₇H₃₈N₃O₆Si₃: [M-H]⁻ requires 464.2074).



2-Azidoethyl 2,3,4-tri-*O*-trimethylsilyl, 6-*O* carboxymethylbromide)-β-*D*-galactopyranoside **2.89**

2-Azidoethyl 2,3,4-tri-*O*-trimethylsilyl-β-*D*-galactopyranoside **2.87** (151 mg, 0.3 mmol) and 4 Å MS was dried on the schlenk, and then dissolved in dry DCM (3 mL) under N₂. Bromoacetic acid (113 mg, 0.8 mmol) 4 Å MS was also dried on the schlenk, and dissolved in dry DCM (2 mL) under N₂. DCC (100 mg, 0.4 mmol) and DMAP (3 mg, 0.01 mmol) were added to the bromoacetic acid solution. The mixture allowed was stirred for 5 min and then the alcohol was added slowly. The reaction mixture was stirred overnight at rt. The solvent was removed under reduced pressure and the resulting residue dissolved in DCM washed with H₂O, dried (MgSO₄). Flash chromatography (3:1, Pet Ether, EtOAc) afforded the pure product **2.89** as viscous clear oil (116 g, 61%); R_f = 0.80 (3:1, Pet Ether:EtOAc); [α]²⁵_D = 4.3 (c, 1.2 in DCM); IR ν_{max} (NaCl plate, DCM): 2958.7, 2924.9, 2104.5, 1745.7, 1441.1, 1402.6, 1344.9, 1373.4, 1279.1, 1250.6, 1171.2, 1116.1, 1076.6, 1051.9, 1024.3, 957.9, 972.8, 894.9, 840.8, 752.1, 685.4 cm⁻¹; ¹H NMR (300 MHz, CDCl₃): δ 4.36-4.30 (m, 1 H, *H*-6), 4.26-4.19 (m, 2 H, overlap of *H*-6' and *H*-1), 4.00-3.93 (m, 1 H, 1 H of OCH₂CH₂NH), 3.80 (s, 2 H, COCH₂Br), 3.78 (d, *J* = 2.1 Hz, 1 H, *H*-4), 3.70-3.60 (m, 3 H, overlap of 1 H of OCH₂CH₂NH, *H*-2 and *H*-5), 3.50-3.46 (m, 2 H, OCH₂CH₂NH), 3.41 (dd, *J* = 2.7 Hz, *J* = 9 Hz, 1 H, *H*-3), 0.16 (s, 9 H, Si(CH₃)₃), 0.14 (s, 18 H, Si(CH₃)₃); ¹³C-NMR (75 MHz, CDCl₃): δ_c 166.4 (CO), 103.4 (*C*-1), 74.3 (*C*-3), 71.4 (*C*-5) 71.0 (*C*-4),

70.7 (C-2), 67.3 (OCH₂CH₂NH), 64.0 (C-6), 50.1 (OCH₂CH₂NH), 24.7 (COCH₂Br), 0.0, 0.02 and -0.2 (Si(CH₃)₃); HRMS m/z (ESI+): 664.0535 (C₁₉H₄₀N₃O₇Si₃: [M+Br]⁻ requires 664.0546).



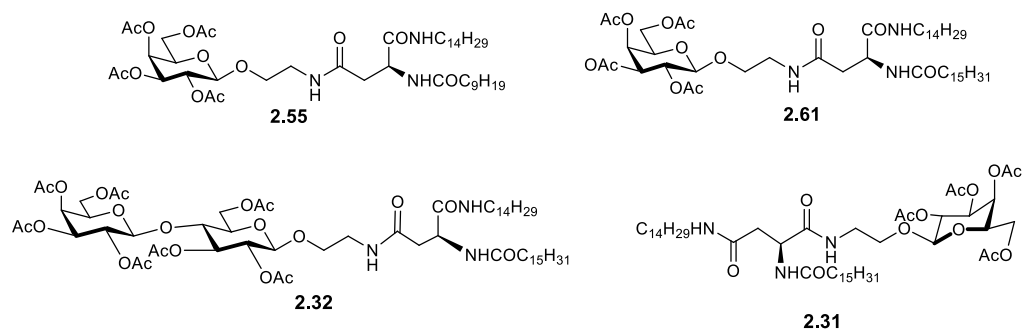
2.93

N-propylhexadecamide

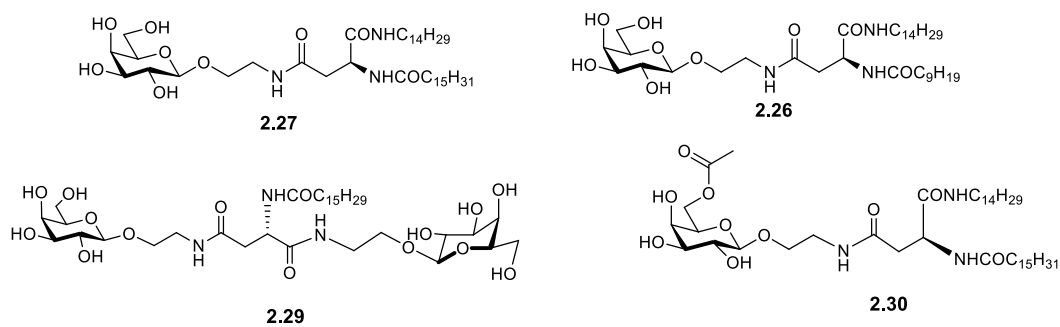
Propyl amine (396 mg, 0.45 mmol) was dissolved in dry DCM (10 mL) under N₂ and hexadecanoyl chloride (0.466 mL, 1.5 mmol) was added. The reaction was left stirring for 10 min and then NEt₃ added (0.235 mL, 1.6 mmol). The reaction mixture was left stirring at rt overnight. Gradient elution chromatography (1:1, Pet Ether:EtOAc) yielded the pure product **2.93** as a white solid (392 mg, 86%); R_f = 0.64 (1:1, Pet Ether:EtOAc); IR ν_{max} (NaCl plate, DCM): 3301.23, 2956.39, 2918.75, 2849.61, 2872.27, 1638.20, 1552.66, 1471.83, 1437.1, 1372.54, 1285.28, 1269.04, 1249.33, 1227.36, 1207.68, 1156.38, 1122.22 and 1080.20 cm⁻¹; ¹H NMR (300 MHz, CDCl₃): δ 5.73 (bs, 1 H, CONHCH₂), 3.24-3.10 (m, 2 H, CONHCH₂C₂H₅), 2.13 (t, *J* = 7.5 Hz, 2 H, NHCOCH₂C₁₄H₂₉), 1.61-1.51 (m, 2 H, NHCH₂CH₂C₁₃H₂₇), 1.53-1.45 (m, 2 H, CONHCH₂CH₂CH₃), 1.25 (s, 24 H, NHCOC₂H₄(CH₂)₁₂CH₃), 0.91-0.82 (m, 6 H, overlap of NHCOC₁₄H₂₈CH₃ and CONHC₂H₄CH₃); ¹³C-NMR (75 Hz, CDCl₃): δ_c 173.2 (CO), 41.1 (CONHCH₂C₂H₅), 36.9 (NHCOCH₂C₁₄H₂₉), 31.9, 29.7, 29.6, 29.6, 29.5, 29.4, 29.3 and 29.3 (NHCOC₂H₄(CH₂)₁₂CH₃), 25.9 (NHCH₂CH₂C₁₃H₂₇), 22.9 (CONHCH₂CH₂CH₃), 22.7 (NHCOC₂H₄(CH₂)₁₂CH₃), 14.1, 11.3 (NHCOC₁₄H₂₈CH₃ and CONHC₂H₄CH₃); HRMS m/z (ESI+): 298.3126 (C₁₉H₄₀NO: [M+H]⁺ requires 298.3104).

The NMR data is in agreement with the literature.^[237]

Solubility of selected aspartic acid analogues



All above compounds are soluble in DCM and EtOAc (**2.55**, **2.61**, **2.31** and **2.32**)

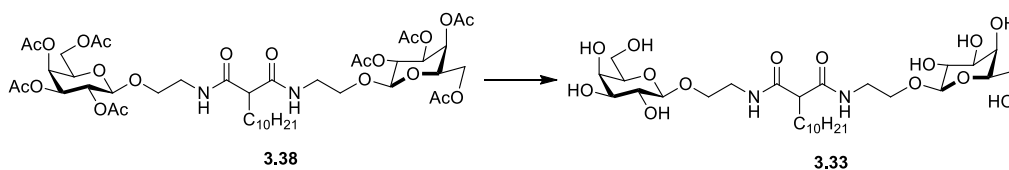


All above compounds are soluble in Pyridine and DMSO (**2.26**, **2.27**, **2.29** and **2.30**)



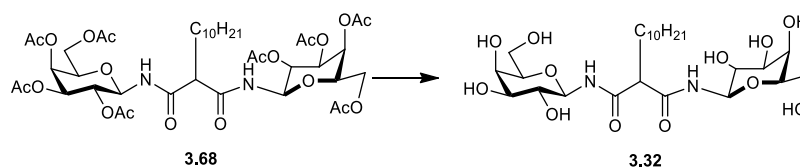
The above compounds are soluble in DCM and EtOAc (**2.91** and **2.75**)

6.2.2 Experimental procedures for Chapter 3



2-Decyl- N^1,N^2 -bis[2-(β -D-galactopyranosyl)ethyl] malonamide **3.33**

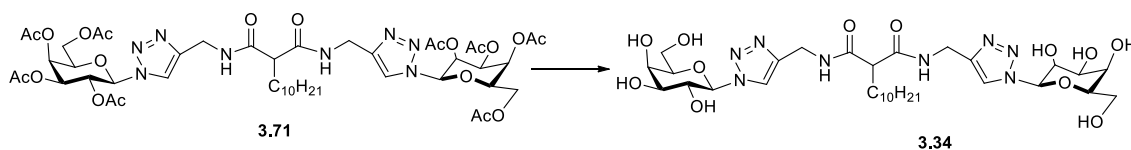
NEt_3 (0.1 mL) was added to a stirring solution of 2-decyl- N^1,N^2 -bis[2-(2,3,4,6-*O*-tetracetyl)- β -D-galactopyranosyl]ethyl malonamide **3.38** (64 mg, 0.064 mmol) dissolved in DCM/MeOH/ H_2O (3 mL/6 mL/3 mL) at 40 °C. The mixture was stirred for 18 h. The reaction mixture was concentrated under reduced pressure to afford the crude solid which was triturated using DCM and EtO_2 to afford **3.33** as a white solid (33 mg, 78%); $[\alpha]_{\text{D}}^{25} = 5$ (c, 0.8 in MeOH); $^1\text{H-NMR}$ (300 MHz, d_5 -Pyr): δ 8.85–8.80 (m, 2 H, $\text{CONHCH}_2\text{CH}_2\text{O}$), 4.79 (dd, $J = 2.0$ Hz, $J = 7.6$ Hz, 1 H, $H-1$), 4.54–4.39 (m, 8 H, overlap of $H-2$, $H-4$, $H-6$, $H-6'$), 4.18–4.07 (m, 6 H, overlap of $H-3$, $H-5$, 1 H of $\text{OCH}_2\text{CH}_2\text{NH}$), 3.99–3.95 (m, 2 H, 1 H of $\text{OCH}_2\text{CH}_2\text{NH}$), 3.78–3.62 (m, 5 H, overlap of $\text{OCH}_2\text{CH}_2\text{NH}$ and $H-\alpha$), 1.54–1.38 (m, 2 H, $\text{NHCOCHCH}_2\text{C}_9\text{H}_{19}$), 1.29–1.06 (m, 16 H, $\text{NHCOCHCH}_2(\text{CH}_2)_8\text{CH}_3$), 0.84 (t, $J = 6.5$ Hz, 3 H, $\text{NHCOCHCH}_2(\text{CH}_2)_8\text{CH}_3$); $^{13}\text{C-NMR}$ (75 MHz, d_5 -Pyr): δ_{c} 171.7, 171.6 (each CO), 105.9 (C-1), 77, 4, 75.6 (C-3, C-5), 72.8, 70.6 (C-2, C-4), 69.9, 69.7 ($\text{OCH}_2\text{CH}_2\text{NH}$), 62.9, 62.8 (C-6), 55.5 (C- α), 40.8 ($\text{OCH}_2\text{CH}_2\text{NH}$), 32.4 ($\text{NHCOCHCH}_2\text{C}_9\text{H}_{19}$), 30.2, 30.1, 30.0, 29.9, 28.4, 23.2 ($\text{NHCOCHCH}_2(\text{CH}_2)_8\text{CH}_3$), 14.6 ($\text{NHCOCHCH}_2(\text{CH}_2)_8\text{CH}_3$); HRMS m/z (ESI $^+$): 655.364 ($\text{C}_{29}\text{H}_{55}\text{N}_2\text{O}_{14}$: $[\text{M}+\text{H}]^+$ requires 655.3648).



2-Decyl- N^1,N^2 -bis(β -D-galactopyranosyl) malonamide **3.32**

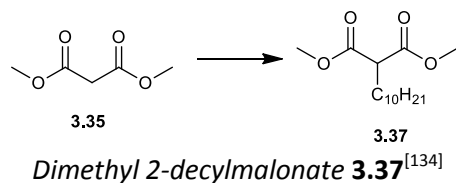
NEt_3 (0.1 mL) was added to a stirring solution of 2-decyl- N^1,N^2 -bis(2,3,4,6-*O*-tetracetyl- β -D-galactopyranosyl) malonamide **3.68** (70 mg, 0.077 mmol) dissolved in DCM/MeOH/ H_2O (3 mL/6 mL/3 mL) at 40 °C. The mixture was stirred for 18 h. The reaction mixture was concentrated under reduced pressure to afford the crude solid which was triturated using DCM and EtO_2 to give **3.32** as a white solid (40 mg, 93%); $[\alpha]_{\text{D}}^{25} = 4.2$ (c, 1.2 in MeOH); $^1\text{H-NMR}$ (300 MHz, d_5 -Pyr): δ 10.03 (d, $J = 9.3$ Hz, 1 H, CONHH-1), 9.92 (d, $J = 9$ Hz, 1 H, CONHH-1), 5.96

(m, 2 H, *H*-1), 4.74–4.50 (m, 4 H, overlap of *H*-2, *H*-4), 4.44–4.32 (m, 4 H, overlap of *H*-6 and *H*-6'), 4.20–4.15 (m, 2 H, overlap of *H*-3), 3.84–3.77 (m, 1 H, *H*- α), 2.29–2.23 (m, 2 H, NHCOCHCH₂C₉H₁₉), 1.58–1.33 (m, 2 H, NHCOCHCH₂CH₂C₈H₁₇), 1.19–1.03 (m, 14 H, NHCOCHCH₂CH₂(CH₂)₇CH₃), 0.83 (t, *J* = 6.5 Hz, 3 H, NHCOCHCH₂CH₂(CH₂)₇CH₃); ¹³C-NMR (75 MHz, *d*₅-Pyr): δ_c 172.6, 172.4 (each CO), 82.3, 82.2 (*C*-1), 79.1, 78.9, 76.6, 76.5 (*C*-3, *C*-5), 72.4, 72.3, 70.8, 70.7 (*C*-2, *C*-4), 62.6 (*C*-6), 55.9 (*C*- α), 32.3 (NHCOCHCH₂C₉H₁₉), 30.1, 29.9, 29.8, 28.4, 23.2 (NHCOCHCH₂(CH₂)₈CH₃), 14.6 (NHCOCHCH₂(CH₂)₈CH₃); HRMS *m/z* (ESI⁺): 567.3125 (C₂₅H₄₇N₂O₁₂: [M+H]⁺ requires 567.3124).



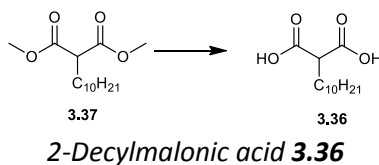
2-Decyl-N¹,N²-bis[(β -D-galactopyranosyl)-1,2,3-triazol-4ylmethylamide] malonamide 3.34

NEt₃ (0.1 mL) was added to a stirring solution of 2-decyl-*N*¹,*N*²-bis[(2,3,4,6-*O*-tetracetyl)- β -D-galactopyranosyl)-1,2,3-triazol-4ylmethylamide] malonamide **3.71** (64 mg, 0.060 mmol) dissolved in DCM/MeOH/H₂O (3 mL/6 mL/3 mL) at 40 °C. The mixture was stirred for 18 h. The reaction mixture was concentrated under reduced pressure to afford the crude solid which was triturated using DCM and EtO₂ to give to afford **3.34** as a white solid (41 mg, 95%); [α]_D²⁵ = 12 (c, 1 in MeOH); ¹H-NMR (300 MHz, *d*₅-Pyr): δ 9.59–9.53 (m, 2 H, CONHCH₂), 8.41 (d, *J* = 2.7 Hz, 1 H, N₃CCH), 6.28 (d, *J* = 9.1 Hz, 2 H, *H*-1), 5.18–5.12 (m, 2 H, *H*-2), 4.81–4.78 (m, 2 H, CONHCH₂), 4.66 (bs, 2 H, *H*-4), 4.47–4.34 (m, 8 H, overlap of *H*-3, *H*-5, *H*-6 and *H*-6'), 3.69 (t, *J* = 7.2 Hz, 1 H, *H*- α), 2.16–2.10 (m, 2 H, NHCOCHCH₂C₉H₁₉), 1.45–1.37 (m, 2 H, NHCOCHCH₂CH₂C₈H₁₇), 1.22–1.08 (m, 14 H, NHCOCHCH₂CH₂(CH₂)₇CH₃), 0.83 (t, *J* = 6.5 Hz, 3 H, NHCOCHCH₂CH₂(CH₂)₇CH₃); ¹³C-NMR (75 MHz, *d*₅-Pyr): δ_c 171.5 (CO), 146.0 (N₃CCH), 122.5 (N₃CCH), 90.5 (*C*-1), 80.7, 76.1 (*C*-3, *C*-5), 71.7, 71.6, 70.6 (*C*-2, *C*-4), 62.6 (*C*-6), 55.6 (*C*- α), 35.9 (CONHCH₂), 32.4 (NHCOCHCH₂C₉H₁₉), 30.2, 30.1, 29.9, 29.8, 28.4, 23.2 (NHCOCHCH₂(CH₂)₈CH₃), 14.6 (NHCOCHCH₂(CH₂)₈CH₃); HRMS *m/z* (ESI⁺): 729.3759 (C₃₁H₅₃N₈O₁₂: [M+H]⁺ requires 729.3777).



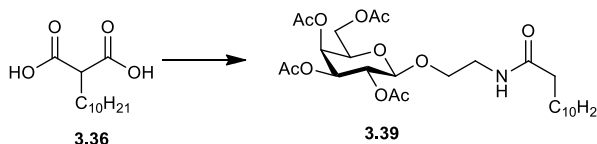
To a solution of dimethyl malonate **3.35** (0.866 mL, 7.5 mmol) and bromodecane (1.61 mL, 98 mmols) in MeCN, K₂CO₃ (4.18 g, 30 mmol) was added and the reaction was refluxed for 24 hrs. The K₂CO₃ was filtered off and the filtrate concentrated under reduced pressure. The resulting liquid was taken up in EtOAc and a wash of H₂O and brine was carried out. It was then dried over MgSO₄ and concentrated under reduced pressure to yield a clear liquid. Flash chromatography (96:4, Hex:EtOAc) afforded the title compound **3.37** as a clear liquid (1.65 g, 80%); R_f = 0.65 (96:4, Hex:EtOAc); IR ν_{max} (NaCl plate, DCM): 2954.9, 2925.8, 2855.3, 1739.8, 1435.8, 1342.3, 1198.8, 1153.5, 1122.9, 1018.3, 804.9, 722.0 cm⁻¹; ¹H NMR (300 MHz, CDCl₃): δ 3.69 (s, 6 H, COOCH₃), 3.30 (t, *J* = 7.5 Hz, 1 H, *H*-α), 1.85-1.81 (m, 2 H, COCHCH₂(CH₂)₈CH₃), 1.29-1.21 (m, 16 H, COCHCH₂(CH₂)₈CH₃), 0.82 (t, *J* = 6.6 Hz, 3 H, COCHCH₂(CH₂)₈CH₃); ¹³C NMR (75 MHz): δ_c 169.8 (CO), 52.2 (OCH₃), 51.6 (α-C), 31.8, 29.5, 29.4, 29.2, 29.1, 28.8, (COCHCH₂(CH₂)₈CH₃), 27.3 (COCHCH₂(CH₂)₈CH₃), 22.6 (COCHCH₂(CH₂)₈CH₃), 13.90 (COCHCH₂(CH₂)₈CH₃); HRMS *m/z* (ESI⁺): 311.1622 (C₁₅H₂₈KO₄: [M+K]⁺ requires 311.1619).

NMR data is in agreement with the literature.^[124]



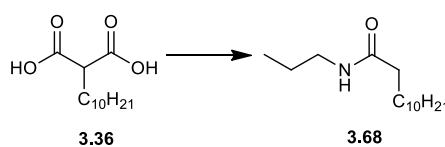
15% NaOH (0.317 mL) was added to dimethyl 2-decylmalonate **3.37** (100 mg, 0.34 mmol) in EtOH (5 mL). The reaction was heated to 80 °C and stirred overnight. H₂O (4 mL) and 2 M HCl was added dropwise until a pH of 1 was reached. The reaction mixture was concentrated *in vacuo*; diluted with EtOAc, washed with brine and H₂O, dried (MgSO₄) and concentrated under reduced pressure to yield **3.36** as a white solid (44 mg, 50%); Mp = 120-118 °C (lit 119.5-118 °C)^[238]; ¹H NMR (300 MHz, CDCl₃): δ 3.44 (t, *J* = 7.5 Hz, 1 H, *H*-α), 1.70-1.68 (m, 2 H, COCHCH₂(CH₂)₈CH₃), 1.30-1.22 (m, 16 H, COCHCH₂(CH₂)₈CH₃), 0.85 (t, *J* = 6.3 Hz, 3 H, COCHCH₂(CH₂)₈CH₃); HRMS *m/z* (ESI⁺): 245.1758 (C₁₃H₂₅O₄: [M+H]⁺ requires 245.1747).

This compounds is mentioned in the literature but no NMR data are given.^[239]



[2-O-(2,3,4,6-O-tetracetyl-β-D-galactopyranose)ethyl]-dodecanamide **3.39**

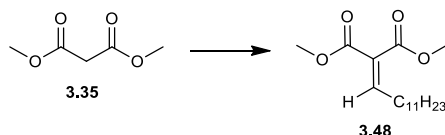
HOBt (116 mg, 0.859 mmol) and NEt₃ (0.228 mL, 1.6 mmol) were added to a stirring solution of 2-decylmalonic acid **3.36** (100 mg, 0.40 mmol) and TBTU (275 mg, 0.85 mmol) dissolved in DMF (12 mL), under N₂ at rt. The mixture was stirred for 20 min and *O*-(2-aminoethyl)-(2,3,4,6-*O*-tetracetyl)-β-D-galactopyranose **2.33** (352 mg, 0.9 mmol) dissolved in DMF (10 mL) was added dropwise. The mixture was stirred overnight. The reaction mixture was concentrated *in vacuo* diluted with EtOAc and washed with brine. Flash chromatography (1:1, Ethyl acetate: Hexane) afforded the title compound **3.39** as an off white solid (180 mg, 78%); R_f = 0.22 (1:1, Hex:EtOAc); [α]²⁵_D = -6.6 (c, 1 in CHCl₂); IR ν_{max} (NaCl plate, DCM): 3409.1, 2958.1, 2925.7, 2854.4, 1751.7, 1547.1, 1465.5, 1436.1, 1379.0, 1221.6, 1172.6, 1221.6, 1059.5, 956.7, 900.9, 799.4, 772.0, 714.1 cm⁻¹; ¹H NMR (300 MHz, CDCl₃): δ 5.84 (t, *J* = 5.1 Hz, 1 H, CONHCH₂CH₂O), 5.38 (d, *J* = 3.3 Hz, 1 H, *H*-4), 5.17 (dd, *J* = 7.8, *J* = 10.5, 1 H, *H*-2), 5.00 (dd, *J* = 3.3 Hz, *J* = 10.5 Hz, 1 H, *H*-3), 4.46 (d, *J* = 7.8 Hz, 1 H, *H*-1), 4.13 (dd, *J* = 2.1 Hz, 2 H, *H*-6, *H*-6'), 3.93-3.82 (m, 2 H, overlap of *H*-5 and 1 H NHCH₂CH₂O), 3.70-3.63 (m, 1 H, 1 H of NHCH₂CH₂O), 3.54-3.34 (m, 2 H, NHCH₂CH₂O), 2.14-1.97 (m, 11 H, overlap of NHCOCH₂C₁₀H₂₁ and O(CO)CH₃), 1.62-1.55 (m, 2 H, NHCOCH₂CH₂C₉H₁₉), 1.29-1.23 (m, 16 H, COCH₂CH₂(CH₂)₉CH₃), 0.85 (t, *J* = 6.3 Hz, 3 H, (COCH₂(CH₂)₉CH₃); ¹³C-NMR (75 MHz, CDCl₃): δ_c 173.2 (CO), 170.3, 170.1, 170.0, 169.6 (O(CO)CH₃) 101.4 (*C*-1), 70.8, 70.7 (*C*-5, *C*-3), 69.2, (*C*-2), 68.9 (OCH₂CH₂NH), 66.9 (*C*-4), 61.3 (*C*-6), 39.0 (OCH₂CH₂NH), 36.7 (NHCOCH₂C₁₀H₂₁), 31.8, 29.6, 29.5, 29.4, 29.3, 29.3, 25.6, (NHCOCH₂(CH₂)₉CH₃), 22.6 20.80, 20.6, 20.5 (each O(CO)CH₃), 14.1 (NHCO(CH₂)₁₀CH₃); HRMS *m/z* (ESI⁺): 574.3231 (C₂₈H₄₈NO₁₁: [M+H]⁺ requires 574.3222).



N-propyldodecanamide **3.68**

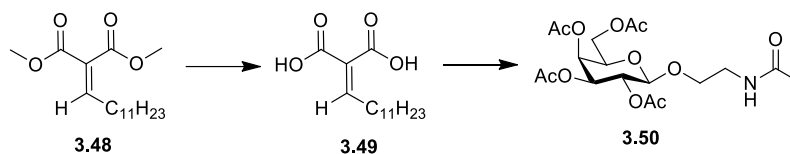
HOBt (81 mg, 0.60 mmol) and NEt₃ (0.076 mL, 0.548 mmol) were added to a stirring solution of 2-decylmalonic acid **3.36** (67 mg, 0.27 mmol) and TBTU (190 mg, 0.60 mmol) dissolved in DMF (10 mL), under N₂ at rt. The mixture was stirred for 20 min and propylamine (0.05 mL, 0.60 mmol) was added dropwise. The mixture was stirred overnight. The reaction mixture was

concentrated *in vacuo* diluted with EtOAc and washed with brine. Flash chromatography (1:1 EtOAc:Hex) afforded **3.68** as a whitish solid (35 mg, 53%); $R_f = 0.63$ (1:1, Hex:EtOAc); $^1\text{H NMR}$ (300 MHz, CDCl_3): δ 5.58 (bs, 1 H, NH), 3.22-3.15 (m, 2 H, $\text{NHCH}_2\text{CH}_2\text{CH}_3$), 2.14 (t, $J = 7.5$ Hz, 2 H, $\text{COCH}_2(\text{CH}_2)_9\text{CH}_3$), 1.62-1.57 (m, 2 H, $\text{COCH}_2\text{CH}_2(\text{CH}_2)_8\text{CH}_3$), 1.53-1.46 (m, 2 H, $\text{NHCH}_2\text{CH}_2\text{CH}_3$), 0.92-0.83 (m, 6 H, overlap of $\text{NHCH}_2\text{CH}_2\text{CH}_3$, $\text{COCH}_2(\text{CH}_2)_9\text{CH}_3$); HRMS m/z (ESI+): 242.2485 ($\text{C}_{15}\text{H}_{31}\text{NO}$: $[\text{M}+\text{H}]^+$ requires 242.2478). NMR data is in agreement with the literature.^[240]



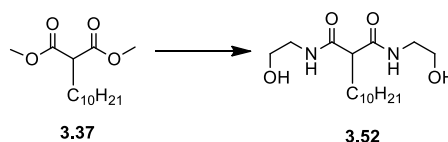
Dimethyl 2-dodecyldenemalonate **3.48**

To a solution of dimethyl malonate **3.35** (0.52 mL, 4.5 mmol) and dodecanal (0.73 mL, 4.5 mmol) in anhydrous DCM (15 mL) on ice, piperidine (2 drops) and acetic acid (2 drops) were added. The reaction was left to stir at 0 °C for 45 min and then 4 Å molecular sieves were added. The reaction was stirred at room temperature for 16 h. The reaction mixture was diluted with Et_2O (40 mL), and washed with H_2O (10 mL portions) until the aqueous phase was neutral. The collected aqueous phase was extracted with Et_2O (15 mL x 3). The combined organic layers were washed with, aqueous sat. NaHCO_3 and brine. The solution was dried over MgSO_4 and solvent removed under reduced pressure to yield a clear liquid. Flash chromatography (5:1, Hex: EtOAc) afforded the title compound **3.48** as a clear liquid (0.516 g, 38%); $R_f = 0.71$ (5:1, Hex:EtOAc); IR ν_{max} (NaCl plate, DCM): 2925.6, 2854.8, 1731.5, 1646.8, 1436.4, 1369.9, 1261.9, 1222.5, 1062.5, 771.1 cm^{-1} ; $^1\text{H NMR}$ (300 MHz, CDCl_3): δ 7.04-6.97 (m, 1 H, $\text{C}=\text{CH}$), 3.80-3.74 (m, 6 H, COOCH_3), 2.31-2.22 (m, 2 H, $\text{CCHCH}_2(\text{CH}_2)_9\text{CH}_3$), 1.51-1.39 (m, 2 H, $\text{CCHCH}_2\text{CH}_2(\text{CH}_2)_8\text{CH}_3$), 1.34-1.19 (m, 16 H, $\text{CCHCH}_2\text{CH}_2(\text{CH}_2)_8\text{CH}_3$), 0.89-0.82 (m, 3 H, $\text{CCHCH}_2\text{CH}_2(\text{CH}_2)_8\text{CH}_3$); $^{13}\text{C NMR}$ (75 MHz, CDCl_3): δ_c 165.9, 164.4 (CO), 150.5 ($\text{C}=\text{CH}$), 127.87 ($\text{C}=\text{CH}$), 52.2, 52.1 (COOCH_3), 31.9, 29.8, 29.6, 29.4, 29.3, 29.2, 29.1, 28.2, 22.6 ($\text{C}=\text{CH}(\text{CH}_2)_{10}\text{CH}_3$), 14.0 ($\text{C}=\text{CH}(\text{CH}_2)_{10}\text{CH}_3$); HRMS m/z (ESI+): 299.2232 ($\text{C}_{17}\text{H}_{31}\text{O}_4$: $[\text{M}+\text{H}]^+$ requires 299.2217).



[2-O(2,3,4,6-O-tetracetyl-β-D-galactopyranosyl)ethyl]-acetamide 3.50

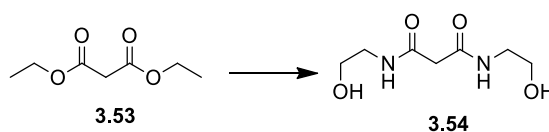
Dimethyl 2-dodecylidenemalonate **3.48** (100 mg, 0.36 mmol) was dissolved in anhydrous EtOAc (2.5 mL) under Ar. The round bottom was wrapped in tinfoil and Lil (396 mg, 1.47 mmol) added. The reaction mixture was heated to 60 °C and stirred overnight. HOBt (148 mg, 1.1 mmol), TBTU (353 mg, 1.1 mmol) and NEt₃ (0.15 mL, 1.1 mmol) were added and the reaction mixture stirred for 5 min. 2-aminoethyl 2,3,4,6-tetra-*O*-acetyl-β-D-galactopyranose **2.33** (431 mg, 1.1 mmol) was dissolved in DMF (3 mL) and added and the resulting solution was stirred for 10 h. The solvent was removed under reduced pressure. The residue obtained was dissolved in DCM and washed with 1M HCl, aqueous sat. NaHCO₃, brine and dried over MgSO₄. Column chromatography afforded the decarboxylated product **3.50** as an oily solid (100 mg, 63%); *R_f* = 0.38 (10:1, DCM:MeOH); [α]_D²⁵ = 4.2 (c, 0.96 in DCM); IR *v*_{max} (NaCl plate, DCM): 3388.3, 3087.6, 2962.9, 2940.2, 1749.7, 1661.5, 1539.0, 1432.0, 1371.1, 1225.8, 1173.3, 1134.7, 1075.9, 956.3, 914.9, 799.9, 753.3, 666.2 cm⁻¹; ¹H NMR (300 MHz, CDCl₃): δ 5.98 (bs, 1 H, CONHCH₂CH₂O), 5.38 (dd, *J* = 1 Hz, *J* = 3.4 Hz, 1 H, *H*-4), 5.17 (dd, *J* = 7.8 Hz, *J* = 10.5 Hz, 1 H, *H*-2), 5.00 (dd, *J* = 3.3 Hz, *J* = 10.5 Hz, 1 H, *H*-3), 4.45 (d, *J* = 7.8 Hz, 1 H, *H*-1), 4.19-4.07 (m, 2 H, *H*-6, *H*-6'), 3.93-3.82 (m, 2 H, overlap of *H*-5 and NHCH₂CH₂O), 3.70-3.64 (m, 1 H, 1 H of NHCH₂CH₂O), 3.54-3.34 (m, 2 H, NHCH₂CH₂O), 2.14, 2.05, 2.03, 1.97 (each s, 3 H, O(CO)CH₃); ¹³C-NMR (75 MHz, CDCl₃): δ_c 173.2 (CO), 170.3, 170.1, 170.0, 169.6 (O(CO)CH₃) 101.4 (*C*-1), 70.8, 70.7 (*C*-5, *C*-3), 69.2, (*C*-2), 68.9 (OCH₂CH₂NH), 66.9 (*C*-4), 61.3 (*C*-6), 39.0 (OCH₂CH₂NH), 23.2, 20.80, 20.6, 20.5 (each O(CO)CH₃); HRMS *m/z* (ESI⁺): 434.1669 (C₁₈H₂₈NO₁₁: [M+H]⁺ requires 434.1657).



2-Decyl-N¹,N³-bis(2-hydroxyethyl)malonamide 3.52 ^[126b]

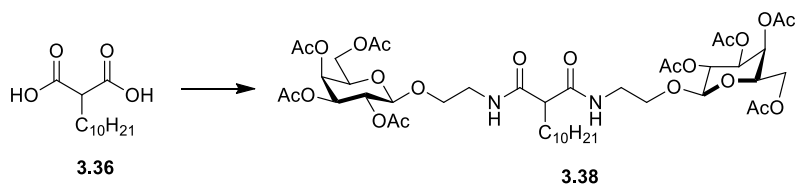
Dimethyl 2-decylmalonate **3.37** (500 mg, 1.8 mmol) and ethanolamine were dissolved in DCM (1 mL) under N₂. The reaction mixture was stirred at rt for 3 days. The solvent was removed in vacuo and the crude residue recrystallised in EtOH and Et₂O (1:1) to yield the desired product **3.52** as white crystals (370 mg, 62%); IR *v*_{max} (NaCl plate, DCM): 3332.9, 2915.7, 2848.6, 1673.9,

16371, 1557.4, 1463.3, 1421.3, 1332.7, 1214.2, 1088.7, 1056.9, 1044.9, 928.0 cm^{-1} ; ^1H NMR (300 MHz, CDCl_3): δ 7.86 (t, $J = 5.4$ Hz, 2 H, NH), 4.70 (t, $J = 5.3$ Hz, 2 H, OH), 3.40-3.35 (m, 4 H, $\text{NHCH}_2\text{CH}_2\text{OH}$), 3.17-3.06 (m, 4 H, $\text{NHCH}_2\text{CH}_2\text{OH}$), 3.30 (t, $J = 7.5$ Hz, 1 H, H- α), 1.67-1.60 (m, 2 H, $\text{COCHCH}_2(\text{CH}_2)_8\text{CH}_3$), 1.33-1.11 (m, 16 H, $\text{COCHCH}_2(\text{CH}_2)_8\text{CH}_3$), 0.85 (t, $J = 6.6$ Hz, 3 H, $\text{COCHCH}_2(\text{CH}_2)_8\text{CH}_3$); ^{13}C NMR (75 MHz, CDCl_3): δ_c 169.8 (CO), 59.7 ($\text{NHCH}_2\text{CH}_2\text{OH}$), 53.0 (α -C), 41.1 ($\text{NHCH}_2\text{CH}_2\text{OH}$), 31.2, 30.4, 28.3, 28.8, 28.7, 26.8, 22.1 ($\text{COCHCH}_2(\text{CH}_2)_8\text{CH}_3$), 13.90 ($\text{COCHCH}_2(\text{CH}_2)_8\text{CH}_3$); HRMS m/z (ESI+): 353.2427 ($\text{C}_{17}\text{H}_{34}\text{NaN}_2\text{O}_4$: $[\text{M}+\text{Na}]^+$ requires 353.2411).



N^1,N^3 -bis(2-hydroxyethyl)malonamide **3.54**^[126b]

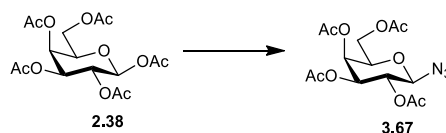
Diethyl malonate **2.53** (476 mL, 3.1 mmol) and ethanolamine (0.386 mL, 6.4 mmol) were dissolved in DCM (1 mL) under N_2 . The reaction mixture was stirred at rt for 2 h. The white solid which had crashed out was filtered and recrystallised from EtOH and Et_2O (1:1) to yield the desired product **3.54** as cream flakes (508 mg, 85%); Mp = 128-125 $^\circ\text{C}$ (lit 126-125 $^\circ\text{C}$)^[126b]; ^1H NMR (300 MHz, CDCl_3): δ 8.01 (bs, 2 H, NH), 4.68 (t, $J = 5.3$ Hz, 2 H, OH), 3.42-3.35 (m, 4 H, $\text{NHCH}_2\text{CH}_2\text{OH}$), 3.15-3.09 (m, 4 H, $\text{NHCH}_2\text{CH}_2\text{OH}$), 3.03 (s, 1 H, H- α); HRMS m/z (ESI+): 213.0844 ($\text{C}_7\text{H}_{15}\text{NaN}_2\text{O}_4$: $[\text{M}+\text{Na}]^+$ requires 213.0846)



*2-Decyl-N¹,N²-bis[2-(2,3,4,6-*O*-tetraacetyl)-β-*D*-galactopyranosyl]ethyl malonamide* **3.38**

The 2-Aminoethyl 2,3,4,6-tetra-*O*-acetyl-β-*D*-galactopyranoside **2.33** (234 mg, 0.59 mmol) and 2-decylmalonic acid **3.36** (73 mg, 0.29 mmol) were dissolved in THF (3 mL) and DMTMM⁽ⁱⁱ⁾ (182 mg, 0.6 mmol) added. The reaction mixture was stirred overnight, and the precipitate filtered off. The filtrate was evaporated under reduced pressure and the residue dissolved in CHCl₃ and washed successively with 0.1 M HCl and H₂O. Column chromatography (EtOAc) yielded the bis substituted product **3.38** (163 mg, 55%); *R*_f = 0.45 (EtOAc); [α]²⁵_D = 1.8 (c, 1.1 in DCM); IR ν_{max} (NaCl plate, DCM): 3336.49, 2927.4, 2855.9, 1752.0, 1669.7, 1529.4, 1433.7, 1370.1, 1224.1, 1173.8, 1135.3, 1060.1, 956.2, 901.8, 803.2, 703.3 cm⁻¹; ¹H NMR (300 MHz, CDCl₃): δ 6.87-6.81 (m, 2 H, CONHCH₂CH₂O), 5.35 (d, *J* = 3.3 Hz, 2 H, *H*-4), 5.15 (dd, *J* = 7.8, *J* = 10.5, 2 H, *H*-2), 5.00-4.95 (m, 2 H, *H*-3), 4.45 (d, *J* = 7.8 Hz, 1 H, *H*-1), 4.15-4.50 (m, 4 H, *H*-6, *H*-6'), 3.92-3.80 (m, 4 H, overlap of *H*-5 and 1 H of OCH₂CH₂NH), 3.63-3.24 (m, 6 H, overlap of 1 H of OCH₂CH₂NH and OCH₂CH₂NH), 2.89 (t, *J* = 7.5 Hz, 1 H, *H*-α), 2.19 (s, 6 H, O(CO)CH₃), 2.06, 2.05 (each s, 3 H, O(CO)CH₃), 2.03, 1.97 (each s, 6 H, O(CO)CH₃), 1.81-1.75 (m, 2 H, COCHCH₂(CH₂)₈CH₃), 1.24-1.20 (m, 16 H, COCH₂(CH₂)₈CH₃), 0.83 (t, *J* = 6.3 Hz, 3 H, COCH(CH₂)₉CH₃); ¹³C-NMR (75 MHz, CDCl₃) δ_c 170.7, 170.6, 170.3, 170.1, 170.0, 169.7, 169.5 (CO), 101.4, 100.9 (C-1), 70.6 (C-5, C-3), 68.6, 68.5 (C-2), 68.2, 68.1 (OCH₂CH₂NH), 66.8 (C-4), 61.1 (C-6), 55.0 (C-α), 39.2, 39.1 (OCH₂CH₂NH), 32.6 (NHCOCHCH₂C₉H₁₉), 31.7, 29.4, 29.3, 29.2, 27.4, 22.6, (each CH₂), 20.7, 20.6, 20.5, 20.4 (each O(CO)CH₃), 14.0 (NHCOCHC₉H₁₈CH₃); HRMS *m/z* (ESI⁺): 992.4522 (C₄₅H₇₁N₂O₂₂: [M+H]⁺ requires 992.4493).

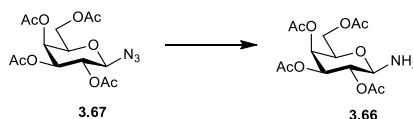
(ii) DMTMM was freshly prepared by reacting *N*-methylmorpholine (NMM) and 2-chloro-4,6-dimethoxy-1,3,5-triazine (CDMT) in THF at rt for 1 h.



1-Azido-2,3,4,6-tetra-O-acetyl- β -D-galactopyranoside **3.67**^[152]

TMSN₃ (2.56 mL, 19.48 mmol) was added to a solution of galactose pentacetate **2.38** (3.04 g, 7.79 mmol) in DCM (30 mL). SnCl₄ (3.90 mL, 3.90 mmol) (1 M solution in DCM) was added to this solution and the reaction mixture stirred for 16 h. Aqueous sat. NaHCO₃ (50 mL) was added and the suspension extracted with DCM (2 x 50 mL). The combined organic layers were dried (MgSO₄), filtered and concentrated *in vacuo* to afford the title compound **3.67** as a white solid (2.65 g, 91%); R_f = 0.55 (1:1, Pet Ether:EtOAc); IR ν_{\max} (NaCl plate, DCM): 3476.5, 3022.0, 2998.2, 2949.7, 2985.9, 2907.2, 2412.9, 2164.2, 2128.3, 1741.3, 1465.4, 1439.2, 1379.9, 1216.0, 1167.4, 118.5, 1085.8, 1057.5, 1022.1, 997.9, 957.9, 902.2 cm⁻¹; ¹H NMR (300 MHz, CDCl₃): δ 5.42 (dd, *J* = 1 Hz, *J* = 3.3 Hz, 1 H, *H*-4), 5.10 (dd, *J* = 8.6 Hz, *J* = 10.3 Hz, 1 H, *H*-2), 5.03 (dd, *J* = 3.3 Hz, *J* = 10.3 Hz, 1 H, *H*-3), 4.59 (d, *J* = 8.6 Hz, 1 H, *H*-1), 4.18-4.15 (m, 2 H, *H*-6 and *H*-6'), 4.03-3.98 (m, 1 H, *H*-5), 2.17, 2.09, 2.06, 1.98 (each s, 3 H, O(CO)CH₃); HRMS *m/z* (ESI⁺): 396.1010 (C₁₄H₁₉N₃NaO₉: [M+Na]⁺ requires 396.1019).

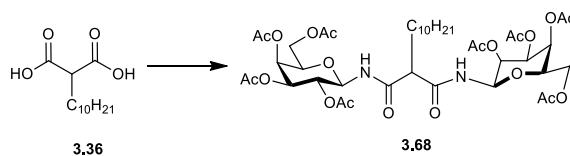
The NMR data is in agreement with the literature.^[152]



1-Amino-2,3,4,6-tetra-O-acetyl- β -D-galactopyranoside **3.66**

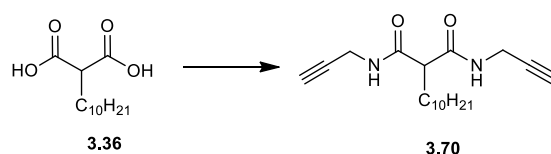
H₂ gas was bubbled through a suspension of 1-azido-2,3,4,6-tetra-O-acetyl- β -D-galactopyranose **3.67** (500 mg, and Pd (C) (50 mg, 10% w/w) in EtOAc (20 mL) at 1 atm. The solution was stirred at rt overnight. The suspension was filtered through Celite and concentrated *in vacuo* to yield the title compound **3.66** as a white foamy solid (450 mg, 97%); ¹H NMR (300 MHz, CDCl₃): δ 5.39 (d, *J* = 1.8 Hz, 1 H, *H*-4), 5.11-5.09 (m, 1 H, *H*-2), 5.04-5.02 (m, 1 H, *H*-3), 4.16 (d, *J* = 8 Hz, 1 H, *H*-1), 4.10-4.08 (m, 2 H, *H*-6 and *H*-6'), 3.91-3.89 (m, 1 H, *H*-5), 2.14, 2.09, 2.06, 1.98 (each s, 3 H, O(CO)CH₃); HRMS *m/z* (ESI⁺): 348.1286 (C₁₄H₂₂NO₉: [M+H]⁺ requires 348.1289).

The NMR data is in agreement with the literature.^[152]



2-Decyl-N¹,N²-bis(2,3,4,6-O-tetracetyl-β-D-galactopyranosyl) malonamide 3.77

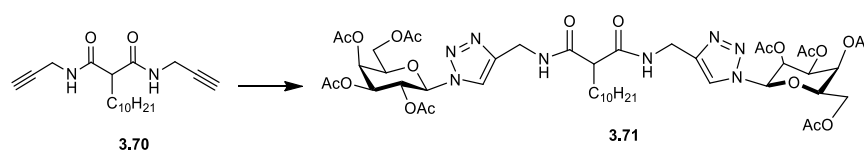
1-Amino-2,3,4,6-tetra-*O*-acetyl-β-D-galactopyranose **3.66** (284 mg, 0.81 mmol) and 2-decylmalonic acid **3.36** (100 mg, 0.40 mmol) were dissolved in THF (3 mL) and DMTMM (249 mg, 0.9 mmol) added. The reaction mixture was stirred overnight, and the precipitate filtered off. The filtrate was evaporated under reduced pressure and the residue dissolved in CHCl₃ and washed successively with 0.1 M HCl and H₂O. Gradient elution chromatography (1:1, EtOAc:Pet Ether- 10:3, EtOAc:Pet Ether) yielded the bis substituted product **3.68** (205 mg, 56%); *R_f* = 0.65 (10:3, EtOAc:Pet Ether); [α]²⁵_D = 22.4 (c, 0.95 in DCM); IR *v*_{max} (NaCl plate, DCM): 3333.7, 2927.7, 2855.9, 2478.8, 1751.4, 1686.1, 1530.0, 1433.2, 1369.9, 1225.7, 1169.2, 11224, 1085.5, 1056.3, 956.1, 907.6 804.7 cm⁻¹; ¹H NMR (300 MHz, CDCl₃): δ 7.79-7.76 (m, 1 H, CONH), 7.01 (d, *J* = 8.7 Hz, 1 H, CONH), 5.39-5.37 (m, 2 H, *H*-4), 5.22-5.07 (m, 6 H, overlap of *H*-1, *H*-2 and *H*-3), 4.08-3.99 (m, 6 H, overlap of *H*-6, *H*-6' and *H*-5), 2.96 (t, *J* = 7.2 Hz, 1 H, *H*-α), 2.12, 2.11 (each s, 3 H, O(CO)CH₃), 2.01 and 2.00 (each s, 6 H, O(CO)CH₃), 1.99, 1.95 (each s, 3 H, O(CO)CH₃), 1.79-1.69 (m, 2 H, NHCOCHCH₂(CH₂)₈CH₃), 1.29-1.11 (s, 16 H, NHCOCHCH₂(CH₂)₈CH₃), 0.83 (t, *J* = 6.3, 3 H, NHCOCHCH₂(CH₂)₈CH₃); ¹³C NMR (75 MHz, CDCl₃) δ_c 171.2, 170.7, 170.5, 170.3, 170.0, 169.9, 169.8, 169.8 (each CO), 78.2, 78.1 (C-1), 72.3, 72.1 (C-5), 70.8, 70.7 (C-3), 67.9, 67.8 (C-2), 66.9, 66.8 (C-4), 60.9, 60.8 (C-6), 54.4 (C-α) 32.5 (NHCOCHCH₂(CH₂)₈CH₃), 31.7, 29.5, 29.4, 29.2, 29.1, 27.0, 22.5 (NHCOCHCH₂(CH₂)₈CH₃), 20.5-20.3 (overlap of O(CO)CH₃), 14.0 (NHCOCHCH₂(CH₂)₈CH₃); HRMS *m/z* (ESI⁺): 941.3534 (C₄₁H₆₂N₂O₂₀: [M+K]⁺ requires 941.3528).



2-Decyl-N¹,N³-bis(propargyl)malonamide 3.70

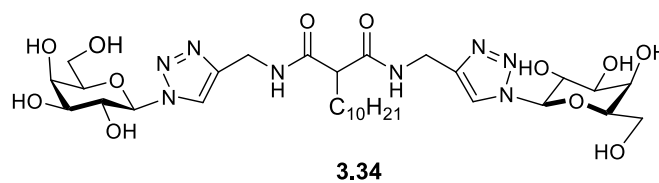
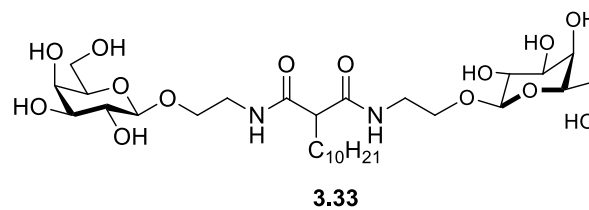
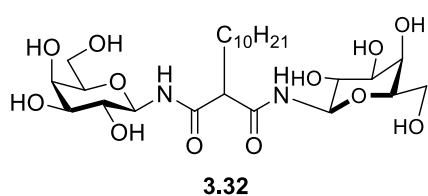
Propargylamine (0.045 mL, 0.70 mmol) and 2-decylmalonic acid **3.36** (78 mg, 0.32 mmol) were dissolved in THF (1.5 mL) and DMTMM (194 mg, 0.7 mmol) added. The reaction mixture was stirred overnight, and the precipitate filtered off. The filtrate was evaporated under reduced pressure and the residue dissolved in CHCl₃ and washed successively with 0.1 M HCl and H₂O. Gradient elution chromatography (1:1, EtOAc:Pet Ether- EtOAc) yielded the bis substituted product **3.70** (79 mg, 78%); *R_f* = 0.83 (EtOAc); IR *v*_{max} (KBr Disc): 3285.2, 3049.5, 2953.3, 2851.3,

2929.7, 2125.1, 1661.4, 1532.6, 1465.9, 1444.1, 1373.7, 1334.5, 1274.6, 1255.9, 1232.9, 1207.3, 1195.2, 1130.2, 1031.7, 1007.8, 921.2, 936.7, 888.7, 847.8, 830.6, 798.2, 721.2, 683.8, 660.5 cm^{-1} ; ^1H NMR (300 MHz, CDCl_3): δ 6.97-6.93 (m, 2 H, CONH), 4.50-4.02 (m, 4 H, NHCH_2CCH), 3.02 (t, $J = 7.8$ Hz, 1 H, $H-\alpha$), 2.23 (t, $J = 2.4$ Hz, 2 H, NHCH_2CCH), 1.89-1.84 (m, 2 H, $\text{NHCOCHCH}_2\text{C}_9\text{H}_{19}$), 1.29-1.11 (m, 16 H, $\text{NHCOCHCH}_2(\text{CH}_2)_8\text{CH}_3$), 0.87 (t, $J = 6.3$, 3 H, $\text{NHCOCHCH}_2(\text{CH}_2)_8\text{CH}_3$); ^{13}C NMR (75 MHz, CDCl_3) δ_c 170.4 (each CO), 78.9 (NHCH_2CCH), 71.8 (NHCH_2CCH), 54.7 ($C-\alpha$) 32.9 ($\text{NHCOCHCH}_2(\text{CH}_2)_8\text{CH}_3$), 31.9, 29.5, 29.4, 29.2, 27.4, 22.7 ($\text{NHCOCHCH}_2(\text{CH}_2)_8\text{CH}_3$), 14.1 ($\text{NHCOCHCH}_2(\text{CH}_2)_8\text{CH}_3$); HRMS m/z (ESI+): 319.239 ($\text{C}_{19}\text{H}_{30}\text{N}_2\text{O}_2$: $[\text{M}+\text{H}]^+$ requires 319.2380).

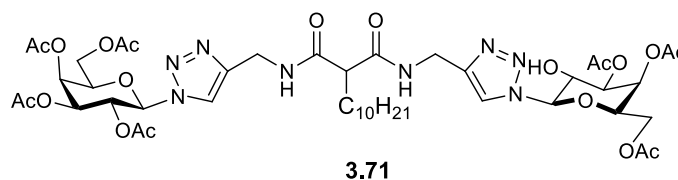
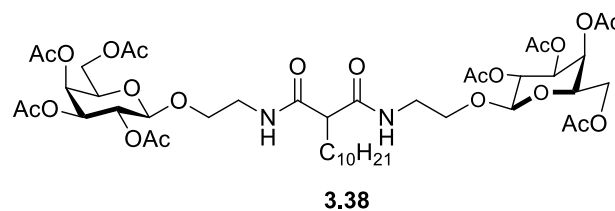
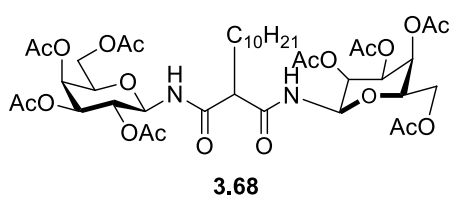


*2-Decyl- N^1,N^3 -bis[(2,3,4,6-*O*-tetraacetyl)- β -*D*-galactopyranosyl]-1,2,3-triazol-4ylmethylamide] malonamide **3.71***

Copper sulphate $\cdot 5\text{H}_2\text{O}$ (2 mg, 0.01 mmol) and sodium ascorbate (4 mg, 0.02 mmol) were added to a solution of 2-decyl- N^1,N^3 -bis(propargyl)malonamide **3.70** (32 mg, 0.1 mmol) and galactosyl azide **3.67** (75 mg, 0.2 mmol) in DCM/Acetone/ H_2O (2:2:1). The reaction was allowed to stir at rt overnight. The solvent was removed *in vacuo*, the residue dissolved in DCM and washed with brine. Column chromatography (EtOAc) afforded the pure product **3.71** as an oily solid (64 mg, 58%); $R_f = 0.57$ (EtOAc); $[\alpha]_D^{25} = -6.6$ (c, 1.1 in DCM); IR ν_{max} (NaCl plate, DCM): 3305.4, 3140.8, 3077.5, 2926.1, 2855.0, 1754.6, 1670.2, 1531.1, 1457.5, 1431.2, 1370.1, 1219.3, 1161.4, 1092.8, 1063.3, 953.2, 924.0, 88.4, 804.2, 747.9 cm^{-1} ; ^1H NMR (300 MHz, CDCl_3): δ 7.82 (d, $J = 3$ Hz, 2 H, N_3CCH), 7.44-7.39 (m, 2 H, CONHCH_2), 5.88 (d, $J = 9.3$ Hz, 2 H, $H-1$), 5.54-5.48 (m, 4 H, overlap of $H-2$ and $H-4$), 5.25 (dd, $J = 2.4$ Hz, $J = 9.3$ Hz, 2 H, $H-3$), 4.56-4.40 (m, 2 H, CONHCH_2), 4.28-4.23 (m, 2 H, $H-5$), 4.16-4.11 (m, 4 H, overlap of $H-6$ and $H-6'$), 3.05 (t, $J = 7.5$ Hz, 1 H, $H-\alpha$), 2.19, 2.04, 1.97 (each s, 6 H, $\text{O}(\text{CO})\text{CH}_3$), 1.81-1.80 (m, 8 H, overlap of $\text{O}(\text{CO})\text{CH}_3$ and $\text{NHCOCHCH}_2\text{C}_9\text{H}_{19}$), 1.31-1.11 (m, 16 H, $\text{NHCOCHCH}_2(\text{CH}_2)_8\text{CH}_3$), 0.82 (t, $J = 6.3$ Hz, 3 H, $\text{NHCOCHCH}_2(\text{CH}_2)_8\text{CH}_3$); ^{13}C NMR (75 MHz, CDCl_3) δ_c 170.6, 170.5, 170.3, 169.9, 169.7, 168.8 (each CO), 145.9 (N_3CCH), 121.1, 121.0 (N_3CCH), 85.9 ($C-1$), 73.7 ($C-5$), 70.6 ($C-3$), 67.8 66.7 ($C-2$, $C-4$), 61.01 ($C-6$), 54.6 ($C-\alpha$), 34.8 (CONHCH_2), 32.1 ($\text{NHCOCHCH}_2\text{C}_9\text{H}_{19}$), 31.7, 29.5, 29.4, 29.2, 29.1 27.4, 22.4 ($\text{NHCOCHCH}_2(\text{CH}_2)_8\text{CH}_3$), 20.6, 20.5 20.4, 20.1 (each $\text{O}(\text{CO})\text{CH}_3$), 14.0 ($\text{NHCOCHCH}_2(\text{CH}_2)_8\text{CH}_3$); HRMS m/z (ESI+): 1065.4642 ($\text{C}_{47}\text{H}_{68}\text{N}_8\text{O}_{20}$: $[\text{M}+\text{H}]^+$ requires 1065.4623).

Solubility of aliphatic based analogues

Compounds **3.32-3.34** are soluble in Pyridine, DMSO and partially soluble in MeOH



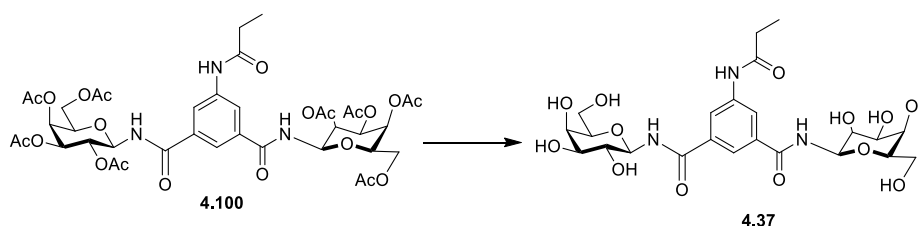
Compounds **3.38, 3.68** and **3.71** are soluble DCM and EtOAc

6.2.3 Experimental procedures for Chapter 4



*N*¹, *N*², di-(β-*D*-galactopyranosyl)-*N*³-hexadecanosyl-5-aminobenzene 1,3,dicarboxamide **4.36**

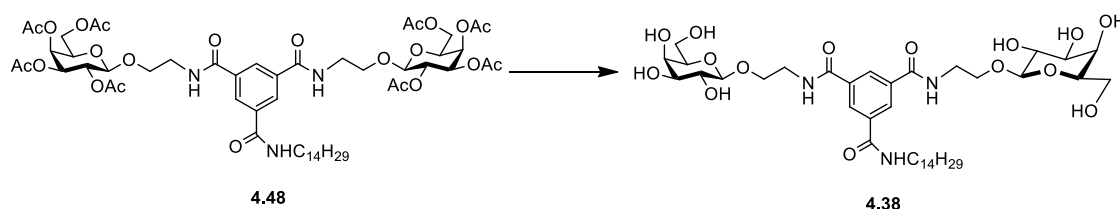
NEt₃ (0.1 mL, 0.016 mmol) was added to a stirring solution of *N*¹,*N*²,di-(2,3,4,6-tetra-*O*-acetyl-β-*D*-galactopyranosyl)-*N*³-hexadecanosyl-5-aminobenzene 1,3,dicarboxamide **4.98** (59 mg, 0.05 mmol) dissolved in DCM/MeOH/H₂O (1 mL/2 mL/1 mL) at 40 °C. The mixture was stirred for 18 h. The reaction mixture was concentrated under reduced pressure and triturated with Et₂O to yield **4.36** as a white solid (10 mg, 93%); [α]²⁵_D = 11.1 (c, 0.72 in MeOH/Pyr); IR ν_{max} (MeOH): 3706.5, 3680.9, 3441.6, 2966.7, 2923.8, 2819.4, 1590.55, 1484.8, 1438.9, 1215.7, 119.1, 1053.8, 1032.9, 997.9 cm⁻¹; ¹H-NMR (300 MHz, *d*₅-Pyr): δ 10.87 (d, *J* = 3.6 Hz, 1 H, NHCOC₁₅H₃₁), 10.41-10.38 (m, 2 H, H₁NHCO), 8.97 (bs, 2 H, Ar), 8.79 (bs, 1 H, Ar), 6.22-6.15 (m, 2 H, *H*-1), 4.76-4.70 (m, 2 H, *H*-2), 4.65-4.60 (m, 2 H, *H*-4), 4.50-4.41 (m, 4 H, overlap of *H*-6, *H*-6'), 4.29-4.25 (m, 4 H, overlap of *H*-3 and *H*-5), 2.53-2.48 (m, 2 H, NHCOCH₂(CH₂)₁₃CH₃), 1.87-1.73 (m, 2 H, NHCOCH₂CH₂(CH₂)₁₂CH₃), 1.41-1.17 (s, 24 H, NHCOCH₂CH₂(CH₂)₁₂CH₃), 0.89-0.81 (m, 3 H, NHCOCH₂CH₂(CH₂)₁₂CH₃); ¹³C NMR (75 MHz, *d*₅-Pyr) δ_c 172.5, 168.7 (CO), 140.9, 137.3 (ArC), 124.1, 122.8 (ArCH), 82.9 (*C*-1), 79.1 (*C*-5), 76.7 (*C*-3), 71.93 (*C*-2), 70.9 (*C*-4), 63.0 (*C*-6), 37.7 (NHCOCH₂(CH₂)₁₃CH₃), 32.4, 30.3, 30.2, 30.1, 30.1, 29.9, 26.3, 23.3 (NHCOCH₂(CH₂)₁₃CH₃), 14.6 (NHCOCH₂(CH₂)₁₃CH₃); HRMS *m/z* (ESI⁺): 742.4099 (C₃₆H₆₀N₃O₁₃: [M+H]⁺ requires 742.4121).



*N*¹, *N*², di-(β-*D*-galactopyranosyl)-*N*³-propyl-5-aminobenzene 1,3, dicarboxamide **4.37**

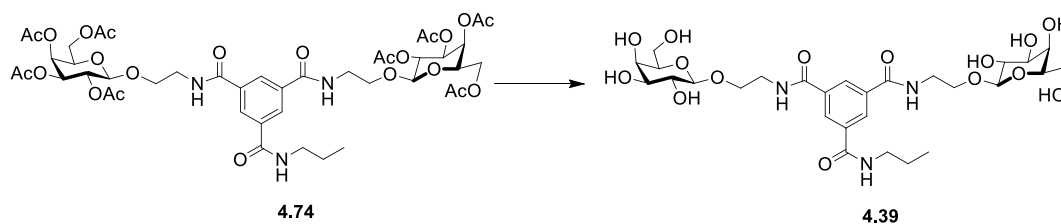
NEt₃ (0.1 mL, 0.016 mmol) was added to a stirring solution *N*¹,*N*²,di-(2,3,4,6-tetra-*O*-acetyl-β-*D*-galactopyranosyl)-*N*³-propyl-5-aminobenzene 1,3, dicarboxamide **4.100** (44 mg, 0.049 mmol) dissolved in DCM/MeOH/H₂O (1 mL/2 mL/1 mL) at 40 °C. The mixture was stirred for 18 h. The reaction mixture was concentrated under reduced pressure to afford the crude mixture which was triturated with Et₂O to yield **4.37** as a white solid (26 mg, 96%); [α]²⁵_D = 10 (c, 1 in MeOH);

$^1\text{H-NMR}$ (300 MHz, $d_5\text{-Pyr}$): δ 10.82-10.80 (m, 1 H, $\text{NHCOCH}_2\text{H}_5$), 10.39 (d, $J = 9.1$ Hz, 2 H, H1NHCO), 8.91 (bs, 2 H, Ar), 8.79 (bs, 1 H, Ar), 6.23-6.17 (m, 2 H, $H-1$), 4.82-4.71 (m, 2 H, $H-2$), 4.65-4.61 (m, 2 H, $H-4$), 4.52-4.43 (m, 4 H, overlap of $H-6$, $H-6'$), 4.30-4.20 (m, 4 H, overlap of $H-3$ and $H-5$), 2.49-2.44 (m, 2 H, $\text{NHCOCH}_2\text{CH}_3$), 0.97 (t, 3 H, $J = 7.1$ Hz, $\text{NHCOCH}_2\text{CH}_3$); $^{13}\text{C NMR}$ (75 MHz, $d_5\text{-Pyr}$) δ_c 173.5, 168.7 (CO), 140.9, 137.3 (ArC), 123.1, 122.8 (ArCH), 82.9 (C-1), 79.1 (C-5), 76.7 (C-3), 71.9 (C-2), 70.9 (C-4), 63.0 (C-6), 30.7 ($\text{NHCOCH}_2\text{CH}_3$), 10.2 ($\text{NHCOCH}_2\text{CH}_3$); HRMS m/z (ESI+): 560.2072 ($\text{C}_{23}\text{H}_{34}\text{N}_3\text{O}_{13}$: $[\text{M}+\text{H}]^+$ requires 560.2086).



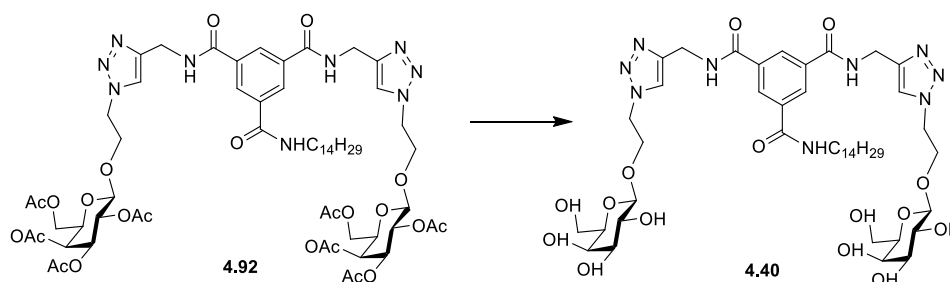
N^1, N^2 , di-[2-*O*-(β -*D*-galactopyranosyl)-ethyl]- N^3 -tetradecyl-benzene 1,3,5 tricarboxamide **4.38**

NEt_3 (0.1 mL, 0.016 mmol) was added to a stirring solution of N^1, N^2 , di-[2-*O*-(2,3,4,6-tetra-*O*-acetyl- β -*D*-galactopyranosyl)-ethyl]- N^3 -tetradecyl-benzene 1,3,5 tricarboxamide **4.29** (19 mg, 0.14 mmol) dissolved in $\text{DCM}/\text{MeOH}/\text{H}_2\text{O}$ (1 mL/2 mL/1 mL) at 40 °C. The mixture was stirred for 18 h. The reaction mixture was concentrated under reduced pressure to afford and triturated with Et_2O to yield **4.38** as a white solid (10 mg, 78%); $[\alpha]_D^{25} = 2.6$ (c, 0.75 in MeOH); $^1\text{H-NMR}$ (300 MHz, $d_5\text{-Pyr}$): δ 9.37-9.34 (m, 1 H, $\text{CONHC}_{14}\text{H}_{29}$), 9.27-9.23 (m, 2 H, $\text{OCH}_2\text{CH}_2\text{NH}$), 9.16 (s, 2 H, Ar), 9.05 (s, 1 H, Ar), 7.38, 6.89, 6.72 and 6.58 (bs, 1 H, OH), 4.85 (d, $J = 7.8$ Hz, 2 H, $H-1$), 4.55-4.42 (m, 8 H, overlap of $H-2$, $H-4$, $H-6$ and $H-6'$), 4.36-4.26 (m, 2 H, 1 H of $\text{OCH}_2\text{CH}_2\text{NH}$), 4.19-4.14 (m, 2 H, $H-3$), 4.12-4.06 (m, 4 H, overlap of 1 H of $\text{OCH}_2\text{CH}_2\text{NH}$ and $H-5$), 3.98-3.84 (m, 4 H, $\text{OCH}_2\text{CH}_2\text{NH}$), 3.72-3.65 (m, 2 H, $\text{NHCH}_2\text{C}_{13}\text{H}_{27}$), 1.78-1.67 (m, 2 H, $\text{NHCH}_2\text{CH}_2\text{C}_{12}\text{H}_{25}$), 1.24 (s, 22 H, $\text{NHC}_2\text{H}_4(\text{CH}_2)_{11}\text{CH}_3$), 0.87 (t, $J = 6.3$ Hz, 3 H, $\text{NHC}_{13}\text{H}_{26}\text{CH}_3$); $^{13}\text{C NMR}$ (75 MHz, $d_5\text{-Pyr}$): δ_c 167.1, 166.9 (CO), 140.9, 136.7 (ArC), 130.0, 129.5 (ArCH), 105.9 (C-1), 77.4 (C-5), 75.6 (C-3), 72.9 (C-2), 70.6 (C-4), 69.5 ($\text{OCH}_2\text{CH}_2\text{NH}$), 62.8 (C-6), 41.4 ($\text{OCH}_2\text{CH}_2\text{NH}$), 32.5 ($\text{NHCH}_2\text{C}_{13}\text{H}_{27}$), 30.4, 30.3, 30.1, 29.9, 23.2 ($\text{NHCOCH}_2(\text{CH}_2)_{12}\text{CH}_3$), 14.7 ($\text{NHCOCH}_2(\text{CH}_2)_{12}\text{CH}_3$); HRMS m/z (ESI+): 662.2754 ($\text{C}_{28}\text{H}_{44}\text{N}_3\text{O}_{15}$: $[\text{M}+\text{H}]^+$ requires 662.2767). HRMS m/z (ESI+): 816.4525 ($\text{C}_{39}\text{H}_{66}\text{N}_3\text{O}_{15}$: $[\text{M}+\text{H}]^+$ requires 816.4488).



*N*¹, *N*², di-[2-*O*-(β-*D*-galactopyranosyl)-ethyl]-*N*³-propyl-benzene 1,3,5 tricarboxamide **4.39**

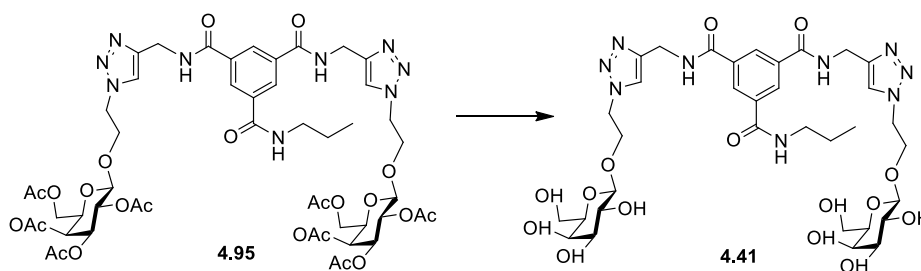
NEt₃ (0.1 mL, 0.016 mmol) was added to a stirring solution of *N*¹,*N*²,di-[2-*O*-(2,3,4,6-tetra-*O*-acetyl-β-*D*-galactopyranosyl)-ethyl]-*N*³-propyl-benzene 1,3,5 tricarboxamide **4.74** (42 mg, 0.42 mmol) dissolved in DCM/MeOH/H₂O (1 mL/2 mL/1 mL) at 40 °C. The mixture was stirred for 18 h. The reaction mixture was concentrated under reduced pressure to afford the crude mixture which was triturated with Et₂O to yield **4.39** as a white solid (26 mg, 96%); [α]²⁵_D = 2.85 (c, 0.7 in MeOH/Pyr); ¹H-NMR (300 MHz, *d*₅-Pyr): δ 9.32-9.22 (m, 3 H, overlap of CONHC₃H₇ and OCH₂CH₂NH), 9.12 (s, 2 H, Ar), 9.05 (s, 1 H, Ar), 4.83 (d, *J* = 7.7 Hz, 2 H, *H*-1), 4.54-4.40 (m, 8 H, overlap of *H*-2, *H*-4, *H*-6 and *H*-6'), 4.33-4.28 (m, 2 H, 1 H of OCH₂CH₂NH), 4.19-4.14 (m, 2 H, *H*-3), 4.08-4.04 (m, 4 H, overlap of 1 H of OCH₂CH₂NH and *H*-5), 3.98-3.81 (m, 4 H, OCH₂CH₂NH), 3.59-3.54 (m, 2 H, NHCH₂C₂H₅), 1.74-1.61 (m, 2 H, NHCH₂CH₂CH₃), 0.87 (t, *J* = 7.1, 3 H, NHC₂H₄CH₃); ¹³C NMR (75 MHz, *d*₅-Pyr): δ_c 167.2, 166.9 (CO), 140.9, 136.7 (ArC), 130.0, 129.5 (ArCH), 105.9 (*C*-1), 77.3 (*C*-5), 75.6 (*C*-3), 72.9 (*C*-2), 70.6 (*C*-4), 69.5 (OCH₂CH₂NH), 62.8 (*C*-6), 42.5 (CONHCH₂C₂H₅), 41.4 (OCH₂CH₂NH), 23.7 (COCH₂CH₂CH₃), 12.0 (NHCOCH₂CH₂CH₃); HRMS *m/z* (ESI⁺): 662.2754 (C₂₈H₄₄N₃O₁₅: [M+H]⁺ requires 662.2767).



*N*¹, *N*², di-[2-*O*-(β-*D*-galactopyranosyl)-ethyl-1,2,3-triazol-4-ylmethylamide]-*N*³-tetradecyl-benzene 1,3,5 tricarboxamide **4.40**

NEt₃ (0.1 mL, 0.016 mmol) was added to a stirring solution of *N*¹,*N*²,di-[2-*O*-(2,3,4,6-tetra-*O*-acetyl-β-*D*-galactopyranosyl)-ethyl-1,2,3-triazol-4-ylmethylamide]-*N*³-tetradecyl-benzene 1,3,5 tricarboxamide **4.92** (40 mg, 0.03 mmol) dissolved in DCM/MeOH/H₂O (1 mL/2 mL/1 mL) at 40 °C. The mixture was stirred for 18 h. The reaction mixture was concentrated under reduced pressure and triturated with Et₂O to give the deprotected glycolipid **4.40** as a white solid (27

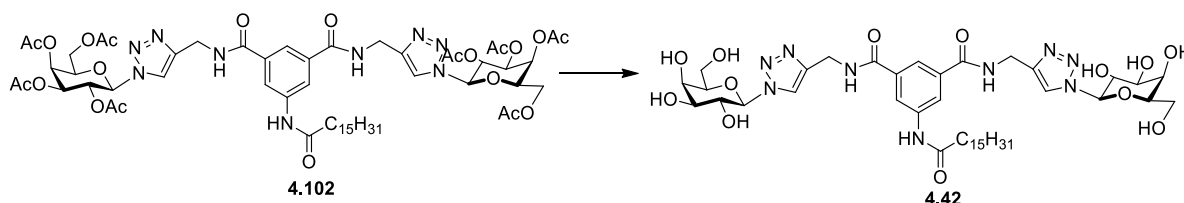
mg, 90%); $[\alpha]_D^{25} = 2.2$ (c, 0.9 in MeOH); $^1\text{H-NMR}$ (300 MHz, d_5 -Pyr): δ 10.20-10.14 (m, 2 H, $\text{NHCH}_2(\text{CCHN}_3)$), 9.38-9.29 (m, 1 H, $\text{CONHC}_{14}\text{H}_{29}$), 9.15 (s, 3 H, Ar), 8.39 (s, 2 H, $\text{NHCH}_2(\text{CCHN}_3)$), 6.96-6.81, 6.66-6.62, 6.53-6.52 (each m, 2 H, OH), 4.95 (d, $J = 5.7$ Hz, 2 H, $\text{CONHCH}_2\text{CN}_3\text{CH}$), 4.77 (d, $J = 7.8$ Hz, 2 H, $H-1$), 4.69-4.64 (m, 4 H, $\text{OCH}_2\text{CH}_2\text{NH}$), 4.57-4.55 (m, 2 H, $H-4$), 4.5-4.33 (m, 8 H, overlap of $\text{OCH}_2\text{CH}_2\text{NH}$, $H-2$, $H-6$ and $H-6'$), 4.18-4.04 (m, 4 H, overlap of $H-5$ and $H-3$), 3.70-3.60 (m, 2 H, $\text{NHCH}_2\text{C}_{13}\text{H}_{27}$), 1.72-1.64 (m, 2 H, $\text{NHCH}_2\text{CH}_2\text{C}_{12}\text{H}_{25}$), 1.24 (s, 22 H, $\text{NHC}_2\text{H}_4(\text{CH}_2)_{11}\text{CH}_3$), 0.89-0.85 (m, 3 H, $\text{NHC}_{13}\text{H}_{26}\text{CH}_3$); $^{13}\text{C NMR}$ (75 MHz, d_5 -Pyr): δ_c 168.1, 167.9 (CO), 146.9 (N_3CCH), 140.9, 136.7 (ArC), 130.9, 130.8 (ArCH), 125.2, (N_3CCH), 105.5 (C-1), 77.5 (C-5), 75.6 (C-3), 72.5 (C-2), 70.5 (C-4), 68.3 ($\text{OCH}_2\text{CH}_2\text{NH}$), 63.6 (C-6), 50.9 ($\text{OCH}_2\text{CH}_2\text{NH}$), 40.8 ($\text{CONHCH}_2\text{C}_{13}\text{H}_{27}$), 36.5 ($\text{CONHCH}_2\text{CN}_3\text{CH}$), 33.4, 30.2, 30.1, 30.0, 29.9, 27.7 ($\text{NHCOCH}_2\text{CH}_2(\text{CH}_2)_{12}\text{CH}_3$), 12.1 ($\text{NHCOCH}_2\text{CH}_2(\text{CH}_2)_{12}\text{CH}_3$); HRMS m/z (ESI+): 978.5149 ($\text{C}_{45}\text{H}_{72}\text{N}_9\text{O}_{15}$: $[\text{M}+\text{H}]^+$ requires 978.5142).



*N*¹, *N*², di-[2-*O*-(β -D-galactopyranosyl)-ethyl-1,2,3-triazol-4-ylmethylamide]-*N*³-propyl-benzene 1,3,5 ticarboxamide **4.41**

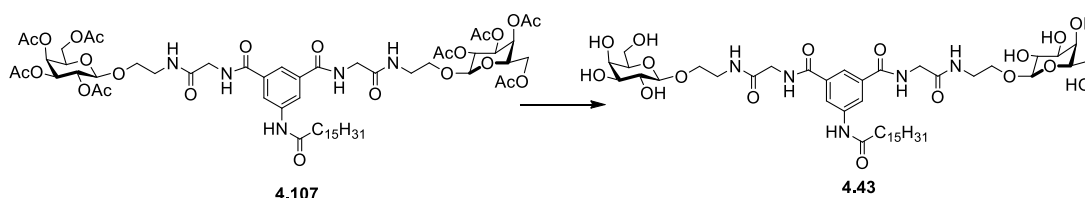
NEt_3 (0.1 mL, 0.016 mmol) was added to a stirring solution of *N*¹,*N*², di-[2-*O*-(2,3,4,6-Tetra-*O*-acetyl- β -D-galactopyranosyl)-ethyl-1,2,3-triazol-4-ylmethylamide]-*N*³-propyl-benzene 1,3,5 ticarboxamide **4.95** (42 mg, 0.036 mmol) dissolved in DCM/MeOH/ H_2O (1 mL/2 mL/1 mL) at 40 °C. The mixture was stirred for 18 h. The reaction mixture was concentrated under reduced pressure to afford the crude mixture which was triturated with Et_2O to yield **4.41** as a white solid (27 mg, 93%); $[\alpha]_D^{25} = 4.2$ (c, 0.95 in MeOH/Pyr); IR ν_{max} (MeOH): 3305.4, 3072.5, 2885.4, 1650.4, 1541.8, 1026.5, 636.8 cm^{-1} ; $^1\text{H-NMR}$ (300 MHz, d_5 -Pyr): δ 10.28-10.05 (m, 2 H, $\text{CONHCH}_2\text{CN}_3\text{CH}$), 9.29-9.24 (m, 1 H, CONHC_3H_7), 9.14-9.08 (m, 3 H, Ar), 8.41-8.36 (m, 2 H, N_3CCH), 4.94 (d, $J = 5.4$ Hz, 4 H, $\text{CONHCH}_2\text{CN}_3\text{CH}$), 4.75 (d, $J = 7.7$ Hz, 2 H, $H-1$), 4.70-4.62 (m, 4 H, $\text{OCH}_2\text{CH}_2\text{NH}$), 4.56-4.51 (m, 2 H, $H-4$), 4.48-4.31 (m, 8 H, overlap of $\text{OCH}_2\text{CH}_2\text{NH}$, $H-2$, $H-6$ and $H-6'$), 4.15-4.11 (m, 2 H, $H-3$), 4.06-4.02 (m, 2 H, $H-5$), 3.58-3.52 (m, 2 H, $\text{NHCH}_2\text{C}_2\text{H}_5$), 1.69-1.57 (m, 2 H, $\text{NHCH}_2\text{CH}_2\text{CH}_3$), 0.86-0.81 (m, 3 H, $\text{NHC}_2\text{H}_4\text{CH}_3$); $^{13}\text{C NMR}$ (75 MHz, d_5 -Pyr): δ_c 167.2, 166.0 (CO), 146.0 (N_3CCH), 140.9, 136.7 (ArC), 130.1, 129.9 (ArCH), 125.2, 124.3

(N_3CCH), 105.5 ($C-1$), 77.5 ($C-5$), 75.6 ($C-3$), 72.6 ($C-2$), 70.5 ($C-4$), 68.4 (OCH_2CH_2NH), 50.9 (OCH_2CH_2NH), 62.7 ($C-6$), 42.5 ($CONHCH_2C_2H_5$), 36.5 ($CONHCH_2CN_3CH$), 23.7 ($COCH_2CH_2CH_3$), 12.0 ($NHCOCH_2CH_2CH_3$); HRMS m/z (ESI+): 824.3417 ($C_{34}H_{50}N_9O_{15}$: $[M+H]^+$ requires 824.3421).



*N*¹, *N*², di-(β-*D*-galactopyranosyl-1,2,3-triazol-4-ylmethylamide)-*N*³-hexadecanosyl-5-aminobenzene 1,3, dicarboxamide **4.42**

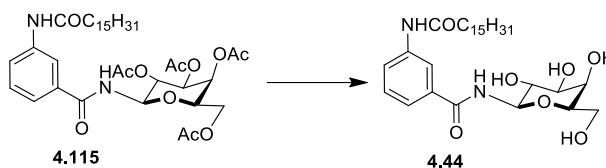
NEt_3 (0.1 mL, 0.016 mmol) was added to a stirring solution of *N*¹, *N*², di-(2,3,4,6-Tetra-*O*-acetyl-β-*D*-galactopyranosyl-1,2,3-triazol-4-ylmethylamide)-*N*³-hexadecanosyl-5-aminobenzene 1,3, dicarboxamide **4.102** (70 mg, 0.056 mmol) dissolved in DCM/MeOH/ H_2O (1 mL/2 mL/1 mL) at 40 °C. The mixture was stirred for 18 h. The reaction mixture was concentrated under reduced pressure to afford the crude mixture which was triturated with Et_2O to yield **4.42** as a white solid (50 mg, 98%); $[\alpha]_D^{25} = 5.4$ (c, 1.1 in MeOH); 1H -NMR (300 MHz, d_5 -Pyr): δ 11.08 (s, 1 H, $NHCOC_{15}H_{31}$), 10.13 (t, $J = 5.6$ Hz, 2 H, $CONHCH_2CN_3CH$), 8.98 (bs, 3 H, Ar), 8.45 (bs, 2 H, N_3CCH), 6.29 (d, $J = 9.1$ Hz, 2 H, $H-1$), 5.10-5.06 (m, 2 H, $H-2$), 4.93 (d, $J = 5.4$ Hz, 4 H, $CONHCH_2CN_3CH$), 4.68 (d, $J = 3.0$ Hz, 2 H, $H-4$), 4.52-4.6 (m, 8 H, overlap of $H-3$, $H-5$, $H-6$ and $H-6'$), 2.50 (t, $J = 7.2$ Hz, 2 H, $NHCOCH_2C_{14}H_{29}$), 1.85-1.78 (m, 26 H, $NHCO(CH_2)_{13}CH_3$), 0.88-0.84 (m, 3 H, $NHCOCH_2(CH_2)_{13}CH_3$); ^{13}C NMR (75 MHz, d_5 -Pyr): δ_c 167.6 (CO), 146.5 (N_3CCH), 140.9, 136.7 (ArC), 130.1, 129.9 (ArCH), 124.7 (N_3CCH), 80.9 ($C-1$), 78.3 ($C-5$), 76.1 ($C-3$), 71.6 ($C-2$), 70.5 ($C-4$), 62.8 ($C-6$), 37.8, 36.4 ($CONHCH_2CN_3CH$ and $NHCOCH_2C_{15}H_{31}$), 32.5, 30.3, 29.9, 23.3 ($NHCOCH_2(CH_2)_{13}CH_3$), 14.8 ($NHCOCH_2(CH_2)_{13}CH_3$); HRMS m/z (ESI+): 904.4758 ($C_{42}H_{66}N_9O_{13}$: $[M+H]^+$ requires 904.4775).



*N*¹, *N*², di-[2-*O*-(β-*D*-galactopyranosyl)-ethyl-glycine]-*N*³-hexadecanosyl-5-aminobenzene 1,3, dicarboxamide **4.43**

NEt_3 (0.1 mL, 0.016 mmol) was added to a stirring solution of *N*¹, *N*², di-[2-*O*-(2,3,4,6-tetra-*O*-acetyl-β-*D*-galactopyranosyl)-ethyl-glycine]-*N*³-hexadecanosyl-5-aminobenzene 1,3,

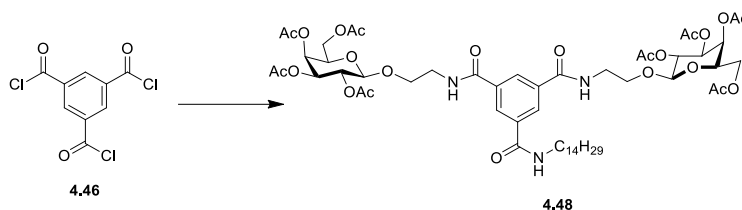
dicarboxamide **4.107** (30 mg, 0.023 mmol) dissolved in DCM/MeOH/H₂O (1 mL/2 mL/1 mL) at 40 °C. The mixture was stirred for 18 h. The reaction mixture was concentrated under reduced pressure to afford the crude mixture which was triturated with Et₂O to yield **4.43** as a white solid (20 mg, 91%); $[\alpha]_D^{25} = 6.4$ (c, 0.75 in DCM); ¹H-NMR (300 MHz, *d*₅-Pyr): δ 10.95 (bs, 1 H, NHCOCH₂H₃₁), 9.69-9.67 (m, 2 H, NHCOCH₂NHCO), 8.94 (s, 3 H, Ar), 8.86 (t, *J* = 5.34 Hz, 2 H, NHCOCH₂NHCO), 4.79 (d, *J* = 7.8 Hz, 1 H, *H*-1), 4.53-4.37 (m, 10 H, overlap of *H*-2, *H*-3, *H*-4, *H*-6 and *H*-6', NHCOCH₂NHCO), 4.20-4.13 (m, 2 H, 1 H of OCH₂CH₂NH), 4.08-4.04 (m, 2 H, *H*-5), 3.99-3.92 (m, 2 H, 1 H of OCH₂CH₂NH), 3.76-3.69 (m, 4 H, OCH₂CH₂NH), 1.84-1.77 (m, 2 H, NHCOCH₂C₁₄H₂₉), 1.40-1.18 (m, 26 H, NHCOCH₂(CH₂)₁₃CH₃), 0.87 (t, *J* = 6.3 Hz, 3 H, NHCOCH₂C₁₄H₂₉); ¹³C NMR (75 MHz, CDCl₃): δ_c 172.9, 171.3, 169.1, 168.3, 167.5 (each CO), 141.1, 140.2 (ArC), 122.8, 121.9 (ArCH), 105.9 (C-1), 77.4 (C-5), 75.6 (C-3), 72.9 (C-2), 70.6 (C-4), 69.7 (OCH₂CH₂NH), 62.8 (C-6), 43.5 (NHCOCH₂NHCO), 40.4 (OCH₂CH₂NH), 37.8 (NHCOCH₂C₁₄H₂₉), 32.4, 30.2, 30.0, 29.8, 26.3, 23.2 (NHCOCH₂(CH₂)₁₃CH₃), 14.5 (NHCOCH₂(CH₂)₁₃CH₃); HRMS *m/z* (ESI+): 966.4912 (C₄₄H₇₃N₅NaO₁₇: [M+Na]⁺ requires 966.4894).



*N*¹-(β-D-galactopyranosyl)-*N*²-hexadecanosyl-3-aminobenzene 1-carboxamide **4.44**

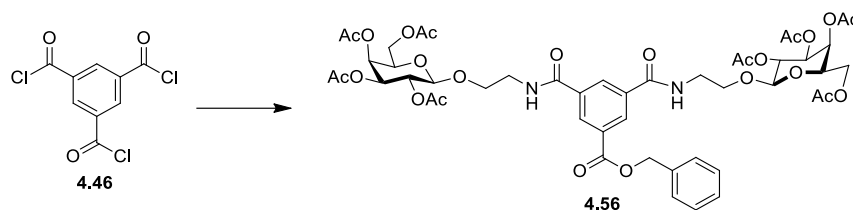
NEt₃ (0.1 mL, 0.016 mmol) was added to a stirring solution of *N*¹-(2,3,4,6-tetra-*O*-acetyl-β-D-galactopyranosyl)-*N*²-hexadecanosyl-3-aminobenzene 1-carboxamide **4.115** (50 mg, 0.07 mmol) dissolved in DCM/MeOH/H₂O (1 mL/2 mL/1 mL) at 40 °C. The mixture was stirred for 18 h. The reaction mixture was concentrated under reduced pressure and triturated with Et₂O and DCM to yield **4.44** as a white solid (35 mg, 92%); $[\alpha]_D^{25} = 2$ (c, 1 in MeOH); ¹H-NMR (300 MHz, *d*₅-Pyr): δ 10.88 (bs, 1 H, NHCOCH₂H₃₁), 10.23 (d, *J* = 9.2 Hz, 1 H, H1NHCO), 8.83 (bs, 1 H, Ar), 8.35-8.32 (m, 1 H, Ar), 7.98-7.95 (m, 1 H, Ar), 7.40-7.35 (m, 1 H, Ar), 6.22 (t, *J* = 9.1 Hz, 1 H, *H*-1), 4.74 (t, *J* = 9.1 Hz, 1 H, *H*-2), 4.65 (d, *J* = 2.7 Hz, 1 H, *H*-4), 4.52-4.46 (m, 2 H, overlap of *H*-6, *H*-6'), 4.30-4.22 (m, 2 H, overlap of *H*-3 and *H*-5), 2.53 (t, *J* = 7.3 Hz, 2 H, NHCOCH₂(CH₂)₁₃CH₃), 1.89-1.79 (m, 2 H, NHCOCH₂CH₂(CH₂)₁₂CH₃), 1.35-1.25 (m, 24 H, NHCOCH₂CH₂(CH₂)₁₂CH₃), 0.87 (t, *J* = 6.4 Hz, 3 H, NHCOCH₂CH₂(CH₂)₁₂CH₃); ¹³C NMR (75 MHz, *d*₅-Pyr): δ_c 172.5, 168.9 (CO), 141.1, 137.2 (ArC), 129.3, 120.4 (ArCH), 82.9 (C-1), 79.1 (C-5), 76.7 (C-3), 72.2 (C-2), 70.9 (C-4), 63.0 (C-6), 37.7 (NHCOCH₂(CH₂)₁₃CH₃), 32.4, 30.3, 30.2, 30.1, 30.1,

29.9, 26.3, 23.3 (NHCOCH₂(CH₂)₁₃CH₃), 14.6 (NHCOCH₂(CH₂)₁₃CH₃); HRMS m/z (ESI⁺): 537.3524 (C₂₉H₄₉N₂O₇: [M+H]⁺ requires 537.3534).



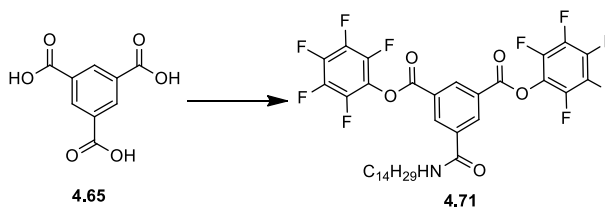
*N*¹, *N*², di-[2-*O*-(2,3,4,6-tetra-*O*-acetyl-β-*D*-galactopyranosyl)-ethyl]-*N*³-tetradecyl-Benzene 1,3,5-tricarboxamide **4.48**

Tetradecylamine (63 mg, 0.29 mmol) and NEt₃ (0.049 mL, 0.35 mmol) dissolved in THF (15 mL) under Ar, was added dropwise over 3 h to 1,3,5-trichloride, tri carbonyl benzene **4.46** (0.052 mL, 0.293 mmol) in THF (37 mL). This mixture was allowed to stir for 3h. 2-Aminoethyl 2,3,4,6-tetra-*O*-acetyl-β-*D*-galactopyranoside **2.33** (230 mg, 0.587 mmol) and NEt₃ (0.09 mL, 0.646 mmol) dissolved in THF (3 mL) was added quickly to the solution. The reaction was left stirring overnight. The solvent was removed under reduced pressure, the residue dissolved in DCM and washed with 0.1 M HCl, aqueous sat. NaHCO₃ solution, brine and dried over MgSO₄. Flash chromatography (9:1, Ethyl Acetate, Hexane) afforded the pure product **4.48** as a white solid (27 mg, 8%); R_f = 0.23 (8:2, Pet Ether:EtOAc); [α]_D²⁵ = -10.5 (c, 0.95 in DCM); IR ν_{max} (NaCl plate, DCM): 3373.6, 2926.2, 2854.7, 1751.2, 1659.4, 1536.2, 1518.6, 1433.3, 1370.4, 1226.5, 1173.3, 1134.4 and 1060.07 cm⁻¹; ¹H NMR (300 MHz, CDCl₃): δ 8.65 (s, 3 H, Ar), 7.07 (t, *J* = 5.1 Hz, 2 H, OCH₂CH₂NH), 6.83 (t, *J* = 5.4 Hz, 1 H, CONHC₁₄H₂₉), 5.39-5.37 (m, 2 H, *H*-4), 5.21 (dd, *J* = 8.1 Hz, *J* = 10.5 Hz, 2 H, *H*-2), 5.02 (dd, *J* = 3.6 Hz, *J* = 10.5, 2 H, *H*-3), 4.50 (d, *J* = 8.1 Hz, 2 H, *H*-1), 4.12-4.09 (m, 4 H, *H*-6 and *H*-6'), 4.01-3.85 (m, 4 H, overlap of *H*-5 and 1 H of OCH₂CH₂NH), 3.85-3.65 (m, 6 H, overlap of 1 H of OCH₂CH₂NH and OCH₂CH₂NH), 3.45- 3.42 (m, 2 H, NHCH₂C₁₃H₂₇), 2.17 (s, 6 H, O(CO)CH₃), 1.98 (s, 12 H, O(CO)CH₃), 1.91 (s, 6 H, O(CO)CH₃), 1.62-1.57 (m, 2 H, NHCH₂CH₂C₁₂H₂₅), 1.24 (s, 22 H, NHC₂H₄(CH₂)₁₁CH₃), 0.86 (t, *J* = 6.9 Hz, 3 H, NHC₁₃H₂₆CH₃); ¹³C NMR (75 MHz, *d*₅-Pyr): δ_c 170.4, 170.3 and 170.1 (OCOCH₃), 165.7 (OCH₂CH₂NHCO) 165.0 (CONHC₁₄H₂₉), 135.7, 134.9 (ArC), 128.5, 128.7 (ArCH), 101.3 (*C*-1), 70.9 (*C*-5), 70.6 (*C*-3), 69.0 (*C*-2) 68.5 (OCH₂CH₂NH), 66.9 (*C*-4), 61.3 (*C*6), 40.4 (NHCH₂C₁₃H₂₇), 39.9 (OCH₂CH₂NH), 31.9, 29.7, 29.6, 29.5, 29.4, 27.0 and 22.7 (NHCH₂(CH₂)₁₂CH₃), 20.7, 20.7, 20.6, 20.6 (O(CO)CH₃), 14.1 (NHC₁₃H₂₆CH₃); HRMS m/z (ESI⁺): 1152.5291 (C₅₅H₈₁N₃O₂₃: [M+H]⁺ requires 1152.5334).



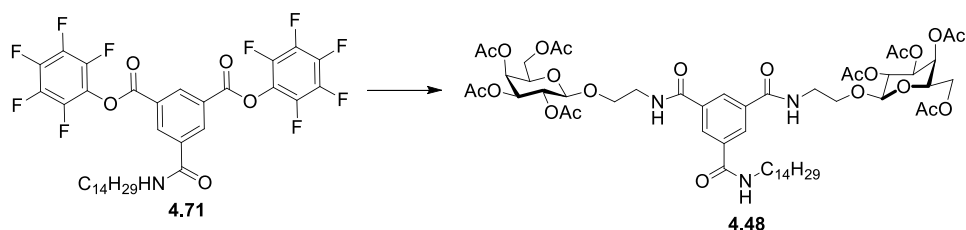
*N*¹, *N*², di-[2-*O*-(2,3,4,6-tetra-*O*-acetyl-β-*D*-galactopyranosyl)-ethyl]-*O*-benzoate-Benzene 1,3, dicarboxamide **4.56**

Benzyl alcohol (0.042 mL, 0.295 mmol) and DIPEA (0.056 mL, 0.322 mmol) dissolved in THF (8 mL) under Ar, were added dropwise over 3h to 1,3,5-benzenetricarbonyl, trichloride **4.46** (0.052 mL, 0.293 mmol) in THF (3.5 mL). This mixture was allowed to stir for 3h. 2-*O*-(2,3,4,6-tetra-*O*-acetyl- β-*D*-galactopyranosyl)-ethyl **2.33** (0.229 g, 0.587 mmol) and DIPEA (0.112 mL, 0.646 mmol) dissolved in THF (3 mL) were added quickly to the solution. The reaction was left stirring overnight. The solvent was removed under reduced pressure, the residue dissolved in DCM and washed with 0.1 M HCl, aqueous sat. NaHCO₃ solution, brine and dried over MgSO₄. Flash chromatography (9:1, Ethyl Acetate, Hexane) afforded the pure product **4.56** as a white solid (22 mg, 7%); *R*_f = 0.57 (1:1, Pet Ether:EtOAc); [α]²⁵_D = -3.6 (c, 0.55 in DCM); IR *v*_{max} (NaCl plate, DCM): 3391.9, 1749.3, 1659.5, 1536.1, 1432.6, 1370.2, 1225.4 cm⁻¹; ¹H NMR (300 MHz, CDCl₃): δ 8.65 (d, *J* = 1.8 Hz, 2 H, Ar), 8.43-8.42 (m, 1 H, Ar), 7.46-7.33 (m, 5 H, Ar), 7.06 (t, *J* = 5.4 Hz, 2 H, NH), 5.39 (bs, 4 H, overlapping of *H*-4 and CH₂Ph), 5.20 (dd, *J* = 7.8 Hz, *J* = 10.5 Hz, 2 H, *H*-2), 5.05 (dd, *J* = 3.6 Hz, *J* = 10.5 Hz, 2 H, *H*-3), 4.49 (d, *J* = 6 Hz, 2 H, *H*-1), 4.12-4.09 (m, 4 H, overlap of *H*-6, *H*-6'), 4.01-3.85 (m, 6 H, overlap of *H*-5 and OCH₂CH₂NH), 3.79-3.66 (m, 4 H, OCH₂CH₂NH), 2.16, 1.98, 1.97, 1.90 (each s, 6 H, O(CO)CH₃); ¹³C NMR (75 MHz, CDCl₃): δ_c 170.4, 170.3, 170.1, 170.1 (OCOCH₃), 165.5 (CH₂NHCO) 165.0 (COOCH₂), 135.4, 135.0 (ArC), 131.4, 131.3 (ArCH), 129.4, 128.7, 128.45 (CH-Ph), 101.4 (*C*-1), 70.9 (*C*-5), 70.7 (*C*-3), 68.9 (*C*-2), 68.6 (OCH₂CH₂NH), 67.4 (CH₂Ph), 66.9 (*C*-4), 61.3 (*C*-6), 39.9 (OCH₂CH₂NH), 20.7, 20.7, 20.6, 20.6 (O(CO)CH₃); HRMS *m/z* (ESI⁺): 1047.3503 (C₄₈H₅₈N₂O₂₄: [M+H]⁺ requires 1047.3452).



*O*¹, *O*²-di[(2,3,4,5,6-pentafluorophenyl)ester], *N*³-tetradecylamide-benzene 1,3 dicarboxylic acid
4.71

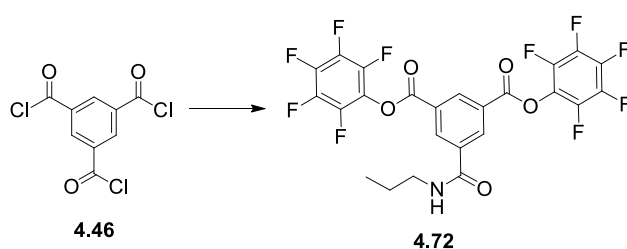
Trimesic acid **4.65** (200 mg, 0.9 mmol), HOBt (128 mg, 0.9 mmol) and TBTU (305 mg, 0.9 mmol) was placed under N₂ and dissolved in DMF (20 mL). NEt₃ (0.16 mL, 1.1 mmol) was added dropwise and the mixture was allowed to stir for 15 min. Tetradecylamine (243 mg, 1.1 mmol) dissolved in DMF (15 mL) was then added. The solution was stirred overnight. The solvent was removed under reduced pressure, and the residue dissolved in MeOH and dried over MgSO₄ to yield a cream solid as the crude product. The crude solid (225 mg, 0.48 mmol) and pentafluorophenol (265 mg, 1.4 mmol) were dissolved in THF (2 mL) under N₂ with 4 Å MS. The solution was placed on ice and DIC (0.30 mL, 1.9 mmol) was added. The mixture was allowed to stir at 0 °C for 1 h and at rt for a further 2 h. The solvent was removed under reduced pressure and gradient elution chromatography (95:5, Pet Ether:EtOAc- 80:20, Pet Ether:EtOAc) afforded the pure product **4.71** as a white solid (84 mg, 24%); R_f = 0.22 (1:1, Pet Ether:EtOAc); mp = 159-161 °C; IR ν_{max} (NaCl plate, DCM): 3285.1, 2921.1, 2852.8, 1765.1, 1645.1, 1546.2, 1519.4, 1470.2, 1278.4, 1196.2, 1152.8, 1099.8 cm⁻¹; ¹H NMR (300 MHz, CDCl₃): δ 9.09 (s, 1 H, Ar), 8.88 (s, 2 H, Ar), 6.46 (t, *J* = 5.4, 1 H, CONHC₁₄H₂₉), 3.52 (q, *J* = 2.3 Hz, 2 H, NHCH₂C₁₃H₂₇), 1.71-1.62 (m, 2 H, NHCH₂CH₂C₁₂H₂₅), 1.24 (s, 22 H, NHC₂H₄(CH₂)₁₁CH₃), 0.86 (t, *J* = 6.6 Hz, 3 H, NHC₁₃H₂₆CH₃); ¹³C NMR (75 MHz, CDCl₃): δ_c 164.5, 160.9 (CO), 139.6, 138.3 (ArC of C₆F₅) 136.9 (ArC of C₆H₃), 134.8, 134.5 (ArCH of C₆H₃), 128.7 (ArC of C₆H₃), 40.7 (NHCH₂C₁₃H₂₇), 31.9, 29.7, 29.6, 29.6, 29.5, 29.4, 29.3, 27.0, 22.7 (NHCH₂(CH₂)₁₂CH₃), 14.1 (NHC₁₃H₂₆CH₃); HRMS *m/z* (ESI⁺): 754.2256 (C₃₅H₃₄F₁₀NO₆: [M+H]⁺ requires 754.377).



$N^1, N^2, di-[2-O-(2,3,4,6-tetra-O-acetyl-\beta-D-galactopyranosyl)-ethyl]-N^3-tetradecyl-benzene$ 1,3,5 tricarboxamide **4.48**

O^1, O^2 -di[(2,3,4,5,6-pentafluorophenyl)ester], N -tetradecylamide-benzene 1,3 dicarboxylic acid **4.71** (75 mg, 0.1 mmol), was dissolved in THF (5 mL) under N_2 with 4Å molecular sieves. 2-Aminoethyl 2,3,4,6-tetra- O -acetyl- β -D-galactopyranoside **2.33** (120 mg, 0.3 mmol) dissolved in THF (5 mL) under N_2 and NEt_3 (0.042 ml, 0.3 mmol) was added and the reaction mixture stirred at rt overnight. The solvent was removed *in vacuo* and the resulting residue purified by flash chromatography (80:20 EtOAc: Pet Ether) to yield compound **4.48** as a clear oily solid (56 mg, 47%).

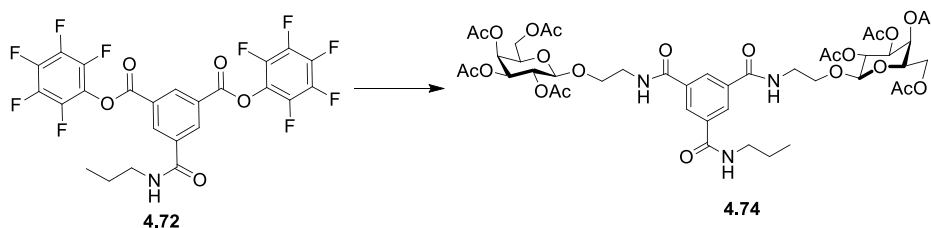
Characterisation as stated previously (pg 229)



$O^1, O^2, di-[(2,3,4,5,6-pentafluorophenyl)ester]-N^3-propyl-benzene$ 1,3, dicarboxylic acid **4.72**

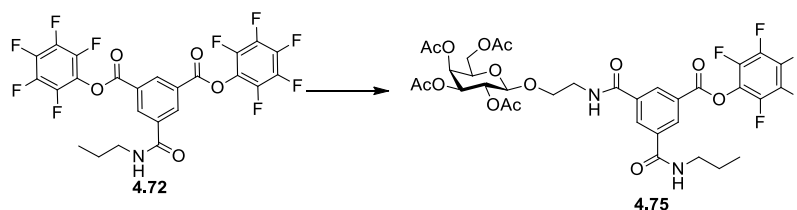
Propylamine (0.092 mL, 1.1 mmol) and DIPEA (0.214 mL, 1.2 mmol) dissolved in THF (10 mL) under Ar, were added dropwise over 3.5 h to 1,3,5- benzenetricarbonyl trichloride **4.46** (0.200 mL, 1.1 mmol) in THF (10 mL). Pentafluorophenol (0.143 mL, 2.2 mmol) and DIPEA (0.427 mL, 2.6 mmol) dissolved in THF (4 mL) were added quickly to the solution. The reaction was left stirring overnight. The solvent was removed under reduced pressure, the residue dissolved in DCM and washed with 1 M HCl, aqueous sat. $NaHCO_3$ solution, brine and dried over $MgSO_4$. Flash chromatography (10:1-1:1, EtOAc:Pet Ether) and recrystallisation in ethyl acetate afforded the pure product **4.72** as a white solid (135 mg, 20%); $R_f = 0.67$ (1:1, EtOAc: Pet Ether); IR ν_{max} (KBr Disc): 3427.0, 2094.9, 1765.7, 1645.3, 1519.4, 1274.4, 1196.5, 1150.3, 1078.0, 995.4 cm^{-1} ; 1H NMR (300 MHz, $CDCl_3$): δ 9.09 (t, $J = 1.8$ Hz, 1 H, Ar), 8.88 (s, 2 H, Ar), 6.38 (bs, 1 H, $CONHC_3H_7$), 3.5-3.46 (m, 2 H, $NHCH_2C_2H_5$), 1.71-1.62 (m, 2 H, $NHCH_2CH_2CH_3$),

1.02 (t, $J = 7.2$ Hz, 3 H, $\text{NHC}_2\text{H}_4\text{CH}_3$); ^{13}C NMR (75 MHz, CDCl_3): δ_{c} 164.4, 160.9 (CO), 139.6, 138.3 (ArC of C_6F_5) 136.9 (ArC), 134.8, 134.4 (ArCH), 128.7 (ArC), 42.3 (NHCH_2), 22.8 (NHCH_2CH_2), 11.4 ($\text{NHCH}_2\text{CH}_2\text{CH}_3$); HRMS m/z (ESI+): 600.0562 ($\text{C}_{24}\text{H}_{12}\text{F}_{10}\text{NO}_6$: $[\text{M}-\text{H}, +\text{H}_2\text{O}]^-$ requires 600.0589) or HRMS m/z (ESI+): 252.0871 ($\text{C}_{12}\text{H}_{14}\text{NO}_5$: $[\text{M}+\text{H}, -\text{PFP ester}]^+$ requires 252.0866).



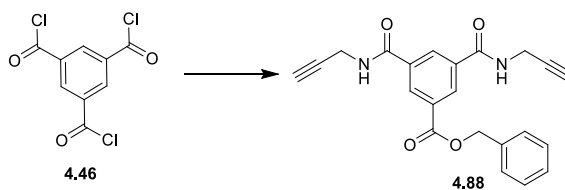
N^1, N^2 , di-[2-*O*-(2,3,4,6-tetra-*O*-acetyl- β -*D*-galactopyranosyl)-ethyl]- N^3 -propyl-benzene 1,3,5 tricarboxamide **4.74**

O^1, O^2 , di-[(2,3,4,5,6-pentafluorophenyl)ester]- N^3 -propyl-benzene 1,3, dicarboxylic acid **4.72** (63 mg, 0.1 mmol), was dissolved in THF (5 mL) under N_2 with 4Å molecular sieves. 2-Aminoethyl 2,3,4,6-tetra-*O*-acetyl- β -*D*-galactopyranoside **2.33** (105 mg, 0.27 mmol) dissolved in THF (5 mL) under N_2 and DIPEA (0.047 ml, 0.27 mmol) was added and the reaction mixture was stirred at rt overnight. The solvent was removed *in vacuo* and the resulting residue purified by flash chromatography (1:1 EtOAc:Pet Ether) to yield compound **4.74** as a clear oil that turned into a solid (43 mg, 40%); $R_f = 0.42$ (EtOAc); $[\alpha]_{\text{D}}^{25} = 7.2$ (c, 1 in DCM); IR ν_{max} (NaCl plate, DCM): 3374.9, 2964.5, 2937.9, 2879.5, 1750.8, 1659.2, 1535.5, 1518.5, 1431.6, 1370.2, 1226.9, 1173.3, 1134.6, 1059.5 cm^{-1} ; ^1H NMR (300 MHz, CDCl_3): δ 8.38-8.36 (m, 3 H, Ar), 7.09 (t, $J = 5.1$ Hz, 2 H, $\text{OCH}_2\text{CH}_2\text{NH}$), 6.83 (t, $J = 5.4$ Hz, 1 H, NHC_3H_7), 5.37 (m, 2 H, *H*-4), 5.14 (dd, $J = 8.1$ Hz, $J = 10.5$ Hz, 2 H, *H*-2), 5.01 (dd, $J = 3.3$ Hz, $J = 10.5$, 2 H, *H*-3), 4.50 (d, $J = 7.8$ Hz, 2 H, *H*-1), 4.13-4.03 (m, 4 H, *H*-6 and *H*-6'), 3.99-3.89 (m, 4 H, overlap of *H*-5 and 1 H of $\text{OCH}_2\text{CH}_2\text{NH}$), 3.85-3.63 (m, 6H, overlap of $\text{OCH}_2\text{CH}_2\text{NH}$ and 1 H of $\text{OCH}_2\text{CH}_2\text{NH}$), 3.46- 3.36 (m, 2 H, $\text{NHCH}_2\text{C}_2\text{H}_5$), 2.15 (s, 6 H, $\text{O}(\text{CO})\text{CH}_3$), 1.97 (s, 12 H, $\text{O}(\text{CO})\text{CH}_3$), 1.91 (s, 6 H, $\text{O}(\text{CO})\text{CH}_3$), 1.65-1.58 (m, 2 H, $\text{NHCH}_2\text{CH}_2\text{CH}_3$), 0.95 (t, $J = 7.5$ Hz, 3 H, $\text{NHC}_2\text{H}_4\text{CH}_3$); ^{13}C NMR (75 MHz, CDCl_3): δ_{c} 170.4, 170.3, 170.0 (OCOCH_3), 165.8, 165.0 (CO), 135.6, 134.9 (*C*-Ar), 128.5, 128.3 (*CH*-Ar), 101.3 (*C*-1), 70.9 (*C*-5), 70.6 (*C*-3), 69.1 (*C*-2) 68.4 ($\text{OCH}_2\text{CH}_2\text{NH}$), 66.9 (*C*-4), 61.3 (*C*-6), 40.4 ($\text{NHCH}_2\text{C}_2\text{H}_5$), 39.9 ($\text{OCH}_2\text{CH}_2\text{NH}$), 22.7 ($\text{NHCH}_2\text{CH}_2\text{CH}_3$), 20.7, 20.6, 20.5, 20.6 ($\text{O}(\text{CO})\text{CH}_3$), 11.4 ($\text{NHC}_2\text{H}_4\text{CH}_3$); HRMS m/z (ESI+): 998.3652 ($\text{C}_{44}\text{H}_{60}\text{N}_3\text{O}_{23}$: $[\text{M}+\text{H}]^+$ requires 998.3652).



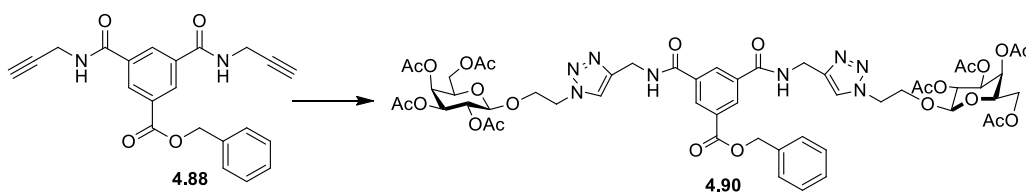
*N*¹-[2-*O*-(2,3,4,6-tetra-*O*-acetyl-β-*D*-galactopyranosyl)-ethyl]-*N*³-propyl-*O*-[(2,3,4,5,6-pentafluorophenyl)ester]-benzene 1,5 dicarboxamide **4.75**

*O*¹,*O*²,di-[(2,3,4,5,6-pentafluorophenyl)ester]-*N*³-propyl-benzene 1,3, dicarboxylic acid **4.72** (207 mg, 0.35 mmol), was dissolved in THF (7 mL) under Ar and 2-aminoethyl 2,3,4,6-tetra-*O*-acetyl-β-*D*-galactopyranoside **2.33** (173 mg, 0.44 mmol) dissolved in THF (5 mL) under Ar was added. The reaction mixture was stirred for 5 min and DIPEA (0.077 ml, 0.44 mmol) was added. The resulting solution was stirred at rt overnight. The solvent was removed *in vacuo* and the resulting residue purified by flash chromatography (1:1 EtOAc: Pet Ether) to yield compound **4.75** as an clear waxy solid (101 mg, 36%); *R*_f = 0.75 (EtOAc); [α]²⁵_D = -8.7 (c, 1.15 in DCM); IR *v*_{max} (NaCl plate, DCM): 3343.6, 3078.0, 2966.4, 2938.6, 2878.8, 1754.4, 1656.7, 1522.5, 1439.7, 1370.4, 1232.2, 1162.3, 1080.8, 1061.4, 995.9, 956.5, 916.5, 801.7, 735.1, 706.3, 677.1, 629.3 cm⁻¹; ¹H NMR (300 MHz, CDCl₃): δ 8.78-8.76 (m, 2 H, Ar), 8.49 (s, 1 H, Ar), 6.95 (t, *J* = 5.4 Hz, 2 H, CONHC₃H₇), 5.38 (d, *J* = 2.7, 1 H, *H*-4), 5.20 (dd, *J* = 7.8 Hz, *J* = 10.5 Hz, 1 H, *H*-2), 5.02 (dd, *J* = 3.3 Hz, *J* = 10.5, 1 H, *H*-3), 4.50 (d, *J* = 7.8 Hz, 1 H, *H*-1), 4.16-4.02 (m, 2 H, *H*-6 and *H*-6'), 3.95-3.90 (m, 2 H, overlap of *H*-5 and 1 H of OCH₂CH₂NH) 3.8-3.62 (m, 3 H, overlap of 1 H of OCH₂CH₂NH and OCH₂CH₂NH), 3.45- 3.40 (m, 2 H, NHCH₂C₂H₅), 2.14, 2.02, 1.97, 1.93 (each s, 3 H, O(CO)CH₃), 1.68-1.61 (m, 2 H, NHCH₂CH₂CH₃), 0.98 (t, *J* = 7.2 Hz, 3 H, NHC₂H₄CH₃); ¹³C NMR (75 MHz, CDCl₃): δ_c 171.3 (CO), 170.5, 170.4, 170.3, 170.0 (OCOCH₃), 165.1, 161.15 (CO), 142.8, 139.7 (ArC of C₆F₅), 136.2, 135.4 (ArC), 132.4, 131.9, 130.6 (ArCH), 128.1 (ArC), 101.3 (C-1), 70.9 (C-5), 70.5 (C-3), 69.2 (C-2) 68.4 (OCH₂CH₂NH), 66.9 (C-4), 61.3 (C-6), 42.1 (NHCH₂C₂H₅), 39.9 (OCH₂CH₂NH), 22.7 (NHCH₂CH₂CH₃), 21.1, 20.8, 20.6, 20.5 (O(CO)CH₃), 11.4 (NHC₂H₄CH₃).



*N*¹, *N*², di-(propargyl)-*O*-benzoate-benzene 1,3, dicarboxamide **4.88**

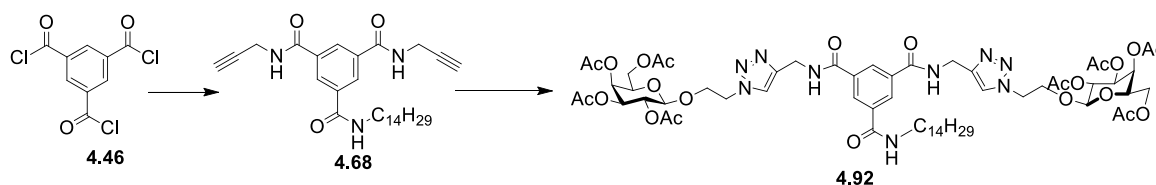
Benzyl alcohol (0.291 mL, 2.8 mmol) and DIPEA (0.538 mL, 3.0 mmol) dissolved in THF (50 mL) under Ar, was added dropwise over 3 h to 1,3,5- benzenetricarbonyl trichloride **4.46** (0.5 mL, 2.8 mmol) in THF (30 mL) at 0 °C. This mixture was allowed to stir for 3 h. Propargylamine (0.359 mL, 5.6 mmol) and DIPEA (1.06 mL, 6.1 mmol) dissolved in THF (10 mL) was added quickly to the solution. The reaction was left stirring overnight. The solvent was removed under reduced pressure, the residue dissolved in DCM and washed with HCl (0.1 M), aqueous sat. NaHCO₃ solution, brine and dried over MgSO₄. Flash chromatography (1:1, EtOAc; Pet Ether) afforded the pure product **4.88** as a white solid (206 mg, 20%); *R*_f = 0.59 (1:1, EtOAc:Pet Ether); IR *v*_{max} (NaCl plate, DCM): 3275.0, 3064.9, 1725.2, 1649.7, 1633.3, 1544.0, 1444.4, 1431.3, 1363.9, 1319.9, 1282.9, 1258.8, 1238.7, 1187.6, 1201.9, 1065.0, 1014.9, 926.8, 914.8, 900.4, 777.2, 748.8, 731.8, 694.2, 645.3, 661.4 cm⁻¹; ¹H NMR (300 MHz, CDCl₃): δ 8.58 (s, 2 H, Ar), 8.46 (s, 1 H, Ar), 7.46-7.33 (m, 5 H, *H*-Ph), 6.62 (bs, 2 H, NHCH₂CCH), 5.44 (s, 2 H, CH₂Ph), 4.28-4.26 (m, 4 H, NHCH₂CCH), 2.31 (t, *J* = 2.4 Hz, 2 H, NHCH₂CCH); ¹³C NMR (75 MHz, CDCl₃): δ_c 165.0 (CONH), 164.9 (COOCH₂), 135.3, 134.7 (ArC), 131.0, 130.2, 128.7, 128.7, 128.6 (ArCH and PhCH), 128.6 (Ph-C), 78.83 (NHCH₂CCH), 72.4 (NHCH₂CCH), 67.6 (CH₂Ph), 30.0 (CONHCH₂CCH); HRMS *m/z* (ESI⁺): 375.133 (C₂₂H₁₉N₂O₂: [M+H]⁺ requires 375.1339).



*N*¹, *N*², di-[2-*O*-(2,3,4,6-tetra-*O*-acetyl-β-*D*-galactopyranosyl)-ethyl-1,2,3-triazol-4-ylmethylamide]-*O*-benzoate-benzene 1,3, dicarboxamide **4.90**

Copper sulphate .5H₂O (11 mg, 0.047 mmol) and sodium ascorbate (18 mg, 0.094 mmol) were added to a solution of *N*¹, *N*², di-(propargyl)-*O*-benzoate-benzene 1,3, dicarboxamide **4.88** (88 mg, 0.2 mmol) and *O*-(azidoethyl)-(2,3,4,6-*O*-tetracetyl)-β-*D*-galactopyranose **2.44** (215 mg, 0.51 mmol) in DCM/Acetone/H₂O (3:1:1). The reaction was allowed to stir at rt overnight. The solvent was removed *in vacuo*, the residue dissolved in DCM and washed with brine. Column

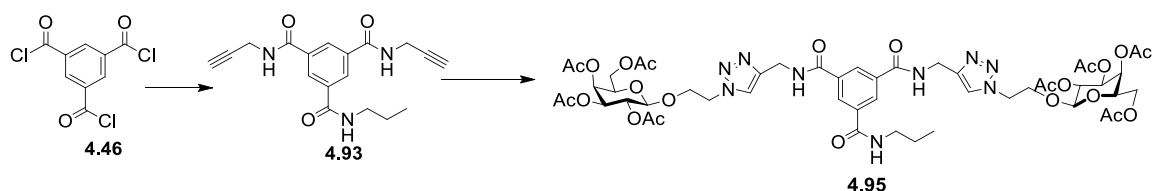
chromatography (8:1:1, DCM:MeOH:Toluene) afforded the pure product **4.90** as a waxy solid (164 mg, 58%); $R_f = 0.52$ (8:1:1, DCM:Toluene:MeOH); $[\alpha]_D^{25} = -5$ (c, 0.8 in DCM); IR ν_{\max} (NaCl plate, DCM): 3317.1, 2925.5, 2854.3, 1750.9, 1660.0, 1536.4, 1432.8, 1370.1, 1223.1, 1174.4, 1057.2 cm^{-1} ; $^1\text{H NMR}$ (300 MHz, CDCl_3): δ 8.67 (s, 2 H, Ar), 8.50-8.40 (m, 1 H, Ar), 7.82-7.72 (m, 2 H, NHCH_2), 7.67 (s, 2 H, CCHN_3), 7.46-7.33 (m, 5 H, H-Ph), 5.37-5.33 (m, 4 H, overlap of CH_2Ph and $H-4$), 5.14 (dd, $J = 7.8$ Hz, $J = 10.5$ Hz, 2 H, $H-2$), 5.00-4.95 (m, 2 H, $H-3$), 4.71-4.69 (m, 4 H, CONHCH_2), 4.58-4.50 (m, 4 H, $\text{OCH}_2\text{CH}_2\text{NH}$), 4.44 (d, $J = 8.1$ Hz, 2 H, $H-1$), 4.25-4.20 (m, 2 H, 1 H of $\text{OCH}_2\text{CH}_2\text{N}$), 4.17-4.03 (m, 4 H, $H-6$ and $H-6'$), 3.97-3.97 (m, 4 H, overlap of 1 H of $\text{OCH}_2\text{CH}_2\text{N}$ and $H-5$), 2.12, 2.02, 1.95, 1.94 (each s, 6 H, $\text{O}(\text{CO})\text{CH}_3$); $^{13}\text{C NMR}$ (75 MHz, CDCl_3): δ_c 170.5, 170.2, 170.1, 169.7 (OCOCH_3), 165.6 (CONHCH_2), 164.5 (COOCH_2), 144.1 (CCHN_3), 135.4, 134.6, 134.6 (ArC, PhC), 131.3, 129.8 (ArCH), 128.7, 128.5, 128.4, 128.3 (PhCH) 123.9 (CCHN_3), 100.9 ($C-1$), 70.9 ($C-5$), 70.5 ($C-3$), 68.6 ($C-2$), 67.6 ($\text{OCH}_2\text{CH}_2\text{NH}$), 67.4 (CH_2Ph), 66.9 ($C-4$), 61.2 ($C-6$), 50.1 ($\text{OCH}_2\text{CH}_2\text{NH}$), 35.6 (CONHCH_2), 20.7, 20.6, 20.6, 20.53 ($\text{O}(\text{CO})\text{CH}_3$); HRMS m/z (ESI⁺): 1209.4106 ($\text{C}_{54}\text{H}_{65}\text{N}_8\text{O}_{24}$: $[\text{M}+\text{H}]^+$ requires 1209.4106).



*N*¹, *N*², di-[2-*O*-(2,3,4,6-tetra-*O*-acetyl- β -*D*-galactopyranosyl)-ethyl-1,2,3-triazol-4-ylmethylamide]-*N*³-tetradecyl-benzene 1,3,5 tricarboxamide **4.92**

Tetradecylamine (0.251 g, 1.1 mmol) and DIPEA (0.214 mL, 1.29 mmol) dissolved in THF (10 mL) under Ar, were added dropwise over 3 h to 1,3,5- benzene tricarbonyl trichloride **4.46** (0.296 mL, 1.1 mmol) in THF (30 mL). This mixture was allowed to stir for 3 h. Propargylamine (0.143 mL, 2.2 mmol) and DIPEA (0.427 mL, 2.6 mmol) dissolved in THF (10 mL) were added quickly to the solution. The reaction was left stirring overnight. The solvent was removed under reduced pressure, the residue dissolved in DCM and washed with HCl (0.1 M), aqueous sat. NaHCO_3 solution, Brine and dried over MgSO_4 . Flash chromatography (1:1, EtOAc:Pet Ether) afforded a mixture of products which was used without further purification. Copper sulphate $\cdot 5\text{H}_2\text{O}$ (4 mg, 0.018 mmol) and sodium ascorbate (7 mg, 0.037 mmol) were added to a solution of **4.92** (50 mg, 0.09 mmol) and 2-azidoethyl 2,3,4,6-tetra-*O*-acetyl- β -*D*-galactopyranoside **2.44** (77 mg, 0.2 mmol) in DCM/Acetone/ H_2O (3 mL, 1 mL, 1 mL). The reaction was allowed to stir at rt overnight. The solvent was removed *in vacuo*, the residue

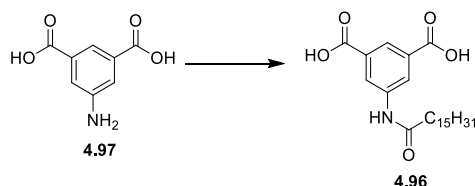
dissolved in DCM and washed with brine. Column chromatography (8:1:1, DCM:MeOH:Toluene) afforded the pure product **4.93** as a waxy solid (64 mg, 54% over two steps); $R_f = 0.45$ (8:1:1, DCM:Toluene:MeOH); $[\alpha]_D^{25} = -3.5$ (c, 0.9 in DCM); IR ν_{\max} (NaCl plate, DCM): 3317.1, 2925.5, 2854.3, 1750.9, 1660.0, 1536.4, 1432.8, 1370.1, 1223.1, 1174.4, 1057.2 cm^{-1} ; ^1H NMR (300 MHz, CDCl_3): δ 8.26-8.25 (m, 3 H, Ar), 8.02 (bs, 2 H, $\text{NHCH}_2(\text{CCHN}_3)$), 7.67 (s, 2 H, CCHN_3), 6.93 (bs, 1 H, $\text{NHC}_{14}\text{H}_{29}$), 5.35 (d, 2 H, $J = 3.3$ Hz, $H-4$), 5.14 (dd, $J = 7.8$ Hz, $J = 10.2$ Hz, 2 H, $H-2$), 4.98 (dd, $J = 3.3$ Hz, $J = 10.5$, 2 H, $H-3$), 4.66 (d, $J = 4.8$ Hz, 4 H, CONHCH_2), 4.58-4.50 (m, 4 H, $\text{OCH}_2\text{CH}_2\text{N}$), 4.45 (d, $J = 7.8$ Hz, 2 H, $H-1$), 4.22-4.16 (m, 2 H, 1 H of $\text{OCH}_2\text{CH}_2\text{N}$), 4.14-4.04 (m, 4 H, $H-6$ and $H-6'$), 3.97-87 (m, 4 H, overlap of $H-5$ and 1 H of $\text{OCH}_2\text{CH}_2\text{N}$), 3.40-3.36 (m, 2 H, $\text{NHCH}_2\text{C}_{13}\text{H}_{27}$), 2.12, 2.01, 1.95, 1.94 (each s, 6 H, $\text{O}(\text{CO})\text{CH}_3$), 1.56 (t, $J = 6.3$, 2 H, $\text{NHCH}_2\text{CH}_2\text{C}_{12}\text{H}_{25}$), 1.23 (s, 22 H, $\text{NHCH}_2\text{CH}_2(\text{CH}_2)_{11}\text{CH}_3$), 0.85 (t, $J = 6.0$ Hz, 3 H, $\text{NHC}_{13}\text{H}_{26}\text{CH}_3$); ^{13}C NMR (75 MHz, CDCl_3): δ_c 170.4, 170.2, 170.0, 169.7 (OCOCH_3), 166.0 (CONHCH_2), 165.9 ($\text{CONHC}_{14}\text{H}_{29}$), 144.4 (CCHN_3) 135.6, 134.6 (ArC), 128.7, 128.0 (ArCH), 123.7 (CCHN_3), 100.9 (C-1), 70.9 (C-5), 70.6 (C-3), 68.6 (C-2), 67.6 ($\text{OCH}_2\text{CH}_2\text{NH}$), 66.9 (C-4), 61.2 (C-6), 50.1 ($\text{OCH}_2\text{CH}_2\text{NH}$), 40.4 ($\text{NHCH}_2\text{C}_{13}\text{H}_{27}$), 35.5 ($\text{NHCH}_2(\text{CCHN}_3)$), 31.9, 29.7, 29.6, 29.5, 29.4, 29.3, 27.1, 22.7 ($\text{NHCH}_2(\text{CH}_2)_{12}\text{CH}_3$), 20.7, 20.7, 20.6 and 20.5 ($\text{O}(\text{CO})\text{CH}_3$), 14.0 ($\text{NHC}_{13}\text{H}_{26}\text{CH}_3$); HRMS m/z (ESI+): 1336.5782 ($\text{C}_{61}\text{H}_{87}\text{N}_9\text{NaO}_{23}$: $[\text{M}+\text{Na}]^+$ requires 1336.5807).



*N*¹, *N*², di-[2-*O*-(2,3,4,6-tetra-*O*-acetyl- β -*D*-galactopyranosyl)-ethyl-1,2,3-triazol-4-ylmethylamide]-*N*³-propyl-benzene 1,3,5 ticarboxamide **4.95**

Propylamine (0.092 mL, 1.1 mmol) and DIPEA (0.214 mL, 1.2 mmol) dissolved in THF (10 mL) under Ar, was added dropwise over 3 h to 1,3,5- benzenetricarbonyl trichloride **4.46** (0.200 mL, 1.1 mmol) in THF (10 mL). The reaction mixture was stirred for 2 h and propargylamine (0.143 mL, 2.2 mmol) and DIPEA (0.427 mL, 2.6 mmol) dissolved in THF (4 mL) were added quickly to the solution. The reaction was left stirring overnight. The solvent was removed under reduced pressure, the residue dissolved in DCM and washed with 1 M HCl, aqueous sat. NaHCO_3 solution, brine and dried over MgSO_4 . Flash chromatography (EtOAc) afforded a mixture of products which was used without further purification (66 mg, 18%). Copper sulphate $\cdot 5\text{H}_2\text{O}$ (18 mg, 0.072 mmol) and sodium ascorbate (29 mg, 0.14 mmol) were added to a solution of 2-

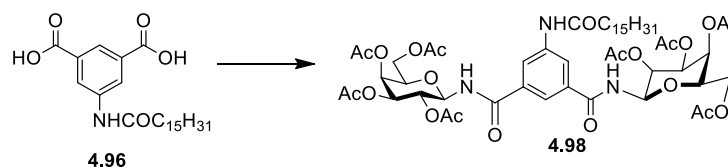
azidoethyl 2,3,4,6-tetra-*O*-acetyl- β -D-galactopyranose **2.44** (166 mg, 0.39 mmol) and alkyne **4.94** (60 mg, 0.18 mmol) in DCM/Acetone/H₂O (3 mL, 1 mL, 1mL). The reaction was allowed to stir at rt overnight. The solvent was removed *in vacuo*, the residue dissolved in DCM and washed with brine. Column chromatography (8:1:1, DCM:MeOH:Toluene) afforded the pure product **4.95** as a waxy solid (120 mg, 57%); $R_f = 0.30$ (8:1:1, DCM:Toluene:MeOH); $[\alpha]_D^{25} = -9$ (c, 1.1 in DCM); IR ν_{\max} (NaCl plate, DCM): 3404.1, 1748.1, 1651.9, 1536.1, 1370.1, 1225.6, 1057.8 cm^{-1} ; $^1\text{H NMR}$ (300 MHz, CDCl₃): δ 8.26 (bs, 3 H, Ar), 8.10 (bs, 2 H, NHCH₂(CCHN₃)), 7.70-7.69 (m, 2 H, CCHN₃), 7.01 (bs, 1 H, NHC₃H₇), 5.38 (d, 2 H, $J = 3$ Hz, *H*-4), 5.15 (dd, $J = 8.1$ Hz, $J = 10.2$ Hz, 2 H, *H*-2), 4.98 (dd, $J = 3.3$ Hz, $J = 10.5$, 2 H, *H*-3), 4.66 (bs, 4 H, NHCH₂(CCHN₃)), 4.61-4.51 (m, 4 H, OCH₂CH₂NH), 4.46 (d, $J = 7.8$ Hz, 2 H, *H*-1), 4.25-4.20 (m, 2 H, OCH₂CH₂NH), 4.16-4.07 (m, 4 H, *H*-6 and *H*-6'), 3.97-3.89 (m, 4 H, overlap of *H*-5 and OCH₂CH₂NH), 3.35 (bs, 2 H, NHCH₂C₂H₅), 2.13, 2.02 (each s, 6 H, O(CO)CH₃), 1.96 (s, 12 H, O(CO)CH₃), 1.63-1.56 (m, 2 H, NHCH₂CH₂CH₃), 0.93 (t, $J = 6$ Hz, 3 H, NHC₂H₄CH₃); $^{13}\text{C NMR}$ (75 MHz, CDCl₃): δ_c 170.5, 170.2, 170.1 (OCOCH₃), 169.7 (CONHCH₂CCHN₃), 166.0 (CONHC₃H₇), 144.4 (CCHN₃) 135.6, 134.6 (ArC), 129.0, 128.2 (ArCH), 125.3 (CCHN₃), 100.9 (*C*-1), 70.9 (*C*-5), 70.6 (*C*-3), 68.6 (*C*-2), 67.5 (OCH₂CH₂NH), 66.9 (*C*-4), 61.2 (*C*-6), 50.2 (OCH₂CH₂NH), 41 (NHCH₂C₂H₅), 35.5 (NHCH₂(CCHN₃)), 22.7 (NHCH₂CH₂CH₃), 20.7, 20.7, 20.6, 20.5 (O(CO)CH₃), 11.5 (NHC₂H₄CH₃); HRMS m/z (ESI⁺): 1160.4295(C₅₀H₆₆N₉NaO₂₃: [M+H]⁺ requires 1160.4266).



*N*³-hexadecanoyl-5-aminobenzene-1,3-dicarboxylic acid **4.96**

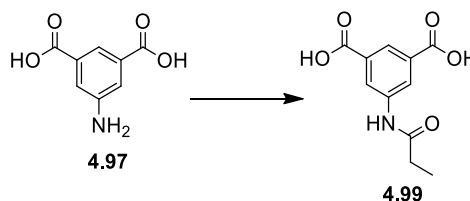
5-aminoisophthalic acid (1 g, 5.5 mmol) was dissolved in DMF (20 mL) and THF (20 mL) under Ar. Hexadecanoyl chloride (1.84 mL, 6 mmol) and NEt₃ (0.92 mL, 6.6 mmol) were added and the reaction mixture stirred overnight. The solvent was removed under reduced pressure. The resulting residue was dissolved in hot MeOH and the insoluble material filtered off. The pure product precipitated out upon cooling, to yield the dicarboxylic acid **4.96** as a white solid (1.86 g, 81%); Mp = Decomposed at 256 °C; IR ν_{\max} (KBr): 3270.3, 2918.0, 2848.8, 1726.6, 1663.28, 1605.1, 1461.87, 1408.3, 1260.2, 1221.9, 1204.7, 967.9, 907.4, 826.1, 751.7 721.7, 671.2 cm^{-1} ; $^1\text{H NMR}$ (300 MHz, DMSO): δ 10.26 (s, 1 H, NHCO), 8.45 (s, 2 H, Ar), 8.14 (s, 1 H, Ar) 3.31 (t, $J = 7.2$ Hz, 2 H, NHCOCH₂C₁₄H₂₉), 1.60-1.56 (m, 2 H, NHCOCH₂CH₂C₁₃H₂₇), 1.18 (s, 24 H,

NHCOC₂H₄(CH₂)₁₂CH₃), 0.82 (t, *J* = 6.3 Hz, 3 H, NHCOC₁₄H₂₈CH₃); ¹³C NMR (75 MHz, CDCl₃): δ_c 171.7, 166.5 (CO), 139.8, 131.6 (ArC), 124.3, 123.3 (ArCH), 36.3 (NHCOCH₂C₁₄H₂₉), 31.3 (NHCOCH₂CH₂C₁₃H₂₆), 29.1, 29.0, 28.9, 28.8, 28.6, 24.9, 24.46, 22.1 (NHCOC₂H₄(CH₂)₁₂CH₃), 13.8 (NHCOC₁₄H₂₉CH₃); HRMS *m/z* (ESI+): 418.2615, (C₂₄H₃₆NO₅: [M-H]⁻ requires 418.2599).



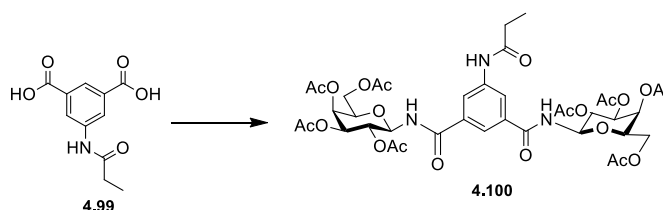
*N*¹, *N*², di-(2,3,4,6-tetra-*O*-acetyl-β-*D*-galactopyranosyl)-*N*³-hexadecanosyl-5-aminobenzene 1,3-dicarboxamide **4.98**

*N*³-hexadecanosyl-5-aminobenzene-1,3-dicarboxylic acid **4.96** (85 mg, 0.2 mmol), was dissolved in THF (5 mL) under N₂ and placed on ice. DMF (2 drops) was added. Oxalyl chloride (0.055 mL, 0.60 mmol) was then added dropwise. The reaction was left stirring for 40 min at 0 °C and a solution of 1-amino-2,3,4,6-tetra-*O*-acetyl-β-*D*-galactopyranoside **3.76** (177 mg, 0.5 mmol) and NEt₃ (0.084 mL, 0.60 mmol) in THF (5 mL) under N₂ was added. The reaction was left stirring overnight at 0 °C. The solvent was removed *in vacuo* and the residue dissolved in DCM and washed successively with 0.1 M HCl, aqueous sat. NaHCO₃ solution, brine and dried over MgSO₄. Flash chromatography (1:1, EtOAc:Pet Ether) afforded the di-substituted product **4.98** as a cream waxy solid (99 mg, 45%); *R*_f = 0.26 (95:5 DCM:MeOH); [α]²⁵_D = -7.3 (c, 1 in DCM); IR *v*_{max} (NaCl plate, DCM): 3325.6, 2925, 2853.9, 1750.4, 1671.4, 1537, 1445.6, 1369.6, 1226.9, 1083.7, 1052.7 cm⁻¹; ¹H NMR (300 MHz, CDCl₃): δ 8.19 (bs, 2 H, Ar), 8.00 (s, 1 H, Ar), 7.88 (s, 1 H, NHCOC₁₅H₃₁), 7.45 (d, *J* = 9 Hz, 2 H, H1NHCO), 5.57-5.44 (m, 4 H, overlap of *H*-1 and *H*-4), 5.30-5.14 (m, 4 H, overlap of *H*-2 and *H*-3), 4.21-4.04 (m, 6 H, overlap of *H*-6, *H*-6' and *H*-5), 2.39 (t, *J* = 7.5 Hz, 2 H, NHCOCH₂(CH₂)₁₃CH₃), 2.18, 2.03, 2.01 and 2.00 (each s, 6 H, O(CO)CH₃), 1.77-1.68 (m, 2 H, NHCOCH₂CH₂(CH₂)₁₂CH₃), 1.24 (s, 24 H, NHCOCH₂CH₂(CH₂)₁₂CH₃), 0.86 (t, *J* = 6.3 Hz, 3 H, NHCOCH₂CH₂(CH₂)₁₂CH₃); ¹³C NMR (75 MHz, CDCl₃): δ_c 172.1, 171.4, 170.9, 170.4, 170.2, 170.0, 165.9, 169.8, 166.1, 156.4 (CO), 139.4, 134.3 (ArC), 121.8, 121.0 (ArCH), 79.0 (*C*-1), 72.4 (*C*-5), 71.0 (*C*-3), 68.6 (*C*-2), 67.3 (*C*-4), 61.3 (*C*-6), 37.6 (NHCOCH₂(CH₂)₁₃CH₃), 31.9, 29.7, 29.5, 29.4, 29.3, 29.3, 25.7 (NHCOCH₂(CH₂)₁₃CH₃), 20.8, 20.7, 20.6, 20.6 (O(CO)CH₃), 14.1 (NHCOCH₂(CH₂)₁₃CH₃); HRMS *m/z* (ESI+): 1078.4966 (C₅₂H₇₆N₃O₂₁: [M+H]⁺ requires 418.2599).



*N*³-propyl-5-aminobenzene-1,3-dicarboxylic acid **4.99**

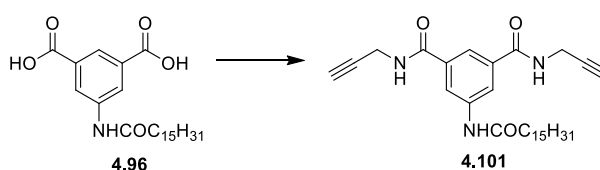
5-Aminoisophthalic acid (1 g, 5.5 mmol) was dissolved in THF (10 mL) and propionyl chloride (0.5 mL, 6.0 mmol) was added dropwise. The mixture was allowed to stir for 5 min and NEt_3 (0.9 mL, 6.6 mmol) was added. The solution was stirred at rt overnight. The reaction was left stirring overnight. The solvent was removed under reduced pressure, and the residue dissolved in hot methanol. The insoluble material was filtered off, and the filtrate recrystallised from EtOAc and Et_2O to yield the title product **4.99** as a cream solid (1.16 g, 89%); ^1H NMR (300 MHz, DMSO): δ 10.48 (s, 1 H, NHCO), 8.47 (s, 2 H, Ar), 8.13 (s, 1 H, Ar), 2.37 (q, $J = 7.5$ Hz, 2 H, $\text{NHCOCH}_2\text{CH}_3$), 1.08 (t, $J = 7.5$ Hz, 3 H, $\text{NHCOCH}_2\text{CH}_3$); ^{13}C NMR (75 MHz, DMSO): δ_c 171.6, 166.5 (CO), 139.9, 131.6 (ArC), 124.2, 123.3 (ArCH), 29.5 ($\text{NHCOCH}_2\text{CH}_3$), 9.4 ($\text{NHCOCH}_2\text{CH}_3$); HRMS m/z (ESI+): 238.0722, ($\text{C}_{11}\text{H}_{12}\text{NO}_5$: $[\text{M}+\text{H}]^+$ requires 238.071).



*N*¹, *N*², di-(2,3,4,6-tetra-*O*-acetyl- β -D-galactopyranosyl)-*N*³-propyl-5-aminobenzene 1,3-dicarboxamide **4.100**

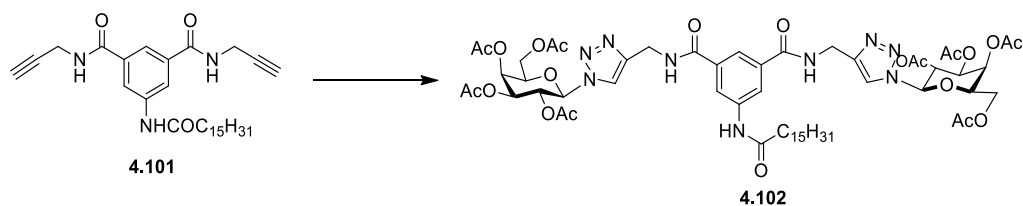
*N*³-propyl-5-aminobenzene-1,3-dicarboxylic acid **4.99** (67 mg, 0.28 mmol), HOBT (84 mg, 0.62 mmol) and TBTU (200 mg, 0.62 mmol) were placed under N_2 and dissolved in DMF (4 mL). NEt_3 (0.16 mL, 1.1 mmol) was added and the mixture was allowed to stir for 15 min. 1-amino-2,3,4,6-tetra-*O*-acetyl- β -D-galactopyranoside **3.76** (248 mg, 0.7 mmol) dissolved in DMF (5 mL) was then added. The solution was stirred overnight. The solvent was removed under reduced pressure and the resulting residue was dissolved in DCM washed with 0.1 M HCl, aqueous sat. NaHCO_3 solution, brine and dried over MgSO_4 . Column chromatography (EtOAc) yielded the pure di-substituted product **4.100** as an oily solid (49 mg, 20%); $R_f = 0.36$ (EtOAc); $[\alpha]_D^{25} = -18.1$ (c, 1.1 in DCM); IR ν_{max} (NaCl plate, DCM): 3338.9, 1750.6, 1676.9, 1602.2, 1535.2, 1370.1, 1228.3, 1083.4, 1052.1, 956.25, 909.15, 802.3 cm^{-1} ; ^1H NMR (300 MHz, CDCl_3): δ 8.23-8.21 (m,

2 H, overlap of Ar and $\text{NHCOCH}_2\text{H}_5$), 7.88 (s, 1 H, Ar), 7.43 (d, $J = 9.3$ Hz, 2 H, $H\text{-1NHCO}$), 5.58-5.48 (m, 4 H, overlap of $H\text{-1}$ and $H\text{-4}$), 5.29-5.27 (m, 4 H, overlap of $H\text{-2}$ and $H\text{-3}$), 4.20-4.05 (m, 6 H, overlap of $H\text{-6}$, $H\text{-6}'$ and $H\text{-5}$), 2.43 (q, $J = 7.5$ Hz, 2 H, $\text{NHCOCH}_2\text{CH}_3$), 2.18, 2.03, 2.01, 1.99 (each s, 6 H, $\text{O}(\text{CO})\text{CH}_3$), 1.27-1.21 (m, 3 H, $\text{NHCOCH}_2\text{CH}_3$); ^{13}C NMR (75 MHz, CDCl_3): δ_c 172.7, 171.4 (CO), 170.5, 170.2, 170.0, 170.1, 170.0 ($\text{O}(\text{CO})\text{CH}_3$), 166.1 (CO), 139.6, 134.3 (ArC), 121.8, 121.8 (ArCH), 79.0 (C-1), 72.4 (C-5), 71.0 (C-3), 68.6 (C-2), 67.3 (C-4), 61.3 (C-6), 30.5 ($\text{NHCOCH}_2\text{CH}_3$), 20.8, 20.7, 20.6, 20.6, 20.5 ($\text{O}(\text{CO})\text{CH}_3$), 14.20 ($\text{NHCOCH}_2(\text{CH}_2)_{13}\text{CH}_3$); HRMS m/z (ESI+): 896.2956, ($\text{C}_{39}\text{H}_{50}\text{N}_3\text{O}_{21}$: $[\text{M}+\text{H}]^+$ requires 896.2931).



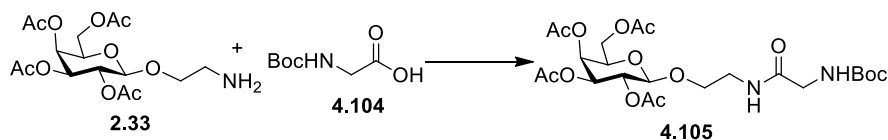
*N*¹,*N*², di-propargyl-*N*³-hexadecanosyl-5-aminobenzene-1,3-dicarboxylic acid **4.101**

*N*³-hexadecanosyl-5-aminobenzene-1,3-dicarboxylic acid **4.96** (200 mg, 0.47 mmol), HOBT (142 mg, 1 mmol) and TBTU (337 mg, 1 mmol) were dissolved in DMF under N_2 and NEt_3 (146 mL, 1 mmol) was added. The mixture was allowed to stir for 10 min and propargylamine (0.07 mL, 1.2 mmol) was added. The solution was stirred at rt overnight. The solvent was removed *in vacuo*, dissolved in DCM washed successively with 0.1 M HCl, aqueous sat. NaHCO_3 solution, brine and dried over MgSO_4 . Column chromatography (1:1, EtOAc: Pet Ether) yielded the product which was recrystallised (EtOAc) as a white solid **4.101** (146 mg, 62%); $R_f = 0.39$ (1:1, EtOAc: Pet EtherDCM); mp = 154- 156 °C; IR ν_{max} (KBr): 3269.08, 3067.5, 2919.0, 2849.6, 2125.93, 1733.94, 1659.0, 1599.1, 1535.7, 1461.3, 1444.6, 1421.6, 1369.2, 1327.4, 1286.6, 1205.6=7, 1221.3, 1187.3, 1112.8, 1065.5, 1050.8, 1013.7, 966.2, 916.1, 888.8 cm^{-1} ; ^1H NMR (300 MHz, CDCl_3): δ 8.54 (s, 1 H, NHCO), 8.28 (s, 2 H, Ar), 7.98 (s, 1 H, Ar) 7.61-7.57 (m, 1 H, Ar), 6.95 (t, $J = 5.1$ Hz, 2 H, NHCH_2CCH), 4.24-4.21 (m, 4 H, NHCH_2CCH), 2.43 (t, $J = 7.5$ Hz, 2 H, $\text{NHCOCH}_2\text{C}_{14}\text{H}_{29}$), 2.27 (t, $J = 2.7$ Hz, 2 H, NHCH_2CCH), 1.73-1.66 (m, 2 H, $\text{NHCOCH}_2\text{CH}_2\text{C}_{13}\text{H}_{27}$), 1.31-1.24 (m, 24 H, $\text{NHCOCH}_2\text{H}_4(\text{CH}_2)_{12}\text{CH}_3$), 0.87 (t, $J = 6.6$ Hz, 3 H, $\text{NHCOCH}_2\text{H}_4(\text{CH}_2)_{12}\text{CH}_3$); ^{13}C NMR (75 MHz, CDCl_3): δ_c 172.7, 166.1 (CO), 139.5, 134.6 (ArC), 121.2, 120.9 (ArCH), 78.9 (NHCH_2CCH), 72.16 (NHCH_2CCH), 37.6 ($\text{NHCOCH}_2\text{C}_{14}\text{H}_{29}$), 31.9 ($\text{NHCOCH}_2\text{CH}_2\text{C}_{13}\text{H}_{26}$), 29.9, 29.7, 29.7, 29.5, 29.4, 29.3, 29.2, 245.4, 22.7 (overlap of NHCH_2CCH and $\text{NHC}_2\text{H}_4(\text{CH}_2)_{12}\text{CH}_3$), 14.1 ($\text{NHC}_{14}\text{H}_{29}\text{CH}_3$).



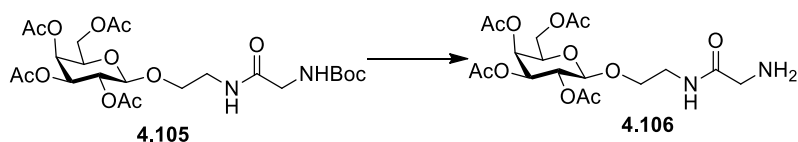
*N*¹, *N*², di-(2,3,4,6-tetra-*O*-acetyl-β-*D*-galactopyranosyl-1,2,3-triazol-4-ylmethylamide)-*N*³-hexadecanosyl-5-aminobenzene 1,3, dicarboxamide **4.102**

Copper sulphate .5H₂O (5 mg, 0.021 mmol) and sodium ascorbate (8 mg, 0.04 mmol) were added to a solution of 1-azido-2,3,4,6-tetra-*O*-acetyl-β-*D*-galactopyranose **3.67** (158 mg, 0.42 mmol) and *N*¹,*N*², di-propargyl-*N*³-hexadecanosyl-5-aminobenzene-1,3-dicarboxylic acid **4.101** (105 mg, 0.21 mmol) in DCM/Acetone/H₂O (3 mL, 1 mL, 1mL). The reaction was allowed to stir at rt overnight. The solvent was removed *in vacuo*, the residue dissolved in DCM, washed with brine and dried over MgSO₄. Gradient elution chromatography (8:1:1, DCM:MeOH:Toluene:EtOAc) afforded the pure product as a clear oil **4.102** (145 mg, 56%); *R*_f = 0.57 (8:1:1, DCM:Toluene:MeOH); [α]²⁵_D = -17.4 (c, 0.87 in DCM); IR *v*_{max} (NaCl plate, DCM): 3291.4, 2924.3, 1754.9, 1649.6, 1599.5, 1537.7, 1446.4, 1425.5, 1369.6, 1092.4, 1062.7, 953.1, 924.1, 897.3, 801.2, 684.3 cm⁻¹; ¹H NMR (300 MHz, CDCl₃): δ 8.12 (s, 1 H, NHCOC₁₅H₃₁), 8.03 (s, 2 H, Ar), 7.96 (CHCN₃), 7.92 (s, 1 H, Ar), 7.71-6.67 (m, 2 H, CONHCH₂), 5.90 (d, *J* = 9 Hz, 1 H, H-1), 5.60-5.40 (m, 4 H, overlap of *H*-4 and *H*-2), 5.27 (dd, *J* = 3.3 Hz, *J* = 10.2 Hz, 2 H, *H*-3), 4.75-4.59 (m, 2 H, CONHCH₂), 4.313-4.27 (m, 2 H, *H*-5), 4.22-4.08 (m, 4 H, *H*-6 and *H*-6'), 2.37 (t, *J* = 7.2 Hz, 2 H, NHCOC₂C₁₄H₂₉), 2.21, 2.01, 1.99, 1.82 (each s, 6 H, O(CO)CH₃), 1.71-1.66 (m, 2 H, NHCOC₂CH₂C₁₃H₂₆), 1.37-1.22 (m, 24 H, NHCOC₂H₄(CH₂)₁₂CH₃), 0.86 (t, *J* = 6.6 Hz, 3 H, NHCOC₁₄H₂₉CH₃); ¹³C NMR (75 MHz, CDCl₃): δ_c 172.2, 170.3, 170.1, 169.8, 169.2, 166.5 (CO), 145.4 (CCHN₃), 139.0, 134.9 (ArC), 121.4, 120.6 (ArCH and CCHN₃), 86.18 (*C*-1), 73.9 (*C*-5), 70.8 (*C*-3), 68.0 (*C*-2), 66.8 (*C*-4), 61.2 (*C*-6), 37.5 (NHCOC₂(CH₂)₁₃CH₃), 35.4 (CONHCH₂), 31.9, 29.7, 29.6, 29.5, 29.4, 29.3, 25.4, 22.7 (NHCOC₂(CH₂)₁₃CH₃), 20.7, 20.6, 20.5, 20.2 (O(CO)CH₃), 14.1 (NHCOC₂(CH₂)₁₃CH₃); HRMS *m/z* (ESI⁺): 1240.5657, (C₅₈H₈₂N₉O₂₁: [M+H]⁺ requires 1240.562).



*N*²-[2-*O*-(2,3,4,6-tetra-*O*-acetyl- β -*D*-galactopyranosyl)-ethyl]- *N*¹-tert-butoxycarbonyl-glycine
4.105

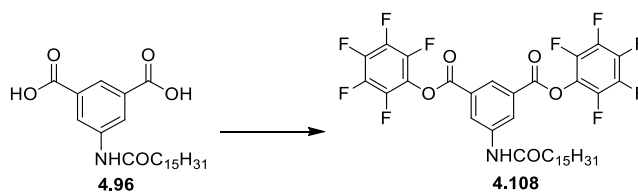
HOBt (0.09 g, 0.69 mmol), followed by NEt₃ (0.12 mL, 0.63 mmol), were added to a stirring solution of *N*-Boc-Glycine-OH **4.104** (0.11 g, 0.63 mmol) and TBTU (0.22 g, 0.69 mmol) dissolved in DMF (10 mL), under N₂ at rt. The mixture was stirred for 30 min and 2-aminoethyl 2,3,4,6-tetra-*O*-acetyl- β -*D*-galactopyranoside **2.33** (0.29 g, 0.75 mmol) dissolved in DMF (2 mL) was added. The mixture was stirred for 18 h. The reaction mixture was concentrated under reduced pressure, diluted with EtOAc and washed successively with HCl 0.1 N, aqueous sat. NaHCO₃ solution, brine and dried over MgSO₄. Flash chromatography (5:1, EtOAc: Pet Ether) afforded **4.105** (0.22 g, 62%); R_f = 0.41 (5:1 EtOAc: Pet Ether); [α]_D²⁵ = 1.97 (c, 1.3 in DCM); IR ν_{\max} (NaCl plate, DCM): 3382, 2978.9, 1752, 1519.7, 1432.6, 1369.3, 1226.3, 1171.1, 1055.8, 955.9 cm⁻¹; ¹H NMR (300 MHz, CDCl₃): δ 6.42 (bs, 1 H, OCH₂CH₂NH), 5.36-5.35 (m, 1 H, *H*-4), 5.26 (s, 1 H, NHCOC(CH₃)₃), 5.13 (dd, *J* = 7.8 Hz, *J* = 10.5 Hz, 1 H, *H*-2), 4.98 (dd, *J* = 3.3 Hz, *J* = 10.5 Hz, 1 H, *H*-3), 4.46 (d, *J* = 7.8 Hz, 1 H, *H*-1), 4.18-4.06 (m, 2 H, *H*-6 and *H*-6'), 3.95-3.79 (m, 2 H, overlap of 1 H of OCH₂CH₂NH and *H*-5), 3.7 (d, *J* = 8.1 Hz, 2 H COCH₂NHCO), 3.70-3.63 (m, 1 H, 1 H of OCH₂CH₂NH), 3.51-3.40 (m, 2 H, OCH₂CH₂NH), 2.12, 2.03, 2.01, 1.95 (each s, 3 H, O(CO)CH₃), 1.42 (s, 9 H, COC(CH₃)₃); ¹³C NMR (75 MHz, CDCl₃): δ_c 170.4, 170.2, 170.0 (O(CO)CH)₃, 169.7, 169.5 (CO), 101.3 (*C*-1), 76.7 (COC(CH₃)₃), 70.9 (*C*-5), 70.72 (*C*-3), 68.9 (*C*-2), 68.6 (OCH₂CH₂NH), 67.0 (*C*-4), 61.4 (*C*-6), 39.2 (OCH₂CH₂NH), 28.3 (COC(CH₃)₃), 20.8, 20.6, 20.6 and 20.5 (O(CO)CH₃); HRMS *m/z* (ESI⁺): 571.211 (C₂₃H₃₆N₂NaO₁₃: [M+H]⁺ requires 571.211).



*N*²-[2-*O*-(2,3,4,6-tetra-*O*-acetyl- β -*D*-galactopyranosyl)-ethyl]-glycine **4.106**

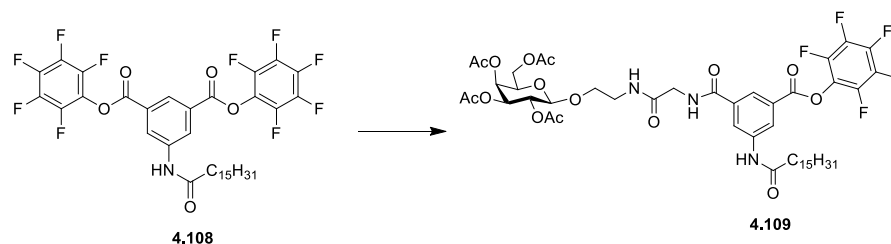
A solution of *N*²-[2-*O*-(2,3,4,6-tetra-*O*-acetyl- β -*D*-galactopyranosyl)-ethyl]- *N*¹-tert-butoxycarbonyl-glycine **4.105** (0.11 g, 0.21 mmol) in DCM (6 mL) was cooled in an ice bath and TFA (0.17 mL, 2.15 mmol) added. The reaction mixture was stirred at 0 °C for 30 min, and for a further 4 h at rt. The organic solvent was removed *in vacuo* and the residue obtained was

diluted with ethyl acetate and washed with aqueous sat. NaHCO_3 solution and brine, dried (MgSO_4) and concentrated to yield the corresponding deprotected amine **4.106** as a brown oil that was used without further purification (0.073 g, 74%); ^1H NMR (300 MHz, CDCl_3): δ 7.43 (bs, 1 H, CH_2NHCO), 5.36-5.35 (m, 1 H, *H*-4), 5.16 (dd, $J = 7.8$ Hz, $J = 10.5$ Hz, 1 H, *H*-2), 4.98 (dd, $J = 3.3$ Hz, $J = 10.5$ Hz, 1 H, *H*-3), 4.46 (d, $J = 7.8$ Hz, 1 H, *H*-1), 4.18-4.05 (m, 2 H, *H*-6 and *H*-6'), 3.91-3.83 (m, 2 H, overlap of 1 H of $\text{OCH}_2\text{CH}_2\text{NH}$ and *H*-5), 3.68-3.61 (m, 2 H, $\text{OCH}_2\text{CH}_2\text{NH}$), 3.54-3.40 (m, 2 H, $\text{OCH}_2\text{CH}_2\text{NH}$), 3.37-3.31 (m, 2 H, COCH_2NH_2) 2.12, 2.03, 2.01, 1.95 (each s, 3H, $\text{O}(\text{CO})\text{CH}_3$).



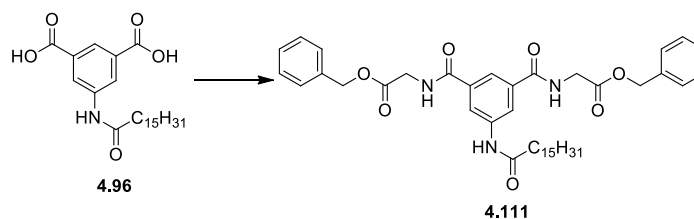
*O*¹,*O*²,*di*-(2,3,4,5,6-pentafluorophenyl) ester -*N*³-hexadecanosyl-5-aminobenzene-1,3-dicarboxylic acid **4.108**

*N*³-hexadecanosyl-5-aminobenzene-1,3-dicarboxylic acid **4.96** (200 mg, 0.47 mmol) and pentafluorophenol (263 mg, 1.4 mmol) was dissolved in THF (5 mL) under N_2 and placed on ice. DIC (0.298 mL, 1.9 mmol) was added and the reaction was stirred for 1 h at 0 °C. The reaction was stirred for a further 4 h at rt. The solvent was removed *in vacuo* and the residue was purified by flash chromatography (10:1, Pet Ether:EtOAc) to yield a white solid which was crystallised in EtOAc to yield the pure product **4.108** as a white solid (167 mg, 46%); $R_f = 0.66$ (7:1, Pet Ether: EtOAc); mp = 151-153 °C; IR ν_{max} (KBr Disc): 3407.5, 2920.0, 2850.7, 1764.4, 1665.3, 1519.1, 1454.7, 1468.8, 1454.7, 1339.4, 1310.4, 1192.8, 1097.3, 1077.32 cm^{-1} ; ^1H NMR (300 MHz, CDCl_3): δ 8.70 (s, 3 H, Ar), 7.47 (s, 1 H, $\text{CNHCOC}_{15}\text{H}_{31}$), 2.43 (t, $J = 7.5$ Hz, 2 H, $\text{NHCOCH}_2\text{C}_{14}\text{H}_{29}$), 1.81-1.71 (m, 2 H, $\text{NHCOCH}_2\text{CH}_2\text{C}_{13}\text{H}_{27}$), 1.24 (s, 24 H, $\text{NHCOCH}_2\text{H}_4(\text{CH}_2)_{12}\text{CH}_3$), 0.86 (t, $J = 6.6$ Hz, 3 H, $\text{NHCOCH}_2\text{C}_{14}\text{H}_{28}\text{CH}_3$); ^{13}C NMR (75 MHz, CDCl_3): δ_c 171.8, 160.9 (CO), 139.6, 138.3 (ArC of C_6F_5) 136.8 (ArC), 134.8, 134.5 (ArCH), 128.7 (ArC), 37.7 ($\text{NHCOCH}_2\text{C}_{14}\text{H}_{29}$), 31.9, 29.7, 29.5, 29.4, 29.2, 25.3, 22.7 ($\text{NHCOCH}_2(\text{CH}_2)_{14}\text{CH}_3$), 14.1 $\text{CONHC}_{14}\text{H}_{28}\text{CH}_3$); HRMS m/z (ESI+): 750.2279 ($\text{C}_{36}\text{H}_{35}\text{F}_{10}\text{NO}_5$: $[\text{M}-\text{H}]^-$ requires 750.2283).



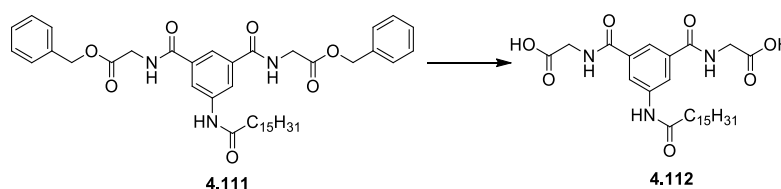
*N*¹-[2-*O*-(2,3,4,6-tetra-*O*-acetyl-β-*D*-galactopyranosyl-ethyl-glycine)-*O*-(2,3,4,5,6-pentafluorophenyl) ester-*N*³-hexadecanosyl-5-aminobenzene 1,3, dicarboxamide **4.109**

*O*¹,*O*²,di-(2,3,4,5,6-pentafluorophenyl) ester -*N*³-hexadecanosyl-5-aminobenzene-1,3-dicarboxylic acid **4.108** (17 mg, 0.02 mmol), was dissolved in THF (5 mL) under N₂ with 4Å molecular sieves. *N*²-[2-*O*-(2,3,4,6-tetra-*O*-acetyl-β-*D*-galactopyranosyl)-ethyl]-glycine **4.106** (25 mg, 0.06 mmol) and DIPEA (0.009 mL, 0.06 mmol) dissolved in THF (2 mL) under N₂ were added and the reaction mixture was stirred at rt overnight. The solvent was removed *in vacuo* and the resulting residue purified by flash chromatography (1:1, EtOAc:Pet Ether) to yield compound **4.109** as a clear oil (10 mg, 45%); *R*_f = 0.57 (EtOAc); [α]²⁵_D = -2 (c, 0.9 in DCM); IR *v*_{max} (NaCl plate, DCM): 3324.9, 3094.0, 2959.1, 2925.7, 2854.5, 1754.3, 1646.9, 1600.2, 1554.2, 1521.0, 1453.5, 1369.1, 1225.5, 1170.9, 1078.9, 997.3, 956.3, 888.6, 802.0, 745.7 cm⁻¹; ¹H NMR (300 MHz, CDCl₃): δ 8.90 (s, 1 H, NHCOC₁₅H₃₁), 8.87 (s, 1 H, Ar), 8.34 (t, *J* = 2.7 Hz, 1 H, Ar), 8.17 (t, *J* = 3.6 Hz, 2 H, Ar) 7.65 (t, *J* = 10.2 Hz 1 H, COCH₂NHCO), 6.74-6.72 (t, *J* = 11.1 Hz, 1 H, OCH₂CH₂NH), 5.41-5.40 (m, 1 H, *H*-4), 5.17 (dd, *J* = 7.8 Hz, *J* = 10.2 Hz, 1 H, *H*-2), 5.05 (dd, *J* = 3.0 Hz, *J* = 10.2 Hz, 1 H, *H*-3), 4.55 (d, *J* = 7.8 Hz, 1 H, *H*-1), 4.23-4.08 (m, 4 H, overlap of *H*-6, *H*-6' and COCH₂NHCO), 3.98-3.94 (m, 1 H, *H*-5), 3.90-3.84 (m, 1 H, 1 H of OCH₂CH₂NH), 3.78-3.70 (m, 1 H, 1 H of OCH₂CH₂NH), 3.57-3.40 (m, 2 H, OCH₂CH₂NH), 2.44 (t, *J* = 7.5 Hz 2 H, NHCOC₂H₁₄CH₃), 2.14, 2.07, 2.05, 1.99 (each s, 3 H, O(CO)CH₃), 1.78-1.70 (m, 2 H, NHCOC₂H₄(CH₂)₁₂CH₃), 1.24 (s, 24 H, NHCOC₂H₄(CH₂)₁₂CH₃), 0.86 (t, *J* = 6.6, 3 H, NHCOC₁₄H₂₈CH₃); ¹³C NMR (75 MHz, CDCl₃): δ_c 170.6, 170.2, 170.2, 169.9 (O(CO)CH₃), 168.9, 166.1, 161.8, 157.2 (CO), 140.0, 135.0, 128.1 (ArC), 124.4, 124.1, 124.0 (ArCH), 101.2 (C-1), 70.9 (C-5), 70.76 (C-3), 69.01 (C-2), 68.46 (OCH₂CH₂NH), 67.0 (C-4), 61.4 (C-6), 43.7 (COCH₂NHCO), 39.6 (OCH₂CH₂NH), 37.6 (NHCOC₂H₄(CH₂)₁₃CH₃), 31.9, 29.7, 29.7, 29.5, 29.4, 29.4, 29.3, 28.3, 25.4, 22.7 (NHCOC₂H₄(CH₂)₁₃CH₃), 21.1, 20.9, 20.7, 20.6 (O(CO)CH₃), 14.1 (NHCOC₂H₄(CH₂)₁₃CH₃); HRMS *m/z* (ESI⁺): 1016.4182 (C₄₈H₆₃F₅N₃O₁₅: [M+H]⁺ requires 1016.4174).



*N*¹,*N*², di-(glycine-benzyl ester)–*N*³-hexadecanosyl-5-aminobenzene-1,3-dicarboxylic acid **4.11**

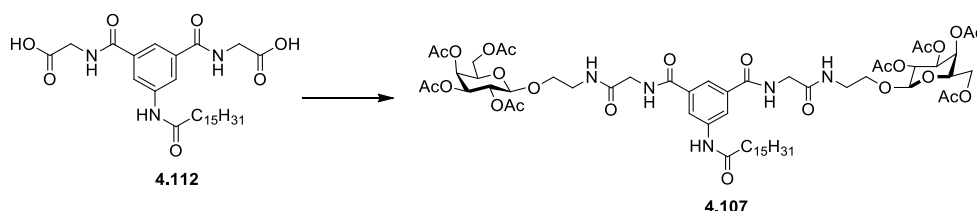
*N*³-hexadecanosyl-5-aminobenzene-1,3-dicarboxylic acid **4.96** (300 mg, 0.7 mmol), HOBT (212 mg, 1.5 mmol) and TBTU (505 mg, 1.5 mmol) was placed under N₂ and dissolved in DMF (10 mL). NEt₃ (0.20 mL, 1.4 mmol) was added and the mixture was allowed to stir for 15 min. Glycine benzyl ester. HCl salt (432 mg, 2 mmol) and NEt₃ (0.298 mL, 2.1 mmol) were dissolved in DMF (5 ml) and added to the reaction mixture, which was stirred overnight. The solvent was removed under reduced pressure, and the resulting residue was dissolved in DCM, washed with 0.1 M HCl, aqueous sat. NaHCO₃ solution, brine and dried over MgSO₄. Recrystallisation in 1:1 (EtOAc:Pet Ether) yielded the pure product **4.11** as a white solid (269 mg, 54%); R_f = 0.9 (1:1, EtOAc:Pet Ether); IR ν_{max} (KBr Disc): 3368.8, 3315.2, 2923.9, 2852.6, 1735.8, 1659.3, 1602.1, 1561.3, 1499.0, 145.5, 1443.3, 1432.3, 1405.6, 1390.2, 1293.0, 1251.3, 1195.8, 1112.9, 1094.7, 1080.8, 1027.03 cm⁻¹; ¹H NMR (300 MHz, CDCl₃): δ 8.52 (bs, 1 H, NHCOC₁₅H₃₁), 7.09 (s, 1 H, Ar), 7.80 (s, 2 H, CONHCH₂), 7.69 (s, 1 H, Ar), 7.35 (s, 10 H, PhH), 5.20 (s, 4 H, CH₂Ph), 4.20 (d, *J* = 5.4, 4 H, COCH₂NHCO), 2.29 (t, *J* = 6.9, 2 H, NHCOCH₂(CH₂)₁₃CH₃), 1.64 (bs, 2 H, NHCOCH₂CH₂(CH₂)₁₂CH₃), 1.24 (s, 24 H, NHCOCH₂CH₂(CH₂)₁₂CH₃), 0.87 (t, *J* = 6.3, 3 H, NHCOCH₂CH₂(CH₂)₁₂CH₃); ¹³C NMR (75 MHz, CDCl₃): δ_c 172.8, 170.8, 167.4 (CO), 139.0, 135.2, 134.5 (ArC) 128.7, 128.5, 128.2 (PhCH), 120.9, 120.6 (ArCH), 67.3 (PhCH₂), 40.4 (COCH₂NHCO), 37.4 (NHCOCH₂(CH₂)₁₃CH₃), 31.9, 29.7, 29.7, 29.6, 29.5, 29.4, 23.3, 22.7, 22.3 (NHCOCH₂(CH₂)₁₃CH₃), 14.3 (NHCOCH₂(CH₂)₁₃CH₃); HRMS *m/z* (ESI⁺): 714.4077 (C₄₂H₅₆N₃O₇: [M+H]⁺ requires 714.4113).



*N*¹,*N*², di-(glycine)-*N*³-hexadecanosyl-5-aminobenzene-1,3-dicarboxylic acid **4.112**

To a solution of *N*¹,*N*², di-(glycine-benzyl ester)–*N*³-hexadecanosyl-5-aminobenzene-1,3-dicarboxylic acid **4.11** (53 mg, 0.07 mmol) in absolute ethanol (5 mL), Pd/C 10% w/w (6 mg) was added. The resulting mixture was stirred under H₂ gas overnight. The mixture was then

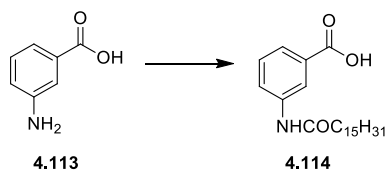
filtered through a Celite cake and the filtrate was concentrated under vacuum to afford the pure product **4.112** as a white solid (32 mg, 78%); IR ν_{\max} (KBr disc): 3326.2, 2922.1, 2853.4, 1732.7, 1714.5, 1682.8, 1638.9, 1600, 1570.7, 1417.7, 1354.8, 1328.3, 1301.1, 1210.84, 1029 cm^{-1} ; HRMS m/z (ESI+): 532.3023 ($\text{C}_{28}\text{H}_{42}\text{N}_3\text{O}_7$: $[\text{M}-\text{H}]^-$ requires 532.3028).



*N*¹, *N*², di-[2-*O*-(2,3,4,6-tetra-*O*-acetyl- β -*D*-galactopyranosyl)-ethyl-glycine]-*N*³-hexadecanosyl-5-aminobenzene 1,3, dicarboxamide **4.107**

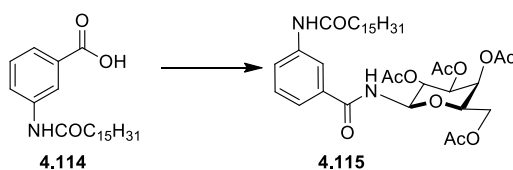
*N*¹,*N*²,di-(glycine)-*N*³-hexadecanosyl-5-aminobenzene-1,3-dicarboxylic acid **4.112** (28 mg, 0.05 mmol), HOBt (15 mg, 1.1 mmol) and TBTU (36 mg, 1.1 mmol) was placed under N_2 and dissolved in DMF (5 mL). NEt_3 (0.016 mL, 1.1 mmol) was added and the mixture was allowed to stir for 15 min. 2-Aminoethyl 2,3,4,6-tetra-*O*-acetyl- β -*D*-galactopyranoside **2.33** (61mg, 0.15 mmol) dissolved in DMF (5 mL) was then added. The solution was stirred overnight. The solvent was removed under reduced pressure and the residue was dissolved in DCM washed with 0.1 M HCl, aqueous sat. NaHCO_3 solution, brine and dried over MgSO_4 . Gradient elution chromatography (98:2-95:5, DCM: MeOH) yielded the pure product **4.107** as an oily solid (11 mg, 15%); $R_f = 0.26$ (95:5 DCM:MeOH); $[\alpha]_D^{25} = -7$ (c, 0.9 in DCM); IR ν_{\max} (NaCl plate, DCM): 3326.2, 2922.1, 2853.4, 1732.7, 1714.5, 1682.8, 1638.9, 1600, 1570.7, 1417.7, 1354.8, 1328.3, 1301.1, 1210.8, 1029 cm^{-1} ; ^1H NMR (300 MHz, CDCl_3): δ 8.69 (bs, 1 H, $\text{NHCOC}_{15}\text{H}_{31}$), 8.07 (s, 2 H, COCH_2NH), 8.01 (s, 2 H, Ar), 7.83 (s, 1 H, Ar), 6.97 (s, 2 H, $\text{CH}_2\text{CH}_2\text{NH}$), 5.39 (d, $J = 3.3$ Hz, 2 H, *H*-4), 5.16 (dd, $J = 7.8$ Hz, $J = 10.5$ Hz, 2 H, *H*-2), 5.06 (dd, $J = 3.3$ Hz, $J = 10.5$ Hz, 2 H, *H*-3), 4.58 (d, $J = 7.8$ Hz, 1 H, *H*-1), 4.21-4.07 (m, 6 H, overlap of *H*-6, *H*-6' and COCH_2NH), 4.0-3.95 (m, 2 H, *H*-5), 3.93-3.85 (m, 1 H, 1 H of $\text{CH}_2\text{CH}_2\text{O}$), 3.81-3.69 (m, 1 H, 1 H of $\text{OCH}_2\text{CH}_2\text{NH}$), 3.57-3.50 (m, 2 H, $\text{OCH}_2\text{CH}_2\text{NH}$), 2.37-2.30 (m, 2 H, $\text{NHCOCH}_2(\text{CH}_2)_{13}\text{CH}_3$), 2.13 (s, 6 H, $\text{O}(\text{CO})\text{CH}_3$), 2.09 (s, 6 H, $\text{O}(\text{CO})\text{CH}_3$), 2.04 (s, 6 H, $\text{O}(\text{CO})\text{CH}_3$), 1.98 (s, 6 H, $\text{O}(\text{CO})\text{CH}_3$), 1.74-1.61 (m, 2 H, $\text{NHCOCH}_2\text{CH}_2(\text{CH}_2)_{12}\text{CH}_3$), 1.24 (s, 24 H, $\text{NHCOCH}_2\text{CH}_2(\text{CH}_2)_{12}\text{CH}_3$), 0.87 (t, $J = 6.3$, 3 H, $\text{NHCOCH}_2\text{CH}_2(\text{CH}_2)_{12}\text{CH}_3$); ^{13}C NMR (75 MHz, CDCl_3): δ_c 178.1, 172.5 (CO), 170.6, 170.2, 170.1, 170.1 ($\text{O}(\text{CO})\text{CH}_3$), 169.9, 167.3 (CO), 135.2, 134 (ArC), 121.9, 121.4 (ArCH), 101.3 (C-1), 70.8 (C-5), 70.8 (C-3), 69.0 (C-2), 68.5 ($\text{OCH}_2\text{CH}_2\text{NH}$), 67.1 (C-4), 61.3 (C-6), 43.8 (COCH_2NHCO), 39.7 ($\text{OCH}_2\text{CH}_2\text{NH}$), 37.5 ($\text{NHCOCH}_2(\text{CH}_2)_{13}\text{CH}_3$), 31.9, 29.7, 29.7, 29.6, 29.5, 29.5, 29.4, 25.4, 22.7

(NHCOCH₂(CH₂)₁₃CH₃), 20.8, 20.7, 20.6, 20.5 (O(CO)CH₃), 14.11 (NHCOCH₂(CH₂)₁₃CH₃); HRMS m/z (ESI+): 1294.6044 (C₆₁H₉₂N₅O₂₅: [M-H]⁻ requires 1294.6044).



*N*³-hexadecanosyl-3-aminobenzoic acid **4.114**

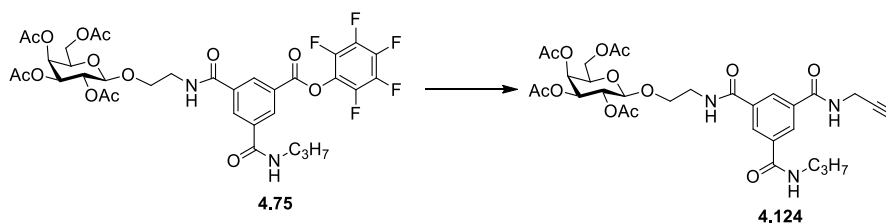
3-Aminobenzoic acid (1 g, 7.2 mmol) was dissolved in DMF (25 mL) and THF (5 mL) under Ar. Hexadecanoyl chloride (2.23 mL, 8 mmol) and NEt₃ (1.2 mL, 8.7 mmol) were added and the reaction mixture stirred overnight. The solvent was removed under reduced pressure. The resulting residue was dissolved in MeOH and the precipitate filtered off. The filtrate was then crystallised in EtOAc to yield the monoacid **4.114** as a cream solid (2.05 g, 75%); Mp = 210- 212 °C; IR ν_{max} (KBr): 3294.1, 2956.8, 2848.7, 2675.7, 1691.2, 1655.9, 1591.9, 1539.4, 1428.3, 1470.7, 1456.3, 1325.7, 1272.5, 1180.6, 1198.4, 1161.6, 111.5, 963.8, 944.4, 894.4, 816.5, 757.4, 718.7, 670.1, cm⁻¹; ¹H NMR (300 MHz, DMSO): δ 10.06 (s, 1 H, NHCO), 8.423 (s, 1 H, Ar), 7.83-7.77 (s, 1 H, Ar) 7.61-7.57 (m, 1 H, Ar), 7.40 (t, *J* = 7.7 Hz, 1 H, Ar), 2.30 (t, *J* = 6.9 Hz, 2 H, NHCOCH₂C₁₄H₂₉), 1.62-1.55 (m, 2 H, NHCOCH₂CH₂C₁₃H₂₇), 1.32-1.19 (m, 24 H, NHCOC₂H₄(CH₂)₁₂CH₃), 0.85 (t, *J* = 8.1 Hz, 3 H, NHCOC₁₄H₂₈CH₃); ¹³C NMR (75 MHz, DMSO): δ_c 171.5, 167.1 (CO), 139.5, 131.1 (ArC), 128.9, 123.7, 123.0, 119.7 (ArCH), 36.3 (NHCOCH₂C₁₄H₂₉), 31.3 (NHCOCH₂CH₂C₁₃H₂₆), 29.0, 28.9, 28.8, 28.7, 28.6, 28.5, 24.9, 22.1 (NHC₂H₄(CH₂)₁₂CH₃), 13.9 (NHC₁₄H₂₉CH₃); HRMS m/z (ESI+): 374.2715, (C₂₃H₃₆NO₃: [M-H]⁻ 374.2701).



*N*¹-(2,3,4,6-tetra-*O*-acetyl-β-*D*-galactopyranosyl)-*N*²-hexadecanosyl-3-aminobenzene 1-carboxamide **4.115**

*N*³-hexadecanosyl-3-aminobenzoic acid **4.114** (157 mg, 0.41 mmol), HOBt (61 mg, 0.45 mmol) and TBTU (145 mg, 0.45 mmol) were placed under N₂ and dissolved in DMF (8 mL). NEt₃ (0.11 mL, 0.82 mmol) was added and the mixture was allowed to stir for 15 min. The 1-amino-2,3,4,6-tetra-*O*-acetyl-β-*D*-galactopyranose **3.76** (215 mg, 0.62 mmol) dissolved in DMF (5 mL) was then added. The solution was stirred overnight. The solvent was removed under reduced pressure and the residue was dissolved in DCM washed with 0.1 M HCl, aqueous sat. NaHCO₃

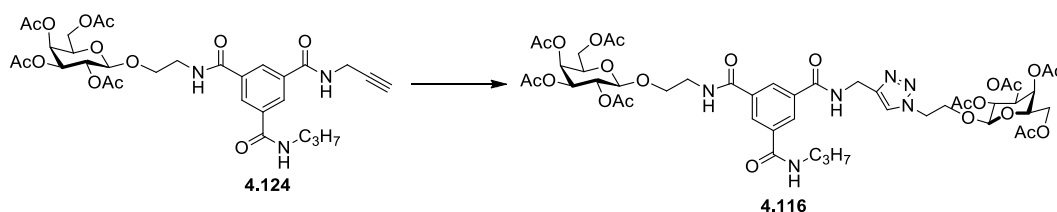
solution, brine and dried over MgSO_4 . Column chromatography (1:1, EtOAc: Pet Ether) yielded the pure monovalent derivative **4.115** as a waxy solid (190 mg, 65%); $R_f = 0.71$ (1:1, Pet Ether: EtOAc); $[\alpha]_D^{25} = 0$ (c, 1.1 in DCM); IR ν_{max} (NaCl plate, DCM): 3317.3, 2923.9, 2853.4, 1751.1, 1665.6, 1610.65, 1592.8, 1547.8, 1486.1, 1467.15, 1433.3, 1369.9, 1227.4, 1084.1, 1053.6, 957.0, 909.3, 805.4, 750.8, 688.3 cm^{-1} ; ^1H NMR (300 MHz, CDCl_3): δ 7.98-7.95 (m, 2 H, Ar), 7.84 (s, 1 H, Ar), 7.37 (s, 1 H, $\text{NHCOC}_{15}\text{H}_{31}$), 7.22 (d, $J = 9$ Hz, 2 H, H1NHCO), 5.56-5.47 (m, 2 H, overlap of $H-1$ and $H-4$), 5.32-5.20 (m, 2 H, overlap of $H-2$ and $H-3$), 4.17-4.05 (m, 3 H, overlap of $H-6$, $H-6'$ and $H-5$), 2.37-2.32 (m, 2 H, $\text{NHCOCH}_2(\text{CH}_2)_{13}\text{CH}_3$), 2.14, 2.01, 2.0 and 1.98 (each s, 3 H, $\text{O}(\text{CO})\text{CH}_3$), 1.71-1.66 (m, 2 H, $\text{NHCOCH}_2\text{CH}_2(\text{CH}_2)_{12}\text{CH}_3$), 1.36-1.15 (s, 24 H, $\text{NHCOCH}_2\text{CH}_2(\text{CH}_2)_{12}\text{CH}_3$), 0.85 (t, $J = 6.6$ Hz, 3 H, $\text{NHCOCH}_2\text{CH}_2(\text{CH}_2)_{12}\text{CH}_3$); ^{13}C NMR (75 MHz, CDCl_3): δ_c 172.0, 171.8, 170.3, 170.4, 170.2, 170.1, 166.8 (CO), 138.9, 133.3 (ArC), 129.5, 123.6, 121.9, 118.7 (ArCH), 79.0 (C-1), 72.2 (C-5), 70.9 (C-3), 68.5 (C-2), 67.3 (C-4), 61.3 (C-6), 37.7 ($\text{NHCOCH}_2(\text{CH}_2)_{13}\text{CH}_3$), 31.9, 29.7, 29.6, 29.5, 29.4, 29.3, 29.3, 25.5, 22.7 ($\text{NHCOCH}_2(\text{CH}_2)_{13}\text{CH}_3$), 20.8, 20.7 ($\text{O}(\text{CO})\text{CH}_3$), 14.1 ($\text{NHCOCH}_2(\text{CH}_2)_{13}\text{CH}_3$), HRMS m/z (ESI+): 705.3993, ($\text{C}_{37}\text{H}_{57}\text{N}_2\text{O}_{11}$: $[\text{M}+\text{H}]^+$ requires 705.3957) .



*N*¹-[2-*O*-(2,3,4,6-tetra-*O*-acetyl- β -*D*-galactopyranosyl)-ethyl]-*N*²-propargyl-*N*³-propyl-Benzene 1,5 dicarboxamide **4.124**

Monovalent derivative **4.75** (99 mg, 0.14 mmol), was dissolved in THF (5 mL) under Ar and propargyl amine (0.016 mL, 0.20 mmol) was added. The reaction mixture was stirred for 5 min and DIPEA (0.036 ml, 0.21 mmol) was added. The resulting solution was stirred at rt for 3 h. The solvent was removed *in vacuo* and the resulting residue purified by column chromatography (EtOAc) to yield compound **4.124** as a clear waxy solid (54 mg, 66%); $R_f = 0.47$ (EtOAc); $[\alpha]_D^{25} = -9.2$ (c, 1.3 in DCM); IR ν_{max} (NaCl plate, DCM): 3296.0, 3071.9, 2965.3, 2937.5, 2877.76, 2122.6, 1751.2, 1659.2, 1532.0, 1431.4, 1369.5, 1226.1, 1173.0, 1135.4, 1058.7, 997.5, 955.9, 914.6, 800.0, 737.3, 706.8, 683.41 cm^{-1} ; ^1H NMR (300 MHz, CDCl_3): δ 8.43 (s, 1 H, Ar), 8.35-8.33 (m, 2 H, Ar), 7.52 (t, $J = 5.1$ Hz, 1 H, NHCH_2CCH), 7.06-6.97 (m, 2 H, overlap of NHC_3H_7 and $\text{OCH}_2\text{CH}_2\text{NH}$), 5.38-5.36 (m, 1 H, $H-4$), 5.18 (dd, $J = 7.8$ Hz, $J = 10.5$ Hz, 1 H, $H-2$), 5.01 (dd, $J = 3.6$ Hz, $J = 10.5$ Hz, 1 H, $H-3$), 4.49 (d, $J = 7.8$ Hz, 1 H, $H-1$), 4.21-4.19 (m, 2 H,

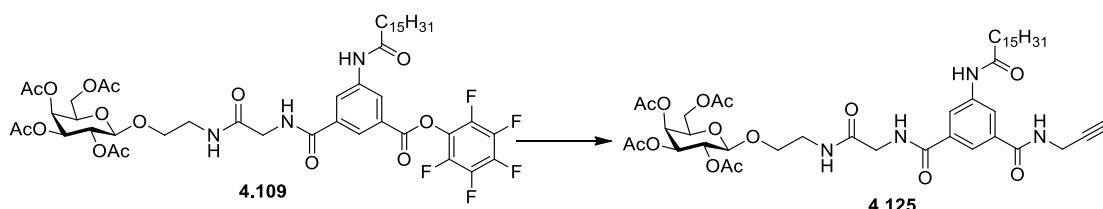
NHCH₂CCH), 4.13-4.05 (m, 2 H, *H*-6 and *H*-6'), 3.99-3.82 (m, 2 H, overlap of *H*-5 and 1 H of OCH₂CH₂NH) 3.8-3.55 (m, 3 H, overlap of 1 H of OCH₂CH₂NH and OCH₂CH₂NH), 3.41-3.34 (m, 2 H, NHCH₂C₂H₅), 2.24 (t, *J* = 2.7, 1 H NHCH₂CCH), 2.16, 2.02, 1.97, 1.91 (each s, 3 H, O(CO)CH₃), 1.63-1.56 (m, 2 H, NHCH₂CH₂CH₃), 0.94 (t, *J* = 7.2 Hz, 3 H, NHC₂H₄CH₃); ¹³C NMR (75 MHz, CDCl₃): δ_c 171.3 (CO), 170.6, 170.5, 170.3, 170.1 (OCOCH₃), 165.9, 161.6 (CO), 135.7, 134.8, 134.6 (ArC), 129.2, 128.5, 128.1 (ArCH), 101.2 (C-1), 79.32 (NHCH₂CCH), 71.78 (NHCH₂CCH), 70.9 (C-5), 70.5 (C-3), 69.2 (C-2) 68.3 (OCH₂CH₂NH), 66.8 (C-4), 61.3 (C-6), 42.13 (NHCH₂C₂H₅), 39.9 (OCH₂CH₂NH), 29.8 (NHCH₂CCH), 22.7 (NHCH₂CH₂CH₃), 21.1, 20.8, 20.6, 20.5 (O(CO)CH₃), 11.5 (NHC₂H₄CH₃); HRMS *m/z* (ESI⁺): 663.2614, (C₃₁H₄₀N₃O₁₃: [M+H]⁺ requires 663.2588).



*N*¹-[2-*O*-(2,3,4,6-tetra-*O*-acetyl-β-*D*-galactopyranosyl)-ethyl]-*N*²-[2-*O*-(2,3,4,6-Tetra-*O*-acetyl-β-*D*-galactopyranosyl)-ethyl-1,2,3-triazol-4-ylmethylamide]-*N*³-propyl-benzene 1,5 dicarboxamide
4.116

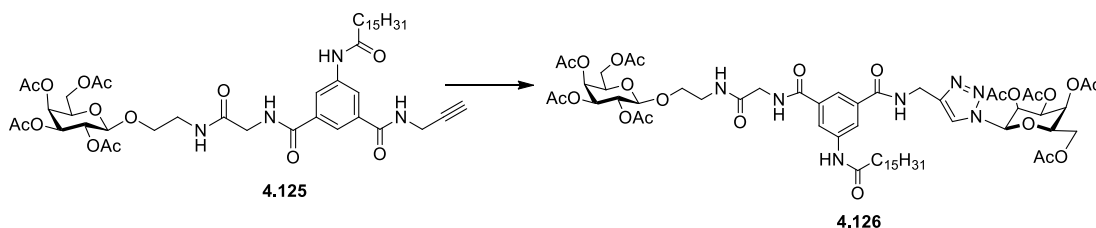
Copper sulphate .5H₂O (2 mg, 0.008 mmol) and sodium ascorbate (3 mg, 0.016 mmol) were added to a solution of 2-aminoethyl 2,3,4,6-tetra-*O*-acetyl-β-*D*-galactopyranoside **2.33** (34 mg, 0.082 mmol) and *O*-(azidoethyl)-(2,3,4,6-*O*-tetracetyl)-β-*D*-galactopyranose **2.44** (54 mg, 0.082 mmol) in DCM/Acetone/H₂O (3 mL, 1 mL, 1mL). The reaction was allowed to stir at rt overnight. The solvent was removed *in vacuo*, the residue dissolved in DCM and washed with brine. Column chromatography (8:1:1, DCM:MeOH:Toluene) afforded the pure product **4.116** as a clear oily solid (68 mg, 72%); *R*_f = 0.34 (8:1:1, DCM:MeOH:Toluene); [α]_D²⁵ = -12 (c, 1 in DCM); IR *v*_{max} (NaCl plate, DCM): 3382.3, 2964.8, 2938.3, 2879.1, 1749.5, 1659.4, 1536.2, 1432.2, 1370.3, 1226.6, 1173.7, 1135.3, 1057.9, 955.7 cm⁻¹; ¹H NMR (300 MHz, CDCl₃): δ 8.39-8.35 (m, 2 H, Ar), 8.29 (s, 1 H, Ar), 7.94-7.87 (m, 1 H, NHCH₂CN₃CH), 7.67 (s, 1 H, CN₃CH), 7.1 (t, *J* = 5.1 Hz, 1 H, OCH₂CH₂NH), 7.0 (t, *J* = 5.4 Hz, 1 H, CONHC₃H₇), 5.37-5.34 (m, 2 H, *H*-4), 5.19-5.10 (m, 2 H, *H*-2), 5.02-4.95 (m, 1 H, *H*-3), 4.72-4.65 (m, 2 H, CONHCH₂CN₃CH), 4.50-4.24 (m, 2 H, *H*-1), 4.13-4.01 (m, 4 H, *H*-6 and *H*-6'), 3.98-3.82 (m, 4 H, overlap of *H*-5 and 1 H of OCH₂CH₂NH) 3.81-3.6 (m, 6 H, overlap of 1 H of OCH₂CH₂NH and OCH₂CH₂NH), 3.39-3.33 (m, 2 H, NHCH₂C₂H₅), 2.15, 2.12, 2.02, (each s, 3 H, O(CO)CH₃) 1.96-1.88 (m, 15 H, O(CO)CH₃), 1.62-1.55 (m, 2 H, NHCH₂CH₂CH₃), 0.93 (t, *J* = 7.2 Hz, 3 H, NHC₂H₄CH₃); ¹³C NMR (75 MHz, CDCl₃): δ_c 171.2 (CO), 170.5, 170.4, 170.3, 170.3, 170.2, 170.11, 170.1 (OCOCH₃), 169.75, 165.83 (CO),

144.3 (CN₃CH), 135.6, 134.8 (ArC), 128.9, 128.3, 128.2 (ArCH), 101.2, 101.9 (C-1), 123.95 (CN₃CH), 70.9 (C-5), 70.5 (C-3), 69.1 (C-2), 68.5, 68.4 (OCH₂CH₂NH), 66.9 (C-4), 61.3, 61.2 (C-6), 42.13 (NHCH₂C₂H₅), 39.9 (OCH₂CH₂NH), 35.6 (NHCH₂CN₃CH), 22.7 (NHCH₂CH₂CH₃), 20.7, 20.7 20.6, 20.6 20.5 (O(CO)CH₃), 11.5 (NHC₂H₄CH₃); HRMS m/z (ESI⁺): 540.7049, (C₄₇H₆₄N₆O₂₃: [M+2H]²⁺ requires 540.7022)



*N*¹-[2-*O*-(2,3,4,6-tetra-*O*-acetyl-β-*D*-galactopyranosyl-ethyl-glycine)-*N*²-propargyl-*N*²-hexadecanosyl-5-aminobenzene 1,3, dicarboxamide **4.125**

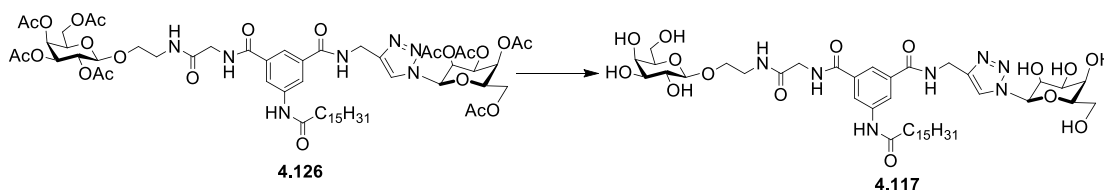
Compound **4.109** (20 mg, 0.019 mmol), was dissolved in THF (3 mL) under Ar and propargyl amine (0.016 mL, 0.0018 mmol) added. The reaction mixture was stirred for 5 min and NEt₃ (0.004 ml, 0.029 mmol) was added. The resulting solution was stirred at rt for 3 h. The solvent was removed *in vacuo* and the resulting residue purified by column chromatography (EtOAc) to yield compound **4.125** as a waxy solid (11 mg, 65%); R_f = 0.29 (EtOAc); [α]_D²⁵ = -3.7 (c, 0.85 in DCM); IR ν_{max} (NaCl plate, DCM): 3287.4, 3086.2, 2924.0, 2853.0, 2140.9, 2119.9, 1751.6, 1648.2, 1549.4, 1447.0, 1369.1, 1259.1, 1227.4, 1070.2, 956.2, 899.9, 800.9 cm⁻¹; ¹H NMR (300 MHz, CDCl₃): δ 8.39 (s, 1 H, CNHCOC₁₅H₃₁), 8.21 (s, 1 H, Ar), 8.05 (s, 1 H, Ar), 7.93 (s, 1 H, Ar) 7.79 (bs, 1 H, COCH₂NHCO), 7.32 (bs, 1 H, NHCH₂CCH), 6.85-6.82 (m, 1 H, OCH₂CH₂NH), 5.39-5.38 (m, 1 H, *H*-4), 5.17 (dd, *J* = 7.8 Hz, *J* = 10.2 Hz, 1 H, *H*-2), 5.08 (dd, *J* = 3 Hz, *J* = 10.2 Hz, 1 H, *H*-3), 4.57 (d, *J* = 7.8 Hz, 1 H, *H*-1), 4.22-4.06 (m, 6 H, overlap of *H*-6, *H*-6', COCH₂NHCO and CONHCH₂CCH), 4.01-3.96 (m, 1 H, *H*-5), 3.91-3.87 (m, 1 H, 1 H of OCH₂CH₂NH), 3.76-3.73 (m, 1 H, 1 H of OCH₂CH₂NH), 3.54-3.50 (m, 2 H, OCH₂CH₂NH), 2.38 (t, *J* = 7.5 Hz, 2 H, NHCOCH₂C₁₄H₂₉), 2.28 (t, *J* = 4.8 Hz, 1 H, NHCH₂CCH), 2.14, 2.07, 2.06, 1.99 (each s, 3 H, O(CO)CH₃), 1.78-1.70 (m, 2 H, NHCOCH₂CH₂C₁₃H₂₇), 1.24 (s, 24 H, NHCOC₂H₄(CH₂)₁₂CH₃), 0.86 (t, *J* = 6.6, 3 H, NHCOC₁₄H₂₈CH₃); ¹³C NMR (75 MHz, CDCl₃): δ_c 173 (CO), 170.8, 170.4, 170.3, 170.2 (O(CO)CH₃), 170.0, 167.4, 166.9 (CO), 139.6, 134.7, 134.2 (ArC), 121.5, 120.6 (ArCH), 101.4 (C-1), 79.9 (NHCH₂CCH), 77.4 (NHCH₂CCH), 71.8 (C-5), 71 (C-3), 69.2 (C-2), 68.6 (OCH₂CH₂NH), 67.2 (C-4), 61.5 (C-6), 60.5 (NHCH₂CCH) 44.0 (COCH₂NHCO), 39.8 (OCH₂CH₂NH), 37.7 (NHCOCH₂(CH₂)₁₃CH₃), 32.1, 30.0, 29.9, 29.8, 29.7, 29.6, 29.5, 25.6, 22.8 (NHCOCH₂(CH₂)₁₃CH₃), 21.0, 20.9, 20.8 and 20.7 (O(CO)CH₃), 14.3 (NHCOCH₂(CH₂)₁₃CH₃); HRMS m/z (ESI⁺): 887.4642 (C₄₅H₆₇N₄O₁₄: [M+H]⁺ requires 887.4648).



*N*¹-[2-*O*-(2,3,4,6-tetra-*O*-acetyl- β -*D*-galactopyranosyl-ethyl-glycine)-*N*²-(2,3,4,6-tetra-*O*-acetyl- β -*D*-galactopyranosyl-1,2,3-triazol-4-ylmethylamide)-*N*³-hexadecanosyl-5-aminobenzene 1,3, dicarboxamide **4.126**

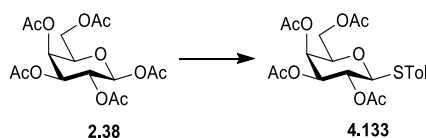
Copper sulphate $\cdot 5\text{H}_2\text{O}$ (2 mg, 0.006 mmol) and sodium ascorbate (3 mg, 0.013 mmol) were added to a solution of 1-azido-2,3,4,6-tetra-*O*-acetyl- β -*D*-galactopyranose **3.67** (29 mg, 0.078 mmol) and *N*¹-[2-*O*-(2,3,4,6-Tetra-*O*-acetyl- β -*D*-galactopyranosyl-ethyl-glycine)-*N*²-propargyl-*N*³-hexadecanosyl-5-aminobenzene 1,3, dicarboxamide **4.125** (58 mg, 0.065 mmol) in DCM/Acetone/ H_2O (3 mL, 1 mL, 1mL). The reaction was allowed to stir at rt overnight. The solvent was removed *in vacuo*, the residue dissolved in DCM and washed with brine. Gradient elution chromatography (EtOAc- 8:1:1, DCM:MeOH:Toluene) afforded the pure product as a clear oily solid **4.126** (53 mg, 65%); $R_f = 0.46$ (8:1:1 DCM:MeOH:Toluene); $[\alpha]_D^{25} = -10.6$ (c, 1 in DCM); IR ν_{max} (NaCl plate, DCM): 3305.1, 3086.7, 2924.3, 2853.5, 1752.3, 1649.6, 1599.4, 1548.2, 1446.7, 1427.6, 1370.2, 1226.2, 171.2, 1060.6, 954.6, 900.0, 802.4, 731.5, 682.0 cm^{-1} ; ¹H NMR (300 MHz, CDCl_3): δ 8.73 (s, 1 H, $\text{CNHCOC}_{15}\text{H}_{31}$), 8.27 (bs, 1 H, COCH_2NHCO), 8.05 (s, 2 H, overlap of CHCN_3 and *H*-Ar), 8.00 (bs, 1 H, $\text{NHCH}_2\text{CN}_3\text{CH}$), 7.84 (s, 1 H, Ar), 7.75 (s, 1 H, Ar), 7.93 (s, 1 H, Ar), 7.00 (bs, 1 H, $\text{OCH}_2\text{CH}_2\text{NH}$), 5.9 (d, $J = 9.3$ Hz, 1 H, *H*-1'), 5.64 (t, $J = 9.9$ Hz, 1 H, *H*-2'), 5.53 (m, 1-H, *H*-4'), 5.39-5.38 (m, 1 H, *H*-4), 5.27 (dd, $J = 3.6$ Hz, 1 H, *H*-3'), 5.15 (dd, $J = 7.8$ Hz, $J = 10.2$ Hz, 1 H, *H*-2), 5.05 (dd, $J = 3.3$ Hz, $J = 10.5$ Hz, 1 H, *H*-3), 4.68 (bs, 1 H, $\text{NHCH}_2\text{CN}_3\text{CH}$), 4.56 (d, $J = 7.8$ Hz, 1 H, *H*-1), 4.32-4.28 (m, 1 H, *H*-5'), 4.22-4.06 (m, 6 H, overlap of *H*-6, *H*-6' and COCH_2NHCO), 3.99-3.95 (m, 1 H, *H*-5), 3.89-3.86 (m, 1 H, 1H of $\text{OCH}_2\text{CH}_2\text{NH}$), 3.71-3.67 (m, 1 H, 1 H of $\text{OCH}_2\text{CH}_2\text{NH}$), 3.49-3.44 (m, 2 H, $\text{OCH}_2\text{CH}_2\text{NH}$), 2.33 (t, $J = 7.2$ Hz, 2 H, $\text{NHCOCH}_2\text{C}_{14}\text{H}_{29}$), 2.15, 2.13, 2.07, 2.03, 2.0, 1.98, 1.97 and 1.83 (each s, 3 H, $\text{O}(\text{CO})\text{CH}_3$), 1.70-1.64 (m, 2 H, $\text{NHCOCH}_2\text{CH}_2\text{C}_{13}\text{H}_{27}$), 1.23 (s, 24 H, $\text{NHCOC}_2\text{H}_4(\text{CH}_2)_{12}\text{CH}_3$), 0.86 (t, $J = 6.6$, 3 H, $\text{NHCOC}_{14}\text{H}_{28}\text{CH}_3$); ¹³C NMR (75 MHz, CDCl_3): δ_c 172.5 (CO), 170.5, 170.3, 170.2, 170.1, 170.1, 170.0, 169.9 ($\text{O}(\text{CO})\text{CH}_3$), 169.3, 167.0, 166.7, 162.61 (CO), 145.6 ($\text{NHCH}_2\text{CN}_3\text{CH}$), 139.1, 134.6, 133.9 (*C*-Ar), 121.5, 120.3 (*CH*-Ar), 120.2 ($\text{NHCH}_2\text{CN}_3\text{CH}$), 101.2 (*C*-1), 86.0 (*C*-1'), 73.9 (*C*-5'), 70.8 (*C*-4'), 70.7 (*C*-3), 70.6 (*C*-5), 68.8 (*C*-2), 68.5 ($\text{OCH}_2\text{CH}_2\text{NH}$), 67.9 (*C*-2'), 66.9 (*C*-4), 66.7 (*C*-4'), 61.2, 61.1 (*C*-6 and *C*-6'), 43.6 (COCH_2NHCO), 39.4 ($\text{OCH}_2\text{CH}_2\text{NH}$), 37.3 ($\text{NHCOCH}_2(\text{CH}_2)_{13}\text{CH}_3$), 35.5 ($\text{NHCH}_2\text{CN}_3\text{CH}$), 31.9, 29.7, 29.6, 29.6, 29.5, 29.3, 29.3, 25.4, 22.6

(NHCOCH₂(CH₂)₁₃CH₃), 20.8, 20.7, 20.6, 20.6, 20.5, 20.2 (O(CO)CH₃), 14.1 (NHCOCH₂(CH₂)₁₃CH₃); HRMS m/z (ESI+): 1260.5813 (C₅₉H₈₆N₇O₂₃: [M+H]⁺ requires 1260.577).



*N*¹-[2-*O*-(2,3,4,6-tetra-*O*-acetyl-β-*D*-galactopyranosyl-ethyl-glycine)-*N*²-(2,3,4,6-tetra-*O*-acetyl-β-*D*-galactopyranosyl-1,2,3-triazol-4-ylmethylamide)-*N*³-hexadecanosyl-5-aminobenzene 1,3-dicarboxamide **4.117**

NEt₃ (0.1 mL, 0.016 mmol) was added to a stirring solution **4.126** (50 mg, 0.04 mmol) dissolved in DCM/MeOH/H₂O (1 mL/2 mL/1 mL) at 40 °C. The mixture was stirred for 18 h. The reaction mixture was concentrated under reduced pressure and triturated with Et₂O to yield compound **4.117** as a white solid (10 mg, 92%); [α]²⁵_D = 2.3 (c, 0.87 in MeOH); ¹H-NMR (300 MHz, *d*₅-Pyr): δ 10.97 (bs, 1 H, NHCOCH₂C₁₅H₃₁), 9.88 (t, *J* = 5.0 Hz, NHCH₂CN₃CH), 9.76 (t, *J* = 5.3 Hz, NHCOCH₂NHCO), 8.97 (s, 1 H, Ar), 8.90 (s, 1 H, AHr), 8.83 (t, *J* = 5.34 Hz, NHCOCH₂NHCO), 8.68 (s, 1 H, Ar), 8.47 (s, 1 H, CN₃CH), 6.28 (d, *J* = 9.15 Hz, H-1'), 5.22-5.13 (m, 1 H, H-2'), 4.93 (d, *J* = 5.3 Hz, NHCH₂CN₃CH), 4.78 (d, *J* = 7.7 Hz, 1 H, H-1), 4.66 (d, *J* = 2.8 Hz, 1 H, H-4'), 4.53-4.34 (m, 11 H, overlap of H-2, H-3, H-3', H-4, H-5, H-6 and H-6', NHCOCH₂NHCO), 4.17-4.13 (m, 1 H, 1 H of OCH₂CH₂NH), 4.07-4.7 (m, 1 H, H-5), 4.12-4.06 (m, 1 H, 1 H, OCH₂CH₂NH), 3.73-3.70 (m, 2 H, OCH₂CH₂NH), 1.87-1.77 (m, 2 H, NHCOCH₂C₁₄H₂₉), 1.32-1.18 (m, 22 H, NHCOCH₂(CH₂)₁₂CH₃), 0.87 (t, *J* = 6.3, 3 H, NHCOCH₂C₁₄H₂₆CH₃); ¹³C NMR (75 MHz, CDCl₃): δ_c 172.8, 170.4, 168.1, 167.5 (each CO), 151.8 (ArC), 146.5 (CN₃CH), 141.1 (ArC), 124.1 (CN₃CH), 124.1, 122.8, 121.9 (ArCH), 105.9 (C-1), 80.9 (C-1'), 77.4 (C-5), 76.1 (C-3'), 75.6 (C-3), 72.9 (C-2), 71.6 (C-2'), 70.6 (C-4, C-4'), 69.7 (OCH₂CH₂NH), 62.8, 62.7 (C-6 and C-6'), 44.4 (NHCOCH₂NHCO), 40.6 (OCH₂CH₂NH), 37.7 (NHCOCH₂C₁₄H₂₉), 32.3, 30.2, 30.0, 29.8, 26.3, 23.2 (NHCOCH₂(CH₂)₁₃CH₃), 14.5 (NHCOCH₂(CH₂)₁₃CH₃); HRMS m/z (ESI+): 924.4895 (C₄₃H₇₀N₇O₁₅: [M+H]⁺ requires 924.4924).

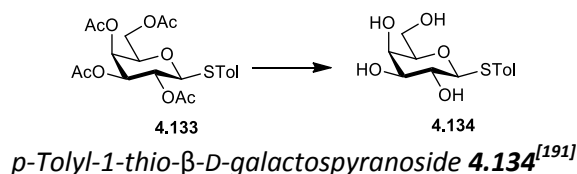


p-Tolyl-2,3,4,6-tetra-*O*-acetyl-1-thio-β-*D*-galactospyranoside **4.133**^[191]

β-*D*-Galactose pentaacetate (5 g, 12.8 mmol) and *p*-toluenethiol (1.8 g, 14.7 mmol) were dissolved in DCM (100 mL) under N₂ and BF₃Et₂O (4.7 mL, 38.4 mmol) added dropwise at 0 °C. The mixture was stirred at rt overnight, diluted with DCM (100 mL) and washed with aqueous

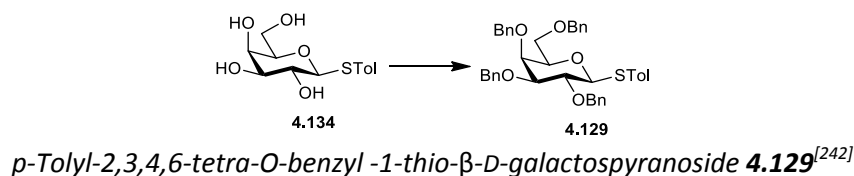
sat. NaHCO₃ solution, dried over MgSO₄, filtered and concentrated. Silica gel column chromatography (2:1, Pet Ether:EtOAc) afforded the pure product **4.133** as a white solid (4.1 g, 69%); $R_f = 0.52$ (2:1, Pet Ether:EtOAc); IR ν_{\max} (NaCl plate, DCM): 3464.4, 3108.1, 3036.3, 3012.4, 2980.4, 2877.9, 1737.7, 1641.4, 1493.8, 1462.8, 1406.4, 1375.4, 1285.1, 1145.8, 1157.0, 1107.6, 1081.9, 1047.7, 1020.4, 946.1, 897.3, 859.1, 805.9, 748.4, 709.5, 650.3 cm^{-1} ; ¹H NMR (300 MHz, CDCl₃): δ 7.40 (d, $J = 8.1$ Hz, 2 H, Ar), 7.11 (d, $J = 8.1$ Hz, 2 H, Ar), 5.39 (d, $J = 3.3$ Hz, 1 H, *H*-4), 5.20 (t, $J = 9.9$ Hz, 1 H, *H*-2), 5.03 (dd, $J = 3.3$ Hz, $J = 9.9$ Hz), 4.64 (d, $J = 9.9$ Hz, 1 H, *H*-1), 4.21-4.07 (m, 2 H, *H*-6 and *H*-6'), 3.90 (t, $J = 6.4$ Hz, 1 H, *H*-5), 2.33 (s, 3 H, SPhCH₃), 2.10, 2.09, 2.03, 1.96 (each s, 3 H, O(CO)CH₃); HRMS m/z (ESI⁺): 477.1210 (C₂₁H₂₆NaO₉S: [M+Na]⁺ requires 477.1195).

NMR data is in agreement with the literature.^[191, 241]



p-Tolyl 2,3,4,6-tetra-*O*-acetyl-1-thio- β -D-galactospyranoside **4.133** (980 mg, 2 mmol) was dissolved in a mixture of DCM/MeOH (10 mL, 7 mL) and 5.14 M NaOMe (0.19 mL, 1 mmol) was added. The mixture was stirred 1 h, neutralised with Amberlite IR-120, filtered and evaporated to dryness to yield the crude product **4.134** as a white solid, which was reacted without further purification (500 mg, 85%); ¹H NMR (300 MHz, MeOD): δ 7.38 (d, $J = 7.9$ Hz, 2 H, Ar), 7.04 (d, $J = 7.9$ Hz, 2 H, Ar), 4.43 (d, $J = 9.5$ Hz, 1 H, *H*-1), 3.8-3.80 (m, 1 H, *H*-4), 3.68-3.64 (m, 2 H, *H*-6 and *H*-6'), 3.54-3.39 (m, 3 H, overlap of *H*-2, *H*-3 and *H*-5), 2.23 (s, 3 H, SPhCH₃); HRMS m/z (ESI⁺): 287.0965 (C₁₃H₁₉O₅S: [M+Na]⁺ requires 287.0948).

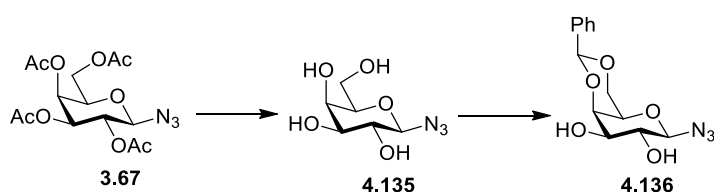
NMR data is in agreement with the literature.^[191]



p-Tolyl 1-thio- β -D-galactospyranoside **4.134** (500 mg, 1.7 mmol) was dissolved in DMF (10 mL) under N₂. The solution was cooled to 0 °C and NaH (419 mg, 17 mmol) was added portionwise. The resulting mixture was allowed to stir for 15 min and BnBr (2 mL, 17 mmol) added. The

reaction mixture was stirred at rt overnight, diluted with EtOAc (20 mL) and washed with aqueous sat. NaHCO₃ sol, H₂O and dried over MgSO₄. Column chromatography (5:1, Pet Ether:EtOAc) afforded the pure product **4.129** as a white solid (905 mg, 80%); *R_f* = 0.75 (5:1, Pet Ether:EtOAc); ¹H NMR (300 MHz, CDCl₃): δ 7.51 (d, *J* = 8.1 Hz, 2 H, Ar), 7.46-7.30 (m, 20 H, Ar), 7.03 (d, *J* = 7.9 Hz, 2 H, Ar), 5.01 (d, *J* = 11.5 Hz, 1 H, *H*-1), 4.86-4.76 (m, 1 H, *H*-4), 4.68-4.62 (m, 1 H, *H*-2), 4.53-4.43 (m, 2H, PhCH₂), 4.01 (m, 1 H, H-3), 3.95 (t, *J* = 6.4 Hz, 1 H, *H*-5), 3.72-3.61 (m, 2 H, H-6 and H-6') 2.32 (s, 3 H, SPhCH₃); HRMS *m/z* (ESI+): 646.2754 (C₄₁H₄₃O₅S: [M+H]⁺ requires 646.2753).

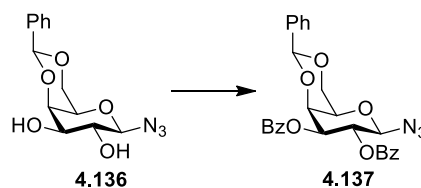
NMR data is in agreement with the literature.^[242]



1-Azido-4,6-O-benzylidene-β-D-galactopyranose **4.136**^[193]

1-Azido-2,3,4,6-tetra-*O*-acetyl-β-D-galactopyranose **3.67** (500 mg, 1.3 mmol) was dissolved in DCM and MeOH (10 mL, 7 mL) and 5.14 M NaOMe (0.124 mL, 0.67 mmol) was added. The mixture was stirred for 1 h, neutralised with Amberlite IR-120, filtered and evaporated to dryness to yield the crude product **4.135** as a white solid. The deprotected galactose azide **4.135** (100 mg, 0.48 mmol) was dissolved in MeCN (1 mL) under Ar, and *p*-TsOH (4 mg, 0.024 mmol) and benzaldehyde dimethyl acetal (370 mg, 2.4 mmol) were added. The reaction mixture was stirred for 24 h, and NEt₃ (0.02 mL) was added. The solvent was removed under reduced pressure and column chromatography (EtOAc) yielded the pure product **4.136** as a clear waxy solid (119 mg, 83%); *R_f* = 0.32 (EtOAc); IR *v*_{max} (NaCl plate, DCM): 3385.7, 2911.5, 2860.8, 2116.6, 1452.4, 1405.8, 1364.9, 1343.9, 1331.0, 1295.6, 1249.7, 1174.5, 1101.6, 1085.8, 1002.4, 963.1, 946.2, 899.4, 820.3, 737.5, 695.7, 597.4 cm⁻¹; ¹H NMR (300 MHz, CDCl₃): δ 7.55-7.42 (m, 2 H, Ar), 7.40-7.35 (m, 3 H, Ar), 5.52 (s, 1 H, COCHPHCO), 4.53 (d, *J* = 8.4 Hz, 1 H, *H*-1), 4.34 (dd, *J* = 1.5 Hz, *J* = 12.6 Hz, 1 H, *H*-6), 4.19-4.18 (m, 1 H, *H*-3), 4.05 (dd, *J* = 2.1 Hz, *J* = 12.9 Hz, 1 H, *H*-6'), 3.71-3.65 (m, 2 H, overlap of *H*-2 and *H*-4), 3.54-3.53 (m, 1 H, *H*-5), 2.89, 2.80 (each bs, 1 H, OH); HRMS *m/z* (ESI+): 328.0725 (C₁₃H₁₅ClN₃O₅: [M+Cl]⁻ requires 328.0706).

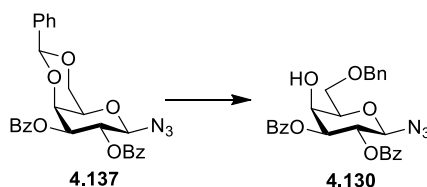
NMR data is in agreement with the literature.^[193]



1-Azido-2,3-O-benzoyl-4,6-O-benzylidene-β-D-galactopyranose **4.137**^[193]

1-Azido-4,6-O-benzylidene-β-D-galactopyranose **4.136** (971 mg, 3.3 mmol), was dissolved in Pyr (10 mL), placed on ice and benzoyl chloride (0.96 mL, 8.2 mmol) was added dropwise. The mixture was allowed to warm to rt and stirred overnight. 1 mL of MeOH was added and the solvent was evaporated under reduced pressure. The residue was dissolved in DCM, washed with aqueous sat. NaHCO₃ and dried MgSO₄. Column chromatography (1:1, Pet Ether:EtOAc) afforded the title compound **4.137** as a white solid (1.39 g, 84%); R_f = 0.74 (1:1, Pet Ether:EtOAc); IR ν_{max} (NaCl plate, DCM): 3036.0, 2982.6, 2862.9, 2119.8, 1727.5, 1601.9, 1584.8, 1492.2, 1451.7, 1403.3, 1368.0, 1340.9, 1315.8, 12748, 1248.8, 1178.1, 1109.6, 1093.8, 1069.8, 1026.2, 999.1, 962.2, 936.8, 835.2, 817.8, 768.9, 738.1, 709.2 cm⁻¹; ¹H NMR (300 MHz, CDCl₃): δ 8.05-7.95 (m, 4 H, Ar), 7.55-7.47 (m, 4 H, Ar), 7.41-7.33 (m, 7 H, Ar), 5.84 (dd, *J* = 8.7 Hz, *J* = 10.2 Hz, 1 H, *H*-2), 5.65 (s, 1 H, COCHPHCO), 5.41 (dd, *J* = 3.3 Hz, *J* = 10.2 Hz, *H*-3), 4.87 (d, *J* = 8.7 Hz, 1 H, *H*-1), 4.63-4.62 (m, 1 H, *H*-4), 4.44 (dd, *J* = 1.5 Hz, *J* = 12.6 Hz, 1 H, *H*-6), 4.17-4.11 (m, 1 H, *H*-6'), 3.79 (d, *J* = 0.9 Hz, 1 H, *H*-5); ¹³C NMR (75 MHz, CDCl₃): δ_c 166.1, 165.1 (CO), 137.3 (ArC), 133.5, 133.4, 129.9, 129.8, 129.1 (each ArCH), 129.1, 128.9, (ArC), 128.5, 128.4, 128.2, 126.3 (ArCH), 101.4 (COCHPHCO), 88.5 (*C*-1), 73.4, (*C*-4), 72.5 (*C*-3), 68.7, 68.4 (*C*-6'), 68.40 (*C*-5, *C*-2); HRMS *m/z* (ESI⁺): 536.1211 (C₂₇H₂₃ClN₃O₇: [M+Cl]⁻ requires 536.123).

This compound is mentioned in the literature but no experimental data is reported.^[189]

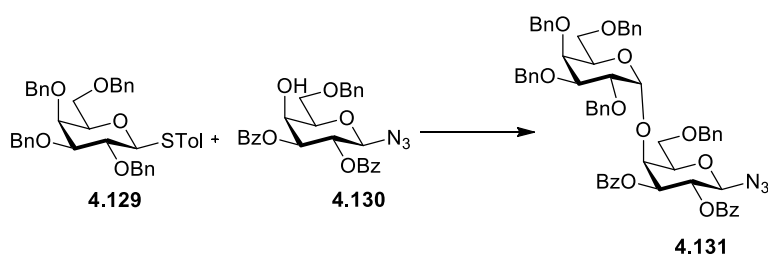


1-azido-2,3-di-O-benzoyl-6-O-benzyl-β-D-galactopyranose **4.208**^[194]

1-azido-2,3-O-benzoyl-4,6-O-benzylidene-β-D-galactopyranose **4.137** (190 mg, 0.37mmol) was dissolved in fresh anhydrous THF (5 mL) containing 4A molecular sieves (500 mg), and stirred for 20 min. NaCNBH₃ (238 mg, 3.7 mmol) and a crystal of methyl orange were added. A

solution of HCl in Et₂O (2 M) was added dropwise until the solution persisted as a pink colour. The reaction mixture was stirred for 90 min and an additional portion of HCl solution in Et₂O (2 M, 0.5 mL) was added. The reaction was stirred for a further 2.5 h. The mixture was filtered into a separating funnel containing a 1:1 mixture of DCM and H₂O (10 mL of each), and the organic layer separated. The aqueous layer was then extracted with DCM (2x5 mL), and the organic layers combined. The combined organic layers were washed successively with aqueous sat. NaHCO₃ and brine, dried over MgSO₄, filtered and concentrated. Column chromatography afforded title glycosyl acceptor **4.130** as colourless oil (138 mg, 73%); *R_f* = 0.15 (5:1, Pet Ether:EtOAc); $[\alpha]_D^{25} = +25.4$ (c, 1.1 in DCM); IR ν_{\max} (NaCl plate, DCM): 3462.6, 3088.4, 3032.9, 3064.0, 2924.6, 2873.9, 2118.4, 1723.6, 1601.8, 1584.7, 1494.5, 1452.1, 1278.1, 1263.8, 1179.1, 110.2, 1071.2, 1028.6, 935.5, 802.9, 709.8 cm⁻¹; ¹H NMR (300 MHz, CDCl₃): δ 7.99-7.93 (m, 4 H, Ar), 7.50-7.25 (m, 11 H, Ar), 5.79 (dd, *J* = 8.8 Hz, *J* = 10.2 Hz, 1 H, *H*-2), 5.33 (dd, *J* = 3.0 Hz, *J* = 10.2 Hz, *H*-3), 4.83 (d, *J* = 8.8 Hz, 1 H, *H*-1), 4.61 (s, 2 H, PhCH₂), 4.41 (t, *J* = 3.2 Hz, 1 H, *H*-4), 3.96 (t, *J* = 5.2 Hz, 1 H, *H*-5), 3.84 (d, *J* = 5.2 Hz, 2 H, *H*-6'), 3.23 (d, *J* = 3.7 Hz, 1 H, OH); ¹³C NMR (75 MHz, CDCl₃): δ_c 165.9, 165.5 (CO), 137.5 (ArC), 133.7, 133.6, 129.9, (ArCH), 129.1, 128.9 (ArC), 128.7, 128.6, 128.5, 128.1, 128.0 (ArCH), 88.7 (C-1), 75.5, (C-5), 74.3 (C-3), 74.0 (CH₂), 69.4 (C-6), 69.0 (C-2), 68.1 (C-4); HRMS *m/z* (ESI+): 504.1774 (C₂₇H₂₆N₃O₇: [M+H]⁺ requires 504.1765).

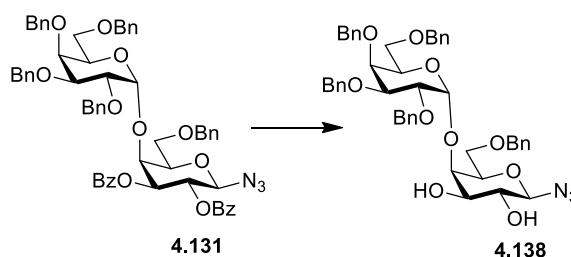
This compound is mentioned in the literature but no experimental data are reported.^[189]



1-azido-2,3,4,6-tetra-O-benzyl- α -D-galactopyranosyl-(1 \rightarrow 4)-2,3-di-O-benzoyl-6-O-benzyl- β -D-galactopyranoside **4.131**

1-Azido-2,3-di-O-benzoyl-6-O-benzyl- β -D-galactopyranose **4.130** (372 mg, 0.73 mmol), *p*-tolyl 2,3,4,6-tetra-O-benzyl-1-thio- β -D-galactopyranoside **4.129** (620 mg, 0.95 mmol) and NIS (453 mg, 2 mmol mmol) were placed under Ar and dissolved in DCM (6 mL), and Et₂O (12 mL) and cooled to -55 °C. TMSOTf (0.03 mL, 0.16 mmol) was added and the mixture was stirred for 1 h. NEt₃ (1.5 mL) was added, and the mixture was further stirred for 1 h at -55 °C. The mixture was warmed to rt, diluted with DCM and washed successively with aqueous sat. NaHCO₃ and

brine, dried over MgSO₄, filtered and concentrated. Gradient elution column chromatography (Pet ether-3:1, Pet Ether:EtOAc) afforded the title glycoside **4.131** as colourless oil (308 mg, 41%); $R_f = 0.63$ (3:1, Pet Ether:EtOAc); $[\alpha]_D^{25} = +63$ (c, 0.95 in CHCl₂); IR ν_{\max} (NaCl plate, DCM): 3063.4, 3030.7, 2923.9, 2868.7, 2116.8, 1730.3, 1601.8, 1584.9, 1452.7, 1360.1, 1314.4, 1452.7, 1360.1, 1275.5, 1098.1, 912.9, 803.4, 741.1, 697.8 cm⁻¹; ¹H NMR (300 MHz, CDCl₃): δ 7.97-7.89 (m, 4 H, Ar), 7.51-7.21 (m, 31 H, Ar), 5.78-5.71 (m, 1 H, *H*-2), 5.26-5.23 (m, 1 H, *H*-3), 4.94 (dd, $J = 3.1$ Hz, 1 H, *H*-1), 4.88-4.87 (m, 1 H, *H*-4'), 4.83 (d, $J = 6$ Hz, *H*-1'), 4.77 (s, 2 H, PhCH₂), 4.63-4.59 (m, 1 H, *H*-2'), 4.49-4.45 (m, 1 H, *H*-3'), 4.41 (bs, 1 H, *H*-4), 4.33-4.28 (m, 1 H, *H*-5'), 4.26 (s, 2 H, PhCH₂), 4.15-3.92 (m, 8 H, overlap of PhCH₂ and *H*-6), 3.71-3.65 (m, 1 H, *H*-5), 3.71-3.65 (m, 1 H, 1 H of *H*-6'), 3.41-3.35 (m, 1 H, of *H*-6'); ¹³C NMR (75 MHz, CDCl₃): δ_c 171.2, 166.2, 165.3 (CO), 138.8, 138.7, 138.6, 138.2, 137.8 (ArC), 133.4, 133.3, 129.8, 129.7, 1290, 128.9 (ArCH), 128.4-127.3 (overlap of ArC and ArCH), 100.3 (*C*-1), 88.7 (*C*-1'), 78.8, 76.4, 76.3 (each CH), 74.9 (PhCH₂), 74.8 (CH), 74.7 (*C*-3), 74.1 (*C*-3'), 73.8, 73.1, 72.8, 72.5 (each CH₂), 69.6 (*C*-2), 69.0 (*C*-2') 67.9, 67.4 (each CH₂); HRMS m/z (ESI⁺): 1048.404 (C₆₁H₅₉N₃NaO₁₂: [M+Na]⁺ requires 1048.3991).

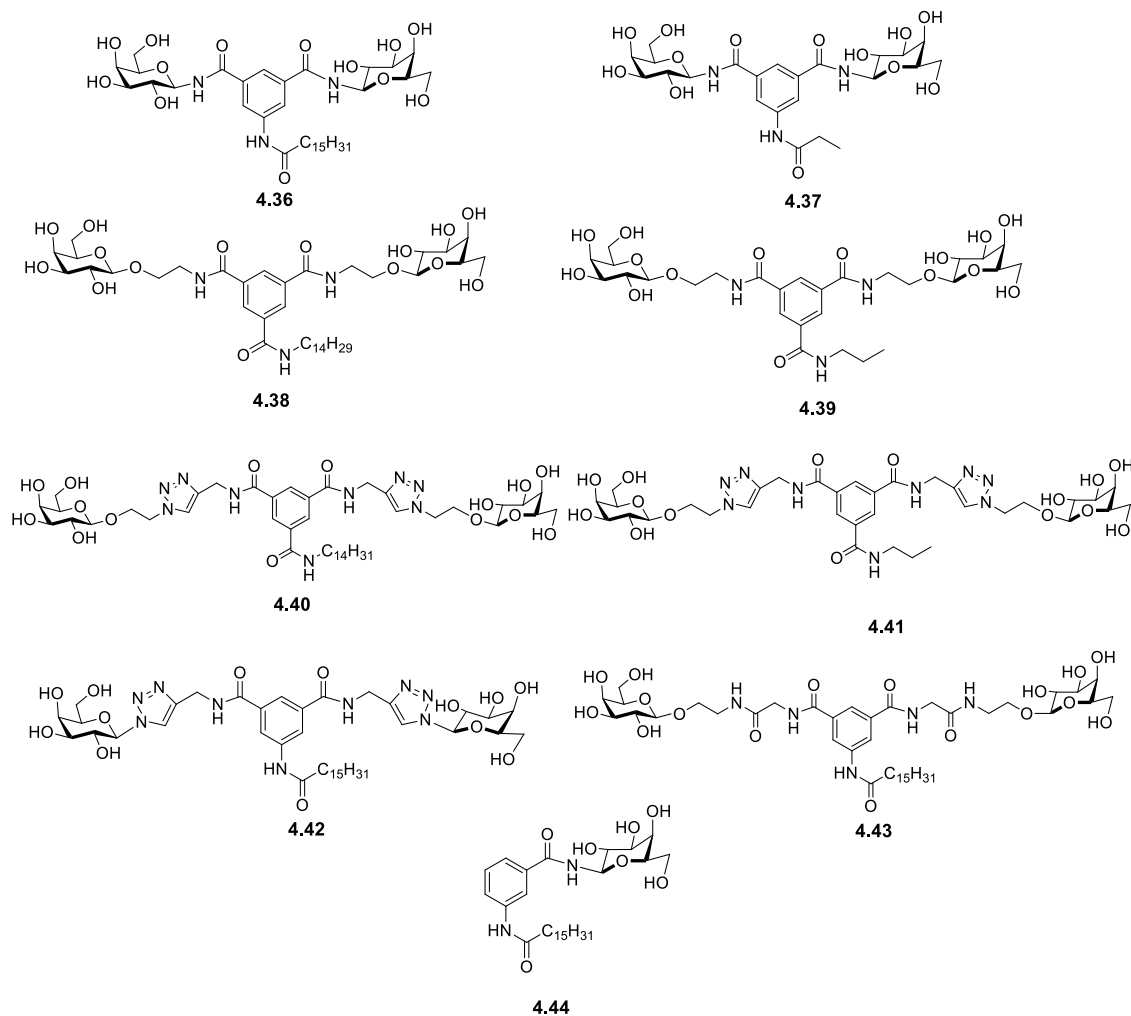


1-Azido-2,3,4,6-tetra-O-benzyl- α -D-galactopyranosyl-(1 \rightarrow 4)-6-O-benzyl- β -D-galactopyranoside
4.138

1-Azido-2,3,4,6-tetra-O-benzyl- α -D-galactopyranosyl-(1 \rightarrow 4)-2,3-di-O-benzoyl-6-O-benzyl- β -D-galactopyranoside **4.131** (308 mg, 0.3 mmol) was dissolved in MeOH (4 mL) and NaOMe added (1 M, 0.094 mL). The solution heated to 90 °C and stirred for 4 h. The mixture was then neutralised using HCl (1 M). Column chromatography (4:1, Toluene:Acetone) afforded the pure product **4.138** as an oily solid (193 mg, 78%); $R_f = 0.22$ (4:1, Toluene:Acetone); $[\alpha]_D^{25} = +63$ (c, 0.95 in CHCl₂); IR ν_{\max} (NaCl plate, DCM): 3444.1, 3088.1, 3063.5, 3030.3, 2919.3, 2870.7, 2114.5, 1496.5, 1453.9, 1366.9, 1334.4, 1260.6, 1208.8, 1097.7, 1053.4, 910.7, 802.6, 736.6, 697.8 cm⁻¹; ¹H NMR (300 MHz, CDCl₃): δ 7.41-7.19 (m, 25 H, Ar), 4.95-4.71 (m, 5 H, overlap of *H*-1 and other signals), 4.66-4.53 (m, 2 H), 4.46-4.29 (m, 5 H, overlap of CH₂Ph, *H*-1' and other signals), 4.08-4.03 (m, 3 H), 3.94-3.56 (m, 7 H), 3.40-3.22 (m, 3 H); ¹³C NMR (75 MHz, CDCl₃): δ_c

170.2, 168.3, 165.3 (CO), 138.4, 138.3, 137.9, 137.2 (ArC), 128.6-127.5 (overlap of ArC and ArCH), 100.4 (C-1), 90.4 (C-1'), 80.9, 78.8, 77.2, 76.4, 76.2 (each CH), 74.5 (PhCH₂), 74.5, 74.3 (each CH), 73.9, 73.8, 73.2, 73.1 (each PhCH₂), 71.6, 71.4, (each CH), 70.33, 69.3 (each CH₂); HRMS m/z (ESI+): 840.3489 (C₄₇H₅₁N₃NaO₁₀: [M+Na]⁺ requires 840.3467).

Solubility of aromatic-based analogues



Compounds **4.36-4.44** are soluble in Pyridine, DMSO and partially soluble in MeOH.

6.2.4 Experimental procedures and materials for Chapter 5

Materials

Phosphate Buffered Saline:

2 PBS tablets were dissolved in 400 mL of distilled H₂O to give a 0.01 M solution. This solution was then sterilised by autoclaving (at 121 °C for 20 mins).

Quarter Strength Ringers Solution:

Quarter Strength Ringers Solution was prepared by dissolving 1 Ringers tablet in 500 mL of distilled H₂O, the solution was then sterilised by autoclaving (at 121 °C for 20 mins).

Invasion Lysis Buffer:

PBS was prepared as before except EDTA was added to give a final concentration of 10 mM. Triton-X 100 was added to the PBS-EDTA to give a 0.25% vol/vol solution. The solution was then autoclaved (at 121 °C for 20 mins).

Coating Solution:

Coating solution was required to aid adherence of the CFBE cells to the tissue culture flasks and 24 well plates. This prepared used 8.8 mL of plain MEM, 1ml of collagen, 100 µl of fibronectin and 100 µl of bovine albumin serum. The 24 well plates and tissue culture flasks were coated with coating solution (500 µl and 3 mL respectively) which was left for 1 min and removed. The 24 well plates tissue culture flasks were allowed to air dry for 1 hour and stored at 4 °C.

LB medium:

LB medium was prepared by dissolving 25 g of LB (Sigma) in 1L of deionised H₂O, the medium was then sterilised by autoclaving (at 121 °C for 20 mins).

LB Agar:

LB Agar was prepared by dissolving 35 g of LB Agar (Sigma) in deionised H₂O, the agar was sterilised by autoclaving (at 121 °C for 20 mins).

BCSA (Burkholderia cepacia selective agar):

BCSA was prepared by adding 5.0 g NaCl, 10.0 g sucrose, 10.0 g lactose, 0.08 g phenol red, 0.02 g crystal violet, 10.0 g trypticase peptone, 1.5 g yeast extract and general agar 14 g to 1 L of deionised H₂O. The media was sterilised by autoclaving, allowed to cool to rt and antibiotics added, (600,000U polymixin B and 10 mg of gentamicin).

Procedures

Freezing cells:

Freezing solution of 10% DMSO, 50% FBS and 40% MEM was used. DMSO is a cryo-protectant which prevents the formation of ice crystals as cells are frozen which would then cause cell lysis upon thawing. It is toxic to cells at rt however, and therefore freezing down and reviving cells should be done as quickly as possible. Cells were frozen down during the log-phase of growth when flakes are approximately 60-80% confluent and not higher. 1×10^6 cells were frozen in each vial. The cells were trypsinised, centrifuged and the pellet resuspended gently but rapidly in the freezing medium above. The vial was frozen at -80 °C and transferred to a nitrogen dewar for long term storage.

Reviving Cells:

The cells were removed from the liquid nitrogen Dewar and thawed rapidly in a H₂O bath at 37 °C and immediately transferred to a universal containing 5 mL of warm culture medium. The cells were centrifuged and the pellet resuspended in 5ml of warm tissue culture medium and transferred to a T25 flask. When this flask was nearly confluent, cells were subcultured into a T75 flask. This was then split into 3 T75 flasks. Cells were not used for any experiment until after three passages.

Subculturing of Epithelial cells:

The cell lines were subcultured once they had reached 80% confluency. Trypsin was warmed to 37 °C. Supernatant was decanted from the T75 flask and the flask washed well with 10ml of sterile PBS to remove any remaining serum. 4ml of trypsin was added to detach the cells from the flask and the flask returned to the incubator for 10 min. After 10 min the flask was taken from the incubator and hit vigorously on the side to see if all cells had dislodged. Once all cells had dislodged the trypsin was inactivated by adding an equivalent amount of tissue culture

medium containing 10% FBS. The cells were centrifuged at 2500 g for 5 min, the pellet collected and resuspended in fresh tissue culture medium at a 1:2 split.

Trypan Blue Exclusion Assay (Cell Counting)

Cells were harvested as usual and resuspended in 5 mL of tissue culture media. Cell suspension (20 μ l) and trypan blue (20 μ l) were added to an eppendorf. 10 μ l of this suspension was pipetted under a coverslip on a haemocytometer. Only viable cells that excluded the dye in a 1mm² area were counted. The number of cells/ml was calculated using the following calculation:

$$\text{No. of cells/mm}^2 \times \text{dilution factor} \times 10^4$$

No. mls added to cells

CFBE41o-:

CFBE cells are transformed bronchial epithelial cells isolated from a CF patient with the F508/F508 deletion.^[243] CFBE cells require coated flasks and plates. CFBEs can be difficult to subculture using trypsin, especially if very confluent. CFBE's cannot be split very low although they should grow very rapidly. CFBE cells can be quite large and a confluent flask might only yield 2x10⁶ cells.

Adhesion Assay:

Lung epithelial cell lines were grown to confluence in sterile T75 flasks at 37 °C under 5% CO₂ and then seeded onto 24 well plates with FBS in the absence of pen/strep at a density of 4x10⁵ cells/1 mL and incubated overnight at 37 °C in 5% CO₂. Bcc strain (LMG13010) were inoculated from BCSA selective agar into 10 mL of LB broth and left shaking at 37 °C overnight. The following day, 10ml of the LMG13010 was inoculated into 100ml of LB and left shaking to reach mid log phase. The bacterial concentration was determined using the growth curve and they were grown to an O.D of 0.6. 1 mL solutions of the relevant concentrations or solvent controls were made up in sterile eppendorfs and bacteria added to a final concentration of 2x10⁷ CFU/ml. The bacteria were then pre-incubated with this inhibitor (shaking at 37 °C, no CO₂, 10 min). The epithelial cells were rinsed with warm MEM to remove serum and 500 μ l of bacterial and inhibitor suspension was added. The plate was centrifuged at 700 g for 5 min to facilitate attachment and incubated for 15 min (no shaking, 37 °C, 5% CO₂). After the 15 mins

the medium was removed from the wells and the cells were washed 3 times with sterile PBS to remove any bacteria which hadn't attached to the epithelial cells. 500 μ l of cell lysis buffer was added for 20 min at room temperature. The resulting lysate was carefully collected with cell scraping to ensure all of the cell lysate is obtained. This was then serially diluted in Ringer's solution and quantified by viable counts of bacteria colonies on LB agar after 48 h.

Bibliography

- [1] A. Cornish-Bowden, A. J. Barrett, R. Cammack, M. A. Chester, D. Horton, C. Liébecq, K. F. Tipton, B. J. Whyte, *Carbohydr. Res.* **1998**, *312*, 167-175.
- [2] T. Róg, I. Vattulainen, A. Bunker, M. Karttunen, *J. Phys. Chem. B* **2007**, *111*, 10146-10154.
- [3] K. Urich, *Comparative Animal Biochemistry*, Springer Verlag, **1994**.
- [4] L.-D. Huang, H.-J. Lin, P.-H. Huang, W.-C. Hsiao, R. L. V. Raghava, S.-L. Fu, C.-C. Lin, *Org. Biomol. Chem.* **2011**, *9*, 2492-2504.
- [5] J. Fantini, N. Garmy, N. Yahy, *Biochemistry*, **2006**.
- [6] B. G. Davis, A. J. Fairbanks, *Carbohydrate Chemistry*, Oxford Chemistry Primers, **2007**.
- [7] G. Toole, S. Toole, *Essential AS Biology*, Nelson Thornes, United Kingdom, **2004**.
- [8] C. Bavington, C. Page, *Respiration* **2005**, *72*, 335-344.
- [9] R. J. Pieters, *Med. Res. Rev.* **2007**, *27*, 796-816.
- [10] J. Ohlsson, A. Larsson, S. Haataja, J. Alajaaeski, P. Stenlund, J. S. Pinkner, S. J. Hultgren, J. Finne, J. Kihlberg, U. J. Nilsson, *Org. Biomol. Chem.* **2005**, *3*, 886-900.
- [11] D. Zopf, S. Roth, *Lancet* **1996**, *347*, 1017-1021.
- [12] N. Sharon, I. Ofek, *Glycoconj. J.* **2000**, *17*, 659-664.
- [13] G. Mulvey, P. I. Kitov, P. Marcato, D. R. Bundle, G. D. Armstrong, *Biochimie* **2001**, *83*, 841-847.
- [14] B. E. Collins, J. C. Paulson, *Curr. Opin. Chem. Biol.* **2004**, *8*, 617-625.
- [15] B. J. L. Jimenez, M. C. Ortiz, F. J. M. Garcia, *Chem. Soc. Rev.* **2013**, *42*, 4518-4531.
- [16] J. B. Corbell, J. J. Lundquist, E. J. Toone, *Tetrahedron Asymmetr.* **2000**, *11*, 95-111.
- [17] Y. C. Lee, R. T. Lee, *Acc. Chem. Res.* **1995**, *28*, 321-327.
- [18] A. Salminen, V. Loimaranta, J. A. F. Joosten, A. S. Khan, J. Hacker, R. J. Pieters, J. Finne, *J. Antimicrob. Chemother.* **2007**, *60*, 495-501.
- [19] R. J. Pieters, *Org. Biomol. Chem.* **2009**, *7*, 2013-2025.
- [20] I. Vrasidas, Nico J. de Mol, Rob M. J. Liskamp, Roland J. Pieters, *Eur. J. Org. Chem.* **2001**, *2001*, 4685-4692.
- [21] T. R. Branson, W. B. Turnbull, *Chem. Soc. Rev.* **2013**, *42*, 4613-4622.
- [22] A. Bernardi, J. Jimenez-Barbero, A. Casnati, C. C. De, T. Darbre, F. Fieschi, J. Finne, H. Funken, K.-E. Jaeger, M. Lahmann, T. K. Lindhorst, M. Marradi, P. Messner, A. Molinaro, P. V. Murphy, C. Nativi, S. Oscarson, S. Penades, F. Peri, R. J. Pieters, O. Renaudet, J.-L. Reymond, B. Richichi, J. Rojo, F. Sansone, C. Schaeffer, W. B. Turnbull, T. Velasco-Torrijos, S. Vidal, S. Vincent, T. Wennekes, H. Zuilhof, A. Imberty, *Chem. Soc. Rev.* **2013**, *42*, 4709-4727.
- [23] T. Mullen, M. Callaghan, S. McClean, *Microb. Pathog.* **2010**, *49*, 381-387.
- [24] C. Wright, R. Leyden, P. V. Murphy, M. Callaghan, T. Velasco-Torrijos, S. McClean, *Molecules* **2012**, *17*, 10065-10071.
- [25] E. Lameignere, L. Malinowska, M. Slavikova, E. Duchaud, E. P. Mitchell, A. Varrot, O. Sedo, A. Imberty, M. Wimmerova, *Biochem. J.* **2008**, *411*, 307-318.
- [26] C. Chemani, A. Imberty, B. S. de, M. Pierre, M. Wimmerova, B. P. Guery, K. Faure, *Infect. Immun.* **2009**, *77*, 2065-2075.
- [27] H.-P. Hauber, M. Schulz, A. Pforte, D. Mack, P. Zabel, U. Schumacher, *Int. J. Med. Sci.* **2008**, *5*, 371-376.
- [28] S. Cecioni, S. Faure, U. Darbost, I. Bonnamour, H. Parrot-Lopez, O. Roy, C. Taillefumier, M. Wimmerova, J.-P. Praly, A. Imberty, S. Vidal, *Chem. Eur. J.* **2011**, *17*, 2146-2159, S2146/2141-S2146/2123.

- [29] I. Otsuka, B. Blanchard, R. Borsali, A. Imberty, T. Kakuchi, *ChemBioChem* **2010**, *11*, 2399-2408.
- [30] F. Pertici, R. J. Pieters, *Chem. Commun. (Cambridge, U. K.)* **2012**, *48*, 4008-4010.
- [31] K. Marotte, C. Preville, C. Sabin, M. Moume-Pymbock, A. Imberty, R. Roy, *Org. Biomol. Chem.* **2007**, *5*, 2953-2961.
- [32] M. Andreini, M. Anderluh, A. Audfray, A. Bernardi, A. Imberty, *Carbohydr. Res.* **2010**, *345*, 1400-1407.
- [33] T. Boehm, *Curr. Biol.* **2012**, *22*, R722-R732.
- [34] R. A. Meyers, *Immunology; From cell biology to disease.*, 1st ed., Wiley-VCH, Weinheim, **2007**.
- [35] Y. Kinjo, B. Pei, S. Bufali, R. Raju, S. K. Richardson, M. Imamura, M. Fujio, D. Wu, A. Khurana, K. Kawahara, C.-H. Wong, A. R. Howell, P. H. Seeberger, M. Kronenberg, *Chem. Biol. (Cambridge, MA, U. S.)* **2008**, *15*, 654-664.
- [36] R. W. Franck, *Comptes Rendus Chimie* **2012**, *15*, 46-56.
- [37] M. Terabe, J. A. Berzofsky, *Adv. Cancer Res.* **2008**, *101*, 277-348.
- [38] T. Natori, Y. Koezuka, T. Higa, *Tetrahedron Lett.* **1993**, *34*, 5591-5592.
- [39] A. Banchet-Cadeddu, E. Henon, M. Dauchez, J.-H. Renault, F. Monneaux, A. Haudrechy, *Org. Biomol. Chem.* **2011**, *9*, 3080-3104.
- [40] P. J. Jervis, L. R. Cox, G. S. Besra, *J. Org. Chem.* **2011**, *76*, 320-323.
- [41] M. Taniguchi, M. Harada, S. Kojo, T. Nakayama, H. Wakao, *Annual Review of Immunology* **2003**, *21*, 483-513.
- [42] E. Kobayashi, K. Motoki, T. Uchida, H. Fukushima, Y. Koezuka, *Oncol. Res.* **1995**, *7*, 529-534.
- [43] F. L. Schneiders, R. J. Scheper, B. B. M. E. von, A. M. Woltman, H. L. A. Janssen, d. E. A. J. M. van, H. M. W. Verheul, G. T. D. de, d. V. H. J. van, *Clin. Immunol. (Amsterdam, Neth.)* **2011**, *140*, 130-141.
- [44] T. Lee, M. Cho, S.-Y. Ko, H.-J. Youn, D. J. Baek, W.-J. Cho, C.-Y. Kang, S. Kim, *J. Med. Chem.* **2007**, *50*, 585-589.
- [45] M. R. Chaulagain, M. H. D. Postema, F. Valeriote, H. Pietraszkewicz, *Tetrahedron Lett.* **2004**, *45*, 7791-7794.
- [46] Y.-J. Chang, J.-R. Huang, Y.-C. Tsai, J.-T. Hung, D. Wu, M. Fujio, C.-H. Wong, A. L. Yu, *Proc. Natl. Acad. Sci. U. S. A.* **2007**, *104*, 10299-10304.
- [47] M. M. Venkataswamy, S. A. Porcelli, *Semin. Immunol.* **2010**, *22*, 68-78.
- [48] M. Trappeniers, B. K. Van, T. Decruy, U. Hillaert, B. Linclau, D. Elewaut, C. S. Van, *J. Am. Chem. Soc.* **2008**, *130*, 16468-16469.
- [49] Y. Liu, R. D. Goff, D. Zhou, J. Mattner, B. A. Sullivan, A. Khurana, C. Cantu, E. V. Ravkov, C. C. Ibegbu, J. D. Altman, L. Teyton, A. Bendelac, P. B. Savage, *J. Immunol. Methods* **2006**, *312*, 34-39.
- [50] a) M. H. Kollef, Y. Golan, S. T. Micek, A. F. Shorr, M. I. Restrepo, *Clin Infect Dis* **2011**, *53 Suppl 2*, S33-55; quiz S56-38; b) L. Freire-Moran, B. Aronsson, C. Manz, I. C. Gyssens, A. D. So, D. L. Monnet, O. Cars, *Drug Resist Updat* **2011**, *14*, 118-124.
- [51] a) D. Kitamoto, T. Morita, T. Fukuoka, M.-a. Konishi, T. Imura, *Curr. Opin. Colloid Interface Sci.* **2009**, *14*, 315-328; b) N. Lourith, M. Kanlayavattanakul, *Int. J. Cosmetic Sci.* **2009**, *31*, 255-261.
- [52] R. Ashby, A. Nuñez, D. Y. Solaiman, T. Foglia, *J. Amer. Oil Chem. Soc.* **2005**, *82*, 625-630.
- [53] a) E. Söderlind, M. Wollbratt, C. von Corswant, *Int. J. Pharm.* **2003**, *252*, 61-71; b) E. Söderlind, L. Karlsson, *Eur. J. Pharmaceut. Biopharmaceut.* **2006**, *62*, 254-259.
- [54] A. Vintiloiu, J.-C. Leroux, *J. Controlled Release* **2008**, *125*, 179-192.
- [55] M. Suzuki, K. Hanabusa, *Chem. Soc. Rev.* **2010**, *39*, 455-463.

- [56] Y. Osada, in *Gels Handbook* (Eds.: O. Yoshihito, K. Kanji, F. Takao, I. Okihiko, H. Yoshitsugu, M. Tsutomu, S. Tadao, W. Lin, K. K. T. F. O. I. Y. H. T. M. T. S. L. W. Hatsuo IshidaA2 - Yoshihito Osada, I. Hatsuo), Academic Press, Burlington, **2001**, pp. 13-25.
- [57] G. Wang, H. Yang, S. Cheuk, S. Coleman, *Beilstein J. Org. Chem.* **2011**, *7*, 234-242, No. 231.
- [58] a) S. Roy, A. Chakraborty, B. Chattopadhyay, A. Bhattacharya, A. K. Mukherjee, R. Ghosh, *Tetrahedron* **2010**, *66*, 8512-8521; b) T. Patra, A. Pal, J. Dey, *J. Colloid Interface Sci.* **2010**, *344*, 10-20; c) P. Mukhopadhyay, N. Fujita, S. Shinkai, in *Annual Review of Nano Research*, pp. 385-428.
- [59] N. M. Sangeetha, U. Maitra, *Chem. Soc. Rev.* **2005**, *34*, 821-836.
- [60] J. G. Hardy, A. R. Hirst, I. Ashworth, C. Brennan, D. K. Smith, *Tetrahedron* **2007**, *63*, 7397-7406.
- [61] R. J. H. Hafkamp, M. C. Feiters, R. J. M. Nolte, *J. Org. Chem.* **1999**, *64*, 412-426.
- [62] J. H. Jung, H. Kobayashi, M. Masuda, T. Shimizu, S. Shinkai, *J. Am. Chem. Soc.* **2001**, *123*, 8785-8789.
- [63] G. L. Patrick, *An Introduction to Medicinal Chemistry*, Oxford University Press, **2009**.
- [64] K. Cantin, S. Rondeau-Gagne, J. R. Neabo, M. Daigle, J.-F. Morin, *Org. Biomol. Chem.* **2011**, *9*, 4440-4443.
- [65] N. Zweep, A. Hopkinson, A. Meetsma, W. R. Browne, B. L. Feringa, E. J. H. van, *Langmuir* **2009**, *25*, 8802-8809.
- [66] K. Murata, M. Aoki, T. Nishi, A. Ikeda, S. Shinkai, *J. Chem. Soc., Chem. Commun.* **1991**, 1715-1718.
- [67] J.-W. Liu, J.-T. Ma, C.-F. Chen, *Tetrahedron* **2011**, *67*, 85-91.
- [68] S. Bhattacharya, A. Pal, *J. Phys. Chem. B* **2008**, *112*, 4918-4927.
- [69] A. R. Hirst, D. K. Smith, M. C. Feiters, H. P. M. Geurts, *Chem. Eur. J.* **2004**, *10*, 5901-5910.
- [70] S. Kiyonaka, S. Shinkai, I. Hamachi, *Chem. Eur. J.* **2003**, *9*, 976-983.
- [71] I. Hamachi, S. Kiyonaka, S. Shinkai, *Chem. Commun. (Cambridge)* **2000**, 1281-1282.
- [72] G. Wang, S. Cheuk, K. Williams, V. Sharma, L. Dakessian, Z. Thorton, *Carbohydr. Res.* **2006**, *341*, 705-716.
- [73] M. J. Clemente, R. M. Tejedor, P. Romero, J. Fitremann, L. Oriol, *RSC Adv.* **2012**, *2*, 11419-11431.
- [74] B. Ernst, J. L. Magnani, *Nat. Rev. Drug Discov.* **2009**, *8*, 661-677.
- [75] X. Chen, Y. Zheng, Y. Shen, *Curr. Med. Chem* **2006**, *13*, 109-116.
- [76] C. U. Kim, W. Lew, M. A. Williams, L. Zhang, H. Liu, S. Swaminathan, N. Bischofberger, M. S. Chen, C. Y. Tai, D. B. Mendel, W. G. Laver, R. C. Stevens, *J. Am. Chem. Soc.* **1997**, *119*, 681-690.
- [77] N. J. Weinreb, J. A. Barranger, J. Charrow, G. A. Grabowski, H. J. Mankin, P. Mistry, *Am. J. Hematol.* **2005**, *80*, 223-229.
- [78] B. E. Maryanoff, S. O. Nortey, J. F. Gardocki, R. P. Shank, S. P. Dodgson, *J. Med. Chem.* **1987**, *30*, 880-887.
- [79] M. Dubber, A. Patel, K. Sadalapure, I. Aumüller, T. K. Lindhorst, *Eur. J. Org. Chem.* **2006**, *2006*, 5357-5366.
- [80] M. Luckey, *Membrane structural biology with biochemical and biophysical foundations.*, Cambridge University Press, New York, **2008**.
- [81] A. S. Ulrich, *Biosci. Rep.* **2002**, *22*, 129-150.
- [82] S. A. DeFrees, L. Phillips, S. Zalipsky, L. Guo, *J. Am. Chem. Soc.* **1996**, *118*, 6101-6104.

- [83] J. Bouckaert, J. Berglund, M. Schembri, G. E. De, L. Cools, M. Wuhrer, C.-S. Hung, J. Pinkner, R. Slaettedgard, A. Zavialov, D. Choudhury, S. Langermann, S. J. Hultgren, L. Wyns, P. Klemm, S. Oscarson, S. D. Knight, G. H. De, *Mol. Microbiol.* **2005**, *55*, 441-455.
- [84] C. Grandjean, V. Santraine, N. Fardel, A. Polidori, B. Pucci, H. Gras-Masse, D. Bonnet, *Tetrahedron Lett.* **2004**, *45*, 3451-3454.
- [85] J. A. Morales-Serna, O. Boutureira, Y. Diaz, M. I. Matheu, S. Castillon, *Carbohydr. Res.* **2007**, *342*, 1595-1612.
- [86] S. C. Ghosh, J. S. Y. Ngiam, A. M. Seayad, D. T. Tuan, C. L. L. Chai, A. Chen, *J. Org. Chem.* **2012**, *77*, 8007-8015.
- [87] C. A. G. N. Montalbetti, V. Falque, *Tetrahedron* **2005**, *61*, 10827-10852.
- [88] I. Abdelmoty, F. Albericio, L. A. Carpino, B. M. Foxman, S. A. Kates, *Lett. Pept. Sci.* **1994**, *1*, 57-67.
- [89] R. R. Schmidt, J. Michel, *Angew. Chem.* **1980**, *92*, 763-764.
- [90] a) M. H. D. Postema, K. TenDyke, J. Cutter, G. Kuznetsov, Q. Xu, *Org. Lett.* **2009**, *11*, 1417-1420; b) G. Zhang, M. Fu, J. Ning, *Carbohydr. Res.* **2005**, *340*, 155-159.
- [91] R. R. Schmidt, M. Stumpp, *Liebigs Annalen der Chemie* **1983**, *1983*, 1249-1256.
- [92] G. T. Noble, S. L. Flitsch, K. P. Liem, S. J. Webb, *Org. Biomol. Chem.* **2009**, *7*, 5245-5254.
- [93] L. Gu, P. G. Luo, H. Wang, M. J. Meziani, Y. Lin, L. M. Veca, L. Cao, F. Lu, X. Wang, R. A. Quinn, W. Wang, P. Zhang, S. Lacher, Y.-P. Sun, *Biomacromolecules* **2008**, *9*, 2408-2418.
- [94] S. Peng, M. Zhao, S. Li, Capital Medical University, Peop. Rep. China . **2012**, p. 18pp.
- [95] D. Pramanik, B. K. Majeti, G. Mondal, P. P. Karmali, R. Sistla, O. G. Ramprasad, G. Srinivas, G. Pande, A. Chaudhuri, *J. Med. Chem.* **2008**, *51*, 7298-7302.
- [96] T. Ziegler, D. Roseling, L. R. Subramanian, *Tetrahedron Asymmetr.* **2002**, *13*, 911-914.
- [97] A. Chaudhary, M. Girgis, M. Prashad, B. Hu, D. Har, O. Repic, T. J. Blacklock, *Tetrahedron Lett.* **2003**, *44*, 5543-5546.
- [98] a) L. Somogyi, G. Haberhauer, J. Rebek, *Tetrahedron* **2001**, *57*, 1699-1708; b) H. M. Muller, O. Delgado, T. Bach, *Angew. Chem., Int. Ed. Engl.* **2007**, *46*, 4771-4774; c) T. Velasco-Torrijos, L. Abbey, R. O'Flaherty, *Molecules* **2012**, *17*, 11346-11362.
- [99] Z. Wang, in *Comprehensive Organic Name Reactions and Reagents*, John Wiley & Sons, Inc., **2010**.
- [100] J. F. Miravet, B. Escuder, *Org. Lett.* **2005**, *7*, 4791-4794.
- [101] C. Fernandez, O. Nieto, E. Rivas, G. Montenegro, J. A. Fontenla, A. Fernandez-Mayoralas, *Carbohydr. Res.* **2000**, *327*, 353-365.
- [102] E. Bialecka-Florjańczyk, *Synth. Commun.* **2000**, *30*, 4417-4424.
- [103] M. A. Witschi, J. Gervay-Hague, *Org. Lett.* **2010**, *12*, 4312-4315.
- [104] A. R. Pinder, *Synthesis* **1980**, 425-452.
- [105] M. Tanaka, T. Ikeda, J. Mack, N. Kobayashi, T. Haino, *J. Org. Chem.* **2011**, *76*, 5082-5091.
- [106] D. Das, A. Dasgupta, S. Roy, R. N. Mitra, S. Debnath, P. K. Das, *Chemistry* **2006**, *12*, 5068-5074.
- [107] M. George, R. G. Weiss, *Molecular Gels, Material with self-assembled fibrillar networks*, Springer, **2006**.
- [108] B. Gao, H. Li, D. Xia, S. Sun, X. Ba, *Beilstein J. Org. Chem.* **2011**, *7*, 198-203, No. 126.
- [109] G. Zhu, J. S. Dordick, *Chem. Mater.* **2006**, *18*, 5988-5995.
- [110] S. Sahoo, N. Kumar, C. Bhattacharya, S. S. Sagiri, K. Jain, K. Pal, S. S. Ray, B. Nayak, *Des. Monomers Polym.* **2011**, *14*, 95-108.
- [111] Y. E. Shapiro, *Prog. Polym. Sci.* **2011**, *36*, 1184-1253.
- [112] T. Kar, S. K. Mandal, P. K. Das, *Chem. Eur. J.* **2011**, *17*, 14952-14961.

- [113] G. Tiwari, R. Tiwari, B. Sriwastawa, L. Bhati, S. Pandey, P. Pandey, S. K. Bannerjee, *Int. J. Pharm. Invest.* **2012**, *2*, 1-11.
- [114] P. Walde, K. Cosentino, H. Engel, P. Stano, *ChemBioChem* **2010**, *11*, 848-865.
- [115] A. D. Bangham, *Bioessays* **1995**, *17*, 1081-1088.
- [116] S. F. Fenz, K. Sengupta, *Integr. Biol.* **2012**, *4*, 982-995.
- [117] G. J. L. Bernardes, R. Kikkeri, M. Maglinao, P. Laurino, M. Collot, S. Y. Hong, B. Lepenies, P. H. Seeberger, *Org. Biomol. Chem.* **2010**, *8*, 4987-4996.
- [118] J. Zhu, J. Xue, Z. Guo, L. Zhang, R. E. Marchant, *Bioconjugate Chem.* **2007**, *18*, 1366-1369.
- [119] G. Sbardella, S. Castellano, C. Vicidomini, D. Rotili, A. Nebbioso, M. Miceli, L. Altucci, A. Mai, *Bioorg. Med. Chem. Lett.* **2008**, *18*, 2788-2792.
- [120] Y. Sun, X. Jiang, S. Chen, B. D. Price, *FEBS Letters* **2006**, *580*, 4353-4356.
- [121] C. L. Peterson, M.-A. Laniel, *Curr. Biol.* **2004**, *14*, R546-R551.
- [122] Y. Liu, A. L. Colosimo, X.-J. Yang, D. Liao, *Mol. Cell. Biol.* **2000**, *20*, 5540-5553.
- [123] C. Hubbert, A. Guardiola, R. Shao, Y. Kawaguchi, A. Ito, A. Nixon, M. Yoshida, X.-F. Wang, T.-P. Yao, *Nature (London, U. K.)* **2002**, *417*, 455-458.
- [124] N. Kolb, M. A. R. Meier, *Green Chem.* **2012**, *14*, 2429-2435.
- [125] G. Kwak, M. Fujiki, *Macromolecules* **2004**, *37*, 2021-2025.
- [126] a) A. Daubinet, P. T. Kaye, *Synth. Commun.* **2002**, *32*, 3207-3217; b) A. Daubinet, P. T. Kaye, *ARKIVOC (Gainesville, FL, U. S.)* **2003**, 93-104.
- [127] S. Fioravanti, A. Morreale, L. Pellacani, F. Ramadori, P. A. Tardella, *Synlett* **2007**, *2007*, 2759-2761.
- [128] S. Fioravanti, S. Gasbarri, A. Morreale, L. Pellacani, F. Ramadori, P. A. Tardella, *Amino Acids* **2010**, *39*, 461-470.
- [129] B. W. Parks, R. D. Gilbertson, D. W. Domaille, J. E. Hutchison, *J. Org. Chem.* **2006**, *71*, 9622-9627.
- [130] H. Kato, C. Böttcher, A. Hirsch, *Eur. J. Org. Chem.* **2007**, *2007*, 2659-2666.
- [131] A. Vasella, P. Uhlmann, C. A. A. Waldraff, F. Diederich, C. Thilgen, *Angew. Chem.* **1992**, *104*, 1383-1385 (See also *Angew. Chem., Int. Ed. Engl.*, 1992, 1331(1310), 1388-1390).
- [132] J. Isaad, M. Rolla, R. Bianchini, *Eur. J. Org. Chem.* **2009**, 2748-2764.
- [133] P. Savarino, S. Parlati, R. Buscaino, P. Piccinini, C. Barolo, E. Montoneri, *Dyes Pigm.* **2006**, *69*, 7-12.
- [134] S. Santra, C. Kaittanis, J. M. Perez, *Langmuir* **2009**, *26*, 5364-5373.
- [135] D. Lafrance, P. Bowles, K. Leeman, R. Rafka, *Org. Lett.* **2011**, *13*, 2322-2325.
- [136] a) J. Blanchet, J. Baudoux, M. Amere, M.-C. Lasne, J. Rouden, *Eur. J. Org. Chem.* **2008**, 5493-5506; b) M. Nejman, A. Śliwińska, A. Zwierzak, *Tetrahedron* **2005**, *61*, 8536-8541.
- [137] P. S. Mahajan, J. P. Mahajan, S. B. Mhaske, *Synth. Commun.* **2013**, *43*, 2508-2516.
- [138] a) J. Walker, J. S. Lumsden, *J. Chem. Soc. London* **1901**, *79*, 1191-1197; b) F. Krafft, R. Seldis, *Ber.*, *33*, 3571-3575.
- [139] B. C. Ranu, R. Jana, *Eur. J. Org. Chem.* **2006**, 3767-3770.
- [140] M. Sylla, D. Joseph, E. Chevallier, C. Camara, F. Dumas, *Synthesis* **2006**, 1045-1049.
- [141] F. D. Popp, A. Catala, *J. Org. Chem.* **1961**, *26*, 2738-2740.
- [142] F. Texier-Boulet, A. Foucaud, *Tetrahedron Lett.* **1982**, *23*, 4927-4928.
- [143] D. Prajapati, K. C. Lekhok, J. S. Sandhu, A. C. Ghosh, *J. Chem. Soc., Perkin Trans. 1* **1996**, 959-960.
- [144] S. Hourcade, A. Ferdenzi, P. Retailleau, S. Mons, C. Marazano, *Eur. J. Org. Chem.* **2005**, 1302-1310.
- [145] S. Mattsson, M. Dahlström, S. Karlsson, *Tetrahedron Lett.* **2007**, *48*, 2497-2499.
- [146] F. Elsinger, J. Schreiber, A. Eschenmoser, *Helv. Chim. Acta* **1960**, *43*, 113-118.

- [147] C. Mayato, R. L. Dorta, J. T. Vázquez, *Tetrahedron Lett.* **2008**, *49*, 1396-1398.
- [148] L. J. Gazzard, E. H. Ha, D. Y. Jackson, J. Um, Genentech, Inc., USA . **2006**, p. 185 pp.
- [149] A. Falchi, G. Giacomelli, A. Porcheddu, M. Taddei, *Synlett* **2000**, 275-277.
- [150] Z. J. Kaminski, P. Paneth, J. Rudzinski, *J. Org. Chem.* **1998**, *63*, 4248-4255.
- [151] a) M. Kunishima, C. Kawachi, J. Monta, K. Terao, F. Iwasaki, S. Tani, *Tetrahedron* **1999**, *55*, 13159-13170; b) M. Kunishima, C. Kawachi, F. Iwasaki, K. Terao, S. Tani, *Tetrahedron Lett.* **1999**, *40*, 5327-5330.
- [152] I. Toth, R. Falconer, Alchemia Pty. Ltd., Australia . **2002**, p. 66 pp.
- [153] P. Arya, K. M. K. Kutterer, H. Qin, J. Roby, M. L. Barnes, S. Lin, C. A. Lingwood, M. G. Peter, *Bioorg. Med. Chem.* **1999**, *7*, 2823-2833.
- [154] Y. M. Chabre, R. Roy, *Chem. Soc. Rev.* **2013**, *42*, 4657-4708.
- [155] M. Bergeron-Brelek, D. Giguere, T. C. Shiao, C. Saucier, R. Roy, *J. Org. Chem.* **2012**, *77*, 2971-2977.
- [156] E. Smits, J. B. F. N. Engberts, R. M. Kellogg, D. H. A. van, *J. Chem. Soc., Perkin Trans. 1* **1996**, 2873-2877.
- [157] D. Page, R. Roy, *Bioorg. Med. Chem. Lett.* **1996**, *6*, 1765-1770.
- [158] R. Leyden, T. Velasco-Torrijos, S. Andre, S. Gouin, H.-J. Gabius, P. V. Murphy, *J. Org. Chem.* **2009**, *74*, 9010-9026.
- [159] a) N. Jayaraman, J. F. Stoddart, *Tetrahedron Lett.* **1997**, *38*, 6767-6770; b) D. Giguere, R. Patnam, M.-A. Bellefleur, C. St-Pierre, S. Sato, R. Roy, *Chem. Commun. (Cambridge, U. K.)* **2006**, 2379-2381; c) Y. M. Chabre, D. Giguere, B. Blanchard, J. Rodrigue, S. Rocheleau, M. Neault, S. Rauthu, A. Papadopoulos, A. A. Arnold, A. Imberty, R. Roy, *Chem. Eur. J.* **2011**, *17*, 6545-6562, S6545/6541-S6545/6134.
- [160] G.-N. Wang, S. Andre, H.-J. Gabius, P. V. Murphy, *Org. Biomol. Chem.* **2012**, *10*, 6893-6907.
- [161] F. Perez-Balderas, J. Morales-Sanfrutos, F. Hernandez-Mateo, J. Isac-Garcia, F. Santoyo-Gonzalez, *Eur. J. Org. Chem.* **2009**, 2441-2453.
- [162] Y. M. Chabre, C. Contino-Pepin, V. Placide, T. C. Shiao, R. Roy, *J. Org. Chem.* **2008**, *73*, 5602-5605.
- [163] a) K. Sato, N. Hada, T. Takeda, *Carbohydr. Res.* **2006**, *341*, 836-845; b) S. M. Dimick, S. C. Powell, S. A. McMahon, D. N. Moothoo, J. H. Naismith, E. J. Toone, *J. Am. Chem. Soc.* **1999**, *121*, 10286-10296.
- [164] Y. Azefu, H. Tamiaki, R. Sato, K. Toma, *Bioorg. Med. Chem.* **2002**, *10*, 4013-4022.
- [165] H. Tamiaki, Y. Azefu, R. Shibata, R. Sato, K. Toma, *Colloids Surf., B* **2006**, *53*, 87-93.
- [166] R. C. T. Howe, A. P. Smalley, A. P. M. Guttenplan, M. W. R. Doggett, M. D. Eddleston, J. C. Tan, G. O. Lloyd, *Chem. Commun. (Cambridge, U. K.)* **2013**, *49*, 4268-4270.
- [167] M. M. Joullie, K. M. Lassen, *ARKIVOC (Gainesville, FL, U. S.)* **2010**, 189-250.
- [168] Y. Nishida, T. Tsurumi, K. Sasaki, K. Watanabe, H. Dohi, K. Kobayashi, *Org. Lett.* **2003**, *5*, 3775-3778.
- [169] W. Chu, Z. Tu, E. McElveen, J. Xu, M. Taylor, R. R. Luedtke, R. H. Mach, *Bioorg. Med. Chem.* **2005**, *13*, 77-87.
- [170] R. Adams, L. H. Ulich, *J. Am. Chem. Soc.* **1920**, *42*, 599-611.
- [171] J. Klosa, *J. Prakt. Chem. (Leipzig)* **1962**, *19*, 45-55.
- [172] K. Oohora, S. Burazerovic, A. Onoda, Y. M. Wilson, T. R. Ward, T. Hayashi, *Angew. Chem., Int. Ed.* **2012**, *51*, 3818-3821.
- [173] C. Meneses, S. L. Nicoll, L. Trembleau, *J. Org. Chem.* **2010**, *75*, 564-569.
- [174] L. Kisfaludy, I. Schon, T. Szirtes, O. Nyeki, M. Low, *Tetrahedron Lett.* **1974**, 1785-1786.
- [175] T. J. Ryan, G. Lecollinet, T. Velasco, A. P. Davis, *Proc. Natl. Acad. Sci. U. S. A.* **2002**, *99*, 4863-4866.

- [176] J. E. Hein, V. V. Fokin, *Chem. Soc. Rev.* **2010**, *39*, 1302-1315.
- [177] V. D. Bock, H. Hiemstra, J. H. van Maarseveen, *Eur. J. Org. Chem.* **2006**, *2006*, 51-68.
- [178] C. W. Tornøe, C. Christensen, M. Meldal, *J. Org. Chem.* **2002**, *67*, 3057-3064.
- [179] V. V. Rostovtsev, L. G. Green, V. V. Fokin, K. B. Sharpless, *Angew. Chem., Int. Ed.* **2002**, *41*, 2596-2599.
- [180] R. Huisgen, *Angew. Chem., Int. Ed. Engl.* **1963**, *2*, 565-598.
- [181] V. O. Rodionov, V. V. Fokin, M. G. Finn, *Angew. Chem., Int. Ed.* **2005**, *44*, 2210-2215.
- [182] F. Himo, T. Lovell, R. Hilgraf, V. V. Rostovtsev, L. Noodleman, K. B. Sharpless, V. V. Fokin, *J. Am. Chem. Soc.* **2005**, *127*, 210-216.
- [183] M. Meldal, C. W. Tornøe, *Chem. Rev.* **2008**, *108*, 2952-3015.
- [184] C. Fasting, C. A. Schalley, M. Weber, O. Seitz, S. Hecht, B. Kocsch, J. Dervede, C. Graf, E.-W. Knapp, R. Haag, *Angew. Chem., Int. Ed.* **2012**, *51*, 10472-10498.
- [185] A. Patel, T. K. Lindhorst, *Eur. J. Org. Chem.* **2002**, 79-86.
- [186] I. Deguise, D. Lagnoux, R. Roy, *New J. Chem.* **2007**, *31*, 1321-1331.
- [187] J. M. Aizpurua, I. Azcune, R. M. Fratila, E. Balentova, M. Sagartzazu-Aizpurua, J. I. Miranda, *Org. Lett.* **2010**, *12*, 1584-1587.
- [188] M. Ortega-Muñoz, F. Perez-Balderas, J. Morales-Sanfrutos, F. Hernandez-Mateo, J. Isac-García, F. Santoyo-Gonzalez, *Eur. J. Org. Chem.* **2009**, *2009*, 2454-2473.
- [189] J. Ohlsson, U. J. Nilsson, *Tetrahedron Lett.* **2003**, *44*, 2785-2787.
- [190] H. C. Hansen, S. Haataja, J. Finne, G. Magnusson, *J. Am. Chem. Soc.* **1997**, *119*, 6974-6979.
- [191] Z. Wang, L. Zhou, K. El-Boubbou, X.-S. Ye, X. Huang, *J. Org. Chem.* **2007**, *72*, 6409-6420.
- [192] C. Wang, Q. Li, H. Wang, L.-H. Zhang, X.-S. Ye, *Tetrahedron* **2006**, *62*, 11657-11662.
- [193] V. Vicente, J. Martin, J. Jimenez-Barbero, J. L. Chiara, C. Vicent, *Chem. Eur. J.* **2004**, *10*, 4240-4251.
- [194] C. Xia, W. Zhang, Y. Zhang, W. Chen, J. Nadas, R. Severin, R. Woodward, B. Wang, X. Wang, M. Kronenberg, P. G. Wang, *ChemMedChem* **2009**, *4*, 1810-1815.
- [195] J. Ohlsson, G. Magnusson, *Carbohydr. Res.* **2000**, *329*, 49-55.
- [196] a) H. K. Chenault, A. Castro, L. F. Chafin, J. Yang, *J. Org. Chem.* **1996**, *61*, 5024-5031; b) K. Fukase, I. Kinoshita, T. Kanoh, Y. Nakai, A. Hasuoka, S. Kusumoto, *Tetrahedron* **1996**, *52*, 3897-3904.
- [197] S. L. Cockroft, J. Perkins, C. Zonta, H. Adams, S. E. Spey, C. M. R. Low, J. G. Vinter, K. R. Lawson, C. J. Urch, C. A. Hunter, *Org. Biomol. Chem.* **2007**, *5*, 1062-1080.
- [198] T.-a. Okamura, K. Kunisue, Y. Omi, K. Onitsuka, *Dalton Trans.* **2013**, *42*, 7569-7578.
- [199] C. Bozkurt-Guezel, A. A. Gerceker, *J. Antibiot.* **2012**, *65*, 83-86.
- [200] M. S. Cartiera, E. C. Ferreira, C. Caputo, M. E. Egan, M. J. Caplan, W. M. Saltzman, *Mol. Pharm.* **2010**, *7*, 86-93.
- [201] B. P. O'Sullivan, S. D. Freedman, *Lancet* **2009**, *373*, 1891-1904.
- [202] F. Stanke, T. Becker, V. Kumar, S. Hedtfeld, C. Becker, H. Cuppens, S. Tamm, J. Yarden, U. Laabs, B. Siebert, L. Fernandez, M. Macek, D. Radojkovic, M. Ballmann, J. Greipel, J.-J. Cassiman, T. F. Wienker, B. Tümmler, *J. Med. Genet.* **2011**, *48*, 24-31.
- [203] A. E. Patrick, P. J. Thomas, *Front. Pharmacol. Ion Channels Channelopathies* **2012**, *3*, 162.
- [204] A. M. George, P. M. Jones, P. G. Middleton, *FEMS Microbiol. Lett.* **2009**, *300*, 153-164.
- [205] R. Tarran, *Proc. Am. Thorac. Soc.* **2004**, *1*, 42-46.
- [206] R. C. Boucher, *Adv. Drug Delivery Rev.* **2002**, *54*, 1359-1371.
- [207] http://highered.mcgraw-hill.com/sites/dl/free/0071402357/156715/figure241_1.html.
- [208] S. A. Sousa, C. G. Ramos, J. H. Leitao, *Int. J. Microbiol.* **2011**, No pp. given.

- [209] a) J. B. Lyczak, C. L. Cannon, G. B. Pier, *Microbes Infect.* **2000**, *2*, 1051-1060; b) D. D. Frangolias, E. Mahenthiralingam, S. Rae, J. M. Raboud, A. G. Davidson, R. Wittmann, P. G. Wilcox, *Am. J. Respir. Crit. Care Med.* **1999**, *160*, 1572-1577.
- [210] A. D. Vinion-Dubiel, J. B. Goldberg, *J. Endotoxin Res.* **2003**, *9*, 201-213.
- [211] J. H. Bowers, J. L. Parke, *Phytopathology* **1993**, *83*, 1466-1473.
- [212] W. J. Janisiewicz, J. Roitman, *Phytopathology* **1988**, *78*, 1697-1700.
- [213] W. H. Burkholder, *Phytopathology* **1950**, *40*, 115-118.
- [214] V. T. Van, O. Berge, S. N. Ke, J. Balandreau, T. Heulin, *Plant Soil* **2000**, *218*, 273-284.
- [215] E. Mahenthiralingam, T. A. Urban, J. B. Goldberg, *Nat. Rev. Microbiol.* **2005**, *3*, 144-156.
- [216] S. McClean, M. Callaghan, *J. Med. Microbiol.* **2009**, *58*, 1-12.
- [217] S. A. Loutet, M. A. Valvano, *Infect. Immun.* **2010**, *78*, 4088-4100.
- [218] J. H. Leitao, S. A. Sousa, M. V. Cunha, M. J. Salgado, J. Melo-Cristino, M. C. Barreto, I. Sa-Correia, *Eur. J. Clin. Microbiol. Infect. Dis.* **2008**, *27*, 1101-1111.
- [219] E. Caraher, G. Reynolds, P. Murphy, S. McClean, M. Callaghan, *Eur. J. Clin. Microbiol. Infect. Dis.* **2007**, *26*, 213-216.
- [220] A. Isles, I. Maclusky, M. Corey, R. Gold, C. Prober, P. Fleming, H. Levison, *J. Pediatr.* **1984**, *104*, 206-210.
- [221] S. Bamford, H. Ryley, S. K. Jackson, *Cell. Microbiol.* **2007**, *9*, 532-543.
- [222] a) I. Ofek, D. L. Hasty, N. Sharon, *FEMS Immunol. Med. Microbiol.* **2003**, *38*, 181-191; b) N. Sharon, *Biochim. Biophys. Acta, Gen. Subj.* **2006**, *1760*, 527-537.
- [223] M. Aronson, O. Medalia, L. Schori, D. Mirelman, N. Sharon, I. Ofek, *J. Infect. Dis.* **1979**, *139*, 329-332.
- [224] F. A. Sylvester, U. S. Sajjan, J. F. Forstner, *Infect. Immun.* **1996**, *64*, 1420-1425.
- [225] H. C. Krivan, D. D. Roberts, V. Ginsburg, *Proc. Natl. Acad. Sci. U. S. A.* **1988**, *85*, 6157-6156.
- [226] C. Wright, G. Herbert, R. Pilkington, M. Callaghan, S. McClean, *Lett. Appl. Microbiol.* **2010**, *50*, 500-506.
- [227] H. C. Kolb, K. B. Sharpless, *Drug Discov. Today* **2003**, *8*, 1128-1137.
- [228] W. C. Still, M. Kahn, A. Mitra, *J. Org. Chem.* **1978**, *43*, 2923-2925.
- [229] J. M. Palomo, M. Filice, R. Fernandez-Lafuente, M. Terreni, J. M. Guisan, *Adv. Synth. Catal.* **2007**, *349*, 1969-1976.
- [230] M. A. Brimble, R. Kowalczyk, P. W. R. Harris, P. R. Dunbar, V. J. Muir, *Org. Biomol. Chem.* **2008**, *6*, 112-121.
- [231] A. J. Ross, O. V. Sizova, A. V. Nikolaev, *Carbohydr. Res.* **2006**, *341*, 1954-1964.
- [232] R. Šardžík, G. T. Noble, M. J. Weissenborn, A. Martin, S. J. Webb, S. L. Flitsch, *Beilstein J. Org. Chem.* **2010**, *6*, 699-703.
- [233] J. L. Xue, S. Cecioni, L. He, S. Vidal, J.-P. Praly, *Carbohydr. Res.* **2009**, *344*, 1646-1653.
- [234] T. Hasegawa, T. Fujisawa, M. Numata, T. Matsumoto, M. Umeda, R. Karinaga, M. Mizu, K. Koumoto, T. Kimura, S. Okumura, K. Sakurai, S. Shinkai, *Org. Biomol. Chem.* **2004**, *2*, 3091-3098.
- [235] A. V. Orlova, A. I. Zinin, N. N. Malysheva, L. O. Kononov, I. B. Sivaev, V. I. Bregadze, *Russ. Chem. B+* **2003**, *52*, 2766-2768.
- [236] L. M. Artner, L. Merkel, N. Bohlke, F. Beceren-Braun, C. Weise, J. Dervedde, N. Budisa, C. P. R. Hackenberger, *Chem. Commun. (Cambridge, U. K.)* **2012**, *48*, 522-524.
- [237] S. Vandevoorde, K.-O. Jonsson, C. J. Fowler, D. M. Lambert, *J. Med. Chem.* **2003**, *46*, 1440-1448.
- [238] a) V. H. Wallingford, A. H. Homeyer, Mallinckrodt Chemical Works . **1945**; b) D. H. Hey, J. I. G. Cadogan, Distillers Co. Ltd. . **1962**, p. 4 pp.
- [239] J. C. Allen, J. I. G. Cadogan, B. W. Harrins, D. H. Hey, *J. Chem. Soc.* **1962**, 4468-4475.

- [240] K. Tanaka, S. Yoshifuji, Y. Nitta, *Chem. Pharm. Bull.* **1987**, *35*, 364-369.
- [241] C.-A. Tai, S. S. Kulkarni, S.-C. Hung, *J. Org. Chem.* **2003**, *68*, 8719-8722.
- [242] Z. Zhang, I. R. Ollmann, X.-S. Ye, R. Wischnat, T. Baasov, C.-H. Wong, *J. Am. Chem. Soc.* **1999**, *121*, 734-753.
- [243] K. Kunzelmann, E. M. Schwiebert, P. L. Zeitlin, W. L. Kuo, B. A. Stanton, D. C. Gruenert, *Am. J. Respir. Cell Mol. Biol.* **1993**, *8*, 522-529.

Author Publications